

# COSMECEUTICALS FROM MEDICINAL PLANTS

EDITED BY: Namrita Lall, Fawzi Mohamad Mahomoodally, Debora Esposito,  
Vanessa Steenkamp and Gokhan Zengin

PUBLISHED IN: Frontiers in Pharmacology





# frontiers

## Frontiers eBook Copyright Statement

The copyright in the text of individual articles in this eBook is the property of their respective authors or their respective institutions or funders. The copyright in graphics and images within each article may be subject to copyright of other parties. In both cases this is subject to a license granted to Frontiers.

The compilation of articles constituting this eBook is the property of Frontiers.

Each article within this eBook, and the eBook itself, are published under the most recent version of the Creative Commons CC-BY licence.

The version current at the date of publication of this eBook is CC-BY 4.0. If the CC-BY licence is updated, the licence granted by Frontiers is automatically updated to the new version.

When exercising any right under the CC-BY licence, Frontiers must be attributed as the original publisher of the article or eBook, as applicable.

Authors have the responsibility of ensuring that any graphics or other materials which are the property of others may be included in the CC-BY licence, but this should be checked before relying on the CC-BY licence to reproduce those materials. Any copyright notices relating to those materials must be complied with.

Copyright and source acknowledgement notices may not be removed and must be displayed in any copy, derivative work or partial copy which includes the elements in question.

All copyright, and all rights therein, are protected by national and international copyright laws. The above represents a summary only. For further information please read Frontiers' Conditions for Website Use and Copyright Statement, and the applicable CC-BY licence.

ISSN 1664-8714

ISBN 978-2-88966-021-6

DOI 10.3389/978-2-88966-021-6

## About Frontiers

Frontiers is more than just an open-access publisher of scholarly articles: it is a pioneering approach to the world of academia, radically improving the way scholarly research is managed. The grand vision of Frontiers is a world where all people have an equal opportunity to seek, share and generate knowledge. Frontiers provides immediate and permanent online open access to all its publications, but this alone is not enough to realize our grand goals.

## Frontiers Journal Series

The Frontiers Journal Series is a multi-tier and interdisciplinary set of open-access, online journals, promising a paradigm shift from the current review, selection and dissemination processes in academic publishing. All Frontiers journals are driven by researchers for researchers; therefore, they constitute a service to the scholarly community. At the same time, the Frontiers Journal Series operates on a revolutionary invention, the tiered publishing system, initially addressing specific communities of scholars, and gradually climbing up to broader public understanding, thus serving the interests of the lay society, too.

## Dedication to Quality

Each Frontiers article is a landmark of the highest quality, thanks to genuinely collaborative interactions between authors and review editors, who include some of the world's best academicians. Research must be certified by peers before entering a stream of knowledge that may eventually reach the public - and shape society; therefore, Frontiers only applies the most rigorous and unbiased reviews.

Frontiers revolutionizes research publishing by freely delivering the most outstanding research, evaluated with no bias from both the academic and social point of view. By applying the most advanced information technologies, Frontiers is catapulting scholarly publishing into a new generation.

## What are Frontiers Research Topics?

Frontiers Research Topics are very popular trademarks of the Frontiers Journals Series: they are collections of at least ten articles, all centered on a particular subject. With their unique mix of varied contributions from Original Research to Review Articles, Frontiers Research Topics unify the most influential researchers, the latest key findings and historical advances in a hot research area! Find out more on how to host your own Frontiers Research Topic or contribute to one as an author by contacting the Frontiers Editorial Office: [researchtopics@frontiersin.org](mailto:researchtopics@frontiersin.org)

# COSMECEUTICALS FROM MEDICINAL PLANTS

Topic Editors:

**Namrita Lall**, University of Pretoria, South Africa

**Fawzi Mohamad Mahomoodally**, University of Mauritius, Mauritius

**Debora Esposito**, North Carolina State University, United States

**Vanessa Steenkamp**, University of Pretoria, South Africa

**Gokhan Zengin**, Selçuk University, Turkey

**Citation:** Lall, N., Mahomoodally, F. M., Esposito, D., Steenkamp, V., Zengin, G., eds. (2020). Cosmeceuticals From Medicinal Plants. Lausanne: Frontiers Media SA. doi: 10.3389/978-2-88966-021-6

# Table of Contents

- 05 Editorial: Cosmeceuticals From Medicinal Plants**  
Namrita Lall, Mohamad Fawzi Mahomoodally, Debora Esposito, Vanessa Steenkamp, Gokhan Zengin, Aimee Steyn and Carel B. Oosthuizen
- 08 Book Review: Cosmeceuticals and Active Cosmetics, Third Edition**  
Marco Nuno De Canha, Analike Blom van Staden, Bianca Daphne Fibrich, Isa Anina Lambrechts, Lilitha Denga and Namrita Lall
- 10 Lamiaceae: An Insight on Their Anti-Allergic Potential and Its Mechanisms of Action**  
Lee Yen Sim, Nur Zahirah Abd Rani and Khairana Husain
- 46 Book Review: Medicinal Plants for Holistic Healing**  
Lyndy J. McGaw, Ajay Kumar Srivastava, Chung-Ho Lin and Vanessa Steenkamp
- 48 Topical Application of KAJD Attenuates 2,4-Dinitrochlorobenzene-Induced Atopic Dermatitis Symptoms Through Regulation of IgE and MAPK Pathways in BALB/C Mice and Several Immune Cell Types**  
Se Hyang Hong, Jin Mo Ku, Hyo In Kim, Tai Young Kim, Hye Sook Seo, Yong Cheol Shin and Seong-Gyu Ko
- 60 Black Walnut (*Juglans nigra*) Extracts Inhibit Proinflammatory Cytokine Production From Lipopolysaccharide-Stimulated Human Promonocytic Cell Line U-937**  
Khanh-Van Ho, Kathy L. Schreiber, Danh C. Vu, Susan M. Rottinghaus, Daniel E. Jackson, Charles R. Brown, Zhentian Lei, Lloyd W. Sumner, Mark V. Coggeshall and Chung-Ho Lin
- 71 Alaskan Berry Extracts Promote Dermal Wound Repair Through Modulation of Bioenergetics and Integrin Signaling**  
Debora Esposito, John Overall, Mary H. Grace, Slavko Komarnytsky and Mary Ann Lila
- 86 Growth Inhibitory Activity of *Callicarpa americana* Leaf Extracts Against *Cutibacterium acnes***  
Rozenn M. Pineau, Sarah E. Hanson, James T. Lyles and Cassandra L. Quave
- 98 In Vitro Antioxidant, Anti-Inflammatory and Skin Permeation of *Myrsine africana* and Its Isolated Compound Myrsinoside B**  
Bianca Fibrich, Xinyi Gao, Ashana Puri, Ajay K. Banga and Namrita Lall
- 106 Book Review: Herbal Principles in Cosmetics: Properties and Mechanisms of Action**  
Marco Nuno De Canha, Aimee Steyn, Analike Blom van Staden, Bianca Daphne Fibrich, Isa Anina Lambrechts, Lilitha Lwando Denga and Namrita Lall
- 109 Exploring the Anti-Acne Potential of *Impepho* [*Helichrysum odoratissimum* (L.) Sweet] to Combat *Cutibacterium acnes* Virulence**  
Marco Nuno De Canha, Slavko Komarnytsky, Lenka Langhansova and Namrita Lall



- 130** *<sup>1</sup>H-NMR Metabolomics and LC-MS Analysis to Determine Seasonal Variation in a Cosmeceutical Plant Leucosidea sericea*  
Phophi Freda Sehlakgwe, Namrita Lall and Gerhard Prinsloo
- 141** *Identification and Quantification of Bioactive Molecules Inhibiting Pro-inflammatory Cytokine Production in Spent Coffee Grounds Using Metabolomics Analyses*  
Khanh-Van Ho, Kathy L. Schreiber, Jihyun Park, Phuc H. Vo, Zhentian Lei, Lloyd W. Sumner, Charles R. Brown and Chung-Ho Lin
- 152** *Biocompatible Nutmeg Oil-Loaded Nanoemulsion as Phyto-Repellent*  
Masturah Mohd Narawi, Hock Ing Chiu, Yoke Keong Yong, Nur Nadhirah Mohamad Zain, Muggundha Raoov Ramachandran, Chau Ling Tham, Siti Fatimah Samsurrijal and Vuanghao Lim
- 167** *Anti-Melanogenic Effect of Dendropanax morbiferus and Its Active Components via Protein Kinase A/Cyclic Adenosine Monophosphate-Responsive Binding Protein- and p38 Mitogen-Activated Protein Kinase-Mediated Microphthalmia-Associated Transcription Factor Downregulation*  
Jung Up Park, Seo Young Yang, Rui Hong Guo, Hong Xu Li, Young Ho Kim and Young Ran Kim



# Editorial: Cosmeceuticals From Medicinal Plants

Namrita Lall<sup>1,2,3\*†</sup>, Mohamad Fawzi Mahomoodally<sup>4†</sup>, Debora Esposito<sup>5†</sup>,  
Vanessa Steenkamp<sup>6†</sup>, Gokhan Zengin<sup>7†</sup>, Aimee Steyn<sup>1†</sup> and Carel B. Oosthuizen<sup>1†</sup>

<sup>1</sup> Department of Plant and Soil Sciences, Faculty of Natural and Agricultural Sciences, University of Pretoria, Pretoria, South Africa, <sup>2</sup> School of Natural Resources, University of Missouri, Columbia, MO, United States, <sup>3</sup> College of Pharmacy, JSS Academy of Higher Education and Research, Mysuru, India, <sup>4</sup> Department of Health Sciences, Faculty of Science, University of Mauritius, Réduit, Mauritius, <sup>5</sup> Department of Animal Science, North Carolina State University, Raleigh, NC, United States, <sup>6</sup> Department of Pharmacology, Faculty of Health Sciences, University of Pretoria, Pretoria, South Africa, <sup>7</sup> Department of Biology, Science Faculty, Selcuk University, Konya, Turkey

## OPEN ACCESS

### Edited and reviewed by:

Javier Echeverría,  
University of Santiago, Chile

### \*Correspondence:

Namrita Lall  
Namrita.Lall@up.ac.za

### †ORCID:

Namrita Lall  
0000-0002-3242-3476  
Mohamad Fawzi Mahomoodally  
0000-0003-3962-8666  
Debora Esposito  
0000-0001-9689-7622  
Vanessa Steenkamp  
0000-0003-3575-0410  
Gokhan Zengin  
0000-0001-6548-7823  
Aimee Steyn  
0000-0002-7398-4659  
Carel B. Oosthuizen  
0000-0003-0940-8099

### Specialty section:

This article was submitted to  
Ethnopharmacology,  
a section of the journal  
Frontiers in Pharmacology

Received: 25 May 2020

Accepted: 15 July 2020

Published: 29 July 2020

### Citation:

Lall N, Mahomoodally MF, Esposito D,  
Steenkamp V, Zengin G, Steyn A and  
Oosthuizen CB (2020) Editorial:  
Cosmeceuticals From  
Medicinal Plants.  
Front. Pharmacol. 11:1149.  
doi: 10.3389/fphar.2020.01149

**Keywords:** cosmeceuticals, medicinal plant, anti-inflammatory, acne (acne vulgaris), skin aging

## Editorial on the Research Topic

### Cosmeceuticals From Medicinal Plants

The use of the word cosmetics comes from *kosmétikos*, an Ancient Greek term. This word can be translated as “skilled in adornment,” with the variant *kosmein* meaning “arrange” or “adorn” and *kosmos* meaning “order”: Further interpretations include “to make for beauty,” especially of the complexion, or beautifying and “done or made for the sake of appearance,” or “correcting defects especially of the face,” primarily it is “decorative” or “ornamental” (Oumeish, 2001). The concept of beauty is one of the aspects of the Greek word *komes*, which means harmony, and was used to attain perfection. Gradually its meaning has changed until it became connected with the idea that was more closely related to the masking, concealing and camouflaging, as true beauty originates from the inner being and could not be created externally. Since primeval time, numerous civilisations have been subjected to the use of herbs as cosmetic applications. Even today, the demand and the utilization of phytocosmetics have increased in the personal care system (Mahomoodally and Ramjuttun, 2016). Research into the value and use of plant and mineral resources in cosmetics continued over the centuries evolving into what we consider to be cosmeceuticals. Interestingly, there is a great tendency of consumers to return to the use of herbs/herbal products for various applications to implement a more natural mode of life (Mahomoodally and Ramjuttun, 2016).

In a similar manner to “drugs,” defined as compounds utilized in the prevention and treatment of diseases, with the inherent potential to modulate physiological and pharmacological functions, so have “cosmetics” been designated as either cleaning or augmenting of skin appearance without therapeutic effects. The word “cosmeceuticals” has been coined to encompass that area which exists between the two aforementioned fields. Cosmeceuticals are hybrids that exist between drug and cosmetic products which are utilized to boost both skin health and beauty through their external and/or internal application. Natural cosmeceuticals include those elements that can have a medicinal effect on acne, pigmentary disorders, melasma (photoprotectants), aging, skin inflammation, wrinkle formation and scarring, as well as hair problems including thinning, and alopecia, to name but a few (Dorni et al., 2017). Resultantly, cosmeceutical research is an emerging field and aligns with health and economic challenges. This Research Topic included studies that provided scientific evidence for the advancement of phytochemicals and traditionally used plants as cosmeceuticals. It is anticipated that such studies will

add to our understanding of the pharmacology and use of medicinal plants, fungi and other organisms used as cosmeceuticals through new and scientifically substantive knowledge.

The statement “there is a plant for every need on every continent,” now appears to be a truism (Cowan, 1999). Traditionally, the use of plants against skin diseases and specifically for cosmeceutical purposes has been a common practice among many cultures. A majority of the plant ingredients (oat, walnuts, chamomile, carrot, almonds, cucumber, lavender, mint, rose, and sweet violet petals) are utilized in modern phytocosmetics, including, shampoos, creams, lotions, and sun care products. Pieroni et al. (2004) documented that much of the external or topical applications of some of these plants have never been scientifically proven before, despite their ability to be used for either dermatological or cosmeceutical purposes.

This unique Research Topic comprises of 14 articles bringing together experimental and review papers on the pharmacology associated with these phyto-cosmeceuticals. The major themes within this topic included anti-acne, anti-inflammatory, pigmentary disorders, allergic reactions, aging, and repellent properties of medicinal plants.

Three book reviews have been included. The first book review; “Herbal Principles in Cosmetics: Properties and Mechanisms of Action” has as a topic a collection of medicinal plants that have been used traditionally as cosmeceuticals (De Canha et al.). The second book that was reviewed, “Cosmeceuticals and Active Cosmetics, Third Edition” provides a collection of medicinal plants that have been used in cosmeceuticals based on their active compounds. The book provides information on various ingredients and commercial products (De Canha et al.). The last book review; “Medicinal Plants for Holistic Healing,” includes a collection of medicinal plants that have been used as a remedy for treating various types of skin cancers, hyperpigmentation, oral disorders, and many others (McGaw et al.).

Sehlagwe et al. focused on a plant, belonging to the Rosaceae family, which has previously been shown to have strong antibacterial properties against *Cutibacterium acnes*. The authors noted that significant differences were observed between the anti-acne activity of plant material collected in different seasons, with the best activity reported for plants collected during the winter period. Proton NMR-based untargeted metabolomic analysis was used to determine the differences in the chemical profiles of samples collected in different seasons. The compound 2-(4-ethoxyphenyl)-5,6,7,8-tetramethoxy-4H-1-benzopyran-4-one was identified in only the winter samples (Sehlagwe et al.).

Pineau et al. investigated the inhibitory activity of *Callicarpa americana* leaves, a native South-Eastern United States shrub historically used by Native Americans to treat fever, stomach-ache, and pruritus against acne vulgaris skin condition. The latter is known to negatively affect adolescents and young adults by impacting self-esteem, self-confidence, and social life. This work highlighted the potential of the extracts as a cosmeceutical ingredient. The authors discussed the need for further research to assess its mechanism of action and *in vivo* efficacy (Pineau et al.).

Another study on ant-acne by De Canha et al. investigated the ability of methanolic extracts of *Helichrysum odoratissimum* to inhibit bacterial growth of *C. acnes* and pathogenic virulence factors thereof. The extract exhibited antimicrobial activity against *C. acnes* by showing high specificity against cell aggregation and preventing biofilm formation. Anti-inflammatory activity was observed by inhibiting cytokine levels of IL-8. This study validated the traditional use of *Impepho* as an ointment for pimples, not only by controlling bacterial proliferation but also due to inhibitory activity on various virulence factors (De Canha et al.).

The study by Ho et al. assessed the anti-inflammatory properties of spent coffee grounds (SCG) belonging to three Arabica cultivars. The extracts were found to exert inhibitory effects on the secretion of inflammatory mediators. Hawaiian Kona exhibited inhibitory effects on the expression of three examined cytokines, whereas Ethiopian Yirgacheffe reduced the secretion of TNF- $\alpha$  and IL-6, and Costa Rican Tarrazu decreased the secretion of IL-6. The anti-inflammatory activity was correlated with 26 identified metabolites quantified by LCMS. Twelve of these had high relative intensities in all of the extracts. The presence of multiple anti-inflammatory compounds in SCG provided a promising natural source for cosmeceutical and pharmaceutical industries (Ho et al.).

Fibrich et al. investigated how dermal aging is characterized by states of oxidative stress, chronic inflammation, and abnormal proteolytic degradation. This study focused on *Myrsine africana* and its active compounds, myrsinoid B and their ability to reduce the activity of hydrogen peroxide, superoxide and 5-lipoxygenase as supplementary mechanisms, ultimately to reduce the appearance of wrinkles. The samples showed the potential to be used as antiwrinkle agents as they indicated promising antioxidant and anti-inflammatory activity (Fibrich et al.).

Black walnut is known to be an excellent source of health-promoting and anti-inflammatory compounds. Ho et al. investigated ‘in-kernel’ extracts of Black walnut belonging to different cultivars and tested their effect on the expression of six human inflammatory cytokines/chemokines using a bead-based, flow cytometric multiplex assay. Certain black walnut cultivars showed promising potential for decreasing the severity of inflammatory skin diseases (Ho et al.).

Esposito et al. focused on Alaskan berries that have traditionally been used to treat skin wounds. The berries were found to contain a variety of bioactive polyphenols which exhibit anti-inflammatory, antioxidant, and antimicrobial properties, making them prime candidates for wound healing. Alaskan berries indicated promise and its usage in regenerative responses and restoring function in a variety of tissues and organs after injury or aging (Esposito et al.).

The paper by Hong et al. focused on atopic dermatitis (AD), of unknown origin. KHU-ATO-JIN-D (KAJD) which is a poly-herbal mixture of extracts from six plants, known to have anti-inflammatory and antiallergic effects, was found to inhibit the development of DNCB-induced AD in BALB/c mice and several immune cell types, suggesting that KAJD might be a useful therapeutic drug for the treatment of AD (Hong et al.).

Sim et al. reviewed the antiallergic potential of the family; Lamiaceae. This included its use as ethnomedicine for treating

inflammatory skin diseases and allergic asthma and in-depth reference to the antiallergic mechanisms related to Lamiaceae species (Sim et al.).

Park et al. investigated the antimelanogenic effect of *Dendropanax morbiferus*. This plant was shown to inhibit tyrosinase activity and melanin formation by reducing melanogenesis-related protein levels. Two active ingredients of *D. morbiferus* were identified, namely, DMW-1 and DMW-2. It was concluded that *D. morbiferus* and DMW-1 may be useful as therapeutic agents for skin hyperpigmentation disorders (Park et al.).

The study by Narawi et al. focused on using nanoemulsions to decrease the volatility of the constituents of essential oils used as repellents. Different formulations were tested for their droplet size and insect repellent activity. A nutmeg oil-loaded nanoemulsion was successfully formulated and controlled release of the essential oil showed mosquito repellent activity, eliminating some of the disadvantages of crude essential oils (Narawi et al.).

These valuable scientific contributions are welcomed by the scientific community, however, the field of cosmeceutical research should be further expanded as one can tap into a wealth of discovery and development of important

cosmeceuticals from natural resources to address consumer and patients demand.

## AUTHOR CONTRIBUTION

All the guest editors and listed authors have made a direct contribution toward this work and approved it for publication.

## ACKNOWLEDGEMENTS

This Research Topic would not have been possible without the contribution of all the researchers and authors. As Guest-Editors, we would like to thank all the authors for their substantial contribution toward the success of this issue. We would like to thank the reviewers for their time and valuable constructive comments and suggestions. Lastly, a special word of appreciation to the members of the Frontiers Editorial Office, for their assistance in making this work a success.

## REFERENCES

- Cowan, M. M. (1999). Plant products as antimicrobial agents. *Clin. Microbiol. Rev.* 12, 564–582. doi: 10.1128/CMR.12.4.564
- Dorni, A. I. C., Amalraj, A., Gopi, S., Varma, K., and Anjana, S. N. (2017). Novel cosmeceuticals from plants—An industry guided review. *J. Appl. Res. Med. Aromat. Plants* 7, 1–26.
- Mahomoodally, M. F., and Ramjuttun, P. (2016). A quantitative ethnobotanical survey of phytocosmetics used in the tropical island of Mauritius. *J. Ethnopharmacol.* 193, 45–59. doi: 10.1016/j.jep.2016.07.039
- Oumeish, O. Y. (2001). The cultural and philosophical concepts of cosmetics in beauty and art through the medical history of mankind. *Clin. Dermatol.* 19, 375–386. doi: 10.1016/S0738-081X(01)00194-8
- Pieroni, A., Quave, C. L., Villanelli, M. L., Mangino, P., Sabbatini, G., Santini, L., et al. (2004). Ethnopharmacognostic survey on the natural ingredients used in

folk cosmetics, cosmeceuticals and remedies for healing skin diseases in the inland Marches, Central-Eastern Italy. *J. Ethnopharmacol.* 91, 331–344. doi: 10.1016/j.jep.2004.01.015

**Conflict of Interest:** The authors declare that the research was conducted in the absence of any commercial or financial relationships that could be construed as a potential conflict of interest.

Copyright © 2020 Lall, Mahomoodally, Esposito, Steenkamp, Zengin, Steyn and Oosthuizen. This is an open-access article distributed under the terms of the Creative Commons Attribution License (CC BY). The use, distribution or reproduction in other forums is permitted, provided the original author(s) and the copyright owner(s) are credited and that the original publication in this journal is cited, in accordance with accepted academic practice. No use, distribution or reproduction is permitted which does not comply with these terms.



# Book Review: Cosmeceuticals and Active Cosmetics, Third Edition

Marco Nuno De Canha<sup>1</sup>, Analike Blom van Staden<sup>1</sup>, Bianca Daphne Fibrich<sup>1</sup>,  
Isa Anina Lambrechts<sup>1</sup>, Lilitha Denga<sup>1</sup> and Namrita Lall<sup>1,2,3\*</sup>

<sup>1</sup> Department of Plant and Soil Sciences, University of Pretoria, Pretoria, South Africa, <sup>2</sup> School of Natural Resources, University of Missouri, Columbia, MO, United States, <sup>3</sup> College of Pharmacy, JSS Academy of Higher Education and Research, Mysuru, India

**Keywords:** cosmeceuticals, cosmetics, skin care, hair care, natural ingredients

## A Book Review on

### Cosmeceuticals and Active Cosmetics, Third Edition

Raja S. Sivamani, Jared Jagdeo, Peter Elsner, Howard I. Maibach, (Boca Raton, FL: CRC Press), 2015, 458 pages, ISBN-13: 978-1-4822-1417-8 (eBook-pdf)

Cosmeceuticals are ingredients or products that possess cosmetic and pharmaceutical benefits, which can be obtained without a prescription (Sharad, 2019). This book (Sivamani et al., 2015) provides the reader with ample information regarding ingredients and commercial products which hail largely from botanical origin, but also includes a chapter on biomarine active ingredients. It not only illustrates the diverse applications of cosmeceutical ingredients in skin, hair, and nail care but also their pharmaceutical indications. The causes and potential mechanisms for the development and progression of several skin conditions and their therapeutic targets are also described.

A general overview of phytochemicals/botanical extracts and their use in skin care is provided in chapters 1, 2, 3, 7, and 10. This includes how certain phytochemicals such as bakuchiol contain functional groups such as terpenic moieties which offer enhanced efficacy when compared to mainstream compounds such as retinol (chapter 1). Compounds such as caffeine which are consumed regularly, offer relief to a plethora of skin conditions when applied topically, with the added benefit of enhanced skin penetration (chapter 2). Chapter 3 delves into the potential of curcumin for the treatment of photocarcinogenesis, validated by clinical trials. The use of hexylrescorinol as an anesthetic in throat lozenges and several additional molecular targets is divulged in chapter 7, while chapter 10 provides a general overview on the use of resveratrol-rich grape skins and seeds and their copious incorporation into commercial products.

Pigmentary aberrations as a function of disorders such as vitiligo or UV-induced hyperpigmentation are discussed in chapters 5, 27, and 29 (Njoo and Westerhof, 2001). Chapter 5 specifically discusses the use of ellagic acid from pomegranate as an agent capable of rectifying UV-induced hyperpigmentation comparable to the efficacy of arbutin.

The pathophysiology of several diseases associated with impaired barrier function and dehydrated skin are elaborated in chapters 19 and 26, which highlight the importance of moisturizers and emollients and the respective mechanisms by which they are able to relieve these conditions. The efficacy of fatty acids such as gamma linoleic acid found in the oils of the genera *Borago*, *Oenothera*, and *Echium* (chapter 6) and amino acids (chapter 15) as wound healing and skin hydration agents is also covered.

Chapter 21, 22, and 23 emphasized how skin homeostasis is disturbed by exposure to UV rays, which may manifest as premature aging and skin cancer. These chapters, along with chapter 16 critically discussed the benefits of topical antioxidants in neutralizing reactive oxygen species and how they can be applied individually or in combination, depending on their chemical properties

## OPEN ACCESS

### Edited and reviewed by:

Michael Heinrich,  
UCL School of Pharmacy,  
United Kingdom

### \*Correspondence:

Namrita Lall  
namrita.lall@up.ac.za

### Specialty section:

This article was submitted to  
Ethnopharmacology,  
a section of the journal  
Frontiers in Pharmacology

**Received:** 18 March 2019

**Accepted:** 26 April 2019

**Published:** 24 May 2019

### Citation:

De Canha MN, Blom van Staden A,  
Fibrich BD, Lambrechts IA, Denga L  
and Lall N (2019) Book Review:  
Cosmeceuticals and Active  
Cosmetics, Third Edition.  
Front. Pharmacol. 10:529.  
doi: 10.3389/fphar.2019.00529



and clinical efficacy. Furthermore, chapter 8, 9, 11, 12, 13, and 14 discusses the use of plant hormones (cytokinins) with high skin penetration and low irritancy as DNA repair agents for aging skin and phenylpropanoids from *Rhodilia rosea*, silymarin from milk thistle, niacinamide, anti-aging peptides and proteins in the prevention of photodamage. Peptides can be carriers of anti-aging ingredients, inhibitors of enzymes contributing to aging or act as signals or neurotransmitters to reverse factors contributing to skin damage. The use of hydroxyacids (both  $\alpha$  and  $\beta$ ), commonly known as fruit acids as common ingredients in skin peeling products and their and potential adverse effects (stinging, irritation, swelling and redness of the skin) is also discussed in chapter 8.

Chapter 28 focused on the cosmeceutical treatment of disorders associated with sebaceous glands and the need for more clinical data while chapter 24 explored the use of botanical extracts such as the feverfew tree, licorice, *Crysanthellum indicum* and *Quassia amara* for rosacea as independent or complementary adjuvant therapies.

This book highlights the potential of phytoconstituents to maintain health across the board but also highlights that the most hindering factor in the development and commercialization of natural products is a lack of efficacy studies in human trials. Even in instances where abundant phytochemicals such as epicatechin-3-gallate which comprises 50–80% of green tea provide sufficient and even surplus information in cell culture and animal studies, the incorporation into cosme- and pharmaceuticals for human consumption is limited (chapter 4). The exploration of marine organisms as a source of active compounds such as fucoidan from brown seaweed may provide a plethora of novel natural actives from which new medicines can be developed (chapter 31).

Non-skin related conditions are discussed in chapter 18, 20, and 25, which includes hair and nail care. Chapter 18 considers hair structure and function and how factors such as hydrophobicity, heat, oil content and the degree of damage govern the ingredients that need to be used in shampoos, conditioners and fixatives. Chapter 25 discusses condition known as androgenic alopecia, which is characterized by hair loss. Various extracts and cosmeceutical compounds involved in hormone and hormone receptor balance are described. Treatments for unhealthy nails and various nail conditions are discussed in chapter 20.

Important concepts in the manufacturing of natural actives including the influence of extraction processes on bioactivity against several conditions are highlighted in chapter 31, while

chapter 33 discusses the use of techniques in the quantification of bioactive compounds from extracts.

Preservatives, antioxidants and natural pigments can also provide crucial functions to the integrity of a formulation as covered in chapters 17, 19, and 26. The use of preservatives and anti-oxidants to prevent bacterial growth and browning in moisturizers is a noteworthy section discussed in chapter 19 and 26. Chapter 17 describes natural pigments, both organic and inorganic in decorative cosmetics like make-up (Parish and Crissey, 1988). Perhaps the highlight of this section in terms of cosmeceutical use, was nano dispersion forms of administration of  $\text{TiO}_2$  and  $\text{ZnO}$  for UVB protection.

Finally, chapter 34 identified legal terms as outlined by the Federal Food, Drug, and Cosmetic Act and what constitutes an agent as a drug or cosmetic which is becoming an increasingly controversial topic.

Although the book provides the reader with extensive scientific data relating to the efficacy of natural products, this limits the readership to researchers in particular fields, requiring some knowledge of associated biological pathways. While the book discusses validation of efficacy, perhaps more focus needs to be placed on other important features of cosmeceuticals, including safety and potential interactions with other products. The quality of the book could also be improved by the inclusion of specific mechanisms of action in addition to the antioxidant data, which has become somewhat over-emphasized in natural product research. The reputation of natural product actives would be valued a great deal more if multiple, concrete mechanisms of action are identified for treating a disorder. Lastly, although a vast amount of information has been superbly summarized in this book, future reviews should perhaps focus on current trends in cosmeceutical and pharmaceutical research that have not been so extensively covered. Cosmeceutical research has entered an era where repeating tedious experiments on new leads, no longer constitutes cutting edge or interesting research. Researchers are more inclined to find alternative methods that enhance the frugality of existing medicinal extracts through a multidisciplinary approach to generate not only revolutionary science, but products too.

## AUTHOR CONTRIBUTIONS

All authors listed have made a substantial, direct and intellectual contribution to the work, and approved it for publication.

## REFERENCES

- Njoo, M. D., and Westerhof, W. (2001). Vitiligo: Pathogenesis and treatment. *Am. J. Clin. Dermatol.* 2, 167–181. doi: 10.2165/00128071-200102030-00006
- Parish, L. C., and Crissey, J. T. (1988). Cosmetics: a historical review. *Clin. Dermatol.* 6, 1–4. doi: 10.1016/0738-081X(88)90024-7
- Sharad, J. (2019). “Cosmeceuticals,” in *Advances in Intergrative Dermatology*, eds K. França and T. Lotti (West Sussex: Wiley Blackwell), 393–411
- Sivamani, R. K., Jagdeo, J. R., Elsner, P., and Maibach, H. I. (2015). *Cosmeceuticals and Active Cosmetics, Third Edition*. Boca Raton, FL: CRC Press.
- Conflict of Interest Statement:** The authors declare that the research was conducted in the absence of any commercial or financial relationships that could be construed as a potential conflict of interest.

Copyright © 2019 De Canha, Blom van Staden, Fibrich, Lambrechts, Denga and Lall. This is an open-access article distributed under the terms of the Creative Commons Attribution License (CC BY). The use, distribution or reproduction in other forums is permitted, provided the original author(s) and the copyright owner(s) are credited and that the original publication in this journal is cited, in accordance with accepted academic practice. No use, distribution or reproduction is permitted which does not comply with these terms.



# Lamiaceae: An Insight on Their Anti-Allergic Potential and Its Mechanisms of Action

Lee Yen Sim, Nur Zahirah Abd Rani and Khairana Husain\*

Drug and Herbal Research Centre, Faculty of Pharmacy, Universiti Kebangsaan Malaysia, Kuala Lumpur, Malaysia

## OPEN ACCESS

### Edited by:

Namrita Lall,  
University of Pretoria,  
South Africa

### Reviewed by:

Helen Skaltsa,  
National and Kapodistrian  
University of Athens,  
Greece  
Funda Nuray Yalcin,  
Hacettepe University,  
Turkey

### \*Correspondence

Khairana Husain  
khairana@ukm.edu.my

### Specialty section:

This article was submitted to  
Ethnopharmacology,  
a section of the journal  
Frontiers in Pharmacology

Received: 29 January 2019

Accepted: 24 May 2019

Published: 19 June 2019

### Citation:

Sim LY, Abd Rani NZ and Husain K  
(2019) Lamiaceae: An Insight on  
Their Anti-Allergic Potential and Its  
Mechanism of Actions.  
Front. Pharmacol. 10:677.  
doi: 10.3389/fphar.2019.00677

The prevalence of allergic diseases such as asthma, allergic rhinitis, food allergy and atopic dermatitis has increased dramatically in recent decades. Conventional therapies for allergy can induce undesirable effects and hence patients tend to seek alternative therapies like natural compounds. Considering the fact above, there is an urgency to discover potential medicinal plants as future candidates in the development of novel anti-allergic therapeutic agents. The Lamiaceae family, or mint family, is a diverse plant family which encompasses more than 7,000 species and with a cosmopolitan distribution. A number of species from this family has been widely employed as ethnomedicine against allergic inflammatory skin diseases and allergic asthma in traditional practices. Phytochemical analysis of the Lamiaceae family has reported the presence of flavonoids, flavones, flavanones, flavonoid glycosides, monoterpenes, diterpenes, triterpenoids, essential oil and fatty acids. Numerous investigations have highlighted the anti-allergic activities of Lamiaceae species with their active principles and crude extracts. Henceforth, this review has the ultimate aim of compiling the up-to-date (2018) findings of published scientific information about the anti-allergic activities of Lamiaceae species. In addition, the botanical features, medicinal uses, chemical constituents and toxicological studies of Lamiaceae species were also documented. The method employed for data collection in this review was mainly the exploration of the PubMed, Ovid and Scopus databases. Additional research studies were obtained from the reference lists of retrieved articles. This comprehensive summarization serves as a useful resource for a better understanding of Lamiaceae species. The anti-allergic mechanisms related to Lamiaceae species are also reviewed extensively which aids in future exploration of the anti-allergic potential of Lamiaceae species.

**Keywords:** Lamiaceae, anti-allergic, allergy, hypersensitivity, mast cell,  $\beta$ -hexosaminidase, eosinophil, histamine

## INTRODUCTION

Allergy is one of the manifestations of an abnormal regulation of the immune system. It can present as a mild to severe disorder, such as allergic rhinitis, food allergies, asthma, conjunctivitis, angioedema, urticaria, eczema, insect allergies and life-threatening anaphylaxis (Galli et al., 2008). Nowadays, allergy has become a global health concern. The cases of allergic disorders are increasingly rising and have reached an alarming rate. This statement is supported by some of the statistical figures provided by Pawankar (2014). According to Pawankar (2014), there are roughly 300 million

individuals experiencing asthma and approximately 200 to 250 million individuals experiencing food allergies around the world. Additionally, 1/10 of the population experienced medication hypersensitivities and around 400 million people suffered from allergic rhinitis. Allergy can be very irritating to an extent that can greatly affect the quality of life, lead to an economic burden and can even jeopardize one's life (Pawankar, 2014). Seeing the staggering pattern of morbidity and mortality caused by allergic disorders, this health issue must not be neglected and must be taken seriously with the active involvement of patients and healthcare professionals.

Currently, there are many treatment options for allergic disorders. Some of the widely used therapeutics are anti-histamine drugs, corticosteroids, leukotriene inhibitors and mast cell stabilizers to treat and control allergic conditions (Cota et al., 2012). All these medications are found to be efficacious in alleviating allergic symptoms. However, the drugs do not actually cure the allergy conditions. Instead, long term consumption of such drugs has been associated with undesirable side effects and sometimes may worsen the conditions (Han et al., 2017). Some examples of common side effects encountered by anti-histamine agents users are dry mouth, drowsiness, gastrointestinal disturbances, headache, agitation, confusion, etc. (Simon and Simons, 2008). As for corticosteroids, they work effectively in relieving allergic disorders, like allergic asthma, eczema, allergic rhinitis, etc. However, they often bring about undesirable side effects to patients in a long-term therapy. For instance, patients who are using inhaled corticosteroids for asthma control are likely to encounter undesirable effects like oral candidiasis (Fukushima et al., 2003) and adrenal suppression (Robert Webb, 1981). Patients with eczema who usually use topical steroidal treatment can develop Cushing's syndrome (Tiwari et al., 2013) and skin thinning (Atherton, 2003) as well as easy bruising (Coondoo et al., 2014). Due to the limitations of modern medicines, there is an increasing interest in using complementary and alternative medicine, particularly herbal medicine for allergy conditions management (Engler et al., 2009).

Undeniably, medicinal plants have been widely utilized as healing modalities for both preventive and curative purposes. They play an extremely crucial role in human health. In recent years, there has been a growing trend in the world population with as many as 80% of people globally relying on the use of herbal medicinal products and supplements for their primary healthcare needs (Schuster, 2001; Ekor, 2013). This increasing demand and interest in the use of herbal medicinal products has encouraged new drug discoveries and developments (Ekor, 2013). In fact, many active ingredients of new drugs are derived from medicinal plants proven to be remarkably important in aiding drug discovery and development (Katiyar et al., 2012). Hence, studies need to be actively conducted on plants in order to identify possible candidates as safer and effective anti-allergic agents in future.

The Lamiaceae family is one of the biggest plant families among flowering plants, consisting of 236 genera with a coverage of more than 7,000 species (Khoury et al., 2016). It is also an important herbal family which comprises a wide array of plants with biological and medical applications (Uritu et al., 2018). Lamiaceae species often have four-angled or quadrangular stems

with the presence of glandular hairs (Harley et al., 2004). Their roots are usually made of branched tap root. Their flowers are typically hypogynous and bilaterally symmetric with five united petals and sepals (Kokkini et al., 2003; Ramasubramania Raja, 2012; Carović-Stanko et al., 2016). The leaves are simple and arranged oppositely, each pair at a right angle to the previous one or whorled (Harley et al., 2004). Fruits are made of four dry one-seeded nutlets (Kokkini et al., 2003). Seeds are non-endospermic (Ramasubramania Raja, 2012). The environment adaptation of Lamiaceae is highly varied. The species predominantly distribute in the summer rainfall areas but also occur in winter rainfall areas. The species usually can be found in habitats which are dry, rocky, woodland or grassland, along forest margins and in fynbos (Will and Claßen-Bockhoff, 2014). The diversity of Lamiaceae species is mainly concentrated in Mediterranean regions and a small portion of them inhabit Australia, Southwest Asia and South America (Kokkini et al., 2003).

Khoury et al. (2016) reported that the high content of volatile compounds has contributed to many medicinal properties in Lamiaceae species. Historically, Lamiaceae plants have been reported to be effective in alleviating a range of conditions like exhaustion, weakness, depression, memory enhancement, circulation improvement, strengthening of fragile blood vessels, skin allergies and asthma (Wang et al., 2004; Naghibi et al., 2010; Ramasubramania Raja, 2012). In the Eastern Himalayan region of India, several Lamiaceae species have been utilized traditionally to treat certain conditions. For instance, the leaves of *Clerodendrum serratum* have been used as a traditional remedy for eye disorders. Moreover, the leaves of *Elsholtzia blanda* is used to relieve itching conditions. The seed of *Perilla frutescens* is also claimed to be effective against fever and headache (Kala, 2005). Meanwhile, in China, the Chinese tea brewed using the leaves of *Salvia officinalis* is used as a traditional remedy to treat tonsillitis and hypertension (Li et al., 2013). Another Lamiaceae species, *Scutellaria baicalensis* has been extensively used as traditional Chinese medicine (TCM) for thousands of years. It is known as Huang Qin in Chinese. The decoction prepared from dried roots is used as a traditional remedy for diarrhea, dysentery, hypertension, hemorrhaging, insomnia, inflammation and respiratory infections (Zhao et al., 2016). In Mediterranean regions, like Lebanon, *Mentha spicata* is formulated into infusions to ease digestive disorders, arthritis, gastritis. The infusion is also used as an antiemetic and antimicrobial agent (Khoury et al., 2016). The medicinal uses of commonly used Lamiaceae species are summarized in Table 1.

This review is particularly focused on the summarization of the anti-allergic activities of the Lamiaceae family linked to the phytochemistry and ethnopharmacology reported in research studies. In addition to anti-allergic activities, toxicological investigations of Lamiaceae species are also highlighted in this review.

## ANTI-ALLERGIC ACTIVITY

The abundance of species within the Lamiaceae family has led to a variety of medicinal uses, making the family pharmacologically



**TABLE 1 |** Medicinal uses of commonly used Lamiaceae species.

Plant name	Country/region	Local name/ common name	Medicinal use	Plant part used	Mode of preparation	References
<i>Clerodendrum petasites</i> (Lour.) S.Moore	Thailand	Thao yaai mom	Asthma	Aerial part	The aerial part is prepared as tea or alcoholic extract.	(Hazekamp et al., 2001)
<i>Clerodendrum serratum</i> (Linn.) Moon	Arunachal Pradesh, India	No information	Eye disorders	Leaves	No information.	(Kala, 2005)
<i>Elsholtzia blanda</i> (Benth.) Benth.	Arunachal Pradesh, India	No information	Itching conditions	Leaves	No information.	(Kala, 2005)
<i>Epimeredi indica</i> (L.) Rothm	China	Guang Fan Feng	Rheumatoid arthritis, bones and muscles ache, skin ulcer, hemorrhoids, eczema	Whole plant	The whole plant is used to prepare as medicinal bath.	(Li et al., 2006)
<i>Mentha arvensis</i> Linn.	Western Himalayas	Pudina	Stomach problems, allergy, liver and spleen disease, asthma, indigestion, rheumatic pains, arthritis	Leaves	Leaves are made as salad and formulated into infusion respectively.	(Khan and Khatoon, 2007)
	Korea	Bak-ha	Analgesic, local vasodilator, skin irritant, antispasmodic agent, acute mastitis, allergic dermatitis and skin itching	Aerial part	Sometimes combine with other herbs as traditional remedy.	(Shin, 2003)
<i>Mentha longifolia</i> (L.) L.	West Bengal, India	Junglipudina	Menstrual disorders, pulmonary infection, congestion, asthma, urinary tract infections, indigestion, back pain, headache and to fasten wound healing process	Leaves	The leaves are formulated into extract.	(Sinhababu and Arpita, 2013)
	India	No information	Carminative, stimulant, antiseptic and febrifuge	Leaves and flower tops	No information.	(Sinhababu and Arpita, 2013)
<i>Mentha spicata</i> Linn.	Thessaloniki, Greece	No information	Common cold and cough	Aerial part	No information.	(Karousou et al., 2007)
	Lebanon	No information	Digestive disorders, arthritis, gastritis, antiemetic and antimicrobial agents	No information	Formulated as infusions.	(Khoury et al., 2016)
<i>Perilla frutescens</i> (Linn.) Britton	India	No information	Arthritis	Seed oil	The oil is extracted from the plant seed and massaged onto the arthritis part.	(Singh, 1997)
	Arunachal Pradesh, India	No information	Fever and headache	Seed	No information.	(Kala, 2005)
<i>Prunella vulgaris</i> Linn.	Iberian Peninsula	No information	External antiseptic	Aerial part	No information.	(Rigat et al., 2015)
<i>Salvia miltiorrhiza</i> Bunge	China	Danshen	Promoting cardiovascular health by improving blood circulation to remove blood stasis, clearing heart heat to relieve restlessness and cooling blood to remove carbuncle	Root	The root is air-dried and made into decoctions and pills. Nowadays, the root is widely formulated into various preparations, such as tablets, capsules, granules, injections, oral liquids, sprays and tea.	(Su et al., 2015)
<i>Salvia officinalis</i> Linn.	China	No information	Tonsillitis and hypertension	Leaves	The leaves are brewed as tea.	(Li et al., 2013)
<i>Salvia plebeia</i> R. Brown	Korea	Baem-Cha-Zu-Ki	Skin inflammatory disease and asthma	No information	No information	(Choi et al., 2014; Shin and Kim, 2002)
<i>Scutellaria baicalensis</i> Georgi	China	Huang Qin	Diarrhea, dysentery, hypertension, hemorrhaging, insomnia, inflammation and respiratory infections	Root	The dried root is used to prepare decoctions.	(Zhao et al., 2016)

TABLE 1 | Continued

Plant name	Country/region	Local name/ common name	Medicinal use	Plant part used	Mode of preparation	References
<i>Thymus serpyllum</i> Linn.	Uttar Pradesh, India	No information	Headache, dysentery and vomiting	No information	Prepared as decoction.	(Singh, 1997)
<i>Thymus vulgaris</i> Linn.	Indonesia	No information	Asthma and other respiratory disorders	Leaves	No information	(Ikawati et al., 2001)
<i>Vitex negundo</i> Linn.	Uttar Pradesh, India	No information	Pain, swelling and eye inflammation	Leaves	The leaves are prepared as paste and applied onto the sprains to relieve pain. The leaf juice is used as drops to reduce eye inflammation.	(Singh, 1997)
<i>Vitex trifolia</i> Linn.	Indonesia	No information	Asthma and other respiratory disorders	Leaves	No information	(Ikawati et al., 2001; Alam et al., 2002)

important. The diversity is believed to be due to the wide variety of biologically active constituents in this plant family. Each species comprises a mixture of phytochemicals which attributes to the bioactivity of the plant (Carović-Stanko et al., 2016). Phytochemical investigations of the Lamiaceae family have demonstrated the presence of various bioactive compounds such as flavonoids (da Silva et al., 2015; Mamadalieva et al., 2017; Aghakhani and Kharazian, 2018), alkaloids (Malik et al., 2003; Asghari et al., 2017), phenolics (Berdowska et al., 2013; Zielińska and Matkowski, 2014; Skendi et al., 2017), lignans (Hong et al., 2009; Brandão et al., 2017), terpenoids (Ye et al., 2018), saponins (Ramasubramania Raja, 2012; Shah et al., 2014), etc. All these chemical constituents contribute to multidirectional pharmacological activities. Some of the remarkable bioactivities reported within this plant family are anti-allergic (Malik et al., 2003; Makino et al., 2003; Kim et al., 2009), anti-inflammatory (Borges et al., 2018), antimicrobial (Khoury et al., 2016; Cocan et al., 2018), free radical scavenging (Khaled-Khodja et al., 2014; Politeo et al., 2018), antinociceptive (Hwang et al., 2018; Uritu et al., 2018), anti-cancer activities (Nguyen et al., 2018; Sajjadi et al., 2018), etc. Many pharmacological activities of the Lamiaceae family have been widely studied and investigated. However, this study is mainly focused on the potential biologically active candidates with promising anti-allergic activity from Lamiaceae species in order to provide a direction in the discovery of potential novel, safe and efficacious natural anti-allergic agents in future. In the past, numerous *in vitro*, *in vivo* and *ex vivo* studies have been conducted and evaluated on the plant parts of Lamiaceae species to investigate the anti-allergic potential of Lamiaceae plants. **Figure 1** and **Table 2** show a summarization of the remarkable anti-allergic activities of the Lamiaceae family. The mechanisms of anti-allergic activities of Lamiaceae species are extensively discussed in this review.

## INHIBITION OF ALLERGEN-SPECIFIC IGE

Immunoglobulin E (IgE) is of central importance in the regulation of immune responses against parasitic infestations and most importantly, it is also recognized as a main mediator for immediate-type allergies or type I hypersensitivity reactions,

such as allergic asthma, rhinitis, atopic diseases, anaphylaxis, etc. (Al-Mughales, 2016). It is a potent mast cell activator able to trigger mast cell degranulation and downstream responses with a minute amount (Actor, 2014). It exists in trace amounts in plasma but the amount can be substantially elevated in allergic reactions (Gould and Beavil, 1998; van der Burg et al., 2014). It possesses an additional constant region, CH<sub>4</sub>, which particularly restricts it to bind to high affinity IgE receptors on mast cells and basophils (Flaherty, 2012). Upon the first encounter with the antigen, the plasma cells start to produce IgE molecules. The secreted IgE molecules bond to the high affinity IgE receptors (FcεRI) on the mast cells and basophils surfaces via their Fc portion, forming IgE-FcεRI complexes. In this form, the half-life of IgE can be prolonged to two to three weeks or sometimes can even be retained on the cell surface for months (Actor, 2014; van der Burg et al., 2014). Upon the re-exposure to the same antigen, the antigen will cross-link with the IgE-FcεRI complexes which then lead to mast cell degranulation (Actor, 2014). Inhibition of IgE production and IgE-mast cell cross-linking are particularly essential to prevent the progression to mast cell degranulation.

There are several studies demonstrating that Lamiaceae species have a suppressive effect on IgE levels and IgE-mast cell cross-linking. These findings could be useful to recognize potential treatment options for allergic disorders. From the study of Sharma et al. (2018), results revealed that the essential oil of *Mentha arvensis* significantly decreased ( $P < 0.001$ ) the serum IgE level in OVA-sensitized mice at a concentration of 200 µl/kg. The study successfully identified three compounds in the essential oil, which are menthol, menthone and 1,8-cineole, with particularly large percentage contents of menthol. However, the compound which contributed to the anti-allergic activity was not known (Sharma et al., 2018). Therefore, this provides a clue for further findings on the possible anti-allergic compound in future. In the work of Lee et al. (2006), it was proposed that the aqueous extract of *Mosla dianthera* exhibited anti-allergic effects through an *in vivo* model. When the mice were sensitized with compound 48/80 and anti-DNP IgE, intraperitoneal pretreatment of 1–1,000 mg/kg of aqueous extract resulted in a dose-related reduction in passive cutaneous anaphylaxis (PCA) reaction (Lee et al., 2006). Similar activities were displayed by the aqueous extract of species *Perilla frutescens* (Shin et al., 2000), *Phlomis umbrosa*

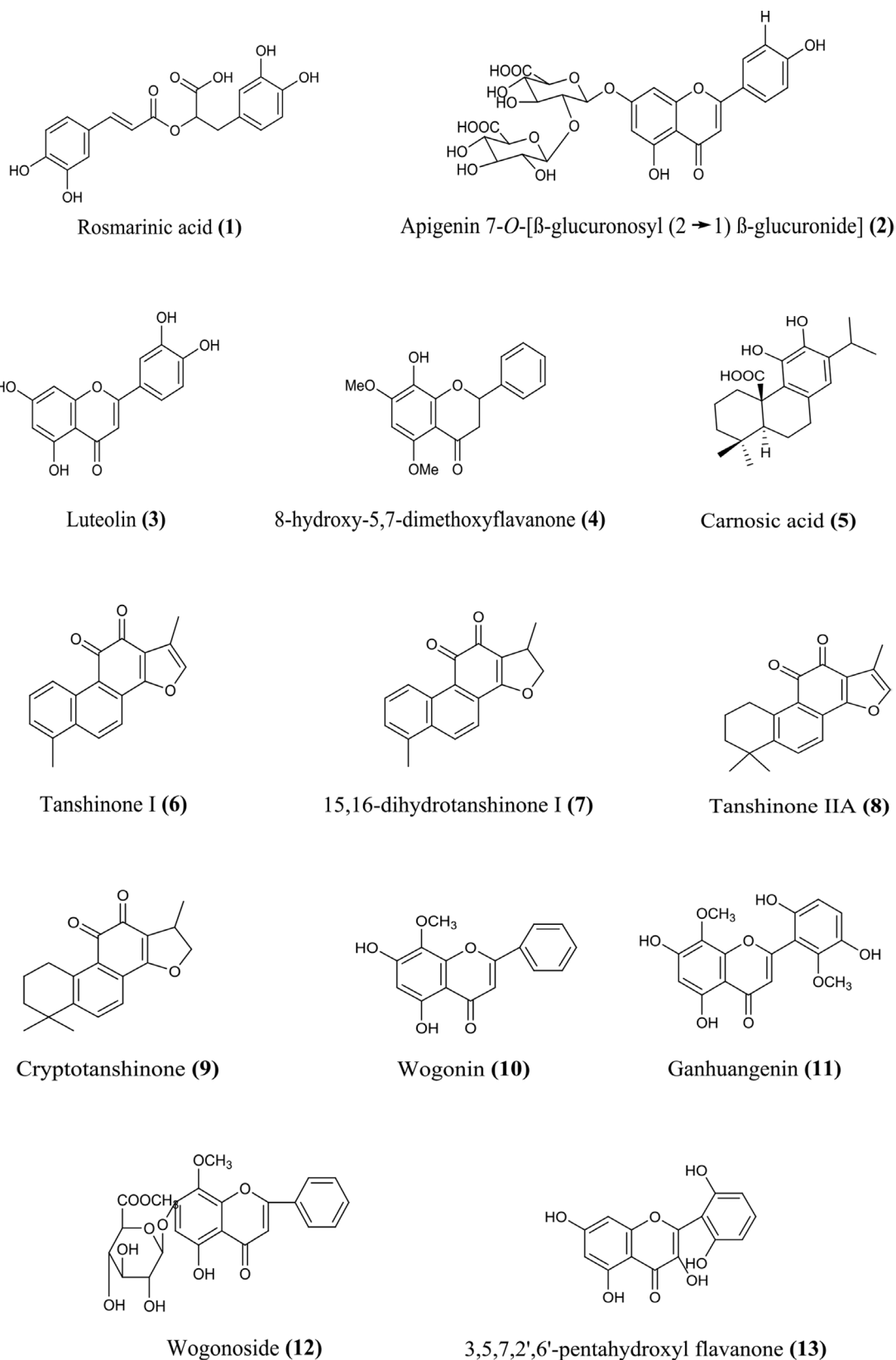
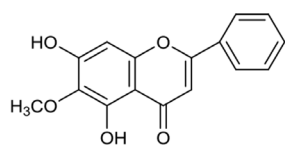
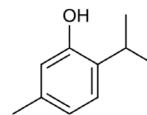


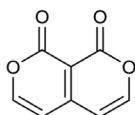
FIGURE 1 | Continued



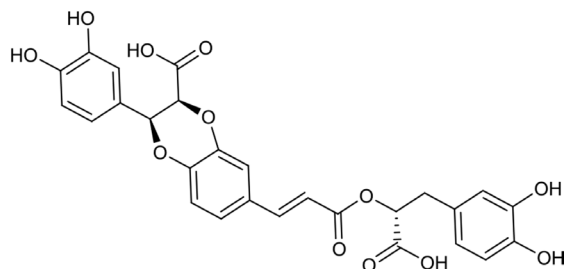
Oroxylin A (14)



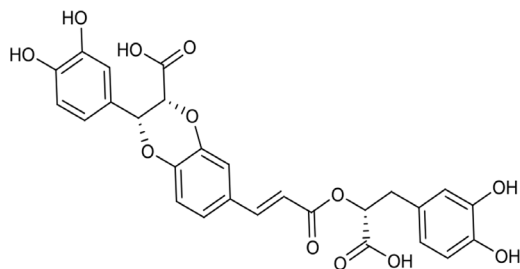
2-isopropyl-5-methylphenol (15)



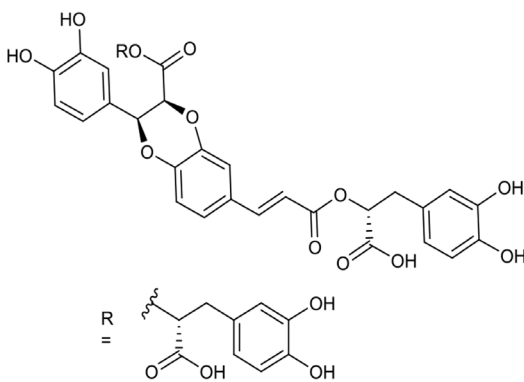
1H,8H-pyrano [3,4-c] pyran-1,8-dione (16)



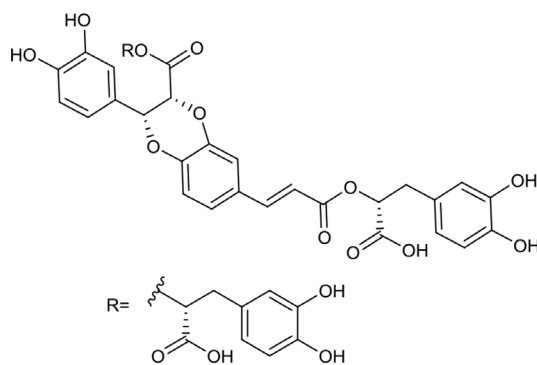
Clinopodic acid C (17)



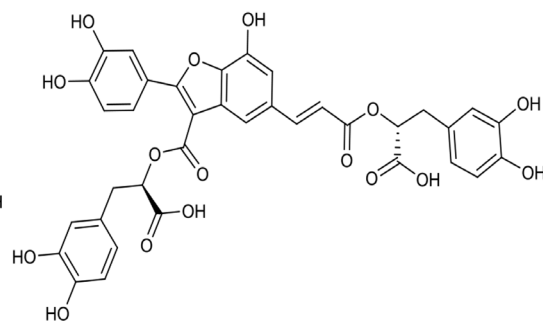
Clinopodic acid E (18)



Lycopic acid A (19)

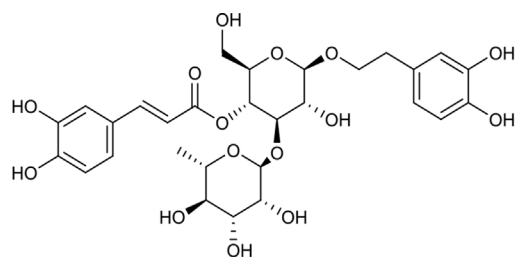


Lycopic acid B (20)

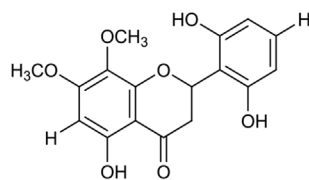


Scizotenuin A (21)

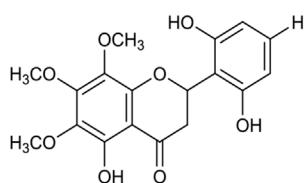
FIGURE 1 | Continued



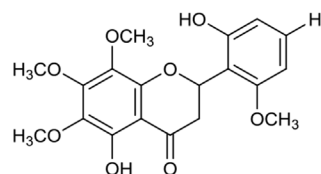
Acteoside (22)



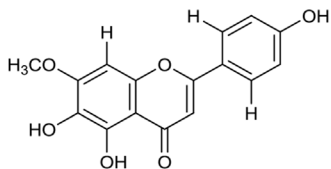
5,2',6'-trihydroxy-7,8-dimethoxyflavanone (23)



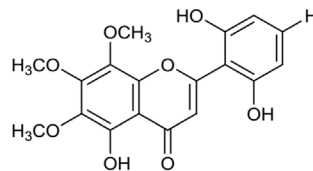
5,2',6'-trihydroxy-6,7,8-trimethoxyflavanone (24)



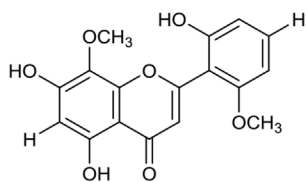
5,2'-dihydroxy-6,7,8,6'-tetramethoxyflavanone (25)



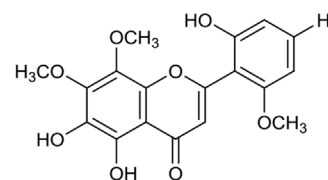
Hispidulin (26)



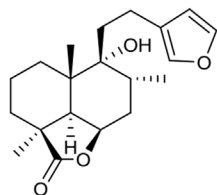
5,2',6'-trihydroxy-6,7,8-trimethoxyflavone (27)



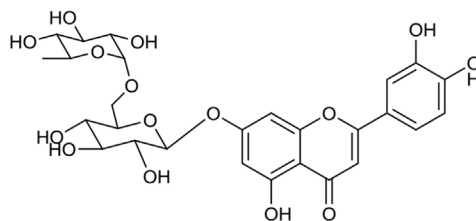
5,7,2'-trihydroxy-8,6'-dimethoxyflavone (28)



5,6,2'-trihydroxy-7,8,6'-trimethoxyflavone (29)

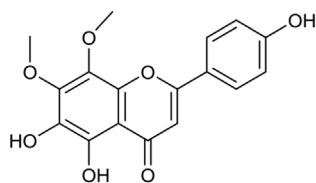


Marrubiin (30)

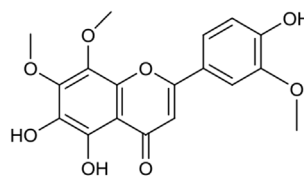


Luteolin-7-O-rutinoside (31)

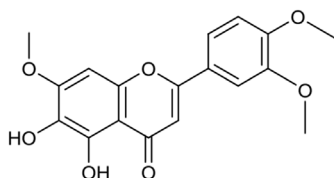
FIGURE 1 | Continued



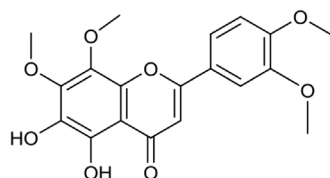
5,6,4'-trihydroxy-7,8-dimethoxyflavone (32)



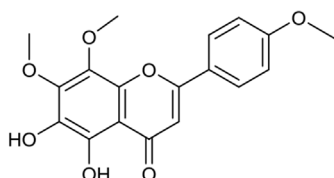
5,6,4'-trihydroxy-7,8,3'-trimethoxyflavone (33)



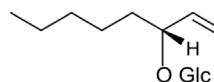
5,6-dihydroxy-7,3',4'-trimethoxyflavone (34)



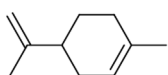
5,6-dihydroxy-7,8,3',4'-tetramethoxyflavone (35)



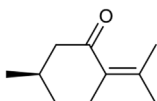
5,6-dihydroxy-7,8,4'-trimethoxyflavone (36)



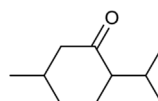
(3R)-1-octan-3-yl β-D-glucopyranoside (37)



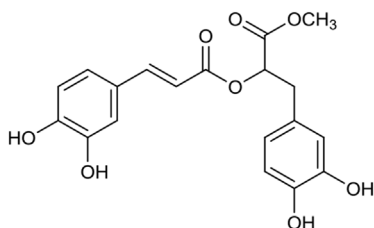
Limonene (38)



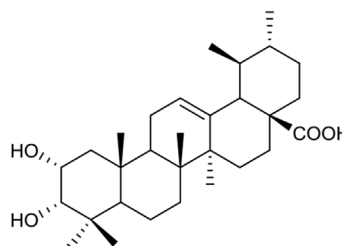
Pulegone (39)



Menthone (40)



Rosmarinic acid methyl ester (41)



2α,3α-dihydroxyurs-12-en-28-oic acid (42)

FIGURE 1 | Continued

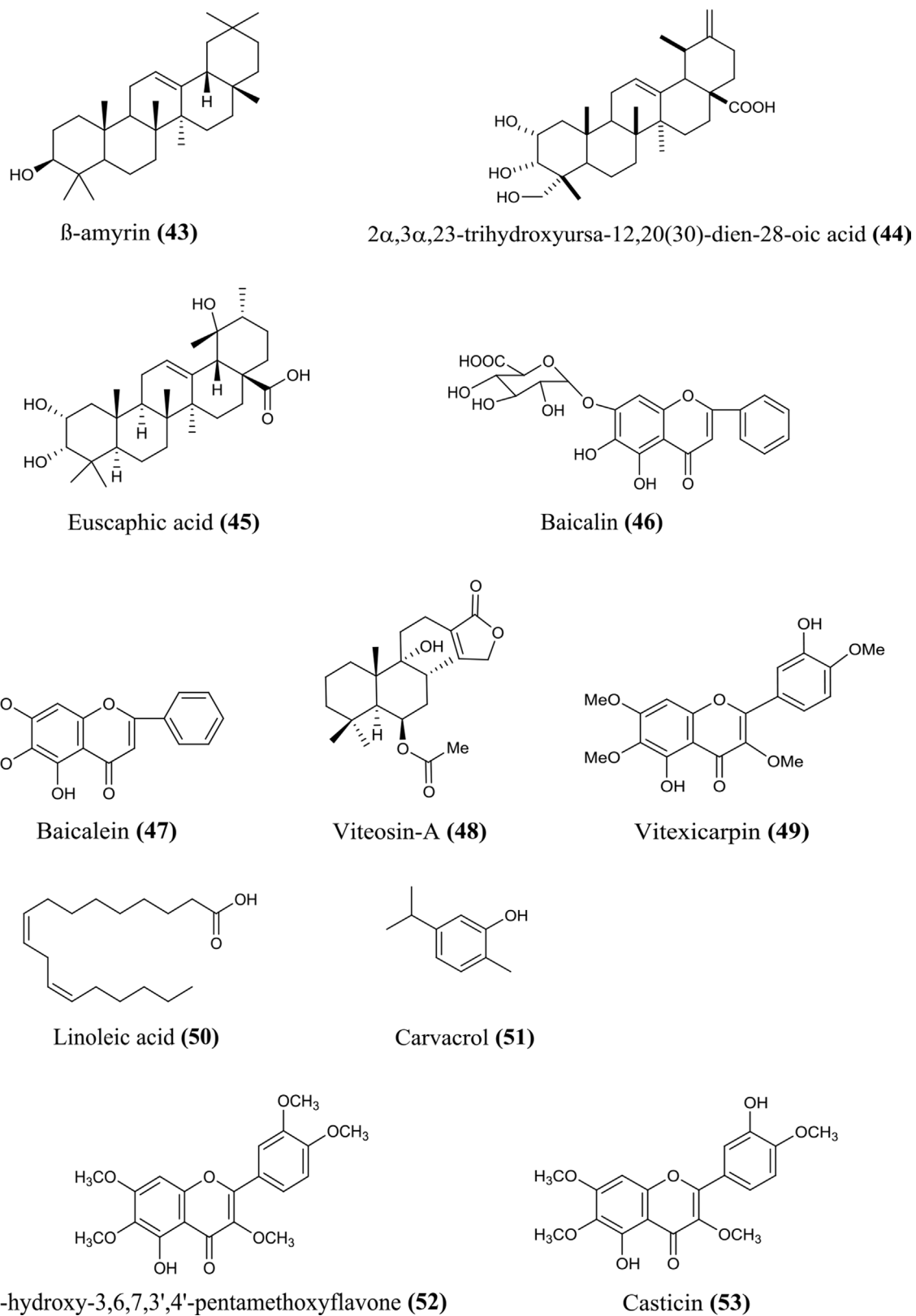


**FIGURE 1 |** Chemical structures of phytochemicals isolated from Lamiaceae species with anti-allergic activity.

**TABLE 2 |** Mechanism of action of extracts and isolates of Lamiaceae species with anti-allergic activity.

Plant name	Plant part used	Isolated compound/ extract used	Chemical class	Assay type	Mechanism of action/conclusion	References
<i>Clerodendron phlomidis</i> Linn.	Leaves	Aqueous extract	–	<i>In vivo</i>	Concentration of 100 mg/kg potently reduced blood eosinophil count, mast cell degranulation and histamine release in sensitized mice.	(Vadnere et al., 2007)
				<i>Ex vivo</i>	Potent antagonizing effect of histamine-induced goat tracheal contraction at doses of 4 mg/ml and 10 mg/ml.	(Vadnere et al., 2007)
<i>Clerodendrum serratum</i> (Linn.) Moon	Root and stem	Aqueous extract	–	<i>In vivo</i>	Root extract resulted in no significant increase of leucocyte and eosinophil count at 260 mg/kg in milk-induced leucocytosis mice and prolonged PCD at 156 mg/kg in egg albumin-sensitized guinea pigs.	(Bhangare et al., 2012)
<i>Clerodendron trichotomum</i> Thunb.	Leaves	Acteoside ( <b>22</b> )	Phenylpropanoid glycoside	<i>In vivo</i>	At dose of 50 mg/kg significantly inhibited eosinophil infiltration, decreased histamine content and phospholipase A <sub>2</sub> activity in BALF while at 25 mg/kg, recruitment of leukocytes was suppressed and inhibited sRaw in both IAR and LAR in sensitized guinea pigs model.	(Lee et al., 2011b)
<i>Clinopodium gracile</i> (Benth.) Matsum var. multicaule	Whole plant	Aqueous extract	–	<i>In vivo</i>	Compound 48/80-induced mice were observed with concentration-dependently reduced anaphylactic death with intraperitoneally administration at concentrations ranging from 1-100 mg/kg and the same reduction manner was seen in IgE-mediated PCA reaction.	(Park et al., 2010)
				<i>In vitro</i>	Dose-dependent inhibition of histamine release inhibition from RPMC and HMC-1 cells respectively across 1-100 µg/ml. Allergic inflammation reduced with the attenuation of intracellular calcium, NF-κB, gene expression and secretion of TNF-α and IL-6 stimulated by PMACI in HMC-1 cells.	(Park et al., 2010)
<i>Dracocephalum argunense</i> Fisch.	Whole plant	Aqueous extract	–	<i>In vivo</i>	Significant inhibition of systemic anaphylaxis with intraperitoneal administration of aqueous extract in mice at concentration range of 0.01–1 g/kg. Serum histamine and PCA inhibition were reduced in a dose-dependent manner.	(Kim et al., 2006; Kim and Shin, 2006)
				<i>In vitro</i>	Decreased intracellular calcium and histamine release from RPMC in dose dependent manner with concentrations of 0.001–1 mg/ml. TNF-α and IL-6 gene expression in HMC-1 cells were inhibited across doses ranging from 0.01–1 mg/ml with the involvement of NF-κB attenuation.	(Kim et al., 2006; Kim and Shin, 2006)



TABLE 2 | Continued

Plant name	Plant part used	Isolated compound/ extract used	Chemical class	Assay type	Mechanism of action/conclusion	References
<i>Elsholtzia ciliata</i> (Thunb.) Hyland	Whole plant	Aqueous extract	–	<i>In vivo</i>	Serum histamine, systemic anaphylaxis and PCA reaction observed with dose-related inhibition at concentrations of 10–1,000 mg/kg.	(Kim et al., 2011)
				<i>In vitro</i>	Significantly inhibited histamine release at 10 and 100 µg/ml of aqueous extract and recorded with reduction of PMACI-stimulated intracellular calcium at 100 µg/ml of aqueous extract pretreatment in HMC-1 cells. Gene expression and production of IL-6, IL-1β and TNF-α were suppressed through inhibition of NF-κB activation and p38 MAPK pathway with concentrations ranging from 1–100 µg/ml.	(Kim et al., 2011)
<i>Isodon japonicas</i> Hara	Whole plant	Aqueous extract	–	<i>In vivo</i>	Challenged-mice protected from systemic allergic death and PCA with intraperitoneal administration of extract at concentration of 0.1 g/kg.	(Kim et al., 2004; Shin et al., 2004)
				<i>In vitro</i>	Dose-dependently decreased histamine release from RPMC stimulated by compound 48/80 or anti-DNP IgE at doses ranging from 0.001–1 mg/ml and reduced gene expression and production of TNF-α and IL-6 in PMACI-stimulated HMC-1 cells.	(Kim et al., 2004; Shin et al., 2004)
<i>Lagochilus leiocanthus</i> Fisch. & C.A.Mey.	Whole plant	5,2',6'-trihydroxy-7,8-dimethoxyflavanone ( <b>23</b> ), 5,2',6'-trihydroxy-6,7,8-trimethoxyflavanone ( <b>24</b> ), 5,2'-dihydroxy-6,7,8,6'-tetramethoxyflavanone ( <b>25</b> ), Oroxylin-A ( <b>14</b> ), Hispidulin ( <b>26</b> ), 5,2',6'-trihydroxy-6,7,8-trimethoxyflavone ( <b>27</b> ), 5,7,2'-trihydroxy-8,6'-dimethoxyflavone ( <b>28</b> ), 5,6,2'-trihydroxy-7,8,6'-trimethoxyflavone ( <b>29</b> )	Flavonoid	<i>In vitro</i>	Significantly inhibited the release of β-hexosaminidase from RBL-2H3 cells with IC <sub>50</sub> values ranging from 13.5–48.9 µM.	(Furukawa et al., 2011)
<i>Lycopus lucidus</i> Turcz.	Aerial part	Rosmarinic acid ( <b>1</b> ), clinopodic acid C ( <b>17</b> ), lycopic acid A ( <b>19</b> ), clinopodic acid E ( <b>18</b> ), lycopic acid B ( <b>20</b> ), scizotenuin A ( <b>21</b> )	Phenylpropanoid	<i>In vitro</i>	Acted as hyaluronidase inhibitor with IC <sub>50</sub> of 309, 80.1, 134, 82.8, 141 and 241 µM respectively.	(Murata et al., 2010)

TABLE 2 | Continued

Plant name	Plant part used	Isolated compound/ extract used	Chemical class	Assay type	Mechanism of action/conclusion	References
<i>Marrubium vulgare</i> Linn.	Whole plant	Aqueous extract	–	<i>In vivo</i>	Systemic anaphylactic death and PCA reaction reduced dose-dependently across concentrations of 0.005–0.1 g/kg in sensitized mice.	(Shin et al., 2005)
				<i>In vitro</i>	Histamine release potentially reduced in compound 48/80 or anti-DNP IgE-stimulated RPMC corresponded to decreased intracellular calcium at dose range of 0.01–1 mg/ml. Attenuation of NF- $\kappa$ B caused a reduction in downstream cytokines, such as TNF- $\alpha$ and IL-6 expression.	(Shin et al., 2005)
	Aerial part	Marrubiin (30)	Furane labdane diterpene	<i>In vitro</i>	Maximal inhibition (67.6 $\pm$ 4%) of OVA-induced allergic oedema was achieved at dose of 100 mg/kg in actively sensitized mice.	(Stulzer et al., 2006)
	Leaves	Rosmarinic acid (1)	Phenylpropanoid	<i>In vitro</i>	Exhibited potent suppressive effect on hyaluronidase with 1.0 $\pm$ 0.3% of enzyme activity.	(Ippoushi et al., 2000)
	Leaves, roots and stem	Ethanollic and aqueous extract	–	<i>In vivo</i>	100 $\mu$ g/ml ethanolic leaf and root extract showed potent histamine inhibition at 57% and 53% respectively in mice.	(Malik et al., 2003)
	Whole plant	Aqueous extract	–	<i>In vivo</i>	Anal administration of 0.05 g/kg extract protected mice from anaphylactic death. PCA reaction reduced dose-dependently with intraperitoneal, oral and intravenous administration of extract.	(Shin, 2003)
–	–	Essential oil	–	<i>In vitro</i>	Significant reduction in histamine release at 0.1 and 1 mg/ml of extract in compound 48/80-induced and anti-DNP IgE-mediated model in RPMC. TNF- $\alpha$ production reduced significantly at concentration of 0.1 mg/ml in RPMC.	(Shin, 2003)
				<i>In vivo</i>	Dose-dependently reduced histamine-induced bronchoconstriction in guinea pigs at 200 and 400 $\mu$ l/kg and significantly reduced eosinophil count, serum IgE level and BALF eosinophils in OVA-sensitized mice at 200 $\mu$ l/kg.	(Sharma et al., 2018)
<i>Mentha haplocalyx</i> Briq.	Aerial part	Ethanollic extract	–	<i>In vivo</i>	Observed with inhibition of eosinophil infiltration, T <sub>H</sub> 2 cytokines (IL-4, IL-5) expression and production in OVA-sensitized mice.	(Lee et al., 2011a)

TABLE 2 | Continued

Plant name	Plant part used	Isolated compound/ extract used	Chemical class	Assay type	Mechanism of action/conclusion	References
<i>Mentha piperita</i> Linn.	Leaves	50% ethanolic eluate	–	<i>In vivo</i>	Decreased nasal responses in antigen-induced rats at 300 and 1,000 mg/kg.	(Inoue et al., 2001)
				<i>In vitro</i>	Recorded with potent inhibition of histamine release from RPMC with IC <sub>50</sub> of 2.55 (1.42–3.94) µg/ml.	(Inoue et al., 2001)
	Leaves	Luteolin-7-O-rutinoside (31)	Flavonoid glycoside	<i>In vivo</i>	Reduced frequency of sneezing at 100 and 300 mg/kg while nasal rubbing was seen in antigen-induced rats at 100 mg/kg or more.	(Inoue et al., 2002)
				<i>In vitro</i>	Suppression of histamine release from compound 48/80-induced RPMC with IC <sub>50</sub> value of 21.9 µM.	(Inoue et al., 2002)
<i>Mentha piperita</i> var. <i>citrata</i> (Ehrh.) Briq.	Leaves	5,6,4'-trihydroxy-7,8-dimethoxyflavone (32), 5,6,4'-trihydroxy-7,8,3'-trimethoxyflavone (33), 5,6-dihydroxy-7,3',4'-trimethoxyflavone (34), 5,6-dihydroxy-7,8,3',4'-tetramethoxyflavone (35), 5,6-dihydroxy-7,8,4'-trimethoxyflavone (36)	Flavonoid	<i>In vitro</i>	Significantly reduction of β-hexosaminidase release from RBL-2H3 at IC <sub>50</sub> range of 2.4–6.7 µM.	(Sato and Tamura, 2015)
<i>Mentha spicata</i> L. var. <i>crispa</i> Benth.	Leaves	5,6-dihydroxy-7,8,3',4'-tetramethoxyflavone (35), 5,6,4'-trihydroxy-7,8,3'-trimethoxyflavone (33), (3R)-1-octan-3-yl β-D-glucopyranoside (37)	Flavonoid and aliphatic glycoside	<i>In vivo</i>	Demonstrated β-hexosaminidase release suppression from rat basophils at 56, 6.4 and 560 µM respectively.	(Yamamura et al., 1998)
<i>Minthostachys verticillata</i> (Griseb.) Epling	Leaves and stems	Essential oil	–	<i>In vitro</i>	β-hexosaminidase release from human basophils was diminished by 32.15% to 39.72% as comparable to dexamethasone and theophylline.	(Cariddi et al., 2007)
	Leaves and stems	Limonene (38), Pulegone (39), Menthone (40)	Monoterpene	<i>In vivo</i>	(38) maximally suppressed PCA reaction in challenged-mice at 250 mg/kg.	(Cariddi et al., 2011)
				<i>In vitro</i>	The combination of the three constituents in essential oil significantly suppressed the production of IL-13 from human PBMC. Potent inhibitory effect on β-hexosaminidase release from human basophils was observed with a concentration range of 10–40 µg/ml.	(Cariddi et al., 2011)
<i>Mosla chinensis</i> Max.	Whole plant	Aqueous extract	–	<i>In vivo</i>	Observed with concentration dependent suppression of systemic anaphylaxis and PCA reaction with doses of ranging from 10–1,000 mg/kg in sensitized mice.	(Kim et al., 2012)
				<i>In vitro</i>	Decreased intracellular calcium caused a dose-dependent reduction of histamine release from RPMC and reduced NF-κB activation resulted in decreased downstream TNF-α, IL-6, IL-8 expression in PMACI-stimulated HMC-1 cells.	(Kim et al., 2012)

TABLE 2 | Continued

Plant name	Plant part used	Isolated compound/ extract used	Chemical class	Assay type	Mechanism of action/conclusion	References
<i>Mosla dianthera</i> Maxim.	Whole plant	Aqueous extract	–	<i>In vivo</i>	Challenged-mice recorded with zero mortality due to systemic shock with pretreatment of 1,000 mg/kg and reduced PCA reaction in a dose-dependent manner across the range of 1–1,000 mg/kg.	(Lee et al., 2006)
				<i>In vitro</i>	Attenuation of histamine release from RPMC at doses ranging from 0.001–1 mg/ml and decreased intracellular calcium, NF- $\kappa$ B activation, gene expression and secretion of TNF- $\alpha$ , IL-6, IL-8 in PMACI-stimulated HMC-1 cells.	(Lee et al., 2006)
<i>Nepeta bracteata</i> Benth.	Whole plant	Crude aqueous extract	–	<i>In vivo</i>	Medium dose (not specified dose) exhibited the most potent reduction in the number of T <sub>H</sub> 17 cells, increased number of Treg cells in OVA-sensitized mice and decreased eosinophil infiltration in BALF.	(Wang et al., 2016)
<i>Ocimum basilicum</i> Linn.	Leaves	Acetone and hydro-methanol extract	–	<i>In vitro</i>	Achieved histamine release suppressive effect of 35.35% and 50.76% respectively at 100 $\mu$ g/ml.	(Kaur et al., 2018)
<i>Ocimum gratissimum</i> Linn.	Leaves	Methanolic extract	–	<i>In vivo</i>	Significantly suppressed number of eosinophils, decreased IL-4 level, reduced level of eosinophil peroxidase in BALF and lungs and decreased airway mucus hypersecretion at 100 mg/kg.	(Costa et al., 2012)
<i>Ocimum sanctum</i> Linn.	Leaves and seeds	Dried and fresh leaves ethanolic extract, volatile oil from fresh leaves and fixed oil from seeds	–	<i>In vivo</i>	Guinea pigs were protected from both histamine-induced and acetylcholine-induced preconvulsive dyspnoea with pretreatment of fresh leaves ethanolic extract, volatile oil and fixed oil.	(Singh and Agrawal, 1991)
	Leaves	Ethanolic extract	–	<i>In vivo</i>	Exhibited significant mast cell stabilizing potential, inhibition of IgE and delayed onset of histamine-induced bronchospasm with 64.25 $\pm$ 9.51%, 25.80 $\pm$ 4.85 ng/ml and 440 s respectively.	(Sridevi et al., 2009)
	Leaves	Ethanolic extract and isolated flavonoidal fraction	–	<i>In vivo</i>	Sensitized rats showed with significant mast cell stabilization of 67.24 $\pm$ 2.94% with extract administration and 60.48 $\pm$ 2.72% with fraction administration.	(Choudhary, 2010)
<i>Perilla frutescens</i> Britton	Whole plant	Aqueous extract	–	<i>In vivo</i>	Exhibited dose-dependent inhibition of compound 48/80-induced plasma histamine release at concentration range of 0.01–1 g/kg in sensitized rats. Marked suppression of PCA reaction at doses of 0.1 and 1 g/kg.	(Shin et al., 2000)
				<i>In vitro</i>	At concentration range of 0.001–1 mg/ml, histamine release and TNF- $\alpha$ production were decreased dose-dependently in stimulated RPMC. cAMP level in RPMC significantly increased at 1 mg/ml.	(Shin et al., 2000)

TABLE 2 | Continued

Plant name	Plant part used	Isolated compound/ extract used	Chemical class	Assay type	Mechanism of action/conclusion	References
	Whole plant	Rosmarinic acid <b>(1)</b> , Apigenin 7-O-[ $\beta$ -glucuronosyl(2 $\rightarrow$ 1) $\beta$ -glucuronide] <b>(2)</b>	Flavonoid and flavonoid glycoside	<i>In vivo</i>	<b>(1)</b> and <b>(2)</b> suppressed PCA reaction in sensitized mice with percentage inhibition of 41% and 32% respectively.	(Makino et al., 2001)
	Leaves	Luteolin <b>(3)</b>	Flavonoid	<i>In vivo</i>	Sensitized mice showed with decreased oxazolone-induced ear edema with oral administration of 1 mg of <b>(3)</b> . Dose-dependent inhibition of TNF- $\alpha$ production occurred at dose range of 1–1,000 $\mu$ g.	(Ueda et al., 2002)
	Leaves	Rosmarinic acid <b>(1)</b>	Phenylpropanoid	<i>In vivo</i>	Equivalent PCA reaction suppression was achieved by 19 mg/kg of <b>(1)</b> as compared to 150 mg/kg of tranilast, the positive control.	(Makino et al., 2003)
	Leaves	Rosmarinic acid <b>(1)</b>	Phenylpropanoid	<i>In vivo</i>	Oral administration of <b>(1)</b> by <i>Der f</i> -sensitized mice caused reduction in allergen-specific immunoglobulin, eosinophil infiltration, eosinophil counts in BALF, eotaxin, IL-4 and IL-5 expression at concentration of 1.5 mg/day.	(Sanbongi et al., 2004)
	Leaves	Ethanol extract	–	<i>In vivo</i>	T <sub>H</sub> 2 cytokines (IL-5 and IL-13), serum IgE level, eosinophil infiltration, histamine and eotaxin in BALF were suppressed in OVA-sensitized BALB/c mice.	(Chen et al., 2015)
	Leaves	Luteolin <b>(3)</b>	Flavonoid	<i>In vivo</i>	Compound 48/80- or serotonin-induced scratching behaviour and vascular permeability were reduced dose-dependently at 5, 10 and 20 mg/kg in sensitized mice.	(Jeon et al., 2014)
				<i>In vitro</i>	Dose-dependent reduction of compound 48/80-induced histamine release from RPMC marked at 5, 10 and 20 $\mu$ M. Diminished production of TNF- $\alpha$ (31.9%–76.8%) and IL-1 $\beta$ (27.3%–81.2%) in PMACI-stimulated HMC-1 cells at a range of 5–20 $\mu$ M of <b>(8)</b> .	(Jeon et al., 2014)
	Leaves	Aqueous fraction	–	<i>In vivo</i>	DNFB-sensitized mice experienced 35% reduction of ear swelling symptom at dose of 100 $\mu$ g/ml.	(Heo et al., 2011)
				<i>In vitro</i>	At 100 $\mu$ g/ml, eosinophil counts reduced by 73.7% accompanied with decreased expression of MMP-9 and IL-31 in mice ear tissues. T-bet protein expression was augmented and resulted in T <sub>H</sub> 1/T <sub>H</sub> 2 balance.	(Heo et al., 2011)
	Leaves	Methanolic extract	–	<i>In vitro</i>	Dose-dependent reduction of IL-4, IL-5, IL-13 and GM-CSF production in DP2-stimulated BEAS-2B cells at concentration range of 5–50 $\mu$ g/ml with involvement of decreased phosphorylation of JNK and p38.	(Liu et al., 2013)
	Leaves	Rosmarinic acid methyl ester <b>(41)</b>	Phenolic compound	<i>In vitro</i>	Possessed potent inhibitory activity on $\beta$ -hexosaminidase from RBL-2H3 cells with IC <sub>50</sub> of 9.9 $\pm$ 0.8 $\mu$ g/ml.	(Zhu et al., 2014)

TABLE 2 | Continued

Plant name	Plant part used	Isolated compound/ extract used	Chemical class	Assay type	Mechanism of action/conclusion	References
<i>Phlomis umbrosa</i> Turcz.	Leaves	8-hydroxy-5,7-dimethoxyflavanone ( <b>4</b> )	Flavanone	<i>In vivo</i>	Oral administration of ( <b>4</b> ) inhibited PCA reaction at dose of 5 mg and allergic nasal response at dose of 1.5 mg.	(Kamei et al., 2017)
				<i>In vitro</i>	Significant suppressive effect on histamine release from RBL-2H3 cells was observed with IC <sub>50</sub> of 68.5 $\mu$ M.	(Kamei et al., 2017)
	Leaves	Crude extract	–	<i>In vivo</i>	Decreased serum IgE level was observed in the blood of <i>Der f</i> -challenged mice.	(Komatsu et al., 2016)
				<i>In vitro</i>	Reduced CD4 <sup>+</sup> /CD8 <sup>+</sup> ratio in splenic T lymphocytes with percentage of 1.50 $\pm$ 0.07%.	(Komatsu et al., 2016)
	Roots	Aqueous extract	–	<i>In vivo</i>	At dose of 1 g/kg, plasma histamine release only recorded with 0.023 $\pm$ 0.002 $\mu$ g/ml in compound 48/80- sensitized mice. Anal, oral and intraperitoneal administration of 0.01–1 g/kg extract resulted in dose-dependent reduction in PCA reaction.	(Shin et al., 2008; Shin and Lee, 2003)
				<i>In vitro</i>	Significant inhibition of histamine release from RPMC activated by compound 48/80 or anti-DNP IgE recorded at doses of 0.1 mg/ml and 1 mg/ml. Extract attenuated the secretion of IL-1 $\beta$ , IL-6 and TNF- $\alpha$ in PMACI-stimulated HMC-1 cells.	(Shin et al., 2008; Shin and Lee, 2003)
				<i>In vivo</i>	Intraperitoneal administration of extract caused a dose-related suppression of systemic anaphylaxis induced by compound 48/80 in sensitized mice across doses of 10–1,000 mg/kg. At doses ranging from 1–1,000 mg/kg, PCA reaction induced by DNP-HSA was reduced in a concentration-dependent manner in sensitized rats.	(Yoon et al., 2016)
				<i>In vitro</i>	Suppressed the release of histamine and $\beta$ -hexosaminidase from RPMC across concentrations of 1–1,000 $\mu$ g/ml. Expression and secretion of TNF- $\alpha$ , IL-6 and IL-8 was inhibited in HMC-1 cells at doses of 1–100 $\mu$ g/ml due to the attenuation of NF- $\kappa$ B activation.	(Yoon et al., 2016)
<i>Pogostemon cablin</i> (Blanco) Benth	–	Aqueous extract	–			
	–	Patchouli oil	–			
				<i>In vivo</i>	Significant reduced PCA reaction in ovalbumin-challenged rats and suppressed delayed-type hypersensitivity at doses of 20, 40 and 80 mg/kg of Patchouli oil.	(He et al., 2013)
				<i>Ex vivo</i>	Decreased contraction responses in guinea pig ileum at concentrations of 0.01, 0.02 and 0.04 mg/ml of Patchouli oil.	(He et al., 2013)

TABLE 2 | Continued

Plant name	Plant part used	Isolated compound/ extract used	Chemical class	Assay type	Mechanism of action/conclusion	References
<i>Prunella vulgaris</i> var. <i>lilacina</i> Nakai	Whole plant	2 $\alpha$ ,3 $\alpha$ -dihydroxyurs-12-en-28-oic acid ( <b>42</b> )	Triterpenoid	<i>In vitro</i>	Significant suppressive effect on $\beta$ -hexosaminidase from RBL-2H3 with IC <sub>50</sub> value of 57 $\mu$ M.	(Ryu et al., 2000)
	Whole plant	Aqueous extract	–	<i>In vivo</i>	At doses of 0.5 and 1 g/kg, sensitized rats completely protected from anaphylactic death. Oral administration of extract with doses ranging from 0.001–1 g/kg dose-dependently reduced PCA reaction.	(Kim et al., 2007; Shin et al., 2001)
				<i>In vitro</i>	Inhibition of intracellular calcium level caused downstream decreased release of histamine from RPMC in a concentration dependent manner with concentration range of 0.001–1 mg/ml. RPMC also showed with significant reduction of TNF- $\alpha$ production with the pretreatment of 0.01 mg/ml and 0.1 mg/ml.	(Kim et al., 2007; Shin et al., 2001)
<i>Rosmarinus officinalis</i> Linn.	Spike	$\beta$ -amyrin ( <b>43</b> ), 2 $\alpha$ ,3 $\alpha$ ,23-trihydroxyursa-12,20(30)-dien-28-oic acid ( <b>44</b> ), Euscaphic acid ( <b>45</b> )	Triterpenoid	<i>In vitro</i>	Observed with inhibition of histamine release from HMC-1 cells with 46.7%, 57.9% and 54.2% respectively.	(Choia et al., 2016)
	Leaves	Carnosic acid ( <b>5</b> )	Polyphenol	<i>In vivo</i>	PCA reaction was significantly suppressed at 100 mg/kg in sensitized mice with percentage inhibition of 67.1%.	(Mizushina et al., 2014)
				<i>In vitro</i>	( <b>5</b> ) inhibited $\beta$ -hexosaminidase release from PMACI A23187-stimulated RBL-2H3 cells at 10 $\mu$ M.	(Mizushina et al., 2014)
<i>Salvia miltiorrhiza</i> Bunge	Roots	15,16-dihydrotanshinone-I ( <b>7</b> ), Cryptotanshinone ( <b>9</b> )	Diterpene	<i>In vitro</i>	( <b>7</b> ) and ( <b>9</b> ) significantly suppressed the release of $\beta$ -hexosaminidase from RBL-2H3 cells with IC <sub>50</sub> values of 16 $\pm$ 2.4 $\mu$ M and 36 $\pm$ 3.7 $\mu$ M respectively.	(Choi and Kim, 2004; Ryu et al., 1999)
	Leaves	Ethanol extract	–	<i>In vivo</i>	Oral administration of 25–100 mg/kg extract dose-dependently inhibited PCA reaction in anti-DNP IgE-stimulated rats.	(Yang et al., 2008)
				<i>In vitro</i>	Dose-related inhibition of COX-1 and COX-2-dependent prostaglandin D <sub>2</sub> production observed with IC <sub>50</sub> values of 3.96 and 21.54 $\mu$ g/ml respectively in BMMC. Suppression of leukotriene C <sub>4</sub> generation and $\beta$ -hexosaminidase release was seen in BMMC with IC value of 2.6 and 22.4 $\mu$ g/ml.	(Yang et al., 2008)
	Rhizome	Tanshinone I ( <b>6</b> ), 15,16-dihydrotanshinone-I ( <b>7</b> ), Tanshinone IIA ( <b>8</b> ), Cryptotanshinone ( <b>9</b> )	Diterpene	<i>In vivo</i>	( <b>6</b> ), ( <b>7</b> ), ( <b>8</b> ) and ( <b>9</b> ) significantly suppressed PCA reaction at dose of 50 mg/kg with percentage inhibition of 59%, 49%, 35% and 32% respectively in sensitized mice.	(Trinh et al., 2010a)
				<i>In vitro</i>	Potent inhibition of IL-4 and TNF- $\alpha$ expression by ( <b>6</b> ), ( <b>7</b> ) and ( <b>8</b> ) at dose of 50 $\mu$ M in RBL-2H3 cells.	(Trinh et al., 2010a)

TABLE 2 | Continued

Plant name	Plant part used	Isolated compound/ extract used	Chemical class	Assay type	Mechanism of action/conclusion	References
	Roots	15,16-dihydrotanshinone-I (7)	Diterpene	<i>In vitro</i>	(7) at 20 $\mu$ M produced 90% suppression on degranulation and generation of prostaglandin D <sub>2</sub> and leukotriene C <sub>4</sub> in IgE/Ag-stimulated BMMC through inhibition of Fc $\epsilon$ RI-mediated Syk-dependent signal pathway.	(Li et al., 2015)
<i>Salvia plebeia</i> R. Brown	Whole plant	Aqueous extract	–	<i>In vivo</i>	No anaphylactic death occurred in compound 48/80-induced rats with intraperitoneal administration of 0.5 and 1 g/kg extract. At doses ranging from 0.01–1 g/kg, intraperitoneal and oral administration of extract showed with dose-dependent inhibition of PCA reaction.	(Shin and Kim, 2002)
				<i>In vitro</i>	Concentration-dependent reduction histamine release from RPMC activated by compound 48/80 or anti-DNP IgE at a concentration range of 0.001–1 mg/ml. TNF- $\alpha$ production from RPMC was significantly inhibited at concentrations of 0.01–1 mg/ml whereas cAMP level in RPMC significantly elevated compared with that of basal cells.	(Shin and Kim, 2002)
	Whole plant	Ethanol extract	–	<i>In vivo</i>	Oral administration of 100 mg/kg extract significantly suppressed serum IgE level, serum histamine, eosinophil count, pro-inflammatory cytokines (IFN- $\gamma$ and TNF- $\alpha$ ) expression, T <sub>H</sub> 1, T <sub>H</sub> 2 and T <sub>H</sub> 17 cytokines expression in <i>Der f</i> -sensitized mice.	(Choi et al., 2014)
<i>Schizonepeta tenuifolia</i> (Benth.) Briq.	Whole plant	Aqueous extract	–	<i>In vivo</i>	100% protection from systemic anaphylaxis was observed with doses of 0.5 and 1 g/kg in compound 48/80-challenged rats whereas a marked suppression in PCA reaction was seen in orally administered of 0.1 and 1 g/kg of anti-DNP IgE-sensitized rats.	(Shin et al., 1999)
				<i>In vitro</i>	Significant inhibition of compound 48/80 or IgE-mediated histamine release from RPMC was marked at concentration range of 0.01–1 mg/ml. A potent inhibition of TNF- $\alpha$ production observed at 1 mg/ml with a content of 0.889 $\pm$ 0.747 ng/ml.	(Shin et al., 1999)
	Whole plant	Extract with phosphate buffered saline/olive oil (P/O) in proportion of (9:1) mixture	–	<i>In vivo</i>	Skin thickening and hyperplasia of epidermis and dermis in DNCB-sensitized mice remarkably decreased by 38.15% and 42.37% respectively with treatment of 1% of extract in P/O (9:1) mixture.	(Choi et al., 2013)
				<i>In vitro</i>	DNCB-induced mice observed with reduced serum levels of IgE, TNF- $\alpha$ and IL-6, recorded with 46.26%, 41.97% and 70.42% inhibition respectively with the treatment of 1% of extract in P/O (9:1) mixture.	(Choi et al., 2013)



TABLE 2 | Continued

Plant name	Plant part used	Isolated compound/ extract used	Chemical class	Assay type	Mechanism of action/conclusion	References
<i>Scutellaria baicalensis</i> Georgi	–	Aqueous extract	–	<i>In vitro</i>	Pro-inflammatory cytokines (IL-6, IFN- $\gamma$ and TNF- $\alpha$ ) and pro-allergic T <sub>H</sub> 2 cytokines (IL-4 and IL-13) in RBL-2H3 were decreased with the treatment of 100 $\mu$ g/ml of aqueous extract. $\beta$ -hexosaminidase release from RBL-2H3 cells reduced significantly at dose of 10 $\mu$ g/ml.	(Lin et al., 2018)
	Roots	Wogonin <b>(10)</b> , Ganhuangenin <b>(11)</b> , Wogonoside <b>(12)</b> , 3,5,7, 2',6'-pentahydroxyflavanone <b>(13)</b>	Flavonoid	<i>Ex vivo</i>	<b>(10)</b> , <b>(11)</b> and <b>(12)</b> significantly inhibited the production of IgE from concanavalin A-stimulated rat spleen lymphocytes at concentrations of 10.0 and 100.0 $\mu$ M. Histamine and leukotriene B <sub>4</sub> release from rat PEC was markedly suppressed at dose of 100 $\mu$ M for all flavonoids.	(Lim, 2003; Lim et al., 2003)
	Roots	Aqueous extract	–	<i>In vivo</i>	Oral administration of 50 mg/kg extract selectively inhibited the release of IL-5 in mice.	(Kim et al., 2010)
	Roots	Baicalin <b>(46)</b>	Flavone glycoside	<i>In vitro</i>	Histamine and leukotriene release from OVA-sensitized guinea pig lung mast cells were potently suppressed at doses of 10, 30 and 60 $\mu$ g. The standardized extract of <b>(46)</b> exhibited a more potent outcome than pure <b>(46)</b> at 60 $\mu$ g only.	(Kim et al., 2010)
	Whole plant	Ethanol extract	–	<i>In vivo</i>	Exhibited 6.6% inhibition of PCA reaction in sensitized-rats at 280 mg/kg.	(Jung et al., 2012)
				<i>In vitro</i>	40% reduction of histamine content in compound 48/80-stimulated RPMC with dose of 10 $\mu$ g/ml. Significant reduced production of TNF- $\alpha$ and IL-8 in PMACI-stimulated HMC-1 cells with inhibition of MAPK activation at concentration range of 1–100 $\mu$ g/ml.	(Jung et al., 2012)
	Roots	Aqueous extract	–	<i>In vivo</i>	Topical application of 5% extract reduced DNFB-induced cutaneous reaction by 31% as compared to control group.	(Kim et al., 2013)
				<i>In vitro</i>	Significantly suppressed $\beta$ -hexosaminidase release from RBL-2H3 at doses of 125, 250 and 500 ppm with percentage inhibition of 19%, 34% and 60% respectively.	(Kim et al., 2013)
	Whole plant	Crude ethanol extract	–	<i>In vivo</i>	OVA-sensitized mice were protected from food allergy anaphylactic death by 60% and observed with significantly suppression of OVA-specific IgE, IL-17, T <sub>H</sub> 2 cytokines (IL-4, IL-5, IL-10, IL-13) and T <sub>H</sub> 1 cytokines (IFN- $\gamma$ and IL-12) with the treatment of 25 mg/kg of extract.	(Shin et al., 2014b)

TABLE 2 | Continued

Plant name	Plant part used	Isolated compound/ extract used	Chemical class	Assay type	Mechanism of action/conclusion	References
–	–	Wogonin <b>(10)</b> , Baicalin <b>(46)</b> , Baicalein <b>(47)</b>	Flavonoid	<i>Ex vivo</i>	<b>(10)</b> suppressed the production of T <sub>H</sub> 2 cytokines (IL-4, IL-5, IL-10, IL-13) and IFN- $\gamma$ without causing cytotoxicity in OVA-sensitized mice splenocytes at 50 $\mu$ mol/ml as compared to <b>(46)</b> and <b>(47)</b> .	(Shin et al., 2014a)
				<i>In vivo</i>	Oral administration of 1 mg/kg of <b>(15)</b> potentially decreased the production of OVA-specific IgE, IL-5, IL-10 and IL-13 in sensitized mice.	(Shin et al., 2014a)
	Roots	Aqueous extract	–	<i>In vivo</i>	Attenuation of DNCB-induced epidermal thickness, leukocytes infiltration, serum IgE, IL-4, IFN- $\gamma$ and TNF- $\alpha$ production in BALB/c mice skin.	(Kim et al., 2016)
Root	Ethanol extract, acetone extract and ethyl acetate extract	–	–	<i>In vivo</i>	The highest inhibitory activity against 4-AP-induced allergic skin pruritus, histamine-induced paw swelling, ear PCA reaction, anaphylaxis ear swelling and total serum IgE level was seen with 1.42 g/kg of ethanol extract in sensitized mice.	(Li et al., 2014)
Rhizome	Baicalin <b>(46)</b> , Baicalein <b>(47)</b> , Oroxylin A <b>(14)</b>	Flavonoid	Flavonoid	<i>In vivo</i>	<b>(46)</b> which was orally administered metabolized into <b>(47)</b> and <b>(14)</b> . Metabolite, <b>(14)</b> possessed a more potent anti-histamine activity, seen with significant reduced histamine-induced scratching behaviour and vascular permeability in sensitized mice at doses of 20 and 50 mg/kg.	(Trinh et al., 2010b)
				<i>In vitro</i>	Metabolite of <b>(46)</b> , <b>(14)</b> remarkably inhibited the contraction of guinea pig ileum with IC <sub>50</sub> value of 0.28 mmol/L.	(Trinh et al., 2010b)
–	Oroxylin A <b>(14)</b>	Flavonoid	Flavonoid	<i>In vivo</i>	Significantly reduced eosinophils infiltration in BALF and airway hyperresponsiveness in OVA-sensitized mice. Potent attenuation of serum IgE level, T <sub>H</sub> 2 cytokines (IL-4, IL-5 and IL-13) production and NF- $\kappa$ B activation with oral administration of 15, 30 and 60 mg/kg.	(Zhou et al., 2016)
Roots	Linoleic acid <b>(50)</b>	Fatty acid	Fatty acid	<i>Ex vivo</i>	Significantly suppressed the production of IL-4, IL-5, IL-10 and IL-13 but enhanced secretion of IFN- $\gamma$ and IL-12, resulted in T <sub>H</sub> 1/T <sub>H</sub> 2 balance at 50 $\mu$ g/L.	(Jung et al., 2017)
–	Baicalein <b>(47)</b>	Flavonoid	Flavonoid	<i>In vivo</i>	<b>(47)</b> induced CD4 <sup>+</sup> FOXP <sub>3</sub> <sup>+</sup> T cell differentiation in ovalbumin-sensitized mice at concentrations of <10 $\mu$ mol/L without causing cell death.	(Bae et al., 2016)

TABLE 2 | Continued

Plant name	Plant part used	Isolated compound/ extract used	Chemical class	Assay type	Mechanism of action/conclusion	References
<i>Stachys riederi</i> var. <i>japonica</i> Miq.	Whole plant	Aqueous extract	–	<i>In vivo</i>	Dose-dependent inhibition was resulted in the occurrence of systemic anaphylaxis at concentration range of 0.005–1 g/kg and significant reduction of PCA reaction at concentrations of 0.1 and 1 g/kg.	(Shin, 2004)
				<i>In vitro</i>	At doses of 0.1 and 1 mg/ml, a significant decrease release of histamine from RPMC and diminished secretion of TNF- $\alpha$ and IL-6 from HMC-1 cells.	(Shin, 2004)
<i>Teucrium japonicum</i> Houttuyn	Whole plant	Aqueous extract	–	<i>In vivo</i>	Serum histamine release was significantly reduced at 100 and 1,000 mg/kg, with 500 mg/kg as the effective dose that completely protected compound 48/80-induced mice from systemic anaphylaxis. At doses ranging from 1–1,000 mg/kg, a dose-dependent inhibition of PCA reaction was resulted in anti-DNP IgE-challenged mice.	(Kim et al., 2009)
				<i>In vitro</i>	Significant reduction of compound 48/80-induced intracellular calcium and downstream histamine release from RPMC was observed at 1 mg/ml. Gene expression of TNF- $\alpha$ was diminished dose-dependently at 0.01–1 mg/ml with the involvement of NF- $\kappa$ B in PMACI-stimulated HMC-1 cells.	(Kim et al., 2009)
<i>Thymus vulgaris</i> Linn.	Leaves	2-isopropyl-5-methylphenol <b>(15)</b>	Monoterpenoid phenolic	<i>In vivo</i>	Dose-dependently inhibited recruitment of inflammatory cells, reduced airway hyperreponsiveness, suppressed level of OVA-specific IgE, T <sub>H</sub> 2 cytokines in BALF at concentrations of 4, 8 and 16 mg/kg.	(Zhou et al., 2014)
	Leaves	n-hexane extract	–	<i>In vivo</i>	Portrayed intermediate inhibitory activity on histamine release with $46.22 \pm 0.08\%$ .	(Ikawati et al., 2001)
	–	2-isopropyl-5-methylphenol <b>(15)</b> , Carvacrol <b>(51)</b>	Monoterpenoid phenolic	<i>In vivo</i>	<b>(15)</b> and <b>(51)</b> reduced delayed-type hypersensitivity by 26% and 50% respectively in ovalbumin-sensitized mice.	(Gholijani and Amirghofran, 2016)
	–	–	–	<i>Ex vivo</i>	Both compounds led to reduction of IL-2, IFN- $\gamma$ , IL-4, IL-17 level and T-bet expression but increased level of IL-10 and TGF- $\beta$ in mice splenocytes cultures.	(Gholijani and Amirghofran, 2016)
<i>Vitex negundo</i> Linn.	Leaves	Aqueous subfraction of ethyl acetate fraction	–	<i>In vitro</i>	Mast cell stabilizing activity with $80.99 \pm 0.7231\%$ was observed in rat mesenteric mast cells at dose of 500 $\mu$ g/ml.	(Patel and Deshpande, 2011)
	Leaves	5-hydroxy-3, 6, 7, 3',4'-pentamethoxyflavone <b>(52)</b>	Flavonoid	<i>In vivo</i>	200 mg/kg extract demonstrated significant reduction of eosinophil count in BALF and serum bicarbonate level in egg albumin sensitized guinea pigs.	(Patel and Deshpande, 2013)

TABLE 2 | Continued

Plant name	Plant part used	Isolated compound/ extract used	Chemical class	Assay type	Mechanism of action/conclusion	References
<i>Vitex rotundifolia</i> Linn.	Fruits	Aqueous extract	–	<i>In vivo</i>	Dose-dependent reduction of systemic anaphylaxis reaction in compound 48/80-induced rats across concentration range of 0.0001–1 g/kg. Significant suppression of PCA reaction marked at doses of 0.5 and 1 g/kg in sensitized rats.	(Shin et al., 2000)
				<i>In vitro</i>	Histamine release from RPMC was reduced in a dose-dependent manner at dose range of 0.001–1 mg/ml and marked inhibition of TNF- $\alpha$ production at 0.001 mg/ml.	(Shin et al., 2000)
	Fruits	1H,8H-pyrano[3,4-c]pyran-1,8-dione <b>(16)</b>	Pyran	<i>In vivo</i>	Serum IgE, eosinophil counts and IL-5 production in BALF were significantly suppressed by 43%, 82% and 34% respectively. IL-4 and IL-5 level significantly decreased in CD4 <sup>+</sup> T cells in T <sub>H</sub> 2 skewed condition with treatment.	(Lee et al., 2009)
				<i>In vitro</i>	Eosinophil migration and eotaxin production were reduced by 48% and 70% respectively at 10 $\mu$ g/ml in A549 cell media.	(Lee et al., 2009)
	Fruits	Casticin <b>(53)</b>	Flavonoid	<i>In vitro</i>	Up to 63% of eosinophil migration inhibition was observed in A549 cell media with pretreatment of 10 $\mu$ g/ml. Eotaxin level was reduced from concentration range of 0.1–10 $\mu$ g/ml in A549 cells.	(Koh et al., 2011)
<i>Vitex trifolia</i> Linn.	–	Aqueous extract	–	<i>In vivo</i>	Oral administration of 100 mg/kg extract caused 86% inhibition of eosinophilia, reduction of T <sub>H</sub> 2 cytokines (IL-4, IL-5, IL-13) and TNF- $\alpha$ level in BALF and decreased serum IgE level in ovalbumin-sensitized mice.	(Bae et al., 2013)
	Leaves	n-hexane and ethanolic extract	–	<i>In vitro</i>	Both n-hexane and ethanolic extract highly suppressed histamine release by 80.13 $\pm$ 3.95 and 81.58 $\pm$ 0.24% respectively in RBL-2H3 cells.	(Ikawati et al., 2001)
	Leaves	Viteosin-A <b>(48)</b> , Vitexicarpin <b>(49)</b>	Flavonoid	<i>Ex vivo</i>	<b>(48)</b> and <b>(49)</b> respectively reduced histamine-induced tracheal contraction by 27.1% and 66.2% at 0.00013 M and percentage increased to 47.9% and 97.2% respectively when raised to 0.0004 M.	(Alam et al., 2002)
	Whole plant	Hydro-ethanolic extract	–	<i>In vitro</i>	Observed with increment of Treg cells, T <sub>H</sub> 1/T <sub>H</sub> 2 ratio, IFN- $\gamma$ /IL-4 ratio, IFN- $\gamma$ and FOXP <sub>3</sub> expression. Significant reduction of T <sub>H</sub> 2 and T <sub>H</sub> 17 cells and decreased expression of IL-4, IL-17 and TGF- $\beta$ occurred in sensitized mice spleen cells.	(Kianmehr et al., 2017)
	Seeds	Hydro-ethanolic extract	–	<i>In vivo</i>	Increased IFN- $\gamma$ and decreased IL-4 were resulted in ovalbumin-sensitized guinea pigs with the oral administration of extract.	(Boskabady et al., 2013)
<i>Zataria multiflora</i> Boiss.	Seeds	Hydro-ethanolic extract	–	<i>In vitro</i>	Achieved T <sub>H</sub> 1/T <sub>H</sub> 2 balance with enhanced ratio of IFN- $\gamma$ /IL-4 in PHA-stimulated hPBMC.	(Boskabady et al., 2013)

(Shin et al., 2008), *Salvia plebeia* (Shin and Kim, 2002), *Schizonepeta tenuifolia* (Shin et al., 1999) and *Teucrium japonicum* aqueous extract (Kim et al., 2009). Sridevi et al. (2009) highlighted that the ethanolic extract of *Ocimum sanctum* at 400 mg/kg effectively reduced mortality (41%) due to anaphylactic shock-induced bronchospasm in tested subjects with a significant drop ( $P < 0.001$ ) in serum IgE level to  $25.80 \pm 4.85$  ng/ml ( $P < 0.001$ ), as compared to sensitized control ( $125.06 \pm 9.66$  ng/ml). These findings confirm that the anti-allergic potential of *O. sanctum* is worthwhile to be further explored.

Over the past two decades, many studies have been conducted on *P. frutescens* species to explore and determine their anti-allergic potential. For example, Makino et al. (2001) isolated rosmarinic acid (1) and apigenin 7-O-[ $\beta$ -glucuronosyl (2 $\rightarrow$ 1)  $\beta$ -glucuronide] (2) from *P. frutescens*, which demonstrated anti-allergic activity with potent suppression of PCA reaction in antigen-challenged mice with inhibition of 41% ( $P < 0.01$ ) and 32% ( $P < 0.05$ ) respectively. Meanwhile, Ueda et al. (2002) isolated rosmarinic acid (1), caffeic acid and luteolin (3) from the leaves of *P. frutescens* and tested them for respective anti-allergic effects with oxazolone-induced ear edema test. Interestingly, only luteolin (3) showed an inhibitory effect on oxazolone-induced ear edema at 1 mg, whereas the other compounds did not show any inhibitory activity (Ueda et al., 2002). However, in a continuation of the work by Makino et al. (2003), the results suggested that the anti-allergic titer of rosmarinic acid (1) was 8 folds higher than the conventional anti-allergic drug tranilast, where 19 mg/kg of rosmarinic acid (1) was sufficient to achieve an equivalent PCA reaction suppression as 150 mg/kg of tranilast. Such a potent anti-allergic effect from rosmarinic acid (1) is certainly exciting and worthy to be further studied in the development of anti-allergic agents. In light of the study by Chen et al. (2015), an OVA-induced murine model of allergic asthma was employed. Results demonstrated a promising reduction in serum IgE level in the OVA-sensitized mice with 320  $\mu$ g of ethanolic extract of *P. frutescens* leaves and hence amelioration of asthmatic symptoms (Chen et al., 2015). A similar reduction outcome was obtained in the study using *Der f* (*Dermatophagoides farinae*) mite-induced atopic dermatitis murine model with oral administration of *P. frutescens* leaves extract (Komatsu et al., 2016). In the latest work by Kamei et al. (2017), a new active principle, 8-hydroxy-5,7-dimethoxyflavanone (PDMF) (4) was isolated from the leaves of *P. frutescens* and demonstrated to have a potent suppressive effect on PCA reaction in anti-DNP IgE-stimulated-BALB/c mice. In addition, sneezing frequency, the allergic rhinitis nasal response, was also reduced with 1.5 mg of PDMF (4) after the BALB/c mice were challenged with Japanese cedar pollen grains (Kamei et al., 2017). Considering all these evidences together, *P. frutescens* possesses a great potential to be developed as an effective anti-allergic agent as shown in allergic asthma, atopic dermatitis and allergic rhinitis models.

According to Mizushina et al. (2014), the isolated compound carnosic acid (5), from the *Rosmarinus officinalis* leaves, possesses the ability to suppress PCA reaction at a dose of 100 mg/kg in sensitized mice with percentage inhibition of 67.1%. Interestingly, the inhibition caused by carnosic acid (5) was greater than that of tranilast, a frequently used anti-allergic drug. In fact, tranilast at

100 mg/kg only inhibited PCA reaction by 23.9% as compared to 67.1% suppression by carnosic acid (5), which was approximately 2.8 folds stronger than tranilast (Mizushina et al., 2014). Hence, it can be assumed that carnosic acid (5) has a strong potential to be used as anti-allergic compound. In another account, *Schizonepeta tenuifolia* demonstrated a 46.26% reduction in serum IgE level with a treatment of 1% of *S. tenuifolia* extract with phosphate buffered saline/olive oil (P/O) in proportion of (9:1) mixture in DNCB-induced BALB/c mice (Choi et al., 2013).

*Salvia miltiorrhiza* is a perennial herb which is well known to have tanshinones as principal bioactives. This plant is widely employed as traditional remedy, particularly in TCM (Li et al., 2015). Over the past decade, researchers have conducted studies to investigate its anti-allergic effect. Yang et al. (2008) proposed that a dose-dependent reduction of PCA reaction occurred at 25–100 mg/kg of ethanol extract of *S. miltiorrhiza* leaves ( $P < 0.001$ ). When the IgE-stimulated rats were fed with 50 mg/kg of extract, the PCA reaction appeared to decrease by approximately 36.4% (Yang et al., 2008). A study conducted by Trinh et al. (2010a) highlighted the potency of the PCA reaction inhibition exhibited by the active principles of *S. miltiorrhiza* in the following manner: tanshinone I (6) (59%) > 15,16-dihydrotanshinone I (7) (49%) > tanshinone IIA (8) (35%) > cryptotanshinone (9) (32%). Another species from the same genus, *S. plebeia*, was reported to suppress *Der f*-induced elevated serum IgE level in BALB/c mice of atopic dermatitis model at a concentration of 100 mg/kg of ethanolic extract (Choi et al., 2014). Therefore, this finding suggests that *S. plebeia* could be a good candidate for atopic dermatitis treatment in future.

For more than 2,000 years, Chinese people have recognized the dried root of *Scutellaria baicalensis* as a very valuable medicinal herb and many people have regarded it as the golden herb due to its diverse medicinal uses. It is traditionally known as Huang-Qin and it is now listed officially in the Chinese Pharmacopoeia (Zhao et al., 2016). It is widely employed in TCM as treatment for cardiovascular diseases and bleeding disorders, such as hematemesis, hematuria and metrorrhagia (Yoon et al., 2009; Chen et al., 2013). In recent years, it has started to emerge as potentially possessing anti-allergic properties as many studies were actively carried out to investigate its anti-allergic effect. Lim et al. (2003) highlighted that *S. baicalensis* root contains active constituents that are particularly useful against allergic diseases. Four flavonoids were isolated from the root of *S. baicalensis*, wogonin (WG) (10), ganhuangenin (GHG) (11), wogonoside (WGS) (12) and 3,5,7,2',6'-pentahydroxyl flavanone (PHF) (13). WG (10), GHG (11) and WGS (12) were found to potently suppress the production of IgE from the concanavalin A (ConA)-stimulated spleen lymphocytes obtained from Sprague-Dawley rats, at 10 and 100  $\mu$ M, except PHF (13), even when tested with the highest dose (Lim et al., 2003). This outcome could be due to the structural differences with methoxy substitution and their respective positions on the polyphenolic ring (Lim, 2002). Meanwhile, Li et al. (2014) evaluated the efficacy of three different extracts (ethanol, acetone and ethyl acetate extract) of *S. baicalensis* against allergic reactions. Result revealed that ethanol extract showed the most promising outcome among the three extracts. It demonstrated the highest inhibitory activity against mice ear PCA reaction with percentage inhibition of 55.17% at a dose of 1.42 g/kg.

With the same dose, the total serum IgE level was recorded at the lowest level ( $3.23 \pm 1.05$  IU/ml) as compared to treatment with the other two extracts and was comparable to the positive control, 0.1 g/kg of sodium cromoglycate ( $3.19 \pm 1.14$  IU/ml) (Li et al., 2014). In the latest work of Zhou et al. (2016), another active constituent, oroxylin A (**14**), isolated from *S. baicalensis*, was reported to cause a potent suppression ( $P < 0.01$ ) in serum IgE levels in OVA-sensitized mice (Zhou et al., 2016). Other than oral administration, the efficacy of topical application on anti-allergic effect was also evaluated. In the study of Kim et al. (2013), the aqueous extract of *S. baicalensis* was topically applied onto DNFB-induced ear swelling and result suggested that the cutaneous reaction significantly reduced ( $P < 0.05$ ) by 31% with 5% of extract (Kim et al., 2013). In a continuation of the study from the same researchers a few years later, in addition to cutaneous reactions, the serum IgE level in DNCB-induced contact dermatitis was also proven to be suppressed by topical treatment of *S. baicalensis* aqueous extract (Kim et al., 2016). Considering these results, *S. baicalensis* showed to be effective against IgE production and thus to have preventive effects towards allergy. Hence, it is suitable to be further developed as natural anti-allergic agent.

Furthermore, Zhou et al. (2014) demonstrated that 2-isopropyl-5-methylphenol (thymol) (**15**) from *Thymus vulgaris* portrayed a dose-dependent reduction trend in the production of IgE with the pretreatment of 4 mg/kg, 8 and 16 mg/kg of thymol (**15**) in OVA-challenged mice. Among the three concentrations used, 16 mg/kg of thymol (**15**) showed a comparable inhibition ( $P < 0.01$ ) of OVA-specific IgE with positive control, dexamethasone (Zhou et al., 2014). Likewise, *Vitex rotundifolia* also showed similar inhibitory activity with 43% suppression in serum IgE level with the treatment of *V. rotundifolia*'s phytoconstituent, 1H,8H-pyrano [3,4-c] pyran-1,8-dione (PPY) (**16**) (Lee et al., 2009).

## INHIBITION OF MAST CELLS AND BASOPHILS DEGRANULATION

A few species of Lamiaceae have successfully displayed compelling mast cell stabilizing activity. For instance, Vadrone et al. (2007) evaluated the mast cell stabilizing activity of *Clerodendron phlomidis* using *in vivo* murine system. The mast cell stabilization was achieved by using leaf aqueous extract of *C. phlomidis* in tested mice. Results revealed that 100 mg/kg of extract was able to confer protection as high as 73.25% from mast cell degranulation which was almost comparable to the standard drug, disodium cromoglycate, that exhibited a protection of 83.75% (Vadrone et al., 2007). Furthermore, *O. sanctum* leaves were also studied for their mast cell stabilization activity in the research of Choudhary (2010). The leaves were prepared into ethanolic extract and flavonoidal fraction isolated from ethanolic extract. The albino rats were fed orally with 100 and 200 mg/kg of leaf ethanolic extract after sensitization. The results demonstrated that  $62.44 \pm 3.80\%$  and  $67.24 \pm 2.94\%$  of mast cell stabilization activity was respectively recorded at 100 and 200 mg/kg of ethanolic extract. Meanwhile, significant inhibition of mast cell degranulation was also seen with 75 and 150 mg/kg of isolated flavonoidal fraction, which marked with  $54.62 \pm 1.76\%$

and  $60.48 \pm 2.72\%$  respectively (Choudhary, 2010). In addition to that, Patel and Deshpande (2011) employed an *in vitro* assay to evaluate the inhibitory activity of mast cell degranulation of *Vitex negundo*. The rat mesenteric mast cells were stimulated with compound 48/80 to induce mast cell degranulation. At the end of experiment, the numbers of intact and disrupted mast cells were counted and compared. Result suggested that the number of intact mast cells was more than that of disrupted mast cells after the pretreatment with 500 µg/ml of aqueous sub-fraction of *V. negundo*. The mast cell protection was significant, which marked with a percentage of  $80.99 \pm 0.7231\%$  ( $P < 0.001$ ) (Patel and Deshpande, 2011).

In a study conducted by Murata et al. (2010), it was found that *Lycopus lucidus* contains bioactive compounds that contribute to anti-allergic activity through inhibition of hyaluronidase enzyme (Murata et al., 2010). Hyaluronidase is an enzyme that cleaves hyaluronic acid in an extracellular matrix of connective tissue and is well known for being involved in allergic reactions by causing increased capillary permeability (Sakamoto et al., 1980). Inhibition of this enzyme is known to have suppressive effect on mast cell degranulation, which is a hallmark manifestation of allergy (Asada et al., 1997). Therefore, inhibition of hyaluronidase enzyme can thus become one of the targets to prevent the occurrence of allergy. Murata et al. (2010) isolated 22 compounds from dried aerial parts of *L. lucidus*. Amongst the 22 compounds isolated, only six of them were identified to possess hyaluronidase inhibitory activity. Isolated rosmarinic acid (**1**) was previously identified as a good hyaluronidase inhibitor. It was set as the positive control in this study and marked with hyaluronidase inhibition with  $IC_{50}$  value of 309 µM. By comparison, the other five constituents were considered as strong hyaluronidase inhibitors with smaller values of  $IC_{50}$  as compared to the positive control. The potencies of inhibition of the six phytoconstituents were arranged in a descending manner: clinopodic acid C (**17**) ( $IC_{50}$  value: 80.1 µM) > clinopodic acid E (**18**) ( $IC_{50}$ : 82.8 µM) > lycopidic acid A (**19**) ( $IC_{50}$ : 134 µM) > lycopidic acid B (**20**) ( $IC_{50}$ : 141 µM) and scizotenuin A (**21**) ( $IC_{50}$ : 241 µM) > rosmarinic acid (**1**) ( $IC_{50}$ : 309 µM) (Murata et al., 2010). This has provided scientific evidence to support future research on *L. lucidus* for its anti-allergic potential. Similarly, in the work of Ippoushi et al. (2000), it was found that the leaf methanolic extract of *Melissa officinalis*, which is also commonly known as lemon balm, possessed the highest hyaluronidase inhibition among 46 plants tested, achieving as low as only  $1.0 \pm 0.3\%$  of enzyme activity (Ippoushi et al., 2000). The potency of lemon balm in suppressing hyaluronidase is worthy to be further explored, so that it can become an anti-allergic therapeutic in future. Taken together, these outcomes suggest that these species can be used as potential novel anti-allergic therapeutic agents through mast cell degranulation inhibition.

## INHIBITION OF ALLERGIC MEDIATORS AND SECRETORY GRANULES

Following mast cell degranulation, various chemical mediators are released from the mast cells or basophils. One of the most



prominent mediators release from mast cells is histamine. Histamine was discovered as a potent vasoactive agent in 1911 by Dale and Laidlaw and recognized as a major contributor to allergic diseases (White, 1990; Xie and He, 2005). Histamine participates in both early and late phase allergic reactions. In the early phase of allergic reactions, the histamine released from degranulated mast cells and basophils triggers an array of acute allergic symptoms which can be seen within minutes. Some of the examples of allergic symptoms are increased vascular permeability causing redness, swelling, itchiness and pain, bronchoconstriction, anaphylaxis, etc. (Jutel et al., 2009). The onset of immediate allergic reactions is followed by the late phase responses (LAR) which contribute to more sustained inflammation. During the LARs, histamine acts as the chemoattractant to effector cells, notably  $T_H2$  lymphocytes, eosinophils, and basophils for recruitment to the inflammatory site and hence is implicated in the pathogenesis of late phase chronic allergic inflammatory reactions (He et al., 1997; Galli et al., 2008).

In addition,  $\beta$ -hexosaminidase is another popular biomarker used to evaluate mast cell degranulation in many the allergy studies (Kuehn et al., 2010). Similar to histamine, it is produced and stored as secretory granules within mast cells and basophils. However, unlike histamine, it does not have any significant involvement or contribution to allergic reactions. Instead,  $\beta$ -hexosaminidase was reported to have the ability to confer host defense against bacterial infection (Fukuishi et al., 2014). Nevertheless, it is widely employed as a mast cell degranulation marker because it is released together with histamine during the degranulation process (Cota et al., 2012; Huang et al., 2016). As compared to histamine, the release of  $\beta$ -hexosaminidase is slower and persists for a longer time. This makes  $\beta$ -hexosaminidase a better indicator for mast cell degranulation detection than histamine (Huang et al., 2016). Apart from histamine and  $\beta$ -hexosaminidase, mast cells also contain other mediators like eicosanoids, such as prostaglandin  $D_2$  and leukotrienes  $C_4$ , chemotactic factors and immunoregulatory cytokines (Xiang et al., 2001; Parikh et al., 2003). During degranulation, these substances are also released from mast cells and basophils through exocytosis. Therefore, they are also used as biomarkers of mast cell degranulation in the allergy studies.

Anti-allergic activity of plants can be evaluated through the potency of the plant in suppressing the mediators, secretory granules or any functional changes induced by the mediators as aforementioned. In a study by Vadnere et al. (2007), a significant inhibition ( $P < 0.05$ ) in histamine-induced tracheal contraction was seen at concentrations of 4 and 10 mg/ml of leaf aqueous extract of *Clerodendron phlomidis* on isolated goat tracheal chain. At the same time, intraperitoneally administered leaf aqueous extract of *C. phlomidis* at concentrations of 100 mg/kg showed a potent reduction ( $P < 0.05$ ) in histamine-induced vascular leakage in sensitized murine model (Vadnere et al., 2007). Lee et al. (2011) explored the possibility of *C. trichotomum* on anti-asthmatic potential employing *in vivo* guinea pig model. A phenylpropanoid glycoside, acteoside (22) was isolated from the ethyl acetate fraction from *C. trichotomum* leaves. At dose 25 mg/kg, specific airway resistance (sRaw) was significantly

( $P < 0.05$ ) inhibited in immediate phase response (IAR) and LAR in ovalbumin-challenged guinea pigs by 32.14% and 55.88% respectively. The result seemed promising as it was superior to positive controls, 5 mg/kg dexamethasone (55.88%) and 10 mg/kg disodium cromoglycate (52.94%) in LAR. Meanwhile, concentration of 50 mg/kg of acteoside (22) was significantly ( $P < 0.05$ ) against the histamine release and phospholipase  $A_2$  ( $PLA_2$ ) activity in BALF in which the histamine content was marked with  $26.40 \pm 1.96\%$  and  $PLA_2$  activity recorded with only  $28.08 \pm 2.05\%$  (Lee et al., 2011b).

Park et al. (2010) investigated the anti-allergic potential of *Clinopodium gracile* using both *in vivo* and *in vitro* studies. In the *in vivo* study, the mice were treated with compound 48/80 to induce systemic anaphylaxis after the pretreatment with intraperitoneal administration of aqueous extract of *C. gracile* with concentrations ranging from 1–100 mg/kg. The mortality of mice due to anaphylactic shock was assessed. Results revealed that the systemic anaphylactic death event was reduced concentration-dependently, in which the doses of 50 mg/kg and above were identified as the effective doses that prevented the mice from fatal anaphylactic shock. The reduction of systemic anaphylaxis corresponded to the reduced serum histamine. On the other hand, aqueous extract of *C. gracile* was also shown to significantly ( $P < 0.05$ ) suppress the release of histamine in *in vitro* RPMC and HMC-1 cells assays. The suppressive effect occurred in a dose-dependent manner with the concentrations ranging from 1–100  $\mu$ g/ml. As aforementioned, calcium influx is pivotal in the releasing of secretory granules and mediators from mast cell degranulation. Therefore, a reduction of intracellular calcium level can result in the inhibition of chemical mediators such as histamine and  $\beta$ -hexosaminidase release (Oka et al., 2005). In the same study, intracellular calcium level was also evaluated in HMC-1 cell line. Results showed that pretreatment with aqueous extract of *C. gracile* caused a suppression in intracellular calcium level induced by PMACI. Hence, this finding is supported by the theory which suggests the involvement of intracellular calcium in the inhibition of histamine release from mast cells. In addition, mast cell-mediated hypersensitivity also occurs with the involvement of NF- $\kappa$ B and inflammatory cytokines. NF- $\kappa$ B activation is essential to regulate downstream pro-inflammatory cytokine expression, such as TNF- $\alpha$  and IL-6 which play a critical role in initiating and sustaining the allergic inflammatory responses (Blackwell and Christman, 1997). Therefore, the attenuation of NF- $\kappa$ B activation causes a reduction in downstream inflammatory cytokines gene expression and hence produces suppressive effects in allergic inflammation. NF- $\kappa$ B-dependent transcriptional activity was evaluated through luciferase activity assay. Results revealed that treatment with aqueous extract significantly ( $P < 0.05$ ) inhibited the activation of NF- $\kappa$ B and its downstream cytokine expression (TNF- $\alpha$  and IL-6) at doses of 1 and 10  $\mu$ g/ml. These findings provide evidence that *C. gracile* has the potential to be developed as an anti-allergic agent in the future, given its potential in reducing allergic inflammation (Park et al., 2010). Similarly, aqueous extracts of *Dracocephalum argunense* (Kim and Shin, 2006; Kim et al., 2006), *Elsholtzia ciliata* (Kim et al., 2011), *Isodon japonicus* (Kim et al., 2004;

Shin et al., 2004), *Lycopus lucidus* (Shin et al., 2005), *Mentha arvensis* (Shin, 2003), *Mosla chinensis* (Kim et al., 2012), *M. dianthera* (Lee et al., 2006), *Perilla frutescens* (Shin et al., 2000), *Phlomis umbrosa* (Shin et al., 2008), *Pogostemon cablin* (Yoon et al., 2016), *Prunella vulgaris* (Shin et al., 2001), *Salvia plebeia* (Shin and Kim, 2002), *Schizonepeta tenuifolia* (Shin et al., 1999), *Stachys riederi* (Shin, 2004), *Teucrium japonicum* (Kim et al., 2009) and *Vitex rotundifolia* (Shin et al., 2000) also exhibited similar outcomes as portrayed in the experiment conducted using *C. gracile*.

In another account, Inoue et al. (2001) prepared four different extracts and separated fractions (50% ethanolic extract, water eluate, 50% ethanolic eluate and ethanolic eluate) from *M. piperita* leaves to investigate their anti-allergic potential on allergic rhinitis. It was found that 50% ethanolic eluate exhibited the most potent inhibition to histamine release, with an  $IC_{50}$  value of 2.55  $\mu$ g/ml and exerted its antagonizing effect on nasal responses at doses of 300 and 1,000 mg/kg in antigen-challenged rats (Inoue et al., 2001). In the continuation of their previous work, Inoue et al. (2002) focused on the 50% ethanolic eluate to isolate the active compounds responsible for the anti-allergic effect. Following the isolation of the compounds, a total of eight chemical constituents were considered. However, among the eight compounds, luteolin-7-*O*-rutinoside (**31**) was found to be the most effective in suppressing histamine release from compound 48/80-induced RPMC with  $IC_{50}$  value of 21.9  $\mu$ M. The nasal responses were reduced at doses of 100 and 300 mg/kg of luteolin-7-*O*-rutinoside (**31**) (Inoue et al., 2002). Recently, Sato and Tamura (2015) evaluated anti-allergic activity of *M. piperita* leaves using  $\beta$ -hexosaminidase assay. Five major flavonoids components, 5,6,4'-trihydroxy-7,8-dimethoxyflavone (**32**), 5,6,4'-trihydroxy-7,8,3'-trimethoxyflavone (**33**), 5,6-dihydroxy-7,3,4'-trimethoxyflavone (**34**), 5,6-dihydroxy-7,8,3,4'-tetramethoxyflavone (**35**) and 5,6-dihydroxy-7,8,4'-trimethoxyflavone (**36**) isolated from leaves dichloromethane extract were all shown to possess potent anti-allergic activity. However, 5,6,4'-trihydroxy-7,8,3'-trimethoxyflavone (**33**) and 5,6-dihydroxy-7,8,3,4'-tetramethoxyflavone (**35**) proved to have the strongest inhibitory activity on  $\beta$ -hexosaminidase release from RBL-2H3 cells, which were recorded with  $IC_{50}$  values of 2.4 and 3.0  $\mu$ M respectively. Their safety profiles also seemed promising as they had relatively lower cytotoxicity than another typical natural anti-allergic substance, luteolin (**3**) (Sato and Tamura, 2015). Therefore, this might indicate that 5,6,4'-trihydroxy-7,8,3'-trimethoxyflavone (**33**) and 5,6-dihydroxy-7,8,3,4'-tetramethoxyflavone (**35**) can be potentially developed into safe and effective anti-allergic agents. Another species from the same genus, *M. spicata*, was shown to have similar activity with its flavones, 5,6,4'-trihydroxy-7,8,3'-trimethoxyflavone (**33**) and 5,6-dihydroxy-7,8,3,4'-tetramethoxyflavone (**35**) and aliphatic glycoside, (3*R*)-1-octan-3-yl  $\beta$ -D-glucopyranoside (**37**). The potency of inhibitory activities was arranged in a descending manner: 5,6,4'-trihydroxy-7,8,3'-trimethoxyflavone (**33**) with  $IC_{50}$  of 6.4  $\mu$ M > 5,6-dihydroxy-7,8,3,4'-tetramethoxyflavone (**35**) with  $IC_{50}$  of 56  $\mu$ M > (3*R*)-1-octan-3-yl  $\beta$ -D-glucopyranoside (**37**) with  $IC_{50}$  of 560  $\mu$ M. Although (3*R*)-1-octan-3-yl  $\beta$ -D-glucopyranoside (**37**) showed the weakest activity, it was however a great discovery as this was the first time an anti-histaminic

activity from an aliphatic glycoside was recorded (Yamamura et al., 1998).

In 2007, Cariddi et al. investigated the anti-allergic activity of *Minthostachys verticillata*. The experiment was conducted using basophils from allergic patients pretreated with essential oil extracted from the stems and leaves of *M. verticillata* and followed by  $\beta$ -hexosaminidase assay. Results suggested that the essential oil showed a promising suppressive effect on  $\beta$ -hexosaminidase release with percentage inhibition ranging from 32.15% to 39.72%, which was comparable to dexamethasone (39.75%) and theophylline (41.63%) (Cariddi et al., 2007). A few years later, Cariddi et al. (2011) carried out an in-depth study on the components of the essential oil extracted from *M. verticillata* to identify the constituent responsible for anti-allergic effect. Limonene (**38**), pulegone (**39**) and menthone (**40**) were found to be present in the essential oil. Results suggested that limonene (**38**) appeared to be the most effective compound in the inhibition of  $\beta$ -hexosaminidase release from human basophils as compared to the other two compounds, pulegone (**39**) and menthone (**40**). It was shown that 20  $\mu$ g/ml of limonene (**38**) was able to achieve inhibitory effect while the other two compounds both required a higher concentration of 40  $\mu$ g/ml to reach the desired inhibition. The inhibitory effect could be achieved at a lower concentration (10  $\mu$ g/ml) when the compounds were used in combination (Cariddi et al., 2011). This can be explained with the synergistic effect of the three compounds.

Jeon et al. (2014) highlighted that luteolin (**3**) isolated from the leaves of *P. frutescens* potently ( $P < 0.05$  to  $P < 0.001$ ) suppressed histamine release from compound 48/80-stimulated RPMC at 5, 10 and 20  $\mu$ M in a dose-related manner. The expression and production of TNF- $\alpha$  and IL-1 $\beta$  were significantly ( $P < 0.05$  to  $P < 0.001$ ) reduced in PMACI-stimulated HMC-1 cells, with inhibition rates of 31.9%–76.8% and 27.3%–81.2% respectively, at the range of 5–20  $\mu$ M of luteolin (**3**) (Jeon et al., 2014). Likewise, Ueda et al. (2002) also reported a similar activity on the TNF- $\alpha$  production with a dose range of 1–1,000  $\mu$ g of luteolin (**3**) in sensitized mice. At the same time, *in vivo* studies conducted on ICR mice demonstrated that compound 48/80- or serotonin-induced scratching behavior and vascular permeability were dose-dependently decreased at concentrations of 5, 10 and 20 mg/kg of luteolin (**3**) (Ueda et al., 2002). According to a study conducted by Heo et al. (2011) on the anti-atopic effect of *P. frutescens*, the aqueous fraction demonstrated a promising outcome whereby the DNFB-sensitized mice experienced a 35% reduction in ear swelling symptoms with the administration of 100  $\mu$ g/ml. In light of the study carried out by Zhu et al. (2014), rosmarinic acid methyl ester (**41**) was found to be able to produce a stronger  $\beta$ -hexosaminidase release inhibition than that of rosmarinic acid (**1**) extract prepared from *P. frutescens* leaves using supramolecular technique, in which the  $IC_{50}$  values were marked with  $9.9 \pm 0.8$  and  $52.9 \pm 6.7$   $\mu$ g/ml respectively. Furthermore, Kamei et al. (2017) suggested that PDMF (**4**) significantly ( $P < 0.05$ ) inhibited histamine release from RBL-2H3 cells with an  $IC_{50}$  value of 68.5  $\mu$ M which was much more potent than other polyphenols. Hence, this finding deduced that PDMF (**4**) is a newly emerged potent anti-allergic component.



In light of a study by Ryu et al. (2000), 2 $\alpha$ ,3 $\alpha$ -dihydroxyurs-12-en-28-oic acid (**42**) isolated from the methanolic extract of *Prunella vulgaris* possessed a significant ( $P < 0.01$ ) inhibitory activity on  $\beta$ -hexosaminidase release from RBL-2H3 cells with  $IC_{50}$  of 57  $\mu$ M. Another histamine release assay conducted recently by Choia et al. (2016) intended to provide more evidence on the anti-allergic effect of *P. vulgaris*. The results suggested that three triterpenoids isolated from the spike of *P. vulgaris* exhibited significant inhibitory effects on histamine release from HMC-1 cells. The active principles represented by  $\beta$ -amyryn (**43**), 2 $\alpha$ ,3 $\alpha$ ,23-trihydroxyursa-12,20(30)-dien-28-oic acid (**44**) and euscaphic acid (**45**) demonstrated a percentage inhibition of 46.7%, 57.9% and 54.2% respectively. It is noteworthy that 2 $\alpha$ ,3 $\alpha$ ,23-trihydroxyursa-12,20(30)-dien-28-oic acid (**44**) was isolated for the first time and possessed promising activity against histamine release (Choia et al., 2016). Putting all the evidence together, *P. vulgaris* is experimentally proven to have high potential to be developed into efficacious anti-allergic agent. On the other hand, Mizushina et al. (2014) highlighted that carnosic acid (**5**) from *Rosmarinus officinalis* leaves significantly inhibited the release of  $\beta$ -hexosaminidase from RBL-2H3 cells at 10  $\mu$ M.

Likewise, Choi and Kim (2004) and Ryu et al. (1999) reported that 15,16-dihydrotanshinone-I (**7**) and cryptotanshinone (**9**) isolated from the root of *S. miltiorrhiza* showed to have  $IC_{50}$  values of  $16 \pm 2.4$  and  $36 \pm 3.7$   $\mu$ M on  $\beta$ -hexosaminidase release. Additionally, the ethanolic extract of *S. miltiorrhiza* also inhibited other chemical mediators, such as leukotriene  $C_4$  with a  $IC_{50}$  value of 2.6  $\mu$ g/ml, COX-1 and COX-2-dependent prostaglandin  $D_4$  with  $IC_{50}$  values of 3.96 and 21.54  $\mu$ g/ml respectively (Yang et al., 2008). With the aid of findings from Yang et al. (2008), Li et al. (2015) successfully identified 15,16-dihydrotanshinone-I (**7**) as the compound responsible for the inhibition of intracellular calcium level, hence suppressing the downstream release of leukotriene  $C_4$  and prostaglandin  $D_4$  from activated bone marrow-derived mast cells (BMMC). The inhibition percentage achieved was as high as 90% with a dose of 20  $\mu$ M of 15,16-dihydrotanshinone-I (**7**) (Li et al., 2015).

In addition, the four active constituents isolated from *Scutellaria baicalensis* root, wogonin (WG) (**10**), ganhuangenin (GHG) (**11**), wogonoside (WGS) (**12**), 3,5,7,2',6'-pentahydroxyflavanone (PHF) (**13**), all showed a significant suppression of histamine ( $P < 0.01$ ) and leukotriene  $B_4$  ( $P < 0.01$ ) release from A23817-induced rat peritoneal exudate cells (PEC) at a concentration of 100  $\mu$ M (Lim, 2003). Moreover, Kim et al. (2010) reported that baicalin (**46**) isolated from the roots of *S. baicalensis* possessed a significant ( $P < 0.001$ ) inhibitory activity of histamine and leukotriene release from OVA-sensitized guinea pig lung mast cells at 10, 30 and 60  $\mu$ g. The histamine inhibition rates recorded with 47.1%, 59.4% and 61.5% while leukotriene production remarkably suppressed by 37.9%, 47.3% and 50.4% with the pretreatment of the three different doses of baicalin (**46**). Interestingly, studies showed that the standardized extract of baicalin (**46**) at high dose produced a greater inhibition on both histamine and leukotriene production as compared to pure baicalin (**46**). Results revealed that 70.4% of histamine suppression and 78% of leukotriene inhibition ( $P < 0.001$ ) were found at high dose (60  $\mu$ g) of standardized extract. However, the percentage inhibitions

produced by low and medium dose standardized extract treatments were smaller than that of pure baicalin (**46**) (Kim et al., 2010). In a very interesting study conducted by (Trinh et al., 2010b), baicalin (**46**) isolated from rhizome of *S. baicalensis* was metabolized into baicalein (**47**) and oroxylin A (**14**) followed by oral administration. All three compounds possessed inhibitory activity against histamine-induced scratching behavior and vascular permeability in *in vivo* ICR mice model at doses of 20 and 50 mg/kg. However, the metabolite, oroxylin A (**14**) showed the most potent inhibition instead of its parent compound, baicalin (**46**). In the study of Li et al. (2014), it was suggested that ethanol extract potently inhibited ( $P < 0.01$ ) 4-AP-induced allergic skin pruritus, histamine-induced mice paw swelling and cutaneous anaphylactic-ear swelling at 1.42 g/kg. For instance, ear swelling inhibition produced by 1.42 g/kg of ethanol extract (47.10%) was superior to that of the positive control, 0.1 g/kg of cromolyn sodium (32.43%) (Li et al., 2014). In a food allergy study, 25 mg/kg of ethanol extract of *S. baicalensis* conferred 60% protection to food allergy anaphylactic death in OVA-sensitized mice (Shin et al., 2014b). Henceforth, these promising experimental outcomes make the anti-allergic potential of *S. baicalensis* worthwhile to be further explored.

## REGULATION OF T CELL RESPONSES

It has been long recognized that allergic sensitization is led by lymphocytes (Zhang et al., 2014). There are various types of T lymphocytes, such as CD4<sup>+</sup>, CD8<sup>+</sup>, and natural killer T cells, in which each population produces response to allergens with different capacities. Among the different types of T lymphocytes, CD4<sup>+</sup> T cells are predominantly implicated in the pathogenesis of allergy. With the expression of major histocompatibility complex (MHC) class II molecules and allergen specific T-cell receptors (TCR), CD4<sup>+</sup> T cells are able to recognize peptide antigen presented by antigen-presenting cells (APCs). Antigen recognition is then led to the activation of downstream immune responses, such as allergic inflammatory cascade (Kallinich et al., 2007; Woodfolk, 2007).

Naive CD4<sup>+</sup> T cells can be differentiated towards T<sub>H</sub>1, T<sub>H</sub>2, T<sub>H</sub>17 and Treg phenotypes (Zhang et al., 2014). T<sub>H</sub>2 subsets are particularly renowned as the major contributors to the immunopathology of allergy. Late-phase allergic responses are provoked by the persistent existence of allergens, leading to T-cell activation (Palomares et al., 2010). Activated T<sub>H</sub>2 lymphocytes play a critical role in the production of T<sub>H</sub>2 cytokines (IL-4, IL-5, IL-9 and IL-13) (Deo et al., 2010; Ozdemir et al., 2010). IL-4 and IL-13 are crucial to the development of T<sub>H</sub>2 cells and induction of IgE isotype switching from B cells, which are the major risk factor for the development of allergic asthma (Steinke and Borish, 2001; Woodfolk, 2007). IL-5 mainly mediates eosinophil recruitment and increases eosinophil survival while IL-9 stimulates mast cells and basophils (Woodfolk, 2007; Ozdemir et al., 2010). In contrast, T<sub>H</sub>1 cells differentiation occurs in response to microbial activation of APC under the influence of IL-12 (Deo et al., 2010). These cells orchestrate the production of IL-2, IFN- $\gamma$  and TNF- $\beta$  (Romagnani, 2004). T<sub>H</sub>1 cytokines tend

to produce pro-inflammatory responses which are important in killing phagocytosed microbes and perpetuating autoimmune responses (Berger, 2000). Recent evidence demonstrate that minimal microbial exposure in early life causes the  $T_H1/T_H2$  balance in the immune system to skew towards the pre-allergic  $T_H2$  response (Berger, 2000; Deo et al., 2010).

Recently, Treg cells emerged as the key component in the sensitization stage of allergy (Zhang et al., 2014). The transcriptional factor, FOXP<sub>3</sub> serves as a lineage specification factor of Treg cells which is required for the differentiation of Treg cells (Rudensky, 2011; Noval Rivas and Chatila, 2016). FOXP<sub>3</sub>, which is dominantly expressed by Tregs, inhibits  $T_H2$  cells activation, thus reducing the production of  $T_H2$  cytokines, which is essential during the effector phase of allergic reactions (Albano et al., 2013). Treg cells also suppress allergic inflammation through direct action on mast cells, basophils and eosinophils (Palomares et al., 2010; Noval Rivas and Chatila, 2016). It has been shown that constitutive FOXP<sup>+</sup> Treg controls the symptomatic phase of mast cell activation and IgE-dependent anaphylaxis in mice (Kanjrawi et al., 2013). Apart from that,  $T_H17$  cells and their corresponding cytokine, IL-17, are also highlighted for their involvement in the progression of  $T_H2$ -mediated allergic disorders (Oboki et al., 2008). A balance between  $T_H17$  and Tregs is essential for immune homeostasis. Excessive or exaggerated  $T_H17$  function and elevated  $T_H17$  cells together with a defect in Treg function or reduction in Treg population lead to the development of allergic disorders, like allergic asthma and rhinitis. Restoring the balance between  $T_H17$  and Treg can promote the resolution of allergic disorders, such as allergic inflammation seen in allergic asthma (Albano et al., 2013).

Natural compounds with the ability to regulate T cell responses have a great potential in the development of novel anti-allergic therapeutic agents. In this review, there are several plants described to have compelling effects on the down-regulation of  $T_H2$  cytokines, re-establishment of  $T_H1/T_H2$  balance,  $T_H17$  inhibition and promotion of Treg cells functions. For example, 100 mg/kg of ethanolic extract of *Mentha haplocalyx* was reported to exhibit significant ( $P < 0.05$ ) inhibition on the expression and production  $T_H2$  cytokines (IL-4 and IL-5) in BALF (Lee et al., 2011a). Besides, Costa et al. (2012) evaluated the effectiveness of *Ocimum gratissimum* in alleviating allergic asthma. Results revealed that *Blomia tropicalis* mite-immunized and challenged mice receiving 100 mg/kg of *O. gratissimum* methanolic extract had a significant reduction ( $P < 0.05$ ) in IL-4 level in BALF in relation to those of the untreated group (Costa et al., 2012). In addition, Trinh et al. (2010a) stated that tanshinone I (6), 15,16-dihydrotanshinone I (7), tanshinone IIA (8) isolated from *Salvia miltiorrhiza* possessed inhibitory activity on IL-4 and TNF- $\alpha$  expression in IgE-antigen complex-stimulated RBL-2H3 cells at a dose of 50  $\mu$ M. The ability of *S. miltiorrhiza* in inhibiting IgE-switching cytokine, IL-4 and pro-inflammatory cytokine, TNF- $\alpha$  is thought to be a spring for allergic reactions improvement (Trinh et al., 2010a). Another species from the same genus, *S. plebeia*, was reported to reduce symptoms of atopic dermatitis through regulation of T cells responses (Choi et al., 2014). At a concentration of 100 mg/kg

of ethanol extract of *S. plebeia*, the expression of  $T_H1$ ,  $T_H2$  and  $T_H17$  cytokines was significantly reduced ( $P < 0.05$ ) in *Der-f*-induced atopic dermatitis-like skin lesions (Choi et al., 2014). On the other hand, *Schizonepeta tenuifolia* demonstrated a significant reduction ( $P < 0.05$ ) of IFN- $\gamma$ , IL-4 and IL-13 in IgE-induced allergic model of RBL-2H3 cells with 100  $\mu$ g/ml of aqueous extract. In the same study, *S. tenuifolia* aqueous extract showed no cytotoxicity even at a higher concentration up to 1,000  $\mu$ g/ml (Lin et al., 2018). However, a more thorough and detailed toxicological investigation is required to develop a more evidence-based safety profile.

In another account, *Perilla frutescens* also suppressed  $T_H2$  responses which then contributed to anti-allergic effect (Sanbongi et al., 2004). Results demonstrated that the expression and production of  $T_H2$  cytokines (IL-4 and IL-5) were potently inhibited by daily oral administration of 1.5 mg of rosmarinic acid (1) from *P. frutescens* ( $P < 0.05$ ) in *in vivo* house mite-challenged murine model (Sanbongi et al., 2004). Meanwhile, Chen et al. (2015) reported that IL-5 and IL-13 were diminished in OVA-induced allergic asthma murine model with ethanolic extract of *P. frutescens* leaves. Interestingly, aqueous fraction of *P. frutescens* leaves showed its effectiveness in alleviating atopic dermatitis through balancing of  $T_H1$  and  $T_H2$  cells (Heo et al., 2011). The effect was achieved by suppressing the release of IL-31, which is a  $T_H2$  cytokine that promotes allergic symptoms like pruritus and allergic skin disorders (Heo et al., 2011; Meng et al., 2018). At the same time, the T-bet protein expression was augmented with 100  $\mu$ g/ml of *P. frutescens* aqueous fraction (Heo et al., 2011). T-bet protein expression is essential for  $T_H1$  cell differentiation (Chatila et al., 2008). Therefore, the combination of suppressed IL-31 and augmented T-bet protein expression resulted in  $T_H1/T_H2$  balance and hence alleviation of allergic symptoms. Besides, Komatsu et al. (2016) suggested that the CD4<sup>+</sup>/CD8<sup>+</sup> ratio in splenic T lymphocytes obtained from *Der f*-induced atopic dermatitis NC/Nga mice was decreased from  $1.82 \pm 0.32\%$  to  $1.50 \pm 0.07\%$  after receiving treatment of *Perilla* leaves extract. This suppression is believed to be associated with the  $T_H1$  and  $T_H2$  balance (Komatsu et al., 2016). Additionally, Liu et al. (2013) employed an *in vitro* assay to investigate the effect of *P. frutescens* extract on *Der p* 2-challenged human bronchial epithelial cells BEAS-2B cells. Result displayed that the pro-allergic cytokines (IL-4, IL-5, IL-13) and GM-CSF productions were all dose-dependently reduced ( $P < 0.05$ ) in *Der p* 2-stimulated BEAS-2B cells with treatment of 5–50  $\mu$ g/ml of methanolic extract of *P. frutescens* leaves (Liu et al., 2013).

In a recent work by Bae et al., 2016, *Scutellaria baicalensis* showed to be effective in ameliorating ovalbumin-induced food allergy murine model through the regulation of Treg cells with its natural flavonoid compound, baicalein (47). Results revealed that baicalein (47) was able to increase Treg cells population through induction of CD4<sup>+</sup> FOXP<sub>3</sub><sup>+</sup> T cell differentiation without causing any cytotoxicity at concentrations smaller than 10  $\mu$ mol/L (Bae et al., 2016). In light of a study by Jung et al. (2017), linoleic acid (50) in hexane fraction from ethanol extract of *S. baicalensis* roots was reported to cause a significant suppression ( $P < 0.05$ ) in the production of pro-allergic cytokines (IL-4, IL-5, IL-10 and IL-13) and enhancement of secretion of  $T_H1$  cytokines (IFN- $\gamma$  ( $P < 0.05$ )).

and IL-12 ( $P < 0.01$ )). The fact that a fatty acid from a plant can contribute anti-allergic effect through restoration of  $T_H1/T_H2$  balance is a new discovery (Jung et al., 2017). A similar outcome was noted in a food allergy murine model conducted by Shin et al. (2014b) with *S. baicalensis* ethanol extract. Interestingly, the ethanol extract also down-regulated the IL-17 level produced by  $T_H17$  and hence produced effective prevention to food allergy (Shin et al., 2014b). Within the same year, the same group of researcher successfully discovered that the active compounds isolated from *S. baicalensis*, represented by wogonin (WG) (10), baicalin (46) and baicalein (47), all inhibited the  $T_H2$  cytokines (IL-4, IL-5, IL-10 and IL-13) and IFN- $\gamma$  at dose of 50  $\mu\text{mol/L}$  in an *ex vivo* study. However, only WG (10) was able to produce inhibition without affecting cell viability as compared to the other two active compounds (Shin et al., 2014a). This finding suggests that WG (10) could be a safer anti-allergic compound at a higher dose, but its toxicity profile should be further investigated with more extensive toxicity testings. Kim et al. (2010) focused on the therapeutic potential of *S. baicalensis* on atopic dermatitis. In the experiment, the male NC/Nga mice were orally fed with aqueous extract of *S. baicalensis* after atopic dermatitis-like skin lesion was conventionally developed in the mice. The feeding process was continued for 6 weeks. After 6 weeks, blood was drawn from the mice and analyzed to measure the level of cytokine release. Interestingly, the results revealed that *S. baicalensis* aqueous extract only exhibited specific inhibition on IL-5 ( $P < 0.05$ ) at a dose of 50 mg/kg. There was no significant change in the level of IL-4 and IL-10 between *S. baicalensis* treatment group and control group (Kim et al., 2010). However, in the study by Kim et al. (2016), it was proposed that topical application of aqueous extract of *S. baicalensis* onto the DNCB-induced contact dermatitis can significantly ( $P < 0.05$ ) reduce the level of IL-4 and IFN- $\gamma$  in BALB/c mice skin cells. Zhou et al. (2016) reported that oroxylin A (14) isolated from *S. baicalensis* was effective against allergic asthma with significant inhibition ( $P < 0.01$ ) of IL-4, IL-5 and IL-13 production at doses of 15, 30 and 60 mg/kg of oroxylin A (14). In conclusion, *S. baicalensis* has good therapeutic potential in allergic diseases, such as atopic dermatitis, food allergy and allergic asthma through regulation of T cell responses.

With the intention to explore the effectiveness of 2-isopropyl-5-methylphenol (thymol) (15) isolated from *Thymus vulgaris* in alleviating allergic asthma, Zhou et al. (2014) employed an *in vivo* allergic murine model of asthma. Results revealed that thymol (15) effectively reduced the symptoms of allergic asthma through dose-dependent inhibition of IL-4, IL-5 and IL-13 production at 4, 8 and 16 mg/kg in OVA-challenged mice. Particularly, a potent reduction ( $P < 0.01$ ) of OVA-induced  $T_H2$  cytokines was recorded at 16 mg/kg of thymol (15) (Zhou et al., 2014). Apart from thymol (15), carvacrol (51) from *T. vulgaris* was reported to effectively inhibit the production of IL-2, IFN- $\gamma$ , IL-4 and IL-17 cytokines as well as T-bet expression in the *ex vivo* splenocytes cultures (Gholijani and Amirghofran, 2016). On the contrary, both thymol (15) and carvacrol (51) led to an increase in the level of IL-10 and TGF- $\beta$  in mice splenocytes cultures (Gholijani and Amirghofran, 2016). Henceforth, the regulation of T cell responses that was shown by thymol (15) and carvacrol (51) suggests that these two compounds potentially benefit allergic disorders. Likewise,

Lee et al. (2009) also highlighted that the active constituent of *Vitex rotundifolia*, 1H,8H-pyrano [3,4-c] pyran-1,8-dione (PPY) (16) potently suppressed the IL-5 production in BALF by 34%. Furthermore, hydro-ethanolic extract prepared from *Zataria multiflora* seeds was reported to restore  $T_H1/T_H2$  balance by enhancing the ratio of IFN- $\gamma$ /IL-4 in *in vivo* and *in vitro* assays (Boskabady et al., 2013). Another study conducted by Kianmehr et al. (2017) further supported the above finding. In addition to enhanced IFN- $\gamma$ /IL-4 ratio, *Z. multiflora* hydro-ethanolic extract also caused potentiation of  $T_H1$  and suppression effect on  $T_H2$  and  $T_H17$  cells, which led to therapeutic effect on allergic asthma in ovalbumin-sensitized BALB/c mice. Results showed that the number of Treg cells ( $P < 0.001$ ),  $T_H1/T_H2$  ratio ( $P < 0.001$ ), IFN- $\gamma$ /IL-4 ratio ( $P < 0.01$ ), IFN- $\gamma$  ( $P < 0.05$ ) and FOXP<sub>3</sub> ( $P < 0.001$ ) expression were increased significantly. Meanwhile,  $T_H2$  and  $T_H17$  cells ( $P < 0.01$  to  $P < 0.001$ ), IL-4, IL-17 and TGF- $\beta$  ( $P < 0.05$  to  $P < 0.001$ ) expressions were significantly reduced in sensitized mice spleen cells (Kianmehr et al., 2017). In conclusion, *Z. multiflora* is able to produce anti-allergic therapeutic effects on type I hypersensitivities like allergic rhinitis, allergic asthma and urticarial by regulating T cell responses.

## SUPPRESSION OF EOSINOPHILS MIGRATION

Eosinophils are long-lived circulating granulocytes which play a central role in promoting allergic reactions. They arise and differentiate in bone marrow and are then widely distributed in the blood, lungs, thymus, uterus, adipose tissues, spleen, etc and lastly readily migrate to the allergic sites (Fulkerson and Rothenberg, 2013; Wen and Rothenberg, 2016). They migrate to the target sites with the influence of chemoattractant, eotaxin and particularly, IL-5 for eosinophil proliferation, survival and priming (Wen and Rothenberg, 2016). Unlike mast cells and basophils with extensive expression of high affinity IgE receptors, eosinophils have a minimal expression of Fc $\epsilon$ RI. Nevertheless, they express a great range of cell surface molecules, such as receptors for IgG and IgA, complement receptors, cytokine receptors, whose aggregation can trigger eosinophils activation and development (Rigoni et al., 2018). Often, the number of eosinophils is greatly elevated in circumstances associated with allergic disorders, such as allergic rhinitis, allergic asthma and atopic dermatitis (Stone et al., 2010). Henceforth, natural products with the ability to suppress eosinophil recruitment or infiltration to allergic sites can be the noteworthy pharmacological therapeutic options for allergic disorders.

Several Lamiaceae plant species have demonstrated their suppressive effects on the eosinophil recruitment. Vadnere et al. (2007) showed that intraperitoneally administration of 100 mg/kg leaf aqueous extract of *Clerodendron phlomidis* produced a potent antagonizing effect towards milk-induced eosinophilia by showing a marked reduction in blood eosinophil count in mice with the value of  $13.8 \pm 2.4$  as compared to the control group ( $43.1 \pm 1.25$ ). This reduction is indicative of the effectiveness of *C. phlomidis* in conferring anti-allergic effect. Another species under the same genus, *C. serratum*, was evaluated by Bhangare et al. (2012) to study the anti-allergic effect of its aqueous extract



prepared from root and stem using different concentrations. Results demonstrated that all extracts used possessed inhibitory activity on milk-induced leukocytosis. However, the most potent activity was shown by high dose (260 mg/kg) aqueous root extract as compared to low dose (130 mg/kg) or any doses of aqueous stem extracts. This extract accorded a more significant protection than the standard used, dexamethasone from milk-induced leukocytosis (Bhangare et al., 2012). This finding suggests that *C. serratum* might be a potential candidate for anti-allergic therapy. Moreover, Lee et al. (2011b) reported that acteoside (**22**) isolated from *C. trichotomum* at 25 mg/kg significantly ( $P < 0.05$ ) reduced total leukocytes in BALF from  $31.25 \pm 6.12 \times 10^5$  to  $25.23 \pm 4.72 \times 10^5$ . At 50 mg/kg, 29.70% of eosinophil infiltration suppression was achieved in guinea pigs model (Lee et al., 2011b). Similar outcome was seen with 200  $\mu$ l/kg of *Mentha arvensis* essential oil (Sharma et al., 2018) and 100 mg/kg of ethanolic extract of *M. haplocalyx* in OVA-challenged mice (Lee et al., 2011a). In an attempt to investigate the effect of *Ocimum gratissimum* in alleviating respiratory allergy, Costa et al. (2012) carried out an experiment through *in vivo* model using male A/J mice. The mice were orally fed with 25, 50 or 100 mg/kg of methanolic leaves extract after subcutaneously injecting *Blomia tropicalis* antigen for respiratory allergy induction. Results revealed that *O. gratissimum* significantly suppressed the eosinophil counts ( $P < 0.05$ ) in BALF as well as eosinophil peroxidase ( $P < 0.01$ ) level at a dose of 100 mg/kg. The same concentration of methanolic extract *O. gratissimum* also attenuated mucus hypersecretion in airway, which is one of the features of allergic asthma (Costa et al., 2012). Henceforth, this suggests that *O. gratissimum* is effective against respiratory allergy disorders, like asthma.

*Perilla frutescens* is a Lamiaceae plant species which has a global distribution, but is especially concentrated in Asian countries, like China, Japan, Korea and Vietnam among others. In an effort to explore the isolate from *P. frutescens* with anti-allergic activity on respiratory allergy, Sanbongi et al. (2004) evaluated the isolate from the leaves of *P. frutescens*. Results from this study suggested that the isolated compound, rosmarinic acid (**1**), can bring about a significant reduction in eosinophil infiltration ( $P < 0.05$ ), BALF eosinophil counts ( $P < 0.01$ ) and eotaxin expression ( $P < 0.05$ ) in the *Der f*-challenged C3H/He mice (Sanbongi et al., 2004). Parallel activity was seen in OVA-sensitized BALB/c mice with its ethanolic extract in the study of Chen et al. (2015). On top of that, in an anti-atopic study carried out by Heo et al. (2011), the immunohistochemistry test showed that the eosinophil count was remarkably reduced by 73.7% and the MMP-9 expression was also decreased significantly ( $P < 0.05$ ) at a 100  $\mu$ g/ml of *P. frutescens* aqueous fraction (Heo et al., 2011). *Scutellaria baicalensis* is another well-known Chinese herb which is widely used as an anti-allergic herb (Li et al., 2014). In light of the study of Zhou et al. (2016), it was proposed that oroxylin A (**14**) from *S. baicalensis* was effective to alleviate allergic asthma. Results demonstrated that oroxylin A (**14**) at doses of 15, 30 and 60 mg/kg were able to inhibit eosinophil infiltration in BALF and consequently led to reduced airway hyperresponsiveness in OVA-challenged BALB/c mice (Zhou et al., 2016). In the same year, Kim et al. (2016) evaluated the efficacy of topical treatment of aqueous extract of *S. baicalensis* on contact dermatitis. Results

revealed that topical application was effective in suppressing leukocytes infiltration and hence ameliorated contact dermatitis symptoms (Kim et al., 2016).

In addition, Zhou et al. (2014) reported that 2-isopropyl-5-methylphenol (thymol) (**15**) from *Thymus vulgaris* produced a dose-dependent reduction of eosinophils infiltration in BALF across concentrations of 4, 8 and 16 mg/kg. A remarkable inhibition ( $P < 0.01$ ) was noted at a dose of 16 mg/kg which was comparable to 2 mg/kg of dexamethasone standard. Consequently, mucus hypersecretion and goblet cell hyperplasia in lung tissues as well as the airway hyperresponsiveness in OVA-sensitized mice in response to methacholine were drastically reduced (Zhou et al., 2014). In 2011, Patel and Deshpande identified the mast cell stabilization potential of *Vitex negundo*. In 2013, they conducted another experiment on *V. negundo*'s leaves to study their anti-asthmatic activity. They successfully isolated a flavonoid compound, 5-hydroxy-3,6,7,3',4'-pentamethoxyflavone (**52**) from the leaves and found that this compound potentially suppressed eosinophil count in BALF ( $9.50 \pm 1.5044$ ;  $P < 0.05$ ) in egg albumin-sensitized guinea pigs. This result was remarkable as the inhibition portrayed was comparable to that of dexamethasone control ( $7.50 \pm 0.5014$ ;  $P < 0.05$ ) at a dose of 200 mg/kg (Patel and Deshpande, 2013). This is indicative of the potential of *V. negundo* in the treatment of allergy diseases like asthma. Meanwhile, Lee et al. (2009) highlighted that 1H,8H-pyrano [3,4-c] pyran-1,8-dione (PPY) (**16**) isolated from *V. rotundifolia* fruits remarkably reduced eosinophil migration and eotaxin production by 48% and 70% respectively at 10  $\mu$ g/ml in human type II-like epithelial lung cells (A549 cell media). In *in vivo* model, the eosinophil count in BALF was also shown to decrease significantly ( $P < 0.05$ ) by 82% (Lee et al., 2009). In 2011, Koh et al. discovered another new compound, casticin (**53**), isolated from the fruits of *V. rotundifolia* which also showed to inhibit 63% of eosinophil infiltration at 10  $\mu$ g/ml while eotaxin production decreased dose-dependently with 0.1–1  $\mu$ g/ml of casticin (**53**) (Koh et al., 2011). In conclusion, the species mentioned above have the potential to fill the knowledge gap of anti-allergy with the inhibition of eosinophil functions.

## TOXICOLOGY

Undeniably, in the past decades, the medicinal potential of Lamiaceae species has captured the attention and interest of many researchers to conduct extensive exploration on their pharmacological properties. Nonetheless, the toxicological aspects of the use of Lamiaceae species have not been studied in-depth. To date, there are several toxicological studies available on Lamiaceae species. For instance, Qi et al. (2009) carried out a toxicological investigation on wogonin (**10**), the active constituent of *Scutellaria baicalensis*, through acute toxicity testing and sub-chronic toxicity testing in murine models. In the acute toxicity testing, the mice were intravenously administered with 350, 315, 283.5, 255.5 and 229.64 mg/kg of wogonin (**10**) respectively. The mice were observed for their general behavior for an hour after the administration and intermittently observed for 24 h for signs of toxicity up to 14-day duration. In the first hour after treatment, the mice showed

decreased locomotor activity, muscle relaxation, catatonia, loss of body-righting reflex and bradypnoea. However, these symptoms diminished within 2 h after treatment. The LD<sub>50</sub> value of wogonin (**10**) determined was 286.15 mg/kg. Meanwhile, in the sub-chronic toxicity study, doses of 30, 60 and 120 mg/kg of wogonin (**10**) were administered daily to the rats through intravenous route and the rats were put under observation for 90 days. Results revealed that a dose of 120 mg/kg of wogonin can cause heart injury with a long period of intravenous administration (**10**) (Qi et al., 2009).

In another account, the essential oil of *Thymus vulgaris* was evaluated on its toxicological profile (Fachini-Queiroz et al., 2012). Acute toxicity was assessed by administering single oral doses of 2,000, 3,000 and 4,000 mg/kg of *T. vulgaris* essential oil and monitoring for any signs of toxicity for seven consecutive days. There were no apparent behavioral side effects observed in the study and the median lethal dose, LD<sub>50</sub>, of *T. vulgaris* essential oil determined was 4,000 mg/kg. The relatively high LD<sub>50</sub> value suggested that *T. vulgaris* essential oil is non-toxic and relatively safe for use (Fachini-Queiroz et al., 2012). Haq et al. (2012) evaluated *Vitex negundo* in an acute neurotoxicity study. Results suggested that no signs of neurotoxicity were seen with doses of 250, 500, 1,000 and 2,000 mg/kg in the tested mice. The LD<sub>50</sub> value determined was greater than 5,000 mg/kg, which indicates the extract of *V. negundo* has a good safety profile (Haq et al., 2012). In term of behavioral symptoms, symptoms started to show at a dose of 2,000 mg/kg, which presented with abdominal contraction, ataxia, reduced spontaneous activity and reduced alertness (Haq et al., 2012).

In China, people have been widely employing *Salvia miltiorrhiza* as a traditional herb for treating a range of cardiovascular disorders (Wang et al., 2012). Therefore, Wang et al. (2012) designed a toxicological study to assess the acute toxicity and sub-chronic toxicity of *S. miltiorrhiza* aqueous extract (Wang et al., 2012). In the acute toxicity investigation, the rats received two doses of 32 g/kg of aqueous extract of *S. miltiorrhiza* through intravenous administration. The sub-chronic toxicity was evaluated by assessment of hematological and biochemical parameters after administering 1.92, 5.76 and 19.20 g/kg of aqueous extract for 13 weeks. At acute doses, no deaths, weight gain or abnormal behavioral changes were observed. The LD<sub>50</sub> value was deduced to be greater than 64 g/kg. At the same time, sub-chronic toxicity demonstrated that there was a significant reduction ( $P < 0.05$ ) in haemoglobin concentration in high dose male rats and a significant decrease ( $P < 0.05$ ) in platelet count, plateletocrit in low dose female rats. The total bilirubin level was also elevated significantly ( $P < 0.05$ ) in all doses received by rats. As for histopathological findings, focal inflammation was observed at the injection site and the severity increased dose-dependently. Other vital organs showed no abnormalities (Wang et al., 2012).

Despite the widespread interest for the use of *Perilla frutescens*, there were only few toxicological studies documenting the toxic potential of *P. frutescens* (Yu et al., 2017). In spite of the diverse medicinal uses of *P. frutescens*, it is actually a medicinal plant with toxic potential, given that certain plant parts contain high concentrations of toxic phytochemicals. According to Kerr et al. (1986), a high concentration of perilla ketone was accumulated in the flowers and seed parts of *P. frutescens*. Perilla ketone has been reported as a potent pulmonary toxin associated with

atypical interstitial pneumonia (Wilson et al., 1977; Guerry-Force et al., 1988; Muller-Waldeck et al., 2010). Furthermore, the toxicological profile of *Mentha arvensis* leaves ethanolic extract was also assessed. The toxic potential of ethanolic leaves extract of *M. arvensis* was tested using brine shrimp cytotoxicity assay. The extracts were serially diluted to concentrations of 1,000, 250, 125, 100 and 75 µg/ml and each extract was added to the tubes containing *Artemia salina*. The number of survivors in each tube was counted after 24 h from the treatment to determine the lethal concentration of ethanolic extract of *M. arvensis* leaves. Result demonstrated that 100 µg/ml as the LD<sub>50</sub> dose caused a significant cytotoxic activity against the brine shrimp, *Artemia salina* (do Nascimento et al., 2009).

## CONCLUSION AND FUTURE PERSPECTIVES

Undeniably, in recent years, there has been an increase in the global demand for natural products for healthcare supplementation. Lamiaceae species have been well known for their culinary values. Nonetheless, they are also a valuable plant family widely employed as medicinal herbs in traditional practices to treat a wide range of allergic inflammatory conditions, such as allergic skin diseases and allergic asthma. Therefore, this plant family may prove to be a diverse source of natural compounds for the development of novel therapeutic agents for allergic disorders. This review conveys deep insights into the botanical features, distribution, medicinal uses, phytochemistry, pharmacology and toxicological investigations conducted, with a particular focus on the anti-allergic activity of Lamiaceae species. A critical analysis of the relationship between phytoconstituents of Lamiaceae species and corresponding anti-allergic activity was done and documented. Currently available *in vitro*, *in vivo* and *ex vivo* studies have provided evidences to support the traditional uses of Lamiaceae species against allergic disorders. Moreover, after a comprehensive summarization, a total of 53 isolated constituents were identified as natural compounds that contribute to anti-allergic effects. In the present review, numerous compounds demonstrated promising anti-allergic activity, such as flavonoids, flavonoid glycosides, diterpenes and phenolics. Some of these constituents were shown to possess comparable anti-allergic activity to the positive control, including carnosic acid (polyphenol), rosmarinic acid, luteolin, oroxylin A, hispidulin and thymol (phenolic), marrubiin (diterpene) and acteoside (phenylpropanoid glycoside). Nevertheless, in the current review, it was found that many studies were conducted using plant extracts. Although the extracts were proven to exhibit anti-allergic effect, the active constituent responsible for the effect is yet to be identified. Therefore, further studies should be carried out on the plant extracts or fractions which exhibited promising experimental results in order to elucidate the exact active principles responsible for anti-allergic activity. With the availability of the information regarding phytochemicals, other studies such as the standardization of extracts and pharmacological studies as well as toxicological investigations of isolated bioactives can be conducted. Meanwhile, the natural compounds that have been

successfully isolated should be further explored and scrutinized for their therapeutic potential to establish a more evidence-based clinical profile. Henceforth, the development of lead molecules for drug discovery can be quicken and accelerated.

## AUTHOR CONTRIBUTIONS

SLY obtained the literatures and wrote the manuscript, while NZAR and KH edited the manuscript.

## REFERENCES

- Actor, J. K. (2014). "The B Lymphocyte and the Humoral Response," in *Introductory Immunology*. Ed. J. K. Actor (Amsterdam: Academic Press).
- Aghakhani, F., and Kharazian, N. (2018). Flavonoid Constituents of *Phlomis* (Lamiaceae) species using liquid chromatography mass spectrometry. *Phytochem. Anal.* 29, 180–195. doi: 10.1002/pca.2733
- Al-Mughales, J. A. (2016). Diagnostic utility of total ige in foods, inhalant, and multiple allergies in Saudi Arabia. *J. Immunol. Res.* 2016, 1–7. doi: 10.1155/2016/1058632
- Alam, G., Wahyuono, S., Ganjar, I. G., Hakim, L., Timmerman, H., and Verpoorte, R. (2002). Tracheospasmodic activity of viteosin-A and vitexicarpin isolated from *Vitex trifolia*. *Planta Med.* 68, 1047–1049. doi: 10.1055/s-2002-35650
- Albano, G. D., Di Sano, C., Bonanno, A., Riccobono, L., and Gagliardo, R. (2013). Th17 immunity in children with allergic asthma and rhinitis: a pharmacological approach. *PLoS One* 8, e58892. doi: 10.1371/journal.pone.0058892
- Asada, M., Sugie, M., Inoue, M., Nakagomi, K., and Hongo, S. (1997). Inhibitory effect of alginic acids on hyaluronidase and on histamine release from mast cells. *Biosci. Biotechnol. Biochem.* 61, 1030–1032. doi: 10.1271/bbb.61.1030
- Asghari, G., Akbari, M., and Asadi-Samani, M. (2017). Phytochemical analysis of some plants from Lamiaceae family frequently used in folk medicine in aligudarz region of lorestan province. *J. Res. Pharm. Pract.* 21, 506. doi: 10.12991/marupj.311815
- Atherton, D. J. (2003). Topical corticosteroids in atopic dermatitis: Recent research reassures that they are safe and effective in the medium term. *BMJ British Med. J.* 327, 942–943. doi: 10.1136/bmj.327.7421.942
- Bae, H., Kim, Y., Lee, E., Park, S., Jung, K. H., Gu, M. J., et al. (2013). Vitex rotundifolia L. prevented airway eosinophilic inflammation and airway remodeling in an ovalbumin-induced asthma mouse model. *Int. Immunol.* 25, 197–205. doi: 10.1093/intimm/dxs102
- Bae, M. J., Shin, H. S., See, H. J., Jung, S. Y., Kwon, D. A., and Shon, D. H. (2016). Baicalein induces CD4<sup>+</sup>Foxp3<sup>+</sup> T cells and enhances intestinal barrier function in a mouse model of food allergy. *Sci. Rep.* 6, 1–11. doi: 10.1038/srep32225
- Berdowska, I., Zieliński, B., Fecka, I., Kulbacka, J., Saczko, J., and Gamian, A. (2013). Cytotoxic impact of phenolics from Lamiaceae species on human breast cancer cells. *Food Chem.* 141, 1313–1321. doi: 10.1016/j.foodchem.2013.03.090
- Berger, A. (2000). Th1 and Th2 responses: what are they? *BMJ* 321, 424. doi: 10.1136/bmj.321.7258.424
- Bhangare, N. K., Pansare, T. A., Ghongane, B. B., and Nesari, T. M. (2012). Screening for anti-inflammatory and anti-allergic activity of *Bharangi* {*Clerodendrum serratum* (Linn.) moon} in animals. *Int. J. Pharma Bio. Sci.* 3, 245–254.
- Blackwell, T. S., and Christman, J. W. (1997). The role of nuclear factor- $\kappa$  b in cytokine gene regulation. *Am. J. Respir. Cell. Mol. Biol.* 17, 3–9. doi: 10.1165/ajrcmb.17.1.f132
- Borges, R. S., Ortiz, B. L. S., Pereira, A. C. M., Keita, H., and Carvalho, J. C. T. (2018). Rosmarinus officinalis essential oil: a review of its phytochemistry, anti-inflammatory activity, and mechanisms of action involved. *J. Ethnopharmacol.* 229, 29–45. doi: 10.1016/j.jep.2018.09.038
- Boskabady, M. H., Mehrjardi, S. S., Rezaee, A., Rafatpanah, H., and Jalali, S. (2013). The impact of *Zataria multiflora* Boiss extract on *in vitro* and *in vivo* Th1/Th2 cytokine (IFN- $\gamma$ /IL4) balance. *J. Ethnopharmacol.* 150, 1024–1031. doi: 10.1016/j.jep.2013.10.003
- Brandão, H. N., Medrado, H. H. S., David, J. P., David, J. M., Pastore, J. F. B., and Meira, M. (2017). Determination of podophyllotoxin and related aryltetralin lignans by HPLC/DAD/MS from lamiaceae species. *Microchem. J.* 130, 179–184. doi: 10.1016/j.microc.2016.09.002
- Cariddi, L. N., Panero, A., Demo, M. S., Sabini, L. I., and Maldonado, A. M. (2007). Inhibition of immediate-type allergic reaction by *minthostachys verticillata* (griseb.) epling essential oil. *J. Essent. Oil Res.* 19, 190–196. doi: 10.1080/10412905.2007.9699257
- Cariddi, L., Escobar, F., Moser, M., Panero, A., and Alaniz, F. (2011). Monoterpenes isolated from *minthostachys verticillata* (Griseb) epling essential oil modulates immediate-type hypersensitivity responses *in vitro* and *in vivo*. *Planta Med.* 77, 1687–1694. doi: 10.1055/s-0030-1271090
- Carović-Stanko, K., Petek, M., Grdiša, M., Pintar, J., Bedeković, D., and Čustić, H. (2016). Medicinal plants of the family Lamiaceae as functional foods – a review. *Czech. J. Food Sci.* 34, 377–390. doi: 10.17221/504/2015-CJFS
- Chatila, T. A., Li, N., Garcia-Lloret, M., Kim, H. J., and Nel, A. E. (2008). T-cell effector pathways in allergic diseases: transcriptional mechanisms and therapeutic targets. *J. Allergy. Clin. Immunol. Pract.* 121, 812–823. doi: 10.1016/j.jaci.2008.02.025
- Chen, M.-L., Wu, C.-H., Hung, L.-S., and Lin, B.-F. (2015). Ethanol extract of *perilla frutescens* suppresses allergen-specific th2 responses and alleviates airway inflammation and hyperreactivity in ovalbumin-sensitized murine model of asthma. *Evid. Based Complementary Altern. Med.* 2015, 8. doi: 10.1155/2015/324265
- Chen, Z., Nihei, K., Tanaka, H., Uda, Y., and Kabuyama, Y. (2013). Identification of a nitric oxide generation-stimulative principle in *scutellariae radix*. *Biosci. Biotechnol. Biochem.* 77, 657–659. doi: 10.1271/bbb.120800
- Choi, H. S., and Kim, K. M. (2004). Tanshinones inhibit mast cell degranulation by interfering with ige receptor-mediated tyrosine phosphorylation of plcgamma2 and mapk. *Planta Med.* 70, 178–180. doi: 10.1055/s-2004-815498
- Choi, J. K., Oh, H. M., Lee, S., Kwon, T. K., Shin, T. Y., Rho, M. C., et al. (2014). Salvia plebeia suppresses atopic dermatitis-like skin lesions. *Am. J. Chin. Med.* 42, 967–985. doi: 10.1142/S0192415X1450061X
- Choi, Y. Y., Kim, M. H., Kim, J. H., Jung, H. S., Sohn, Y., Choi, Y. J., et al. (2013). Schizonepeta tenuifolia inhibits the development of atopic dermatitis in mice. *Phytother. Res.* 27, 1131–1135. doi: 10.1002/ptr.4833
- Choia, H. G., Kim, T. H., Kim, S. H., and Kim, J. A. (2016). Anti-allergic Inflammatory Triterpenoids Isolated from the Spikes of *Prunella vulgaris*. *Nat. Prod. Commun.* 11, 31–32. doi: 10.1177/1934578X1601100111
- Choudhary, G. P. (2010). Mast cell stabilizing activity of *Ocimum sanctum* leaves. *Int. J. Pharma. Bio. Sci.* 1, 1–11.
- Cocan, I., Alexa, E., Danciu, C., Radulov, I., and Galuscan, A. (2018). Phytochemical screening and biological activity of Lamiaceae family plant extracts. *Exp. Ther. Med.* 15, 1863–1870. doi: 10.3892/etm.2017.5640
- Coondoo, A., Phiske, M., Verma, S., and Lahiri, K. (2014). Side-effects of topical steroids: a long overdue revisit. *Indian Dermatol. Online J.* 5, 416–425. doi: 10.4103/2229-5178.142483
- Costa, R. S., Carneiro, T. C., Cerqueira-Lima, A. T., Queiroz, N. V., Alcantara-Neves, N. M., Pontes-De-Carvalho, L. C., et al. (2012). *Ocimum gratissimum* linn. and rosmarinic acid, attenuate eosinophilic airway inflammation in an experimental model of respiratory allergy to *blomia tropicalis*. *Int. Immunopharmacol.* 13, 126–134. doi: 10.1016/j.intimp.2012.03.012
- Cota, B., Bertollo, M., and De Oliveira, D. M. (2012). Anti-allergic potential of herbs and herbal natural products - activities and patents. *Recent Pat. Endocr. Metab. Immune Drug Discov.* 7 (1), 26–56.

## FUNDING

This study was financially supported by Universiti Kebangsaan Malaysia (UKM) under grant number GUP- 2018-138.

## ACKNOWLEDGMENTS

We are grateful to Universiti Kebangsaan Malaysia (UKM) for allowing us to use all its facilities.



- da Silva, L. A. L., Pezzini, B. R., and Soares, L. (2015). Spectrophotometric determination of the total flavonoid content in *Ocimum basilicum* L. (Lamiaceae) leaves. *Pharmacogn. Mag.* 11, 96–101. doi: 10.4103/0973-1296.149721
- Deo, S. S., Mistry, K. J., Kakade, A. M., and Niphadkar, P. V. (2010). Role played by Th2 type cytokines in IgE mediated allergy and asthma. *Lung India* 27, 66–71. doi: 10.4103/0970-2113.63609
- do Nascimento, E. M. M., Rodrigues, F. F. G., Campos, A. R., and Da Costa, J. G. M. (2009). Phytochemical prospection, toxicity and antimicrobial activity of *mentha arvensis* (labiateae) from northeast of Brazil. *J. Young Pharm.* 1, 210–212. doi: 10.4103/0975-1483.57066
- Ekor, M. (2013). The growing use of herbal medicines: issues relating to adverse reactions and challenges in monitoring safety. *Front. Pharmacol.* 4, 177. doi: 10.3389/fphar.2013.00177
- Engler, R. J., With, C. M., Gregory, P. J., and Jellin, J. M. (2009). Complementary and alternative medicine for the allergist-immunologist: where do I start? *J. Allergy. Clin. Immunol. Pract.* 123, 309–316. doi: 10.1016/j.jaci.2009.01.001
- Fachini-Queiroz, F. C., Kummer, R., Estevão-Silva, C. F., Carvalho, M. D. D. B., and Cunha, J. M. (2012). Grespan, R. et al. (2012). Effects of thymol and carvacrol, constituents of thymus vulgaris L. essential oil, on the inflammatory response. *Evid. Based Complementary Altern. Med.: eCAM.* 2012, 657026–657026. doi: 10.1155/2012/657026
- Flaherty, D. K. (2012). "Chapter 9 - Antibodies," in *Immunology for Pharmacy* (Saint Louis: Mosby).
- Fukuishi, N., Murakami, S., Ohno, A., Yamanaka, N., Matsui, N., Fukutsuji, K., et al. (2014). Does  $\beta$ -hexosaminidase function only as a degranulation indicator in mast cells? the primary role of  $\beta$ -hexosaminidase in mast cell granules. *Journal. Immunol.* 193, 1886–1894. doi: 10.4049/jimmunol.1302520
- Fukushima, C., Matsuse, H., Tomari, S., Obase, Y., Miyazaki, Y., Shimoda, T., et al. (2003). Oral candidiasis associated with inhaled corticosteroid use: comparison of fluticasone and beclomethasone. *Ann. Allergy Asthma Immunol.* 90, 646–651. doi: 10.1016/S1081-1206(10)61870-4
- Fulkerson, P. C., and Rothenberg, M. E. (2013). Targeting eosinophils in allergy, inflammation and beyond. *Nat. Rev. Drug. Discov.* 12, 117–129. doi: 10.1038/nrd3838
- Furukawa, M., Suzuki, H., Makino, M., Ogawa, S., Iida, T., and Fujimoto, Y. (2011). Studies on the constituents of *lagochilus leiocanthus* (Labiatae). *Chem. Pharm. Bull.* 59, 1535–1540. doi: 10.1248/cpb.59.1535
- Galli, S. J., Tsai, M., and Piliponsky, A. M. (2008). The development of allergic inflammation. *Nature* 454, 445–454. doi: 10.1038/nature07204
- Gholijani, N., and Amirghofran, Z. (2016). Effects of thymol and carvacrol on T-helper cell subset cytokines and their main transcription factors in ovalbumin-immunized mice. *J. Immunotoxicol.* 13, 729–737. doi: 10.3109/1547691X.2016.1173134
- Gould, H. J., and Beavil, R. L. (1998). "IgE," in *Encyclopedia of Immunology*, 2nd ed. Ed. P. J. Delves (Oxford: Elsevier). doi: 10.1006/rwei.1999.0312
- Guerry-Force, M. L., Coggeshall, J., Snapper, J., and Meyrick, B. (1988). Morphology of noncardiogenic pulmonary edema induced by *Perilla* ketone in sheep. *Am. J. Pathol.* 133, 285–297.
- Han, S., Sun, L., He, F., and Che, H. (2017). Anti-allergic activity of glycyrrhizic acid on IgE-mediated allergic reaction by regulation of allergy-related immune cells. *Sci Rep.* 7, 7222. doi: 10.1038/s41598-017-07833-1
- Haq, R. U., Shah, A. U., Khan, A. U., Ullah, Z., Khan, H. U., Khan, R. A., et al. (2012). Antitussive and toxicological evaluation of *Vitex negundo*. *Nat. Prod. Res.* 26, 484–488. doi: 10.1080/14786419.2010.534472
- Harley, R. M., Atkins, S., Budantsev, A. L., Cantino, P. D., Conn, B. J., Grayer, R. et al., (2004). "The Families and Genera of Vascular Plants," in *Labiatae*. Ed. K. Kubitzki (Berlin, Heidelberg, New York: Springer-Verlag).
- Hazekamp, A., Verpoorte, R., and Panthong, A. (2001). Isolation of a bronchodilator flavonoid from the Thai medicinal plant *clerodendrum petasites*. *J. Ethnopharmacol.* 78, 45–49. doi: 10.1016/S0378-8741(01)00320-8
- He, S., Peng, Q., and Walls, A. F. (1997). Potent induction of a neutrophil and eosinophil-rich infiltrate *in vivo* by human mast cell tryptase: selective enhancement of eosinophil recruitment by histamine. *J. Immunol. Res.* 159, 6216–6225.
- He, J. J., Chen, H. M., Li, C. W., Wu, D. W., Wu, X. L., Shi, S. J., et al. (2013). Experimental study on antinociceptive and anti-allergy effects of patchouli oil. *J. Essent. Oil Res.* 25, 488–496. doi: 10.1080/10412905.2013.809319
- Heo, J. C., Nam, D. Y., Seo, M. S., and Lee, S. H. (2011). Alleviation of atopic dermatitis-related symptoms by *perilla frutescens* Britton. *Int. J. Mol. Med.* 28, 733–737. doi: 10.3892/ijmm.2011.763
- Hong, S. S., Lee, C., Lee, C. H., Park, M., Lee, M. S., Hong, J. T., et al. (2009). A new furofuran lignan from *Isodon japonicus*. *Arch. Pharm. Res.* 32, 501–504. doi: 10.1007/s12272-009-1404-x
- Huang, L., Pi, J., Wu, J., Zhou, H., Cai, J., Li, T., et al. (2016). A rapid and sensitive assay based on particle analysis for cell degranulation detection in basophils and mast cells. *Pharmacol. Res.* 111, 374–383. doi: 10.1016/j.phrs.2016.05.033
- Hwang, S. H., Kim, S. B., Jang, S. P., Wang, Z., Suh, H. W., and Lim, S. S. (2018). Anti-nociceptive effect and standardization from mixture of *agrimonia pilosa* Ledeb and *Salvia miltiorrhiza* Bunge extracts. *J. Med. Food* 21, 596–604. doi: 10.1089/jmf.2017.4077
- Ikawati, Z., Wahyuno, S., and Maeyama, K. (2001). Screening of several Indonesian medicinal plants for their inhibitory effect on histamine release from RBL-2H3 cells. *J. Ethnopharmacol.* 75, 249–256. doi: 10.1016/S0378-8741(01)00201-X
- Inoue, T., Sugimoto, Y., Masuda, H., and Kamei, C. (2001). Effects of peppermint (*Mentha piperita* L.) extracts on experimental allergic rhinitis in rats. *Biol. Pharm. Bull.* 24, 92–95. doi: 10.1248/bpb.24.92
- Inoue, T., Sugimoto, Y., Masuda, H., and Kamei, C. (2002). Antiallergic effect of flavonoid glycosides obtained from *Mentha piperita* L. *Biol. Pharm. Bull.* 25, 256–259. doi: 10.1248/bpb.25.256
- Ippoushi, K., Yamaguchi, Y., Itou, H., Azuma, K., and Higashio, H. (2000). Evaluation of inhibitory effects of vegetables and herbs on hyaluronidase and identification of rosmarinic acid as a hyaluronidase inhibitor in lemon balm (*Melissa officinalis* L.). *Food Sci. Technol. Res.* 6, 74–77. doi: 10.3136/fstr.6.74
- Jeon, I. H., Kim, H. S., Kang, H. J., Lee, H. S., Jeong, S. I., Kim, S. J., et al. (2014). Anti-inflammatory and antipruritic effects of luteolin from *Perilla* (*P. frutescens* L.) leaves. *Molecules* 19, 6941–6951. doi: 10.3390/molecules19066941
- Jung, H. S., Kim, M. H., Gwak, N. G., Im, Y. S., Lee, K. Y., Sohn, Y., et al. (2012). Antiallergic effects of *Scutellaria baicalensis* on inflammation *in vivo* and *in vitro*. *J. Ethnopharmacol.* 141, 345–349. doi: 10.1016/j.jep.2012.02.044
- Jung, S. Y., Lee, S. Y., Choi, D. W., See, H. J., Kwon, D. A., Do, J. R., et al. (2017). Skullcap (*scutellaria baicalensis*) hexane fraction inhibits the permeation of ovalbumin and regulates Th1/2 immune responses. *Nutrients* 9, 1–12. doi: 10.3390/nu9111184
- Jutel, M., Akdis, M., and Akdis, C. A. (2009). Histamine, histamine receptors and their role in immune pathology. *Clin. Exp. Allergy* 39, 1786–1800. doi: 10.1111/j.1365-2222.2009.03374.x
- Kala, C. P. (2005). Ethnomedicinal botany of the Apatani in the Eastern Himalayan region of India. *J. Ethnobiol. Ethnomed.* 1, 11. doi: 10.1186/1746-4269-1-11
- Kallinich, T., Beier, K. C., Wahn, U., Stock, P., and Hamelmann, E. (2007). T-cell co-stimulatory molecules: their role in allergic immune reactions. *Eur. Respir. J.* 29, 1246. doi: 10.1183/09031936.00094306
- Kamei, R., Fujimura, T., Matsuda, M., Kakiyama, K., Hirakawa, N., Baba, K., et al. (2017). A flavanone derivative from the Asian medicinal herb (*Perilla frutescens*) potentially suppresses IgE-mediated immediate hypersensitivity reactions. *Biochem. Biophys. Res. Commun.* 483, 674–679. doi: 10.1016/j.bbrc.2016.12.083
- Kanjarawati, R., Dy, M., Bardel, E., Sparwasser, T., Dubois, B., Mecheri, S., et al. (2013). Regulatory CD4+Foxp3+ T cells control the severity of anaphylaxis. *PLoS One* 8, e69183. doi: 10.1371/journal.pone.0069183
- Karousou, R., Balta, M., Hanlidou, E., and Kokkini, S. (2007). "Mints," smells and traditional uses in Thessaloniki (Greece) and other Mediterranean countries. *J. Ethnopharmacol.* 109, 248–257. doi: 10.1016/j.jep.2006.07.022
- Katiyar, C., Gupta, A., Kanjilal, S., and Katiyar, S. (2012). Drug discovery from plant sources: an integrated approach. *Int. J. Ayurveda. Res.* 33, 10–19. doi: 10.4103/0974-8520.100295
- Kaur, M., Singh, V., and Shri, R. (2018). Evaluation of mast cell stabilizing activity of *Camellia sinensis* and *Ocimum basilicum* and correlation with their antioxidant property. *Pharma. Innovation.* 7, 69–73.
- Kerr, L. A., Johnson, B. J., and Burrows, G. E. (1986). Intoxication of cattle by *Perilla frutescens* (purple mint). *Vet. Hum. Toxicol.* 28, 412–416.
- Khaled-Khodja, N., Boulekbache-Makhlouf, L., and Madani, K. (2014). Phytochemical screening of antioxidant and antibacterial activities of methanolic extracts of some Lamiaceae. *Ind. Crops. Prod.* 61, 41–48. doi: 10.1016/j.indcrop.2014.06.037



- Khan, S., and Khatoon, S. (2007). Ethnobotanical studies on some useful herbs of haramosh and bugrote valleys in gilgit, Northern areas of Pakistan. *Pak. J. Bot.* 40, 43–58.
- Khoury, M., Stien, D., Eparvier, V., Ouaini, N., and El Beyrouthy, M. (2016). Report on the medicinal use of eleven lamiaceae species in lebanon and rationalization of their antimicrobial potential by examination of the chemical composition and antimicrobial activity of their essential oils. *Evid. Based Complementary Altern. Med.: eCAM.* 2016, 2547169. doi: 10.1155/2016/2547169
- Kianmehr, M., Haghmorad, D., Nosratabadi, R., Rezaei, A., Alavinezhad, A., and Boskabady, M. H. (2017). The effect of zataria multiflora on th1/th2 and th17/t regulatory in a mouse model of allergic asthma. *Front. Pharmacol.* 8, 458. doi: 10.3389/fphar.2017.00458
- Kim, S. H., and Shin, T. Y. (2006). Effect of dracocephalum argunense on mast-cell-mediated hypersensitivity. *Int. Arch. Allergy Immunol.* 139, 87–95. doi: 10.1159/000090383
- Kim, H. H., Yoo, J. S., Shin, T. Y., and Kim, S. H. (2012). Aqueous extract of Mosla chinensis inhibits mast cell-mediated allergic inflammation. *American. J. Chin. Med.* 40, 1257–1270. doi: 10.1142/S0192415X12500930
- Kim, T. W., Choi, J. M., Kim, M. S., Son, H. Y., and Lim, J. H. (2016). Topical application of Scutellaria baicalensis suppresses 2,4-dinitrochlorobenzene-induced contact dermatitis. *Nat. Prod. Res.* 30, 705–709. doi: 10.1080/14786419.2015.1038812
- Kim, H. H., Yoo, J. S., Lee, H. S., Kwon, T. K., Shin, T. Y., and Kim, S. H. (2011). Elsholtzia ciliata inhibits mast cell-mediated allergic inflammation: role of calcium, p38 mitogen-activated protein kinase and nuclear factor- $\kappa$ B. *Exp. Biol. Med.* 236, 1070–1077. doi: 10.1258/ebm.2011.011017
- Kim, D. S., Son, E. J., Kim, M., Heo, Y. M., Nam, J. B., Ro, J. Y., et al. (2010). Antiallergic herbal composition from scutellaria baicalensis and phyllostachys edulis. *Planta Med.* 76, 678–682. doi: 10.1055/s-0029-1240649
- Kim, S. H., Kim, S. H., Kim, S. H., Moon, J. Y., Park, W. H., Kim, C. H., et al. (2006). Action of dracocephalum argunense on mast cell-mediated allergy model. *Biol. Pharm. Bull.* 29, 494–498. doi: 10.1248/bpb.29.494
- Kim, S. H., Park, S. B., Kang, S. M., Jeon, H., Lim, J. P., Kwon, T. K., et al. (2009). Anti-allergic effects of Teucrium japonicum on mast cell-mediated allergy model. *Food Chem Toxicol.* 47, 398–403. doi: 10.1016/j.fct.2008.11.030
- Kim, S. Y., Choi, Y. G., Kim, S. H., Shin, H. Y., Ahn, M. K., Kim, H. M., et al. (2004). Isodon japonicus inhibits mast cell-mediated immediate-type allergic reactions. *Immunopharmacol. Immunotoxicol.* 26, 273–284. doi: 10.1081/IPH-120037725
- Kim, S. Y., Kim, S. H., Shin, H. Y., Lim, J. P., Chae, B. S., Park, J. S., et al. (2007). Effects of prunella vulgaris on mast cell – mediated allergic reaction and inflammatory cytokine production. *Exp. Biol. Med.* 232, 921–926. doi: 10.3181/00379727-232-2320921
- Kim, T. W., Song, I. B., Lee, H. K., Kim, M. S., Ham, S. H., Cho, J. H., et al. (2013). Assessment of dermal safety of scutellaria baicalensis aqueous extract topical application on skin hypersensitivity. *Planta Med.* 79, 959–962. doi: 10.1055/s-0032-1328714
- Koh, D. J., Ahn, H. S., Chung, H. S., Lee, H., Kim, Y., Lee, J. Y., et al. (2011). Inhibitory effects of casticin on migration of eosinophil and expression of chemokines and adhesion molecules in A549 lung epithelial cells via NF- $\kappa$ B inactivation. *J. Ethnopharmacol.* 136, 399–405. doi: 10.1016/j.jep.2011.01.014
- Kokkini, S., Karousou, R., and Hanlidou, E. (2003). “HERBS | Herbs of the Labiatae,” in *Encyclopedia of Food Sciences and Nutrition*, 2nd ed. Ed. B. Caballero (Oxford: Academic Press). doi: 10.1016/B0-12-227055-X/00593-9
- Komatsu, K., Takanari, J., Maeda, T., Kitadate, K., Sato, T., Mihara, Y., et al. (2016). Perilla leaf extract prevents atopic dermatitis induced by an extract of Dermatophagoides farinae in NC/Nga mice. *Asian Pac. J. Allergy Immunol.* 34, 272–277. doi: 10.12932/AP0717
- Kuehn, H. S., Radinger, M., and Gilfillan, A. M. (2010). Measuring mast cell mediator release. *Curr. Protoc. Immunol.* 91, 7.38.1–7.38.9. CHAPTER 7, Unit7.38. doi: 10.1002/0471142735.im0738s91
- Lee, D. H., Kim, S. H., Eun, J. S., and Shin, T. Y. (2006). Mosla dianthera inhibits mast cell-mediated allergic reactions through the inhibition of histamine release and inflammatory cytokine production. *Toxicol. Appl. Pharmacol.* 216, 479–484. doi: 10.1016/j.taap.2006.06.007
- Lee, J. K., Lee, J. A., Seo, C. S., Ha, H., Lee, N., and Shin, H. K. (2011a). Protective effects of mentha haplocalyx ethanol extract (mh) in a mouse model of allergic asthma. *Phytother. Res.* 25, 863–869. doi: 10.1002/ptr.3341
- Lee, J. Y., Lee, J. G., Sim, S. S., Whang, W. K., and Kim, C. J. (2011b). Anti-asthmatic effects of phenylpropanoid glycosides from Clerodendron trichotomum leaves and Rumex gmelini herbes in conscious guinea-pigs challenged with aerosolized ovalbumin. *Phytomedicine* 18, 134–142. doi: 10.1016/j.phymed.2010.06.014
- Lee, H., Han, A. R., Kim, Y., Choi, S. H., Ko, E., Lee, N. Y., et al. (2009). A new compound, 1H,8H-pyrano[3,4-c]pyran-1,8-dione, suppresses airway epithelial cell inflammatory responses in a murine model of asthma. *Int. J. Immunopathol. Pharmacol.* 22, 591–603. doi: 10.1177/039463200902200305
- Li, X., Wang, J., Shi, H., Gao, L., and Wang, X. (2014). Inhibition of three novel Radix Scutellariae extracts on immediate hypersensitivity. *Afr. J. Tradit. Complement. Altern. Med.* 11, 54–60. doi: 10.4314/ajtcam.v11i5.9
- Li, M., Li, Q., Zhang, C., Zhang, N., Cui, Z., Huang, L., et al. (2013). An ethnopharmacological investigation of medicinal Salvia plants (Lamiaceae) in China. *Acta. Pharm. Sin.* B. 3, 273–280. doi: 10.1016/j.apsb.2013.06.001
- Li, S., Long, C., Liu, F., Lee, S., Guo, Q., Li, R., et al. (2006). Herbs for medicinal baths among the traditional Yao communities of China. *J. Ethnopharmacol.* 108, 59–67. doi: 10.1016/j.jep.2006.04.014
- Li, X., Yang, J. H., Jin, Y., Jin, F., Kim, D. Y., Chang, J. H., et al. (2015). 15,16-Dihydrotanshinone I suppresses IgE-Ag stimulated mouse bone marrow-derived mast cell activation by inhibiting Syk kinase. *J. Ethnopharmacol.* 169, 138–144. doi: 10.1016/j.jep.2015.04.022
- Lim, B. O. (2002). Effect of ganhuangenin obtained from scutellaria radix on the chemical mediator production of peritoneal exudate cells and immunoglobulin e level of mesenteric lymph node lymphocytes in sprague-dawley rats. *Phytother. Res.* 16, 166–170. doi: 10.1002/ptr.1034
- Lim, B. O. (2003). Effects of wogonin, wogonoside, and 3,5,7,2',6'-pentahydroxyflavone on chemical mediator production in peritoneal exudate cells and immunoglobulin E of rat mesenteric lymph node lymphocytes. *J. Ethnopharmacol.* 84, 23–29. doi: 10.1016/S0378-8741(02)00257-X
- Lim, B. O., Choue, R. W., Lee, H. Y., Seong, N. S., and Kim, J. D. (2003). Effect of the flavonoid components obtained from Scutellaria radix on the histamine, immunoglobulin E and lipid peroxidation of spleen lymphocytes of Sprague-Dawley rats. *Biosci. Biotechnol. Biochem.* 67, 1126–1129. doi: 10.1271/bbb.67.1126
- Lin, Y.-H., Chen, H.-Y., Chiu, J.-C., Chen, K.-J., Ho, H.-Y., and Yang, S.-H. (2018). Immunomodulation effects of schizonepeta tenuifolia briq. on the IgE-induced allergic model of RBL-2H3 cells. *Evid. Based Complementary Altern. Med.* 2018, 7. doi: 10.1155/2018/6514705
- Liu, J. Y., Chen, Y. C., Lin, C. H., and Kao, S. H. (2013). Perilla frutescens leaf extract inhibits mite major allergen Der p 2-induced gene expression of pro-allergic and pro-inflammatory cytokines in human bronchial epithelial cell BEAS-2B. *PLoS One.* 8, e77458. doi: 10.1371/journal.pone.0077458
- Makino, T., Furuta, Y., Fujii, H., Nakagawa, T., and Wakushima, H. (2001). Effect of oral treatment of perilla frutescens and its constituents on type-i allergy in mice. *Biol. Pharm. Bull.* 24, 1206–1209. doi: 10.1248/bpb.24.1206
- Makino, T., Furuta, Y., Wakushima, H., Fujii, H., Saito, K., and Kano, Y. (2003). Anti-allergic effect of Perilla frutescens and its active constituents. *Phytother. Res.* 17, 240–243. doi: 10.1002/ptr.1115
- Malik, F., Hussain, S., Sadiq, A., Parveen, G., Wajid, A., Shafat, S., et al. (2003). Phyto-chemical analysis, anti-allergic and anti-inflammatory activity of Mentha arvensis in animals. *Afr. J. Pharm. Pharmacol.* 6 (9), 613–619. ISSN 1996-0816 © 2012 Academic Journals. doi: 10.5897/AJPP11.702
- Mamadaliyeva, N. Z., Akramov, D. K., Ovidi, E., Tiezzi, A., Nahar, L., Azimova, S. S., et al. (2017). Aromatic medicinal plants of the lamiaceae family from uzbekistan: ethnopharmacology, essential oils composition, and biological activities. *Medicines* 4, 8. doi: 10.3390/medicines4010008
- Meng, J., Moriyama, M., Feld, M., Buddenkotte, J., Buhl, T., Szöllösi, A., et al. (2018). New mechanism underlying IL-31 – induced atopic dermatitis. *J. Allergy. Clin. Immunol. Pract.* 141, 1677–1689. doi: 10.1016/j.jaci.2017.12.1002
- Mizushima, Y., Onodera, T., Kuriyama, I., Nakayama, H., Sugimoto, K., and Lee, E. (2014). Screening of mammalian DNA polymerase inhibitors from rosemary leaves and analysis of the anti-inflammatory and antiallergic effects of the isolated compounds. *Food Sci. Technol. Res.* 20, 829–840. doi: 10.3136/fstr.20.829
- Muller-Waldeck, F., Sitzmann, J., Schnitzler, W. H., and Grassmann, J. (2010). Determination of toxic perilla ketone, secondary plant metabolites and antioxidative capacity in five Perilla frutescens L. varieties. *Food Chem. Toxicol.* 48, 264–270. doi: 10.1016/j.fct.2009.10.009

- Murata, T., Watahiki, M., Tanaka, Y., Miyase, T., and Yoshizaki, F. (2010). Hyaluronidase inhibitors from *Takuran*, *Lycopus lucidus*. *Chem. Pharm. Bull.* 58, 394–397. doi: 10.1248/cpb.58.394
- Naghibi, F., Mosaddegh, M., Mohammadi Motamed, M., and Ghorbani, A. (2010). Labiatae family in folk medicine in Iran: from ethnobotany to pharmacology. *Iran J. Pharm. Res.* 4, 63–79. doi: 10.22037/IJPR.2010.619
- Nguyen, H. T., Tran, L. T. T., Ho, D. V., Le, D. V., Raal, A., and Morita, H. (2018). Pogostemins A-C, three new cytotoxic meroterpenoids from *Pogostemon auricularius*. *Fitoterapia* 130, 100–104. doi: 10.1016/j.fitote.2018.08.015
- Noval Rivas, M., and Chatila, T. A. (2016). Regulatory T cells in allergic diseases. *J. Allergy. Clin. Immunol. Pract.* 138, 639–652. doi: 10.1016/j.jaci.2016.06.003
- Oboki, K., Ohno, T., Saito, H., and Nakae, S. (2008). Th17 and allergy. *Allergol. Int.* 57, 121–134. doi: 10.2332/allergolint.R-07-160
- Oka, T., Hori, M., and Ozaki, H. (2005). Microtubule disruption suppresses allergic response through the inhibition of calcium influx in the mast cell degranulation pathway. *J. Immunol.* 174, 4584. doi: 10.4049/jimmunol.174.8.4584
- Ozdemir, C., Akdis, M., and Akdis, C. A. (2010). T-cell response to allergens. *Chem. Immunol. Allergy* 95, 22–44. doi: 10.1159/000315936
- Palomares, O., Yaman, G., Azkur, A. K., Akkoc, T., Akdis, M., and Akdis, C. A. (2010). Role of Treg in immune regulation of allergic diseases. *Eur. J. Immunol.* 40, 1232–1240. doi: 10.1002/eji.200940045
- Parikh, S. A., Cho, S. H., and Oh, C. K. (2003). Preformed enzymes in mast cell granules and their potential role in allergic rhinitis. *Curr. Allergy Asthma Rep.* 3, 266–272. doi: 10.1007/s11882-003-0049-y
- Park, S. B., Kim, S. H., Suk, K., Lee, H. S., Kwon, T. K., Ju, M. G., et al. (2010). Clinopodium gracile inhibits mast cell-mediated allergic inflammation: involvement of calcium and nuclear factor- $\kappa$ B. *Exp. Biol. Med.* 235, 606–613. doi: 10.1258/ebm.2010.009292
- Patel, J. I., and Deshpande, S. S. (2011). Mast cell stabilising activity of various subfractions of leaves of vitex negundo. *Int. J. Green Pharm.* 5, 273–275. doi: 10.4103/0973-8258.94346
- Patel, J. I., and Deshpande, S. S. (2013). Antieosinophilic activity of various subfractions of leaves of Vitex negundo. *Int. J. Nutr. Pharmacol. Neurol. Dis.* 3, 135–141. doi: 10.4103/2231-0738.112839
- Pawankar, R. (2014). Allergic diseases and asthma: a global public health concern and a call to action. *World Allergy Organ. J.* 7, 1–3. doi: 10.1186/1939-4551-7-12
- Politeo, O., Bektasevic, M., Carev, I., Jurin, M., and Roje, M. (2018). Phytochemical Composition, antioxidant potential and cholinesterase inhibition potential of extracts from mentha pulegium L. *Chem. Biodivers.* 15 (12), 1–25. doi: 10.1002/cbdv.201800374
- Qi, Q., Peng, J., Liu, W., You, Q., Yang, Y., Lu, N., et al. (2009). Toxicological studies of wogonin in experimental animals. *Phytother. Res.* 23, 417–422. doi: 10.1002/ptr.2645
- Ramasubramania Raja, R. (2012). Medicinally potential plants of labiatae (Lamiaceae) family: an overview. *J. Med. Plant Res.* 6, 203–213. doi: 10.3923/rjmp.2012.203.213
- Rigat, M., Vallès, J., D'Ambrosio, U., Gras, A., Iglésias, J., and Garnatje, T. (2015). Plants with topical uses in the ripollès district (pyrenees, catalonia, iberian peninsula): ethnobotanical survey and pharmacological validation in the literature. *J. Ethnopharmacol.* 164, 162–179. doi: 10.1016/j.jep.2015.01.055
- Rigoni, A., Colombo, M. P., and Pucillo, C. (2018). Mast cells, basophils and eosinophils: from allergy to cancer. *Semin. Immunol.* 35, 29–34. doi: 10.1016/j.smim.2018.02.001
- Robert Webb, D. (1981). Steroids in allergic disease. *Med. Clin. North Am.* 65, 1073–1081. doi: 10.1016/S0025-7125(16)31490-0
- Romagnani, S. (2004). Immunologic influences on allergy and the TH1/TH2 balance. *J. Allergy. Clin. Immunol. Pract.* 113, 395–400. doi: 10.1016/j.jaci.2003.11.025
- Rudensky, A. Y. (2011). Regulatory T cells and Foxp3. *Immunol. Rev.* 241, 260–268. doi: 10.1111/j.1600-065X.2011.01018.x
- Ryu, S. Y., Oak, M. H., and Kim, K. M. (1999). Inhibition of mast cell degranulation by tanshinones from the roots of salvia miltiorrhiza. *Planta Med.* 65, 654–655. doi: 10.1055/s-2006-960839
- Ryu, S. Y., Oak, M. H., Yoon, S. K., Cho, D. I., Yoo, G. S., Kim, T. S., et al. (2000). Anti-allergic and anti-inflammatory triterpenes from the herb of prunella vulgaris. *Planta Med.* 66, 358–360. doi: 10.1055/s-2000-8531
- Sajjadi, S. E., Delazari, Z., Aghaei, M., and Ghannadian, M. (2018). Flavone constituents of *Phlomis bruguieri* Desf. with cytotoxic activity against MCF-7 breast cancer cells. *Res. Pharm. Sci.* 13, 422–429. doi: 10.4103/1735-5362.236835
- Sakamoto, K., Nagai, H., and Koda, A. (1980). Role of hyaluronidase in immediate hypersensitivity reaction. *Immunopharmacology.* 2, 139–146. doi: 10.1016/0162-3109(80)90006-5
- Sanbongi, C., Takano, H., Osakabe, N., Sasa, N., and Natsume, M. (2004). Yanagisawa, R. et al. Rosmarinic acid in perilla extract inhibits allergic inflammation induced by mite allergen, in a mouse model. *Clin. Exp. Allergy* 34, 971–977. doi: 10.1111/j.1365-2222.2004.01979.x
- Sato, A., and Tamura, H. (2015). High antiallergic activity of 5,6,4'-trihydroxy-7,8,3'-trimethoxyflavone and 5,6-dihydroxy-7,8,3,4'-tetramethoxyflavone from eau de cologne mint (*Mentha x piperita citrata*). *Fitoterapia* 102, 74–83. doi: 10.1016/j.fitote.2015.02.003
- Schuster, B. G. (2001). A new integrated program for natural product development and the value of an ethnomedical approach. *J. Altern. Complement. Med.* 7 Suppl 1, S61–72. doi: 10.1089/107555301753393823
- Shah, S. M. M., Sadiq, A., Shah, S. M. H., and Khan, S. (2014). Extraction of saponins and toxicological profile of *Teucrium stocksianum* boiss extracts collected from District Swat, Pakistan. *Biol. Res.* 47, 65–69. doi: 10.1186/0717-6287-47-65
- Sharma, S., Rasal, V. P., Patil, P. A., and Joshi, R. K. (2018). *Mentha arvensis* essential oil suppressed airway changes induced by histamine and ovalbumin in experimental animals. *Nat. Prod. Res.* 32, 468–472. doi: 10.1080/14786419.2017.1311891
- Shin, T. Y. (2003). Inhibition of immunologic and nonimmunologic stimulation-mediated anaphylactic reactions by the aqueous extract of *Mentha arvensis*. *Immunopharmacol. Immunotoxicol.* 25, 273–283. doi: 10.1081/IPH-120020475
- Shin, T. Y. (2004). *Stachys riederi* inhibits mast cell-mediated acute and chronic allergic reactions. *Immunopharmacol. Immunotoxicol.* 26, 621–630. doi: 10.1081/IPH-200042365
- Shin, T. Y., and Kim, H. M. (2002). Inhibition of immediate-type allergic reactions by the aqueous extract of *Salvia plebeia*. *Immunopharmacol. Immunotoxicol.* 24, 303–314. doi: 10.1081/IPH-120003763
- Shin, T. Y., and Lee, J. K. (2003). Effect of *phlomis umbrosa* root on mast cell-dependent immediate-type allergic reactions by anal therapy. *Immunopharmacol. Immunotoxicol.* 25, 73–85. doi: 10.1081/IPH-120018285
- Shin, T. Y., Kim, Y. K., and Kim, H. M. (2001). Inhibition of immediate-type allergic reactions by *Prunella vulgaris* in a murine model. *Immunopharmacol. Immunotoxicol.* 23, 423–435. doi: 10.1081/IPH-100107341
- Shin, H. S., Bae, M. J., Choi, D. W., and Shon, D. H. (2014a). Skullcap (*scutellaria baicalensis*) extract and its active compound, wogonin, inhibit ovalbumin-induced th2-mediated response. *Molecules* 19, 2536–2545. doi: 10.3390/molecules19022536
- Shin, H. S., Bae, M. J., Jung, S. Y., and Shon, D. H. (2014b). Preventive effects of skullcap (*Scutellaria baicalensis*) extract in a mouse model of food allergy. *J. Ethnopharmacol.* 153, 667–673. doi: 10.1016/j.jep.2014.03.018
- Shin, T. Y., Kim, S. H., Kim, D. K., Leem, K. H., and Park, J. S. (2008). *Phlomis umbrosa* root inhibits mast cell-dependent allergic reactions and inflammatory cytokine secretion. *Phytother. Res.* 22, 153–158. doi: 10.1002/ptr.2164
- Shin, T. Y., Kim, S. H., Choi, C. H., Shin, H. Y., and Kim, H. M. (2004). *Isodon japonicus* decreases immediate-type allergic reaction and tumor necrosis factor- $\alpha$  production. *Int. Arch. Allergy Immunol.* 135, 17–23. doi: 10.1159/000080038
- Shin, T. Y., Jeong, H. J., Jun, S. M., Chae, H. J., Kim, H. R., Baek, S. H., et al. (1999). Effect of *Schizonepeta tenuifolia* extract on mast cell-mediated immediate-type hypersensitivity in rats. *Immunopharmacol. Immunotoxicol.* 21, 705–715. doi: 10.3109/08923979909007136
- Shin, T. Y., Kim, S. H., Kim, S. H., Kim, Y. K., Park, H. J., Chae, B. S., et al. (2000). Inhibitory effect of mast cell-mediated immediate-type allergic reactions in rats by *Perilla frutescens*. *Immunopharmacol. Immunotoxicol.* 22, 489–500. doi: 10.3109/08923970009026007
- Shin, T. Y., Kim, S. H., Suk, K., Ha, J. H., Kim, I., Lee, M. G., et al. (2005). Anti-allergic effects of *Lycopus lucidus* on mast cell-mediated allergy model. *Toxicol. Appl. Pharmacol.* 209, 255–262. doi: 10.1016/j.taap.2005.04.011
- Simon, F. E. R., and Simons, K. J. (2008). H(1)Antihistamines: current status and future directions. *World Allergy Organ. J.* 1, 145–155. doi: 10.1186/1939-4551-1-9-145

- Singh, K. K. (1997). Studies on Native Medicine of Jaunsari Tribe of Dehradun District, Uttar Pradesh, India. *Int. J. Pharmacogn.* 35, 105–110. doi: 10.1076/phbi.35.2.105.13289
- Singh, S., and Agrawal, S. S. (1991). Anti-asthmatic and anti-inflammatory activity of ocimum sanctum. *Int. J. Pharmacogn.* 29, 306–310. doi: 10.3109/13880209109082904
- Sinhababu, A., and Arpita, B. (2013). documentation of some ethno-medicinal plants of family lamiaceae in bankura district, west bengal, india. *Int. Res. J. Biol. Sci.* 2, 63–65.
- Skendi, A., Irakli, M., and Chatzopoulou, P. (2017). Analysis of phenolic compounds in Greek plants of Lamiaceae family by HPLC. *J. Appl. Res. Med. Aromat. Plants* 6, 62–69. doi: 10.1016/j.jarmap.2017.02.001
- Sridevi, G., Gopkumar, P., Ashok, S., and Shastry, C. S. (2009). Pharmacological basis for antianaphylactic, antihistaminic and mast cell stabilization activity of Ocimum sanctum. *Int. J. Pharmacol.* 7. doi: 10.5580/bc4
- Steinke, J. W., and Borish, L. (2001). Th2 cytokines and asthma. Interleukin-4: its role in the pathogenesis of asthma, and targeting it for asthma treatment with interleukin-4 receptor antagonists. *Respir. Res.* 2, 66–70. doi: 10.1186/rr40
- Stone, K. D., Prussin, C., and Metcalfe, D. D. (2010). IgE, Mast Cells, Basophils, and Eosinophils. *J. Allergy Clin. Immunol. Pract.* 125, S73–S80. doi: 10.1016/j.jaci.2009.11.017
- Stulzer, H. K., Tagliari, M. P., Zampirolo, J. A., Cechinel-Filho, V., and Schlemper, V. (2006). Antioedematogenic effect of marrubiin obtained from Marrubium vulgare. *J. Ethnopharmacol.* 108, 379–384. doi: 10.1016/j.jep.2006.05.023
- Su, C. Y., Ming, Q. L., Rahman, K., Han, T., and Qin, L. P. (2015). Salvia miltiorrhiza: traditional medicinal uses, chemistry, and pharmacology. *Chin. J. Nat. Med.* 13, 163–182. doi: 10.1016/S1875-5364(15)30002-9
- Tiwari, A., Goel, M., Pal, P., and Gohiya, P. (2013). Topical-steroid-induced iatrogenic Cushing syndrome in the pediatric age group: a rare case report. *Indian J. Endocrinol. Metab.* 17, S257–S258. doi: 10.4103/2230-8210.119593
- Trinh, H. T., Chae, S. J., Joh, E. H., Son, K. H., Jeon, S. J., and Kim, D. H. (2010a). Tanshinones isolated from the rhizome of Salvia miltiorrhiza inhibit passive cutaneous anaphylaxis reaction in mice. *J. Ethnopharmacol.* 132, 344–348. doi: 10.1016/j.jep.2010.07.037
- Trinh, H. T., Joh, E. H., Kwak, H. Y., L. B. N., and Kim, D. H. (2010b). Anti-pruritic effect of baicalin and its metabolites, baicalein and oroxylin a, in mice. *Acta Pharmacol. Sin.* 31 (6), 718–724. doi: 10.1038/aps.2010.42
- Ueda, H., Yamazaki, C., and Yamazaki, M. (2002). Luteolin as an anti-inflammatory and anti-allergic constituent of Perilla frutescens. *Biol. Pharm. Bull.* 25, 1197–1202. doi: 10.1248/bpb.25.1197
- Uritu, C. M., Mihai, C. T., Stanciu, G.-D., Dodi, G., Alexa-Stratulat, T. Luca, A. et al. (2018). Medicinal plants of the family lamiaceae in pain therapy: a review. *Pain Res. Manag.* 2018, 44. doi: 10.1155/2018/7801543
- Vadnere, G. P., Somani, R. S., and Singhai, A. K. (2007). Studies on antiasthmatic activity of aqueous extract of clerodendron phlomidis. *Pharmacologyonline* 1, 487–494.
- van der Burg, M., Weemaes, C. M. R., and Cunningham-Rundles, C. (2014). "Chapter 16 - Isotype Defects," in *Stiehm's Immune Deficiencies*. Eds. K. E. Sullivan and E. R. Stiehm (Amsterdam: Academic Press). doi: 10.1016/B978-0-12-405546-9.00016-9
- Wang, H., Provan, J., and Helliwell, K. (2004). Determination of rosmarinic acid and caffeic acid in aromatic herbs by HPLC. *Food Chem.* 87, 307–311. doi: 10.1016/j.foodchem.2003.12.029
- Wang, J., Li, F. S., Pang, N. N., Tian, G., Jiang, M., Zhang, H. P., et al. (2016). Inhibition of asthma in ova sensitized mice model by a traditional uyghur herb nepeta bracteata benth. *Evid. Based Complementary Altern. Med.* 2016, 8. doi: 10.1155/2016/5769897
- Wang, M., Liu, J., Zhou, B., Xu, R., Tao, L., Ji, M., et al. (2012). Acute and sub-chronic toxicity studies of Danshen injection in Sprague-Dawley rats. *J. Ethnopharmacol.* 141, 96–103. doi: 10.1016/j.jep.2012.02.005
- Wen, T., and Rothenberg, M. E. (2016). The Regulatory Function of Eosinophils. *Microbiol. Spectr.* 4, 1–12. doi: 10.1128/microbiolspec.MCHD-0020-2015
- White, M. V. (1990). The role of histamine in allergic diseases. *J. Allergy. Clin. Immunol. Pract.* 86, 599–605. doi: 10.1016/S0091-6749(05)80223-4
- Will, M., and Claßen-Bockhoff, R. (2014). Why Africa matters: evolution of Old World Salvia (Lamiaceae) in Africa. *Ann. Bot.* 114, 61–83. doi: 10.1093/aob/mcu081
- Wilson, B. J., Garst, J. E., Linnabary, R. D., and Channell, R. B. (1977). Perilla ketone: a potent lung toxin from the mint plant, Perilla frutescens Britton. *Science* 197, 573–574. doi: 10.1126/science.877573
- Woodfolk, J. A. (2007). T-cell responses to allergens. *J. Allergy. Clin. Immunol. Pract.* 119, 280–294. doi: 10.1016/j.jaci.2006.11.008
- Xiang, Z., Block, M., Löfman, C., and Nilsson, G. (2001). IgE-mediated mast cell degranulation and recovery monitored by time-lapse photography. *J. Allergy Clin. Immunol. Pract.* 108, 116–121. doi: 10.1067/mai.2001.116124
- Xie, H., and He, S.-H. (2005). Roles of histamine and its receptors in allergic and inflammatory bowel diseases. *World J. Gastroenterol.* 11, 2851–2857. doi: 10.3748/wjg.v11.i19.2851
- Yamamura, S., Ozawa, K., Ohtani, K., Kasai, R., and Yamasaki, K. (1998). Antihistaminic flavones and aliphatic glycosides from Mentha spicata. *Phytochemistry* 48, 131–136. doi: 10.1016/S0031-9422(97)01112-6
- Yang, J. H., Son, K. H., Son, J. K., and Chang, H. W. (2008). Anti-allergic activity of an ethanol extract from Salvia miltiorrhiza. *Arch. Pharm. Res.* 31, 1597–1603. doi: 10.1007/s12272-001-2157-3
- Ye, Q., Qiu, X., Wu, Y., Ban, Y., Ai, H., Huang, B., et al. (2018). Sesquiterpenoids from Vitex pterisantha. *Fitoterapia* 130, 175–179. doi: 10.1016/j.fitote.2018.08.028
- Yoon, S. B., Lee, Y. J., Park, S. K., Kim, H. C., Bae, H., Kim, H. M., et al. (2009). Anti-inflammatory effects of Scutellaria baicalensis water extract on LPS-activated RAW 264.7 macrophages. *J. Ethnopharmacol.* 125, 286–290. doi: 10.1016/j.jep.2009.06.027
- Yoon, S. C., Je, I. G., Cui, X., Park, H. R., Khang, D., Park, J. S., et al. (2016). Anti-allergic and anti-inflammatory effects of aqueous extract of Pogostemon cablin. *Int. J. Mol. Med.* 37, 217–224. doi: 10.3892/ijmm.2015.2401
- Yu, H., Qiu, J.-F., Ma, L.-J., Hu, Y.-J., Li, P., and Wan, J.-B. (2017). Phytochemical and phytopharmacological review of Perilla frutescens L. (Labiatae), a traditional edible-medicinal herb in China. *Food Chem. Toxicol.* 108, 375–391. doi: 10.1016/j.fct.2016.11.023
- Zhang, H., Kong, H., Zeng, X., Guo, L., Sun, X., and He, S. (2014). Subsets of regulatory T cells and their roles in allergy. *J. Transl. Med.* 12, 125. doi: 10.1186/1479-5876-12-125
- Zhao, Q., Chen, X.-Y., and Martin, C. (2016). Scutellaria baicalensis, the golden herb from the garden of Chinese medicinal plants. *Sci. Bull.* 61, 1391–1398. doi: 10.1007/s11434-016-1136-5
- Zhou, D. G., Diao, B. Z., Zhou, W., and Feng, J. L. (2016). Oroxylin a inhibits allergic airway inflammation in ovalbumin (ova)-induced asthma murine model. *Inflammation* 39, 867–872. doi: 10.1007/s10753-016-0317-3
- Zhou, E., Fu, Y., Wei, Z., Yu, Y., Zhang, X., and Yang, Z. (2014). Thymol attenuates allergic airway inflammation in ovalbumin (OVA)-induced mouse asthma. *Fitoterapia* 96, 131–137. doi: 10.1016/j.fitote.2014.04.016
- Zhu, F., Asada, T., Sato, A., Koi, Y., Nishiwaki, H., and Tamura, H. (2014). Rosmarinic acid extract for antioxidant, antiallergic, and  $\alpha$ -glucosidase inhibitory activities, isolated by supramolecular technique and solvent extraction from perilla leaves. *J. Agric. Food Chem.* 62, 885–892. doi: 10.1021/jf404318j
- Zielińska, S., and Matkowski, A. (2014). Phytochemistry and bioactivity of aromatic and medicinal plants from the genus Asgastache (Lamiaceae). *Phytochem. Rev.* 13, 391–416. doi: 10.1007/s11101-014-9349-1.

**Conflict of Interest Statement:** The authors declare that the research was conducted in the absence of any commercial or financial relationships that could be construed as a potential conflict of interest.

Copyright © 2019 Sim, Abd Rani and Husain. This is an open-access article distributed under the terms of the Creative Commons Attribution License (CC BY). The use, distribution or reproduction in other forums is permitted, provided the original author(s) and the copyright owner(s) are credited and that the original publication in this journal is cited, in accordance with accepted academic practice. No use, distribution or reproduction is permitted which does not comply with these terms.



# Book Review: Medicinal Plants for Holistic Healing

Lyndy J. McGaw<sup>1\*</sup>, Ajay Kumar Srivastava<sup>2</sup>, Chung-Ho Lin<sup>3</sup> and Vanessa Steenkamp<sup>4</sup>

<sup>1</sup> Phytomedicine Programme, Department of Paraclinical Sciences, Faculty of Veterinary Science, University of Pretoria, Pretoria, South Africa, <sup>2</sup> Department of Botany, St Xavier's College, Ranchi, India, <sup>3</sup> Phytochemistry and Bioremediation, Center for Agroforestry, School of Natural Resources, University of Missouri, Columbia, MO, United States, <sup>4</sup> Department of Pharmacology, Faculty of Health Sciences, University of Pretoria, Pretoria, South Africa

**Keywords:** medicinal plants, cosmeceutics, skin cancer, skin infections, tuberculosis

## A Book Review on

### Medicinal Plants for Holistic Healing

Namrita Lall (London, United Kingdom: Elsevier Academic Press), 2018, 312 pages, ISBN 978-0-12-812475-8

## OPEN ACCESS

### Edited and reviewed by:

Benedict Green,  
United States Department of  
Agriculture, United States

### \*Correspondence:

Lyndy J. McGaw  
lyndy.mcgaw@up.ac.za

### Specialty section:

This article was submitted to  
Ethnopharmacology,  
a section of the journal  
Frontiers in Pharmacology

**Received:** 14 March 2019

**Accepted:** 20 August 2019

**Published:** 18 September 2019

### Citation:

McGaw LJ, Srivastava AK, Lin C-H  
and Steenkamp V (2019) Book  
Review: Medicinal Plants  
for Holistic Healing.  
Front. Pharmacol. 10:1053.  
doi: 10.3389/fphar.2019.01053

It is undeniable that medicinal plants have played, and continue to play, a major role in the lives of people worldwide. This book appropriately opens with a fascinating and concise, though comprehensive, history of traditional medicine and its African heritage, starting approximately 4,000 years ago. The reader is taken on a journey through the use of medicinal plants for specific diseases, which originated from trial and error to the development of modern herbal preparations or drugs with specific treatment targets. The book concludes by focussing on realizing the potential of medicinal plants. In essence, the book comes full circle, portraying global interests and highlighting the importance of medicinal plant usage in health and well-being. The intense pace of today's lifestyle has led to a dramatic rise in the incidence of many ailments, such as cancer, cardiovascular disease, and diabetes. This book mentions several diseases of present and future significance including cancer, tuberculosis, and skin infections and potential plant-based medications against them. All remedies require varying lead times to enable development, and by then, casualties may rise. However, this book has given a useful background and highlighted research opportunities aimed at maximizing the realization of the potential of plants found in South Africa. Such disease threats include various types of skin cancers, hyper-pigmentation, oral disorders (with changing food and eating styles), and many others. This textbook provides a thorough and detailed description of many classes of plant-derived natural products for medical use, particularly regarding nutraceutical and cosmeceutical applications. Functional foods are foods consumed frequently that have potential health benefits, and nutraceuticals refer to products sold over the counter containing phytochemicals putatively enhancing health. The use of these purportedly beneficial foods and supplements is particularly relevant in the field of cancer prevention, as covered in the second chapter of the book. In this chapter, it is noted that substances found in plants may be able to prevent, inhibit, or even reverse formation of cancerous cells. Skin infections, acne, and aging negatively affect confidence, and plants have been used for centuries as natural cosmeceuticals to enhance beauty and combat infections. The interest of international cosmetics enterprises has been stirred by the possibilities in this sphere. An example mentioned in Chapter 3 is the incorporation of *Mesembryanthemum crystallinum* into an antiaging formulation by a renowned cosmetics company.



Edited by a renowned expert in the field, Professor Namrita Lall of the University of Pretoria, the book comprises a collection of chapters on diverse areas of the potential application of medicinal plants. It covers a variety of topics with a major focus comprising the traditional use of medicinal plants and their potential application. The book consists of 10 insightful and well-written chapters supported by neat and appropriate illustrations. The book has a two pronged approach, with holistic health reflecting on healing from the point of view of traditional healers on the one hand and health and well-being directed at practitioners in orthodox medical fields on the other. Traditional healers have a long history of using medicinal plants and trust their effectiveness, while orthodox medical professionals may view the use of plants in medicine with some scepticism in light of the general paucity of scientific data supporting the safety and efficacy of these remedies. Books such as this, combining traditional knowledge of plants with Western scientific methods evaluating their use in accepted model assay systems, will go a long way toward building bridges between the two modes of thinking.

The body of the book comprises thought-provoking and diverse chapters on the potential for utilization of plants in treating diseases of the skin and use of traditional medicine as anticancer, anti-aging, and anti-infective agents. Chapters on oral care, progressive macular hypomelanosis, and tuberculosis are included, with the useful addition of a chapter on garlic and its many uses. Each topic is introduced by providing a background on the disease, which contains updated statistics on the prevalence thereof, followed by the associated pathology, pharmacologically approved drugs currently on the market used for treatment of the disease, an array of medicinal plants used for treatment accompanied with a list of their active phytoconstituents and chemical structures thereof, as well as scientific evidence for use. Additionally, photographic plates of the most commonly used plants are provided, which serve as useful aids in plant identification. For example, a large number of plant species are used for antiaging properties such as *Aloe vera*, *Aspalathus linearis*, and *Populus nigra*, and photographs of these and many other species are provided. Most likely owing to space constraints, the pictures are small, but the plates illustrate the diversity of plants used to treat the targeted conditions.

The book concludes with an extremely useful chapter on maximizing the value of medicinal plants in terms of commercialization. This is an oft-neglected aspect of medicinal plant research highly deserving of increased attention, as much potential value is locked in plants that have been used for centuries for cosmetic or medicinal treatments. Thus, this book contributes toward bridging the gap between the traditional healer and the modern scientist, as consumers are increasingly combining treatments sourced from both traditional and orthodox spheres. It not only calls for an enhanced understanding and appreciation

of medicinal plant usage but also cautions that natural does not imply safe or that no side effects will be experienced, thereby clearly indicating the need for scientific testing to validate efficacy and safety.

Cognisance should be taken of the important role of plants in drug development—they remain sources of treatment that are desperately needed. Emphasis should be placed on integrating the knowledge of traditional healers and verifying activity using modern techniques. The knowledge of traditional healers includes treatment with medicinal plants as well as psychological aspects that cannot be tested in a laboratory. However, scientific techniques involving targeted bioassay screening, synergistic studies, and detailed mechanism of action investigations may go a long way toward assisting with validation of traditional remedies as well as identifying potential future drug leads. Reanalyzing medicinal plants using this perspective could reveal a world of knowledge encompassing valuable potential sources of drugs and hope for future medications for currently incurable diseases.

The work presented in this book will be most advantageous for undergraduate and postgraduate students as well as academic staff researching plants for medicinal and cosmetic purposes in South Africa and indeed the rest of the world. The authors' unbiased approach in guiding the reader through fundamental chemical principles, modes of action, and product formulation of bioactive natural products for medical applications, ranging from treatment and prevention of skin disorders, infections, and aging to dental disease, makes this a useful reference for students and pharmacognosists, pharmacists, medicinal chemists, phytochemists, dermatologists, and cosmetic chemists. The accessible and informative writing style, which is consistent throughout the chapters, also lends itself to being of interest to lay people with a particular interest in medicinal plants and how they work. The writing is pitched at a level to provide the specialist with intriguing information, updated facts and references but will also resonate with the novice who would like to gain more in-depth information on the highlighted topics.

## AUTHOR CONTRIBUTIONS

All authors contributed to writing the book review. LM edited the manuscript and submitted it.

**Conflict of Interest Statement:** The authors declare that the research was conducted in the absence of any commercial or financial relationships that could be construed as a potential conflict of interest.

Copyright © 2019 McGaw, Srivastava, Lin and Steenkamp. This is an open-access article distributed under the terms of the Creative Commons Attribution License (CC BY). The use, distribution or reproduction in other forums is permitted, provided the original author(s) and the copyright owner(s) are credited and that the original publication in this journal is cited, in accordance with accepted academic practice. No use, distribution or reproduction is permitted which does not comply with these terms.



# Topical Application of KAJD Attenuates 2,4-Dinitrochlorobenzene-Induced Atopic Dermatitis Symptoms Through Regulation of IgE and MAPK Pathways in BALB/C Mice and Several Immune Cell Types

Se Hyang Hong<sup>1</sup>, Jin Mo Ku<sup>1</sup>, Hyo In Kim<sup>2</sup>, Tai Young Kim<sup>1</sup>, Hye Sook Seo<sup>1</sup>, Yong Cheol Shin<sup>1</sup> and Seong-Gyu Ko<sup>1\*</sup>

<sup>1</sup> Department of Preventive Medicine, College of Korean Medicine, Kyung Hee University, Seoul, South Korea, <sup>2</sup> Department of Science in Korean Medicine, Graduate School, Kyung Hee University, Seoul, South Korea

## OPEN ACCESS

### Edited by:

Vanessa Steenkamp,  
University of Pretoria, South Africa

### Reviewed by:

Chung-Ho Lin,  
University of Missouri, United States  
Jesper Grønlund Holm,  
Bispebjerg Hospital, Denmark

### \*Correspondence:

Seong-Gyu Ko  
epiko@khu.ac.kr

### Specialty section:

This article was submitted to  
Ethnopharmacology,  
a section of the journal  
Frontiers in Pharmacology

**Received:** 13 February 2019

**Accepted:** 26 August 2019

**Published:** 19 September 2019

### Citation:

Hong SH, Ku JM, Kim HI, Kim TY,  
Seo HS, Shin YC and Ko S-G  
(2019) Topical Application of KAJD  
Attenuates 2,4-Dinitrochlorobenzene-  
Induced Atopic Dermatitis Symptoms  
Through Regulation of IgE and MAPK  
Pathways in BALB/C Mice and  
Several Immune Cell Types.  
Front. Pharmacol. 10:1097.  
doi: 10.3389/fphar.2019.01097

Atopic dermatitis (AD) is a frequent skin complication that is caused by unknown reasons. KHU-ATO-JIN-D (KAJD) is a new drug aimed at AD composed of a mixture of extracts from six plants known to have anti-inflammatory and antiallergic effects. This study investigated whether KAJD alleviates 2,4-dinitrochlorobenzene (DNCB)-induced AD in BALB/c mice and several immune cell types. We applied KAJD to DNBCB-induced AD-like skin lesions in BALB/c mice, phorbol myristate acetate/ionomycin-stimulated human mast cells (HMC-1), and lipopolysaccharide (LPS)-stimulated macrophages and splenocytes. Histological, ELISA, PCR, and Western blot experiments were performed. The application of KAJD significantly attenuated the lesion severity and skin thickness and inhibited the infiltration of inflammatory cells, mast cells, and CD4+ T cells into the sensitized skin of mice. Reduced leukocyte numbers and proinflammatory cytokine and IgE levels were also observed in the sera of KAJD-treated mice. Moreover, *in vitro* studies demonstrated that KAJD treatment reduced the LPS-induced expression of proinflammatory cytokines and nitric oxide (NO) production in RAW 264.7 cells. The regulation of IL-4 and IL-6 mRNA and MAPK pathways was also detected in agonist-induced isolated splenocytes and HMC-1 cells by the addition of KAJD. Taken together, our results demonstrate that KAJD inhibits the development of DNBCB-induced AD in BALB/c mice and in several immune cell types, suggesting that KAJD might be a useful therapeutic drug for the treatment of AD.

**Keywords:** atopic dermatitis, mast cell, splenocyte, macrophage, IgE, CD4+ T cells, MAPK pathway

## INTRODUCTION

Atopic dermatitis (AD) is a common chronic inflammatory skin disease and often causes other allergic disorders, such as food allergies, asthma, and rhinitis (Leung and Bieber, 2003; Spergel and Paller, 2003). Atopic dermatitis is characterized by eczematous skin lesions, pruritic folliculitis, and increased serum immunoglobulin E (IgE) levels, which are associated with infiltration of inflammatory

cells, such as lymphocytes, macrophages, eosinophils, and mast cells (Rousset et al., 1991; Simon et al., 2004; Marsella et al., 2011).

Mast cells are activated through Th2 cytokines or cross-linking of their high-affinity surface receptors with IgE (FcεRI), thereby leading to cell degranulation and production of inflammatory mediators (Novak et al., 2004; Ong and Leung, 2006; Theoharides et al., 2012). Atopic dermatitis is also associated with elevated levels of Th2 cytokines, IL-4, IL-5, and IL-13 in blood (Homey et al., 2006) and infiltration of CD4+ T cells into AD skin lesions (Leung and Bieber, 2003). Corticosteroids are one of the most common topical medications for treating AD, but their long-term use produces undesired side effects (Lubach et al., 1989; Blume-Peytavi and Wahn, 2011). Although topical immunosuppressants such as tacrolimus (TAC) have been introduced as an alternative steroid-free anti-inflammatory agent for the safe and effective treatment of patients with AD (Akhavan and Rudikoff, 2008), several side effects of TAC, such as itching, burning sensation of the skin, flu-like symptoms, headache, cough, and burning eyes, have also been reported (Hanifin et al., 2005). Consequently, the development of new useful drugs that efficiently manage AD and have reduced side effects is urgently needed.

In this study, we introduce KHU-ATO-JIN-D (KAJD), which is a mixture of extracts from six plants (*Phellodendri cortex*, *Schizonepetae spica*, *Sophorae radix*, *Glycyrrhizae radix*, *Liriodendri tuber*, and *Radix rehmanniae* Exsiccata), as a novel medication for treating AD. Each extract has been shown to demonstrate anti-inflammatory and antiallergic activity (Ho-Sub et al., 2001; Lee et al., 2005; Shin et al., 2008; Ra et al., 2011; Han et al., 2012; Choi et al., 2014). We used BALB/c mice as a model animal because they exhibited symptoms very similar to those of human AD, including an increased IgE level and chronic dryness (Dearman et al., 1995), and 2,4-dinitrochlorobenzene (DNCB) was used to induce AD in BALB/c mice (Kim et al., 2014; Wang et al., 2015; Yoon et al., 2015).

In the present study, we sought to explore the therapeutic effects of KAJD on DNCB-induced AD-like symptoms in BALB/c mice. In addition, we investigated the anti-inflammatory effects of KAJD on macrophages, mast cells, and splenocytes. Our results demonstrate that KAJD inhibits the development of DNCB-induced AD-like symptoms, suggesting that KAJD might be a useful therapeutic drug for the treatment of AD.

## MATERIALS AND METHODS

### Preparation of KAJD and HPLC Analysis

KHU-ATO-JIN-D, prepared by Hanpoong Pharm and Foods Company (Jeon-ju, Korea) in accordance with good manufacturing practice (GMP) protocols, is a water-extracted brown-colored mixture composed of *Phellodendri amurense*, *Schizonepetae spica*, *Sophorae radix*, *Glycyrrhizae radix*, *Liriodendri tuber*, and *Radix rehmanniae*

Exsiccata (Figure 1A). High-performance liquid chromatography (HPLC) was performed to confirm the characteristics of herbal mixtures, including each component (Hanpoong Pharm and Foods Company) (Figure 1B). KHU-ATO-JIN-D was passed through a 0.2-μm membrane filter, and 20 μl aliquots of the filtrate were injected into the HPLC. The Hypersil GOLD C18 analytical column (250 mm × 4.6 mm; particle size 5 μm) was used, and the mobile phases consisted of solvent A (DI water) and solvent B (acetonitrile), which were applied at a flow rate of 1 ml/min. The column temperature was set at 30°C. The injection volume was 10 μl, and content analysis was performed at 280 nm. Glycyrrhizin and berberine were used as standard compounds (Sigma, St. Louis, MO, USA) at a concentration of 1 mg/ml to identify the peaks [Figure 1B (lower panel)]. The total glycyrrhizin and berberine contents in the extracts were 8.05 and 4.8 mg/g, respectively (Figure 1B (upper panel)). More information on the KAJD production processes can be obtained upon request from Hanpoong Pharm and Foods Company (<http://hpeng.hanpoong.co.kr/>). The KAJD cream was made by ATEC & Co. (Seoul, Korea) in accordance with cosmetic guidelines on good manufacturing practice (CGMP) protocols for animal experiments. More information on the KAJD cream production processes can be obtained upon request from ATEC & Co. (<http://www.atecltd.com/>).

### Animal Studies

Six-week-old male BALB/c mice (20 ± 2 g) were purchased from Orient (Sung-nam, Korea) and randomly assigned into four groups (no treatment, DNCB, DNCB + TAC, DNCB + KAJD); each group included five mice. All mice were housed in a pathogen-free environment and provided *ad libitum* access to food and water. Our methods were executed in accordance with relevant guidelines, and regulations and procedures involving mice were approved by the animal care center of Kyung Hee University (approval number KHUASP (SE)-14-014).

### Sensitization and Treatment

To promote the development of AD-like skin lesions, the mouse back skin was shaved and sensitized twice a week by applying 100 μl of 2% DNCB in acetone using 1 × 1 cm patches and followed with a second challenge of 100 μl of 0.2% DNCB twice a week. Control mice were painted with acetone alone. Next, KAJD or TAC was applied to the sensitized mouse skin regularly for 2 weeks. On day 28, all mice were sacrificed by CO<sub>2</sub> inhalation, and blood samples were collected. The method was performed as described previously (Ku et al., 2017).

### Clinical Skin Score

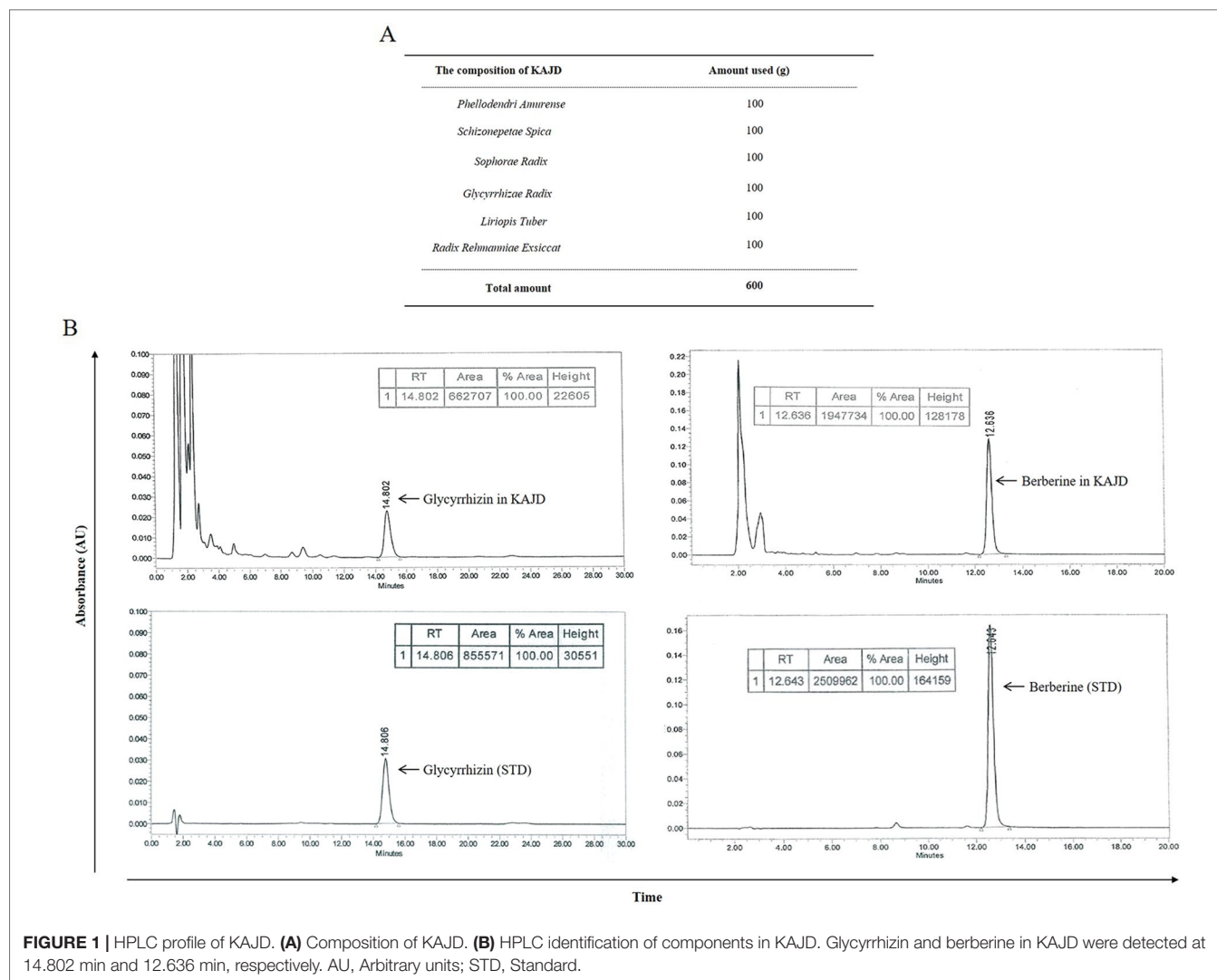
Clinical observation to assess changes in the skin of BALB/c mice was performed once a week for 4 weeks. The severity of AD-like dorsal skin lesions was evaluated based on four symptoms, including erythema/hemorrhage, scarring/dryness, edema, and excoriation/erosion; each of which was graded on a scale from 0 to 3 (none, 0; mild, 1; moderate, 2; severe, 3). The clinical skin score was defined as the sum of the individual scores and ranged from 0 to 12.

### Skin Thickness and Spleen Weight

Before sacrifice, the epidermal thickness at three different mouse back skin sites was measured with a digital caliper (Mitutoyo,

**Abbreviations:** PUL, *Pyrus ussuriensis* Maxim. Leaves; AD, Atopic dermatitis; NO, Nitric oxide; IL-6, Interleukin 6; IL-1β, Interleukin 1β; TNF-α, tumor necrosis factor; DNCB, 2, 4-dinitrochlorobenzene; IgE, Immunoglobulin E; IL-4, Interleukin 4; IL-13, Interleukin 13; HPLC, High performance liquid chromatography; TEWL, Transepidermal water loss; DMEM, Dulbecco's modified Eagle's medium; FBS, Fetal bovine serum; LPS, Lipopolysaccharide; DMSO, Dimethyl sulfoxide; PBS, phosphate-buffered saline; H&E, Hematoxylin and eosin; SEM, Standard error of the mean; ANOVA, Analysis of variance.





Kawasaki, Japan). The spleens from all mice were removed and weighed immediately.

## Histological Analysis

Portions of the skin biopsies were fixed in 4% paraformaldehyde (PFA) and embedded in Frozen Section Compound (FSC22 Clear, Surgipath, Leica Biosystem, Wetzlar, Germany) on dry ice. Skin sections of 20  $\mu$ m thickness were cut and stained with hematoxylin and eosin (H&E) to detect inflammatory cells or with toluidine blue (T. B) to detect mast cells. The stained tissues were examined under a light microscope (Olympus, Tokyo, Japan), and the inflammatory or mast cells were counted in 10 random high-power field (HPF) sections at 400 $\times$  magnification.

## Immunohistochemistry

We performed immunohistochemical analysis to detect CD4+ lymphocytes using the anti-CD4+ antibody. Briefly, the skin sections were hydrated, and after heating, the sections were incubated with 3% hydrogen peroxide (PBS) for 15 min to prohibit endogenous peroxidase activity in blood cells. Next, the skin sections were treated

with a blocking solution [5% bovine serum albumin (BSA) in PBS] for 1 h at room temperature. The sections were then treated with a mouse monoclonal CD4+ antibody overnight at 4°C and incubated with secondary biotinylated anti-rabbit IgG for 1 h at room temperature. The skin sections were next treated with an avidin-biotin horseradish peroxidase (HRP) complex (VECTASTAIN ABC Kit, Vector Labs, Burlingame, CA, USA) for 30 min at 4°C and stained with diaminobenzidine tetrachloride (DAB) as a substrate. The sections were counterstained with hematoxylin, mounted with an aqueous mounting solution (Permount, Fisher Scientific, Waltham, MA, USA), and coverslipped. The skin sections were analyzed using an Olympus microscope, and images were captured using a digital video camera. The CD4+ lymphocytes were counted in 10 random HPF sections at 400 $\times$  magnification.

## Blood Analysis

Whole blood samples were collected from mice by cardiac puncture under anesthesia and placed in Vacutainer TM tubes containing EDTA (BD Science, NJ, USA). To determine the hematological parameters [white blood cells (WBC), lymphocytes, monocytes,

eosinophils, basophils, and neutrophils] of the blood samples, a HEMAVET 950 hematology analyzer (Drew Scientific, Inc., Oxford, Dallas, TX, USA) was used in accordance with the manufacturer's recommendation.

## Enzyme-Linked Immunosorbent Assay

The levels of cytokines and total IgE in the sera of mice and the expression levels of cytokines in cell lines, including RAW264.7 cells, HMC-1 cells, and splenocytes, were measured by sandwich ELISA using the BD Pharmingen mouse or human ELISA Set (Pharmingen, San Diego, CA, USA). Briefly, plates were coated with a capture antibody in ELISA coating buffer (Sigma, Louis, MO, USA) and incubated overnight at 4°C. The plates were washed with PBS-Tween 20 (0.05%) and subsequently blocked [10% fetal bovine serum (FBS) in PBS] for 1 h at 20°C. Serial dilutions of standard antigen or sample in dilution buffer (10% FBS in PBS) were added to the plates and incubated for 2 h at 20°C. After washing, biotin-conjugated anti-mouse IgE and streptavidin-HRP conjugate (Sav-HRP) were added to the plates and incubated for 1 h at 20°C. Finally, tetramethylbenzidine (TMB) substrate solution was added to the plates for 15 min in the dark, followed by the addition of 2N H<sub>2</sub>SO<sub>4</sub> to stop the reaction. Optical densities were measured at 450 nm on an automated ELISA reader (Versa Max, Molecular Devices, Sunnyvale, CA, USA).

## Cell Culture

The RAW 264.7 murine macrophage cell line and the human mast cell (HMC-1) line were purchased from the Korea Cell Line Bank (Seoul, Korea). Each cell line was grown in Dulbecco's modified Eagle's medium (DMEM, Welgene, Daegu, Korea) or Iscove's Modified Dulbecco's Medium (IMDM, Welgene, Daegu, Korea) supplemented with 10% heat-inactivated FBS (Welgene, Daegu, Korea) and 1% antibiotics (Ab, Welgene, Daegu, Korea) at 37°C and 5% CO<sub>2</sub>.

## Splenocyte Isolation

Splenic cell suspensions from BALB/c mice were prepared in RPMI-1640 medium (containing 10% FBS, 1% Ab, and 0.05 mM mercaptoethanol) by homogenization under aseptic conditions. The contaminating red blood cells were removed using red blood cell lysis buffer (Sigma, St. Louis, MO, USA). The suspension was centrifuged and resuspended in complete RPMI-1640. The isolated spleen cells were maintained at 37°C in an incubator humidified at 5% CO<sub>2</sub>.

## Cell Viability Assay

RAW 264.7 cells, HMC-1 cells, and splenocytes (1 × cells/well) were plated in 96-well culture plates and incubated for 24 h. RAW264.7 cells and splenocytes were treated with 1 µg/ml LPS, and HMC-1 cells were treated with 5 ng/ml phorbol-12-myristate (PMA) and 500 ng/ml ionomycin (Ion) in the presence or absence of various concentrations of KAJD. After 24 h of incubation, 10 µl of water-soluble tetrazolium (WST) solution was added to each well of the plate, which was incubated in the dark at 37°C for another 1 h. Optical density was measured at 450 nm using an ELISA Plate Reader (Versa Max, Molecular Devices, Sunnyvale, CA, USA).

## Detection of Nitric Oxide

Nitric oxide (NO) production was measured in the RAW 264.7 culture supernatant using a Griess Reagent Kit (Promega, Madison, WI, USA). In brief, 150 µl of culture supernatant was transferred to a 96-well plate and then mixed with 150 µl of Griess reagent solution. The mixtures were then incubated for 30 min at room temperature, and optical density was determined at 570 nm using a microplate reader.

## Reverse Transcription-Polymerase Chain Reaction

Cells were harvested by centrifugation, and the pellet was washed with ice-cold PBS. RNA was isolated from the pellet using an easy-BLUE RNA Extraction Kit (iNtRON Biotech, Sungnam, Korea) according to the manufacturer's instructions. The quantity of the isolated RNA was measured using the NanoDrop ND-1000 Spectrophotometer (NanoDrop Technologies Inc., Wilmington, DE, USA). cDNA was synthesized from 2 µg of total RNA using a cDNA Synthesis Kit (TaKaRa, Otsu, Shinga, Japan). RT-PCR was performed in a 20 µl reaction mixture consisting of DNA template, 10 pM of each gene-specific primer, 10× Taq buffer, 2.5 mM dNTP mixture, and 1 unit of Taq DNA polymerase (Takara, Otsu, Shinga, Japan). The primer sequences used for human and/or mouse IL-4, IL-6, and GAPDH are shown in Table 1.

## Western Blot Analysis

Cells were harvested, and cell pellets were incubated in one volume of lysis buffer containing 20 mM Tris-HCl (pH 7.5), 150 mM NaCl, 1 mM EDTA, 1 mM Na<sub>2</sub>EDTA, 1 mM EGTA, 1% NP-40, 1% sodium deoxycholate, 1 mM Na<sub>3</sub>VO<sub>4</sub>, 1 mM DTT, 1 mM NaF, 1 mM PMSF, and propidium iodide (PI) cocktail on ice for 30 min, centrifuged at 13,000 rpm for 20 min at 4°C, aliquoted to 20 µl, and transferred onto nitrocellulose membranes (Protran Nitrocellulose Membrane, Whatman, UK). The membranes were blocked with 5% nonfat milk and probed with specific primary antibodies. After washing, the membranes were incubated with diluted enzyme-linked secondary antibodies, and the protein bands were detected using an EZ-Western Chemiluminescence Detection Kit and visualized by exposing the membranes to X-ray films. In a parallel experiment, cytoplasmic and nuclear proteins were extracted using NE-PER® Nuclear and Cytoplasmic Extraction Reagents (Pierce Biotechnology, Rockford, IL, USA) according to the manufacturer's instructions. Each protein was appropriately detected with the following antibodies: anti-p-EKR1/2, p-P38, and p-JNK antibodies (all purchased from Santa Cruz Biotechnology [Santa Cruz, CA, USA]) and anti-GAPDH antibodies (purchased from Cell Signaling Technology [Danvers, MA, USA]).

## Statistical Analysis

All quantitative data derived from this study were analyzed statistically. The results are expressed as the mean ± standard deviation (SD) or mean ± SEM of at least three separate tests. Statistical significance was determined using one-way analysis of variance followed by the Tukey-Kramer multiple comparisons post-test to analyze differences between groups. P < 0.05 was considered to indicate a statistically significant difference, and

**TABLE 1 |** PCR primer sequences.

Primer type	Primer name	Primer sequence
Mouse	IL-4	F: 5'-TCG GCA TTT TGA ACG AGG TC-3'
		R: 5'-GAA AAG CCC GAA AGA GTC TC-3'
	IL-6	F: 5'-CAA GAG ACT TCC ATC CAG TTG C-3'
		R: 5'-TTG CCG AGT TCT CAA AGT GAC-3'
	GAPDH	F: 5'-GAG GGG CCA TCC ACA GTC TTC-3'
		R: 5'-CAT CAC CAT CTT CCA GGA GCG-3'
Human	IL-4	F: 5'-TGC CTC CAA GAA CAC AAC TG-3'
		R: 5'-CTC TGG TTG GCT TCC TTC AC-3'
	IL-6	F: 5'-AAC CTT CCA AAG ATG GCT GAA-3'
		R: 5'-CAG GAA CTG GAT CAG GAC TTT-3'
	GAPDH	F: 5'-CGT CTT CAC CAC CAT GGA GA-3'
		R: 5'-CGG CCA TCA CGC CAC AGT TT-3'

$P < 0.05$ ,  $<0.01$ , and  $<0.001$  are assigned respective symbols in the figures. All experiments were performed at least three times. All statistical analyses were performed using PRISM software (version 5.0; GraphPad Software Inc., La Jolla, CA, USA).

## RESULTS

### Topical Application of KAJD Suppresses DNCB-Induced AD in Mice

To investigate the effects of KAJD on DNCB-induced AD-like symptoms, BALB/c mice were first sensitized with multiple applications of DNCB on their skin and then treated with KAJD or TAC ointment as a control on a regular basis for 2 weeks (**Figure 2A**). All mice developed significant skin hypersensitivity reactions after the DNCB application, showing severe erythema/hemorrhage, scarring/dryness, edema, and excoriation/erosion (**Figure 2B**). Scoring of the skin lesion severity revealed that the wounds were very severe and lasted until the mice were sacrificed. However, subsequent topical application of KAJD or TAC on the sensitized skin markedly reduced the skin severity. On day 28, the clinical scores of  $3.13 \pm 1.27$  in the KAJD-treated group and  $3.29 \pm 0.76$  in the TAC-treated group were significantly lower than that of  $5.5 \pm 1.38$  in DNCB-treated mice (**Figure 2C**). Moreover, the skin thickness was increased by DNCB and markedly reduced by the application of KAJD or TAC (**Figure 2D**). It is well known that the weights of some immune organs increase in response to the topical application of agents that have allergenic or sensitizing potential (Stahlmann et al., 2006; Bae et al., 2010). Similarly, the increased spleen weight in DNCB-treated mice was slightly decreased in response to KAJD or TAC treatment (**Figure 2E**). Notably, KAJD exhibited a greater potential for ameliorating the DNCB-induced increase in skin thickness and spleen weight than TAC. Taken together, these results demonstrate that KAJD effectively attenuates DNCB-induced AD-like symptoms and is superior to TAC in some ways. We also monitored the mouse body weight changes and food intake twice a week throughout the study. Mice treated with DNCB did not show any changes in food intake, but their body weight was decreased by 15% compared with that of vehicle-treated mice. Treatment with KAJD or TAC did not markedly alter the index of DNCB-treated mice (**Supplementary Figure 1**).

### KAJD Decreases the DNCB-Induced Infiltration of Inflammatory Cells, Mast Cells, and CD4<sup>+</sup> T Cells Into AD Skin Lesions

Next, we examined the recruitment of inflammatory cells to sensitized skin by H&E staining. While repeated cutaneous application of DNCB induced the infiltration of inflammatory cells into both the epidermis and dermis, subsequent application of KAJD to the allergic skin inhibited their recruitment (**Figure 3A**). Mast and CD4<sup>+</sup> T cells are well known to be involved in allergenic reactions and inflammation (Ahmadzadeh et al., 2001; Liu et al., 2011). T. B staining showed that DNCB increased the number of dermal mast cells on the treated skin, and this increase was attenuated by KAJD (**Figure 3B**). Moreover, DNCB increased the number of CD4<sup>+</sup> T cells, while KAJD decreased this number in the skin epidermis and dermis (**Figure 3C**). Bar graphs indicate the average number of cells counted in a random field of view (**Figure 3D**). Notably, although TAC also reduced the recruitment of inflammatory cells, mast cells, and CD4<sup>+</sup> T cells to the skin, KAJD was more effective for the inhibition of mast cell and CD4<sup>+</sup> T cell recruitment than TAC.

### KAJD Suppresses the DNCB-Induced Increase in Mouse WBCs

Since the numbers of most types of WBCs are increased in patients with AD (Lubach et al., 1989; Hanifin et al., 2005), we determined the number of WBCs in mouse blood using a HEMAVET 950 Hematology Analyzer. In mice treated with DNCB, the total number of WBCs was increased up to 3.5-fold compared with that in vehicle-treated mice, but this number was dramatically reduced by treatment with KAJD or TAC (**Figure 4**). Counting each subtype of WBCs, including granulocytes (neutrophils, basophils, eosinophils), monocytes, and lymphocytes, showed that KAJD and TAC suppressed the DNCB-induced increases in the numbers of each WBC cell type to similar extents. In particular, both KAJD and TAC effectively decreased the eosinophil cell count, which is correlated with the severity of AD (Reitamo et al., 1998).

### KAJD Decreases Serum IgE and Inflammatory Cytokine Levels in DNCB-Treated Mice

To understand the mechanisms underlying the anti-inflammatory activity of KAJD, we examined its effects on the production of serum IgE and several proinflammatory cytokines in the blood of mice by ELISA, as a high serum IgE level is a major characteristic of AD. The DNCB application increased the IL-6, IL-10, and IL-12 levels, with a major increase in the serum IgE level. However, KAJD and TAC significantly suppressed the production of inflammatory cytokines and serum IgE (**Figure 5**). Note that KAJD was more effective at suppressing the DNCB-induced production of IgE and IL-6 than TAC. These results suggest that KAJD suppresses skin inflammation by inhibiting the DNCB-stimulated increase in serum IgE and proinflammatory cytokine concentrations.

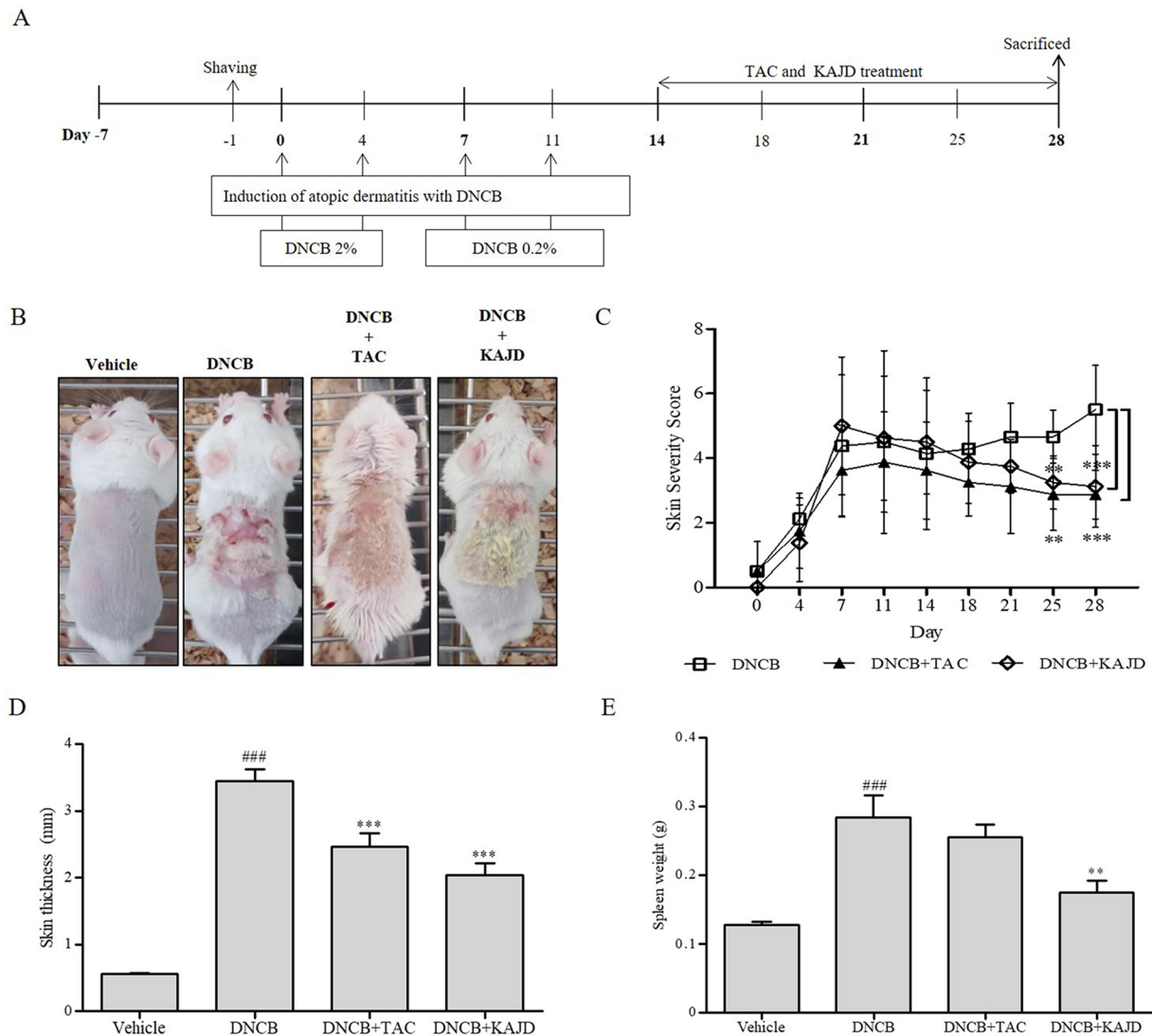


**FIGURE 2 |** KAJD suppresses DNCB-induced atopic dermatitis-like symptoms. **(A)** BALB/c mice were sensitized with the sequential application of 2% and 0.2% DNCB for 2 weeks. KAJD or tacrolimus was regularly applied to the sensitized skin for an additional 2 weeks. **(B)** Photographs were taken at the end of the experiment to show the appearance of skin lesions ( $n=8$ ). **(C)** Skin severity scores of AD-like skin lesions in BALB/c mice. The total score is the sum of individual scores determined based on the symptoms of erythema/hemorrhage, edema, scaling/dryness, and excoriation/erosion. **(D, E)** The dorsal skin thickness **(D)** and spleen weights **(E)** of BALB/c mice were measured at the end of treatment. ###  $P < 0.001$  compared to the vehicle group. \*\*  $P < 0.01$  and \*\*\*  $P < 0.001$  compared to the DNCB-stimulated group. Vehicle, no treatment; DNCB, 2,4-dinitrochlorobenzene; TAC, tacrolimus.

## KAJD Suppresses the Agonist-Induced Production of Cytokines and Inhibits the MAPK Pathway in Several Immune Cell Types

Given the marked inhibitory effects of KAJD on cytokine production in mice, we next examined its effect on the expression of proinflammatory cytokines in RAW264.7 murine macrophage cells. LPS-mediated stimulation of RAW264.7 cells significantly promoted the expression of IL-6 and TNF- $\alpha$  and NO production. However, the addition of KAJD significantly reduced the expression of these cytokines and NO production in a dose-dependent

manner (Figure 6). Moreover, we examined the role of KAJD in the suppression of cytokine expression in other immune cell types, including isolated mouse splenocytes and human mast cells (HMC-1). Similar to RAW264.7 cells, KAJD cotreatment significantly reduced agonist-stimulated IL-6 production in both cell types (Figures 7B and 8B). We further tested whether KAJD regulates the expression of cytokines at the transcriptional level (Figures 7A and 8A). RT-PCR analysis showed that both the IL-4 and IL-6 mRNA levels were induced by agonist treatment and decreased by KAJD cotreatment in both splenocytes and HMC-1 cells. Specifically, KAJD treatment at a concentration of 500  $\mu\text{g/ml}$  reduced both IL-4



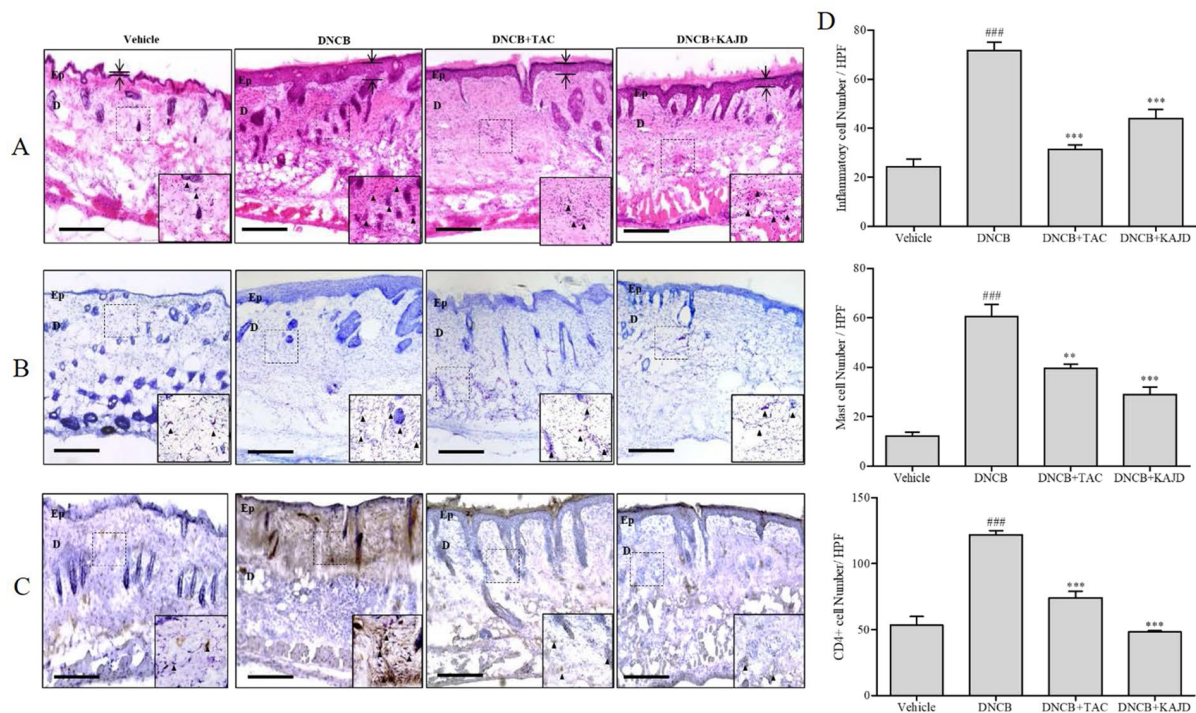


**FIGURE 3 |** KAJD reduces the dermal infiltration of inflammatory cells and mast cells in DNCB-treated BALB/c mice. **(A, B, and C)** Dorsal skin sections were stained with hematoxylin and eosin to show inflammatory cells as indicated by the purple spot **(A)**, stained with toluidine blue to show mast cells as indicated by the purple spot **(B)**, or stained with diaminobenzidine tetrachloride (DAB) and hematoxylin to show CD4+ T cells as indicated by the brown spot **(C)**. The arrows and bars indicate the thickness of the epidermis. **(D)** The stained inflammatory cells (upper panel), mast cells (middle panel), and CD4+ cells (lower panel) were counted, and the results are presented in a graph. Sections were evaluated using a microscope at an original magnification of 400 $\times$ . The data are shown as the mean  $\pm$  SEM. <sup>###</sup>  $P < 0.001$  compared to the vehicle group. <sup>\*\*</sup>  $P < 0.01$  and <sup>\*\*\*</sup>  $P < 0.001$  compared to the DNCB-stimulated group. Bar = 50  $\mu$ m. Vehicle, no treatment; DNCB, 2,4-dinitrochlorobenzene; TAC, tacrolimus; Ep, epidermis; D, dermis.

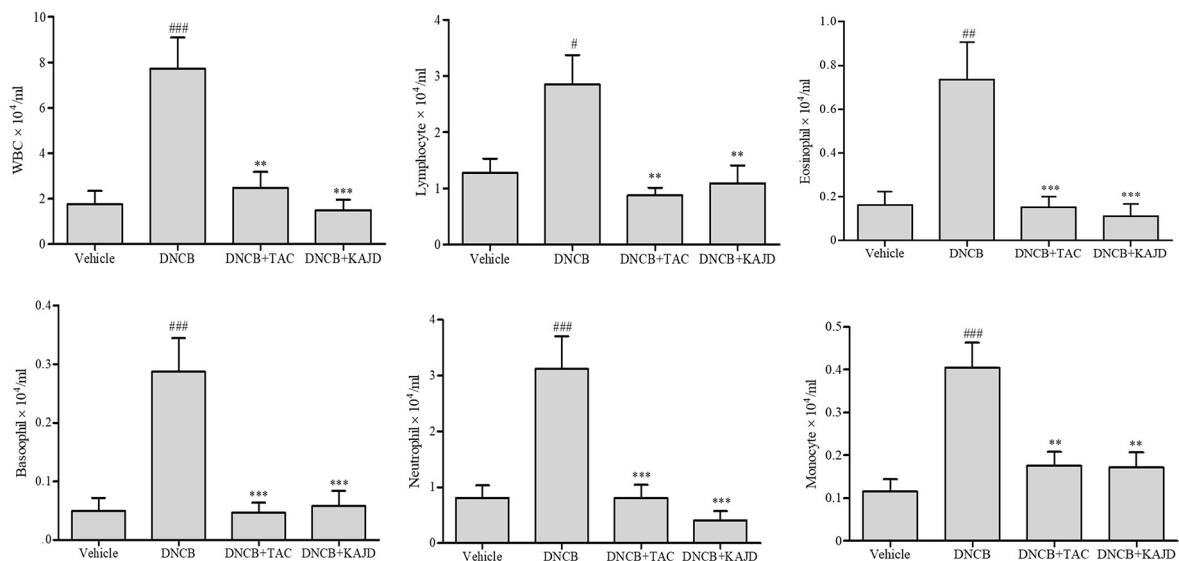


**FIGURE 4 |** KAJD suppresses the number of WBCs. WBCs in each group of mice were analyzed for subtype cell numbers using a HEMAVET hematology analyzer. The data are presented as the mean  $\pm$  SEM. <sup>#</sup>  $P < 0.05$  and <sup>###</sup>  $P < 0.001$  compared to the vehicle group. <sup>\*\*</sup>  $P < 0.01$  and <sup>\*\*\*</sup>  $P < 0.001$  compared to the DNCB-stimulated group. Vehicle, no treatment; DNCB, 2,4-dinitrochlorobenzene; TAC, tacrolimus.

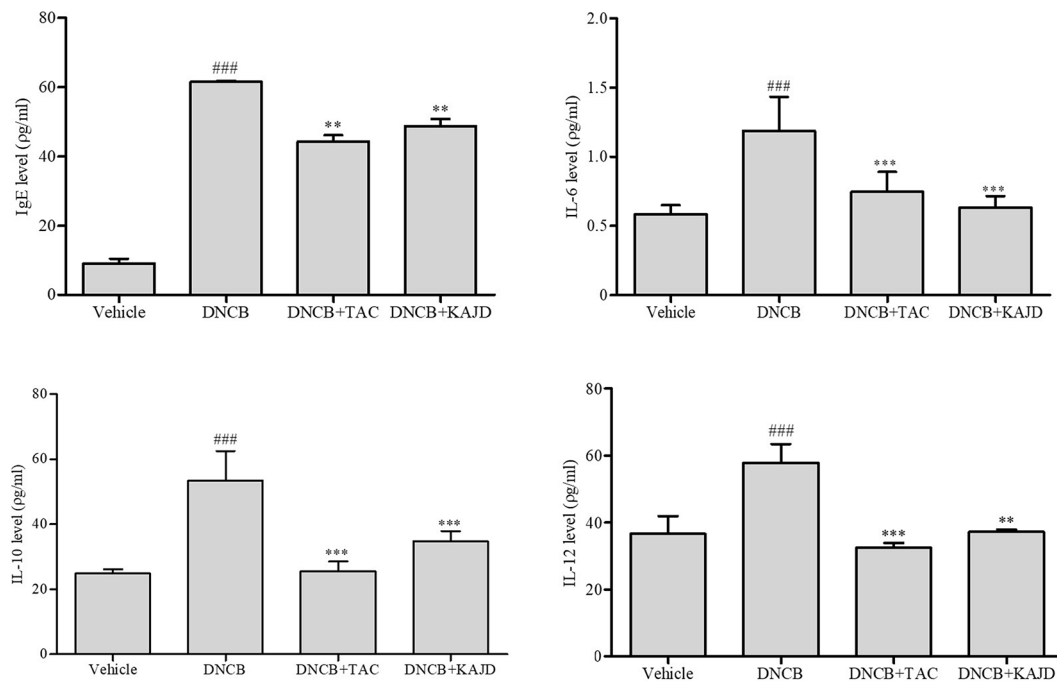


**FIGURE 5 |** KAJD decreases the levels of serum IgE and proinflammatory cytokines. Blood samples were collected from each mouse, and the levels of serum IgE and cytokines IL-6, IL-10, and IL-12 were quantified by ELISA. ###  $P < 0.001$  compared to the vehicle group. \*\* $P < 0.01$  and \*\*\* $P < 0.001$  compared to the DNCB-stimulated group. Vehicle, no treatment; DNCB, 2,4-dinitrochlorobenzene; TAC, tacrolimus.

and IL-6 to the control levels. Next, we examined the viabilities of several immune cell types (RAW264.7, HMC-1, and splenocytes) following treatment with various concentrations of KAJD (**Supplementary Figures 2–4**). KHU-ATO-JIN-D did not induce any cytotoxicity in several immune cell types over a 24-h period. Furthermore, KAJD was shown to regulate the phosphorylation of ERK, JNK, and p38, and the inflammatory response reportedly results in the activation of MAPK pathways (Saklatvala, 2004). ERK, JNK, and p38 phosphorylation was marginally increased after treatment with 500  $\mu\text{g/ml}$  KAJD (**Figures 7C and 8C**). KHU-ATO-JIN-D regulated the phosphorylation of ERK, JNK, and p38 in a dose-dependent manner. These results suggest that KAJD suppresses proinflammatory cytokine production and inhibits MAPK pathways in several immune cell types, thereby suppressing AD-like symptoms caused by DNCB.

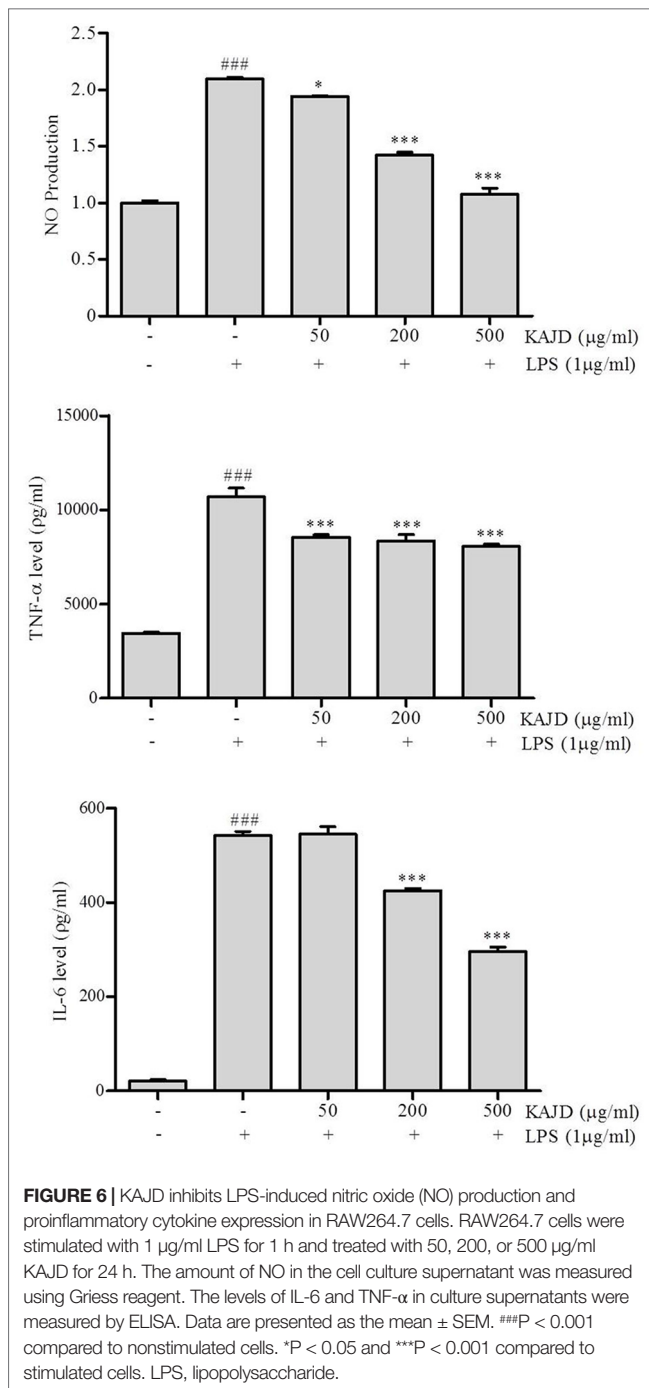
## DISCUSSION

Atopic dermatitis is an inflammatory skin disease that is caused by immune dysregulation associated with various environmental and genetic factors (Schultz Larsen, 1993). The current treatments for AD include antihistamines, steroids, and immune suppressants, but side effects are very common with long-term usage of these medications (Prabhakaran et al., 1999; Simpson, 2010). The ratio and concentration of KAJD, which was used in this experiment, most suitable for cream manufacture were set after various attempts (data not shown). In this study, we showed that KAJD, herbal extracts,

inhibited various AD-like skin hypersensitivity reactions, such as erythema/hemorrhage, scarring/dryness, edema, and excoriation/erosion, in BALB/c mice exposed to DNCB. Treatment with KAJD suppressed not only the infiltration of inflammatory immune cells into AD skin lesions but also the levels of several proinflammatory cytokines in the blood. Therefore, our results suggest that KAJD can be an effective treatment option for AD. Moreover, KAJD shows no toxicity and effectively attenuates AD symptoms; thus, developing this extract as a treatment for AD is important. It should be noted that KAJD performs better than TAC.

Since many reports have demonstrated that Th2-type immune responses play significant roles in the pathogenesis of AD; Th2 cytokines are considered to be attractive therapeutic targets for AD treatment. In AD skin lesions, Th2 lymphocytes produce high levels of IL-4, IL-5, IL-6, IL-10, and IL-13, which induce IgE production by B cells. IgE, in turn, binds to the high-affinity IgE-Fc receptor type I (Fc $\epsilon$ RI) on the surface of mast cells, leading to the release of various types of inflammatory mediators, such as histamine, chemokines, and cytokines. Eosinophil recruitment to inflamed skin *via* Th2-type cytokines is another important characteristic of AD. Our findings showed that KAJD reduced the serum levels of IgE and Th2 cytokines, such as IL-6 and IL-10, and the infiltration of mast cells and leukocytes, including eosinophils and monocytes, into AD skin lesions.

In addition to Th2 cytokines, proinflammatory cytokines such as TNF- $\alpha$  are also known to play important roles in AD



pathogenesis by disrupting skin barrier function. A recent study showed that TNF-α alone or in combination with Th2 cytokines changes the skin barrier lipid composition and epidermal morphogenesis, leading to skin barrier perturbation (Danso et al., 2014). The disrupted barrier in AD skin becomes vulnerable to the penetration of allergens through the skin. In response to these stimuli, keratinocytes are able to secrete proinflammatory mediators, which increase the recruitment and activation of T cells and dendritic cells (DCs) (Pastore et al., 2006). Moreover, keratinocytes in the disrupted skin

produce thymic stromal lymphopoietin (TSLP), an epithelial cell-derived cytokine that strongly activates DCs, which prime naïve CD4<sup>+</sup> T cells to differentiate into Th2 cells (Liu, 2009). Therefore, in AD, the skin forms a positive feedback loop between cytokines and barrier-disrupted skin with highly elevated levels of proinflammatory and Th2 cytokines. In this study, we showed that KAJD treatment suppressed both the infiltration of T cells and the expression of the TNF-α and Th2 cytokines, indicating that KAJD might inhibit some point in this positive feedback loop in AD skin.

Macrophages are also involved in skin inflammation in AD. Although macrophage activation is beneficial for eliminating inflammatory stimuli during acute inflammatory responses, persistent macrophage activation results in the development of chronic inflammatory skin diseases, including psoriasis and AD (Valledor et al., 2010). Activated macrophages produce proinflammatory cytokines, including IL-1, IL-6, IL-12, and TNF-α, and high levels of inducible nitric oxide synthase (iNOS), thus contributing to the pathogenesis of AD (Kasraie and Werfel, 2013). Similarly, Th2 cells release various cytokines, such as IL-4, IL-6, and IL-10, to induce B cells to produce IgE, which, in turn, activates mast cells for histamine release (Hammad and Lambrecht, 2008; Holgate and Polosa, 2008). Moreover, the spleen, the largest lymphatic organ in the body, acts as storage for inflammatory monocytes and differentiates into macrophages to participate in both anti-inflammatory and anti-inflammatory reactions (Auffray et al., 2007; Hiroyoshi et al., 2012; Robbins et al., 2012; Wystrychowski et al., 2014). Notably, topical application of KAJD on BALB/c mice suppressed the levels of IL-12, which were increased by exposure to DNCB (Figure 5). Moreover, ELISA analysis of murine macrophage RAW 264.7 cells revealed that KAJD inhibited the LPS-induced production of IL-6, TNF-α, and NO. The MAPK pathway is essential for the pathogenesis of the inflammatory response (Wu, 2004). As mentioned in previous studies, MAPK inhibition attenuates severe inflammatory responses in the dermis (Ipaktchi et al., 2006). In our attempt to investigate the molecular mechanisms by which KAJD inhibits the production of Th2 cytokines, we found that KAJD dramatically downregulates IL-4 and IL-6 mRNA expressions and inhibits the MAPK (p38, ERK, and JNK) pathways in immune cells, such as murine splenocytes and human mast cells stimulated with LPS, indicating that KAJD alleviates several AD symptoms by controlling the transcriptional expression of Th2 cytokines. However, further studies are needed to identify signaling pathways that govern the KAJD-mediated transcriptional control of these Th2 cytokines.

Notably, KAJD was more effective at alleviating several AD symptoms, including skin thickness and infiltration of mast cells and CD4<sup>+</sup> T cells, than TAC, which was used as a control in this study. In addition, KAJD did not show cell toxicity in multiple cells at the concentration used in our experiments.

Taken together, these results demonstrate that KAJD is very effective for the treatment of AD by suppressing the recruitment of numerous inflammatory cells, the production of proinflammatory cytokines, and the MAPK pathway. Further studies are warranted to investigate the clinical usefulness of KAJD.



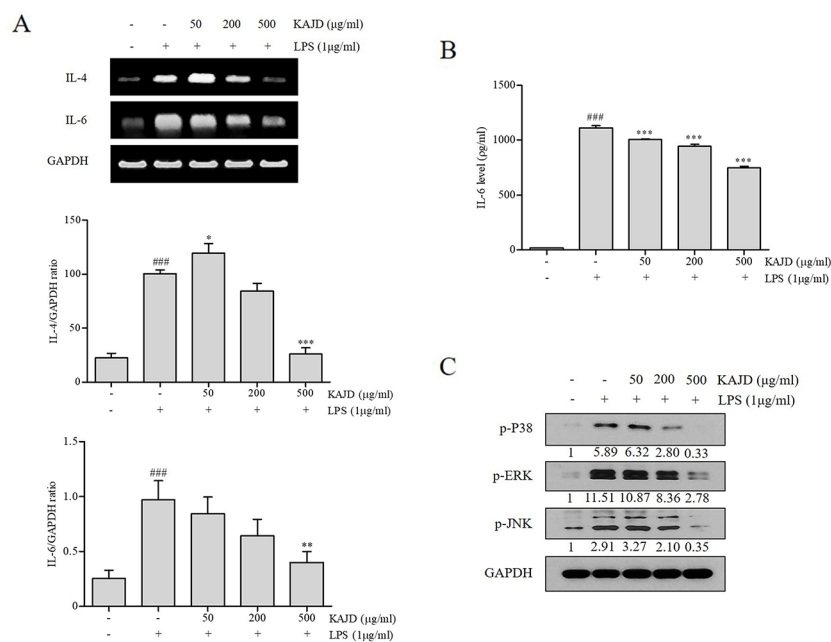


**FIGURE 7 |** KAJD inhibits MAPK pathways and suppresses the mRNA and protein expression of proinflammatory molecules in splenocytes. **(A)** The IL-4 and IL-6 mRNA levels in splenocytes were measured by RT-PCR analysis. The bar graphs represent the quantitation of RT-PCR data. **(B)** The level of IL-6 in cell culture supernatants was measured by ELISA. Splenocytes stimulated with LPS for 1 h were treated with varying concentrations of KAJD for 24 h. **(C)** Phosphorylated ERK1/2, p38, and JNK levels in cell lysates were determined by immunoblot analysis. GAPDH was used as an internal control. Data are presented as the mean  $\pm$  SEM. <sup>###</sup> $P < 0.001$  compared to nonstimulated cells. <sup>\*</sup> $P < 0.05$ , <sup>\*\*</sup> $P < 0.01$ , and <sup>\*\*\*</sup> $P < 0.001$  compared to stimulated cells. LPS, lipopolysaccharide.

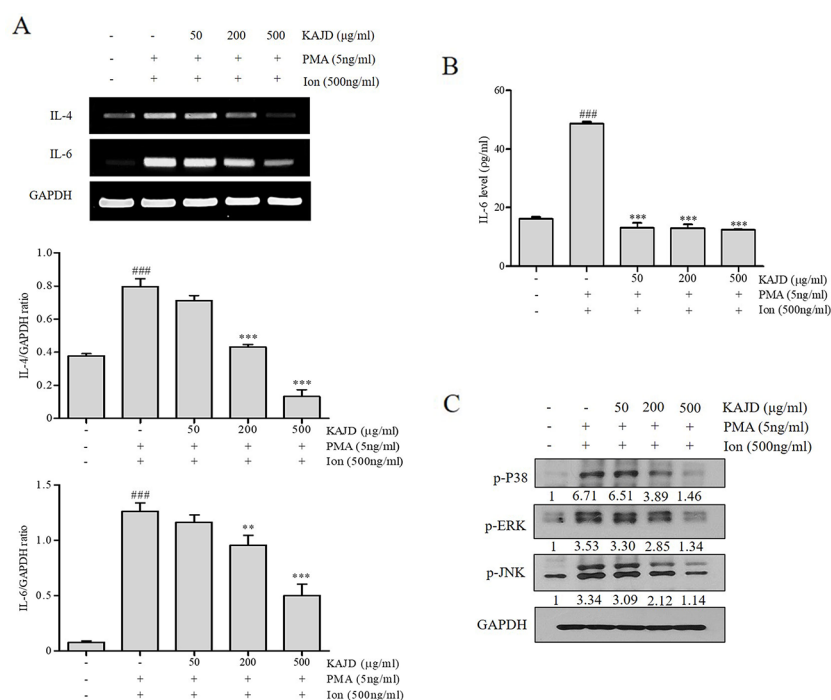


**FIGURE 8 |** KAJD inhibits MAPK pathways and suppresses the mRNA and protein expression of proinflammatory molecules in HMC-1 cells. **(A)** The IL-4 and IL-6 mRNA levels were measured by RT-PCR in HMC-1 cells treated with the reagents described in **Figure 7 (A)**. The bar graphs represent the quantitation of RT-PCR data. **(B)** The level of IL-6 in cell culture supernatants was measured by ELISA. HMC-1 cells were stimulated with both 5 ng/ml PMA and 500 ng/ml Ion for 1 h and treated with varying concentrations of KAJD for 24 h. **(C)** Phosphorylated ERK1/2, p38, and JNK levels in cell lysates were determined by immunoblot analysis. GAPDH was used as an internal control. Data are presented as the mean  $\pm$  SEM. <sup>###</sup> $P < 0.001$  compared to nonstimulated cells. <sup>\*</sup> $P < 0.05$ , <sup>\*\*</sup> $P < 0.01$  and <sup>\*\*\*</sup> $P < 0.001$  compared to stimulated cells. PMA, phorbol-12-myristate-13-acetate; Ion, ionomycin.

## DATA AVAILABILITY

The raw data supporting the conclusions of this manuscript will be made available by the authors, without undue reservation, to any qualified researcher.

## ETHICS STATEMENT

All the experiments were performed in accordance with the protocols approved by the Institutional Animal Care and Use Committees of Kyung Hee University (Approval Number KHUASP (SE)-14-014). The authors highly acknowledged the Department of Preventive Medicine for providing lab facilities.

## AUTHOR CONTRIBUTIONS

SH carried out the experiment and drafted the manuscript. SH, JK and HK revised the research and manuscript and assisted in the research work. SH, TK, HS and YS guided the research and revised and submitted the manuscript. S-GK supervised the research. All the authors read and approved the final manuscript.

## FUNDING

This research was supported by a grant from the Korean Medicine R&D Project of the Ministry of Health and Welfare (HI12C1889 and HI13C0530, HI11C2110). The funding sponsors had no role in the study design, performance, data collection and analysis, decision to publish, or preparation/writing of the manuscript.

## REFERENCES

- Ahmadzadeh, M., Hussain, S. F., and Farber, D. L. (2001). Heterogeneity of the memory CD4 T cell response: persisting effectors and resting memory T cells. *J. Immunol.* 166, 926–935. doi: 10.4049/jimmunol.166.2.926
- Akhavan, A., and Rudikoff, D. (2008). Atopic dermatitis: systemic immunosuppressive therapy. *Semin Cutan Med. Surg.* 27, 151–155. doi: 10.1016/j.sder.2008.04.004
- Auffray, C., Fogg, D., Garfa, M., Elain, G., Join-Lambert, O., Kayal, S., et al. (2007). Monitoring of blood vessels and tissues by a population of monocytes with patrolling behavior. *Science* 317, 666–670. doi: 10.1126/science.1142883
- Bae, C. J., Shim, S. B., Jee, S. W., Lee, S. H., Kim, M. R., Lee, J. W., et al. (2010). IL-6, VEGF, KC and RANTES are a major cause of a high irritant dermatitis to phthalic anhydride in C57BL/6 inbred mice. *Allergol. Int.* 59, 389–397. doi: 10.2332/allergolint.10-OA-0207
- Blume-Peytavi, U., and Wahn, U. (2011). Optimizing the treatment of atopic dermatitis in children: a review of the benefit/risk ratio of methylprednisolone aceponate. *J. Eur. Acad. Dermatol. Venerol.* 25, 508–515. doi: 10.1111/j.1468-3083.2010.03942.x
- Choi, Y. Y., Kim, M. H., Han, J. M., Hong, J., Lee, T. H., Kim, S. H., et al. (2014). The anti-inflammatory potential of Cortex Phellodendron *in vivo* and *in vitro*: down-regulation of NO and iNOS through suppression of NF-kappaB and MAPK activation. *Int. Immunopharmacol.* 19, 214–220. doi: 10.1016/j.intimp.2014.01.020

## ACKNOWLEDGMENTS

The authors are very grateful for the Department of Preventive Medicine for providing laboratory facilities.

## SUPPLEMENTARY MATERIAL

The Supplementary Material for this article can be found online at: <https://www.frontiersin.org/articles/10.3389/fphar.2019.01097/full#supplementary-material>

**FIGURE S1** | Changes in (A) mouse body weight and (B) food intake during treatment with KAJD. Values are expressed as the mean  $\pm$  SEM (n=8). Vehicle, no treatment; DNCB, 2,4-dinitrochlorobenzene; TAC, tacrolimus.

**FIGURE S2** | Effect of KAJD on LPS-stimulated RAW264.7 cell viability. RAW264.7 cells were treated with various concentrations of KAJD for 24 h after vehicle (upper panel) or LPS (lower panel) pretreatment for 1 h (upper panel). After treatment, cell viability was measured using a WST assay. Data are presented as the mean  $\pm$  SEM. \*\*\*P < 0.001 compared to nonstimulated cells. \*\*\*P < 0.001 compared to stimulated cells. LPS, lipopolysaccharide.

**FIGURE S3** | Effect of KAJD on LPS-stimulated splenocyte cell viability. Splenocytes were treated with various concentrations of KAJD for 24 h after vehicle (upper panel) or LPS (lower panel) pretreatment for 1 h (upper panel). After treatment, cell viability was measured using a WST assay. Data are presented as the mean  $\pm$  SEM. \*\*P < 0.01 and \*\*\*P < 0.001 compared to nonstimulated cells. \*\*P < 0.01 compared to stimulated cells. LPS, lipopolysaccharide.

**FIGURE S4** | Effect of KAJD on PMA and ionomycin-stimulated HMC-1 cell viability. HMC-1 cells were treated with various concentrations of KAJD for 24 h after the pretreatment of vehicle (upper panel) or PMA plus Ion (lower panel) for 1 h (upper panel). After treatment, cell viability was measured using a WST assay. Data are presented as the mean  $\pm$  SEM. \*\*\*P < 0.001 compared to nonstimulated cells. \*P < 0.05 and \*\*\*P < 0.001 compared to stimulated cells. PMA, phorbol-12-myristate-13-acetate; Ion, ionomycin.

- Danso, M. O., Van Drongelen, V., Mulder, A., Van Esch, J., Scott, H., Van Smeden, J., et al. (2014). TNF-alpha and Th2 cytokines induce atopic dermatitis-like features on epidermal differentiation proteins and stratum corneum lipids in human skin equivalents. *J. Invest. Dermatol.* 134, 1941–1950. doi: 10.1038/jid.2014.83
- Dearman, R. J., Basketter, D. A., and Kimber, I. (1995). Differential cytokine production following chronic exposure of mice to chemical respiratory and contact allergens. *Immunology* 86, 545–550.
- Hammad, H., and Lambrecht, B. N. (2008). Dendritic cells and epithelial cells: linking innate and adaptive immunity in asthma. *Nat. Rev. Immunol.* 8, 193–204. doi: 10.1038/nri2275
- Han, Y., Jung, H. W., Lee, J. Y., Kim, J. S., Kang, S. S., Kim, Y. S., et al. (2012). 2,5-dihydroxyacetophenone isolated from Rehmannia radix Preparata inhibits inflammatory responses in lipopolysaccharide-stimulated RAW264.7 macrophages. *J. Med. Food* 15, 505–510. doi: 10.1089/jmf.2011.1940
- Hanifin, J. M., Paller, A. S., Eichenfield, L., Clark, R. A., Korman, N., Weinstein, G., et al. (2005). Efficacy and safety of tacrolimus ointment treatment for up to 4 years in patients with atopic dermatitis. *J. Am. Acad. Dermatol.* 53, S186–S194. doi: 10.1016/j.jaad.2005.04.062
- Hiroyoshi, T., Tsuchida, M., Uchiyama, K., Fujikawa, K., Komatsu, T., Kanaoka, Y., et al. (2012). Splenectomy protects the kidneys against ischemic reperfusion injury in the rat. *Transpl. Immunol.* 27, 8–11. doi: 10.1016/j.trim.2012.03.005

- Ho-Sub, L., Kwan-Ha, P., Kang-Beom, K., Byeong-Sun, M., Cheol-Min, S., Yong-Seon, S., et al. (2001). Anti-allergic activity of the Sophorae radix water extract in experimental animals. *Am. J. Chin. Med.* 29, 129–139. doi: 10.1142/S0192415X01000149
- Holgate, S. T., and Polosa, R. (2008). Treatment strategies for allergy and asthma. *Nat. Rev. Immunol.* 8, 218–230. doi: 10.1038/nri2262
- Homey, B., Steinhoff, M., Ruzicka, T., and Leung, D. Y. (2006). Cytokines and chemokines orchestrate atopic skin inflammation. *J. Allergy Clin. Immunol.* 118, 178–189. doi: 10.1016/j.jaci.2006.03.047
- Ipaktchi, K., Mattar, A., Niederbichler, A. D., Hoesel, L. M., Hemmila, M. R., Su, G. L., et al. (2006). Topical p38MAPK inhibition reduces dermal inflammation and epithelial apoptosis in burn wounds. *Shock* 26, 201–209. doi: 10.1097/01.shk.0000225739.13796.f2
- Kasraie, S., and Werfel, T. (2013). Role of macrophages in the pathogenesis of atopic dermatitis. *Mediators Inflamm.* 2013, 942375. doi: 10.1155/2013/942375
- Kim, S. R., Choi, H. S., Seo, H. S., Ku, J. M., Hong, S. H., Yoo, H. H., et al. (2014). Oral Administration of herbal mixture extract inhibits 2,4-dinitrochlorobenzene-induced atopic dermatitis in BALB/c mice. *Mediators Inflamm.* 2014, 319–438. doi: 10.1155/2014/319438
- Ku, J. M., Hong, S. H., Kim, H. I., Seo, H. S., Shin, Y. C., and Ko, S. G. (2017). Effects of Angelicae dahuricae radix on 2, 4-dinitrochlorobenzene-induced atopic dermatitis-like skin lesions in mice model. *BMC Complement. Altern. Med.* 17, 98. doi: 10.1186/s12906-017-1584-8
- Lee, Y. C., Lee, J. C., Seo, Y. B., and Kook, Y. B. (2005). Liriodopsis tuber inhibit OVA-induced airway inflammation and bronchial hyperresponsiveness in murine model of asthma. *J. Ethnopharmacol.* 101, 144–152. doi: 10.1016/j.jep.2005.04.030
- Leung, D. Y., and Bieber, T. (2003). Atopic dermatitis. *Lancet* 361, 151–160. doi: 10.1016/S0140-6736(03)12193-9
- Liu, F. T., Goodarzi, H., and Chen, H. Y. (2011). IgE, mast cells, and eosinophils in atopic dermatitis. *Clin. Rev. Allergy Immunol.* 41, 298–310. doi: 10.1007/s12016-011-8252-4
- Liu, Y. J. (2009). TSLP in epithelial cell and dendritic cell cross talk. *Adv. Immunol.* 101, 1–25. doi: 10.1016/S0065-2776(08)01001-8
- Lubach, D., Bensmann, A., and Bornemann, U. (1989). Steroid-induced dermal atrophy. Investigations on discontinuous application. *Dermatologica* 179, 67–72. doi: 10.1159/000248314
- Marsella, R., Olivry, T., Carlotti, D. N., and De, I. T. F. O. C. A. (2011). Current evidence of skin barrier dysfunction in human and canine atopic dermatitis. *Vet. Dermatol.* 22, 239–248. doi: 10.1111/j.1365-3164.2011.00967.x
- Novak, N., Valenta, R., Bohle, B., Laffer, S., Haberstok, J., Kraft, S., et al. (2004). FcεpsilonRI engagement of Langerhans cell-like dendritic cells and inflammatory dendritic epidermal cell-like dendritic cells induces chemotactic signals and different T-cell phenotypes in vitro. *J. Allergy Clin. Immunol.* 113, 949–957. doi: 10.1016/j.jaci.2004.02.005
- Ong, P. Y., and Leung, D. Y. (2006). Immune dysregulation in atopic dermatitis. *Curr. Allergy Asthma. Rep.* 6, 384–389. doi: 10.1007/s11882-996-0008-5
- Pastore, S., Mascia, F., and Girolomoni, G. (2006). The contribution of keratinocytes to the pathogenesis of atopic dermatitis. *Eur. J. Dermatol.* 16, 125–131.
- Prabhakaran, K., Lau, H. T., Wise, B., Schwarz, K., and Colombani, P. M. (1999). Incidence of allergic symptoms in pediatric liver transplant recipients treated with tacrolimus based immunosuppression. *Pediatrics* 104, 786–787.
- Ra, J., Chung, J. H., Lee, H., and Kim, J. (2011). Reduction of interleukin-1β induced matrix metalloproteinase-3 release by extracts of six plants: inhibitory screening of 35 traditional medicinal plants. *Immunopharmacol. Immunotoxicol.* 33, 461–465. doi: 10.3109/08923973.2010.537663
- Reitamo, S., Rissanen, J., Remitz, A., Granlund, H., Erkkö, P., Elg, P., et al. (1998). Tacrolimus ointment does not affect collagen synthesis: results of a single-center randomized trial. *J. Invest Dermatol.* 111, 396–398. doi: 10.1046/j.1523-1747.1998.00323.x
- Robbins, C. S., Chudnovskiy, A., Rauch, P. J., Figueiredo, J. L., Iwamoto, Y., Gorbato, R., et al. (2012). Extramedullary hematopoiesis generates Ly-6C(high) monocytes that infiltrate atherosclerotic lesions. *Circulation* 125, 364–374. doi: 10.1161/CIRCULATIONAHA.111.061986
- Rousset, F., Robert, J., Andary, M., Bonnin, J. P., Souillet, G., Chretien, I., et al. (1991). Shifts in interleukin-4 and interferon-gamma production by T cells of patients with elevated serum IgE levels and the modulatory effects of these lymphokines on spontaneous IgE synthesis. *J. Allergy Clin. Immunol.* 87, 58–69. doi: 10.1016/0091-6749(91)90213-8
- Saklatvala, J. (2004). The p38 MAP kinase pathway as a therapeutic target in inflammatory disease. *Curr. Opin. Pharmacol.* 4, 372–377. doi: 10.1016/j.coph.2004.03.009
- Schultz Larsen, F. (1993). The epidemiology of atopic dermatitis. *Monogr. Allergy* 31, 9–28.
- Shin, E. M., Zhou, H. Y., Guo, L. Y., Kim, J. A., Lee, S. H., Merfort, I., et al. (2008). Anti-inflammatory effects of glycyrrhizic acid isolated from Glycyrrhiza uralensis in LPS-stimulated RAW264.7 macrophages. *Int. Immunopharmacol.* 8, 1524–1532. doi: 10.1016/j.intimp.2008.06.008
- Simon, D., Braathen, L. R., and Simon, H. U. (2004). Eosinophils and atopic dermatitis. *Allergy* 59, 561–570. doi: 10.1111/j.1398-9995.2004.00476.x
- Simpson, E. L. (2010). Atopic dermatitis: a review of topical treatment options. *Curr. Med. Res. Opin.* 26, 633–640. doi: 10.1185/03007990903512156
- Spergel, J. M., and Paller, A. S. (2003). Atopic dermatitis and the atopic march. *J. Allergy Clin. Immunol.* 112, S118–S127. doi: 10.1016/j.jaci.2003.09.033
- Stahlmann, R., Wegner, M., Riecke, K., Kruse, M., and Platzeck, T. (2006). Sensitising potential of four textile dyes and some of their metabolites in a modified local lymph node assay. *Toxicology* 219, 113–123. doi: 10.1016/j.tox.2005.11.005
- Theoharides, T. C., Alysandratos, K. D., Angelidou, A., Delivanis, D. A., Sismanopoulos, N., Zhang, B., et al. (2012). Mast cells and inflammation. *Biochim. Biophys. Acta* 1822, 21–33. doi: 10.1016/j.bbdis.2010.12.014
- Valledor, A. F., Comalada, M., Santamaria-Babi, L. F., Lloberas, J., and Celada, A. (2010). Macrophage proinflammatory activation and deactivation: a question of balance. *Adv. Immunol.* 108, 1–20. doi: 10.1016/B978-0-12-380995-7.00001-X
- Wang, H., Zhang, J. X., Li, S. L., Wang, F., Zha, W. S., Shen, T., et al. (2015). An animal model of trichloroethylene-induced skin sensitization in BALB/c Mice. *Int. J. Toxicol.* 34, 442–453. doi: 10.1177/1091581815591222
- Wu, G. S. (2004). The functional interactions between the p53 and MAPK signaling pathways. *Cancer Biol. Ther.* 3, 156–161. doi: 10.4161/cbt.3.2.614
- Wystrychowski, W., Filipczyk, L., Cierpka, L., Obuchowicz, E., Wiecek, A., and Wystrychowski, A. (2014). Splenectomy attenuates the course of kidney ischemia-reperfusion injury in rats. *Transplant Proc.* 46, 2558–2561. doi: 10.1016/j.transproceed.2014.09.056
- Yoon, H. J., Jang, M. S., Kim, H. W., Song, D. U., Nam, K. I., Bae, C. S., et al. (2015). Protective effect of diet supplemented with rice prolamin extract against DNCB-induced atopic dermatitis in BALB/c mice. *BMC Complement. Altern. Med.* 15, 353. doi: 10.1186/s12906-015-0892-0

**Conflict of Interest Statement:** The authors declare that the research was conducted in the absence of any commercial or financial relationships that could be construed as a potential conflict of interest.

Copyright © 2019 Hong, Ku, Kim, Kim, Seo, Shin and Ko. This is an open-access article distributed under the terms of the Creative Commons Attribution License (CC BY). The use, distribution or reproduction in other forums is permitted, provided the original author(s) and the copyright owner(s) are credited and that the original publication in this journal is cited, in accordance with accepted academic practice. No use, distribution or reproduction is permitted which does not comply with these terms.



# Black Walnut (*Juglans nigra*) Extracts Inhibit Proinflammatory Cytokine Production From Lipopolysaccharide-Stimulated Human Promonocytic Cell Line U-937

Khanh-Van Ho<sup>1,2</sup>, Kathy L. Schreiber<sup>3</sup>, Danh C. Vu<sup>1</sup>, Susan M. Rottinghaus<sup>3</sup>, Daniel E. Jackson<sup>3</sup>, Charles R. Brown<sup>4</sup>, Zhentian Lei<sup>5,6</sup>, Lloyd W. Sumner<sup>5,6</sup>, Mark V. Coggeshall<sup>7</sup> and Chung-Ho Lin<sup>1\*</sup>

## OPEN ACCESS

### Edited by:

Namrita Lall,  
University of Pretoria,  
South Africa

### Reviewed by:

Lyndy Joy McGaw,  
University of Pretoria,  
South Africa  
Sefirin Djiogue,  
University of Yaounde I,  
Cameroon

### \*Correspondence:

Chung-Ho Lin  
LinChu@missouri.edu

### Specialty section:

This article was submitted to  
Ethnopharmacology,  
a section of the journal  
Frontiers in Pharmacology

**Received:** 15 March 2019

**Accepted:** 20 August 2019

**Published:** 19 September 2019

### Citation:

Ho K-V, Schreiber KL, Vu DC, Rottinghaus SM, Jackson DE, Brown CR, Lei Z, Sumner LW, Coggeshall MV and Lin C-H (2019) Black Walnut (*Juglans nigra*) Extracts Inhibit Proinflammatory Cytokine Production From Lipopolysaccharide-Stimulated Human Promonocytic Cell Line U-937. *Front. Pharmacol.* 10:1059. doi: 10.3389/fphar.2019.01059

<sup>1</sup> Center for Agroforestry, School of Natural Resources, University of Missouri, Columbia, MO, United States, <sup>2</sup> Department of Food Technology, Can Tho University, Can Tho, Vietnam, <sup>3</sup> Cell and Immunobiology Core, University of Missouri, Columbia, MO, United States, <sup>4</sup> Department of Veterinary Pathobiology, University of Missouri, Columbia, MO, United States, <sup>5</sup> Metabolomics Center, University of Missouri, Columbia, MO, United States, <sup>6</sup> Department of Biochemistry, Bond Life Sciences Center, University of Missouri, Columbia, MO, United States, <sup>7</sup> United States Northern Research Station, USDA-Forest Service, West Lafayette, IN, United States

Black walnut (*Juglans nigra* L.) is an excellent source of health-promoting compounds. Consumption of black walnuts has been linked to many health benefits (e.g., anti-inflammatory) stemming from its phytochemical composition and medicinal properties, but these effects have not been systematically studied or characterized. In this study, potential anti-inflammatory compounds found in kernel extracts of 10 black walnut cultivars were putatively identified using a metabolomic profiling analysis, revealing differences in potential anti-inflammatory capacities among examined cultivars. Five cultivars were examined for activities in the human promonocytic cell line U-937 by evaluating the effects of the extracts on the expression of six human inflammatory cytokines/chemokines using a bead-based, flow cytometric multiplex assay. The methanolic extracts of these cultivars were added at four concentrations (0.1, 0.3, 1, and 10 mg/ml) either before and after the addition of lipopolysaccharide (LPS) to human U-937 cells to examine their effect on cytokine production. Results from cytotoxicity and viability assays revealed that the kernel extracts had no toxic effect on the U-937 cells. Of the 13 cytokines [interleukin (IL)-1 $\beta$ , tumor necrosis factor alpha (TNF- $\alpha$ ), monocyte chemoattractant protein (MCP)-1, IL-6, IL-8, IL-10, IL-12, IL-17, IL-18, IL-23, IL-33, interferon (IFN)- $\alpha$ , IFN- $\gamma$ ] measured, only six were detected under the culture conditions. The production of the six detected cytokines by phorbol 12-myristate 13-acetate (PMA)-differentiated, LPS-stimulated U-937 was significantly inhibited by the kernel extracts from two cultivars Surprise and Sparrow when the extracts were added before the addition of LPS. Other cultivars (Daniel, Mistry, and Sparks) showed weak or no significant effects on cytokine production. In contrast, no inhibitory effect was observed on the production of cytokines by PMA-differentiated, LPS-stimulated U-937 when the



kernel extracts were added after the addition of LPS. The findings suggest that the extracts from certain black walnut cultivars, such as Sparrow and Surprise, are promising biological candidates for potentially decreasing the severity of inflammatory disease.

**Keywords:** black walnut, *Juglans nigra*, metabolomic profiling, cytokine suppression, potential anti-inflammatory compounds

## INTRODUCTION

Inflammation is a complex pathophysiological response of the immune system in response to infections of harmful stimuli or tissue damage (Medzhitov, 2010). An uncontrolled inflammatory response might result in development of a variety of chronic inflammatory diseases such as rheumatoid arthritis (RA). RA is the most common inflammatory arthritis affecting ~1% of population worldwide (Firestein, 2003). This inflammatory disease is associated with articular inflammation and synovial joint damage that can result in disability and increased mortality. In synovial tissues, several cytokines are released and are functionally active in mediating immune responses associated with the pathogenesis of RA (McInnes and Schett, 2007). Cytokines are therapeutic targets for the treatment of patients with RA [tumor necrosis factor (TNF)] and in RA clinical trials [e.g., interleukin (IL)-1, IL-6, IL-27] (McInnes et al., 2016).

Black walnut (*Juglans nigra* L.) is one of the most economically valuable hardwood species in the United States (Randolph et al., 2013). Native Americans traditionally valued kernels of black walnut as a food source and utilized leaves for medical purposes to treat diarrhea, bilious, and cramp colic (Nolan and Robbins, 1999). A recent report indicated that the kernels of black walnut contain a wealth of phytochemical substances (Vu et al., 2018), and many of these phenolic compounds are associated with a variety of biological functions such as antioxidant, antimicrobial, and anti-inflammatory properties. Our previous study demonstrated antibacterial activities of the kernels from black walnut against a Gram-positive bacterium (*Staphylococcus aureus* RN6390), and its antibacterial compounds (e.g., glansreginin A, azelaic acid) were successfully identified (Ho et al., 2018).

Anti-inflammatory capacities of another common *Juglans* species, English walnut (*Juglans regia* L.) have been well established *in vitro* and *in vivo*. Willis et al. (2010) reported that kernel extracts of English walnut reduced production of TNF- $\alpha$  and nitric oxide synthase induced by BV-2 murine microglial cells stimulated with lipopolysaccharide (LPS) when the cells were pretreated with the extract before stimulation with LPS. Papoutsis et al. (2008) also documented that extracts of English walnut decreased expression of TNF- $\alpha$ -induced endothelial vascular cell adhesion molecule (VCAM)-1 and intracellular adhesion molecule (ICAM)-1 expression in human aortic endothelial cells. *In vivo*, consumption of English walnut was associated with multiple health benefits with respect to alleviating inflammation and oxidative stress and improving vascular function in both animals and human clinical trials (Ros, 2015). In fact, the consumption of English walnut was associated with a lowered risk of type 2 diabetes (Pan et al., 2013) and a reduction in the

incidence of major cardiovascular events (Estruch et al., 2013) in two randomized clinical trials of 137,956 women aged 35–77 over 10 years and of 7,447 participants aged 55–80 (47% were men), respectively. Anti-inflammatory functions of English walnut are likely associated with its phytochemical compounds. Remarkably, English walnut and black walnut share a similar phytochemical profile, revealing potential anti-inflammatory capacities of black walnut extracts. In fact, 16 phenolic compounds characterized in English walnut are also found in black walnut (Vu et al., 2018). Nonetheless, anti-inflammatory properties of black walnut have never been characterized yet. Exploring the anti-inflammatory properties of black walnut might point to novel uses of black walnut and its by-products, promoting development of new biological agents for the prevention or even treatment of inflammation as well as increasing the value of black walnuts by identifying new applications and health benefits.

In the present study, we first examined and compared effects of kernel extracts from 10 black walnut cultivars *via* a global metabolomic profiling approach. We then characterized possible anti-inflammatory properties in kernel extracts of five selective cultivars by evaluating the expression of six inflammatory mediators (IL-1 $\beta$ , TNF- $\alpha$ , MCP-1, IL-6, IL-8, and IL-10) using the human promonocytic cell line U-937.

## MATERIALS AND METHODS

**Black walnut cultivars.** The nuts of 10 black walnut cultivars including Daniel, Davidson, Hay, Jackson, Kwik Krop, Mystry, Schessler, Sparks, Sparrow, and Surprise were collected at the University of Missouri, Horticulture and Agroforestry Research Center (New Franklin, MO, USA). The black walnuts were hulled mechanically and hung up to dry at 24°C for 15 days. The hulled nuts were then stored at –20°C until analysis.

**Sample preparation.** The hulled nuts were cracked manually and the kernels removed from the shell and homogenized using a coffee grinder (CBG100S, Black + Decker, Beachwood, OH, USA). For metabolomic analysis, the kernels (2.5 g, 20–30 mesh) from 10 cultivars were extracted by sonication in 15 ml methanol. The methanolic extract was sonicated in a water bath (4°C) for 60 min followed by centrifugation for 10 min at 8,000 rpm. The supernatant was collected and filtered through a 0.2- $\mu$ m Whatman Anotop syringe membrane filter (Sigma-Aldrich, St. Louis, MO, USA) and then injected into ultra high-performance liquid chromatography tandem mass spectrometry (UHPLC-MS). For assays, the kernels (2.5 g) from five selective cultivars (i.e., Daniel, Mystry, Sparks, Sparrow, and Surprise) were extracted by sonication in 10 ml of methanol. The extract was sonicated for

60 min followed by centrifugation for 10 min at 4,000 rpm, and the supernatant was collected. Subsequently, the supernatant was filtered through the syringe membrane filter (0.2  $\mu$ m, Whatman). The aqueous extract was evaporated until dryness under a flow of nitrogen and was resuspended with 0.125 ml of dimethyl sulfoxide (DMSO) (Sigma-Aldrich, USA), and then, the resulting extract was concentrated 40 times to achieve the concentration of 10,000 mg/ml. Cytokine-modulating activities of the extract were identified using multiplex bead-based cytokine assay kits (BioLegendplex™ Human Inflammation panel kits, BioLegend, San Diego, CA, USA).

**UHPLC-QTOF-MS analysis to examine metabolite profiles of black walnut.** The kernel extracts (2  $\mu$ l per injection) from 10 black walnut cultivars were analyzed by UHPLC coupled to a maXis impact quadrupole time-of-flight mass spectrometer (Bruker Co., Billerica, MA, USA). Separations were achieved on a Waters Acquity UHPLC BEH C18 column (2.1  $\times$  150 mm, 1.7  $\mu$ m particle size) using a linear gradient of 95%/5–30%/70% eluents A/B (A: 0.1% formic acid and B: acetonitrile) in 30 min. Subsequently, the separation was followed by a linear wash gradient as follows: 70–95% B (30–33 min), 95% B (33–35 min), 95–5% B (35–36 min), and 5% B (37–40 min), respectively. The column temperature was kept at 60°C, and the flow rate was 0.56 ml/min. Mass spectrometry was performed in both negative and positive electrospray ionization modes with the nebulization gas pressure at 43.5 psi, dry gas of 12 l/min, dry temperature of 250°C, and a capillary voltage of 4,000 V. Mass spectral data were collected automatically from 100 to 1,500 m/z; three precursors were selected for auto MS/MS and m/z range auto-calibrated using sodium formate after data acquisition. Each cultivar was analyzed in triplicate along with methanol blank used as a control.

**Cell culture and differentiation induction.** The human monocyte cell line U-937 was purchased from American Type Culture Collection (ATCC) (CRL-1593.2, ATCC, Manassas, VA, USA). U-937 cells were cultured in complete Roswell Park Memorial Institute (RPMI) medium (RPMI 1640, ATCC) supplemented with 10% fetal bovine serum (FBS, Sigma-Aldrich) and 100  $\mu$ g/ml gentamicin, and then incubated at 37°C in a 5% CO<sub>2</sub> humidified atmosphere. U-937 cells were seeded at  $2 \times 10^5$  cells/well in 96-well plates in a 200- $\mu$ l volume in the presence of 50 nM of phorbol 12-myristate 13-acetate (PMA, Sigma-Aldrich) for 48 h (Rovera et al., 1979) to induce differentiation. After washing the PMA-differentiated cells twice, fresh media was added, and the cultures were incubated for an additional 18 h at 37°C in a 5% CO<sub>2</sub> humidified atmosphere before the addition of extracts. Subsequently, the cultures were pretreated with extract dilutions from five cultivars (Daniel, Mystry, Sparks, Sparrow, and Surprise) at four final concentrations (0.1, 0.3, 1, and 10 mg/ml) for 2 h before stimulation with 1  $\mu$ g/ml LPS (*Escherichia coli* 0127:B8, Sigma-Aldrich). In some experiments, the PMA-differentiated cells were stimulated with LPS for 2 h before the addition of two cultivar extracts (Sparrow and Surprise). Extracts were prepared in tissue-culture-grade DMSO, and the highest concentration of DMSO in any cultivar sample was 0.1%. An immunosuppressant drug, cyclosporin A (CSA, Sigma-Aldrich), was added at a final concentration of 0.002 mg/ml in 0.02% DMSO and served as a positive control for the inhibition of cytokine secretion. Samples

without CSA or cultivars were supplemented with 0.1% DMSO and served as vehicle controls. Twenty-four hours after the addition of LPS and extracts, the triplicate culture supernatants from each group were pooled, spun to remove cell debris, transferred to new tubes, and stored at –20°C until analysis. Cytokine secretion levels in LPS-stimulated, cultivar-treated cultures were compared to samples containing DMSO but not cultivars. Viability of the attached cells was determined using a 3-(4, 5-dimethylthiazol-2-yl)-2, 5-diphenyltetrazolium bromide (MTT) assay (see methods section below).

A macrophage model system was chosen to investigate the anti-inflammatory potential of black walnut extracts because macrophages are central to the inflammatory response and are active during all phases of inflammation. The U-937 cell line can be induced to differentiate with PMA, and the addition of LPS derived from Gram-negative bacterial cell walls results in the release of numerous inflammatory mediators. These cytokines include, but are not limited to, TNF- $\alpha$ , IL-1 $\beta$ , and IL-6, which in turn contribute to the recruitment and activation of other immune cells against bacterial infections (Gordon, 2002). Since cytokines such as TNF, IL-6, and IL-1 $\beta$  play primary roles in the pathogenesis of RA (Smolen and Aletaha, 2015), they can be used as key biomarkers of RA.

**Quantification of secretion of cytokines/chemokines by macrophages.** The LEGENDplex™ human inflammation bead-based immunoassay was used to quantitate the secretion of cytokines in the U-937 culture model system in the absence or presence of black walnut extract, according to the manufacturer's procedure. Initial experiments were performed using a predefined panel of 13 inflammatory analytes (IL-1 $\beta$ , TNF- $\alpha$ , MCP-1, IL-6, IL-8, IL-10, IL-12, IL-17, IL-18, IL-23, IL-33, IFN- $\alpha$ , and IFN- $\gamma$ ), but subsequent experiments focused on a subset of six cytokines. Data were collected on a BD LSR Fortessa™ X-20 cell analyzer (BD Biosciences, San Jose, CA, USA) using instrument settings recommended by BioLegend. A cytokine standard curve was included in each experiment, and cytokine levels were calculated from a five-parameter logistic curve using the software provided in the BioLegend kit. Triplicates were collected at each cultivar concentration in multiple experiments.

**Effects of black walnut extracts on cell viability.** The MTT assays were performed to evaluate the effect of black walnut extracts on cytotoxicity and/or cell loss at the time of supernatant collection. A colorimetric cell viability assay (CGD1-1KT, Sigma-Aldrich) using MTT as the substrate (Mosmann, 1983) was carried out after collection of the supernatants. The ability of the cells to convert MTT to formazan crystals indicates mitochondrial activity and cell viability. Dulbecco's modified eagle medium high-glucose phenol red free media (Fisher Scientific, Pittsburgh, PA, USA) containing 1% FBS and MTT was added to each well, and the plates were incubated for 3 h at 37°C until precipitates were observed. An acidified isopropanol solvent was then added to dissolve the formazan crystals, and the samples were pipetted several times to completely dissolve the crystals. Absorbance was measured within 30 min after solvent addition using a BioTek ELx808 microplate reader (BioTek, Winooski, Vermont, USA). Formazan crystals were detected at a wavelength of 570 nm, and background absorbance was measured at 630 nm.

## Statistical Analysis

For the metabolic analyses, the original UHPLC-MS data were converted into a format (\*.cdf) that is compatible with XCMS Online (<http://xcmsonline.scripps.edu>) (Tautenhahn et al., 2012), and they were processed using the XCMS Online algorithms. This web-based tool for metabolomics data allows converting data file for peak detection, peak grouping, retention time correction, and alignment. Pairwise analyses between each black walnut cultivar and the control (methanol) were performed to identify single ion ( $m/z$ ) features that were significantly different at  $p < 0.005$  and intensity  $\geq 10,000$  across the chromatographic time domain. The metabolites of the significant ion features were putatively identified based on the accurate mass of the molecular ions, referenced to METLIN metabolite mass spectral database containing over 1 million molecules (<http://metlin.scripps.edu>) (Guijas et al., 2018). Metabolites that have been reported to possess anti-inflammatory activities based on a literature search (Supplementary Table 1) were selected to initially examine profiles of black walnut cultivars and to identify potential anti-inflammatory compounds in each cultivar. Multivariate analyses such as partial least squares discriminant analysis (PLS-DA) and heat map were performed using MetaboAnalyst (Chong et al., 2018) to reveal differences in metabolic profiles among black walnut cultivars.

Relative cell viability was measured with the MTT assay according to the manufacturer's protocol. The amount of MTT conversion was determined by subtracting the background absorbance (630 nm) from the absorbance of formazan crystals at 570 nm ( $A_{570\text{ nm}} - A_{630\text{ nm}}$  = specific MTT absorbance). Cell viability was expressed relatively to the PMA-differentiated, LPS-stimulated sample (control sample) in the absence of black walnut cultivars. The percentage of cell viability (%) was calculated by dividing the specific MTT absorbance of the treated sample by the specific MTT absorbance of the control sample and multiplying by 100. The control sample was set at 100%.

Cytokine concentrations were determined in the multiplex bead-based assay by extrapolating the concentration from a five-parameter logistic standard curve using curve-fitting software. The absolute concentrations of each cytokine from treated samples were then compared to the control samples, as described above for the MTT assay. The relative percentage (%) was obtained by dividing the cytokine concentration of the treated sample by the cytokine concentration of the control sample and multiplying by 100. The PMA-differentiated, LPS-stimulated sample served as the control sample and was set at 100%.

The data were analyzed as a randomized complete block design using PROC MIXED in SAS 9.4 (SAS Institute, Cary, NC). The black walnut extract was the fixed effect, and replication was the random variable. Differences between extracts were determined using Fisher's least significant difference at  $p < 0.01$ .

## RESULTS

**Anti-inflammatory profiles of black walnut.** The anti-inflammatory profiles of the kernel extracts from 10 black walnut cultivars were characterized using data acquired from

liquid chromatography–high-resolution MS (LC-HRMS). The UHPLC-HRMS data processed with XCMS Online provided 650 and 420 significant features in positive and negative modes, respectively, which were further annotated using METLIN metabolite database. This resulted in the identification of 26 substances with known anti-inflammatory activities. These metabolites included flavanols, hydroxybenzoic acids, and ellagitannins (Supplementary Table 1). The PLS-DA score plot showed significant differences in anti-inflammatory profiles among 10 black walnut cultivars (Figure 1A). In the score plot, Sparrow and Schessler, Mystry and Sparks, and Daniel and Davidson were distributed separately on quadrants I, II, and IV, respectively, whereas other four cultivars including Kwik Krop, Jackson, Hay, and Surprise roughly clustered together in the intersection of quadrants I and IV. Five cultivars (Daniel, Mystry, Sparks, Sparrow, and Surprise) were chosen as representative examples for further examined for their ability to alter cytokine production using human promonocytic cell line U-937 because they were selected from different groups distributed in four distinct quadrants (I, II, IV, or the intersection of I and IV). This approach was utilized to select cultivars that capture the most potentially diverse set of anti-inflammatory compounds.

Each black walnut cultivar contained several potential anti-inflammatory compounds, and the relative concentrations of many compounds were distinct within specific cultivars (Figures 1B, C). Sparks and Mystry contained the highest relative abundance of gallic acid and four ellagitannins including tellimagrandin I isomer 1 and 3, punicalin isomer 1, and pedunculagin isomer 1, while cinnamic acid and quercetin neohesperidoside were relatively dominant in Daniel and Davidson. The highest relative abundance of ellagic acid was found in Surprise, and this cultivar also contained procyanidin dimer, quercetin neohesperidoside, and pedunculagin isomer 1 as major components. Kwik Krop contained the highest relative abundance of myricetin hexoside, procyanidin dimer, punicalin isomer 3, and dicaffeoylquinic acid isomer 2. Schessler and Sparrow also contained a variety of bioactive compounds. Quercetin glucoside, myricetin, and pedunculagin isomer 3 were presented dominantly in Sparrow, while vanillic acid and dicaffeoylquinic acid isomer 3 were major compounds in Schessler.

**Cell viability assays.** The cell viability assays were performed to address possible cytotoxic effects of the black walnut cultivars. A reduction in MTT absorbance could point to a decrease in cell viability, a decrease in mitochondrial activity, and/or cell loss, resulting in a concomitant decrease in cytokine secretion. MTT viability assays were performed at the same time cell supernatants were collected. CSA, a potent immunosuppressive agent capable of inhibiting cytokine production and release, was included in the experiments as a positive control. Black walnut extracts were resuspended in DMSO, and all experimental groups contained up to 0.1% DMSO. Control groups without extracts were supplemented with 0.1% DMSO to account for any adverse effects of the DMSO vehicle. The results indicated that the viability was not significantly different in any of the groups analyzed (Figure 2). These groups include no treatment (none, no LPS, and no black walnut extracts, with DMSO), LPS control



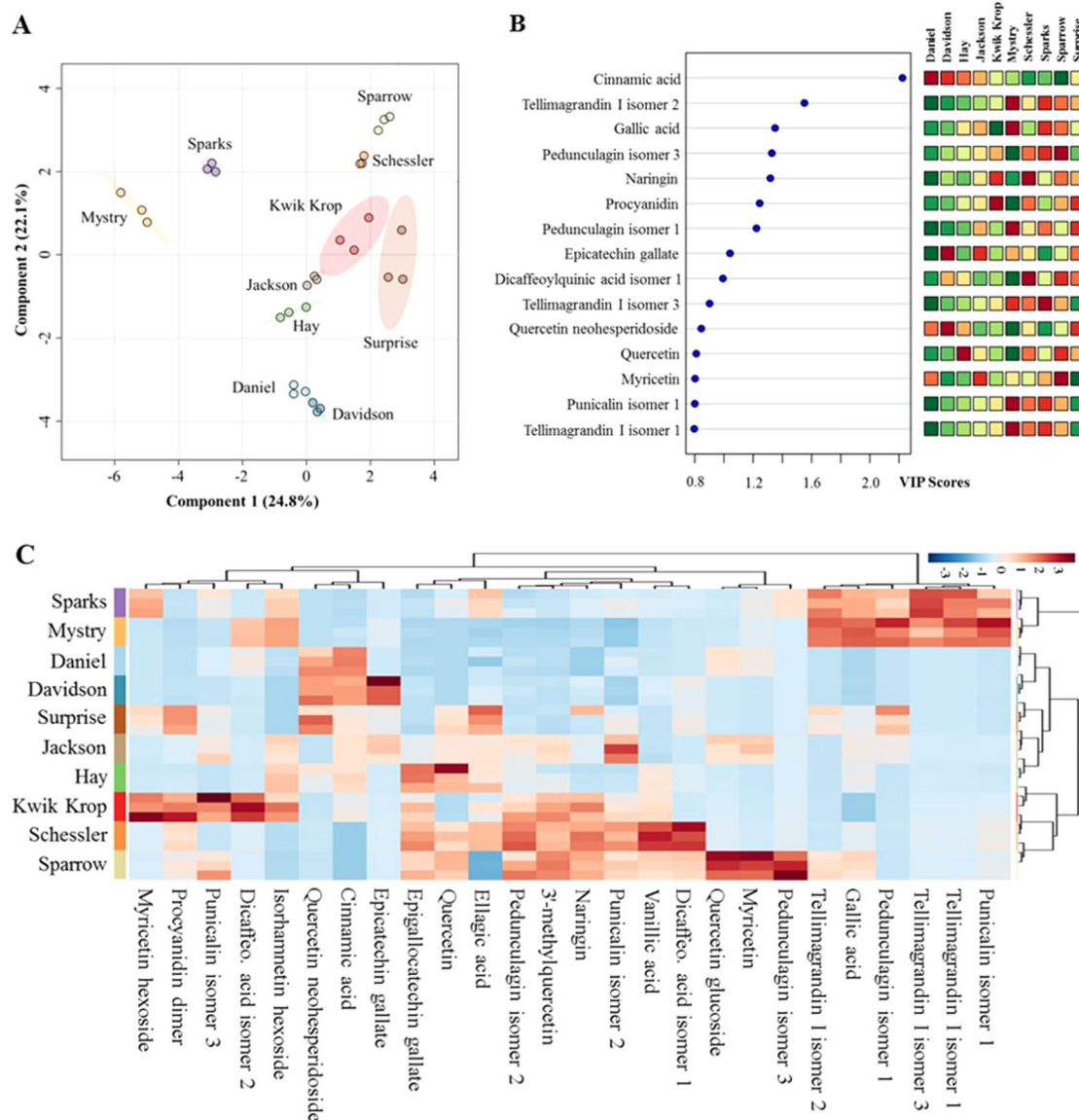


**FIGURE 1 |** Differences in metabolic profiles of black walnut cultivars. **(A)** Partial least squares discriminant analysis (PLS-DA). **(B)** Variable importance in projection (VIP) and **(C)** heat map. In the PLS-DA plot, circles with same colors represent replicates of metabolic profiles for each cultivar. The colored ellipses indicate 95% confidence regions of metabolic profiles for each cultivar. In the VIP score plot, 15 out of 26 metabolites in total were shown, and the colored boxes on the right indicate the relative abundance of the corresponding metabolite in each cultivar. Red represents higher relative abundance, whereas green and blue represent lower relative abundance in the VIP score plot and the heat map, respectively.

cultures (LPS: LPS and DMSO, no extract), treated cells (Daniel, Mystry, Sparks, Sparrow, and Surprise: extracts, DMSO, and LPS), and CSA (CSA: CSA, DMSO, and LPS). Since the extracts of all five cultivars and CSA at all the concentrations tested were nontoxic to the PMA-differentiated U-937 cells, they were selected for examining their effect on cytokine production.

**Secretion of cytokines.** Secreted cytokine levels were quantified in PMA-differentiated, LPS-stimulated U-937 cells after pretreatment with five representative cultivars at four concentrations. A predefined human inflammation bead-based multiplex kit was chosen because it could be used to detect

multiple cytokines simultaneously from the same sample with a small amount of the sample. The panel was comprised of 13 cytokines involved in various aspects of the inflammatory process, and many of these were studied previously in the U-937 model system. Of the six cytokines initially detected in the supernatants, five (TNF- $\alpha$ , IL-1 $\beta$ , IL-6, IL-8, and MCP-1) are proinflammatory and one (IL-10) is anti-inflammatory. Subsequent experiments focusing on these cytokines showed that secretion by PMA-differentiated, LPS-stimulated U-937 cells was significantly and dose-dependently attenuated by pretreatment with extracts derived from Sparrow and Surprise

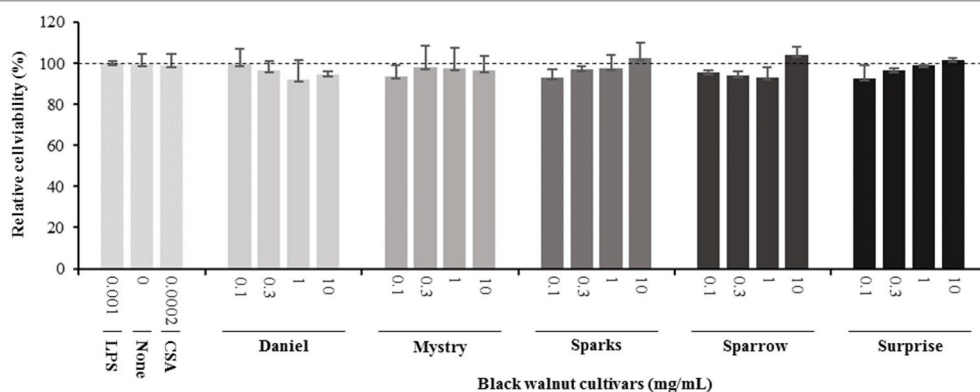


**FIGURE 2 |** Effect of lipopolysaccharide (LPS), an immune suppressor drug (cyclosporin A, CSA), and black walnut extracts on the viability of PMA-differentiated U-937 cells. None: PMA-differentiated cells in the absence of black walnut extract and LPS. Mean  $\pm$  SEM.

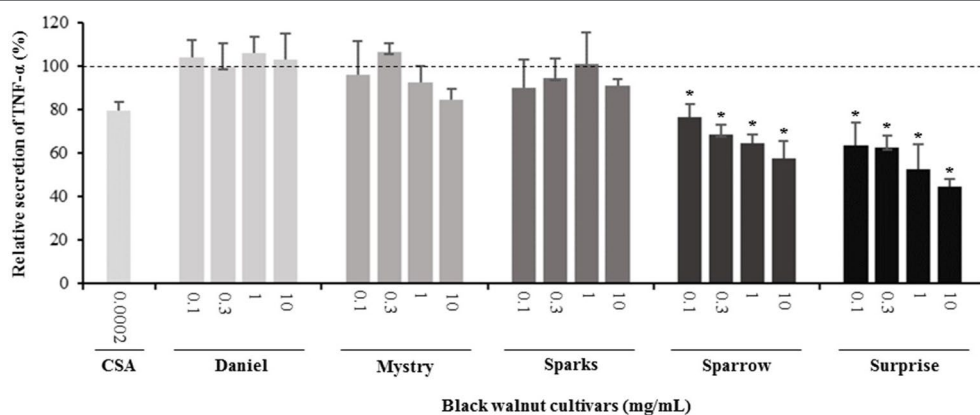


**FIGURE 3 |** Effect of black walnut extracts on the secretion of TNF- $\alpha$  by PMA-differentiated, LPS-stimulated U937 cells. Cyclosporin A (CSA) was used as a positive control. (\*) Significant decrease ( $p < 0.01$ ) compared to PMA-differentiated, LPS-stimulated U937 cells in the absence of extract. Mean  $\pm$  SEM.

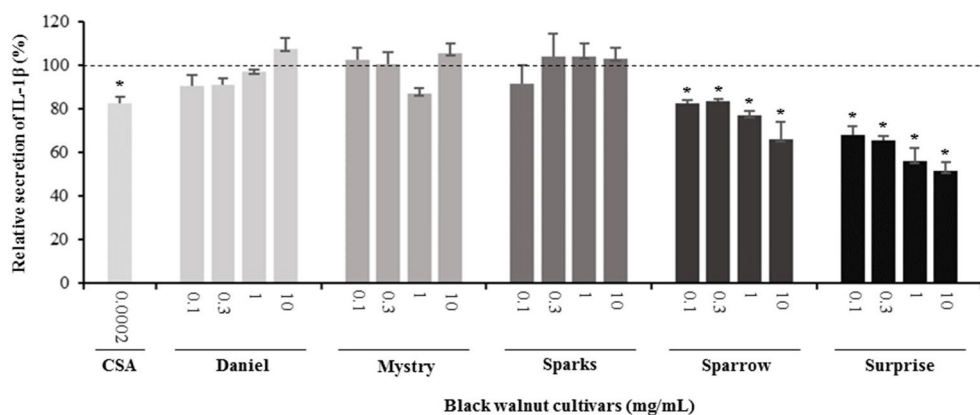


**FIGURE 4 |** Effect of black walnut extracts on the secretion of IL-1 $\beta$  by PMA-differentiated, LPS-stimulated U937 cells. Cyclosporin A (CSA) was used as a positive control. (\*) Significant decrease ( $p < 0.01$ ) compared to PMA-differentiated, LPS-stimulated U937 cells in the absence of extracts. Mean  $\pm$  SEM.

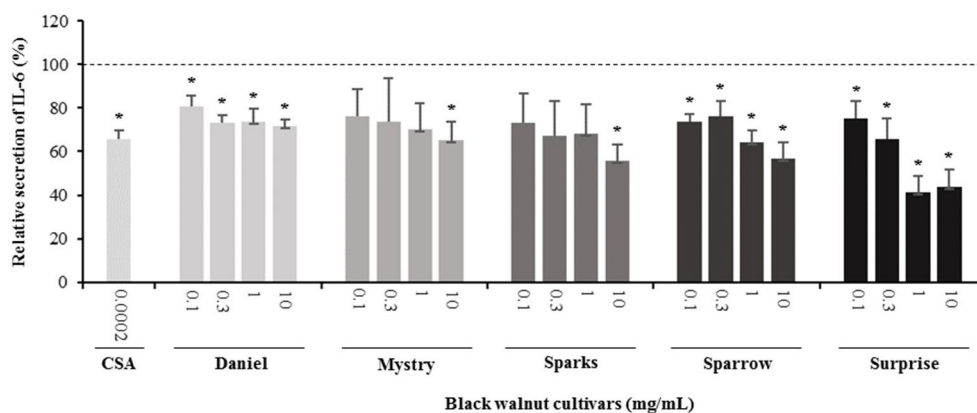


**FIGURE 5 |** Effect of black walnut extracts on the secretion of IL-6 by PMA-differentiated, LPS-stimulated U937 cells. Cyclosporin A (CSA) was used as a positive control. (\*) Significant decrease ( $p < 0.01$ ) compared to PMA-differentiated, LPS-stimulated U937 cells in the absence of extract. Mean  $\pm$  SEM.

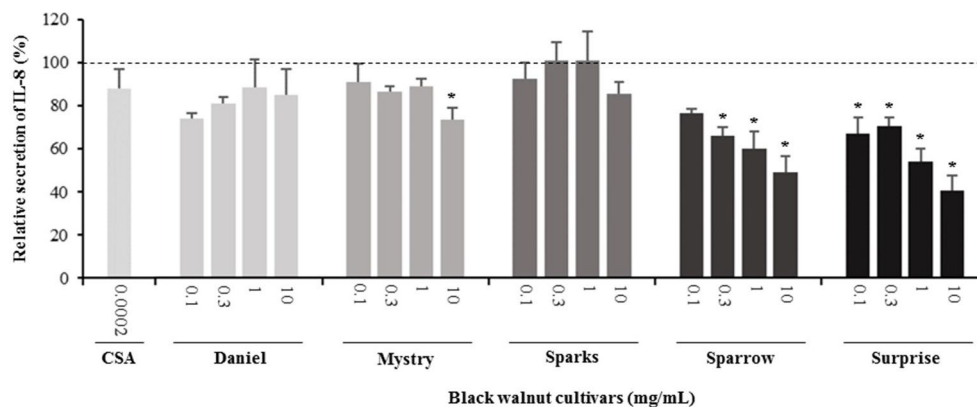


**FIGURE 6 |** Effect of black walnut extracts on the secretion of IL-8 by PMA-differentiated, LPS-stimulated U937 cells. Cyclosporin A (CSA) was used as a positive control. (\*) Significant decrease ( $p < 0.01$ ) compared to PMA-differentiated, LPS-stimulated U937 cells in the absence of extract. Mean  $\pm$  SEM.

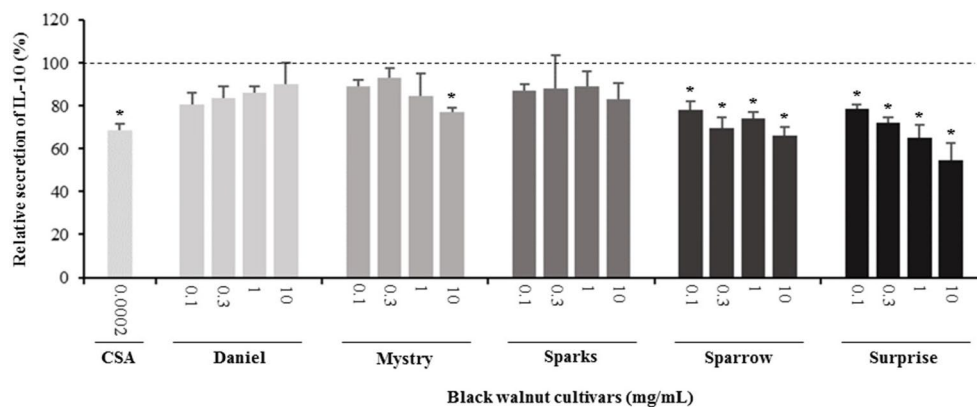


**FIGURE 7 |** Effect of black walnut extracts on the secretion of IL-10 by PMA-differentiated, LPS-stimulated U937 cells. Cyclosporin A (CSA) was used as a positive control. (\*) Significant decrease ( $p < 0.01$ ) compared to PMA-differentiated, LPS-stimulated U937 cells in the absence of extract. Mean  $\pm$  SEM.

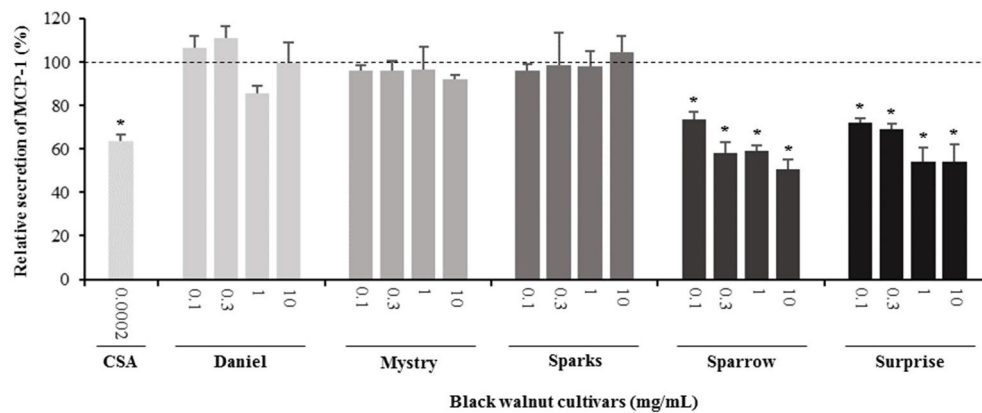


**FIGURE 8 |** Effect of black walnut extracts on the secretion of MCP-1 by PMA-differentiated, LPS-stimulated U937 cells. Cyclosporin A (CSA) was used as a positive control. (\*) Significant decrease ( $p < 0.01$ ) compared to PMA-differentiated, LPS-stimulated U937 cells in the absence of extract. Mean  $\pm$  SEM.

compared to control cells (Figures 3–8). More specifically, cultures pretreated with Sparrow extracts at the concentrations of 0.1, 0.3, 1, and 10 mg/ml reduced the secretion of TNF- $\alpha$  by 23.9%, 31.7%, 35.5%, and 42.7%, respectively; IL-1 $\beta$  by 17.7%, 16.4, 23.1, and 34.1%, respectively; IL-6 by 26.3%, 23.7%, 35.6%, and 43.3%, respectively; IL-8 by 23.4%, 34.1%, 39.8%, and 51.1%, respectively; IL-10 by 22.0%, 30.1%, 25.6%, and 33.9%, respectively; and MCP-1 by 26.5%, 41.9%, 40.8%, and 49.1%, respectively (Figures 3–8). Similarly, at the concentrations of 0.1, 0.3, 1, and 10 mg/ml, cultures pretreated with Surprise extracts also reduced the secretion of TNF- $\alpha$  by 36.4%, 37.6%, 47.8%, and 55.7%, respectively; IL-1 $\beta$  by 32.1%, 34.8%, 44.0%, and 48.7%, respectively; IL-6 by 24.9%, 34.3%, 58.9%, and 56.3%, respectively; IL-8 by 33.1%, 29.3%, 45.9%, and 59.3%, respectively; IL-10 by 21.2%, 27.8%, 34.9%, and 45.5%, respectively; and MCP-1 by 27.8%, 30.7%, 45.6%, and 46.0%, respectively (Figures 3–8).

Minor to no effects were observed in IL-1 $\beta$ , TNF- $\alpha$ , and MCP-1 cytokine levels following pretreatment with Daniel, Mystry, and Sparks at all four concentrations tested. The secretion of IL-6 was significantly inhibited by extracts derived from Daniel ( $\geq 0.1$  mg/ml), Mystry (10 mg/ml), and Spark (10 mg/ml). More specifically, the extracts of Daniel at the concentrations of 0.1, 1, 0.3, and 10 mg/ml, Mystry and Sparks at a concentration of 10 mg/ml significantly reduced the secretion of IL-6 by 19.5%, 26.7%, 26.5%, 28.5%, 34.9%, and 44.1%, respectively (Figure 5). In addition, the extract of Mystry at a concentration of 10 mg/ml reduced the secretion of IL-8 (26.3%) and IL-10 (22.8%) by PMA-differentiated, LPS-stimulated U-937 cells (Figures 6 and 7).

In order to gain insight into potential mechanism(s) of action, parallel experiments whereby LPS was added 2 h before exposure to extracts were conducted. These experiments focused on Sparrow or Surprise cultivars because of their strong inhibitory effect on cytokine secretion among examined cultivars when the extracts were added before the addition of LPS. In these experiments, the cell stimulation and cytokine secretion were initiated before the extracts were added. The results showed that Sparrow and Surprise extracts had no inhibitory effect on the secretion of the

six cytokines (TNF- $\alpha$ , IL-1 $\beta$ , IL-6, IL-8, IL-10, and MCP-1) when LPS was added before the extracts (data not shown).

## DISCUSSION

The results of this study demonstrated for the first time that black walnut possesses compounds that exert an inhibitory effect on the secretion of six measured cytokines (TNF- $\alpha$ , IL-1 $\beta$ , IL-6, IL-8, IL-10, and MCP-1) induced by a human promonocytic cell line differentiated with PMA and stimulated with LPS. Cytokines play vital roles in mediating pathological responses in RA. TNF, IL-1, and IL-6 are pivotal cytokines in regulating innate and adaptive immune responses associated with the disease onset and persistence, and TNF and IL-1 are signature innate cytokines in RA. TNF is functionally central to RA pathophysiology and is involved in leukocyte activation, adhesion, and migration, in endothelial-cell adhesion molecule expression, and in stromal-cell, chondrocyte, and osteoclast activation (McInnes et al., 2016); IL-1 plays a role in destruction of bone at inflammatory joint sites, such as in RA, *via* activation, differentiation, and survival of osteoclasts (Kim et al., 2009), and it also mediates secretion of cytokines from synovial fibroblasts and monocytes and induces endothelial-cell adhesion molecule expression (McInnes and Schett, 2007). IL-6 is a key player in innate and adaptive immune responses, including proliferation, differentiation, cytotoxic T cell activity, antibody production, generation of blood cells and platelets, hepatic acute-phase responses, and neuroendocrine effects (McInnes and Schett, 2007). The two proinflammatory cytokines, TNF and IL-6, are therapeutic targets for the treatment of RA (Smolen and Aletaha, 2015), whereas inhibition of IL-1 using biological therapies has not been effective in preventing RA (McInnes et al., 2016). In the present study, we showed that black walnut cultivars Sparrow and Surprise significantly and dose-dependently reduced the secretion of three proinflammatory cytokines (TNF- $\alpha$ , IL-1 $\beta$ , and IL-6) in the U-937 model system. Additionally, other

cultivars also had an inhibitory effect on IL-6 secretion. Our findings suggest that the extracts from certain black walnut cultivars, such as Sparrow and Surprise, might be promising biological agents for future investigation on the prevention of inflammatory diseases, such as RA in animal model studies.

Our results also revealed the inhibitory effects of black walnut extracts on three other cytokines/chemokines (MCP-1, IL-8, and IL-10) in the U-937 model system. MCP-1 and IL-8, members of the CC and CXC chemokine family, respectively, play important roles in acute inflammation. The expression of MCP-1 regulates migration and infiltration of monocytes, memory T cells, and dendritic cells (Carr et al., 1994, Deshmane et al., 2009), whereas IL-8 recruits neutrophils and other granulocytes to the site of infection and stimulates phagocytosis (Harada et al., 1994). IL-10 is a potent immune-modulatory cytokine with broad anti-inflammatory properties (O'garra et al., 2008) and is produced by a variety of cells including B cells, Th1, Th2, Th17, T reg, CD8+ T cells, and myeloid cells (Saraiva and O'garra, 2010). During inflammation, IL-10 can be produced by regulatory B cells and inhibit the production of TNF (Smallie et al., 2010) as well as inhibit the infiltration and activation of neutrophils in the synovial tissue (Bober et al., 2000). Interestingly, Sparrow and Surprise exhibited inhibitory effects not only on MCP-1 and IL-8 but also on IL-10. Black walnut extracts contain many possible anti-inflammatory metabolites (Figure 1) that might exert the inhibitory effect on the production of IL-8 and MCP-1 (Figure 1) as well as other unidentified metabolites. Some anti-inflammatory compounds might have broad cytokine suppressive effect that might inhibit the production of IL-10 in the U-937 model system.

Our results indicated a rich source of possible anti-inflammatory bioactive compounds in black walnut. These compounds were tentatively identified through a metabolomics analysis (Figure 1), and many of them, including gallic acid, vanillic acid, ellagic acid, quercetin, quercetin 3-O-glucoside, naringin, and cinnamic acid, have been confirmed and quantified in black walnut kernels using LC-MS/MS analysis with authentic standards (Vu et al., 2018). The presence of multiple compounds in certain cultivars raises the possibility of synergistic effects on cytokine secretion. We previously identified multiple bioactive compounds (e.g., glansreginin A, azelaic acid, and quercetin) in black walnut that are responsible for antibacterial activities against a Gram-positive bacterium (*S. aureus* RN6390) (Ho et al., 2018). Bioassay-guided fractionation was utilized to isolate and identify the bioactive compounds (based on MS/MS fragmentation data of ions) by a metabolomics approach using high-resolution MS/MS databases (e.g., METLIN, MassBank of North America, MetFrag). Future research will focus on purification, validation, and characterization of compounds responsible for cytokine suppressive activities in Surprise and Sparrow utilizing the same metabolomics strategy. The compounds in black walnut might be useful as natural anti-inflammatory agents to mitigate inflammation.

Interestingly, the inhibitory effect of Surprise and Sparrow cultivars was only observed when U-937 were pretreated with the extracts of these cultivars before the addition of LPS,

whereas the suppressive activity did not occur when U-937 were stimulated with LPS before addition of the extract. These findings suggest the possibility that the extracts are inhibiting cell activation at the level of the receptor rather than affecting downstream signaling pathways. The observed decrease in cytokine levels in the pretreated experiments could result from the ability of the extract to interfere with the interaction between LPS and its receptor TLR4 and/or coreceptor CD14, or from the direct binding of the extract to the LPS receptor, thereby blocking cell activation. In other words, the extracts might function by preventing LPS from activating U-937 cells. Importantly, TLR4 receptors are expressed in U-937 cells, and receptor activation leads to a dose-dependent induction of certain inflammatory markers (Vogel et al., 2012). When U-937 were stimulated with LPS before the addition of the extracts, LPS might bind to its receptor and initiate the signaling cascade before the addition of the extracts. Additionally, the active compounds may be effective against other receptors and/or affect intracellular signaling pathways. The mechanism of action is not fully understood at this point. Future experiments will be required to elucidate how the active compounds are carrying out their effect.

We also documented that cytokine suppressive activities of black walnut were variable among tested cultivars. Two cultivars (Sparrow and Surprise) exhibited inhibitory effect on the secretion of six detected cytokines induced by U-937 differentiated with PMA and stimulated with LPS, while other cultivars (Daniel, Mystry, and Sparks) reduced the secretion of IL-6 alone. Mystry also reduced the secretion of IL-10 and MCP-1, but no inhibitory effect of Mystry on TNF- $\alpha$ , IL-1 $\beta$ , and IL-8 was observed. Differences in the suppressive properties of black walnut are likely due to the differences in the composition and proportions of different compounds among these cultivars (Figure 1A). In our previous studies, we also found differences in antibacterial properties among black walnut cultivars (Ho et al., 2018). In fact, Surprise and Mystry exhibited the strongest antibacterial capacities against *S. aureus* among 22 tested cultivars, while Daniel, Davidson, Hay, Jackson, Kwik Krop, Schessler, Sparks, and Sparrow cultivars showed no effect on the inhibition of *S. aureus*. Health-promoting characteristics of black walnut (e.g., anti-inflammatory and antibacterial capacities) could potentially be used to select traits to improve nut quality. Over 700 black walnut cultivars have been recorded, and many of them were selected for nut production in the past century (Williams, 1990). Current nut production criteria include yield, percent kernel, leafing date, flowering dates, growth habit, disease resistance, precocity, productivity, and shelling quality (Reid et al., 2004).

## CONCLUSION

We demonstrated cytokine suppressive properties of black walnut extracts using the human promonocytic cell line U-937. Black walnut kernels contain a wealth of bioactive metabolites putatively identified through a metabolomics approach. The five cultivars (Daniel, Mystry, Sparks, Sparrow, and Surprise)



tested showed differences in their ability to inhibit the secretion of six cytokines/chemokines (TNF- $\alpha$ , IL-1 $\beta$ , IL-6, IL-8, IL-10, and MCP-1). Sparrow and Surprise showed the strongest inhibitory effects on the secretion of all measured cytokines. Mystry reduced the secretion of IL-6, IL-10, and MCP-1, while Daniel and Sparks only reduced the production of IL-6. Our findings reveal that certain black walnut cultivars may represent promising preventive agents for inflammatory diseases. In addition, this could potentially have an application in the cosmeceutical field related to inflammatory skin disorders.

## DATA AVAILABILITY

All datasets generated for this study are included in the manuscript and the **Supplementary files**.

## AUTHOR CONTRIBUTIONS

C-HL contributed to conception of the study. K-VH wrote the first draft of the manuscript. K-VH and KS designed the experiments and performed the analyses. K-VH, KS, and DV performed the experiments. KS, ZL, LS, MC, and C-HL provided

materials required for the experiments. All authors edited and approved the final version of the manuscript.

## ACKNOWLEDGMENTS

The authors would like to thank the Center of Agroforestry, University of Missouri and Missouri Department of Agriculture Specialty Crop Block Grant Program for supporting this research. The Sumner Lab and the MU Metabolomics Center have been graciously supported by several entities over the years for the development of natural products profiling and plant metabolomics. These specifically include support from the University of Missouri, The Samuel Roberts Noble Foundation, Bruker Daltonics GmbH, Agilent Technologies, US National Science Foundation (NSF)-JST Metabolomics for a Low Carbon Society #1139489, NSF MRI DBI #1126719, NSF RCN #1340058, and NSF MCB #1024976.

## SUPPLEMENTARY MATERIAL

The Supplementary Material for this article can be found online at: <https://www.frontiersin.org/articles/10.3389/fphar.2019.01059/full#supplementary-material>

## REFERENCES

- Bober, L. A., Rojas-Triana, A., Jackson, J. V., Leach, M. W., Manfra, D., Narula, S. K., et al. (2000). Regulatory effects of interleukin-4 and interleukin-10 on human neutrophil function ex vivo and on neutrophil influx in a rat model of arthritis. *Arthritis Rheum.* 43 (12), 2660–2667. doi: 10.1002/1529-0131(200012)43:12<2660::AID-ANR5>3.0.CO;2-4
- Carr, M. W., Roth, S. J., Luther, E., Rose, S. S., and Springer, T. A. (1994). Monocyte chemoattractant protein 1 acts as a T-lymphocyte chemoattractant. *Proc. Natl. Acad. Sci. U.S.A.* 91 (9), 3652–3656. doi: 10.1073/pnas.91.9.3652
- Chong, J., Soufan, O., Li, C., Caraus, I., Li, S., Bourque, G., et al. (2018). MetaboAnalyst 4.0: towards more transparent and integrative metabolomics analysis. *Nucleic Acids Res.* 46, W486–W494. doi: 10.1093/nar/gky310
- Deshmane, S. L., Kremlev, S., Amini, S., and Sawaya, B. E. (2009). Monocyte chemoattractant protein-1 (MCP-1): an overview. *J. Interferon Cytokine Res.* 29 (6), 313–326. doi: 10.1089/jir.2008.0027
- Estruch, R., Ros, E., Salas-Salvadó, J., Covas, M.-I., Corella, D., Arós, F., et al. (2013). Primary prevention of cardiovascular disease with a Mediterranean diet. *N. Engl. J. Med.* 368 (14), 1279–1290. doi: 10.1056/NEJMoa1200303
- Firestein, G. S. (2003). Evolving concepts of rheumatoid arthritis. *Nature* 423 (6937), 356. doi: 10.1038/nature01661
- Gordon, S. (2002). Pattern recognition receptors: doubling up for the innate immune response. *Cell* 111 (7), 927–930. doi: 10.1016/S0092-8674(02)01201-1
- Guijas, C., Montenegro-Burke, J. R., Domingo-Almenara, X., Palermo, A., Warth, B., Hermann, G., et al. (2018). METLIN: a technology platform for identifying knowns and unknowns. *Anal. Chem.* 90 (5), 3156–3164. doi: 10.1021/acs.analchem.7b04424
- Harada, A., Sekido, N., Akahoshi, T., Wada, T., Mukaida, N., and Matsushima, K. (1994). Essential involvement of interleukin-8 (IL-8) in acute inflammation. *J. Leukoc. Biol.* 56 (5), 559–564. doi: 10.1002/jlb.56.5.559
- Ho, K.-V., Lei, Z., Sumner, L., Coggeshall, M., Hsieh, H.-Y., Stewart, G., et al. (2018). Identifying antibacterial compounds in black walnuts (*Juglans nigra*) using a metabolomics approach. *Metabolites* 8 (4), 58. doi: 10.3390/metabo8040058
- Kim, J. H., Jin, H. M., Kim, K., Song, I., Youn, B. U., Matsuo, K., et al. (2009). The mechanism of osteoclast differentiation induced by IL-1. *J. Immunol.* 183, 1862–1870. doi: 10.4049/jimmunol.0803007
- McInnes, I. B., Buckley, C. D., and Isaacs, J. D. (2016). Cytokines in rheumatoid arthritis—shaping the immunological landscape. *Nat. Rev. Rheumatol.* 12 (1), 63. doi: 10.1038/nrrheum.2015.171
- McInnes, I. B., and Schett, G. (2007). Cytokines in the pathogenesis of rheumatoid arthritis. *Nat. Rev. Immunol.* 7 (6), 429. doi: 10.1038/nri2094
- Medzhitov, R. (2010). Inflammation 2010: new adventures of an old flame. *Cell* 140 (6), 771–776. doi: 10.1016/j.cell.2010.03.006
- Mosmann, T. (1983). Rapid colorimetric assay for cellular growth and survival: application to proliferation and cytotoxicity assays. *J. Immunol. Methods* 65 (1–2), 55–63. doi: 10.1016/0022-1759(83)90303-4
- Nolan, J. M., and Robbins, M. C. (1999). Cultural conservation of medicinal plant use in the Ozarks. *Hum. Organ.* 58, 67–72. doi: 10.17730/humo.58.1.k1854516076003p6
- O'garra, A., Barrat, F. J., Castro, A. G., Vicari, A., and Hawrylowicz, C. (2008). Strategies for use of IL-10 or its antagonists in human disease. *Immunol. Rev.* 223 (1), 114–131. doi: 10.1111/j.1600-065X.2008.00635.x
- Pan, A., Sun, Q., Manson, J. E., Willett, W. C., and Hu, F. B. (2013). Walnut consumption is associated with lower risk of type 2 diabetes in women. *J. Nutr.* 143 (4), 512–518. doi: 10.3945/jn.112.172171
- Papoutsis, Z., Kassi, E., Chinou, I., Halabalaki, M., Skaltsounis, L., and Moutsatsou, P. (2008). Walnut extract (*Juglans regia* L.) and its component ellagic acid exhibit anti-inflammatory activity in human aorta endothelial cells and osteoblastic activity in the cell line KS483. *Br. J. Nutr.* 99 (4), 715–722. doi: 10.1017/S0007114507837421
- Randolph, K. C., Rose, A. K., Oswalt, C. M., and Brown, M. J. (2013). Status of black walnut (*Juglans nigra* L.) in the eastern United States in light of the discovery of thousand cankers disease. *Castanea* 78 (1), 2–14. doi: 10.2179/12-024
- Reid, W., Coggeshall, M. V., and Hunt, K. L. (2004). "Cultivar evaluation and development for black walnut orchards," in *Black Walnut in a New Century*. Eds. Michler, C. H., Pijut, P. M., van Sambeek, J. W., Coggeshall, M. V., Seifert, J., Woeste, K. Square, PA, USA: U.S. Department of Agriculture, Forest Service, (North Central Research Station), 18–24.
- Ros, E. (2015). Nuts and CVD. *Br. J. Nutr.* 113 (S2), S111–S120. doi: 10.1017/S0007114514003924
- Rovera, G., Santoli, D., and Damsky, C. (1979). Human promyelocytic leukemia cells in culture differentiate into macrophage-like cells when treated with a phorbol diester. *Proc. Natl. Acad. Sci. U.S.A.* 76 (6), 2779–2783. doi: 10.1073/pnas.76.6.2779

- Saraiva, M., and O'garra, A. (2010). The regulation of IL-10 production by immune cells. *Nat. Rev. Immunol.* 10 (3), 170. doi: 10.1038/nri2711
- Smallie, T., Ricchetti, G., Horwood, N. J., Feldmann, M., Clark, A. R., and Williams, L. M. (2010). IL-10 inhibits transcription elongation of the human TNF gene in primary macrophages. *J. Exp. Med.* 207 (10), 2081–2088. doi: 10.1084/jem.20100414
- Smolen, J. S., and Aletaha, D. (2015). Rheumatoid arthritis therapy reappraisal: strategies, opportunities and challenges. *Nat. Rev. Rheumatol.* 11 (5), 276. doi: 10.1038/nrrheum.2015.8
- Tautenhahn, R., Patti, G. J., Rinehart, D., and Siuzdak, G. (2012). XCMS Online: a web-based platform to process untargeted metabolomic data. *Anal. Chem.* 84 (11), 5035–5039. doi: 10.1021/ac300698c
- Vogel, C. F., Garcia, J., Wu, D., Mitchell, D. C., Zhang, Y., Kado, N. Y., et al. (2012). Activation of inflammatory responses in human U937 macrophages by particulate matter collected from dairy farms: an *in vitro* expression analysis of pro-inflammatory markers. *Environ. Health* 11, 17. doi: 10.1186/1476-069X-11-17
- Vu, D. C., Vo, P. H., Coggeshall, M. V., and Lin, C. H. (2018). Identification and characterization of phenolic compounds in black walnut kernels. *J. Agric. Food Chem.* 66 (17), 4503–4511. doi: 10.1021/acs.jafc.8b01181
- Williams, R. D. (1990). "*Juglans nigra* L., black walnut," in *Silvics of North America*, vol. 2. Eds. R. M. Burns and B. H. Honkala (Washington, D.C., USA: U. S. Department of Agriculture, Forest Service), 391–399.
- Willis, L. M., Bielinski, D. F., Fisher, D. R., Matthan, N. R., and Joseph, J. A. (2010). Walnut extract inhibits LPS-induced activation of BV-2 microglia via internalization of TLR4: possible involvement of phospholipase D2. *Inflammation* 33 (5), 325–333. doi: 10.1007/s10753-010-9189-0.

**Conflict of Interest Statement:** The authors declare that the research was conducted in the absence of any commercial or financial relationships that could be construed as a potential conflict of interest.

At least a portion of this work is authored by Mark V. Coggeshall on behalf of the U.S. Government and, as regards Dr. Coggeshall and the U.S. Government, is not subject to copyright protection in the United States. Foreign and other copyrights may apply. This is an open-access article distributed under the terms of the Creative Commons Attribution License (CC BY). The use, distribution or reproduction in other forums is permitted, provided the original author(s) and the copyright owner(s) are credited and that the original publication in this journal is cited, in accordance with accepted academic practice. No use, distribution or reproduction is permitted which does not comply with these terms.



# Alaskan Berry Extracts Promote Dermal Wound Repair Through Modulation of Bioenergetics and Integrin Signaling

Debora Esposito<sup>1,2\*</sup>, John Overall<sup>1,3</sup>, Mary H. Grace<sup>1,3</sup>, Slavko Komarnytsky<sup>1,3</sup> and Mary Ann Lila<sup>1,3</sup>

<sup>1</sup> Food Bioprocessing and Nutrition Sciences Department, Plants for Human Health Institute, North Carolina State University, Kannapolis, NC, United States, <sup>2</sup> Department of Animal Science, North Carolina State University, Raleigh, NC, United States, <sup>3</sup> Department of Food, Bioprocessing, and Nutrition Sciences, North Carolina State University, Raleigh, NC, United States

## OPEN ACCESS

### Edited by:

Luc Pieters,  
University of Antwerp, Belgium

### Reviewed by:

José M. Alvarez-Suarez,  
University of the Americas,  
Ecuador

Ana María González-Paramas,  
University of Salamanca,  
Spain

Carel Basson Oosthuizen,  
University of Pretoria,  
South Africa

### \*Correspondence:

Debora Esposito  
daesposi@ncsu.edu

### Specialty section:

This article was submitted to  
Ethnopharmacology,  
a section of the journal  
Frontiers in Pharmacology

**Received:** 13 March 2019

**Accepted:** 20 August 2019

**Published:** 27 September 2019

### Citation:

Esposito D, Overall J, Grace MH,  
Komarnytsky S and Lila MA (2019)  
Alaskan Berry Extracts Promote  
Dermal Wound Repair Through  
Modulation of Bioenergetics and  
Integrin Signaling.  
Front. Pharmacol. 10:1058.  
doi: 10.3389/fphar.2019.01058

Various wild berry species endemic to Alaska and the circumpolar North that exhibit unique medicinal properties have long been appreciated by indigenous Arctic communities. Traditional use of Alaskan berry preparations in the treatment of skin wounds is recorded but has not been scientifically evaluated. Alaskan wild berries feature diverse phytochemical compositions that contain a variety of bioactive polyphenols exhibiting anti-inflammatory, antioxidant, and antimicrobial properties, making them ideal for wound healing interventions and natural anti-aging cosmeceutical formulations. Given increasing interest in identifying biologically active plant constituents for wound care and cosmeceutical applications, the objective of this study was to screen several wild berry species endemic to Alaska and the circumpolar Arctic for wound healing and in the crude, polyphenol-enriched, and further fractionated extracts of: *Empetrum nigrum* (crowberry), *Vaccinium uliginosum* (bog blueberry), and *V. vitis-idaea* (low-bush cranberry or lingonberry). A cell migration assay with human dermal fibroblasts (HDFa) was performed to model promotion of wound closure, revealing that bog blueberry extract most actively promoted migration, whereas divergent effects observed with other berry extracts were related to compositional disparities. Lipopolysaccharide (LPS)-stimulated inflammatory response variables measured in RAW 264.7 macrophages [reactive oxygen species (ROS), NO production, prostaglandin-endoperoxide synthase 2 (COX-2), and inducible nitric oxide synthase (iNOS) expression] were suppressed by most extracts/fractions, but especially bog blueberry and proanthocyanidin (PAC) fractions. Wild berry germplasm contained abundant complex flavonoid structures such as PAC and anthocyanins (ANCs), associated with enhanced repair and inflammatory resolution in these models. Next, underlying mechanisms by which PACs and bioactive metabolites (B2 dimer and epicatechin) could influence wound repair and tissue regeneration were examined. PAC metabolites promoted scratch-wound closure and appeared to exert the highest impacts on early stages of wound healing through stimulating mitochondrial bioenergetics (basal respiration, ATP production, and maximum respiratory capacity) and upregulating expression of important extracellular matrix (ECM) proteins (integrin-β1

and collagen type I  $\alpha 2$  chain). Targeting cellular bioenergetics and integrin-mediated cell–ECM signaling with bioactives from Alaskan wild berries shows considerable therapeutic promise to treat chronic skin wounds and inflammatory skin disorders, as well as more generally to support regenerative healing responses and restore function in a variety of tissue and organ settings after injury or aging.

**Keywords:** skin regeneration, wound healing, Alaskan berries, integrins, proanthocyanidins, epicatechins

## INTRODUCTION

Wild berries contain an impressive array of bioactive phytochemical compounds, which collectively present a range of biological activities targeting key mechanisms involved in healthy tissue development and aging (Paredes-Lopez et al., 2010; Li et al., 2016). The human health–relevant bioactive properties of wild berries can be primarily attributed to their considerable diversity of polyphenolic constituents, typically exhibiting antioxidant, anti-inflammatory, and antimicrobial capabilities (Seeram, 2008; Nile and Park, 2014). Wild berries contain complex mixtures of polyphenolic compounds in relatively dense concentrations, especially major flavonoid subclasses with well-documented health benefits such as proanthocyanidin (PAC) and anthocyanin (ANC) (Esposito et al., 2014). Interspecific differences, as well as environmental factors such as geographic location and climatic variation, substantially influence the accumulation of berry phytochemicals and thus likely alter their profile of health-related bioactivities (Howard et al., 2003; Lila, 2006; Karppinen et al., 2016).

Our previous work extensively characterized and cross-compared the phenolic profiles of Alaskan wild berry species with commercially cultivated species (Grace et al., 2014), demonstrating key qualitative differences between wild and cultivated berries with regard to phytochemical composition and contents. Wild species demonstrated unique compositional profiles with respect to key polyphenolic classes, especially PAC, and generally exhibited quantitative superiority with regard to total phenolic concentrations. Such compositional diversity is interesting in light of the hypothesis that wild species exhibit robust and distinctive bioactivity profiles due to disparities among major bioactive compounds such as PAC and ANC. These findings prompted further investigation of Alaskan wild berries to identify opportunities for biomedical application and commercial product formulation.

The traditional application of Alaskan wild berry preparations for skin wound care has been documented (Kellogg et al., 2010). Corroborating traditional accounts of their efficacy in skin wound healing, there is widespread literature indication that many other plant-derived compounds that bear similar structural principles likewise exhibit physiological benefits in skin homeostasis, skin inflammation, and related disorders, and in wound healing (Dawid-Pač, 2013; Budovsky et al., 2015; Działo et al., 2016).

Wound healing and skin repair are primary therapeutic targets for regenerative as well as cosmetic interventions, which aim to facilitate restoration of normal tissue architecture and function. Wound repair is a highly complex, multifaceted response, which is temporally and spatially coordinated across multiple stages

through cooperative actions of diverse cell types, extracellular matrix (ECM) molecules, cytokines, and growth factors (Walraven and Hinz, 2018). Cell–ECM interactions provide critical feedback during wound healing, which is primarily accomplished through dynamic signaling between ECM proteins, particularly collagens and laminins, with cell surface adhesion receptors such as integrins (Manninen, 2015). Integrins are heterodimeric transmembrane glycoproteins formed by differentially associated  $\alpha$  and  $\beta$  subunits (Schnittert et al., 2018). Human epithelial cells are known to express seven distinct types of integrins:  $\alpha 2\beta 1$ ,  $\alpha 3\beta 1$ ,  $\alpha 5\beta 1$ ,  $\alpha 9\beta 1$ ,  $\alpha 6\beta 4$ ,  $\alpha v\beta 1$ , and  $\alpha v\beta 6$  (Larjava et al., 2011). In view of their fundamental role in regulating cell–ECM communication and mechanical homeostasis of the ECM, which provides the structural context for cell adhesion, migration, proliferation, and differentiation during epithelial and connective tissue development and repair, integrins represent an exceptionally attractive molecular target for corrective modulation with novel therapeutic agents derived from whole botanical sources or extracts.

The aim of the current study was to explore the influence of compositionally diverse Alaskan berry extracts on critical processes underpinning constructive wound repair and tissue regeneration. We examined the extent to which different berry extract/fraction conditions modulated macrophage inflammatory activation, reflecting the early pro-inflammatory phase of repair, as well as evaluating effects on human skin cell migration into the wound as a reflection of the efficiency of wound closure and granulation tissue formation, employing a monolayer exclusion zone assay to model the rate of wound closure and stimulate migration of human dermal fibroblasts (HDFa) into the wound site. Additional mechanistic investigations were conducted in order to elucidate the molecular pathways through which Alaskan wild berry compounds could effectively modulate gene expression networks regulating inflammatory response, wound repair, and tissue regeneration; to that end, individual bioactive principles were selected for testing in a separate scratch-wound healing assay, and bioenergetic measurements were conducted to determine whether these structures modulated integrin–ECM signaling through cellular metabolic adaptations imposed *via* changes in mitochondrial function.

## MATERIALS AND METHODS

### Reagents and Materials

Reference compounds procyanidin A2 (PAC-A2), procyanidin B2 (PAC-B2), catechin, and epicatechin were purchased from



Chromadex (Irvine, CA, USA). 4-Dimethylaminocinnamaldehyde (DMAC), Folin–Ciocalteu reagent, Sephadex LH-20, and Supelco LC-18 12 ml solid-phase extraction (SPE) cartridges were purchased from Sigma-Aldrich Inc. (St. Louis, MO, USA). All organic solvents were high pressure liquid chromatography (HPLC) grade and obtained from VWR International (Suwanee, GA, USA).

## Berry Sources

Three wild Alaskan berry species, bog blueberry (*Vaccinium uliginosum* L.), crowberry (*Empetrum nigrum* L.), and lingonberry (*Vaccinium vitis-idaea* L.), were handpicked when fully ripe (mid-September 2015) from the greater Fairbanks area, specifically in Skiland (about 10 to 15 miles northeast of Fairbanks, on mostly north-facing slopes with a few scattered tree stands), as well as on Murphy Dome (about 15 miles west of Fairbanks, on mostly northeast-facing slopes without trees) see **Supplementary Material**. Upon collection, berries were immediately frozen and stored at  $-80^{\circ}\text{C}$  prior to freeze-drying. Freeze-dried berries were ground immediately prior to extraction.

## Extraction and Polyphenol Enrichment

Ground, freeze-dried berries (8.0 g each) were blended (Waring, Inc., Torrington, CT, USA) with 70 ml acidified 70% aqueous methanol (0.5% acetic acid) for 2 min. The mixture was centrifuged (Sorvall RC-6 plus, Asheville, NC, USA) for 20 min at 4,000 rpm [2,688 relative centrifugal force (RCF)], and the supernatant was transferred to 250 ml volumetric flasks. The pellets were re-extracted two additional times, and the combined extracts from each berry were brought to a final volume of 250 ml. An aliquot of 20 ml from each extract was evaporated and freeze-dried to afford the crude extract. The remaining volume from each berry extract (220 ml) was evaporated to about 25 ml before loading onto two Supelclean™ LC-18 SPE cartridges 12 ml (2 g) preconditioned with methanol and acidified water [0.05% trifluoroacetic acid (TFA)]. The adsorbed extract on the cartridges was washed with 50 ml acidified water to remove free sugars and organic acids before eluting the polyphenols with 100% methanol. The methanol eluate was evaporated and freeze-dried to afford the polyphenol-enriched extracts (370, 220, and 321 mg for bog blueberry, crowberry, and lingonberry, respectively). About 50 mg from each extract was stored for phytochemical analysis and biochemical assays.

## Fractionation of Polyphenol-Enriched Extract

The remaining polyphenol-enriched extracts were dissolved in about 10 ml of 20% methanol in water (0.05% TFA) and applied to a column packed with Sephadex LH-20 preconditioned with the same solvent mixture. Isocratic elution of ANC-enriched fractions, fractions 1 and 2 (Fr 1 and Fr 2), continued until the color of eluate faded, at which time the columns were then washed with 70% acetone in water to collect the third PAC-enriched fraction (Fr 3). Solvents were evaporated, and the remaining aqueous extracts were freeze-dried. Bog blueberry extract afforded Fr 1 (120 mg), Fr 2 (50 mg), and Fr 3 (128 mg); crowberry Fr 1 (80 mg), Fr 2 (39 mg), and Fr 3 (60 mg); and lingonberry Fr 1 (80 mg), Fr 2

(24 mg), and Fr 3 (163 mg). Between approximately 6 and 8 mg of each crude extract and fraction in triplicate were dissolved in 60% methanol in water at a concentration of 5 mg/ml and filtered using a 0.20  $\mu\text{m}$  polytetrafluoroethylene (PTFE) syringe filter (Fisher Scientific, Pittsburg, PA, USA) before further analyses.

## Total Phenolic and PAC Determination

Total phenolics were determined with Folin–Ciocalteu reagent (Singleton et al., 1999). Concentrations were expressed as mg/g extract as gallic acid equivalents based on a gallic acid standard curve. Total PAC was determined colorimetrically using the DMAC method (Prior et al., 2010). A series of dilutions of standard procyanidin B2 dimer were prepared in 80% ethanol ranging from 1 to 100  $\mu\text{g/ml}$ . Blank, standard, and diluted samples were analyzed in triplicate. The plate reader protocol was set to read the absorbance (640 nm) of each well in the plate every minute for 30 min (SpectraMax M3, Sunnyvale, CA, USA). PAC concentration was expressed as mg/g extract procyanidin B2 equivalent.

## ANC Determination via HPLC and LC-MS

HPLC analysis for ANC identification and quantification was conducted using an Agilent 1200 HPLC (Agilent Technologies, Santa Clara, CA, USA), according to our previously published protocol (Grace et al., 2014). Quantification was performed using the peak areas recorded at 520 nm to construct the calibration curve for cyanidin-3-O-glucoside. liquid chromatography-mass spectrometry (LC-MS) analysis was performed using a Shimadzu liquid chromatography-mass spectrometry ion trap time of flight (LC-MS-IT-TOF) instrument (Shimadzu, Tokyo, Japan) equipped with a Prominence HPLC system. The LC separation was done using a Shim-pack XR-ODS column (50 mm  $\times$  3.0 mm  $\times$  2.2  $\mu\text{m}$ ) at  $40^{\circ}\text{C}$  with a binary solvent system comprised of 0.1% formic acid in water (A) and methanol (B). Compounds were eluted into the ion source at a flow rate of 0.35 ml/min with a step gradient of B of 5–8% (0–5 min), 8–14% (10 min), 14% (15 min), 20% (25 min), 25% (85 min), 5% (35 min), and 5% (40 min). Ionization was performed using an electrospray ionization (ESI) source in the negative ion mode. Compounds were characterized and identified by their MS, MS/MS spectra, and LC retention times and by comparison with available reference samples and our previous analyses (Grace et al., 2014).

## PAC Composition by Normal-Phase HPLC–FLD Analysis

Chromatographic separation of oligomeric PACs was conducted using an Agilent 1200 HPLC with fluorescence detector (FLD) according to the previously reported method (Grace et al., 2014). Separation was performed using a Develosil Diol column, 250 mm  $\times$  4.6 mm  $\times$  5  $\mu\text{m}$  (Phenomenex). The mobile phase consisted of (A) 2% acetic acid in acetonitrile and (B) 95% methanol, 3% water, and 2% acetic acid using a linear gradient from 0% to 40% B, in 35 min; 40% to 100% B, in 40 min; 100% to 100% isocratic B, in 45 min; and 100% to 0% B, in 50 min. Fluorescence of the procyanidins was monitored at excitation and emission wavelengths of 230 and 321 nm. PACs were identified



by comparison with available standards, our previous analyses (Grace et al., 2014), reported literature (Hollands et al., 2017), and LC-ESI-MS. Percentages of PACs were calculated based on peak area measurements, relative to total area measurements.

## In Vitro Cell Culture

The mouse macrophage cell line RAW 264.7 (ATCC TIB-71, obtained from American Type Culture Collection, Livingstone, MT, USA) was maintained in Dulbecco's modified Eagle's medium (DMEM, Life Technologies, Grand Island, NY, USA), supplemented with 100 IU/ml penicillin, 100 µg/ml streptomycin (Thermo Fisher Scientific, Waltham, MA, USA), and 10% fetal bovine serum (FBS) (Life Technologies, Grand Island, NY, USA), not exceeding 80% confluency at 37°C in a humidified incubator with 5% CO<sub>2</sub>. Primary human dermal fibroblasts isolated from adult skin (HDFa, Invitrogen C-013-5C) were cultured in Medium 106 (Invitrogen M-106-500) with Low Serum Growth Supplement (LSGS, Invitrogen S-003-10) and antibiotic penicillin/streptomycin solution 100 IU/100 µg/ml (Fisher MT-30-002-CI).

## Cell Viability and Dose Range Determination

The cytotoxic activity against HDFa was evaluated by MTT ([3-(4,5-dimethylthiazol-2-yl)-2,5-diphenyl-tetrazolium bromide] colorimetric assay performed according to manufacturer protocol and quantified spectrophotometrically at 550 nm using a microplate reader SynergyH1 (BioTek, Winooski, VT, USA). Inhibition was calculated as a percentage against vehicle control, and absolute IC<sub>50</sub> values were calculated by non-linear regression using twofold serial dilutions of the treatment samples. Treatment concentrations showing no changes in cell viability compared with that of vehicle control were considered optimal and selected for use in subsequent experimental assays.

## ROS and NO Inhibition Assays

To evaluate treatment effects on *in vitro* reactive oxygen species (ROS) production after lipopolysaccharide (LPS) stimulation, an adapted fluorescent dye protocol was used (Choi et al., 2007). RAW 264.7 macrophages seeded at a concentration of  $5 \times 10^5$  cells per well into a 24-well plate were incubated overnight at 37°C. Fresh fluorescent medium [50 µM solution of dichlorodihydrofluorescein diacetate acetylmethyl ester (H<sub>2</sub>DCFDA) in sterile phosphate-buffered saline (PBS), Molecular Probes, Eugene, OR, USA] was added to cells for 30 min. After aspiration of the medium, cells received new medium and 1 µl of treatments (all achieving a final concentration of 50 µg/ml) in triplicate and were stimulated with 10 µl of LPS (from *Escherichia coli* 026:B6) prior to incubation for 24 h, to a final volume of 500 µl per well. Fluorescence of 2',7'-dichlorofluorescein (DCF) was measured at 485/515 nm (excitation/emission) *via* microplate reader (Synergy H1, Biotek, Winooski, VT, USA). LPS induction (no treatment) and vehicle controls were included for reference, along with a positive control containing dexamethasone (DEX), a well-known antioxidant. ROS concentrations were calculated relative to LPS induction control.

Next, the ability of treatment samples to inhibit LPS-stimulated NO radical formation in RAW 264.7 cells was evaluated *via* colorimetric assay in accordance with a protocol that has been previously reported (Van de Velde et al., 2016). Briefly, 100 µl of cell culture medium was added to 100 µl of Griess reagent (1% sulfanilamide and 0.1% naphthylethylenediamine in 5% phosphoric acid), and the mixture was incubated in the dark at room temperature for 10 min. The absorbance at 540 nm was read (Synergy H1, Biotek, Winooski, VT, USA), and a calibration curve built with serial dilutions of sodium nitrite ( $R^2 = 0.990$ ) was used to express results as NO concentration relative to LPS induction control.

## Inflammatory Gene Expression Assay and Real-Time Quantitative PCR Analysis

Effects of enriched extract and fraction treatments on LPS-stimulated inflammatory gene expression (COX-2, iNOS) were evaluated in RAW 264.7 cells. Treatments were administered 1 h prior to LPS stimulation (1 µg/ml) for 4 h, followed by RNA extraction and purification, cDNA synthesis, and quantitative polymerase chain reaction (qPCR) analysis. Positive (DEX at 10 µM) and negative (vehicle) controls were included in every experiment, and triplicates were made for all treatments and control conditions. Cells were harvested using TRIzol reagent for extraction of cellular RNA, and spectrophotometric quantification was performed using the SynergyH1/Take 3 Reader (Biotek). cDNA synthesis was conducted with 2 µg of RNA from each treatment sample, using a high-capacity cDNA reverse transcription kit (Life Technologies, CA, USA) according to manufacturer protocol, on an ABI GeneAmp 9700 (Life Technologies).

The resulting cDNA was amplified by real-time qPCR using PowerUp SYBR PCR Master Mix (Life Technologies) according to a protocol previously reported (Esposito et al., 2014). Samples were subjected to a melting curve analysis to confirm the amplification specificity. Changes in target gene expression relative to the endogenous genetic control were determined using the  $2^{-\Delta\Delta CT}$  method (Livak and Schmittgen, 2001).

## Cell Migration Assay and Fluorescence Imaging Analysis

HDFa was seeded into 96-well Oris plates (Platypus Technologies, LLC, Madison, WI, USA) at a concentration of  $3 \times 10^4$  cells/ml and cultured to near confluence in cell monolayers. Cells were labeled with fluorescent dyes (NucBlue Live Cell Stain and CellTracker Red CMTPX, at 1 µM). Once confluence was reached, wound induction through removal of well inserts and growth media exposed a central, cell-free zone initiating cell migration. This was immediately followed by the rapid removal of free cellular debris through single wash with sterile PBS, and addition of fresh growth medium containing various test and control treatments; treatments were administered to cells in groups of four wells per treatment condition and included enriched extracts and fractions (each at a final concentration of 50 µg/ml), blank (cell-free) and vehicle (0.5% ethanol) controls, and a positive control (10% FBS) serving as a reference for robust induction of migration.

Cell migration into the central zone was quantitatively assessed by cell-specific fluorescence measurement 0, 24, and 48 h post-wounding at excitation/emission wavelengths of 360/460 and 577/605 nm. Fluorescence image analysis was conducted with the EVOS FL Auto Cell Imaging System (Life Technologies), by capturing bright field and fluorescent images at well centers (for consistency) 0, 24, and 48 h after insert removal. EVOS software analysis allowed for parallel assessment of cell migration during wound closure across treatments in real time, providing an illustration of differential capacities for dermal repair promotion. Wound closure as cell migration rate was calculated relative to vehicle control treatment.

## Scratch-Wound Healing Assay and qPCR Array Transcription Profiling

We additionally employed a scratch-wound closure model to test effects of selected Alaskan berry compounds in the interest of generating a diverse bioactivity profile relevant to wound repair. HDFa seeded in 24-well plates were grown to near confluence in cell monolayers, and identical linear wounds were generated in each well using sterile 100  $\mu$ l plastic pipette tips. After sterile PBS wash removed free cellular debris, fresh growth medium was added to wells in triplicate per treatment, containing either vehicle control (0.1% ethanol) or treatment compounds [procyanidin B2, epicatechin, 3,4-dihydroxyphenylacetic acid, and 3-(3,4-dihydroxyphenyl) propionic acid, all at 10  $\mu$ M]. Treated cells were then incubated for 24 h prior to pharmacogenomic profiling of genes associated with wound healing and regeneration. Using RT<sup>2</sup> Profiler PCR Array PAHS-121Z (Qiagen, Hilden, Germany), we examined expression profiles of 84 genes pertinent to ECM, cell adhesion, inflammatory cytokine/chemokine, growth factor, *MAPK*, *TGFB*, and *WNT* signaling pathways. RNA isolation, template cDNA synthesis and qPCR analysis were performed, and relative gene expression levels were normalized to those of five housekeeping genes [ $\beta$ -actin (*ACTB*),  $\beta$ -2-microglobulin (*B2M*), hypoxanthine phosphoribosyltransferase 1 (*HPRT1*), lactate dehydrogenase A (*LDHA*), and large ribosomal protein P1 (*RPLP1*)]. The RT<sup>2</sup> Profiler PCR Array Data Analysis Tool (v3.5, default settings) was used to generate clustergrams to identify co-regulated genes across treatments, and volcano plots were generated to determine significant expression changes across individual gene targets.

## Measurement of Cellular Bioenergetics

HDFa was seeded into a 24-well XF assay plate ( $2 \times 10^4$  cells per well) overnight and subjected to real-time measurements of oxygen consumption rate (OCR) and extracellular acidification rate (ECAR), using Agilent Seahorse XF24 Extracellular Flux Analyzer (Seahorse Biosciences, North Billerica, MA, USA). Cells were then transferred to 500  $\mu$ l of XF assay medium (DMEM without  $\text{NaHCO}_3$ , 10 mM glucose, 2 mM pyruvate, pH 7.4) and equilibrated in a non- $\text{CO}_2$  incubator at 37°C for 1 h. OCR and ECAR were automatically recorded by Seahorse XF24 software v1.8. Basal OCR and ECAR rates were determined by averaging the last four basal measurements. Next, following a triplicate treatment with vehicle (0.1% EtOH) or test compounds

as indicated (10  $\mu$ M), eight subsequent measurements were performed every 15 min. For mitochondrial stress tests, the mitochondrial complex inhibitors were then injected sequentially in the following order: oligomycin (1  $\mu$ M), FCCP (0.75  $\mu$ M), and antimycin A/rotenone (1  $\mu$ M each). Four readings were taken after administration of each inhibitor.

**Statistical analysis.** Statistics were performed using the software GraphPad Prism v7 (GraphPad Software Inc., La Jolla, CA, USA). All data were analyzed by one-way or two-way ANOVA as appropriate. Post hoc analyses were conducted using the Dunnett's multiple comparison tests at 5% level of significance. All results are expressed as means  $\pm$  standard error of the mean (SEM).

## RESULTS

### Extraction and Polyphenolic Enrichment of Alaskan Wild Berries

Crude extracts were prepared from freeze-dried whole berries using successive enrichment (Grace et al., 2009; Yousef et al., 2013). Crude extracts were purified using C18 SPE to afford the polyphenol-enriched extracts. These polyphenol-enriched extracts of bog blueberry, crowberry, and lingonberry showed substantial enrichment of total phenolics (20-, 10- and 11-fold), ANC (26-, 7.5-, and 14-fold), and PAC (11-, 6.6-, and 8-fold), respectively. Each berry polyphenol-enriched extract was loaded on a Sephadex LH-20 column and eluted with 20% acidified methanol, affording two fractions (Fr 1 and Fr 2) specifically enriched in ANC. Elution with 70% acetone afforded a third fraction (Fr 3) specifically enriched in PAC. For bog blueberry, ANC constituted 52% (Fr 1) and 70% (Fr 2); for crowberry, ANC constituted 98% (Fr 1) and 77% (Fr 2); and for lingonberry, ANC constituted 14% (Fr 1) and 64% (Fr 2). In Fr 3, PAC represented 22% (bog blueberry), 34% (crowberry), and 52% (lingonberry). The results of total phenolic, ANC, and PAC concentrations for the extracts and fractions obtained from each berry are listed in Table 1.

### ANC Determination and Quantification

ANCs were identified based on LC-MS analysis as well as previous reports (Grace et al., 2014) and in comparison with available standards. Quantitative analysis was performed based on HPLC peak areas recorded at 520 nm and expressed as cyanidin-3-glucoside equivalents. Glucosides of malvidin and delphinidin represented over 70% of total ANCs present in crude and polyphenol-enriched extracts of bog blueberry. Malvidins were the major ANC in Fr 1 (47% of total ANCs), while delphinidins dominated Fr 2 (62%). Fr 3 contained negligible concentrations of ANC. Crude and polyphenol-enriched extracts of crowberry exhibited high concentrations of cyanidins (37% of total ANC), and delphinidins (24%) as well as malvidins (18%) to lesser extents. Malvidins and cyanidins constituted 50% of total ANC in Fr 1, whereas in Fr 2, 85% of ANCs were delphinidins and cyanidins. Lingonberry exhibited a very distinct ANC profile, in which cyanidins were overwhelmingly predominant throughout

**TABLE 1** | Polyphenol composition of crude, polyphenol-enriched, and Sephadex LH-20 fractionated extracts from wild Alaskan berries.

	<b>Polyphenol class</b>	<b>Crude extract</b>	<b>Polyphenol-enriched extract</b>	<b>Fraction 1 (ANC-enriched)</b>	<b>Fraction 2 (ANC-enriched)</b>	<b>Fraction 3 (PAC-enriched)</b>
Crowberry	TP <sup>1</sup>	101 ± 4.7	723 ± 5.8	544 ± 22	598 ± 7.6	692 ± 1.4
	ANC <sup>2</sup>	104 ± 6.0	780 ± 19	984 ± 31	774.2 ± 16	41.1 ± 2.2
	PAC <sup>3</sup>	30.3 ± 1.9	189 ± 19	19.7 ± 0.5	25.1 ± 1.2	339 ± 11
Bog blueberry	TP <sup>1</sup>	52.6 ± 3.0	601 ± 18	403 ± 20	584 ± 22	733 ± 9.0
	ANC <sup>2</sup>	18.1 ± 0.8	484 ± 11	522 ± 21	701 ± 20	43.5 ± 4.5
	PAC <sup>3</sup>	10.0 ± 0.4	113 ± 6.6	28.3 ± 7.2	90.6 ± 6.6	220 ± 21
Lingonberry	TP <sup>1</sup>	70.0 ± 0.4	610 ± 10	160 ± 5.2	518 ± 11	700 ± 9.1
	ANC <sup>2</sup>	6.9 ± 0.2	97.0 ± 4.0	140 ± 9.0	696 ± 23	2.4 ± 0.5
	PAC <sup>3</sup>	46.0 ± 1.7	364 ± 11	11.2 ± 0.5	20.8 ± 0.4	521 ± 12

<sup>1</sup>TP, total phenolics, measured by Folin–Ciocalteu assay as mg/g dry extract and expressed as gallic acid equivalent.

<sup>2</sup>ANC, anthocyanins, measured by HPLC as mg/g dry extract and expressed as cyanidin-3-glucoside equivalent.

<sup>3</sup>PAC, proanthocyanidins, measured by dimethylaminocinnamaldehyde (DMAC) assay as mg/g dry extract and expressed as procyanidin B2 equivalent.

all extracts/fractions (>95% of total ANC). **Figure 1** shows the HPLC profile, identified peaks, and concentrations of ANC in each berry extract/fraction.

## PACs Compositional Analysis

Normal-phase HPLC with FLD was able to separate proanthocyanin components in the PAC-rich fraction (Fr 3) from the three Alaskan berries according to their degree of polymerization (**Figure 2**). Total peak areas indicated that lingonberry had the highest value, followed by crowberry, and the least was bog blueberry (data not shown); this agrees well with the PAC content measured by the DMAC assay (**Table 1**). All berries contained both type-A and type-B dimers. The normal-phase method cannot not distinguish between the B-types of procyanidins, however our previous study indicated that procyanidin B2 was a common compound in all berries investigated, including Alaskan lingonberry and bog blueberry, utilizing LC-MS on a reversed phase column (Grace et al., 2014). PAC-dimer B constituted 6.09% and 9.30% of total PAC area for bog blueberry and crowberry, respectively, while it constituted 12.3% in lingonberry (**Table 2**). PAC-A dimers constituted 10.41%, 10.18%, and 4.8% for bog blueberry, crowberry, and lingonberry, respectively. These ratios are not consistent with our previous report, which might be due to a different harvest year, where water fall and climate conditions might have been different.

## Impacts on LPS-Stimulated Inflammatory Response Variables

Capacities of Alaskan berry treatments (polyphenol-enriched extracts and specifically ANC- or PAC-enriched fractions) to inhibit production of intracellular ROS and NO were investigated in LPS-stimulated RAW 264.7 macrophages. As shown in **Figure 2A**, polyphenol-enriched extract treatments did not reduce ROS production in activated macrophages, whereas ANC- and PAC-enriched fractions (Fr 1–3) were associated with a 25% reduction ( $p \leq 0.05$ ), with the exception of F1 of lingonberry. Berry extracts and fractions at 50 µg/ml slightly suppressed NO synthesis (> 25%), as shown in **Figure 2B**, a level of inhibition that was maintained across all treatments. Notably, the highest

relative suppression of NO synthesis was achieved by treatment with PAC-enriched fractions of each berry.

The effects of berry extract/fraction treatments on COX-2 expression are shown in **Figure 2C**. Treatments with bog blueberry polyphenol-enriched extract and all of its fractions induced pronounced inhibition of COX-2 mRNA expression, particularly in comparison with other berry treatments, which showed weaker impacts. Of exception, the PAC-enriched fractions of lingonberry and crowberry were associated with significant reduction of COX-2 expression. Interestingly, treatment with the PAC-enriched fraction of bog blueberry produced the greatest COX-2 inhibition (45%). The impacts of berry treatments on iNOS mRNA expression are shown in **Figure 2D**. All berry extracts and fractions significantly attenuated iNOS expression (>25%).

## Cell Viability Assay in HDFa and Dose Determination

MTT assay was used to evaluate the viability of HDFa after 24 h incubation with treatments at different concentrations. Alaskan berry extracts in the range of 50–250 µg/ml had nonsignificant effects on cell viability ( $p > 0.05$ ; data not shown). Based on these data, all subsequent experiments in this work were performed with treatment concentrations of 50 µg/ml.

## Berry Extract/Fraction Effects on HDFa Migration in Exclusion Zone Wound Healing Assay

To determine the effects of wild berry extracts on fibroblast migration in skin wound healing, an exclusion zone–based wound healing model (Oris Migration Assay) was conducted with HDFa in a 96-well plate. Prior to cell seeding, each well was populated with inserts (silicone-based stoppers), which inhibit cell adherence to a central zone. After cells seeded and completely adhered around this zone, wounding was induced through removal of inserts to reveal a 2-mm-diameter unseeded area into which migration could proceed. Cell migration could be visualized by fluorescence imaging as cell movement into the unseeded area (**Figure 3A** shows migration at 24 h post-wounding) and rates of migration

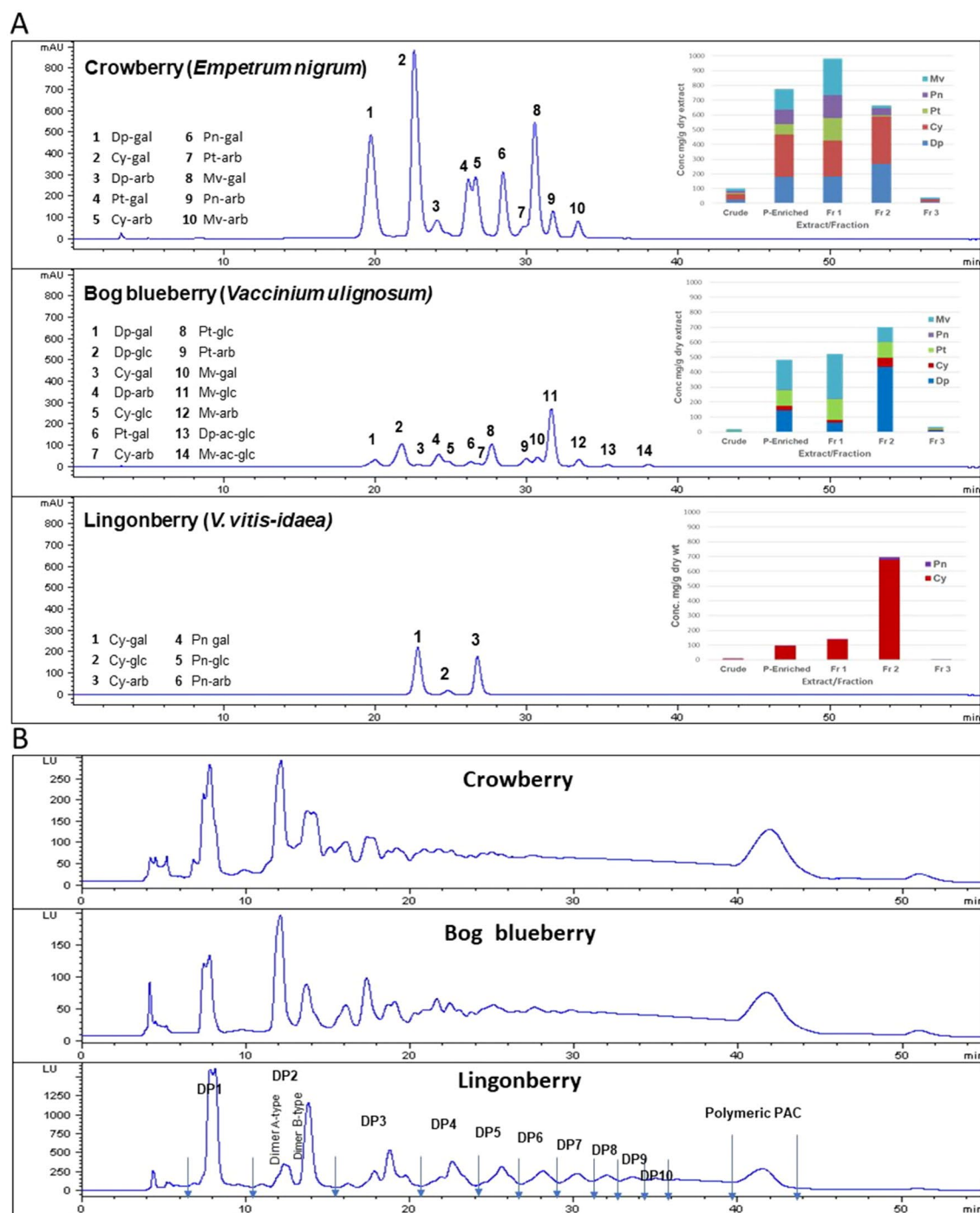


**FIGURE 1 |** Anthocyanin (ANC) and proanthocyanidin (PAC) compositions of Alaskan berry crude extracts, polyphenol-enriched extracts, ANC-enriched fractions (Fr 1 and Fr 2), and PAC-enriched fraction (Fr 3). Dp, delphinidin glycosides; Cy, cyanidin glycosides; Pt, petunidin glycosides; Pn, peonidin glycosides; Mv, malvidin glycosides. **(A)** The HPLC chromatograms presented here represent the polyphenol-enriched extracts, recorded at 520 nm. Concentrations (mg/g dry extract/fractions) were expressed as cyanidin-3-glucoside equivalents. **(B)** HPLC–fluorescence detection (FLD) profiles for proanthocyanidins in fraction 3 from Alaskan berries (excitation, 230 nm; emission, 320 nm).

associated with treatments were quantitatively assessed by measuring increases in cell fluorescence within the central exclusion zone across 48 h (**Figure 3B**), normalized to vehicle control treatment.

In a separate study, phenolic compounds extracted from black soybeans similarly demonstrated the ability to stimulate skin cell migration, an effect that could be attributed to ANC (Nizamutdinova et al., 2009). The authors found that treatment



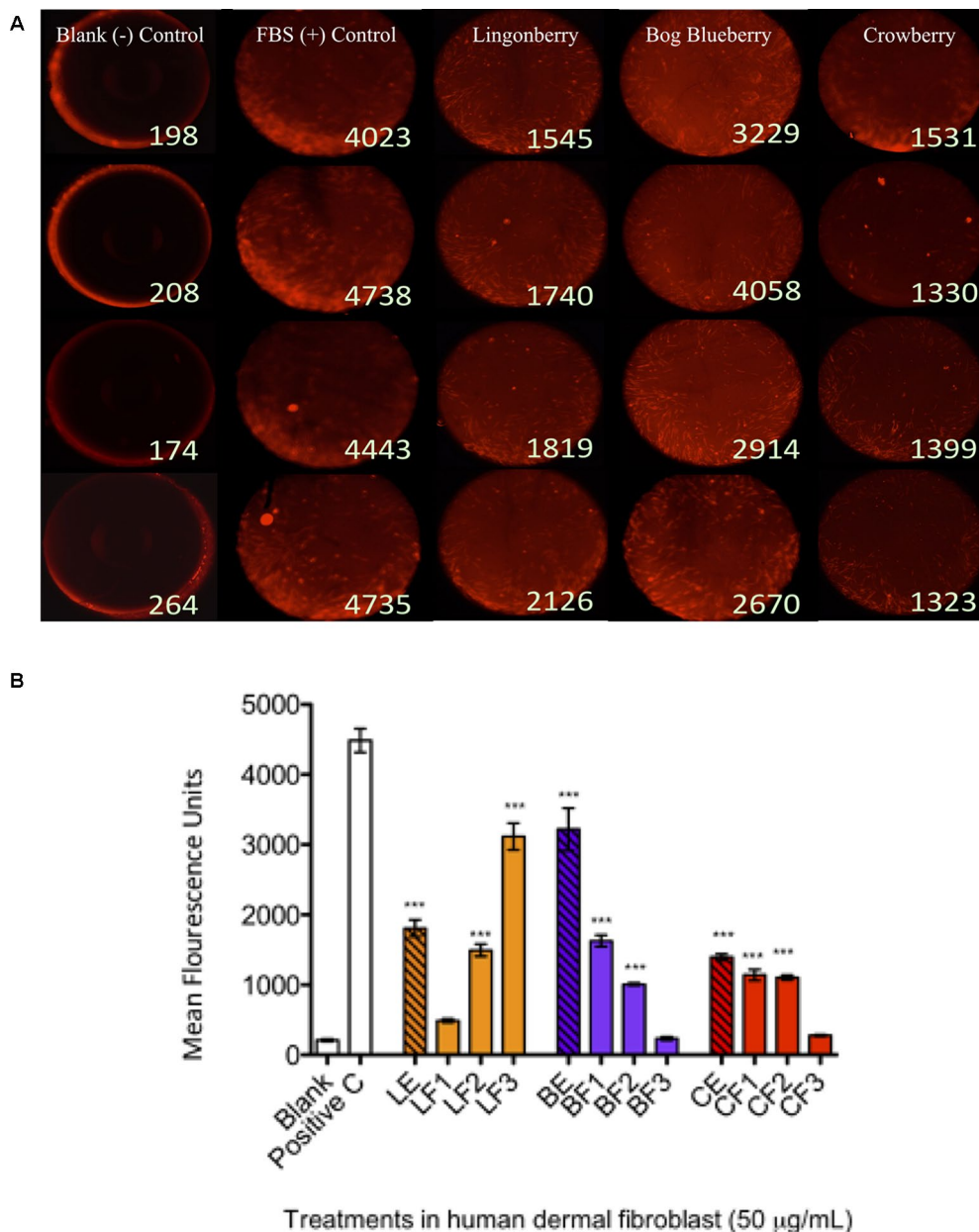


**FIGURE 2 |** Wound healing assay and cell migration end point detection. Wells were seeded with 50,000 human dermal fibroblast (HDFa) cells. Cells adhered after 18 h and stoppers were removed. All wells received CellTracker Red dye to fluorescently stain the cells prior to 24 h incubation with berry extract treatments to permit cell migration; the fluorescence signals in the detection zones were measured using a plate reader. Pictures demonstrate visualization of cell migration after 24 h treatments in HDFa. **(A)** First column shows the cell-free control (blank); second column shows positive control group [10% fetal bovine serum (FBS)]; third column shows migration associated with bog blueberry (*Vaccinium uliginosum* L.) polyphenol-enriched extract; fourth column shows migration associated with crowberry (*Empetrum nigrum*) polyphenol-enriched extract; fifth column shows migration associated with the lingonberry (*Vaccinium vitis-idaea* L.) polyphenol-enriched extract. All extract treatments were tested at a final concentration of 50 µg/ml. The data represent the average of two experiments ± standard error of the mean (SEM). \* $P < 0.05$ ; \*\* $P < 0.01$ ; \*\*\* $P < 0.001$  ( $n = 3$ ) using one-way ANOVA and Dunnett's post-test. All images are taken at a magnification of 4×. Cells are stained with CellTracker CMPTX fluorescence dye. **(B)** The graph illustrates representative cell fluorescence measurements for post-migration ( $t = 48$  h) per treatment ( $n = 4$  wells). *Blank*: cell-free negative control; *Positive C*: FBS positive control; *LE/BE/CE*: lingonberry, bog blueberry, and crowberry polyphenol-enriched extracts, respectively; *F1–F3*: ANC-enriched and PAC-enriched fractions. All extracts were tested at a final concentration of 50 µg/ml.

over 48 h with 50 and 100 µg/ml of ANC from black soybean, comprising glucosides of cyanidin (72%), delphinidin (20%),

and petunidin (6%), induced human dermal fibroblast and keratinocyte migration *in vitro*; furthermore, black soybean



**TABLE 2 |** Analysis of proanthocyanidins oligomers and determination of degrees of polymerization (DPs) in fraction 3 of Alaskan berries by normal-phase HPLC–fluorescence analysis (excitation, 230 nm, emission, 320 nm).

Degree of polymerization	Bog blueberry %*	Crowberry %*	Lingonberry %*
DP1	6.93	10.09	17.95
DP2: Dimer A-type	(10.41)	(10.18)	(4.80)
Dimer B-type	(6.09)	(9.30)	(12.43)
Total DP2	13.07	22.78	16.57
DP3	13.70	9.53	10.44
DP4	8.59	10.28	8.30
DP5	11.35	6.97	6.81
DP6	5.94	7.08	5.78
DP7	5.64	2.90	4.88
DP8	3.51	4.18	4.20
DP9	3.73	3.76	3.74
DP10	2.86	3.67	3.27
DP11	3.95	2.30	2.93
DP≥12	7.95	4.25	5.67
Polymeric PACs	11.04	12.20	9.46

\*Results were calculated based on peak area measurements relative to total area measurements.

ANC treatment increased the production of vascular endothelial growth factor (VEGF), a key cytokine that stimulates early wound angiogenesis in the initiation of wound repair (Galiano et al., 2004). Thus, ANCs are suggested to potentiate wound healing through facilitating cell proliferation and migration and through increasing proangiogenic VEGF production to accelerate the early stages of wound healing. Another study investigated the effects of several well-known bioactive compounds, including resveratrol, phloretin, and ferulic acid, on the proliferation and migration of human oral fibroblasts (San Miguel et al., 2011). Intriguingly, only high or low ( $10^{-3}$ – $10^{-5}$ M) concentrations exhibited beneficial effects on functional mechanisms regulating fibroblast migration and proliferation during gingival healing or periodontal tissue repair. Evidence from these studies and ours supports the feasibility of bioactive compound delivery to sites of tissue damage/injury as a potential therapeutic strategy to support active tissue repair and encourage regenerative healing through promoting skin cell proliferation and migration. It is virtually certain that the promotion of HDFa migration by enriched and fractionated berry extracts, as observed in the current work, is underpinned by enhanced accumulation of TP, ANC, and/or PAC (Table 1), although specific connections between individual classes or compounds with cell migration promotion are unclear.

## Pharmacogenomic Evaluation of Procyanidin B2 and Its Structural Units

The phytochemical analysis for PAC composition (Table 2 and Figure 1B) indicated that procyanidin B2 is a common component in the investigated berries. To further elucidate the involvement of procyanidin B2 and its structural metabolites (Figure 4A) in wound healing pathways in HDFa, pooled RNA samples were used to measure gene expression changes in ECM and cell adhesion, inflammatory cytokines and chemokines, growth factors, *MAPK*,

*TGFB*, and *WNT* signaling pathways in response to each compound. The RT<sup>2</sup> Profiler clustergram (Figure 4B) showed moderate effects of procyanidin B2 on gene expression levels in the HDFa cells, potentiated by epicatechin or homoprotocatechuic acid (HPCA). All structures modulated nearly identical sets of genes, suggesting that they share a structural moiety responsible for mediating the conserved functional effects. 3-(3,4-dihydroxyphenyl)propionic acid clustered together with procyanidin B2, as both compounds showed relatively weaker impacts on repair and regeneration pathways. A volcano plot was constructed from the RT Profiler data (Figure 4C). Three genes were upregulated by the majority of treatments: *COL1A2* (pro- $\alpha$ 2 chain of type I collagen), *ITGB1* (integrin receptor subunit beta 1), and *RHOA* (ras homolog family member A), suggesting that procyanidin-based treatments modulate a complex interplay between ECM proteins (*COL1A2* and *ITGB1*) and *RHO* guanosine triphosphate phosphatase (GTPase) that regulates cell–ECM signaling to support cell adhesion and migration during active tissue repair *via* mechanosensitive reorganization of the actin cytoskeleton (Figure 4D).

Another group of prominently downregulated genes across treatments included *MMP2* (matrix metalloproteinase 2) and *CCL2* (C-C motif chemokine ligand 2, also known as *MCP1* [monocyte chemoattractant protein 1]). *MMP2* expression offers a reliable indicator for clinical wound healing and is induced in the inflammatory phase before being suppressed in downstream stages of tissue repair (Karim et al., 2006). Moreover, MMPs are known to mediate aberrant ECM remodeling and potentially contribute to the progressive fragmentation of dermal collagen that is considered as a major driver of skin aging (Qin et al., 2017). *CCL2* promotes monocyte infiltration and macrophage response in wounds early after injury and is similarly suppressed in the subsequent stages of tissue repair (Wood et al., 2014). Reduced expression of both genes strongly suggests that procyanidin and its metabolites may have promoted scratch-wound closure through an acceleration or shortening of the early inflammatory phase. Thus, PAC-based structures from Alaskan berries may impact the trajectory of wound healing and tissue regeneration by promoting earlier inflammatory resolution. Weak simultaneous suppression of multiple genes responsible for the early inflammatory phase of wound healing (*IFNG* [interferon gamma], *IL1B* [interleukin 1 beta], *IL6* [interleukin 6], *HGF* [hepatocyte growth factor], *MIF* [macrophage migration inhibitory factor]) further supports this conclusion.

Among the phenolic metabolites tested, only procyanidin B2 showed moderate suppression of *MAPK3* (mitogen activated protein kinase 3, also known as *ERK1*) and *TGFB1* (transforming growth factor beta 1) signaling (Figure 4D), which possibly explains its weaker effects on scratch-wound healing due to attenuated activation of the signal transduction pathways leading to cellular proliferation, differentiation, and growth. As such, direct comparisons between procyanidin B2 and its structural units in equimolar concentrations revealed that epicatechin and its metabolite HPCA were associated with superior scratch-wound healing activity *in vitro*. These results are in agreement with those obtained in previous studies. Epicatechin ester of gallic acid (epicatechin gallate) displayed promising wound healing effects in a 3T3 mouse fibroblast model (Schmidt et al., 2010), as well as *in vivo* in a full-thickness incisional model of wound

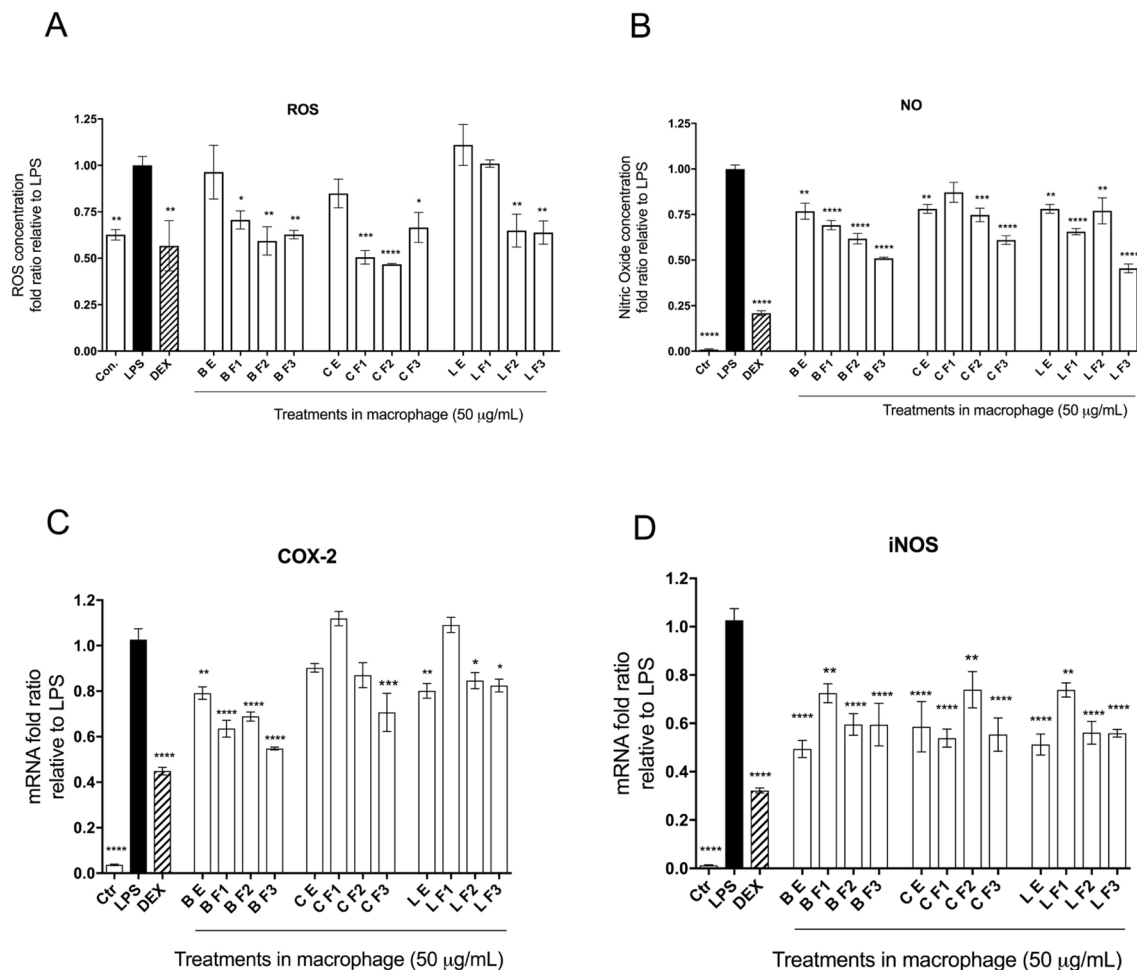


**FIGURE 3 |** Anti-inflammatory bioactivity of polyphenol-enriched extracts (PE) of Alaskan berries, ANC-enriched (Fr 1, Fr 2), and PAC-enriched (Fr 3). Effects on the expression of the inflammatory biomarker genes in the lipopolysaccharide (LPS)-stimulated RAW264.7 macrophages at 50 µg/ml. Genes involved in the inflammatory response are represented: interleukin *IL-1β* assay (**A**), prostaglandin-endoperoxide synthase 2 *COX-2* assay (**B**), inducible nitric oxide synthase *iNOS* assay (**C**), and interleukin *IL-6* assay (**D**). Changes in gene expression were measured by comparing mRNA quantity relative to LPS. A value of less than 1.0 indicates transcriptional downregulation (inhibition of gene expression) compared with LPS, which shows maximum genetic induction (1.0). Ctrl: cell treatment with vehicle only; Dex: dexamethasone at 10 µM used as positive control. The data represent the average of two experiments ± standard error of the mean (SEM). \**P* < 0.05; \*\**P* < 0.01; \*\*\**P* < 0.001 (*n* = 3) using one-way ANOVA and Dunnett's post-test.

healing in rats (Kapoor et al., 2004). The predominant green tea polyphenol, epigallocatechin-3-gallate (EGCG), also elicited growth and differentiation of pooled normal human primary epidermal keratinocytes (Hsu et al., 2003). Although the present study did not examine the effects of bioactive structures on epidermal repair functions during wound healing (i.e., keratinocyte proliferation and re-epithelization) based on the above evidence, it is likely that Alaskan berry bioactive compounds could also modulate keratinocyte activities and mediate improvement of epidermal proliferation during re-epithelization, which occurs in conjunction with dermal fibroblast migration and granulation tissue formation to facilitate wound closure. Highlighting their interconnected functionality, fibroblasts and keratinocytes are known to engage in cross-talk, which may act as an important regulator of their respective dermal and epidermal repair functions during skin wound healing.

## Bioenergetic Characterization of Procyanidin B2 and Its Metabolites in Fibroblasts

To determine whether the beneficial effects of procyanidin B2 and its structural units on wound healing are mediated by changes in mitochondrial function and bioenergetics, we examined the activity of two major pathways of cellular respiration, glycolysis and oxidative phosphorylation in mitochondria, by directly measuring cellular bioenergetics coupled with mitochondrial stress tests using an XF24 Extracellular Flux Analyzer (Figure 5). Under basal conditions, all groups showed comparable OCRs (Figure 5C). Treatment with procyanidin B2 elevated fibroblast mitochondrial function without reaching significance. This effect could be largely attributed to its structural subunits, as epicatechin and, to a certain degree, HPCA (3,4-dihydroxyphenylacetic acid) tested in the equimolar

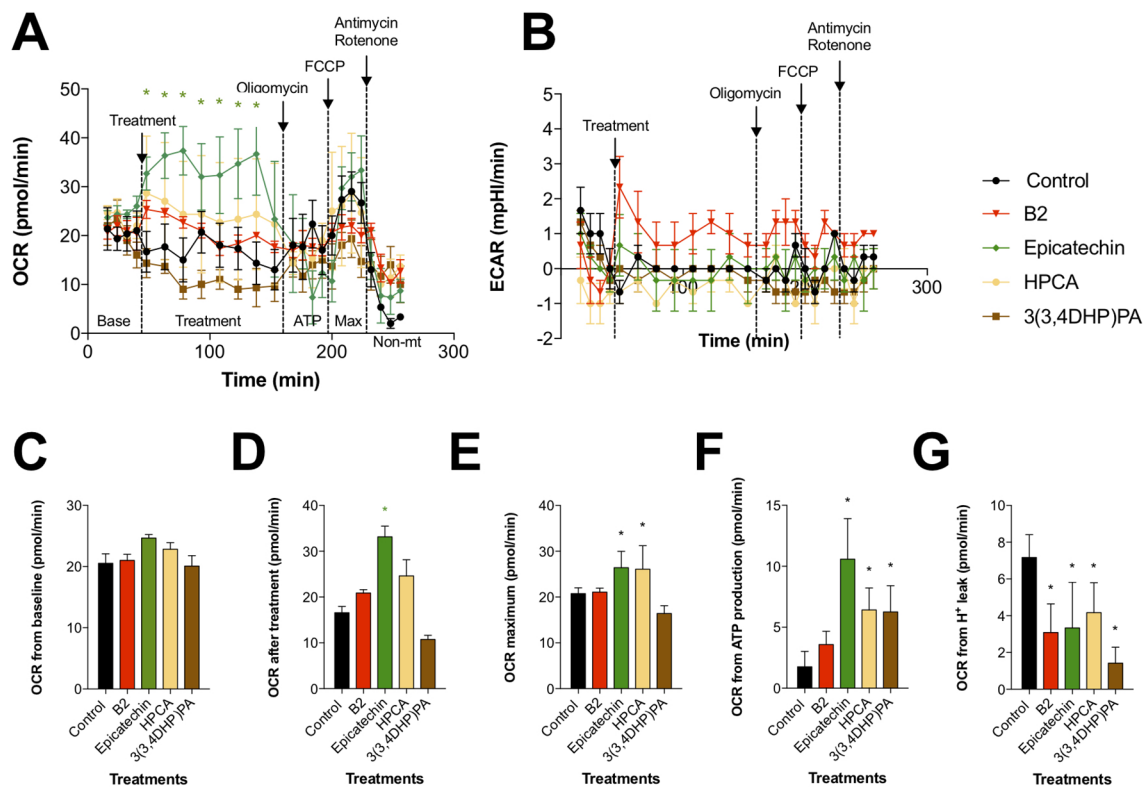


**FIGURE 4 |** Effects of procyanidin B2 and its metabolites on mitochondrial respiration in HDFa. Changes in (A) oxidative phosphorylation and (B) glycolysis rates in response to 10  $\mu$ M of all tested compounds. (C) Cells were subjected to six baseline bioenergetics readings, followed by (D) eight readings of the corresponding treatments. Next, mitochondrial complex inhibitors were injected to all treatments sequentially, and four readings were taken after each inhibitor. Calculations of (E) maximal oxygen consumption rate (OCR), (F) OCR from ATP production, and (G) OCR from proton leak were expressed as means  $\pm$  SEM. \* $P < 0.05$  ( $n = 3$ ).

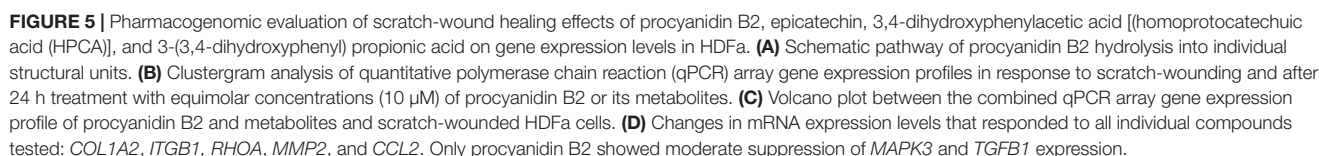
concentration produced marked elevation of mitochondrial function by increasing maximal OCR (Figure 5E), OCR directed at ATP production (Figure 5F), and decreased proton leak (Figure 5G). Modification of HPCA to 3-(3,4-dihydroxyphenyl)propionic acid reduced these effects, as chain length extension possibly enabled this compound to reach the mitochondrial membrane and to partially uncouple the mitochondrial electron transport chain. On the other hand, glycolysis was elevated only by procyanidin B2 treatment alone, and this effect could not be attributed to any of its functional groups, suggesting that an intact procyanidin dimer was required for this activity (Figure 5B).

Mitochondria have critical roles in regulating cellular metabolism, signaling, ROS production, and calcium homeostasis during tissue repair; productive healing depends on mitochondrial calcium uptake, induced after injury, which consequently stimulates ROS generation, causing RhoA activation and actin accumulation at the wound, which ultimately leads to the initiation of membrane repair (Horn et al., 2017). Our observations in the current work suggest that procyanidin B2 and its bioactive structural metabolites promoted wound repair by stimulating oxidative phosphorylation, thereby increasing mitochondrial ATP synthesis and ROS signaling, which are highly implicated in the initiation of cell repair and regenerative responses at the injury site. We speculate that this, in turn, promoted further association of cellular f-actin filaments

with upregulated integrins and induced integrin-dependent fibroblast-like migration (Vicente-Manzanares et al., 2009) as we observed *in vitro*. Mitochondria fundamentally participate in metabolic regulation during tissue repair processes, and it has been suggested that dysfunctional shifts of metabolic programming in immune and nonimmune cells may represent a driving force behind impaired wound healing, failed regenerative outcomes, as well as fibrosis and scarring (Eming et al., 2017). The conserved role of mitochondria in repair and regeneration across many different types of cells and tissues further supports the notion that bioactive polyphenolic compounds of botanical origin, specifically procyanidin B2 and its structural metabolites present in Alaskan wild berries, may promote early phases of wound repair and regeneration, critically dependent on mitochondrial respiration and increased expression of the ECM proteins such as integrins and collagens.

## DISCUSSION

In summary, our results revealed a protective role for polyphenols from three compositionally diverse Alaskan wild berries in signaling and mitochondrial function in cellular wound repair. In general, similar phenolic structures and metabolites are widely distributed across the plant kingdom, which greatly broadens the





applicability of the current work. Principal bioactive phenolic components in these berries may possess immunomodulatory properties, encouraging inflammatory resolution and transition across early stages of repair, as well as potentially protecting against proteolytic degradation of ECM, which is often associated with skin aging. Procyanidin B2 and its structural metabolites demonstrated anti-inflammatory activities but appeared to promote wound repair *via* increasing mitochondrial basal respiration, ATP production, and maximum respiratory capacity, potentially contributing to upregulated expression of integrins and other molecules regulating the ECM. Thus, manipulation of mitochondrial function and integrin signaling with epicatechin and HPCA may be of interest in the development of novel wound therapeutics and skincare products aimed at improving skin repair and regenerative functions.

Integrins and their receptors mechanically link ECM and the actin cytoskeleton, therefore playing a fundamental role in maintaining mechanical homeostasis and detecting mechanical properties of the ECM, such as stiffness, in a process known as mechanosensing. Integrin signaling importantly mediates cell–ECM interactions and regulation of ECM remodeling in repair, regeneration, and aging (Humphrey et al., 2014; De Pascalis and Etienne-Manneville, 2017). On the other hand, spatial activation of Rho-family GTPases is involved in immune-competent cell migration to sites of tissue injury *via* chemoattractant cues, highlighting their importance in the infiltration of inflammatory cells such as macrophages during the early inflammatory phase of wound healing (Eming et al., 2017).

The inflammatory response after injury is divided into multiple phases, and ordered progression through these phases is crucial for constructive tissue repair and regeneration of normal tissue architecture (Landen et al., 2016). A preliminary pro-inflammatory phase stimulates an innate immune response to induce infiltration of key inflammatory cells, particularly macrophages, into the wound site. Next, transition to a secondary phase occurs with progressive abatement of pro-inflammatory processes as macrophages switch to reparative phenotypes. In the final phase, termination of the inflammatory response is accomplished through diminishment of macrophages and other inflammatory cells at the wound site through apoptosis and clearance, thus paving the way for transition into the proliferative phase of repair.

Most berry extract and fraction treatments showed moderate effectiveness in inhibiting inflammatory response variables (ROS and NO production) and gene expression (COX-2 and *i*NOS) in LPS-stimulated macrophages. It is likely that Alaskan berry extracts reduce ROS production in activated macrophages by inducing upregulation of endogenous antioxidant enzyme activities, including glutathione reductase (GSR), glutathione *s*-transferase (GST), and superoxide dismutase (SOD), which represents a virtually ubiquitous mechanism by which polyphenolic-rich berry extracts are known to provide protection against oxidative stress and redox imbalance (Kelly et al., 2017). Broadly, our observations provide evidence for a reasonable degree of anti-inflammatory bioactivity associated with the majority of tested extract and fraction conditions. However, this was by far the most

pronounced in the PAC-enriched fractions. Moreover, the relatively divergent impacts on inflammatory response variables observed with respect to individual extraction/enrichment conditions, and across species, render difficult the discernment of precise structural trends underlying anti-inflammatory potency. Bioactive disparities most likely relate to specific differences in phytochemical profile and quantitative composition of the berries tested in this study. It is generally accepted that the immunomodulatory and/or anti-inflammatory effectiveness associated with any given plant-derived phytochemical mixture is typically determined not only by the presence of specific bioactive constituents and their proportional concentrations but also by the numerous physicochemical interactions that potentially occur between individual bioactive constituents, or between individual constituents and inert components of the plant matrix; while often faithfully presumed to be synergistic or additive in nature, the specific biological consequences of these interactions are not well understood but are appreciated to potentially contribute to bioactivity and target tissue accessibility (Liu, 2004; Phan et al., 2018).

Alaskan wild berries and other botanicals continue to be held in high regard by Alaska native communities for their unique medicinal benefits as well as nutritive qualities (Flint et al., 2011). Medicinal plant usage encompasses an integral element of the traditional ecological knowledge (TEK) of indigenous Arctic communities, and the rich ethnobotanical heritage of indigenous Alaskan communities has largely eluded scientific attention until recently. Moving forward, an overarching scientific priority is the integration of ethnobotanical knowledge with modern biomedical principles, which will likely generate major scientific innovations and lead to novel research avenues in the future (Finn et al., 2017). Interestingly, several Alaskan wild berries tested in this study, lowbush cranberry and bog blueberry, have recently demonstrated benefits *in vitro* for neuronal changes associated with neurodegenerative conditions (Scerbak et al., 2016; Maulik et al., 2018; Scerbak et al., 2018).

Future investigations should explore the influence of 3-D matrices on the effects of these bioactive compounds on fibroblast migration and integrin-mediated mechanosensitive ECM signaling, as these are known to be considerably altered between 2-D and 3-D matrices (Tschumperlin, 2013). Furthermore, it warrants consideration for design for future studies that these experiments were performed in a homogenous cell population, which may not reflect physiological relevance to the same degree as in a heterogeneous co-culture, including keratinocytes, immune cells, and/or endothelial cells, all of which cooperatively coordinate wound healing and tissue repair.

Taken together, these findings point to the attractive possibility of using PAC and bioactives such as epicatechins derived from Alaskan wild berries to promote cellular and molecular responses underpinning regenerative wound healing and constructive tissue repair outcomes. Ultimately, their therapeutic utility in skin repair and regeneration appears to be mediated through several distinct but potentially complementary mechanisms of action, which principally include: immunomodulation to attenuate dysregulated inflammatory response and encourage timely inflammatory resolution; modulation of cell–ECM interaction dynamics



via integrin signaling to optimize cell behaviors, particularly adhesion and migration, which govern regenerative capacity; and regulation of proteolytic tissue factors that contribute to aberrant ECM remodeling and collagen fragmentation in chronic wounds or aging (Pang et al., 2017).

## DATA AVAILABILITY

The raw data supporting the conclusions of this manuscript will be made available by the authors, without undue reservation, to any qualified researcher.

## ETHICS STATEMENT

All work was carried out in accordance with Biosafety Level 2 (BSL-2) Biological use authorization (BUA) 2018-11-688.

## AUTHOR CONTRIBUTIONS

DE and SK contributed the conception and design of the study. DE and SK performed the statistical analysis. DE and JO wrote the first draft of the manuscript. DE, SK, JO, MG, and ML wrote sections of the manuscript. All authors

contributed to manuscript revision and read and approved the submitted version.

## FUNDING

This work is supported by North Carolina State University—Hatch Project no. NC02671 from the United States Department of Agriculture (USDA) National Institute of Food and Agriculture.

## ACKNOWLEDGMENTS

We are very thankful to professor Thomas Kuhn, from the University of Alaska Fairbanks and the Alaska Nature Tribal Health Consortium Program, for providing the wild berries used for this study, and Dr. Jia Xiong for her technical assistance with cell culture and RNA extraction.

## SUPPLEMENTARY MATERIAL

The Supplementary Material for this article can be found online at: <https://www.frontiersin.org/articles/10.3389/fphar.2019.01058/full#supplementary-material>

## REFERENCES

- Budovsky, A., Yarmolinsky, L., and Ben-Shabat, S. (2015). Effect of medicinal plants on wound healing. *Wound Repair Regen.* 23 (2), 171–183. doi: 10.1111/wrr.12274
- Choi, S. Y., Hwang, J. H., Ko, H. C., Park, J. G., and Kim, S. J. (2007). Nobiletin from citrus fruit peel inhibits the DNA-binding activity of NF-kappaB and ROS production in LPS-activated RAW 264.7 cells. *J. Ethnopharmacol.* 113 (1), 149–155. doi: 10.1016/j.jep.2007.05.021
- Dawid-Pač, R. (2013). Medicinal plants used in treatment of inflammatory skin diseases. *Postepy Dermatol. Alergol.* 30 (3), 170–177. doi: 10.5114/pdia.2013.35620
- De Pascalis, C., and Etienne-Manneville, S. (2017). Single and collective cell migration: the mechanics of adhesions. *Mol. Biol. Cell* 28 (14), 1833–1846. doi: 10.1091/mbc.e17-03-0134
- Działo, M., Mierziak, J., Korzun, U., Preisner, M., Szopa, J., and Kulma, A. (2016). The potential of plant phenolics in prevention and therapy of skin disorders. *Int. J. Mol. Sci.* 17 (2), 160. doi: 10.3390/ijms17020160
- Eming, S. A., Wynn, T. A., and Martin, P. (2017). Inflammation and metabolism in tissue repair and regeneration. *Science (New York, N.Y.)* 356 (6342), 1026–1030. doi: 10.1126/science.aam7928
- Esposito, D., Chen, A., Grace, M. H., Komarnytsky, S., and Lila, M. A. (2014). Inhibitory effects of wild blueberry anthocyanins and other flavonoids on biomarkers of acute and chronic inflammation *in vitro*. *J. Agric Food Chem* 62 (29), 7022–7028. doi: 10.1021/jf4051599
- Finn, S., Herne, M., and Castille, D. (2017). The value of traditional ecological knowledge for the environmental health sciences and biomedical research. *Environ. Health Perspect* 125 (8), 085006. doi: 10.1289/EHP858
- Flint, C. G., Robinson, E. S., Kellogg, J., Ferguson, G., Boufajreldin, L., Dolan, M., et al. (2011). Promoting wellness in Alaskan villages: integrating traditional knowledge and science of wild berries. *Ecohealth* 8 (2), 199–209. doi: 10.1007/s10393-011-0707-9
- Galiano, R. D., Tepper, O. M., Pelo, C. R., Bhatt, K. A., Callaghan, M., Bastidas, N., et al. (2004). Topical vascular endothelial growth factor accelerates diabetic wound healing through increased angiogenesis and by mobilizing and recruiting bone marrow-derived cells. *Am. J. Pathol.* 164 (6), 1935–1947. doi: 10.1016/S0002-9440(10)63754-6
- Grace, M. H., Esposito, D., Dunlap, K. L., and Lila, M. A. (2014). Comparative analysis of phenolic content and profile, antioxidant capacity, and anti-inflammatory bioactivity in wild Alaskan and commercial *Vaccinium* berries. *J. Agric Food Chem* 62 (18), 4007–4017. doi: 10.1021/jf403810y
- Grace, M. H., Ribnicky, D. M., Kuhn, P., Poulev, A., Logendra, S., Yousef, G. G., et al. (2009). Hypoglycemic activity of a novel anthocyanin-rich formulation from lowbush blueberry, *Vaccinium angustifolium* Aiton. *Phytomedicine* 16 (5), 406–415. doi: 10.1016/j.phymed.2009.02.018
- Hollands, W. J., Voorspoels, S., Jacobs, G., Aaby, K., Meisland, A., Garcia-Villalba, R., et al. (2017). Development, validation and evaluation of an analytical method for the determination of monomeric and oligomeric procyanidins in apple extracts. *J. Chromatogr. A* 1495, 46–56. doi: 10.1016/j.chroma.2017.03.030
- Horn, A., Van der Meulen, J. H., Defour, A., Hogarth, M., Sreetama, S. C., Reed, A., et al. (2017). Mitochondrial redox signaling enables repair of injured skeletal muscle cells. *Sci. Signal* 10 (495), eaaj1978. doi: 10.1126/scisignal.aaj1978
- Howard, L. R., Clark, J. R., and Brownmiller, C. (2003). Antioxidant capacity and phenolic content in blueberries as affected by genotype and growing season. *J. Sci. Food Agric.* 83 (12), 1238–1247. doi: 10.1002/jsfa.1532
- Hsu, S., Bollag, W. B., Lewis, J., Huang, Q., Singh, B., Sharawy, M., et al. (2003). Green tea polyphenols induce differentiation and proliferation in epidermal keratinocytes. *J. Pharmacol. Exp. Ther.* 306 (1), 29–34. doi: 10.1124/jpet.103.049734
- Humphrey, J. D., Dufresne, E. R., and Schwartz, M. A. (2014). Mechanotransduction and extracellular matrix homeostasis. *Nat. Rev. Mol. Cell Biol.* 15 (12), 802–812. doi: 10.1038/nrm3896
- Kapoor, M., Howard, R., Hall, I., and Appleton, I. (2004). Effects of epicatechin gallate on wound healing and scar formation in a full thickness incisional wound healing model in rats. *Am. J. Pathol.* 165 (1), 299–307. doi: 10.1016/S0002-9440(10)63297-X
- Karim, R. B., Brito, B. L., Dutrieux, R. P., Lassance, F. P., and Hage, J. J. (2006). MMP-2 assessment as an indicator of wound healing: a feasibility study. *Adv. Skin Wound Care* 19 (6), 324–327. doi: 10.1097/00129334-200607000-00011
- Karppinen, K., Zoratti, L., Nguyenquynh, N., Haggman, H., and Jaakola, L. (2016). On the developmental and environmental regulation of secondary metabolism in *Vaccinium* spp. berries. *Front. Plant Sci.* 7, 655. doi: 10.3389/fpls.2016.00655

- Kellogg, J., Wang, J., Flint, C., Ribnick, D., Kuhn, P., De Mejia, E. G., et al. (2010). Alaskan wild berry resources and human health under the cloud of climate change. *J. Agric Food Chem* 58 (7), 3884–3900. doi: 10.1021/jf902693r
- Kelly, E., Vyas, P., and Weber, J. (2017). Biochemical properties and neuroprotective effects of compounds in various species of berries. *Molecules* 23, 26. doi: 10.3390/molecules23010026
- Landen, N. X., Li, D., and Stahle, M. (2016). Transition from inflammation to proliferation: a critical step during wound healing. *Cell Mol. Life Sci.* 73 (20), 3861–3885. doi: 10.1007/s00018-016-2268-0
- Larjava, H., Koivisto, L., Hakkinen, L., and Heino, J. (2011). Epithelial integrins with special reference to oral epithelia. *J. Dent. Res.* 90 (12), 1367–1376. doi: 10.1177/0022034511402207
- Li, Y., Zhang, J. J., Xu, D. P., Zhou, T., Zhou, Y., Li, S., et al. (2016). Bioactivities and health benefits of wild fruits. *Int. J. Mol. Sci.* 17 (8), 1258. doi: 10.3390/ijms17081258
- Lila, M. A. (2006). The nature-versus-nurture debate on bioactive phytochemicals: the genome versus terroir. *J. Sci. Food Agric.* 86 (15), 2510–2515. doi: 10.1002/jsfa.2677
- Liu, R. H. (2004). Potential synergy of phytochemicals in cancer prevention: mechanism of action. *J. Nutr.* 134 (12 Suppl), 3479s–3485s. doi: 10.1093/jn/134.12.3479s
- Livak, K. J., and Schmittgen, T. D. (2001). Analysis of relative gene expression data using real-time quantitative PCR and the 2(-Delta Delta C(T)) Method. *Methods* 25 (4), 402–408. doi: 10.1006/meth.2001.1262
- Manninen, A. (2015). Epithelial polarity—generating and integrating signals from the ECM with integrins. *Exp Cell Res.* 334 (2), 337–349. doi: 10.1016/j.yexcr.2015.01.003
- Maulik, M., Mitra, S., Hunter, S., Hunstiger, M., Oliver, S. R., Bult-Ito, A., et al. (2018). Sir-2.1 mediated attenuation of  $\alpha$ -synuclein expression by Alaskan bog blueberry polyphenols in a transgenic model of *Caenorhabditis elegans*. *Sci. Rep.* 8 (1), 10216. doi: 10.1038/s41598-018-26905-4
- Nile, S. H., and Park, S. W. (2014). Edible berries: bioactive components and their effect on human health. *Nutrition* 30 (2), 134–144. doi: 10.1016/j.nut.2013.04.007
- Nizamutdinova, I. T., Kim, Y. M., Chung, J. I., Shin, S. C., Jeong, Y.-K., Seo, H. G., et al. (2009). Anthocyanins from black soybean seed coats stimulate wound healing in fibroblasts and keratinocytes and prevent inflammation in endothelial cells. *Food Chem. Toxicol.* 47 (11), 2806–2812. doi: 10.1016/j.fct.2009.08.016
- Pang, C., Ibrahim, A., Bulstrode, N. W., and Ferretti, P. (2017). An overview of the therapeutic potential of regenerative medicine in cutaneous wound healing. *Int. Wound J.* 14 (3), 450–459. doi: 10.1111/iwj.12735
- Paredes-Lopez, O., Cervantes-Ceja, M. L., Vigna-Perez, M., and Hernandez-Perez, T. (2010). Berries: improving human health and healthy aging, and promoting quality life—a review. *Plant Foods Hum. Nutr.* 65 (3), 299–308. doi: 10.1007/s11130-010-0177-1
- Phan, M. A. T., Paterson, J., Bucknall, M., and Arcot, J. (2018). Interactions between phytochemicals from fruits and vegetables: effects on bioactivities and bioavailability. *Crit. Rev. Food Sci. Nutr.* 58 (8), 1310–1329. doi: 10.1080/10408398.2016.1254595
- Prior, R. L., Fan, E., Ji, H., Howell, A., Nio, C., Payne, M. J., et al. (2010). Multi-laboratory validation of a standard method for quantifying proanthocyanidins in cranberry powders. *J. Sci. Food Agric.* 90 (9), 1473–1478. doi: 10.1002/jsfa.3966
- Qin, Z., Balimunkwe, R. M., and Quan, T. (2017). Age-related reduction of dermal fibroblast size upregulates multiple matrix metalloproteinases as observed in aged human skin *in vivo*. *Br. J. Dermatol.* 177 (5), 1337–1348. doi: 10.1111/bjd.15379
- San Miguel, S. M., Opperman, L. A., Allen, E. P., Zielinski, J., and Svoboda, K. K. (2011). Bioactive antioxidant mixtures promote proliferation and migration on human oral fibroblasts. *Arch. Oral Biol.* 56 (8), 812–822. doi: 10.1016/j.archoralbio.2011.01.001
- Scerbak, C., Vayndorf, E., Hernandez, A., McGill, C., and Taylor, B. (2018). Lowbush cranberry acts through DAF-16/FOXO signaling to promote increased lifespan and axon branching in aging posterior touch receptor neurons. *Geroscience* 40 (2), 151–162. doi: 10.1007/s11357-018-0016-0
- Scerbak, C., Vayndorf, E. M., Hernandez, A., McGill, C., and Taylor, B. E. (2016). Mechanosensory neuron aging: differential trajectories with lifespan-extending Alaskan berry and fungal treatments in *Caenorhabditis elegans*. *Front. Aging Neurosci.* 8, 173. doi: 10.3389/fnagi.2016.00173
- Schmidt, C. A., Murillo, R., Bruhn, T., Bringmann, G., Goettert, M., Heinzmann, B., et al. (2010). Catechin derivatives from *Parapiptadenia rigida* with *in vitro* wound-healing properties. *J. Nat. Prod.* 73 (12), 2035–2041. doi: 10.1021/np100523s
- Schnitter, J., Bansal, R., Storm, G., and Prakash, J. (2018). Integrins in wound healing, fibrosis and tumor stroma: high potential targets for therapeutics and drug delivery. *Adv. Drug Deliv. Rev.* 129, 37–53. doi: 10.1016/j.addr.2018.01.020
- Seeram, N. P. (2008). Berry fruits: compositional elements, biochemical activities, and the impact of their intake on human health, performance, and disease. *J. Agric. Food Chem.* 56 (3), 627–629. doi: 10.1021/jf071988k
- Singleton, V. L., Orthofer, R., and Lamuela-Raventós, R. M. (1999). “[14] Analysis of total phenols and other oxidation substrates and antioxidants by means of Folin–Ciocalteu reagent,” in *Methods in Enzymology*. (Academic Press), 152–178. doi: 10.1016/S0076-6879(99)99017-1
- Tschumperlin, D. J. (2013). Fibroblasts and the ground they walk on. *Physiology (Bethesda, Md.)* 28 (6), 380–390. doi: 10.1152/physiol.00024.2013
- Van de Velde, F., Grace, M. H., Esposito, D., Pirovani, M., Elida and Lila, M. A. (2016). Quantitative comparison of phytochemical profile, antioxidant, and anti-inflammatory properties of blackberry fruits adapted to Argentina. *J. Food Compos. Anal.* 47, 82–91. doi: 10.1016/j.jfca.2016.01.008
- Vicente-Manzanares, M., Choi, C. K., and Horwitz, A. R. (2009). Integrins in cell migration—the actin connection. *J. Cell Sci.* 122 (Pt 2), 199–206. doi: 10.1242/jcs.018564
- Walraven, M., and Hinz, B. (2018). Therapeutic approaches to control tissue repair and fibrosis: extracellular matrix as a game changer. *Matrix Biol.* 71–72, 205–224. doi: 10.1016/j.matbio.2018.02.020
- Wood, S., Jayaraman, V., Huelsmann, E. J., Bonish, B., Burgad, D., Sivaramakrishnan, G., et al. (2014). Pro-inflammatory chemokine CCL2 (MCP-1) Promotes healing in diabetic wounds by restoring the macrophage response. *PLoS One* 9 (3), e91574. doi: 10.1371/journal.pone.0091574
- Yousef, G. G., Brown, A. F., Funakoshi, Y., Mbeunkui, F., Grace, M. H., Ballington, J. R., et al. (2013). Efficient quantification of the health-relevant anthocyanin and phenolic acid profiles in commercial cultivars and breeding selections of blueberries (*Vaccinium* spp.). *J. Agric. Food Chem.* 61 (20), 4806–4815. doi: 10.1021/jf400823s

**Conflict of Interest Statement:** The authors declare that the research was conducted in the absence of any commercial or financial relationships that could be construed as a potential conflict of interest.

Copyright © 2019 Esposito, Overall, Grace, Komarnytsky and Lila. This is an open-access article distributed under the terms of the Creative Commons Attribution License (CC BY). The use, distribution or reproduction in other forums is permitted, provided the original author(s) and the copyright owner(s) are credited and that the original publication in this journal is cited, in accordance with accepted academic practice. No use, distribution or reproduction is permitted which does not comply with these terms.



# Growth Inhibitory Activity of *Callicarpa americana* Leaf Extracts Against *Cutibacterium acnes*

Rozenn M. Pineau<sup>1†</sup>, Sarah E. Hanson<sup>2†</sup>, James T. Lyles<sup>2</sup> and Cassandra L. Quave<sup>2,3,4\*</sup>

<sup>1</sup> School of Biological Sciences, Georgia Institute of Technology, Atlanta, GA, United States, <sup>2</sup> Center for the Study of Human Health, Emory College of Arts and Sciences, Atlanta, GA, United States, <sup>3</sup> Department of Dermatology, Emory University School of Medicine, Atlanta, GA, United States, <sup>4</sup> Emory University Herbarium, Atlanta, GA, United States

## OPEN ACCESS

### Edited by:

Namrita Lall,  
University of Pretoria, South Africa

### Reviewed by:

Adam Matkowski,  
Wroclaw Medical University, Poland  
Hemant K. Gautam,  
Institute of Genomics and  
Integrative Biology (CSIR), India  
Sefirin Djogoue,  
University of Yaounde I, Cameroon

### \*Correspondence:

Cassandra L. Quave  
cquave@emory.edu

<sup>†</sup>These authors have contributed  
equally to this work and share  
first authorship

### Specialty section:

This article was submitted to  
Ethnopharmacology,  
a section of the journal  
Frontiers in Pharmacology

**Received:** 16 April 2019

**Accepted:** 19 September 2019

**Published:** 15 October 2019

### Citation:

Pineau RM, Hanson SE, Lyles JT and  
Quave CL (2019) Growth Inhibitory  
Activity of *Callicarpa americana*  
Leaf Extracts Against  
*Cutibacterium acnes*.  
Front. Pharmacol. 10:1206.  
doi: 10.3389/fphar.2019.01206

Acne vulgaris is a common skin disease affecting adolescents and young adults of all ethnic groups, negatively impacting self-esteem, self-confidence, and social life. The Gram-positive bacteria *Cutibacterium acnes* colonizes the sebum-rich follicle and contributes to inflammation of the pilosebaceous gland. Long-term antibiotic therapies targeting *C. acnes* lead to the development of antimicrobial resistance, and novel acne vulgaris therapies are needed. This study investigated the *C. acnes* inhibitory activity of *Callicarpa americana* leaves, a native Southeastern United States shrub historically used by Native Americans to treat fever, stomachache, and pruritis. Flash chromatography fractions of the ethyl acetate-soluble *C. americana* ethanol leaf extract (649C-F9 and 649C-F13) exhibited MICs ranging from 16 to 32  $\mu\text{g ml}^{-1}$  and  $\text{IC}_{50}$  range of 4–32  $\mu\text{g ml}^{-1}$  against a panel of 10 distinct *C. acnes* isolates. Cytotoxicity against an immortalized human keratinocyte cell line (HaCaTs) skin was detected at more than eight times the dose required for growth inhibitory activity ( $\text{IC}_{50}$  of 256  $\mu\text{g ml}^{-1}$  for 649C-F9 and  $\text{IC}_{50}$  of >512  $\mu\text{g ml}^{-1}$  for 649C-F13). This work highlights the potential of *C. americana* leaf extracts as a cosmeceutical ingredient for the management of acne vulgaris. Further research is necessary to assess its mechanism of action and *in vivo* efficacy.

**Keywords:** medicinal plants, MIC, phytochemicals, acne, *Cutibacterium acnes*, biofilm, cosmeceutical

## INTRODUCTION

### Pathogenesis of Acne Vulgaris

Acne vulgaris is a common skin disease affecting the vast majority of adolescents and a significant proportion of young adults. Approximately 85% of the population suffers from acne vulgaris at some point in their lives (Shah and Peethambaran, 2018). Acne negatively impacts self-esteem, self-confidence, and social life as it specifically affects the skin of the face, the chest, and the back—areas where the pilosebaceous gland concentration is the highest (Thomas, 2004; Titus and Hodge, 2012). Four processes characterize acne pathogenesis: 1) follicular hyperkeratinization, 2) excess of sebum, 3) colonization of *Cutibacterium acnes*, and 4) inflammation and immune response (Toyoda and Morohashi, 2001). *C. acnes* is a Gram-positive aero-tolerant anaerobic bacteria found in the sebaceous follicle. The oxygen-poor area formed by the lipid-rich obstructed follicle makes an ideal environment for the bacteria to proliferate. Other factors such as hormonal fluctuations or imbalance, stress, and pollution can also increase inflammation by providing a suitable environment for *C. acnes* growth (Bhambri et al., 2009).

## Current Treatment and Limitations

Current treatments for acne vulgaris include the use of topical antibiotics and/or chemical peeling agents. Treatments can also include daily oral antibiotics, retinoids, or hormones. In the United States, topical agents predominantly prescribed in the treatment of mild to moderate acne are composed of retinoids such as differin, tazorac, or retin-A, in combination with antibiotics such as clindamycin and erythromycin (Titus and Hodge, 2012). Benzoyl peroxide and salicylic acid are non-antibiotic therapies frequently added to creams to decrease the risk of developing antibiotic resistance and to reduce inflammation (Thiboutot et al., 2009). The most commonly used oral therapies include the tetracyclines (tetracycline, minocycline, and doxycycline), trimethoprim/sulfamethoxazole, and macrolides (erythromycin and azithromycin) (Leyden and Del Rosso, 2011).

A major disadvantage of current treatments is that daily intake of antibiotics places great selective pressure on bacteria to develop multidrug resistance (Van Den Bergh et al., 2016). Many countries have reported increasing resistance of *C. acnes* strains to topical macrolides (Walsh et al., 2016). Application of an active antibiotic gel increased resistance to erythromycin after only 12 weeks of treatment (Mills et al., 2002). The treatment of an individual's acne can also have unintended effects on the microbiome, resulting in antibiotic resistance and proliferation of opportunistic pathogens elsewhere in the body. Margolis et al. reported that development of upper respiratory tract infections and pharyngitis was more likely in patients receiving oral antibiotics (Margolis et al., 2005; Margolis et al., 2012). In light of the growing concern for increasing antibiotic resistance of *C. acnes* and other bacteria due to antibiotic use in acne treatment, alternative therapies are urgently needed.

## Ethnopharmacological Relevance of *Callicarpa americana*

Ethnobotany is the study of plants used in different cultures, and it is a valuable framework from which to pursue drug discovery (Cox, 1994). Botanical therapies are a mixture of many active and non-active components, thus potentially having several modes of action, both direct and synergistically. The Quave Natural Product Library (QNPL) is a chemical library composed of over 1,900 plant extracts derived from 600 plant and fungal species, largely representing plants used in the traditional treatment of infectious and inflammatory skin disease. A screen of the QNPL against *C. acnes* revealed the growth inhibitory bioactivity of a crude leaf extract from *Callicarpa americana* L. (Lamiaceae), a native Southeastern American shrub. The *Callicarpa* genus has a rich history of use in traditional medicine and is characterized by the presence of biologically active terpenoids, such as monoterpenoids and diterpenoids (Kadereit, 2004). The fruits are the most striking elements of the plants in this genus—hence the genus name '*Callicarpa*,' meaning "beautiful fruit," and the common name, 'Beauty Berry.' The Alabama, Choctaw, Creek, Koasati, Seminole, and other Native American tribes used preparations of the roots, leaves, and branches for various medicinal purposes, including to treat fevers, stomachaches, and skin cancers (Taylor, 1940; Jones and Kinghorn, 2008).

Interestingly, *Callicarpa* species are also a key component of Asian traditional medicines (Tu et al., 2013). *C. arborea* Roxb. was traditionally used in India to heal cuts and wounds, and *C. tomentosa* Lam. was used to cure boils and eczema. In China, *C. macrophylla* Vahl, *C. pedunculata* R.Br., and *C. cathayana* C.H.Chang were applied to the skin to heal burns and bleeds (Jones and Kinghorn, 2008), highlighting the potential effectiveness of the *Callicarpa* genus to treat skin diseases (Gupta et al., 2010; Bhat et al., 2014).

## *Callicarpa americana* as a Source of Antimicrobial Therapies for Acne

Few studies have reported the bioactivity of the species *C. americana*. Three diterpenes (genkwanin, 16 $\xi$ -hydroxycleroda-3,13-dien-15,16-olide, and 2-formyl-16 $\xi$ -hydroxy-3-A-norcleroda-2,13-dien-15,16-olide) were isolated from the combined fruits, leaves, and twigs (fruiting branches) of *C. americana* and exhibit activity against human cancer cell lines (Jones et al., 2007). Intermedeol and callicarpenal (3,14,15,16-tetranorclerodane) compounds were found in essential oils from the leaves and acted as effective deterrents of *Aedes stephensi* and *Aedes aegypti* mosquitos (Cantrell et al., 2005). Research focused on other species within the same genus, and leaf extracts of *C. longifolia* Lam. in a gel preparation were recently found to exhibit antibacterial and wound healing effects on rabbit skin (Susilawati et al., 2018). A retinoid-containing gel in combination with a *C. nudiflora* Hook. & Arn. extract tablet was used in a clinical research study on acne vulgaris and was demonstrated to be more effective than the gel alone (Yang et al., 2010). These studies highlight the need for further research on *C. americana* extracts. In the present work, we demonstrate the promising growth inhibitory activity of *C. americana* on *C. acnes*.

## MATERIALS AND METHODS

### Plant Collection and Identification

Fresh leaves of *C. americana* were harvested from wild populations in Atlanta, GA, in June and August 2017. Voucher specimens (Table 1) were deposited at the Emory University Herbarium (GEO), and species identity was confirmed by botanist Tharanga Samarakoon, Ph.D. Specimens were digitized and are available for viewing on the SERNEC portal (Sernec, 2019). Bulk plant material was dried in a dehumidification chamber and then ground into a fine powder through a 2-mm mesh with a Thomas Scientific Wiley Mill (Swedesboro, NJ). Retention vouchers of dried and ground material were prepared for future reference and stored in The Quave Research Laboratories at Emory University.

### Preparation of Extracts

Dry, ground plant biomass was double macerated in 95% ethanol at a 1:10 ratio (w/v) for 72 h of maceration with daily agitation. The liquid was then decanted and vacuum filtered, then concentrated by rotary evaporation at  $\leq 40^{\circ}\text{C}$ . Extracts were redissolved in  $\text{dH}_2\text{O}$ , shell frozen in a dry ice-acetone bath, and lyophilized overnight on a Labconco FreeZone 2.5 Lyophilizer (Kansas



**TABLE 1** | List of *Callicarpa americana* specimens harvested from wild populations in Atlanta, GA.

GEO accession number	Collection date	Collection location	Location coordinates
22044	June 26, 2017	Hahn Wood, Emory University; USA, Georgia, DeKalb County	33.8036944440 N, -84.3230833330 W
22204	Aug. 11, 2017	Coralwood Centre School; USA, Georgia, DeKalb County	33.8281800000 N, -84.2872430000 W
22205	Aug. 11, 2017	Coralwood Centre School; USA, Georgia, DeKalb County	33.8281800000 N, -84.2872430000 W

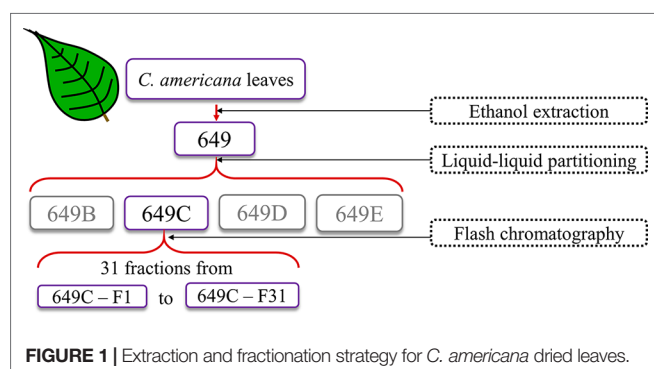
Voucher specimens of all populations harvested were collected and deposited at the Emory University Herbarium (Index Herbariorum Code: GEO). Digitized specimens are available for viewing online through the SERNEC portal (Serneec, 2019).

City, MO). Dry crude extract (Extract ID: 649) was scraped into scintillation vials and stored at  $-20^{\circ}\text{C}$  until microbiological testing, at which time they were dissolved in DMSO to a stock concentration of  $10\text{ mg ml}^{-1}$ .

## Fractionation Strategy

The crude extract (649) was partitioned against hexanes, ethyl acetate, *n*-butanol, and water following a modified Kupchan scheme. Subsequently, the ethyl acetate partition (649C) was determined to be the most active partition by antimicrobial bioassays and was further fractionated *via* flash chromatography. The full fractionation strategy is detailed in **Figure 1**.

Briefly, to prepare the sample, 15.36 g of the extract was dissolved in methanol, Celite was added at a 1:4 ratio (*w/w*), the mixture was concentrated *in vacuo*, and the dry preparation was loaded into a Teledyne solid-phase load cartridge. A 330-g RediSep Rf Gold Silica column was used with the CombiFlash Rf+ (Teledyne ISCO) flash chromatography system. Three mobile phases—hexanes, ethyl acetate, and methanol—were used to perform the separation (**Table 2** and **Figure 2**). The resulting tubes were combined into 31 fractions, dried *in vacuo*, lyophilized, scraped into scintillation vials, and then stored at  $-20^{\circ}\text{C}$  until testing.

**FIGURE 1** | Extraction and fractionation strategy for *C. americana* dried leaves.**TABLE 2** | Gradient table for the flash chromatography separation of extract 649C.

Minutes	% Hexane	% Ethyl Acetate	% Methanol
0	100	0	0
4.4	100	0	0
8.2	99	1	0
12	98	2	0
15.8	96	4	0
19.6	91.9	8.1	0
24.3	85.4	14.9	0
38.9	68.1	31.9	0
54.3	35.9	64.1	0
69.8	0	100	0
88.2	0	100	0
88.4	0	100	0
92.2	0	99	1
96	0	98	2
99.8	0	96	4
103.6	0	92	8
107.4	0	84	16
111.2	0	70	30
129.7	0	70	30
133.3	0	0	100
146.6	0	0	100

The flow rate for the 330-g RediSep Rf Gold Silica column was  $200\text{ ml min}^{-1}$ .

## Antibacterial Testing

### Bacterial Strains and Cultures

Extracts were first tested against a *C. acnes* isolate obtained from the American Type Culture Collection (strain ATCC6919). Based on these results, the most active fractions and their parent extracts were tested for growth inhibitory activity in nine additional clinical isolates of *C. acnes*; strain and source details are provided in **Table 3**. All bacteria were streaked onto tryptic soy agar (TSA) plates supplemented with 5% sheep blood (Hardy). Plates were incubated at  $37^{\circ}\text{C}$  until individual colonies were visible (72 h for most isolates and 120 h for the slowest growers) before individual colonies were transferred into Brain Heart Infusion broth supplemented with 1% dextrose (BHId). Liquid cultures were incubated for an additional 72 h before preparation of a working culture for biological assays. An EZ Anaerobe Chamber and GasPak EZ Anaerobe (BD) container sachets were used to create the anaerobic conditions required for *C. acnes* growth.

### Growth Inhibition Assays

As no Clinical and Laboratory Standards Institute (CLSI) guidelines for MIC testing in *C. acnes* have been published, we followed a previously described microtiter broth method (Nelson et al., 2016). Liquid cultures were standardized to an optical density of 0.05 at 590 nm ( $\text{OD}_{590\text{nm}}$ ), which corresponds to  $5 \times 10^7\text{ CFU ml}^{-1}$ , using a Cytation-3 multimode plate reader (BioTek). This was further confirmed by plate counts. BHId was used for adjusting the final inoculum density.

The growth inhibition assay was performed in a sterile 96-well plate (Falcon 351172) in a total well volume of  $200\text{ }\mu\text{L}$ . The dose tested ranged from  $0.125$  to  $64\text{ }\mu\text{g ml}^{-1}$  for ATCC6919 and from  $2$  to  $64\text{ }\mu\text{g ml}^{-1}$  for all other clinical isolates. Negative controls



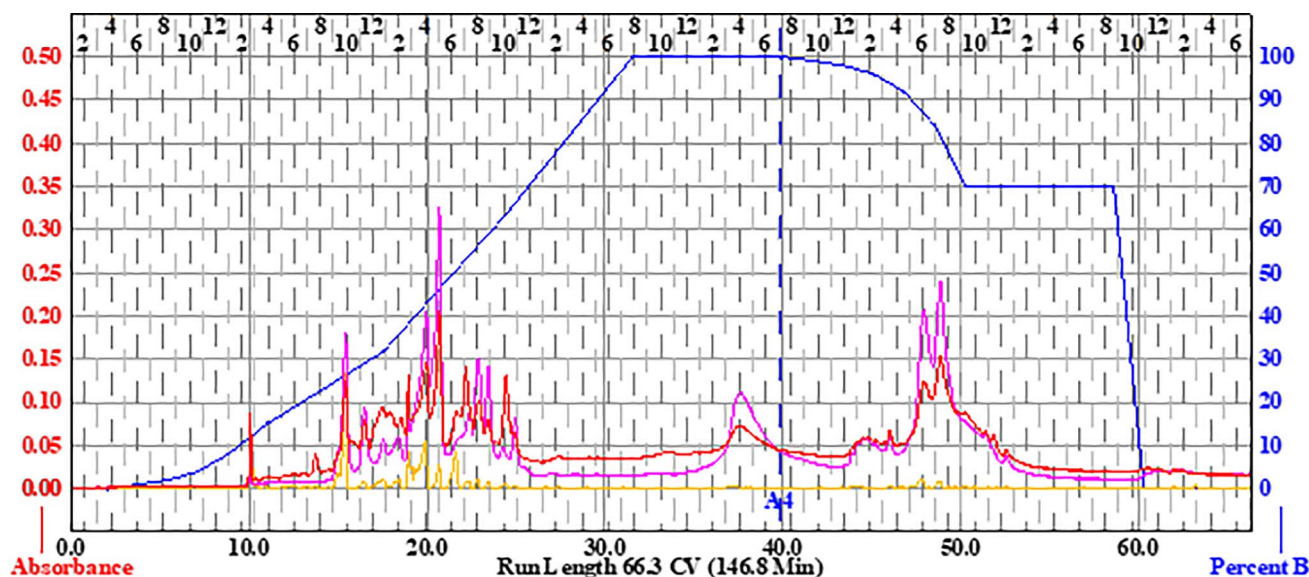


**FIGURE 2 |** Flash chromatogram of 649C fraction. A 330-g Gold Silica column was loaded with 15.36 g of the 649C fraction. Three mobile phases— hexanes, ethyl acetate, and methanol—were used to perform the separation. The blue line details the percent of ethyl acetate mobile phase. In total, 31 fractions were decided based on the chromatogram, with each peak being assigned to a unique fraction if possible. Absorbance of the extract is read on the left axis (red, orange, and pink lines for three wavelengths: 254 nm, 320 nm, and total absorbance of 200–780 nm, respectively). The x-axis corresponds to column volumes (CV) with a total run length of 66.3 CV.

(no treatment and DMSO vehicle treatment), positive control (clindamycin treatment), and a media control (BHId alone) were included, and all treatments were conducted in triplicate and repeated on two separate days. A first  $OD_{600nm}$  determination was conducted immediately following plate setup, prior to a 72-h incubation period at 37°C in an anaerobe chamber. A second  $OD_{600nm}$  determination was taken 72 h post-inoculation, and the final percent inhibition of growth was determined following a previously reported formula, which takes into account the effect

of the extract color (Quave et al., 2008). The  $IC_{50}$  and MIC are the minimal concentrations to inhibit at least 50% and 90% of the growth, respectively.

### Biofilm Eradication

Liquid cultures were standardized to an optical density at 590 nm ( $OD_{590nm}$ ) of 0.05, which corresponds to  $5 \times 10^7$  CFU  $ml^{-1}$ , and pipetted into a 96-well tissue culture plate (TPP92097). After a 24-h incubation period at 37°C in an anaerobic chamber, the media was gently removed using a single-channel micropipette without disturbing the biofilm. Fresh BHId and treatment was added to each well. The plate was incubated for an additional 24 h at 37°C in an anaerobe chamber. The media was gently removed before fixing the biofilms in two steps: adding 100% ethanol to each well, removing it, and then heat fixing at 60°C for 60 min. Crystal violet was then added to each well for 5 min to stain the biofilms and was subsequently gently rinsed out under tap water. Plates were dried overnight, then a solution of 2.5% Tween 80 in ethanol was added to elute the stain for 15 min, the eluent transferred to a new 96-well plate, and an  $OD_{595nm}$  obtained to determine total biofilm mass in each well. The minimal biofilm eradication concentration ( $MBEC_{50}$ ) was defined as the minimal concentration of extract required to eradicate at least 50% of the preformed biofilm.

### Mammalian Cytotoxicity Assay

Mammalian cytotoxicity of extracts was assessed using human keratinocytes (HaCaTs) and a lactate dehydrogenase (LDH) test kit (G-Biosciences, St. Louis, MO) as previously described (Quave et al., 2015). Extracts were sterile-filtered with 0.2- $\mu m$

**TABLE 3 |** *C. acnes* strain details.

Strain ID	Strain genotype	Type of isolate	Body site
ATCC6919	–	Laboratory strain	Facial acne
B104.1	Ribotype 3	Clinical isolate	Nasal microcomedone
B104.2	Ribotype 3	Clinical isolate	Nasal microcomedone
B104.4	Ribotype 3	Clinical isolate	Nasal microcomedone
B104.5	Ribotype 3	Clinical isolate	Nasal microcomedone
B104.6	Ribotype 1	Clinical isolate	Nasal microcomedone
B104.7	Ribotype 1	Clinical isolate	Nasal microcomedone
B104.8	Ribotype 3	Clinical isolate	Nasal microcomedone
HL013PA1;	–	Clinical isolate	–
HM-497; EU-09	–	Clinical isolate	–
HL030PA1;	–	Clinical isolate	–
HM-504; EU-16	–	Clinical isolate	–

Clinical isolates B104.1 to B104.8 were obtained from Dr. Laura Marinelli (Marinelli et al., 2012). Clinical isolates EU-09 and EU-16 were obtained through BEI Resources, NIAID, NIH as part of the Human Microbiome Project. – indicates unknown information from the strain providers.

syringe filters and tested at a concentration range of 2–1024  $\mu\text{g ml}^{-1}$ . Percent DMSO (v/v) in the wells was <2% for all tests.

## Chemical Characterization

### LC-FTMS Analysis

Liquid chromatography–Fourier transform mass spectrometry (LC-FTMS) was performed on 649C fractions using a Shimadzu SIL-ACHT (Columbia, MD) and Dionex (San Jose, CA) 3600SD HPLC pump. The stationary phase was a Phenomenex Kinetex C18 150  $\times$  2.1 mm, 2.5  $\mu\text{m}$  with guard column at room temperature. Mobile phases were Optima LC/MS (Fisher Scientific, Waltham, MA) consisting of (A) 0.1% formic acid in water (B) and 0.1% formic acid in methanol at a flow rate of 0.15 ml/min. The gradient profile consisted of initial conditions of 70:30 A/B which was held until 2.6 min., then a linear gradient applied until 5:95 A/B was reached at 52.7 min—this was held until 61.6 min—then a step gradient applied to 0:100 A/B, which was held until 70.4 min, and then the column returned to initial conditions prior to the next injection. A 20- $\mu\text{l}$  injection of each fraction was applied onto the column. The chromatography was monitored at 190–600 nm by a Dionex DAD detector. The MS data was acquired in MS<sup>1</sup> mode scanning a  $m/z$  of 150–1,500 on a Thermo Scientific LTQ-FT Ultra MS in positive ESI mode and processed with Thermo Scientific Xcalibur 2.2 SP1.48 software (San Jose, CA). The capillary temperature was 275.0°C, sheath gas of 40, source voltage and current of 5.0 kV and 100.0  $\mu\text{A}$ , and capillary voltage of 29.0 V.

Putative formulas and compounds were determined for peaks of the bioactive fractions of 649C with greater than 1% relative abundance by area in the MS total ion chromatograph (TIC). Scifinder (Chemical Abstracts Service) was searched in July 2019 to identify putative matches. The (M+1)<sup>+</sup> from the MS data was used to calculate the accurate mass of the parent ion and the databases searched for small molecules from the genus *Callicarpa* within  $\pm 1.0$  Da. The molecular formulas of the hits were compared to empirical formulas derived from the experimental MS data. Database hits that matched the experimentally calculated empirical formula,  $\pm 10$  ppm, were evaluated further. Publications on the remaining small molecules were reviewed and the presence of the compound in the genus was verified. The resulting putative compound matches are in Table 5. Only an empirical formula is reported for ions that do not have a match in the database.

## RESULTS

### Growth Inhibitory Activity Against *P. acnes*

Growth inhibitory effects of the crude extract and partitions of *C. americana* leaves were determined using a static MIC assay. The initial screen was performed on ATCC6919 and demonstrated that the ethyl acetate partition (649C) was the most effective inhibitor of *C. acnes* growth with an IC<sub>50</sub> value of 32  $\mu\text{g ml}^{-1}$ . 649C was subjected to flash chromatography to yield 31 fractions. Eight out of the 31 fractions exhibited 100% growth inhibition at 64  $\mu\text{g ml}^{-1}$  against ATCC6919 (Figure 3). Dose-dependent growth inhibition of the most active fractions

was then conducted on ATCC6919 as well as nine other clinical isolates of *C. acnes* (Figures 4 and 5). Growth inhibitory activity was observed for each of the 10 isolates of *C. acnes* tested. The most active fractions were 649C-F9 and 649C-F13, with IC<sub>50</sub> values ranging from 4 to 32  $\mu\text{g ml}^{-1}$  and MIC values ranging from 16 to 32  $\mu\text{g ml}^{-1}$  across all isolates (Table 4 and Figure 6). Although no interpretive standards from the CLSI for antibiotic resistance exist for *C. acnes*, it is noteworthy that seven of the nine clinical isolates tested exhibited MICs >4  $\mu\text{g ml}^{-1}$  for the antibiotic control (clindamycin), which is commonly used in both oral and topical therapies for the management of acne vulgaris. Furthermore, six of the nine clinical isolates tested did not achieve even 50% growth inhibition at the maximum concentration of clindamycin tested (4  $\mu\text{g ml}^{-1}$ ).

### Biofilm Eradication Activity in *C. acnes*

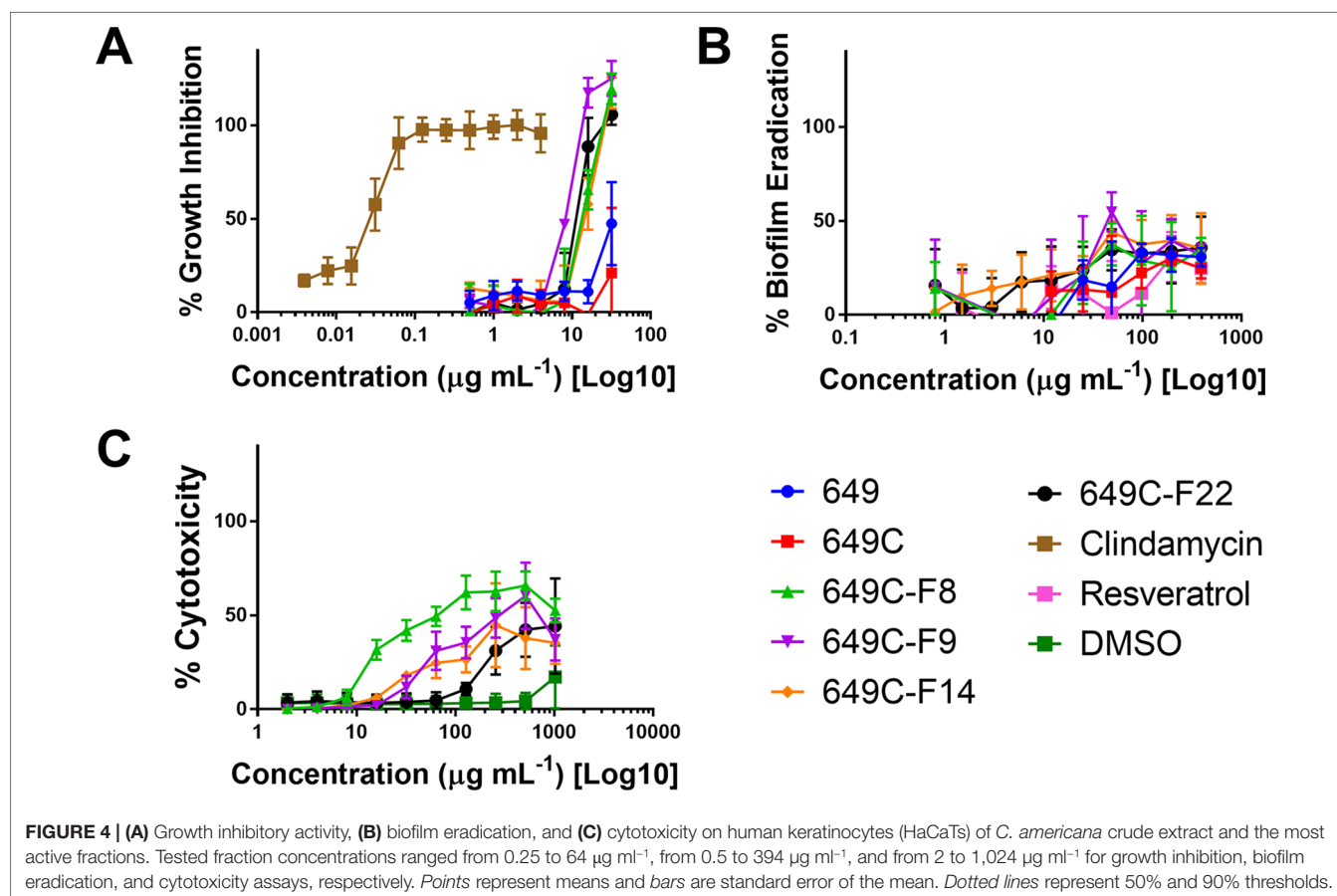
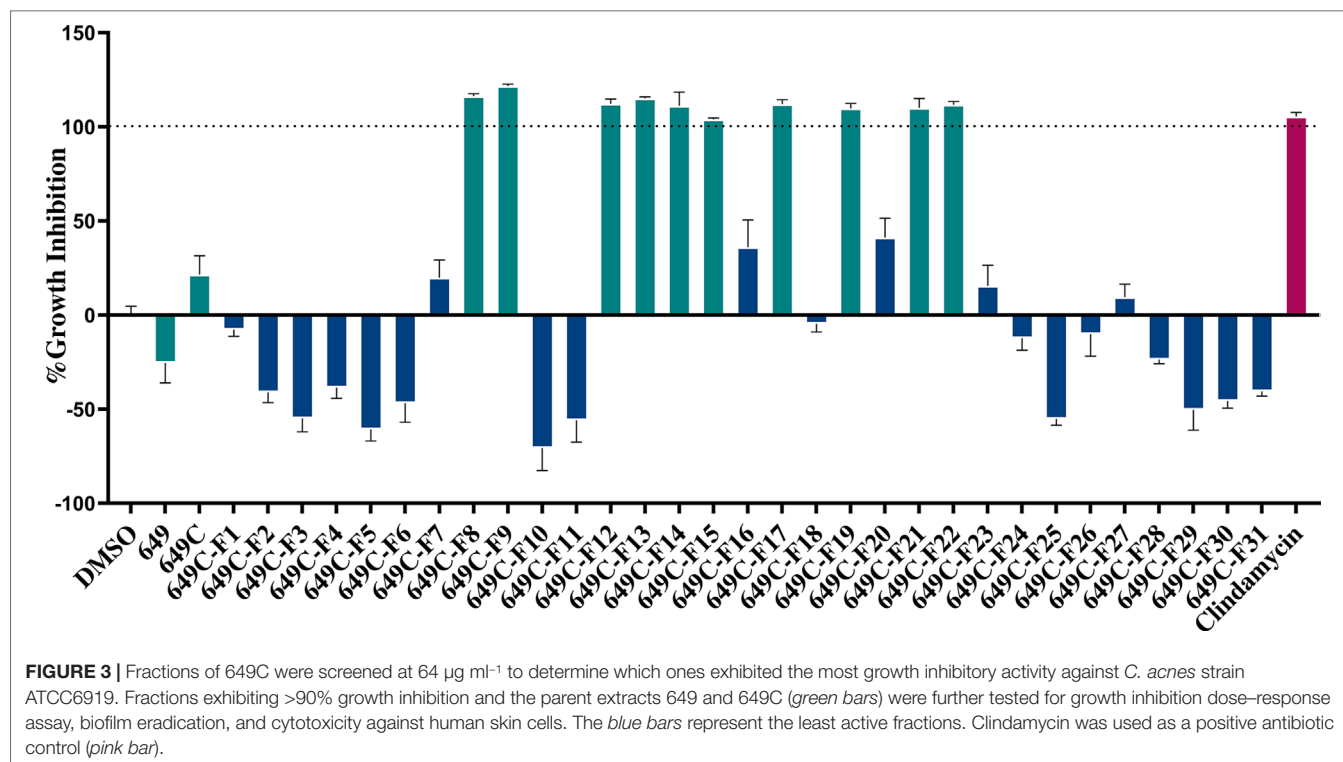
Biofilm eradication activity was assessed, and none of the fractions were found to significantly eradicate the biofilm. A decrease in 30–40% of biofilm was observed for the highest concentration tested (394  $\mu\text{g ml}^{-1}$ ). Resveratrol, a previously reported candidate for *C. acnes* biofilm eradication, reached 30% eradication at a concentration of 394  $\mu\text{g ml}^{-1}$ .

### *C. americana* Extracts Exhibit Low Toxicity to Human Keratinocytes

To examine possible cytotoxic effects of the extracts in mammalian cells, HaCaT cells were treated at concentrations ranging from 2 to 1,024  $\mu\text{g ml}^{-1}$ . For all tested fractions, cytotoxicity (IC<sub>50</sub>) was only observed at more than eight times the dose required for inhibitory activity when compared to the IC<sub>50</sub> values for *C. acnes* strain ATCC6919 (Table 4). Fractions 649C-F8 and 649C-F9 were the most cytotoxic to the HaCaTs, with IC<sub>50</sub> values at 28 and 256  $\mu\text{g ml}^{-1}$ , respectively. The therapeutic index (TI) was calculated by dividing the IC<sub>50</sub> for mammalian cytotoxicity by the IC<sub>50</sub> for *C. acnes* growth inhibition, and the TI range for each fraction is reported in Table 4.

### Chemical Characterization of Extracts

The LC-FTMS ESI-positive mass spectral chromatograms of the ethyl acetate partition (649C) and the bioactive fractions (649C-F9 and 649C-F13) are shown in Figure 7. The ions with greater than a 1% abundance in the LC-FTMS ESI-positive mode analysis are tabulated in Table 5. Fraction 649C-F9 is the least complex fraction, with over 56% consisting of a compound with  $m/z$  637.4457 eluting at 51.3 min. A total of nine ions were identified as having greater than 1% relative abundance. Putative matches were only obtained for peak number 1 with an empirical formula of C<sub>20</sub>H<sub>29</sub>O<sub>3</sub>, which corresponded to 14 compounds in Scifinder: 16 $\xi$ -hydroxycyclohexa-3,11(E),13-trien-15,16-olide (CAS #935527-99-4), seco-hinokiol (834870-61-0), angustanoic acid F (104998-60-9), 7-hydroxydehydroabiatic acid (95416-24-3), 11-hydroxylsugiol (88664-08-8), 3,4-dihydroxyphenethyl glucoside (76873-99-9), 7 $\alpha$ -hydroxydehydroabiatic acid (76235-98-8), 7 $\beta$ -hydroxydehydroabiatic acid (73609-55-9), 15-hydroxydehydroabiatic acid (54113-95-0), maingayic acid (34327-14-5), 11-hydroxy-13-(1-hydroxy-1-methylethyl)-podocarpa-8,11,13-trien-7-one (16755-58-1), 11-hydroxy-12-methoxyabietatriene



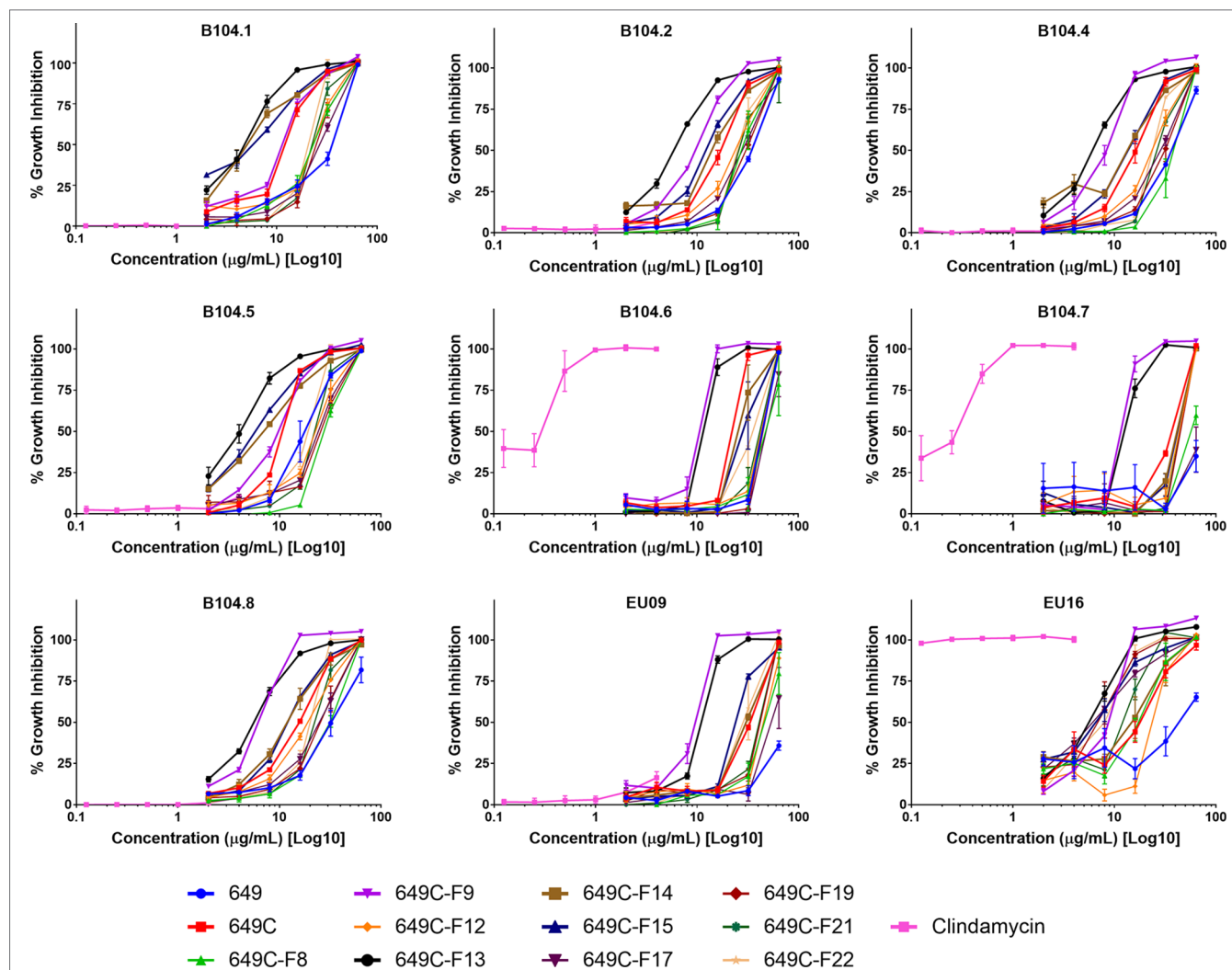


**FIGURE 5 |** Growth inhibitory activity of extracts and fractions against a panel of nine clinical isolates of *C. acnes*.

(16755-54-7), methyltrans-communate (15798-13-7), and methyl isopimarate (1686-62-0).

Fraction 649-F13 was more diverse, with 19 ions having greater than 1% relative abundance by LC-MS analysis. As before, a single ion dominates,  $m/z$  669.4379 eluting at 49.6 min. There are no putative matches for this ion in Scifinder. However, putative matches were obtained for five other ions from 649C-F13, identified as peaks 2–6 in **Figure 7**. Peak 2 has  $m/z$  376.2583 and empirical formula  $C_{23}H_{36}O_4$  and corresponds to [5'aS-(5'aa,7'aa,9'a,10'a,12'aa,12'bβ)]-decahydro-2,2,5',5',12'b-pentamethyl-spiro[1,3-dioxolane-4,9'(8'H)]-[7a,10]methano[7aH]cyclohepta[g][2]benzoxepin-3'(2'H)-one (CAS #49817-39-2). Peak 3 has  $m/z$  301.2152 and empirical formula  $C_{20}H_{29}O_2$  which corresponds to (5α,9α,10β)-3-oxo-kaur-15-en-17-al (CAS #878000-26-1), 18-oxoferruginol (108904-92-3), 4-epidehydroabiatic acid (5155-70-4), and dehydroabiatic acid (1740-19-8). Peak 4 has  $m/z$  303.2309 and empirical formula  $C_{20}H_{31}O_2$  and corresponds to callicarpic acid A (CAS

#1130124-82-1), 1-[2-(3-furanyl)ethyl]-1,3,4,7,8,8a-hexahydro-1,2,5-trimethyl-4a(2H)-naphthalenemethanol (35319-12-1), isopimaric acid (5835-26-7), and cryptopimaric acid (471-74-9). Peak 5 has  $m/z$  305.2464 and empirical formula  $C_{20}H_{33}O_2$  which corresponds to [4aS-(4aa,4bβ,8aa,10aβ)]-4a,4b,5,6,7,8,8a,9,10,10a-decahydro-2-(1-hydroxy-1-methylethyl)-4b,8,8-trimethyl-4(1H)-phenanthrenone (CAS #121926-95-2), [1R-(1α,4aβ,4bα,7α,8α,10aa)]-7-ethenyl-1,2,3,4,4a,4b,5,6,7,8,10,10a-dodecahydro-8-hydroxy-1,4a,7-trimethyl-1-phenanthrenemethanol (101467-73-6), 15,16-dihydroisopimaric acid (5673-36-9), 15,16-dihydrosandaracopimaric acid (4807-69-6), and arachidonic acid (506-32-1). Peak 6 has  $m/z$  319.2257 and empirical formula  $C_{20}H_{31}O_3$  and corresponds to 4-[2-[(1S,4aR,6S,8aR)-1,4,4a,5,6,7,8,8a-octahydro-6-hydroxy-2,5,5,8a-tetramethyl-1-naphthalenyl]ethyl]-2(5H)-furanone (CAS #2305691-63-6), 4-[2-[(1S,4aR,6S,8aR)-decahydro-6-hydroxy-5,5,8a-trimethyl-2-methylene-1-naphthalenyl]ethyl]-2(5H)-furanone (2305691-62-5), nudiflopene B (2226250-84-4), (1S,



**TABLE 4 |** *C. americana* extract, partition, and fraction growth inhibition (IC<sub>50</sub> and MIC) and HaCat cytotoxicity IC<sub>50</sub> values (in µg ml<sup>-1</sup>).

		649	649C	649C-F8	649C-F9	649C-F12	649C-F13	649C-F14	649C-F15	649C-F17	649C-F19	649C-F21	649C-F22	Cli-
<b>IC<sub>50</sub> for <i>C. acnes</i> growth</b>	<b>ATCC6919</b>	32	32	16	8	16	16	16	16	16	16	16	16	0.0625
	<b>B104.1</b>	64	16	32	16	32	8	8	8	32	32	32	32	>4
	<b>B104.2</b>	64	32	32	32	32	8	16	16	32	32	32	32	>4
	<b>B104.4</b>	64	16	64	8	32	8	16	16	32	32	32	32	>4
	<b>B104.5</b>	32	16	32	16	32	4	8	8	32	32	32	32	>4
	<b>B104.6</b>	64	32	64	16	64	16	32	32	64	64	64	64	0.5
	<b>B104.7</b>	>64	64	64	16	64	16	64	64	>64	64	64	64	0.5
	<b>B104.8</b>	64	16	32	8	32	8	16	16	32	32	32	32	>4
	<b>EU-09</b>	>64	32	64	16	64	16	32	32	64	64	64	32	>4
	<b>EU-16</b>	64	32	32	16	32	8	16	8	8	8	16	16	<
<b>MIC for <i>C. acnes</i> growth</b>	<b>ATCC6919</b>	>32	>32	32	16	16	16	32	32	16	16	16	16	0.125
	<b>B104.1</b>	64	32	64	32	64	16	32	32	64	64	64	64	>8
	<b>B104.2</b>	64	32	64	32	64	16	64	32	64	64	64	64	>4
	<b>B104.4</b>	64	32	64	16	64	16	64	32	64	64	64	64	>4
	<b>B104.5</b>	64	32	64	32	64	16	32	32	64	64	64	32	>4
	<b>B104.6</b>	64	32	>64	16	64	16	64	64	>64	64	64	64	0.5
	<b>B104.7</b>	>64	64	>64	16	64	32	64	64	>64	64	64	64	1
	<b>B104.8</b>	>64	32	64	16	64	16	32	32	64	64	64	32	>4
	<b>EU-09</b>	>64	64	>64	16	64	16	64	64	>64	64	64	64	>4
	<b>EU-16</b>	>64	64	32	16	64	16	64	32	32	16	32	16	0.125
<b>HaCat</b>	<b>IC<sub>50</sub></b>	>	>	128	256	>512	>512	>	>	512	>512	>512	1024	–
		1024	1024					1024	512					
<b>TI</b>	<b>Lower range</b>	16	32	2	8	8	32	16	8	8	8	8	16	–
	<b>Upper range</b>	>32	>64	8	32	32	128	128	64	64	64	32	64	–

All values were determined as compared to the vehicle control for at least three replicates. The therapeutic index (TI) is reported as a range of values for the 10 *C. acnes* isolates (cytotoxicity IC<sub>50</sub> divided by growth inhibition IC<sub>50</sub>).

Cli clindamycin, antibiotic control.

4aS,4bS,7S,8S,10aS)-7-ethenyl-1,2,3,4,4a,4b,5,6,7,8,10,10a-dodecahydro-8-hydroxy-1,4a,7-trimethyl-1-phenanthrenecarboxylic acid (**2137490-87-8**), callilongisin D (**1367097-06-0**), callilongisin C (**1367097-03-7**), callilongisin B (**1367097-00-4**), (1S,2S,8aS)-1,2,3,7,8,8a-hexahydro-8a-hydroxy-1-methyl-2-(1-methylethenyl)-6-(1-methylethyl)-1-naphthalenepropanoic acid (**1123207-97-5**), 12(S)-hydroxycyclohexa-3,13-dien-16,15-olide (**935293-68-8**), 12(S)-hydroxycyclohexa-3,13-dien-15,16-olide (**935293-66-6**), 16ξ-hydroxycyclohexa-3,13-dien-15,16-olide (**141979-19-3**), 7α-hydroxysandaracopimaric acid (**122537-68-2**), [4aS-(4αα,7αα,8αα,9bβ)]-2,3,4,4a,5,6,7,7a,8a,9b-decahydro-7a-(1-hydroxy-1-methylethyl)-4,4,9b-trimethylphenanthro[2,3-b]oxirene-9(1H)-one (**121926-98-5**), calliphyllin (**101467-72-5**), and 3-oxoanticalpic acid (**83997-21-1**).

## DISCUSSION

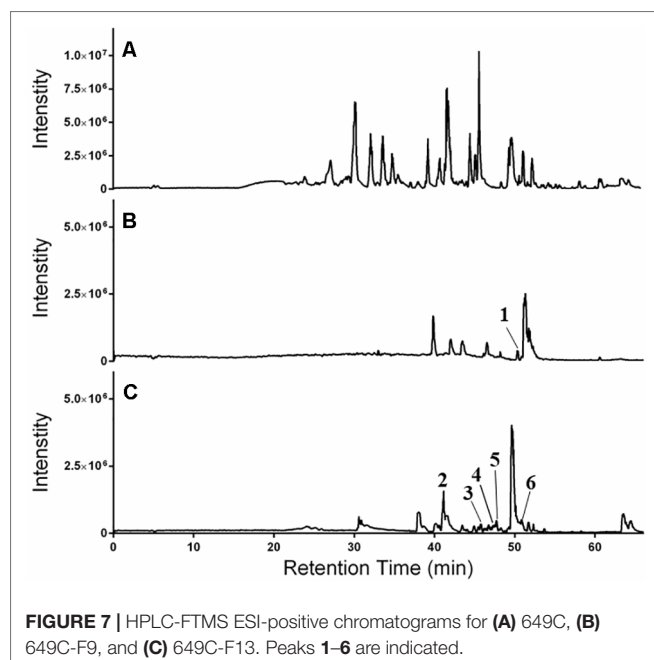
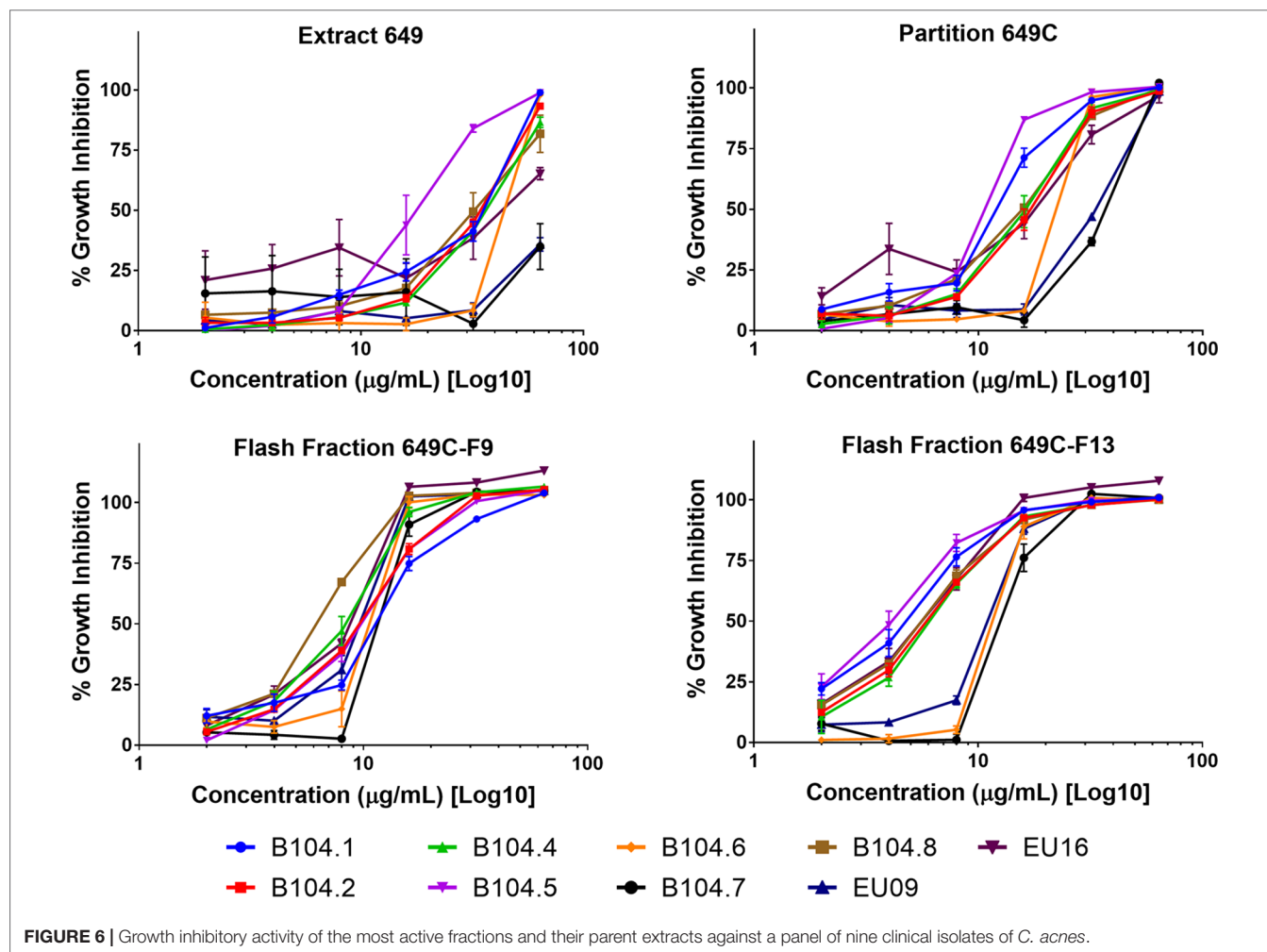
The most active fractions of the *C. americana* leaf extracts exhibited MICs against *C. acnes* isolates at concentrations as low as 0.016 mg ml<sup>-1</sup>, which is 30 times less than the lowest MIC value found for other botanical extracts previously investigated, including Jeju (*Thymus quinquecostatus* Celak., Lamiaceae—MIC of 0.5 mg ml<sup>-1</sup>), Damask Rose (*Rosa x damascene* Herrm., Rosaceae—MIC of 2 mg ml<sup>-1</sup>), Duzhong (*Eucommia ulmoides* Oliv., Eucommiaceae—MIC

of 0.5 mg ml<sup>-1</sup>), and Maté (*Ilex paraguariensis* A.St.-Hil.—MIC of 1 mg ml<sup>-1</sup>) (Oh et al., 2009; Tsai et al., 2010). In comparison to the growth inhibition activity, the *C. americana* extracts were less effective at the eradication of existing biofilm. Following the result reported by Coenye et al., we included resveratrol as a biofilm eradication control (Coenye et al., 2012). At the highest concentration tested (394 µg ml<sup>-1</sup>), only 21% inhibition was achieved by resveratrol. However, the previous 80% biofilm eradication reported for resveratrol was at a concentration of 3,200 µg ml<sup>-1</sup>.

The cytotoxicity (IC<sub>50</sub>) of the most active fractions, 649C-F9 and 649C-F13, were at concentrations 32 and >128 times greater than that required for *C. acnes* growth inhibition (IC<sub>50</sub>). These results demonstrate the strong potential of *C. americana* fractions to reduce *C. acnes* fitness at a good therapeutic index ratio of mammalian toxicity to antimicrobial activity.

In other studies, bioassay-guided fractionation of the dried leaf, twigs, and fruits of *C. americana* extracts led to the isolation of six clerodane diterpenes (Jones et al., 2007). Flavonoids including genkwanin, 5-hydroxy-7,4'-dimethoxyflavone, and luteolin were also found in these extracts. The leaf essential oil contained lipids [(E)-2-hexenal and 1-octen-3-ol] as well as monoterpenoids (nopinone, α-pinene, and β-pinene), sesquiterpenoids (α-cadinol, caryophyllene oxide, 7-epi-α-eudesmol, α-humulene, humulene epoxide II, intermediol, khusinol, valencene, α-selinene, and





7-*epi*- $\alpha$ -selinene), and triterpenoids (euscaphic acid) (Tellez et al., 2000; Kobaisy et al., 2002; Cantrell et al., 2005; Jones et al., 2007). Some compounds were active against human cancer cell lines with a cytotoxic activity below  $5 \mu\text{g ml}^{-1}$ . These include 12(S),16-dihydroxycyclo-3,13-dien-15,16-olide, 2-formyl-16-hydroxy-3- $\alpha$ -norcleroda-2,13-dien-15,16-olide, genkwanin, 12(S)-hydroxycyclo-3,13-dien-16,15-olide, 16-hydroxycyclo-3,13-dien-15,16-olide, and 16-hydroxy-cleroda-3,11(E),13-trien-15,16-olide. Intermedeol and callicarpal were demonstrated to be effective deterrents of *A. stephensi* and *A. aegypti* mosquitos, and clerodane diterpenes are also known to have insect antifeedant properties (Gebbinck et al., 2002). To the best of the authors' knowledge, this is the first report on the antibacterial activity of *C. americana* extracts against *C. acnes*.

By colonizing the pilosebaceous follicle and inducing the production of reactive oxygen species highly toxic to the cells (Shalita et al., 2011), *C. acnes* exacerbates the inflammation associated with acne vulgaris. *C. acnes* also worsens the symptoms by inducing immune cells to produce pro-inflammatory cytokines including interleukins and tumor necrosis factors (Vowels et al., 1995). Prior studies on

**TABLE 5 |** Tabulated (M+H)<sup>+</sup> ions, empirical formulas, for the bioactive 649C fractions.

Peak number	Retention time (min)	m/z	Relative abundance (%)	Empirical formula Δ (ppm)
<b>Fraction 649C-F9</b>				
<b>1</b>	33	371.0991	1.4	C <sub>16</sub> H <sub>19</sub> O <sub>10</sub> (4.7)
	39.8	376.2581	15.49	C <sub>23</sub> H <sub>36</sub> O <sub>4</sub> (−6.8)
	42.1	368.2422	7.55	C <sub>17</sub> H <sub>36</sub> O <sub>8</sub> (5.2)
	43.4	368.2426	8.19	C <sub>17</sub> H <sub>36</sub> O <sub>8</sub> (5.9)
	46.5	718.449	5.73	C <sub>37</sub> H <sub>66</sub> O <sub>13</sub> (−1.1)
	48.2	371.0994	0.92	C <sub>19</sub> H <sub>17</sub> O <sub>7</sub> N (−1.6)
	50.3	<b>317.2099</b> , 650.4375	2.89	C <sub>20</sub> H <sub>29</sub> O <sub>3</sub> (−3.8)
	51.3	637.4457	56.4	C <sub>40</sub> H <sub>61</sub> O <sub>6</sub> (−1.0)
	60.6	630.504	1.24	C <sub>36</sub> H <sub>70</sub> O <sub>8</sub> (−4.0)
<b>Fraction 649C-F13</b>				
<b>2</b>	24.2	608.3806	2.09	C <sub>30</sub> H <sub>56</sub> O <sub>12</sub> (6.5)
	30.6	371.0994	1.66	C <sub>16</sub> H <sub>19</sub> O <sub>10</sub> (5.7)
	30.9	371.0993	1.04	C <sub>16</sub> H <sub>19</sub> O <sub>10</sub> (5.5)
	38.0	384.2368	7.89	C <sub>17</sub> H <sub>36</sub> O <sub>9</sub> (3.7)
	40.2	384.2374, 782.4683	2.23	C <sub>38</sub> H <sub>70</sub> O <sub>16</sub> (2.8)
	41.1	376.2583	6.92	C <sub>23</sub> H <sub>36</sub> O <sub>4</sub> (−6.8)
	41.6	715.4025	6.76	C <sub>40</sub> H <sub>59</sub> O <sub>11</sub> (−3.8)
	43.5	718.4499	1.39	C <sub>37</sub> H <sub>66</sub> O <sub>13</sub> (0.2)
	44.9	718.4499	1.01	C <sub>37</sub> H <sub>66</sub> O <sub>13</sub> (−1.5)
	45.8	301.2152	1.48	C <sub>20</sub> H <sub>29</sub> O <sub>2</sub> (−3.5)
<b>3</b>	47.5	<b>303.2309</b> , 605.4541,	1.52	C <sub>20</sub> H <sub>31</sub> O <sub>2</sub> (−3.3)
<b>4</b>		750.4388		
<b>5</b>	47.7	<b>305.2464</b> , 609.4851	1.64	C <sub>20</sub> H <sub>33</sub> O <sub>2</sub> (−3.5)
	49.6	669.4379	36.27	C <sub>40</sub> H <sub>61</sub> O <sub>8</sub> (2.7)
<b>6</b>	50.9	<b>319.2257</b> , 659.4258	2.03	C <sub>20</sub> H <sub>31</sub> O <sub>3</sub> (−3.3)
	51.7	654.4701	1.51	C <sub>37</sub> H <sub>66</sub> O <sub>9</sub> (0)
	63.5	621.302	6.87	C <sub>43</sub> H <sub>41</sub> O <sub>4</sub> (3.2)
	64.5	621.3017	4.05	C <sub>43</sub> H <sub>41</sub> O <sub>4</sub> (2.8)
	67.2	621.3037	2.19	C <sub>36</sub> H <sub>45</sub> O <sub>9</sub> (−3.4)
	76.3	371.0991	5.02	C <sub>16</sub> H <sub>19</sub> O <sub>10</sub> (5.0)

ND, formula not determined.

\*Percent relative abundance is determined by peak area.

†The putative formula is reported for bold ion.

ethanolic extracts of rosemary demonstrated a significant reduction of cytokine production *in vitro* and attenuation of swelling and inflammation in a mouse model (Tsai et al., 2010). The minimum inhibitory concentration was 4 mg ml<sup>−1</sup>, which is 250 times more than the lowest MIC reported in the present paper. By effectively reducing *C. acnes* growth and proliferation, *C. americana* leaf extracts may also impact inflammatory processes. Further research is needed to evaluate this aspect of *C. americana* treatments with *in vivo* infection models.

While treating acne with antibiotics, such as erythromycin and clindamycin, was shown to significantly reduce inflammation, extensive use of oral and/or topical antibiotics since the 1960s has led to the emergence of resistant strains (Eady et al., 1989). This underlines the need for alternative compounds for acne therapy. Other factors such as androgens, poor digestion, or smoking habits (Leyden, 1995) are also important in the development and persistence of the disease. Treatments should focus not only on the consequences but also on the causes of acne and could combine cross-acting compounds to reduce sebum production, correct stomach acidity for better digestion, while also reducing inflammation (Yarnell and Abascal, 2006). Previous studies reported the interesting potential of botanical combinations in

treatments to reduce acne (Lalla et al., 2001; Kılıç et al., 2019). Our study highlights the potential of *C. americana* leaf extracts to efficiently reduce bacterial proliferation and lessen acne vulgaris symptoms.

## CONCLUSION

Our work has demonstrated the promising antibacterial potential of *C. americana* constituents against *C. acnes* growth. Fractions 649C-F9 and 649C-F13 exhibited growth inhibitory activity against a panel of 10 *C. acnes* isolates and with a good therapeutic index of 32 and >128, respectively). Future studies should pursue isolation and structural determination of active components, further examination of the efficacy and safety of the compounds, and examine the mechanism of action for these observed antibacterial effects.

## DATA AVAILABILITY STATEMENT

The raw data supporting the conclusions of this manuscript will be made available by the authors, without undue reservation, to any qualified researcher.

## AUTHOR CONTRIBUTIONS

RP prepared the extracts and fractions and performed HaCaT cytotoxicity experiments. RP and SH performed antibacterial assays. JL performed the chemical analysis of the extracts. CQ designed and directed the study. RP and CQ analyzed the data and wrote the manuscript. All authors read, revised, and approved the final manuscript.

## FUNDING

This work was supported by faculty development funds from the Emory University School of Medicine, Department of

Dermatology and Emory College of Arts and Sciences, Center for the Study of Human Health.

## ACKNOWLEDGMENTS

The following reagent was obtained through BEI Resources, NIAID, NIH as part of the Human Microbiome Project: HL013PA1 and HL030PA1. We thank Dr. Laura Marinelli for the provision of the following clinical isolates: B104.1, B104.2, B104.4, B104.5, B104.6, B104.7, and B104.8. We thank Dr. T. Samarakoon (Emory University Herbarium) for assistance with the collection and identification of the study species, Dr. F. Chassagne for assistance with the cell culture assays, and M. Dettweiler for assistance with the growth inhibition plates setup.

## REFERENCES

- Bhambri, S., Del Rosso, J. Q., and Bhambri, A. (2009). Pathogenesis of acne vulgaris: recent advances. *J. Drugs Dermatol.* 8, 615–618.
- Bhat, P., Hegde, G. R., Hegde, G., and Mulgund, G. S. (2014). Ethnomedicinal plants to cure skin diseases—an account of the traditional knowledge in the coastal parts of Central Western Ghats, Karnataka, India. *J. Ethnopharmacol.* 151, 493–502. doi: 10.1016/j.jep.2013.10.062
- Cantrell, C. L., Klun, J. A., Bryson, C. T., Kobaisy, M., and Duke, S. O. (2005). Isolation and identification of mosquito bite deterrent terpenoids from leaves of American (*Callicarpa americana*) and Japanese (*Callicarpa japonica*) Beautyberry. *J. Agric. Food Chem.* 53, 5948–5953. doi: 10.1021/jf0509308
- Coenye, T., Brackman, G., Rigole, P., De Witte, E., Honraet, K., Rossel, B., et al. (2012). Eradication of *Propionibacterium* acnes biofilms by plant extracts and putative identification of icariin, resveratrol and salidroside as active compounds. *Phytomedicine* 19, 409–412. doi: 10.1016/j.phymed.2011.10.005
- Cox, P. A. (1994). “The ethnobotanical approach to drug discovery: strengths and limitations,” in *Ethnobotany and the search for new drugs* (Chichester: Wiley).
- Eady, E. A., Cove, J., Holland, K., and Cunliffe, W. (1989). Erythromycin resistant *propionibacteria* in antibiotic treated acne patients: association with therapeutic failure. *Br. J. Dermatol.* 121, 51–57. doi: 10.1111/j.1365-2133.1989.tb01399.x
- Gebbinck, E. A. K., Jansen, B. J., and De Groot, A. (2002). Insect antifeedant activity of clerodane diterpenes and related model compounds. *Phytochemistry* 61, 737–770. doi: 10.1016/S0031-9422(02)00174-7
- Gupta, A., Nagariya, A., Mishra, A., Bansal, P., Kumar, S., Gupta, V., et al. (2010). Ethno-potential of medicinal herbs in skin diseases: an overview. *J. Pharm. Res.* 3, 435–441. doi: 10.1186/s12906-019-2605-6
- Jones, W. P., and Kinghorn, A. D. (2008). Biologically active natural products of the genus *Callicarpa*. *Curr. Bioact. Compd.* 4, 15–32. doi: 10.2174/157340708784533393
- Jones, W. P., Lobo-Echeverri, T., Mi, Q., Chai, H.-B., Soejarto, D. D., Cordell, G. A., et al. (2007). Cytotoxic constituents from the fruiting branches of *Callicarpa americana* collected in southern Florida. *J. Nat. Prod.* 70, 372–377. doi: 10.1021/np060534z
- Kadereit, J. W. (2004). *Flowering Plants: Dicotyledons: Lamiales (except Acanthaceae including Avicenniaceae)*. Berlin: Springer. doi: 10.1007/978-3-642-18617-2
- Kılıç, S., Okullu, S. Ö., Kurt, Ö., Sevinç, H., Dündar, C., Altınordu, F., et al. (2019). Efficacy of two plant extracts against acne vulgaris: initial results of microbiological tests and cell culture studies. *J. Cosmet. Dermatol.* 18, 1061–1065. doi: 10.1111/jocd.12814
- Kobaisy, M., Tellez, M. R., Dayan, F. E., and Duke, S. O. (2002). Phytotoxicity and volatile constituents from leaves of *Callicarpa japonica* Thunb. *Phytochemistry* 61, 37–40. doi: 10.1016/S0031-9422(02)00207-8
- Lalla, J., Nandedkar, S., Paranjape, M., and Talreja, N. (2001). Clinical trials of ayurvedic formulations in the treatment of acne vulgaris. *J. Ethnopharmacol.* 78, 99–102. doi: 10.1016/S0378-8741(01)00323-3
- Leyden, J. J. (1995). New understandings of the pathogenesis of acne. *J. Am. Acad. Dermatol.* 32, S15–S25. doi: 10.1016/0190-9622(95)90416-6
- Leyden, J. J., and Del Rosso, J. Q. (2011). Oral antibiotic therapy for acne vulgaris: pharmacokinetic and pharmacodynamic perspectives. *J. Clin. Aesthet. Dermatol.* 4, 40–47.
- Margolis, D. J., Bowe, W. P., Hoffstad, O., and Berlin, J. A. (2005). Antibiotic treatment of acne may be associated with upper respiratory tract infections. *Arch. Dermatol.* 141, 1132–1136. doi: 10.1001/archderm.141.9.1132
- Margolis, D. J., Fanelli, M., Kupperman, E., Papadopoulos, M., Metlay, J. P., Xie, S. X., et al. (2012). Association of pharyngitis with oral antibiotic use for the treatment of acne: a cross-sectional and prospective cohort study. *Arch. Dermatol.* 148, 326–332. doi: 10.1001/archdermatol.2011.355
- Marinelli, L. J., Fitz-Gibbon, S., Hayes, C., Bowman, C., Inkeles, M., Loncaric, A., et al. (2012). *Propionibacterium acnes* bacteriophages display limited genetic diversity and broad killing activity against bacterial skin isolates. *mBio* 3, e00279–e00212. doi: 10.1128/mBio.00279-12
- Mills, O., Jr., Thornsberry, C., Cardin, C. W., Smiles, K. A., and Leyden, J. J. (2002). Bacterial resistance and therapeutic outcome following three months of topical acne therapy with 2% erythromycin gel versus its vehicle. *Acta. Derm. Venereol.* 82, 260–265. doi: 10.1080/000155502320323216
- Nelson, K., Lyles, J. T., Li, T., Saitta, A., Addie-Noye, E., Tyler, P., et al. (2016). Anti-acne activity of Italian medicinal plants used for skin infection. *Front. Pharmacol.* 7, 425–425. doi: 10.3389/fphar.2016.00425
- Oh, T.-H., Kim, S.-S., Yoon, W.-J., Kim, J.-Y., Yang, E.-J., Lee, N. H., et al. (2009). Chemical composition and biological activities of Jeju Thymus quinquecostatus essential oils against *Propionibacterium* species inducing acne. *J. Gen. Appl. Microbiol.* 55, 63–68. doi: 10.2323/jgam.55.63
- Quave, C. L., Lyles, J. T., Kavanaugh, J. S., Nelson, K., Parlet, C. P., Crosby, H. A., et al. (2015). Castanea sativa (European chestnut) leaf extracts rich in ursene and oleanene derivatives block *Staphylococcus aureus* virulence and pathogenesis without detectable resistance. *PLOS ONE* 10, e0136486. doi: 10.1371/journal.pone.0136486
- Quave, C. L., Plano, L. R., Pantuso, T., and Bennett, B. C. (2008). Effects of extracts from Italian medicinal plants on planktonic growth, biofilm formation and adherence of methicillin-resistant *Staphylococcus aureus*. *J. Ethnopharmacol.* 118, 418–428. doi: 10.1016/j.jep.2008.05.005
- Sernec. (2019). *Southeast Regional Network of Expertise and Collections [Online]*. <http://sernecportal.org/portal/>. Available: <http://sernecportal.org/portal/> (Accessed May 15 2019).
- Shah, R., and Peethambaran, B. (2018). “Chapter 19—Anti-inflammatory and antimicrobial properties of Achillea millefolium in acne treatment,” in *Immunity and inflammation in health and disease*. Eds. S. Chatterjee, W. Jungraithmayr, and D. Bagchi. San Diego, CA, United States (Academic Press). 241–248. doi: 10.1016/B978-0-12-805417-8.00019-6
- Shalita, A. R., Del Rosso, J. Q., and Webster, G. (2011). *Acne vulgaris*. London: CRC Press. doi: 10.3109/9781616310097
- Susilawati, E., Aligita, W., Adnyana, I. K., and Sukmawati, I. K. (2018). Activity of Karehau (*Callicarpa longifolia* Lamk.) leaves ethanolic extract as a wound healing. *J. Pharm. Sci. Res.* 10, 1243–1247.

- Taylor, L. A. (1940). *Plants used as curatives by certain southeastern tribes*. Cambridge, MA: Botanical Museum of Harvard University.
- Tellez, M. R., Dayan, F. E., Schrader, K. K., Wedge, D. E., and Duke, S. O. (2000). Composition and some biological activities of the essential oil of *Callicarpa americana* (L.). *J. Agric. Food Chem.* 48, 3008–3012. doi: 10.1021/jf991026g
- Thiboutot, D., Gollnick, H., Bettoli, V., Dréno, B., Kang, S., Leyden, J. J., et al. (2009). New insights into the management of acne: an update from the Global Alliance to Improve Outcomes in Acne group. *J. Am. Acad. Dermatol.* 60, S1–50. doi: 10.1016/j.jaad.2009.01.019
- Thomas, D. R. (2004). Psychosocial effects of acne. *J. Cutan. Med. Surg.* 8, 3–5. doi: 10.1007/s10227-004-0752-x
- Titus, S., and Hodge, J. (2012). Diagnosis and treatment of acne. *Am. Fam. Physician* 86, 734–740.
- Toyoda, M., and Morohashi, M. (2001). Pathogenesis of acne. *Med. Electron. Microsc.* 34, 29–40. doi: 10.1007/s007950100002
- Tsai, T.-H., Tsai, T.-H., Wu, W.-H., Tseng, J. T.-P., and Tsai, P.-J. (2010). *In vitro* antimicrobial and anti-inflammatory effects of herbs against *Propionibacterium acnes*. *Food Chem.* 119, 964–968. doi: 10.1016/j.foodchem.2009.07.062
- Tu, Y., Sun, L., Guo, M., and Chen, W. (2013). The medicinal uses of *Callicarpa* L. in traditional Chinese medicine: an ethnopharmacological, phytochemical and pharmacological review. *J. Ethnopharmacol.* 146, 465–481. doi: 10.1016/j.jep.2012.12.051
- Van Den Bergh, B., Michiels, J. E., Wenseleers, T., Windels, E. M., Boer, P. V., Kestemont, D., et al. (2016). Frequency of antibiotic application drives rapid evolutionary adaptation of *Escherichia coli* persistence. *Nat. Microbiol.* 1, 16020. doi: 10.1038/nmicrobiol.2016.20
- Vowels, B. R., Yang, S., and Leyden, J. J. (1995). Induction of proinflammatory cytokines by a soluble factor of *Propionibacterium acnes*: implications for chronic inflammatory acne. *Infect. Immun.* 63, 3158–3165.
- Walsh, T. R., Efthimiou, J., and Dreno, B. (2016). Systematic review of antibiotic resistance in acne: an increasing topical and oral threat. *Lancet Infect. Dis.* 16, e23–e33. doi: 10.1016/S1473-3099(15)00527-7
- Yang, D., Zhou, C., and Bai, Y. (2010). Clinical research on acne vulgaris treated by *Callicarpa nudiflora* tablet combined with adapalene gel. *World J. Integr. Tradit. West. Med.* 5, 45–47.
- Yarnell, E., and Abascal, K. (2006). Herbal medicine for acne vulgaris. *Altern. Complement Ther.* 12, 303–309. doi: 10.1089/act.2006.12.303

**Conflict of Interest:** The authors declare that the research was conducted in the absence of any commercial or financial relationships that could be construed as a potential conflict of interest.

Copyright © 2019 Pineau, Hanson, Lyles and Quave. This is an open-access article distributed under the terms of the Creative Commons Attribution License (CC BY). The use, distribution or reproduction in other forums is permitted, provided the original author(s) and the copyright owner(s) are credited and that the original publication in this journal is cited, in accordance with accepted academic practice. No use, distribution or reproduction is permitted which does not comply with these terms.



# In Vitro Antioxidant, Anti-Inflammatory and Skin Permeation of *Myrsine africana* and Its Isolated Compound Myrsinoside B

Bianca Fibrich<sup>1</sup>, Xinyi Gao<sup>2</sup>, Ashana Puri<sup>2</sup>, Ajay K. Banga<sup>2</sup> and Namrita Lall<sup>1,3\*</sup>

<sup>1</sup> Department of Plant and Soil Sciences, University of Pretoria, Pretoria, South Africa, <sup>2</sup> Center for Drug Delivery Research, Department of Pharmaceutical Sciences, College of Pharmacy, Mercer University, Atlanta, GA, United States, <sup>3</sup> School of Natural Resources, University of Missouri, Columbia, MO, United States

## OPEN ACCESS

### Edited by:

Andrei Mocan,  
Iuliu Hațieganu University of Medicine  
and Pharmacy, Romania

### Reviewed by:

Helen Skaltsa,  
National and Kapodistrian  
University of Athens, Greece  
Adeyemi Oladapo Aremu,  
North-West University, South Africa

### \*Correspondence:

Namrita Lall  
Namrita.lall@up.ac.za

### Specialty section:

This article was submitted to  
Ethnopharmacology,  
a section of the journal  
Frontiers in Pharmacology

**Received:** 16 July 2019

**Accepted:** 06 November 2019

**Published:** 08 January 2020

### Citation:

Fibrich B, Gao X, Puri A,  
Banga AK, and Lall N (2020) In Vitro  
Antioxidant, Anti-Inflammatory and Skin  
Permeation of *Myrsine africana* and Its  
Isolated Compound Myrsinoside B.  
Front. Pharmacol. 10:1410.  
doi: 10.3389/fphar.2019.01410

Dermal aging is characterized by states of oxidative stress, chronic inflammation, and abnormal proteolytic degradation due to the action of hydrogen peroxide, superoxide, 5-lipoxygenase, and elastase, respectively. Noteworthy elastase inhibition has previously been reported, and so this study aimed to investigate the ability of *Myrsine africana* and myrsinoside B to reduce the activity of hydrogen peroxide, superoxide, and 5-lipoxygenase as supplementary mechanisms of action by which *M. africana* may reduce the appearance of wrinkles. The use of maltose microneedles were also investigated as a means to enhance the delivery of myrsinoside B into the skin as this is a crucial aspect to investigate when characterizing the efficacy of an active ingredient. *Myrsine africana* has traditionally been used for skin allergies, boils, and to purify blood (as an astringent) and was selected for this study based on its use in skincare. The crude extract exhibited IC<sub>50</sub>'s of 56.08 ± 2.88 and 132.74 ± 1.64 µg/ml against the hydrogen peroxide and superoxide radicals, while myrsinoside B exhibited IC<sub>50</sub>'s of 52.19 ± 4.16 and 192.14 ± 3.52 µg/ml, respectively. The IC<sub>50</sub> of the extract and compound against 5-lipoxygenase was 29.65 ± 2.92 and 29.33 ± 3.08 µg/ml, respectively. No toxicity was observed *in vitro* at the highest concentration tested. Microneedle treatment increased the permeation of the active through the skin after 24 h to 12.46 ± 5.14 µg/cm<sup>2</sup> compared to the passive group (1.30 ± 0.85 µg/cm<sup>2</sup>). The amount of active retained in the epidermis and dermis was 8.97 ± 0.90 and 6.98 ± 0.73 µg/cm<sup>2</sup> respectively, greater than the retention observed in the passive group (3.24 ± 1.41 and 3.27 ± 1.47 µg/cm<sup>2</sup>, respectively). *M. africana* and myrsinoside B showed promising antioxidant and anti-inflammatory activity thus supporting the potential of *M. africana* and myrsinoside B as anti-wrinkle agents. Further, treatment of dermatomed human skin with maltose microneedles facilitated topical delivery of myrsinoside B and provided an effective means for compound delivery to ensure maximum effect.

**Keywords:** *Myrsine africana*, myrsinoside B, lipoxygenase, skin delivery, maltose microneedles



## INTRODUCTION

The science of aging skin has long been a topic of interest with the demand for effective botanical actives a particular area of curiosity. Dermal aging may arise from either intrinsic or extrinsic factors and is characterized by states of oxidative stress, abnormal degradation of structural components housed within the dermis, and chronic inflammation. Specifically, hydrogen peroxide and superoxide are produced in this process and interact undesirably with biological molecules to enhance the activity of proteases such as elastase which proceed to degrade structural components. Simultaneously, inflammatory enzymes such as 5-lipoxygenase are recruited to the affected site and further elicit a stress response. Coupled to this, reduced cellular turnover rates, abridged production of structural components, and the naturally diminishing capacity of the skin to maintain homeostasis contribute synergistically to the formation of wrinkles (Pillai et al., 2005; Pandel et al., 2013; Peng et al., 2014; Ryu et al., 2014).

The ability of biologically active molecules to penetrate the skin is equally significant to ensure delivery to the targeted site. Microneedles comprise a commonly used physical enhancement technology for topical and transdermal delivery of hydrophilic drugs. These work by creating aqueous micron-sized channels in the skin that enable transportation of active constituents into the skin or systemic circulation (Chen et al., 2008). The use of microneedles in cosmetics is promising, however, the therapeutic efficacy of microneedle-based products is still under investigation in clinical trials. Microneedles are actively employed in the cosmetic industry and are even available for home use, making their potential particularly promising (Bhatnagar et al., 2017).

*Myrsine africana* L. (Primulaceae) is a shrub commonly known as the African Boxwood. It is found throughout Asia, Macaronesia, and Africa and has a wealth of traditional knowledge alluding to its applications. Traditionally, a leaf decoction is prepared for the treatment of acne, pigmentation disorders, wound healing, cellulitis, and as a blood purifier by the Southern Sotho, Kwenya, and Tswana tribes of South Africa. Similarly, a leaf decoction is prepared for the treatment of skin allergies and as a blood purifier in Pakistan. In Kenya, people of the Samburu district prepare a decoction from ground seeds for the treatment of wounds. Chinese folklore also indicates that it is traditionally used for the treatment of diarrhea, pulmonary tuberculosis, rheumatism, toothache, and hemorrhaging (Kang et al., 2007). It is also used in various culinary applications as a fragrance, flavoring agent, spice, and appetizer (Ahmad et al., 2011b). Additional uses include as an anthelmintic, antibacterial, for the treatment of boils, and scanty urine (Watt and Breyer-Brandwijk, 1962; Killick, 1969; Githiori et al., 2002; Abbasi et al., 2010). The reported use of *M. africana* as a blood purifier spurs interest around its potential application as an anti-wrinkle agent as such agents often play an important role in maintaining healthy skin (Kishore et al., 2018).

Previous studies have identified and characterised myrsinoside B (94.39% purity) amongst other compounds (Kishore et al., 2018). Lall et al. (2017) reported noteworthy elastase inhibition for *M. africana* (28.04 µg/ml) and myrsinoside B (4.69 µg/ml). The aim of this study was therefore extrapolate on the anti-aging activity of *M. africana* and myrsinoside B by determining the ability of the crude extract and compound to respectively scavenge hydrogen

peroxide and superoxide radicals, and inhibit 5-lipoxygenase. Further, this study aimed to characterize and identify a means of delivery of myrsinoside B into the skin. The extract and isolated myrsinoside B samples used in this study were the same as that produced in previous studies (Lall et al., 2017; Kishore et al., 2018).

## MATERIALS

Ethanol, methanol (M), ethyl-acetate (EA) and hydrogen peroxide were purchased from Associated Chemical Enterprises Chemicals (Southdale, South Africa). XTT cell proliferation kit II, actinomycin D, soybean lipoxygenase (type V), linoleic acid, xylenol orange, ferrous sulphate, nitroblue tetrazolium chloride, dimethyl sulfoxide (DMSO), propylene glycol (PG) and 10X Phosphate-buffered saline, pH 7.4 (PBS) were obtained from Sigma-Aldrich (St Louis, MO, USA). The HaCat cell line was purchased from Highveld Biological (Pty) Ltd. (South Africa). Dulbecco's Modified Eagle's Medium (DMEM), trypsin-EDTA, fetal bovine serum (FBS), phosphate buffer saline (PBS), and antibiotics were supplied by Thermofisher scientific (Modderfontein, Johannesburg, South Africa). Citric acid, disodium hydrogen phosphate, triethanolamine (TEA) and formic acid were obtained from Fisher Scientific (Fair Lawn, NJ, USA). Carbopol 980NF was procured from Lubrizol Corporation (Wickliffe, Ohio, USA). Dermatomed human cadaver skin was purchased from the New York Fire Fighter (NY, USA). All other reagents were of analytical grade.

## METHODS

### Plant Collection and Extract Preparation

*M. africana* was collected in 2011 from the Manie van der Schijff Botanical Garden in Pretoria, South Africa (S25° 45' 21" E28° 13' 51") and identified by Ms. Magda Nel at the H.G.W.J. Schweickerdt Herbarium (PRU) where a voucher specimen (MA-S-2013-1) was deposited. The preparation of a crude ethanolic extract and isolation of myrsinoside B were exactly as previously reported (Lall et al., 2017; Kishore et al., 2018).

### Hydrogen Peroxide Scavenging

Hydrogen peroxide scavenging potential was determined according to the method of Kumar et al. (2012). Briefly, the ethanolic extract of *M. africana* and the positive drug control, L-ascorbic acid, were prepared to stock concentrations of 10,000 µg/ml and serially diluted in Eppendorf tubes to yield a concentration range of 400–3.125 µg/ml. To this, hydrogen peroxide (10 mM) prepared in potassium phosphate buffer (pH 7, 50 mM) was added and the reaction mixture incubated at room temperature in the dark. The FOX reagent was prepared using sulfuric acid (0.025 M), D-sorbitol (0.1 M), xylenol orange ( $1 \times 10^{-3}$  M), ferrous sulphate (250 mM), and methanol:water 9:1, and added to the reaction mixture which was incubated for a further 20 min in the dark at room temperature. The Eppendorf tubes were then centrifuged for 1 min to remove flocculation and the supernatant removed. The absorbance of the supernatant was measured at 580 nm using a BIO-TEK Power-Wave XS multi-well plate reader (A.D.P,

Weltevreden Park, South Africa) and KC Junior software. The  $IC_{50}$  values were calculated using GraphPad Prism 4 software.

## Superoxide Radical Scavenging

The alkaline DMSO method of Kumar et al. (2012) was used to determine the superoxide radical scavenging potential of *M. africana* and myrsinoside B. These samples and the positive control, Quercetin, were prepared to stock concentrations in DMSO and serially diluted to yield a range of concentrations (400–3.125  $\mu\text{g/ml}$ ). Alkaline DMSO was prepared by dissolving sodium hydroxide in DMSO (0.2 mg/ml). In a 96-well microtiter plate, alkaline DMSO was added to the plant extract of *M. africana*, myrsinoside B and quercetin. A color control, negative control, and vehicle control containing DMSO were included. Nitro blue tetrazolium (NBT) chloride was dissolved in DMSO at a 1:1 ratio and this was added to the test samples, including the vehicle control and the plates were read immediately at 560 nm using a BIO-TEK Power-Wave XS multi-well plate reader (A.D.P, Weltevreden Park, South Africa) and KC Junior software. The  $IC_{50}$  values were calculated using GraphPad Prism 4 software.

## 5-Lipoxygenase Inhibition

The 5-LOX inhibition was investigated according to the method of Chung et al. (2009) in which lipoxygenase from soybean (type V) (100 ng/ml) prepared in Tris-HCl (pH 7.4, 50 mM) was incubated for 5 min at room temperature with the test samples and positive control respectively. All test samples were prepared to stock concentrations of 20 mg/ml in DMSO and serially diluted to a concentration range of 400–3.125  $\mu\text{g/ml}$ . A vehicle control containing 0.2% DMSO, a blank containing 5-LOX to which linoleic acid was added after the addition of the FOX reagent, positive control containing caffeic acid at the same concentration range as the extracts, and color controls containing the plant extract and Tris-HCl buffer were included. The reaction was then initiated by the addition of linoleic acid (140  $\mu\text{M}$ ) prepared in Tris-HCl (pH 7.4, 50 mM) and incubated for 20 min at room temperature in the dark. The reaction was terminated through the addition of freshly prepared FOX reagent (30 mM sulfuric acid; 100  $\mu\text{M}$  xylenol orange; 100  $\mu\text{M}$  ferrous sulphate, and methanol: water (9:1). The formation of a color complex was allowed to develop for 30 min at room temperature, and the absorbance was measured at 560 nm using a BIO-TEK Power-Wave XS multi-well plate reader (A.D.P, Weltevreden Park, South Africa) and KC Junior software. The  $IC_{50}$  values were calculated using GraphPad Prism 4 software.

## Cell Culture and Cytotoxicity

Human keratinocytes were maintained in Dulbecco's Modified Eagle's Medium supplemented with 10% Fetal Bovine Serum and 1% antibiotics (100 U/ml penicillin, 100  $\mu\text{g/ml}$  streptomycin, and 250  $\mu\text{g/ml}$  fungizone). The cells were grown statically at 37°C in a humidified incubator set at 5%  $\text{CO}_2$  "CO<sub>2</sub>:Carbon dioxide". Once confluent, the cells were sub-cultured by treating them with trypsin-EDTA (0.25% trypsin containing 0.01% EDTA) for a maximum of 10 min. The cytotoxicity was evaluated using the XTT cell proliferation Kit II according to the method of Zheng et al. (2001). Cells ( $1 \times 10^5$  cells/ml) were seeded in a 96-well microtitre plate and allowed to attach for 24 h at 37°C and 5%  $\text{CO}_2$ . *M. africana* and myrsinoside B were prepared to stock concentrations of 20 mg/ml DMSO and the cells were treated at concentrations ranging from

400–3.13  $\mu\text{g/ml}$  for test samples and concentrations ranging between 0.5 and 0.002  $\mu\text{g/ml}$  for the positive drug control, Actinomycin D. A vehicle control was included where cells were treated with 2% DMSO. The treated cells were further incubated for 72 h followed by the addition of 50  $\mu\text{l}$  XTT to a final concentration of 0.3 mg/ml. The plates were incubated with the viability reagent for 2 h and the absorbance of the color complex measured at 490 nm with a reference wavelength set at 690 nm for XTT using KC Junior software and a BIO-TEK Power-Wave XS multi-well plate reader (A.D.P, Weltevreden Park, South Africa). The  $IC_{50}$  values were calculated using GraphPad Prism 4 software.

## Determination of Myrsinoside B Concentration in the *Myrsine africana* Extract and Formulation Into a Hydrogel

The concentration of myrsinoside B in the *M. africana* extract was determined by preparing stock concentrations of the extract (10mg/ml, 24.5 mg/ml, and 45 mg/ml) in propylene glycol. The concentrations were agitated at 150 rpm overnight and centrifuged at 13,400 rpm for 10 min to remove undissolved constituents. The supernatant of each concentration was then dissolved in 10 ml PBS and filtered using a 0.22  $\mu\text{m}$  syringe (Cell treat Scientific Products, Shirley, MA, USA). The concentration of myrsinoside B was determined using HPLC. For the formulation of the hydrogel, *M. africana* was dissolved in propylene glycol according to the method of Gao (2018). The agitated at 150 rpm overnight. The mixture was centrifuged at 13,400 rpm for 30 min to remove undissolved constituents and filtered through a 0.45  $\mu\text{m}$  syringe filter followed by a 0.22  $\mu\text{m}$  syringe filters and collected in a scintillation vial. A hydrogel was prepared by adding Carbopol 980 NF (1% w/v) to the solution slowly and stirred using a magnetic stirrer overnight at room temperature (VWR, Radnor, PA, USA). The mixture was neutralized with TEA to form a transparent gel matrix with a pH of approximately 5.5. The concentration of myrsinoside B in the hydrogel formulation was determined by sampling 10  $\mu\text{l}$  of the formulation from three different locations in the container. These samples were diluted 200 times in PBS and injected for HPLC analysis.

## Microneedle Treatment and Confocal Microscopy

Eighty one sharp tipped maltose microneedles (500  $\mu\text{m}$  in length) arranged in three parallel rows were used to physically enhance the delivery of myrsinoside B into dermatomed human skin. Parafilm was used to support the skin. The maltose microneedles were injected vertically into the skin for one minute and removed. The depth of the microchannels created by the microneedle injection was measured using a computerized Leica SP8 confocal laser scanning microscope (Leica Microsystems, Heerbrugg, Switzerland) with the 10X objective. Fluoresoft® (0.35%) solution was applied to the treatment site for one minute and thoroughly wiped off using kimwipes and alcohol swabs. The skin sample was scanned under the confocal microscope at an excitation wavelength of 496 nm. X-Z sectioning was used to estimate the depth of the microchannels by capturing a series of images at the same location but from different depths (from the skin surface to the point where no fluorescent signal was observed) (Puri et al., 2016).

## In Vitro Skin Permeation, Skin Extraction and HPLC Analysis

The permeation of myrsinoside B through dermatomed human skin was studied *in vitro* using static vertical Franz diffusion cells ( $n \geq 3$ ). The temperature of the receptor compartment was set at 37°C using a circulating water bath to maintain the temperature of the surface of the skin at 32°C. Non-treated and maltose microneedle treated skin was mounted on the Franz cells with the stratum corneum facing up. The *M. africana* extract hydrogel (200  $\mu$ l) was applied in the donor chamber, and the receptor chamber was filled with 5 ml 1 X PBS (pH 7.4 buffer). The receptor buffer (300  $\mu$ l) was withdrawn at pre-determined time points and replaced with 300  $\mu$ l fresh buffer solution. Samples were filtered using a 0.22  $\mu$ m syringe filter and analyzed using HPLC. After the 24 h permeation study, the remaining hydrogel in the donor compartment was removed using Q tips and the surface of the skin cleaned properly. The epidermis was removed from the skin using forceps and minced. The underlying dermis was cut into small pieces using scissors. The epidermis and dermis samples were transferred into a 6-well plate to which 2 ml PBS was added and maintained on a shaker (New Brunswick Scientific Co. Inc., Edison, NJ, USA) at 150 rpm for 4 h. The samples were then filtered through 0.22  $\mu$ m syringe filter (Celltreat Scientific Products, Shirley, MA, USA) and analyzed using HPLC using Waters Alliance HPLC system (e2695 separation module) (Waters Co., Milford, MA, USA) coupled to a 2996 photodiode array detector (Waters Co., Milford, MA, USA). Reverse-phase high-performance liquid chromatography (RP-HPLC) was used to determine the levels of myrsinoside B. A Kinetex Luna Phenyl-Hexyl (150 x 4.6 mm, 2.6 $\mu$ m) column was used at room temperature with methanol and 0.01% v/v formic acid in deionised water (30:70% v/v) as the mobile phase. A sample volume of 30  $\mu$ l was injected at a flow rate of 0.5 ml/min and analyzed at the detection wavelength of 278 nm.

## Data Analysis

The cytotoxicity, hydrogen peroxide scavenging, superoxide scavenging, and 5-lipoxygenase inhibitory results are depicted as the mean  $\pm$  SD ( $n = 3$ ). Statistical analysis was done using one-way analysis of variance (ANOVA) followed by Tukey's multiple comparison test using the GraphPad Prism statistical software to determine the statistical differences observed. All statistical evaluations for the results from the permeation studies were performed using Student's t-test and  $p$ -value  $< 0.05$  was considered for concluding significant difference ( $n \geq 3$ ).

## RESULTS

### In Vitro Biological Activity

The results for the *in vitro* biological activity investigated are summarized in **Table 1**.

### Hydrogen Peroxide and Superoxide Radical Scavenging

*M. africana* scavenged 50% of the hydrogen peroxide free radical at a concentration of  $56.08 \pm 2.88$   $\mu$ g/ml, not significantly different

from myrsinoside B which exhibited an  $IC_{50}$  of  $52.19 \pm 4.16$   $\mu$ g/ml. Both of these were found to be significantly higher ( $p < 0.01$ ) than the positive control, L-ascorbic acid which exhibited an  $IC_{50}$  of  $47.62 \pm 3.34$   $\mu$ g/ml. The *M. africana* ethanolic extract scavenged 50% of the superoxide radical at a concentration of  $132.74 \pm 1.64$   $\mu$ g/ml, significantly lower than the  $IC_{50}$  of Myrsinoside B ( $192.14 \pm 3.34$   $\mu$ g/ml), but significantly higher than the positive drug control quercetin ( $15.29 \pm 3.68$   $\mu$ g/ml) ( $p < 0.01$ ) (**Table 1**).

### 5-LOX Inhibition

The results indicate that both the crude extract of *M. africana* and myrsinoside B showed inhibition of 5-LOX, with  $IC_{50}$ 's of  $29.65 \pm 2.92$  and  $29.23 \pm 3.08$   $\mu$ g/ml respectively, not significantly different from one another, but significantly higher ( $p < 0.01$ ) than caffeic acid ( $14.87 \pm 0.69$   $\mu$ g/ml) (**Table 1**).

### In Vitro Cytotoxicity

The *in vitro* cytotoxicity investigation on human keratinocytes showed the ethanolic extract of *M. africana*, as well as myrsinoside B to be non-toxic to human keratinocytes *in vitro* at the highest concentration tested (400  $\mu$ g/ml). The positive control, Actinomycin D, exhibited an  $IC_{50}$  of  $< 5 \times 10^{-3}$   $\mu$ g/ml, lower than the lowest concentration investigated (**Table 1**).

### Myrsinoside B Concentration in M. africana Extract and Formulation Into a Hydrogel

Different amounts of the *M. africana* extract (10, 24.5 and, 45 mg) were added to 1 ml of PG to determine the content of myrsinoside B in the extract. For each concentration, the test was performed in triplicate. The average concentration of myrsinoside B in *M. africana* extract was found to be  $26.99 \pm 0.18\%$ . Once *M. africana* was formulated into a hydrogel for the permeation study, three locations within the hydrogel were sampled and the average concentration of myrsinoside was found to be  $5.06 \pm 0.12$  mg/ml (**Supplementary Data Sheet 1**).

### Depth of Microchannels Created by Maltose Microneedles

The depth of the micropores were estimated using confocal microscopy z-stack which captured a sequence of the images at the same horizontal position (x, y) at different depths (z). The results (**Figure 1**) indicated that the microchannels created by maltose microneedles in dermatomed human skin were approximately 110  $\mu$ m deep.

### In Vitro Permeation and Skin Extraction Studies

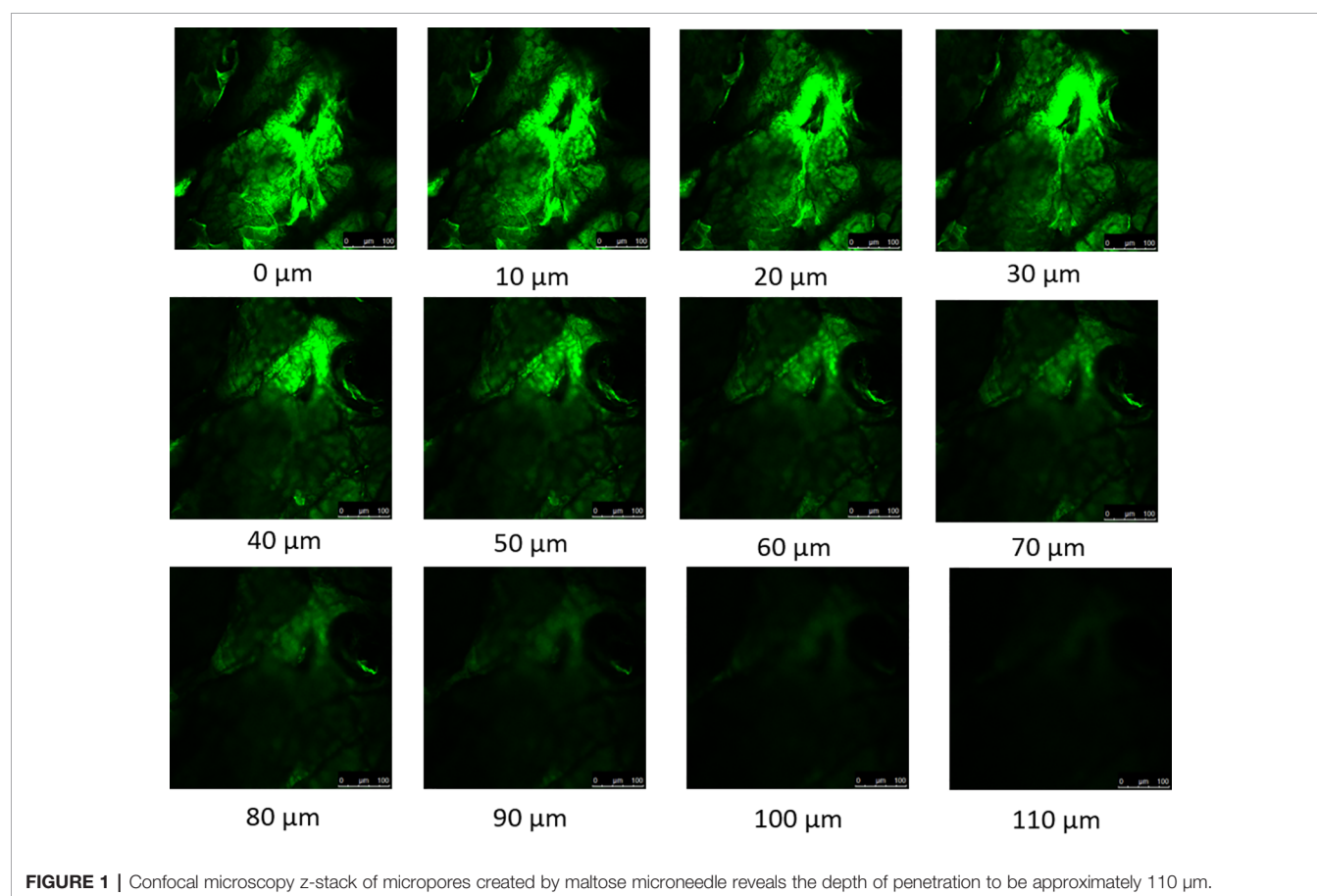
The control permeation study indicated low passive permeability of myrsinoside B after 24 h ( $1.30 \pm 0.85$   $\mu$ g/cm<sup>2</sup>) due to its hydrophilic nature. Maltose microneedle treatment significantly increased the permeation of myrsinoside B to  $12.46 \pm 5.14$   $\mu$ g/cm<sup>2</sup> ( $p < 0.05$ ) (**Figure 2**). The lag time for permeation was also significantly reduced to 1 h, compared to the passive group (more than 10 h). The drug amount retained in the epidermis after 24 h for the microneedle treatment group was observed to be  $8.97 \pm 0.90$   $\mu$ g/cm<sup>2</sup>, significantly



**TABLE 1 |** The *in vitro* cytotoxicity, 5-lipoxygenase inhibitory, hydrogen peroxide and superoxide scavenging activity of the ethanolic extract of *Myrsine africana* and its isolated compound, myrsinoside B.

	H <sub>2</sub> O <sub>2</sub> <sup>a</sup> scavenging (IC <sub>50</sub> <sup>e</sup> in µg/ml ± SD <sup>l</sup> )	O <sub>2</sub> <sup>-b</sup> scavenging (IC <sub>50</sub> <sup>e</sup> in µg/ml ± SD <sup>l</sup> )	5-LOX <sup>c</sup> inhibition (IC <sub>50</sub> <sup>f</sup> in µg/ml ± SD <sup>l</sup> )	Cytotoxicity <sup>d</sup> (IC <sub>50</sub> <sup>g</sup> in µg/ml ± SD <sup>l</sup> )
<i>Myrsine africana</i> ethanolic extract	56.08 ± 2.88 <sup>A</sup>	132.74 ± 1.64 <sup>A</sup>	29.65 ± 2.92 <sup>A</sup>	>400
Myrsinoside B	52.19 ± 4.16 <sup>A</sup>	192.14 ± 3.52 <sup>B</sup>	29.23 ± 3.08 <sup>A</sup>	>400
Positive drug control	47.62 ± 3.34 <sup>h,B</sup>	15.29 ± 3.68 <sup>i,C</sup>	14.87 ± 0.69 <sup>j, B</sup>	<5 × 10 <sup>-3</sup> k

Hydrogen peroxide<sup>a</sup>, Superoxide<sup>b</sup>, 5-Lipoxygenase<sup>c</sup>, Tested against Human Keratinocytes<sup>d</sup>, Fifty percent scavenging concentration<sup>e</sup>, Fifty percent inhibitory concentration<sup>f</sup>, Concentration at which fifty percent of the cell population remains viable<sup>g</sup>, L-Ascorbic Acid<sup>h</sup>, Quercetin<sup>i</sup>, Caffeic acid<sup>j</sup>, Actinomycin D<sup>k</sup>. Values are expressed as mean ± SD (n = 3). Statistical analysis was done using one-way analysis of variance (ANOVA) with Tukey's multiple comparison test, where A, B and C represent significant differences (p < 0.01).

**FIGURE 1 |** Confocal microscopy z-stack of micropores created by maltose microneedle reveals the depth of penetration to be approximately 110 µm.

greater than in the control group ( $3.24 \pm 1.41 \mu\text{g}/\text{cm}^2$ ,  $p < 0.05$ ). However, the drug amount in dermis layer for microneedle group ( $6.98 \pm 0.73 \mu\text{g}/\text{cm}^2$ ) was not significantly different than the control group ( $3.27 \pm 1.47 \mu\text{g}/\text{cm}^2$ ,  $p > 0.05$ ) (**Figure 3**).

## DISCUSSION

Three conditions of the skin make it especially vulnerable to the effects of reactive oxygen species; firstly, it is exposed to high doses of UV radiation often. Secondly, it has a high oxygen

tension, and thirdly, it is rich in unsaturated fatty acids. Phagocytic and polymorphonuclear cells, such as neutrophils and monocytes, produce superoxide, molecular oxygen, hydroxyl radicals, and hydrogen peroxide in response to inflammation. Furthermore, infiltrating leukocytes also expose the skin to a respiratory burst, producing elevated levels of superoxide. During this process, catalytic iron is also released from ferritin which causes additional damage. The effects of the hydroxyl radical include damaging biological macromolecules and releasing cellular components, ultimately leading to cell death. In addition, ROS activate transcription factors such as AP-1 and

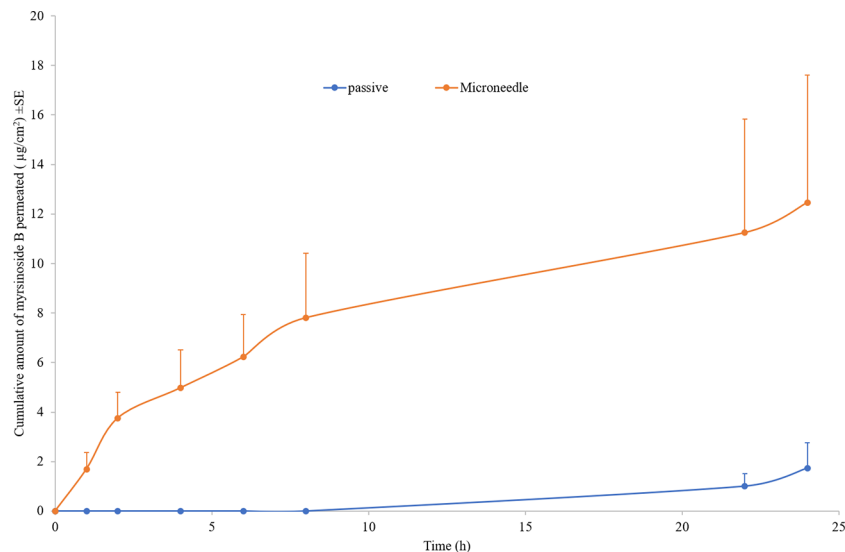


**FIGURE 2 |** Cumulative quantities of permeated myrsinoid B for the maltose microneedle treated skin compared to passive delivery ( $\mu\text{g}/\text{cm}^2 \pm \text{SE}$ ,  $n \geq 3$ ). Maltose microneedle treatment significantly increases the quantity of myrsinoid B permeated and reduces lag time ( $n \geq 3$ , Student's t-test  $p < 0.05$  indicates significant difference).

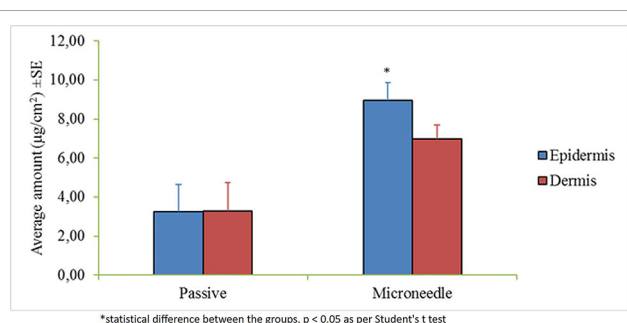


**FIGURE 3 |** Average amount of myrsinoid B retained in the epidermis and dermis of the human dermatomed skin ( $\mu\text{g}/\text{cm}^2 \pm \text{SE}$ ). The epidermis of the maltose microneedle treated group retained significantly greater amounts of myrsinoid B compared to the epidermis of the passive delivery group, however, no statistical difference was observed for the dermis ( $n \geq 3$ , Student's t-test  $p < 0.05$  indicates significant difference).

NF $\kappa$ B, which are regulated by cellular redox levels, to further stimulate the aging process (Peng et al., 2014). Antioxidant investigations have been conducted on various extracts of *M. africana*, which suggest that *M. africana* holds a higher affinity for scavenging superoxide and hydrogen peroxide than alternative radicals such as nitric oxide (Ahmad et al., 2011b). Gul et al. (2017) investigated the antioxidant propensity of various extracts of *M. africana* including an ethanolic extract, using hydrogen peroxide, and superoxide radicals amongst others (DPPH and ABTS). From their study, the findings indicate the ethanolic extract of *M. africana* to have an  $\text{IC}_{50}$  of  $46.61 \pm 0.08 \mu\text{g}/\text{ml}$  against the hydrogen peroxide free radical and  $122.64 \pm 1.55 \mu\text{g}/\text{ml}$  against the superoxide free radical, which supports the findings of the current study. Further investigations into the phytochemistry of *M. africana* revealed

the presence of a range of secondary metabolites including flavonoids and polyphenols, which may contribute to the antioxidant activity observed in both studies (Gul et al., 2017). By inactivating specific free radicals such as hydrogen peroxide and superoxide, the initiation of the aging cascade is diminished and the states of oxidative stress which continue to fuel the process reduced.

Inflammation is a complex biological response to external stimuli such as UV-radiation, pathogens, and irritants. Compromised cell membranes resulting from this damage release arachidonic acid that is then processed by either the cyclooxygenase or lipoxygenase pathway. The COX pathway involves two isoforms of the cyclooxygenase enzyme which act to produce thromboxane's and prostaglandins, while the lipoxygenase pathway produces a range of leukotrienes. Of these leukotrienes, leukotriene B<sub>4</sub> (LTB<sub>4</sub>) has been noted to produce the most pronounced effect in the inflammatory response and is produced predominantly by 5-LOX. By diminishing the inflammatory response, the production of reactive oxygen species and free radicals is curbed, reducing activation of cellular components which are mediated by the cellular redox potential (Pillai et al., 2005). Thus, the inflammatory response extends to the processes involved with oxidative stress and abnormal proteolytic degradation, to form an interlinked network that is collectively targeted. A study by Ahmad et al. (2011a) investigated a crude methanolic extract and various fractions of the aerial parts of *M. africana* for their anti-inflammatory activity in a phagocyte induced human neutrophil model which measures the production of reactive oxygen species. The ethyl acetate and n-hexane fractions of the plant showed the highest percentage inhibition at 500  $\mu\text{g}/\text{ml}$  (44.8 and 40.9%, respectively). The data in the current study indicates the extract of *M. africana* may be a potential anti-inflammatory agent with a more specific mechanism of action towards inflammatory



enzymes such as lipoxygenase, but future studies should investigate additional inflammatory enzymes such as cyclooxygenase-II. By targeting both classes of inflammatory enzymes the manifestation of inflammation will be more significantly reduced.

Edible plants, culinary plants and spices are considered highly toxic when exhibiting an  $IC_{50}$  lower than 50 µg/ml, moderately toxic 50–200 µg/ml, low toxicity between 200–1,000 µg/ml, and non-toxic >1,000 µg/ml (Kuethe and Efferth, 2015). Low levels of toxicity as observed in the present study were similarly found in a study by Gul et al. (2017) as well as irritancy studies in a clinical trial setting in an investigation by Lall et al. (2017).

As the largest organ of the human body, the most important function of the skin is to protect the underlying tissues and internal organs from external stimuli. This barrier function is achieved mainly by the topmost layer of the skin, stratum corneum, which is composed of layers of dead, flattened, keratin-filled cells and has lipophilic nature. For most hydrophilic drugs, like myrsinoid B, passive permeation efficiency is usually very low as observed (Log P -0.69), and enhancement techniques are needed to disrupt the skin barrier and facilitate delivery. The microneedle technique has been found to facilitate many molecules through skin previously by creating micro-sized channels through stratum corneum and epidermis. Microneedles are well investigated and have been demonstrated to significantly enhance the intradermal delivery of recombinant HIV-1 CN54gp, Nile red-loaded nano-particles, 5-aminolevulinic acid, DNA vaccine, botulinum toxin A, nano-encapsulated rhodamine B dye, and epigallocatechin-3-gallate (Nguyen and Banga, 2015; Puri et al., 2017). In our study, the depth of the microchannels created by the maltose microneedles was found to be around 110 nm, indicating the successful disruption of the stratum corneum and epidermis without reaching deep dermis nerves which stimulate pain. A significantly higher amount of myrsinoid B permeated the aqueous channels created by the microneedles than passive application on intact skin, which continued to accumulate over the 24 h period at a greater rate than passive application. More importantly, the lag time for skin permeation of the active was dramatically shortened by microneedles. By delivering myrsinoid B directly into the skin the efficacy of the active is enhanced. The slow rate of penetration and accumulation observed in the passive application suggests that the majority of the active is not absorbed and will ultimately be lost through sweating or touching the skin. Although the quantity of myrsinoid B retained within the dermis and epidermis is at concentration higher than its reported elastase inhibitory activity as reported by Lall et al. (2017), it is lower than the active concentrations obtained in the present study, suggesting that additional means to improve the delivery of myrsinoid B should be investigated. When comparing the amount of myrsinoid B in the dermis and epidermis, only the epidermis of the microneedle treated skin showed significantly higher amounts of myrsinoid B. The dermis of the microneedle treated skin retained less myrsinoid B than the epidermis, suggesting a barrier preventing the efficient transport of

myrsinoid B across the dermal-epidermal junction. Future investigations should focus on the delivery of myrsinoid B to the dermis where its efficacy would be most pronounced, which may be achieved by increasing the length of the microneedle channels to penetrate deeper into the epidermis.

The results indicate *M. africana* and myrsinoid B are capable of targeting numerous facets of the aging pathway, however, investigating additional major targets would further characterize any additional mechanisms of action by which this plant extract and its isolated compound may exert their action. While significant differences were observed in the superoxide scavenging investigation, the activity profiles of *M. africana* and myrsinoid B were similar for the other investigations, and suggest that the whole extract or a semi-pure fraction can be used for anti-aging therapies as a cost-effective alternative to compound isolation. Myrsinoid B could be used as a biomarker. Clinical studies by Lall et al. (2017) indicate even with passive application, the appearance of wrinkles is visibly reduced after 14–28 d of consecutive application, however, maltose microneedle treatment delivers a higher active load to the epidermis and dermis in a shorter time that would ultimately improve the efficacy of the treatment. To further improve the delivery of *M. africana* or myrsinoid B to the dermis, additional techniques such as nanoencapsulation should be investigated.

## CONCLUSION

The findings in the current study supports the use of *M. africana* and myrsinoid B as agents capable of diminishing the aging cascade by targeting the three critical processes associated with aging skin: oxidative stress, abnormal proteolytic degradation, and chronic inflammation. Further to this, *in vitro* investigations confirm the potential of these agents to be assimilated into the skin by implementing microneedle technology, where their efficacy will be most exerted. Prospective studies should investigate the application of the crude extract and myrsinoid B against additional targets implicated in the aging cascade such as AP-1, NF-κB, TGF-β, and additional inflammatory cytokines, as well as investigate the potential of nanoparticle technology for the enhancement of drug delivery and observed efficacy *in vitro*.

## DATA AVAILABILITY STATEMENT

The raw data supporting the conclusions of this manuscript will be made available by the authors, without undue reservation, to any qualified researcher.

## ETHICS STATEMENT

Human skin was procured from New York firefighters skin bank as per a memorandum of understanding with Mercer University

and was reviewed by University Institutional Review Board (IRB Ref No. H0303041).

## AUTHOR CONTRIBUTIONS

BF conducted the *in vitro* biological investigations and conducted the analysis for these results. XG, AP, and AB conducted the permeation studies and analyzed the results. NL supervised the project and provided resources for the project. All authors contributed towards and edited the final manuscript as well as provided final approval of the manuscript.

## REFERENCES

- Abbasi, A. M., Khan, M. A., Ahmed, M., and Zafar, M. (2010). Herbal medicines used to cure various ailments by the inhabitants of Abbottabad district, North West Frontier Province, Pakistan. *Indian J. Traditional Knowl.* 9, 175–183.
- Ahmad, B., Azam, S., Bashir, S., Hussain, F., and Chaudhary, M. I. (2011a). Insecticidal, brine shrimp cytotoxicity, antifungal and nitric oxide free radical scavenging activities of the aerial parts of *Myrsine africana* L. *Afr. J. Biotechnol.* 10 (8), 1448–1453. doi: 10.5897/AJB10.1652
- Ahmad, B., Azam, S., Bashir, S., Adhikari, A., and Hussain, F. (2011b). Anti-inflammatory activity and a new compound isolated from aerial parts of *Myrsine africana*. *Afr. J. Biotechnol.* 10, 8465–8470. doi: 10.5897/AJB11.115
- Bhatnagar, S., Dave, K., and Venuganti, V. V. K. (2017). Microneedles in the clinic. *J. Controlled Release* 260, 164–182. doi: 10.1016/j.jconrel.2017.05.029
- Chen, B., Wei, J., Tay, F., Wong, Y. T., and Iliescu, C. (2008). Silicon microneedles array with biodegradable tips for transdermal drug delivery. *Microsys. Technol.* 14, 1015–1019. doi: 10.1007/s00542-007-0530-y
- Chung, L. Y., Soo, W. K., Chan, K. Y., Mustafa, M. R., Goh, S. H., and Imiyabir, Z. (2009). Lipooxygenase inhibiting activity of some Malaysian plants. *Pharm. Biol.* 47 (12), 1142–1148. doi: 10.3109/13880200903008724
- Gao, X. (2018). *Skin delivery of natural compounds by enhancement technologies*. Atlanta, GA, USA: Mercer University.
- Githiori, J. B., Höglund, J., Waller, P. J., and Baker, R. L. (2002). Anthelmintic activity of preparations derived from *Myrsine africana* and *Rapanea melanophloeos* against the nematode parasite, *Haemonchus contortus*, of sheep. *J. Ethnopharmacol.* 80, 187–191. doi: 10.1016/S0378-8741(02)00030-2
- Gul, H., Ahmad, M., Zafar, M., Ahmad, S., Abid, A., Hira, S., et al. (2017). The *in vitro* and *in vivo* biological activities of the leaf of cape Myrtle, *Myrsine africana* L. *Phytother. Res.* 31 (9), 1305–1309. doi: 10.1002/ptr.5853
- Kang, L., Zhou, J. X., and Shen, Z. W. (2007). Two novel antibacterial flavonoids from *Myrsine africana* L. *Chin. J. Chem.* 25, 1323–1325. doi: 10.1002/cjoc.2007902455
- Killick, D. J. B. (1969). *Myrsine africana*. *Flowering Plants Afr.* 40, 1564. South Africa: Government Printer.
- Kishore, N., Twilley, D., Blom van Staden, A., Verma, P., Singh, B., Cardinali, G., et al. (2018). Isolation of flavonoids and flavonoid glycosides from *Myrsine africana* and their inhibitory activities against mushroom Tyrosinase. *J. Natural Prod.* 81 (1), 49–56. doi: 10.1021/acs.jnatprod.7b00564
- Kuete, V., and Efferth, T. (2015). African flora has the potential to fight multidrug resistance of cancer. *BioMed. Res. Int.* 15, 914813. doi: 10.1155/2015/914813
- Kumar, R. S., Rajkapoor, B., and Perumal, P. (2012). Antioxidant activities of *Indigofera cassioides* Rottl. Ex. DC. using various *in vitro* assay models. *Asian Pacific. J. Trop. Biomed.* 2, 256–261. doi: 10.1016/S2221-1691(12)60019-7
- Lall, N., Kishore, N., Fibrich, B., and Lambrechts, I. (2017). *In vitro* and *in vivo* activity of *Myrsine africana* on elastase inhibition and anti-wrinkle activity. *Pharmacogn. Mag.* 13 (52), 583–589. doi: 10.4103/pm.pm\_145\_17

## FUNDING

The authors acknowledge the University of Pretoria, Mercer University, and the National Research Foundation.

## SUPPLEMENTARY MATERIAL

The Supplementary Material for this article can be found online at: <https://www.frontiersin.org/articles/10.3389/fphar.2019.01410/full#supplementary-material>

- Nguyen, H. X., and Banga, A. K. (2015). Enhanced skin delivery of vismodegib by microneedle treatment. *Drug Delivery Trans. Res.* 5, 407–423. doi: 10.1007/s13346-015-0241-3
- Pandel, R. D., Poljšak, B., Godic, A., and Dahmane, R. (2013). Skin photoaging and the role of antioxidants in its prevention. *ISRN Dermatol.* 12, 930164. doi: 10.1155/2013/930164
- Peng, C., Wang, X., Chen, J., Jiao, R., Wang, L., Li, Y. M., et al. (2014). Biology of aging and role of dietary antioxidants. *BioMed. Res. Int.* 2014, 13 doi: 10.1155/2014/831841.
- Pillai, S., Oresajo, C., and Hayward, J. (2005). Ultraviolet radiation and skin aging: roles of reactive oxygen species, inflammation and protease activation, and strategies for prevention of inflammation induced matrix degradation - a review. *Int. J. Cosmetic Sci.* 27 (1), 17–34. doi: 10.1111/j.1467-2494.2004.00241.x
- Puri, A., Nguyen, H. X., and Banga, A. K. (2016). Microneedle-mediated intradermal delivery of epigallocatechin-3-gallate. *Int. J. Cosmetic Sci.* 38 (5), 512–523. doi: 10.1111/ics.12320
- Puri, A., Murnane, K. S., Blough, B. E., and Banga, A. K. (2017). Effects of chemical and physical enhancement techniques on transdermal delivery of 3-fluoroamphetamine hydrochloride. *Int. J. Pharm.* 528 (1–2), 452–462. doi: 10.1016/j.jpharm.2017.06.041
- Ryu, S., Kim, J., Kim, Y., Lee, S., Cho, Y., Lee, H., et al. (2014). Negligible pharmacokinetic interaction of red ginseng and antihypertensive agent amlodipine in Sprague-Dawley rats. *J. Toxicol. Environ. Health* 77, 1372–1383. doi: 10.1080/15287394.2014.951594
- Watt, J. M., and Breyer-Brandwijk, M. G. (1962). *The medicinal and poisonous plants of Southern and Eastern Africa being an account of their medicinal and other uses, chemical composition, pharmacological effects and toxicology in man and animal* Vol. 2. Edinburgh: E. & S. Livingstone Ltd., p. 1457.
- Zheng, Y. T., Chan, W. L., Chan, P., Huang, H., and Tam, S. C. Y. (2001). Enhancement of the anti-herpetic activity of trichosanthin by acyclovir and interferon. *FEBS Lett.* 496, 139–142. doi: 10.1016/S0014-5793(01)02391-2

**Conflict of Interest:** The authors declare that the research was conducted in the absence of any commercial or financial relationships that could be construed as a potential conflict of interest.

Copyright © 2020 Fibrich, Gao, Puri, Banga and Lall. This is an open-access article distributed under the terms of the Creative Commons Attribution License (CC BY). The use, distribution or reproduction in other forums is permitted, provided the original author(s) and the copyright owner(s) are credited and that the original publication in this journal is cited, in accordance with accepted academic practice. No use, distribution or reproduction is permitted which does not comply with these terms.



# Book Review: Herbal Principles in Cosmetics: Properties and Mechanisms of Action

Marco Nuno De Canha<sup>1</sup>, Aimee Steyn<sup>1</sup>, Analike Blom van Staden<sup>1</sup>, Bianca Daphne Fibrich<sup>1</sup>, Isa Anina Lambrechts<sup>1</sup>, Lilitha Lwando Denga<sup>1</sup> and Namrita Lall<sup>1,2,3\*</sup>

<sup>1</sup> Department of Plant and Soil Sciences, University of Pretoria, Pretoria, South Africa, <sup>2</sup> School of Natural Resources, University of Missouri, Columbia, MO, United States, <sup>3</sup> College of Pharmacy, JSS Academy of Higher Education and Research, Mysuru, India

**Keywords:** cosmeceuticals, monographs, mechanism of action, skin care, natural actives

## OPEN ACCESS

### Edited by:

Karl Tsim,  
Hong Kong University  
of Science and Technology,  
Hong Kong

### Reviewed by:

Nattaya Lourith,  
Mae Fah Luang University,  
Thailand  
Helen Skaltsa,  
National and Kapodistrian  
University of Athens, Greece

### \*Correspondence:

Namrita Lall  
namrita.lall@up.ac.za

### Specialty section:

This article was submitted to  
Ethnopharmacology,  
a section of the journal  
Frontiers in Pharmacology

**Received:** 28 August 2019

**Accepted:** 21 November 2019

**Published:** 09 January 2020

### Citation:

De Canha MN, Steyn A,  
Blom van Staden A, Fibrich BD,  
Lambrechts IA, Denga LL and Lall N  
(2020) Book Review: Herbal  
Principles in Cosmetics: Properties  
and Mechanisms of Action.  
Front. Pharmacol. 10:1513.  
doi: 10.3389/fphar.2019.01513

## A Book Review on

## Herbal Principles in Cosmetics: Properties and Mechanisms of Action

Burlando, B., Verotta, L., Cornara, L., Bottini-Massa, E., (Boca Raton, FL: CRC Press), 2010, 460 pages, ISBN 9781439812143, 1439812144 (eBook-pdf).

This book forms part of the series Traditional Herbal Medicines for Modern Times, and includes cosmeceuticals used in traditional Chinese medicine, Japanese Kampo medicine, and Indian Ayurvedic practices (Burlando et al., 2010). Consumer demand for cosmetic ingredients from natural sources, with comparable efficacy and safety features of synthetic ingredients, is becoming progressively more popular. In the past, cosmetics were restricted to aesthetic and decorative applications; however, modern cosmeceuticals are defined as cosmetics with the ability to alter skin functionality and improve health, eliminating any ambiguity between cosmetology and dermatology (Taofiq et al., 2018).

Chapter 1 of this book describes skin morphology, cell types, and structural features responsible for maintaining healthy skin. Chapter 2 focuses on the major phytochemical classes, their synthesis in plant cells, and their medicinal uses. Briefly, fatty acids and triglycerides act as emollients and emulsifiers providing the skin with moisture and adding to the waterproofing effect by interacting with the lipophilic fraction of the skin. Terpenoids commonly found in the essential oils of plants have preservative effects due to their ability to cause damage to prokaryote cell walls. They are often also used as antioxidants and for flavoring. Phenolic compounds from plants act as UV filters due to the presence of benzene ring structures. Alkaloids such as vincristine and vinblastine act as chemotherapeutic agents by affecting microtubule formation in cancer cells. Carbohydrates such as glucans act as skin moisturizing agents by preventing epidermal water loss. O-glycosides are cardioactive compounds that can prevent heart failure by stimulating the sodium/potassium ATPase pump. Hydroxy acids increase skin desquamation and exfoliate the skin for cell renewal. Chapter 3 provides valuable information to potential formulators searching for emulsifiers, humectants, and emollients from natural sources by arranging the plant species alphabetically using their common names. It includes herbal preservatives and agents enhancing skin penetration. Valuable insights into the side effects of topical formulations, even of those

containing natural ingredients and their role as comedogenic and acneogenic agents, are mentioned in this section.

Chapter 4 of this book comprises of 70 plant species summarized in the form of monographs. These provide the reader with a botanical description, region of origin, phytochemical constituents, and their therapeutic properties, as well as their current dermatological and cosmetic uses. They also include a section outlining the side effects and toxicological data associated with the use of these extracts.

Several well-known plant species including *Aloe vera*, *Argania spinosa* (argan), *Azadirachta indica* (neem), *Ginkgo biloba* (gingko), and *Moringa oleifera* (Moringa) are described. These species are used extensively as active ingredients in cosmetic products.

Numerous species used as flavor enhancers in cuisine are also described. *Cinnamomum verum* (cinnamon) containing cinnamaldehyde is largely used in cosmetics for its fragrance, most commonly in the form of an oil. *Rosmarinus officinalis* (rosemary), high in caffeol derivatives such as rosmarinic acid, is used to treat acne by reducing swelling. Rosemary essential oil is common in perfumery and hair care. Hops (*Humulus lupulus*), popular in beer flavoring and preservation, contains several constituents including  $\alpha$ - and  $\beta$ -acids and prenylnaringenin, contributing to the photoprotecting and regenerative activity of this species. The multi-purpose hydrodistilled oil of lemon balm (*Melissa officinalis*) used as a perfuming, antimicrobial, and antiviral agent is said to be due to the presence of citronellal.

Edible berries including those from *Sambucus nigra* (European elder), *Vaccinium myrtillus* (bilberry), and *Vitex agnus-castus* (chasteberry) are used for various disorders associated with the skin and are often used to protect the skin from the harsh effects of the sun.

The versatility of various plant parts of common fruit producing species including *Mangifera indica* (mango tree) and *Punica granatum* (pomegranate) are discussed. They are rich in bioactive phenolic compounds. Mangiferin and ellagic acid are highlighted in the monographs of these two species. The fruit and seeds of *Cocos nucifera* (coconut palm) is used in several cosmetic formulations and soaps for its hydrating and regenerating properties attributed to the compound, lauric acid. Olive oil, produced from the fruit of *Olea europaea*, has hydrating, photoprotective, and soothing effects on the skin. Interestingly, species like *Plukenetia volubilis* (Inca peanut) and *Lentinula edodes* (shiitake mushroom) contribute to enhancing skin barrier function and hydration due to the presence of essential lipids and amino acids. Similarly, *Sclerocarya birrea* (marula) fruits and seeds are rich in vitamin, minerals, and proteins. Red grape (*Vitis vinifera*) extracts rich in polyphenols, including resveratrol, are widely used to improve skin health and protect from UV radiation. *Macadamia integrifolia* (macadamia nut) oil high in palmitoleic acid is used as a natural preservative of cosmetic ingredients, inhibiting Gram-positive bacterial growth. *Glycyrrhiza glabra* (licorice) mimics cortisol activity and is, therefore, used for inflammatory skin disorders.

Alkaloid compounds produced in well-known species are discussed, with a particular focus on caffeine, theobromine,

and theophylline. *Coffea arabica* (coffee plant), *Cola acuminata*, and *Cola nitida* (Cola) are producers of caffeine while *Camellia sinensis* (green tea) and *Theobroma cacao* (cocoa plant) produce theobromine and theophyllines. *Paullinia cupana* (guarana) produces all three of these compounds. In general, these compounds show lipolytic activity, with the cosmetic potential to treat cellulite.

*Plectranthus barbatus* (Indian coleus), a forskolin producing species, is also used in cellulite treatment; however, it has several other applications including acne, psoriasis, and oral hygiene products. *Trichilia emetica* (mafura) seed oil forms a butter at room temperature. This butter is used to moisturize skin and improve wound healing and skin health due to the presence of essential fatty acids. The oil of *Aesculus hippocastanum* (horse chestnut), containing the complex saponin escin, is used to soothe erythema caused by inflammatory skin disorders.

The book highlights several algal species used in cosmetics. *Fucus vesiculosus* and *Laminaria digitata* and *Undaria pinnatifida* are all brown alga. These organisms are high in polysaccharides alginic acid, for example, which can be used as a thickening and emulsifying agent in cosmetic formulations. These polysaccharides are also emollients and increase skin hydration, preventing ageing. These polysaccharides are also in *Palmaria palmata*, a red algae. *Lithothamnion corallioides* and *Phymatolithon calcareum* (Maërl) are calcareous red algae used as exfoliants for skin rejuvenation. *Chlorella vulgaris* (green algae) has anti-ageing effects through metalloproteinase inhibition and cell regenerating properties by stimulating collagen synthesis. Two mosses, *Cetraria islandica* (Iceland moss) and *Chondrus crispus* (Irish moss), are also discussed, which have similar cosmetic applications to the algal species and act as skin hydrating agents and emollients.

Perhaps one of the major criticisms of this book is the lack of clarity of whether the cosmetic and dermatologic use of these herbal principles is based on their use in commercially available products or whether it is solely based on *in vitro* and *in vivo* data or records of traditional uses. From this book review, the authors would like to suggest that subsequent published books of this nature include cosmetic products where these ingredients are being used as the active ingredient and perhaps some form of clinical data to support the use of these herbal principles.

The monograph section of this book covered most cosmetic uses and included applications in skin care, hair care, oral care, as well as functional cosmetic ingredients with potential pharmaceutical applications. The authors successfully keep readers interested by describing actives from plant, algal, and fungal species.

## AUTHOR CONTRIBUTIONS

All the listed authors have made a direct, substantial, and intellectual contribution to the work and have approved it for publication. MDC edited and submitted the manuscript.

## REFERENCES

- Burlando, B., Verotta, L., Cornara, L., and Bottini-Massa, E. (2010). *Herbal Principles in Cosmetics: Properties and Mechanisms of Action* (Boca Raton, FL: CRC Press).
- Taofiq, O., Heleno, S. A., Calhelha, R. C., Fernandes, I. P., Alves, M. J., Barros, L., et al. (2018). Mushroom-based cosmeceutical ingredients: microencapsulation and *in vitro* release profile. *Ind. Crop Prod.* 124, 44–52. doi: 10.1016/j.indcrop.2018.07.057

**Conflict of Interest:** The authors declare that the research was conducted in the absence of any commercial or financial relationships that could be construed as a potential conflict of interest.

Copyright © 2020 De Canha, Steyn, Blom van Staden, Fibrich, Lambrechts, Denga and Lall. This is an open-access article distributed under the terms of the Creative Commons Attribution License (CC BY). The use, distribution or reproduction in other forums is permitted, provided the original author(s) and the copyright owner(s) are credited and that the original publication in this journal is cited, in accordance with accepted academic practice. No use, distribution or reproduction is permitted which does not comply with these terms.





# Exploring the Anti-Acne Potential of Impepho [*Helichrysum odoratissimum* (L.) Sweet] to Combat *Cutibacterium acnes* Virulence

Marco Nuno De Canha<sup>1</sup>, Slavko Komarnytsky<sup>2</sup>, Lenka Langhansova<sup>3</sup>  
and Namrita Lall<sup>1,4,5\*</sup>

<sup>1</sup> Department of Plant and Soil Sciences, University of Pretoria, Pretoria, South Africa, <sup>2</sup> Department of Food, Bioprocessing and Nutrition Sciences, Plants for Human Health Institute, North Carolina State University, Kannapolis, NC, United States, <sup>3</sup> Laboratory of Plant Biotechnologies, Institute of Experimental Botany, The Czech Academy of Sciences, Prague, Czechia, <sup>4</sup> School of Natural Resources, University of Missouri, Columbia, MO, United States, <sup>5</sup> College of Pharmacy, JSS Academy of Higher Education and Research, Mysuru, India

## OPEN ACCESS

### Edited by:

Andrei Mocan,  
Iuliu Hajeganu University of Medicine  
and Pharmacy, Romania

### Reviewed by:

Nokwanda Makunga,  
Stellenbosch University,  
South Africa  
Jolene Brooks,  
Stellenbosch University,  
South Africa  
François Chassagne,  
Emory University, United States

### \*Correspondence:

Namrita Lall  
namrita.lall@up.ac.za

### Specialty section:

This article was submitted to  
Ethnopharmacology,  
a section of the journal  
Frontiers in Pharmacology

**Received:** 25 June 2019

**Accepted:** 03 December 2019

**Published:** 30 January 2020

### Citation:

De Canha MN, Komarnytsky S,  
Langhansova L and Lall N (2020)  
Exploring the Anti-Acne Potential of  
Impepho [*Helichrysum odoratissimum*  
(L.) Sweet] to Combat *Cutibacterium*  
*acnes* Virulence.  
Front. Pharmacol. 10:1559.  
doi: 10.3389/fphar.2019.01559

The Gram-positive bacterium *Cutibacterium acnes* (previously *Propionibacterium acnes*), plays an important role in the pathogenesis and progression of the dermatological skin disorder acne vulgaris. The methanolic extract of *Helichrysum odoratissimum* (L.) Sweet (HO-MeOH) was investigated for its ability to target bacterial growth and pathogenic virulence factors associated with acne progression. The gas chromatography–mass spectrometry (GC-MS) analysis of HO-MeOH identified  $\alpha$ -humulene (3.94%),  $\alpha$ -curcumene (3.74%), and caryophyllene (8.12%) as major constituents, which correlated with previous reports of other *Helichrysum* species. The HO-MeOH extract exhibited potent antimicrobial activity against *C. acnes* (ATCC 6919) with a minimum inhibitory concentration (MIC) of 7.81  $\mu$ g/ml. It enhanced the antimicrobial activity of benzoyl peroxide (BPO). The extract showed high specificity against *C. acnes* cell aggregation at sub-inhibitory concentrations, preventing biofilm formation. Mature *C. acnes* biofilms were disrupted at a sub-inhibitory concentration of 3.91  $\mu$ g/ml. At 100  $\mu$ g/ml, HO-MeOH reduced interleukin-1 $\alpha$  (IL-1 $\alpha$ ) cytokine levels in *C. acnes*-induced human keratinocytes (HaCaT) by 11.08%, highlighting its potential as a comedolytic agent for the treatment of comedonal acne. The extract exhibited a 50% inhibitory concentration (IC<sub>50</sub>) of 157.50  $\mu$ g/ml against lipase enzyme activity, an enzyme responsible for sebum degradation, ultimately causing inflammation. The extract's anti-inflammatory activity was tested against various targets associated with inflammatory activation by the bacterium. The extract inhibited pro-inflammatory cytokine levels of IL-8 by 48.31% when compared to *C. acnes*-induced HaCaT cells at 7.81  $\mu$ g/ml. It exhibited cyclooxygenase-II (COX-II) enzyme inhibition with an IC<sub>50</sub> of 22.87  $\mu$ g/ml. Intracellular nitric oxide (NO) was inhibited by 40.39% at 7.81  $\mu$ g/ml when compared with NO production in lipopolysaccharide (LPS)-induced RAW264.7 cells. The intracellular NO inhibition was potentially due to the 2.14 fold reduction of inducible nitric oxide synthase (iNOS) gene expression. The HO-MeOH extract exhibited an IC<sub>50</sub> of 145.45  $\mu$ g/ml against virulent hyaluronidase enzyme activity,

which is responsible for hyaluronan degradation and scar formation. This study provides scientific validation for the traditional use of *H. odoratissimum* as an ointment for pimples, not only due to its ability to control *C. acnes* proliferation but also due to its inhibitory activity on various targets associated with bacterial virulence leading to acne progression.

**Keywords:** *Helichrysum odoratissimum* (L.) Sweet, *Cutibacterium acnes*, anti-acne, antibiofilm, pathogenesis

## INTRODUCTION

Acne vulgaris (AV) is a chronic inflammatory skin disorder of the pilosebaceous, localized on the face, chest, and back. This skin condition affects approximately 85% of people but is particularly common among adolescents. The disorder is characterized by the formation of non-inflammatory comedone lesions, more commonly referred to as blackheads or whiteheads. In more severe cases, the formation of inflammatory papules, pustules, nodules, and cysts is common. Acne vulgaris persistence and unresponsiveness to antibiotic treatments can result in the formation of atrophic (sunken) and hypertrophic scars. The formation of lesions and scars on visible areas of the skin not only affect aesthetic beauty but contribute to psychological problems affecting self-confidence and self-esteem. The progression of AV arises from four main events, including abnormal keratinocyte proliferation, increases in sebum production, increased *Cutibacterium acnes* proliferation, and activation of inflammatory cascades. The Gram-positive rod, *C. acnes* is of particular importance in acne progression. This bacterium contributes to disease progression with its ability to modulate keratinocyte proliferation, secrete virulent enzymes involved in sebum degradation (lipase) and tissue injury (hyaluronidase) and activating skin innate immunity through the activation of keratinocytes, sebocytes, and peripheral blood mononuclear cells resulting in the production of pro-inflammatory cytokines interleukin-1 $\beta$  (IL-1 $\beta$ ), IL-6, IL-8, IL-12, IL-17, TNF- $\alpha$ , and GM-CSF (granulocyte-macrophage colony-stimulating factor) (Dessinioti and Katsambas, 2017; Jeong and Kim, 2017; Han et al., 2018). The biofilm growth form of *C. acnes* is a major contributor to antibiotic resistance and pathogenesis, with biofilm-forming strains of the bacterium being associated with more severe AV (Coenye et al., 2008). The genome sequence of *C. acnes* has provided substantial evidence with regards to the presence of genes that contribute to the ability of this microorganism to form biofilms. In the early stages of biofilm development, the attachment of bacterial cells is an important step preceding the maturation of the biofilm structure. Gene clusters coding for the formation of polysaccharide capsule biosynthesis made up of glycocalyx polymers are said to contribute to *C. acnes* adhesion to surfaces (Burkhart and Burkhart, 2007). The attachment of *C. acnes* is not only limited to structures found on the skin, but this growth form has also been identified on orthopedic bone implants made from polymethylmethacrylate, titanium alloys, silicone, and even steel indicating the adaptive adhesion ability of this microorganism (Ramage et al., 2003; Achermann et al., 2014). Abnormal keratinocyte proliferation plays a crucial role

in the pathogenesis of *C. acnes*. Hyper-keratinization results in an imbalance of the shedding to proliferating keratinocyte ratio, clogging the pilosebaceous follicle, ultimately resulting in the formation of micro-comedones (De Medeiros-Ribeiro et al., 2015). The cytokine interleukin-1 $\alpha$  (IL-1 $\alpha$ ) has been detected in both diseased and healthy epidermis in the keratinocytes (Walters et al., 1995). *C. acnes* is known to possess a glycerol-ester hydrolase A (GehA) lipase enzyme involved in the degradation of sebum triacylglycerides resulting in the release of glycerol and free fatty acids. Glycerol is used as a nutrient source for the *C. acnes* bacterium, and the free fatty acids arrange themselves between keratinocytes, increasing bacterial cell adhesion, and enhancing biofilm formation within the pilosebaceous unit (Falcocchio et al., 2006). It is, therefore, an important target to consider when testing extracts or compounds for anti-acne activity. Sebocytes are specialized cells forming part of the pilosebaceous unit. These cells are responsible for the production of lipid droplets, functioning as a moisturizer for the skin. They are also immunocompetent cells contributing to immune responses in the skin, including the production of cytokines and other inflammatory mediators. Alongside their contribution to skin barrier function, keratinocytes also form part of many pathophysiological processes acting as a bridge between the external environment and the host. Keratinocytes elicit and maintain the skin immune response through the secretion of soluble factors, including cytokines, as well as antimicrobial peptides (Nagy et al., 2005). Sebocytes in follicles colonized with *C. acnes* have shown increased cyclooxygenase-II (COX-II) expression (Makrantonaki et al., 2011; Mattii et al., 2018). The production of excess PGE<sub>2</sub> results in sebaceous gland enlargement and increased sebum production, favoring *C. acnes* proliferation (Ottaviani et al., 2010). *C. acnes* results in the production of nitric oxide (NO) through chemotaxis and activation of neutrophil cells. These increased levels of NO production within the pilosebaceous follicles causes irritation and rupture of the follicular wall, ultimately leading to the formation of inflammatory lesions (Portugal et al., 2007). Hyaluronic acid (HA) is a glycosaminoglycan molecule made up of repeating disaccharide units of  $\beta$ -1,4-glucuronic acid and 1,3-*N*-acetylglucosamine connected *via* a  $\beta$ -linkage. Approximately 56% of the body's hyaluronic acid resides in the skin, with high abundance of this extracellular polysaccharide being found in the epidermis and the dermis. This polysaccharide is produced by epidermal keratinocytes and dermal fibroblasts. Bacterial hyaluronidases (HYALs) are distributed widely among Gram-positive microorganisms including *Cutibacterium* species. Hyaluronidases act by completely degrading HA into disaccharides or by degradation

into a mixture of unsaturated oligosaccharides. These enzymes contribute to bacterial virulence through tissue injury, facilitating bacterial spread to deeper tissues (Kumar et al., 2016; Nazipi et al., 2017). The inhibition of hyaluronidase activity, therefore, provides an important target for scar prevention and bacterial spread.

*Helichrysum odoratissimum* (L.) Sweet is a perennial shrub of the genus *Helichrysum*, consisting of approximately 500–600 species, of which approximately 244–250 are found in South Africa (Lourens et al., 2008). The vernacular name “Impepho” is common among species of this genus and are commonly used medicinal plants. This species is well distributed in South Africa and neighboring African countries, including Lesotho, Swaziland, Mozambique, and Zimbabwe (Swelankomo, 2004). This species has a plethora of traditional uses in the treatment of wounds, burns, eczema, and as an ointment for pimples (Hutchings et al., 1996; Akaberi et al., 2019). *H. odoratissimum* is among one of the most popular species within the *Helichrysum* genus and has been traditionally used as an application for pimples and to treat other skin dermatoses, however, it was yet to be tested for its antimicrobial activity against *C. acnes* (Hutchings et al., 1996; Lourens et al., 2011; Mabona and Van Vuuren, 2013).

This study aimed to investigate the potential of *H. odoratissimum* for its ability to treat acne by directly targeting *C. acnes* growth and indirectly by targeting the virulence factors involved in the progression of AV as a result of bacterial activity, therefore, providing scientific evidence to support traditional uses.

## MATERIALS AND METHODS

### Materials

#### Chemical Reagents

Tetracycline, erythromycin, benzoyl peroxide, crystal violet, actinomycin D, dimethyl sulfoxide (DMSO), Tris, KCl, 5,5'-dithio-bis-(2-nitrobenzoic acid) (DTNB), DMPTB, Triton X-100, ibuprofen, porcine hematin, L-epinephrine, formic acid, Na<sub>2</sub>EDTA, Griess reagent, citric acid, Na<sub>2</sub>HPO<sub>4</sub>, NaCl, BSA, NaOH, and CTAB were purchased from Merck SA (Pty) Ltd. (Sandton, Johannesburg, SA). PrestoBlue was purchased from Thermo Fisher Scientific (Randburg, South Africa). TRIzol and molecular grade water were purchased from Thermo Fisher Scientific (Waltham, Massachusetts, USA). Dexamethasone was purchased from Sigma Chemicals Co. (St. Louis, Missouri, USA). Ultra pure liquid chromatography water and acetonitrile (Romil-UpS™) were purchased from Microsep, South Africa. Formic acid (99% purity) was purchased from Thermo Scientific, South Africa. Fluka® Analytical Ammonium hydroxide ≥ 25% in H<sub>2</sub>O, eluent additive for liquid chromatography (LC) was purchased from Sigma-Aldrich, South Africa.

#### Microorganisms and Cell Culture Reagents

The *C. acnes* strain (ATCC 6919), brain heart infusion (BHI) agar, and BHI broth were purchased from Anatech Instruments (Pty) Ltd (Randburg, South Africa). Human keratinocytes

(HaCaT) were donated by Dr. Lester Davids (Department of Human Biology, University of Cape Town). Murine macrophages (RAW264.7), glucose, and lipopolysaccharide (LPS) (*Escherichia coli* 0127: B8) were purchased from Merck SA (Pty) Ltd. (Sandton, Johannesburg, SA). DMEM, trypsin, PBS, FBS, penicillin-streptomycin, and amphotericin B (Fungizone) were purchased from Thermo Fisher Scientific ZA (Johannesburg, RSA). TrypLE was purchased from Thermo Fisher Scientific (Waltham, Massachusetts, USA).

### Enzymes and Kits

Human recombinant COX-II, hyaluronidase from *Streptococcus pyogenes*, and lipase from *Candida rugosa* were all purchased from Merck SA (Pty) Ltd. (Sandton, Johannesburg, SA). The XTT cell proliferation kit II was purchased from Merck SA (Pty) Ltd. (Sandton, Johannesburg, SA). The IL-1α and PGE<sub>2</sub> ELISA kits were purchased from Biocom Africa (Pty) Ltd (Centurion, Pretoria, RSA). The CBA Human Inflammatory Cytokine kit was purchased from BD Biosciences (Woodmead, Pretoria, RSA). The Promega Griess Reagent System was purchased from Promega Corporation (Madison, Wisconsin, USA). The complementary DNA (cDNA) reverse transcriptase kit and the SYBR Green PCR Master Mix kits were purchased from Thermo Fisher Scientific (Waltham, Massachusetts, USA). Primers were purchased from Integrated DNA Technologies (Skokie, Illinois, USA).

## Methods

### Plant Extraction and Identification

*H. odoratissimum* L. Sweet was collected in the December from Durban (KwaZulu, South Africa) global positioning system (GPS) coordinates: grid 2931CC 29°00'S, 31°00'E. Taxonomical species identification was performed by Ms. Magda Nel from the H. G. W. J. Schweickerdt Herbarium at the University of Pretoria, and a voucher specimen number was deposited (PRU 118963). Shade-dried plant material (leaves and stems) was ground to a fine powder. Plant material (100 g) was extracted with methanol (1:5 w/v) for 72 h with constant agitation on a shaker. The maceration was filtered through a Buchner funnel (Whatman 1.0 filter). The filtrate was then concentrated under vacuum using a Rotary evaporator (Buchi-R-200). The crude extract was then stored at 4°C until use.

### Extract Characterization Using Gas Chromatography–Mass Spectrometry and Liquid Chromatography–Mass Spectrometry

The gas chromatography–mass spectrometry (GC-MS) analysis of methanolic extract of *H. odoratissimum* (L.) Sweet (HO-MeOH) (1 mg/ml, 0.22 μm filtered) was performed using a LECO Pegasus 4D GC-TOFMS (LECO Africa (Pty) Ltd., Kempton Park, South Africa) equipped with a GC Rxi-5SilMS (30 m, 0.25 mm ID, 0.2 μm film thickness) column (Restek, Bellefonte, PA, USA). The temperature of the injector and the interface were kept at 250°C. The following temperature program was used for analysis: 40°C (hold for 3 min) at 10°C/min to 300°C (hold for 5 min). Helium was used as a



carrier gas at a constant flow rate of 1 ml.min<sup>-1</sup>. Splitless injection with a 30 s splitless time was used. The first 5 min of the analysis was considered as solvent delay and omitted from the final GC-MS chromatograms. The MS transfer line temperature was set at 280°C. The mass spectrometer was operated in electron impact ionization mode (EI +) at 70 eV. Detector voltage was set to 1,750 V. The scan range was set at 40–550 Da with a data acquisition rate of 10 spectra/s. Peaks were identified by mass matching to the NIST05 database.

Compound separation and peak detection of HO-MeOH using LC-MS was performed using the Waters® Synapt G2 high definition mass spectrometry (HDMS) system (Waters Inc., Milford, Massachusetts, USA). The system includes a Waters Acquity Ultra Performance Liquid Chromatography (UPLC®) system linked with a quadrupole-time-of-flight (QTOF) instrument. MassLynx™ (version 4.1) software (Waters Inc., Milford, Massachusetts, USA) was used for data acquisition and processing. The internal lock mass control standard was a 2 pg/μl solution of leucine enkephalin (m/z 555.2693). Sodium formate clusters and Intellistart functionality was used to calibrate the instrument (mass range 112.936–1.132.688 Da). Resolution of 20,000 at m/z 200 [full width at half maximum (FWHM)] and mass error within 0.4 mDa were obtained.

The HO-MeOH extracts was prepared to a 1 mg/ml stock concentration and filtered using a 0.2 μm syringe filter to remove any particulates. A Kinetex® 1.7 μm EVO C18 100 Å (2.1 mm ID x 100 mm length) column was used for separation. A volume of 5 μl was injected into the system using an autosampler. A reverse phase step gradient elution scheme from 97% H<sub>2</sub>O (0.1% formic acid) to 100% acetonitrile (0.1% formic acid) was used as the mobile phase. The gradient started with an isocratic flow (hold 0.1 min) followed by a linear increase to 100% ACN; subsequently the column was washed for 1 min followed by conditioning and re-establishing of initial conditions to allow for equilibration before the start of the next run for the complete elution scheme. The column temperature was kept constant at 40°C and the flow rate was set at 0.4 ml/min for the each run, giving a total run time of 20 min. The positive and negative ion mass spectra were collected in separate chromatographic runs (employing the same separation conditions). Mass spectral scans were collected every 0.3 s. The raw data was collected in the form of a continuous profile. Mass to charge ratios (m/z) between 50 and 1,200 Da were recorded. Quantitative data-independent acquisition (DIA) was done using two simultaneous acquisition functions with low and high collision energy (MSE approach) with a QTOF instrument. The fragmentation energy was set at 1 and 4 V (positive mode) and 1.8 and 6 V (negative mode) for the trap and collision energies, respectively. The ramping was set from 3 to 4 V and 20 to 30 V for both modes for the trap and transfer collision energy, respectively. The electrospray ionization (ESI) mode conditions were set as follows; capillary voltage for ESI was 2.6 and 2.0 kV for positive and negative mode ionization, respectively. The source temperature for both modes was set at 120°C. the sampling cone voltage at 25 V for negative mode and 40 V for positive mode.

The extraction cone voltage was set at 4.0 V for both modes. Cone gas (nitrogen) flow was set at 10.0 L/Hr for both modes. The desolvation temperature was set at 300°C with a gas (nitrogen) flow of 600.0 L/h.

### Determination of Minimum Inhibitory Concentration

Susceptibility of the *C. acnes* (ATCC 6919) strain was tested using the microdilution broth assay as described by Lall et al. (2013). Briefly, 100 μl of HO-MeOH and tetracycline were serially diluted in BHI broth in a 96-well plate. Concentrations of plant extract ranged from 3.91 to 500 μg/ml, while tetracycline was tested from 0.39 to 50 μg/ml and was used as the positive control. Cultures of *C. acnes* grown for 72 h were then inoculated in BHI broth at a concentration of  $1.5 \times 10^8$  CFU/ml (OD<sub>600</sub> = 0.132). To each test well 100 μl of bacterial suspension was added. The 96-well plates were then incubated in an Anaerocult® jar with Anaerocult® A for the generation of CO<sub>2</sub>. Control plates were included and consisted of *C. acnes* alone, an extract vehicle DMSO treatment (2.5% v/v), and a growth media control only. After 72 h, 20 μl of PrestoBlue® reagent was added. The MIC (minimum inhibitory concentration) was then determined visually after 1 h of incubation. An MIC of less than 100 μg/ml was considered as potent anti-microbial activity.

### Combinations of *Helichrysum odoratissimum* (L.) Sweet Methanol With Benzoyl Peroxide, Erythromycin, and Tetracycline

The interaction between the HO-MeOH (component A) extract and commercial agents (component B) were determined using the variable ratio method described by De Rapper et al. (2012). The commercial agents and HO-MeOH extract were prepared to a stock concentration of 2 mg/ml (10% DMSO v/v). In a 96-well micro-titer plate, 100 μl of BHI broth was added to all the wells. Each component (A and B) was then added in varying ratios (9A:1B; 8A:2B; 7A:3B; 6A:4B; 5A:5B; 4A:6B; 3A:7B; 2A:8B; and 1A:9B). The combined ratios were then serially diluted two-fold. Cultures of *C. acnes* grown for 72 h were then inoculated in BHI broth at a concentration of  $1.5 \times 10^8$  CFU/ml (0.132 at OD<sub>600</sub>). To each test well, 100 μl of bacterial suspension was added. The 96-well plates were then incubated in an Anaerocult® jar with Anaerocult® A for the generation of CO<sub>2</sub>. Control plates were included and consisted of *C. acnes* only (no treatment) and a solvent control (2.5% v/v DMSO). After 72 h, 20 μl of PrestoBlue® reagent was added and following an hour incubation the MIC was determined. The MIC of HO-MeOH (component A) and antibiotic (component B) in combination, were then used to determine the sum of the fractional inhibitory concentrations (Σ FIC) using the following equation:

$$\sum \text{FIC} = \text{FIC A} + \text{FIC B} = \frac{\text{MIC in combination}}{\text{MIC A alone}} + \frac{\text{MIC in combination}}{\text{MIC B alone}}$$

An FIC value ≤ 0.5 was considered a synergistic combination, an FIC of 0.5 ≤ 1 was considered as additive, an FIC of 1 < 4 was considered non-interactive, and finally an FIC > 4 was considered antagonistic.

## Biofilm Prevention and Disruption

The bacterial adhesion assay for *C. acnes* (ATCC 6919) was previously performed by Coenye et al. (2007). Actively growing cultures of *C. acnes* were inoculated in sterile 96-well plates by adding 100  $\mu$ l (0.132 at OD<sub>600</sub>) in BHI to each well. Following bacterial plating, 100  $\mu$ l of plant extract and tetracycline were added to achieve concentrations of 0.24–31.25 and 0.02–3.13  $\mu$ g/ml, respectively. Controls including 100% adhesion (untreated *C. acnes*) and 0% adhesion (BHI media only) were included. Plates were then incubated anaerobically for 72 h. Following incubation, the BHI media was removed, and plates were gently washed with 100  $\mu$ l phosphate buffered saline (PBS) three times. Adhered cells were then fixed using 100  $\mu$ l of 99% methanol for 15 min. The MeOH was aspirated, and plates were allowed to air dry for 20 min. Quantification of adhered cells was then performed by the addition of 100  $\mu$ l of a 0.5% crystal violet for 20 min. The plates were then gently rinsed with distilled water to remove the excess crystal violet and allowed to air dry. The bound crystal violet was then dissolved using 160  $\mu$ l of a 33% acetic acid solution. The optical density was then measured at 590 nm using a BIO-TEK Power-Wave XS multi-well reader (A.D.P., Weltevreden Park, South Africa). For the biofilm disruption, *C. acnes* were plated as described in the adhesion protocol. After the 72 h adhesion, BHI media was removed, and the plates were gently washed three times with PBS to remove planktonic cells. Following the wash step, 200  $\mu$ l of fresh BHI was added, and plates were then incubated for an additional 72 h to allow for biofilm maturation. After incubation, the media was removed and replaced with 200  $\mu$ l of the test sample in BHI broth. After 24 h of treatment, the biofilm was quantified using crystal violet.

## Cytotoxicity Analysis

### Human Immortalized Keratinocytes

HaCaT were cultured in Dulbecco's modified Eagle's medium (DMEM) supplemented with 10% fetal bovine serum (FBS), 100  $\mu$ g/ml penicillin, 100  $\mu$ g/ml streptomycin, and 250  $\mu$ g/ml fungizone and incubated at 37°C and 5% CO<sub>2</sub>. Cells were grown to 80% confluency, in vented cell culture flasks (T-75) before subculture. Adhered cells were sub-cultured by cell detachment using trypsin-ethylenediaminetetraacetic acid (EDTA) followed by the addition of fresh media into new growing flasks. Cytotoxicity was determined using the XTT Cell Proliferation Kit II. In a 96-well plate, 100  $\mu$ l of ( $1 \times 10^6$  cells/ml) cell suspension was added, and cells were incubated for 24 h. The HO-MeOH extract was added at a concentration ranging from 3.125 to 400  $\mu$ g/ml. Actinomycin D was used as the toxic inducer and was tested from 0.05 to 3.91  $\mu$ g/ml. Treated cells were then incubated for 72 h. An untreated cell control and a 2% v/v DMSO vehicle control were also included. Following incubation, 50  $\mu$ l of activated XTT was added to all the test and control wells and further incubated for 2 h. The optical density was read at 490 nm with a reference wavelength of 690 nm to remove background. Tests were performed in triplicate and the percentage viability was then calculated. The 50% inhibitory concentration (IC<sub>50</sub>) was then calculated using GraphPad Prism 4.0 software (Lall et al., 2013).

### Murine Macrophage Cells (RAW264.7)

Murine macrophages (RAW264.7) cells were cultured in DMEM supplemented with 10% fetal bovine serum (FBS) and 1% penicillin-streptomycin and incubated at 37°C and 5% CO<sub>2</sub>. Cells were grown to 85% confluency in 100 mm cell culture dishes to prevent contact inhibition. Adhered cells were then sub-cultured by cell detachment using TrypLE followed by the addition of fresh media into new 100 mm cell culture dishes. Cytotoxicity was determined using the 3-(4,5-dimethylthiazol-2-yl)-2,5-diphenyltetrazolium bromide (MTT) reagent. In a 96-well plate, 100  $\mu$ l of a  $1 \times 10^5$  cells/ml was added and incubated for 24 h. The HO-MeOH extract was tested at a concentration range from 3.91 to 125  $\mu$ g/ml. A 5% DMSO (v/v) was added as the toxic inducer. An untreated cell control was also included in the assay. Following incubation, 20  $\mu$ l of MTT (5 mg/ml in PBS) was added to the test and control wells and incubated for 4 h. This was followed by the addition of 200  $\mu$ l of acidified isopropanol (0.1% HCl). Plates were covered in foil and placed on a rotating platform for 10 min. The optical density was then read at 560 nm with a reference wavelength of 670 nm to remove background. Tests were performed in triplicate, and the percentage viability was then calculated. The IC<sub>50</sub> was then calculated using GraphPad Prism 4.0 software (Esposito et al., 2014).

### Inhibition of Interleukin-1 $\alpha$

The effect of HO-MeOH on secreted IL-1 $\alpha$  levels in human keratinocytes was investigated at non-lethal concentrations determined from the cell viability assay (3.125–400  $\mu$ g/ml). Human keratinocytes were plated in a 24-well plate at a seeding density of  $1 \times 10^5$  cells per well and incubated for 24 h. The cells were stimulated with 100  $\mu$ g/ml of heat-killed *C. acnes* and 100 ng/ml of LPS from *E. coli*, independently. The HO-MeOH was added together with the stimulating factor to determine inhibitory activity for 24 h. An untreated cell control, LPS only and *C. acnes* only controls were also included. Plates were incubated for 24 h in a humidified incubator with 5% CO<sub>2</sub> and then centrifuged (980 rpm for 5 min) before the supernatant was collected, aliquoted, and stored at –80°C until use. The quantification of IL-1 $\alpha$  was performed using an Elabscience ELISA kit (Biocom Africa, Pretoria, SA) according to the manufacturer protocol. The IL-1 $\alpha$  concentration was calculated using a standard curve.

### Inhibition of Lipase Activity

The inhibitory effect of HO-MeOH against lipase was determined described by Choi et al. (2003). Ellman's reagent (DTNB) was dissolved in isobutanol to prepare a stock concentration of 40 mM. A stock concentration 10 mM of 2,3-dimercapto-1-propanol tributyrat (DMPTB) was then prepared in a solution of 6% Triton v/v, 50 mM Tris-Cl at a pH of 7.2. These were then stored at –20°C until the assay was performed. The lipase buffer was then prepared with 10 mM KCl and 10 mM Tris-Cl at pH 7.5 and was used to dissolve the lipase enzyme from *C. rugosa* (Sigma Aldrich, Johannesburg, South Africa). A stock solution of 0.5 M EDTA, 10% v/v Triton X-100, and 1 M



Tris-Cl were also prepared and made up the reaction mixture. The reaction mixture consisted of the following volumes, 20  $\mu$ l of 40 mM DTNB, 2  $\mu$ l of 0.5 M EDTA, 5  $\mu$ l of 10% v/v Triton X-100, and 50  $\mu$ l of 1 M Tris-Cl, pH 7.5. The reaction mixture was added to a 15 ml centrifuge tube, and the volume adjusted to 900  $\mu$ l with distilled water. For the enzyme inhibition assay, 160  $\mu$ l of the reaction mixture was added to a 96-well plate with 10  $\mu$ l of inhibitor (test sample in DMSO) and 20  $\mu$ l of enzyme solution (10 U/ml). The plates were then incubated at 37°C for 5 min to allow for inhibitor-enzyme interaction. The reaction was initiated by the addition of 10  $\mu$ l of a 4 mM DMPTB solution. For tests with no inhibitor, 10  $\mu$ l of lipase buffer was added. The assay controls included enzyme and substrate (no inhibitor), DMSO (5% v/v) only, no DTNB, no DMPTB, and no enzyme (substrate only). The plates were then incubated for 30 min at 37°C in a BIO-TEK Power-Wave XS multi-well reader (A.D.P., Weltevreden Park, South Africa) while performing a kinetic read at 405 nm. The IC<sub>50</sub> was then calculated using GraphPad Prism 4.0 software.

## Anti-Inflammatory Targets Associated With Acne Progression

### Pro-Inflammatory Cytokine Inhibition

The levels of pro-inflammatory cytokine (IL-1 $\beta$ , IL-6, IL-8, IL-10, IL-12p70, and TNF- $\alpha$ ) production in HaCaT cells induced with heat-killed *C. acnes* was determined from cell culture supernatants using flow cytometry. The BD Cytometric Bead Array (CBA) Human Inflammatory Cytokine kit was used to detect cytokine production according to the manufacturer's protocol (Cat. No. 551811) (BD Biosciences, San Jose, USA). HaCaT were seeded in 24-well plates at a density of  $1 \times 10^5$  cells/well in DMEM supplemented with 10% FBS, 100  $\mu$ g/ml penicillin, 100  $\mu$ g/ml streptomycin, and 250  $\mu$ g/ml fungizone and incubated at 37°C and 5% CO<sub>2</sub> for 24 h. After incubation, plating media was removed and replaced with 1 ml fresh culture media. Test samples were prepared in 1 ml of DMEM to yield final concentrations of 7.81  $\mu$ g/ml (HO-MeOH), 0.78  $\mu$ g/ml (tetracycline), *C. acnes* (100  $\mu$ g/ml), and LPS (100 ng/ml) in test wells. The HO-MeOH was added at the MIC to *C. acnes*-stimulated cells to determine inhibition of cytokines produced by *C. acnes*. LPS-stimulation was used as a control for cytokine induction. Untreated cells were also included as a control. Following 24 h of incubation plates were centrifuges at 980 rpm for 5 min, and cell-free supernatants were collected and stored at -80°C until use. Cytokine analysis was performed using the Accuri C6 cytometer (BD, Biosciences, USA). Inhibition of cytokines was calculated as a percentage (%) reduction from cytokine levels in *C. acnes*-stimulated HaCaT cells.

### Nitric Oxide Scavenging Activity and Intracellular Nitric Oxide Inhibition

The NO radical scavenging activity of HO-MeOH was determined using the methods described by Boora et al. (2014), adapted for a microtiter plate. In a 96-well plate, 90  $\mu$ l of distilled water was added to the first row, and 50  $\mu$ l of distilled water was added to the subsequent wells. A stock solution of HO-MeOH (10 mg/ml in methanol) was prepared. Serial dilutions of

HO-MeOH were then prepared by adding 10  $\mu$ l of the prepared stock solution to the first row and transferring 50  $\mu$ l to subsequent wells. The test concentration of HO-MeOH ranged from 15.625 to 2,000  $\mu$ g/ml. Ascorbic acid was used as the positive control and tested at the same concentrations. Methanol was used as the solvent control. The NO production was then initiated with the addition of 50  $\mu$ l of 10 mM sodium nitroprusside to each well. To account for the effect of the color of the extract, an extract blank was prepared using distilled water. The plates were then incubated for 90 min at room temperature in the dark. For NO quantification, 100  $\mu$ l of Griess reagent was added to all the wells and the OD<sub>546</sub> was then determined immediately using the BioTek Power Wave XS (A.D.P. Veltevreden Park, South Africa). The IC<sub>50</sub> was then calculated using GraphPad Prism 4.0 software.

The cellular NO scavenging activity of HO-MeOH using stimulated murine macrophages (RAW264.7) was performed according to the methods described by Esposito et al. (2014). Cell cultures were maintained as described above [*Murine Macrophage Cells (RAW264.7)*]. Cells were then seeded in a 96-well plate, at a density of ( $1 \times 10^4$  cells per well) and allowed to attach for 24 h prior to treatment. The HO-MeOH was tested at non-lethal concentrations obtained from the MTT cell viability assay (3.91–31.25  $\mu$ g/ml). The positive control dexamethasone was tested at 4  $\mu$ g/ml (10  $\mu$ M), and the negative control was DMSO (0.1% v/v). The cells were pre-treated with test samples for 2 h before the induction of NO with 1  $\mu$ g/ml of LPS (*E. coli* 0127: B8). Plates were then incubated overnight at 37°C in a humidified incubator with 5% CO<sub>2</sub>. The amount of NO produced in treated cells was detected using 50  $\mu$ l of cell supernatant using the manufacturer's protocol described in the Promega Griess Reagent System (Promega Corporation, WI, USA). The optical density was then read at 530 nm using a BioTek Synergy H1 microplate reader. The IC<sub>50</sub> was then calculated using GraphPad Prism 4.0 software.

### Cyclooxygenase-II Inhibition

Inhibition of human recombinant COX-II activity was investigated using the methods described by Reiningger and Bauer (2006). Briefly, 5  $\mu$ l of COX-II (0.5 U/well) was added to 180  $\mu$ l of 100 mM Tris buffer (pH 8.0) containing cofactors as follows: 5  $\mu$ M porcine hematin, 18 mM L-epinephrine, and 50  $\mu$ M Na<sub>2</sub>EDTA in a 96-well plate. Stock concentrations of HO-MeOH and Ibuprofen were prepared in DMSO, and 10  $\mu$ l of inhibitor was added to obtain final concentrations of 2.5–160  $\mu$ g/ml for HO-MeOH and 0.4–10  $\mu$ M (0.01–0.15  $\mu$ g/ml) for ibuprofen, the positive control. After 5 min incubation with the test inhibitors, 5  $\mu$ l of 10  $\mu$ M arachidonic acid substrate was added to initiate the reaction. The test plate was incubated at 37°C for 20 min. Following incubation, 10  $\mu$ l of 10% formic acid was added as a stop solution. The production of PGE<sub>2</sub> was quantified using the PGE<sub>2</sub> ELISA kit according to the manufacturer's protocol (Cat. No. ADI-900-001) (Enzo Life Sciences, New York, USA). The quantification of PGE<sub>2</sub> in test inhibitors and controls was determined from the PGE<sub>2</sub> standard curve. The IC<sub>50</sub> values for test inhibitors were calculated using GraphPad Prism 4.0 software.

### Inhibition of Inflammatory Gene Expression

Murine macrophages (RAW264.7) were maintained as in the section *Murine Macrophage Cells* (RAW264.7). Cells were seeded in a 24-well plate at a cell density of  $5 \times 10^5$  cells/ml and incubated for 24 h in a humidified incubator with 5% CO<sub>2</sub>. Cells were then treated with non-lethal concentrations of HO-MeOH (3.91–31.25 µg/ml) and dexamethasone was used as the positive control tested at 4 µg/ml (10 µM). Treatments with the extract and positive control were performed for 2 h before the addition of 1 µg/ml of LPS. Controls with untreated cells, 0.1% v/v DMSO and LPS only were also included. Plates were then incubated overnight. The total RNA was then isolated using the TRIzol reagent. Briefly, 330 µl of TRIzol was added to each replicate and combined in a sterile Eppendorf tube. Samples were then frozen at –20°C overnight. Following incubation, samples were thawed before the addition of 200 µl chloroform and vortexing for 30 s. Eppendorf tubes were then centrifuged (12,000 g) for 15 min. Samples were then carefully removed and the clear upper layer (~400 µl) was pipetted and transferred to a clean, sterile Eppendorf tube, without disturbing the pink TRIzol layer. To the supernatant layer, 500 µl of ice-cold isopropanol was added, vortexing briefly and storing on ice for 10 min. Samples were then centrifuged and supernatants discarded. Pellets were washed with 1 ml of 70% ethanol (using absolute ethanol and molecular grade water) followed by brief vortexing and storage on ice for 10 min before centrifuging (7,500 g) for 5 min. The supernatant was decanted without disturbing the pelleted RNA pellet. The Eppendorf tubes were air-dried for 15–20 min to allow residual ethanol to evaporate. Samples were stored in 40 µl of molecular grade water and stored at –80°C until use. RNA was quantified using the BioTek Synergy H1/Take 3 spectrophotometer to determine the OD<sub>260</sub>/OD<sub>280</sub> ratio. The cDNA was synthesized using 2 µg for each test sample and the controls using the cDNA Reverse Transcriptase Kit (Life Technologies, California, USA) on the ABI Applied Biosystems GeneAmp 9700 thermal cycler (Life Technologies, California, USA). Synthesized cDNA was amplified in duplicate using real-time quantitative PCR using SYBR green PCR Master Mix (Life Technologies, California, USA). The effects of genomic DNA contamination were overcome by selective use of intron-overlapping primers selected using Primer Express version 2.0 software (ABI Applied Biosystems, California, USA). The quantitative PCR amplifications were performed using the ABI Applied Biosystems 7500 Fast Real-Time PCR System (Life Technologies, California, USA) with 1 cycle at 50°C for 2 min and 1 cycle at 95°C for 10 min, subsequently followed by 40 cycles of 15 s at 95°C and 1 min at 60°C. Dissociation curves were completed with a single cycle of 1 min at 95°C, 30 s at 55°C, and finally 30 s at 95°C. The mRNA expression was determined using  $\Delta\Delta CT$  analysis with data normalized against the  $\beta$ -actin housekeeping gene using the 7500 Fast System SDS software v1.3.0. Inhibition of gene expression was compared with LPS-stimulated gene expression, where values < 1 indicated inhibition of gene expression and values > 1 indicated the overexpression of the gene of interest in excess of that of LPS stimulation. Melting curve profiles for the specific transcripts were also obtained. The forward primers sequences for each gene were as follows:  $\beta$ -actin (5'-AAC CGT GAA AAG ATG ACC CAG AT-3'), COX-II (5'-

TGG TGC CTG GTC TGA TGA TG-3'), and inducible nitric oxide synthase (iNOS) (5'-CCC TCC TGA TCT TGT GTT GGA-3'). The reverse primers for each gene were as follows:  $\beta$ -actin (5'-CAC AGC CTG GAT GGC TAC GT-3'), COX-II (5'-GTG GTA ACC GCT CAG GTG TTG-3'), and iNOS (5'-TCA ACC CGA GCT CCT GGA A-3') (Integrated DNA Technologies, Illinois, USA).

### Inhibition of Hyaluronidase Activity

The turbidometric assay described by Hofinger et al. (2007) was used to determine the hyaluronidase inhibitory activity. A citrate-phosphate buffer (McIlvaine's buffer) was prepared by mixing a solution of 0.2 M Na<sub>2</sub>HPO<sub>4</sub> with 0.1 M NaCl and 0.1 M citric acid with 0.1 M NaCl to pH 5.0. The hyaluronic acid substrate stock solution was prepared to 2 mg/ml (in distilled water). A stock solution of 0.2 mg/ml (in distilled water) bovine serum albumin (BSA) was also prepared. The hyaluronidase from *Streptococcus pyogenes* was optimized to 1 U/ml. In a 96-well plate, 136 µl of citrate-phosphate buffer was added to the first row. To all the subsequent wells 70 µl of buffer was added. The HO-MeOH extract was diluted in DMSO, and 4 µl was added to the first row in triplicate, followed by a two-fold serial dilution to obtain final concentrations ranging from 1.95 to 250 µg/ml. Ten microliters (10 µl) of BSA and 10 µl of hyaluronidase enzyme were then added. The negative control was DMSO without sample. The plates were then incubated for 15 min at 37°C. The reaction was then initiated by the addition of 10 µl of hyaluronic acid and further incubation for 30 min at 37°C. The reaction was then stopped with the addition of 200 µl of 2.5% (w/v) cetyltrimethylammonium bromide (CTAB) in 0.5 M NaOH and incubated at room temperature for 20 min. The turbidity was then measured by obtaining the optical density at 355 nm using the BioTek PowerWave XS (A.D.P. Veltevreden Park, South Africa). Additional controls included an extract color control, a substrate only control (100% enzyme inhibition), an enzyme and substrate only control (0% inhibition), and a no substrate control. The IC<sub>50</sub> was then calculated using GraphPad Prism 4.0 software.

### Statistical Analyses

Results for each experiment were determined using data obtained in triplicate with three independent assay repeats. One-way analysis of variance (ANOVA) was used to determine the differences in means and the Dunnett's multiple comparison post-test was used to determine significant differences between the means of treated and untreated groups as identified in each bioassay. For enzyme assays a four parameter logistic equation with a 95% confidence interval was performed to determine the IC<sub>50</sub>.

## RESULTS AND DISCUSSION

### Gas Chromatography–Mass Spectrometry and Liquid Chromatography–Mass Spectrometry Analysis

The major constituents in the extract were oleic acid amide (11.33%), linoleic acid (9.16%), palmitic acid (8.52%),

caryophyllene (8.13%), oxalic acid allyl nonyl ester (8.13%), 5,5-diethoxy-2-pentanone (4.74%), stigmaterol (4.36%),  $\alpha$ -sitosterol (4.28%),  $\alpha$ -humulene (3.94%),  $\alpha$ -curcumene (3.74%), and valencen (3.23%) (Table 1) (Figure S1). Lower levels of linoleic acid have been detected in acne patients. This fatty acid is of particular interest as it cannot be synthesized in human body and is generally obtained through diet. In sebaceous gland cells, low levels of linoleic acid influence linoleate concentrations in sebum, which translate to a fatty acid deficiency in the cells of the follicular epithelium leading to hyperkeratinization (Downing et al., 1986; Makrantonaki et al., 2011). This could contribute to the treatment of comedonal acne. The presence of stigmaterol and  $\alpha$ -sitosterol may contribute to HO-MeOH biological activity as previously isolated plant sterols isolated from green tea have shown therapeutic effects for acne vulgaris (Saric et al., 2016).

The HO-MeOH shared common compounds with other *Helichrysum* species, including *Helichrysum aureonitens* ( $\alpha$ -humulene and *para*-cymene). Hydrodistilled *Helichrysum leucocephalum* and *Helichrysum artemisioides* led to the

identification of  $\beta$ -caryophyllene and  $\alpha$ -humulene as major components of the oils of both species. These species also contained other constituents like hexadecanoic acid and E, E-farnesene present in HO-MeOH (Yani et al., 2005; Javidnia et al., 2009). A study by Bougatsos et al. (2003) reported that *Helichrysum kraussii* and *Helichrysum rugulosom* both contained  $\beta$ -caryophyllene as a major constituent. The *H. kraussii* oil also contained 9.8%  $\alpha$ -humulene, which was present in HO-MeOH. This study also reported the antibacterial activity of the individual component  $\beta$ -caryophyllene against *Staphylococcus aureus* and *Staphylococcus epidermidis* and showed that the crude essential oil exhibited better activity. This could explain the potent antimicrobial activity of HO-MeOH. Kuate et al. (1999) reported the presence of  $\alpha$ -curcumene and  $\beta$ -caryophyllene in *H. odoratissimum* L. Less. This study also reported the presence of  $\alpha$ -humulene in smaller quantities. Gundidza and Zwaving (1993) reported similar results in a Zimbabwean *H. odoratissimum* species with  $\alpha$ -humulene (13%) and  $\beta$ -caryophyllene (9.6%) as a major components. Valencene (1.9%), *para*-cymene (0.3%), and  $\alpha$ -cubebene (0.1%) were also present in the oil showing good correlation with the HO-MeOH components. Lawal et al. (2015) who tested a South African *H. odoratissimum* L. Sweet species, found that  $\alpha$ -humulene (5.6%) and  $\beta$ -caryophyllene (4.7%) were the major sesquiterpene compounds present.

The LC-MS data of the negative ionization mode, identified a caffeoylquinic acid derivative as a possible constituent in the crude methanolic extract (Table 2, Figure S2 and Figure S3). The identified mass fragment  $m/z$  515.1223 making up the peak at 3.71 min (Figure S4—Supplementary Data) was of particular interest since the possible compound hits included some caffeoylquinic acid derivatives which have been previously identified in other *Helichrysum* species, including *Helichrysum italicum*, *Helichrysum populifolium*, and *Helichrysum stoechas* (Barroso et al., 2014; Heyman et al., 2015; Maksimovic et al., 2017; Pereira et al., 2017). The mass fragments  $m/z$  353.1017 and 191.0762 corresponded to previous data on *Helichrysum obconicum* reported by Gouveia and Castilho (2011) corresponding to some caffeoyl-quinic acid derivatives. The 4,5-O-dicaffeoylquinic acid derivative was determined as the most probable compound match after comparison of the MS fragmentation pattern given for this derivative on the METLIN database (Figure S5).

## Antimicrobial Activity and Interaction With Benzoyl Peroxide, Erythromycin, and Tetracycline

The antibacterial activity of the methanolic leaf and stem extract of *H. odoratissimum* (HO-MeOH) exhibited an MIC of 7.81  $\mu\text{g/ml}$  against *C. acnes*, while the positive control tetracycline, exhibited an MIC of 0.78  $\mu\text{g/ml}$ . The minimum bactericidal concentration (MBC) activity was also determined with the HO-MeOH exhibiting a bactericidal effect at 250  $\mu\text{g/ml}$ , compared with tetracycline at 1.56  $\mu\text{g/ml}$ . The effect of the combination of HO-MeOH and the macrolide antibiotic, erythromycin, was also antagonistic to a much larger degree. The general trend observed for the combination of HO-MeOH and benzoyl peroxide (BPO)

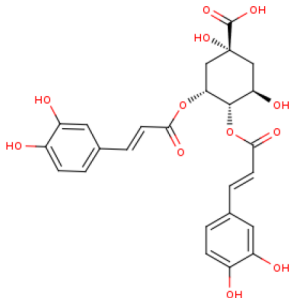
**TABLE 1 |** Compounds present in the methanolic extract of *Helichrysum odoratissimum* identified through gas chromatography–mass spectrometry.

Retention time (min)	Abundance (%)	Formula	Molecular weight (g/mol)	Compound name
6.24	1.9744	C <sub>9</sub> H <sub>20</sub>	128	Pentane, 2,2,4,4-tetramethyl-
7.07	2.1806	C <sub>7</sub> H <sub>6</sub> NS	135	Benzothiazole
7.23667	2.0781	C <sub>8</sub> H <sub>14</sub> O <sub>2</sub>	142	2,7-Octanedione
5.32667	0.84052	C <sub>8</sub> H <sub>18</sub> O <sub>2</sub>	146	Propane, 1,1-diethoxy-2-methyl-
6.77167	1.9106	C <sub>11</sub> H <sub>24</sub>	156	Undecane
6.13	4.742	C <sub>9</sub> H <sub>18</sub> O <sub>3</sub>	174	2-Pentanone, 5,5-diethoxy-
10.3967	3.7395	C <sub>15</sub> H <sub>22</sub>	202	$\alpha$ -Curcumene
11.5583	3.2313	C <sub>15</sub> H <sub>22</sub>	202	Valencen
8.99333	2.0484	C <sub>15</sub> H <sub>24</sub>	204	$\alpha$ -Cubebene
9.94667	3.9443	C <sub>15</sub> H <sub>24</sub>	204	Humulene
9.505	8.1263	C <sub>15</sub> H <sub>24</sub>	204	Caryophyllene
12.0883	1.7008	C <sub>15</sub> H <sub>24</sub> O	220	11,11-Dimethyl-4,8-dimethylenebicyclo[7.2.0]undecan-3-ol
22.3183	1.8196	C <sub>15</sub> H <sub>26</sub> O	222	trans-Farnesol
15.2583	0.6965	C <sub>14</sub> H <sub>28</sub> O <sub>2</sub>	228	Tridecanoic acid, methyl ester
15.685	8.5215	C <sub>16</sub> H <sub>32</sub> O <sub>2</sub>	256	Palmitic acid
9.51667	8.1263	C <sub>14</sub> H <sub>24</sub> O <sub>4</sub>	256	Oxalic acid, allyl nonyl ester
15.3767	1.301	C <sub>20</sub> H <sub>30</sub>	270	Gerany-P-cymene
17.1767	9.1583	C <sub>18</sub> H <sub>32</sub> O <sub>2</sub>	280	Linoleic acid
22.0833	11.329	C <sub>18</sub> H <sub>35</sub> NO	281	Oleic acid amide
16.91	2.2018	C <sub>20</sub> H <sub>40</sub> O	296	Phytol
17.6117	2.0086	C <sub>20</sub> H <sub>40</sub> O <sub>2</sub>	312	Butyl palmitate
19.2683	2.9919	C <sub>22</sub> H <sub>42</sub> O <sub>4</sub>	370	Hexanedioic acid, bis(2-ethylhexyl) ester
19.385	1.8204	C <sub>27</sub> H <sub>56</sub>	380	Heptacosane
24.7767	4.3613	C <sub>29</sub> H <sub>48</sub> O	412	Stigmaterol
23.365	0.45973	C <sub>26</sub> H <sub>38</sub> O <sub>4</sub>	414	Lupulon
23.4467	2.2776	C <sub>26</sub> H <sub>38</sub> O <sub>4</sub>	414	Lupulon
22.9983	2.1277	C <sub>27</sub> H <sub>55</sub> Cl	414	Heptacosane, 1-chloro-
25.135	4.282	C <sub>29</sub> H <sub>50</sub> O	414	$\alpha$ -Sitosterol



**TABLE 2 |** Identified compound match present in the methanolic extract of *Helichrysum odoratissimum* using negative ionization mode liquid chromatography–mass spectrometry data.

Peak	Retention time	Molecular mass (g/mol)	Elemental composition from MassLynx	Corrected mass fragments (m/z)	Potential compound match
1.	3.71	516.40	C <sub>25</sub> H <sub>24</sub> O <sub>12</sub>	515.1223 353.1017 191.0762	4,5-Di-O-caffeoylquinic acid



was that lower concentrations of HO-MeOH (sub-MIC) meant that less BPO was needed to produce an antimicrobial effect. The MIC of BPO alone was 31.25 µg/ml, but with the addition of the HO-MeOH extract in three combinations, antimicrobial activity of BPO was observed at concentrations as low as 5.47, 6.25, and 7.03 µg/ml (**Table 3**).

The antimicrobial activity of *H. odoratissimum* has, however, been tested previously against other microorganisms that have been linked to acne progression. The antibacterial activity of 3-O-methylquercetin isolated from the methanolic flower extract of *H. odoratissimum* showed selectivity against the Gram-positive bacteria *Bacillus subtilis* and *S. aureus* with an MIC of 50 and 6.25 µg/ml, respectively (Van Puyvelde et al., 1989). Although the flowers were not included in this study, a review by Lourens et al. (2008) indicated the presence of other flavonoid derivatives including chalcones and flavonols found in the aerial parts and roots of *H. odoratissimum*. The presence of pyrone, phloroglucinols, and diterpenes were mentioned and could be responsible for the observed antimicrobial activity against Gram-positive *C. acnes*. The antimicrobial activity of the acetone extract of *H. odoratissimum* also showed antimicrobial activity

against *S. aureus*, with an MIC of 15.63 µg/ml (Lourens et al., 2004). The antimicrobial activity of *H. odoratissimum* against *C. acnes*, was more potent when compared to other *Helichrysum* species. *Helichrysum pallidum*, *H. aureonitens*, and *H. splendidum* showed poor inhibition of the bacterium with MICs at ≥ 500 µg/ml, while *H. kraussii* exhibited an MIC of 61.25 µg/ml (De Canha et al., 2018; Lall et al., 2019).

The acetone shoot extract of *H. odoratissimum* which excluded the flowers was prepared by Mathekgga and Meyer (1998) and reported antibacterial activity against *S. aureus* and *B. subtilis* at 10 µg/ml. The choloform:methanol (1:1) leaf and stem extract of *H. odoratissimum* exhibited no activity against *S. epidermidis*, another microorganism which has been implicated in the pathogenesis of acne with an MIC of 4 mg/ml but was active against *S. aureus* with an MIC of 20 µg/ml (Lourens et al., 2011; Kumar et al., 2016). Previous reports on the antimicrobial activity of *H. odoratissimum* suggested that this plant contains compounds that are more selective toward Gram-positive bacteria, and showed better activity against *C. acnes* when compared to other acne related Gram-positive microorganisms used in previous studies. These results provide scientific evidence

**TABLE 3 |** Biological activity of *Helichrysum odoratissimum* methanolic extract against important targets of *Cutibacterium acnes* associated with acne progression.

Sample	MIC (µg/ml)	MBC (µg/ml)	Bacterial adhesion IC <sub>50</sub> (µg/ml)	Biofilm disruption IC <sub>50</sub> (µg/ml)	Nitric oxide scavenging IC <sub>50</sub> (µg/ml)	COX-II IC <sub>50</sub> (µg/ml)	Lipase IC <sub>50</sub> (µg/ml)	Hyaluronidase IC <sub>50</sub> (µg/ml)
HO-MeOH	7.81	250	<0.24	7.65 ± 0.60	214.90 ± 13.27	22.87 ± 6.48	157.50 ± 6.85	145.45 ± 6.22
Combination 1: 3:7 dilution 7	2.34 HO 5.47 BPO	*0.48	–	–	–	–	–	–
Combination 2: 2:8 dilution 7	1.56 HO 6.25 BPO	*0.40	–	–	–	–	–	–
Combination 3: 1:9 dilution 7	0.78 HO 7.03 BPO	*0.33	–	–	–	–	–	–
L-ascorbic acid	–	–	–	–	35.24 ± 7.85	–	–	–
Benzoyl peroxide	31.25	–	–	–	–	–	–	–
Erythromycin	0.06	–	–	–	–	–	–	–
Ibuprofen	–	–	–	–	–	0.15 ± 0.002	–	–
Tetracycline	0.78	1.56	0.32 ± 0.11	>3.125	–	–	>50	>250

\*ΣFIC (sum fractional inhibitory concentration) for synergistic combinations of HO-MeOH and BPO showing synergistic antibacterial activity (ΣFIC < 0.5).



for the application of the extract to pimples, as it potentially reduces *C. acnes* load within the acne lesions.

Antibiotic resistance is often linked with extensive use of antibiotics as a treatment option. The topical use and oral administration of antibiotics are common practice in acne treatment. Reports suggest that more than 50% of clinical isolates of *C. acnes* are resistant to topical macrolide antibiotics such as erythromycin. The use of broad-spectrum antibiotics also disturbs the delicate balance of the skin microbiome and can promote the growth of opportunistic bacteria. The use of topical compounds such as benzoyl peroxide (BPO), has therefore been prescribed as a solution for using antibiotic monotherapies or concurrent topical and oral antibiotic therapies in isolation. This compound is often used when long-term antibiotic use is prescribed for the treatment of acne patients. While macrolide antibiotics are the most common topical antibiotics, cyclines are the most common orally prescribed antibiotics. The burden of antibiotic resistance is escalated by the long treatment regimens often lasting between 3 and 6 months (Walsh et al., 2016). The combination of the HO-MeOH extract with erythromycin, tetracycline, and BPO was investigated to determine what type of interaction occurs and whether the interaction could potentiate antimicrobial activity against *C. acnes*. The MICs for erythromycin and BPO were determined independently and were shown to inhibit *C. acnes* growth at 0.061 and 31.25 µg/ml, respectively. The HO-MeOH extract showed an overall antagonistic effect when combined with the cycline antibiotic, tetracycline. The general trend of the results suggested that a decrease in HO-MeOH will always require more antibiotic to show the same antimicrobial activity (**Table 2**).

The tested *C. acnes* strain ATCC 6919 was more susceptible to erythromycin than to tetracycline and BPO. Macrolides such as erythromycin can reversibly bind to the 50S ribosomal subunit of bacteria and inhibit protein translocation, and tetracycline binds to the 30S ribosomal subunit preventing the synthesis of proteins essential for bacterial cell function (Chukwudi, 2016; Fox et al., 2016). The compounds present in the HO-MeOH extract could potentially interfere with the binding of tetracycline and erythromycin to the ribosomal subunits, decreasing their antimicrobial activity. Studies investigating the *in vitro* effects of combinations of antibiotics and plant extracts on *C. acnes* specifically, are not common. However, there are numerous scientific reports of combinations of plant essential oils and antibiotics on other acne-associated bacteria.

Oliveira et al. (2006) reported antagonistic effects for combinations of the essential oils of *Plectranthus amboinicus* and *Eucalyptus citriodora* with gentamicin against *S. epidermidis*. Combinations of *E. citriodora* oils with gentamicin, chloramphenicol, and ampicillin were all antagonistic against *S. aureus*. Several antagonistic effects were also observed for combinations of the oils of *Lippia sidoides* with gentamicin, *P. amboinicus* with chloramphenicol and gentamicin and *Conyza bonariensis* with chloramphenicol and gentamicin with regards to antimicrobial activity against *S. aureus*. Although it is an aminoglycoside antibiotic, gentamicin, much like tetracycline, affects protein synthesis by binding to the 16S A-site, which forms part of the 30S ribosomal subunit (Kotra et al., 2000). A

study by Van Vuuren et al. (2009) also showed the antagonistic effects of commercial tea tree essential oil when combined with ciprofloxacin against *S. aureus*, using the ratio method. *H. odoratissimum* is a highly aromatic species with several volatile constituents such as oxygenated monoterpenes (Asekun et al., 2007) which could potentially explain the antagonistic activity. The emergence of resistant strains of bacteria has encouraged the investigation of combinations of current antibiotic compounds with plant extracts and plant compounds. However, many of these reports focus on the publication of data where positive combinations are observed while ignoring the relevance of potentially antagonistic combinations (Sibanda and Okoh, 2007).

Benzoyl peroxide itself does not show potent antimicrobial activity, according to previously reported studies on 44 clinical isolates of *C. acnes* the MIC of BPO ranged between 128 and 256 µg/ml for all the isolates (Okamoto et al., 2016a; Okamoto et al., 2016b). In this study, the MIC was reported as 31.25 µg/ml against the type strain of *C. acnes* (ATCC 6919), which is particularly more susceptible to antimicrobial compounds. The potent antimicrobial activity of erythromycin can also be used to explain the susceptibility of the tested strain because clinical isolates of *C. acnes* commonly have higher resistance toward both erythromycin and clindamycin (Dessinioti and Katsambas, 2017). It is therefore expected that BPO would show a lower MIC against the type strain. This study showed that three concentrations of HO-MeOH resulted in better synergistic activity by keeping the BPO concentrations well below its MIC. The antibacterial activity of BPO is based on the breakdown of this compound into benzoic acid and hydrogen peroxide oxidative free radicals. These are highly reactive compounds that can affect *C. acnes* growth by damaging cellular constituents (Kosmadaki and Katsambas, 2017). Plants from the *Helichrysum* genus are known to possess many anti-oxidant compounds which can neutralize reactive oxygen species. The constituents found in the HO-MeOH extract could, therefore, be interacting with oxidative free radicals produced by the breakdown of the peroxide bond in BPO, which is known to be very unstable. This could potentially explain why at lowered concentrations of HO-MeOH show better synergistic potential (Albayrak et al., 2010). In this study the mechanism of antimicrobial activity was not tested. However, it is possible that the HO-MeOH extract targets the synthesis of enzymes responsible for protection against oxidative stress, resulting in increased susceptibility to BPO generated radicals (Nusbaum et al., 2012). It is important to note that combining components to achieve a desired effect; in this case, antimicrobial activity, is highly dependent on the selection of specific concentrations of each component.

## Biofilm Prevention and Disruption

A study by Coenye et al. (2007) reported the ability of the ATCC 6919 strain of *C. acnes* to attach to polystyrene prior to the development of a mature biofilm *in vitro*. The HO-MeOH extract exhibited high anti-adherence activity even at concentrations well below the MIC. Inhibition of attachment observed at 15.63 and 31.25 µg/ml is most likely due to the antimicrobial activity affecting

*C. acnes* growth. All the concentrations of HO-MeOH showed statistically significant differences when compared with the *C. acnes* untreated control, which was defined as the 100% adherence (**Figure 1A**). The BHI only control retained no crystal violet and indicated that no contaminants were present in the growth media. Bacterial adherence is often due to charge, hydrophobicity, or production of extracellular polysaccharides of cells (Zeraik and Nitschke, 2012). A study by Nostro et al. (2004), which tested the effect of *Helichrysum italicum* on the adherence of *Streptococcus mutans*, observed that the extract was able to reduce adherence by causing changes in the hydrophobicity index to a hydrocarbon surface. Styrene, the component making up the polystyrene plates, is itself a hydrocarbon and therefore, suggests that the attachment of *C. acnes* to this surface is due to hydrophobic bonding (Rosenberg, 2017). The formation of biofilm is largely dependent on the ability of the microorganism to adhere to the substrate or surface. This adhesive ability is, therefore, one of the targets available for the prevention of biofilm formation and is of particular importance, because mature biofilm structures play a crucial part in disease development.

Studies on the polar constituents of some *Helichrysum* species through hydro-methanolic, hydro-alcoholic, or methanol have identified caffeoylquinic and flavonoid derivatives as major

constituents (Mari et al., 2014; Silva et al., 2017). The quinic acid derivative chlorogenic acid isolated from the methanol extract of *H. italicum* exhibited anti-adhesive activity against *Pseudomonas aeruginosa* (D'Ambrosia et al., 2013). The results observed in this study suggested that HO-MeOH contained an active constituent or a number thereof, which could potentially disrupt hydrophobic interactions between the polystyrene surface and the *C. acnes* cells. The drug control tetracycline was also tested for its ability to inhibit the attachment of *C. acnes*. Tetracycline was not as effective as the HO-MeOH extract with regards to the inhibition of bacterial cell adhesion. Tetracycline exhibited an  $IC_{50}$  of  $0.32 \pm 0.11$   $\mu\text{g/ml}$  (**Figure S8A**), which indicates anti-adhesion activity was not due to bacterial cell death as this was below the MIC of 1.56  $\mu\text{g/ml}$  (**Figure 1B**). The results suggested that tetracycline is used solely for its ability to inhibit excessive proliferation of the bacterial cells, targeting protein synthesis. In a clinical setting, *C. acnes* thrives within a biofilm and often results in reduced activity of antibiotic therapies. The addition of sub-MIC concentrations of tetracycline does not inhibit the attachment of *C. acnes* cells as well as the HO-MeOH. Tetracycline tested at a sub-inhibitory concentration of 0.02–0.2  $\mu\text{g/ml}$  was not able to inhibit biofilm formation after 72 h of treatment, suggesting that bacterial

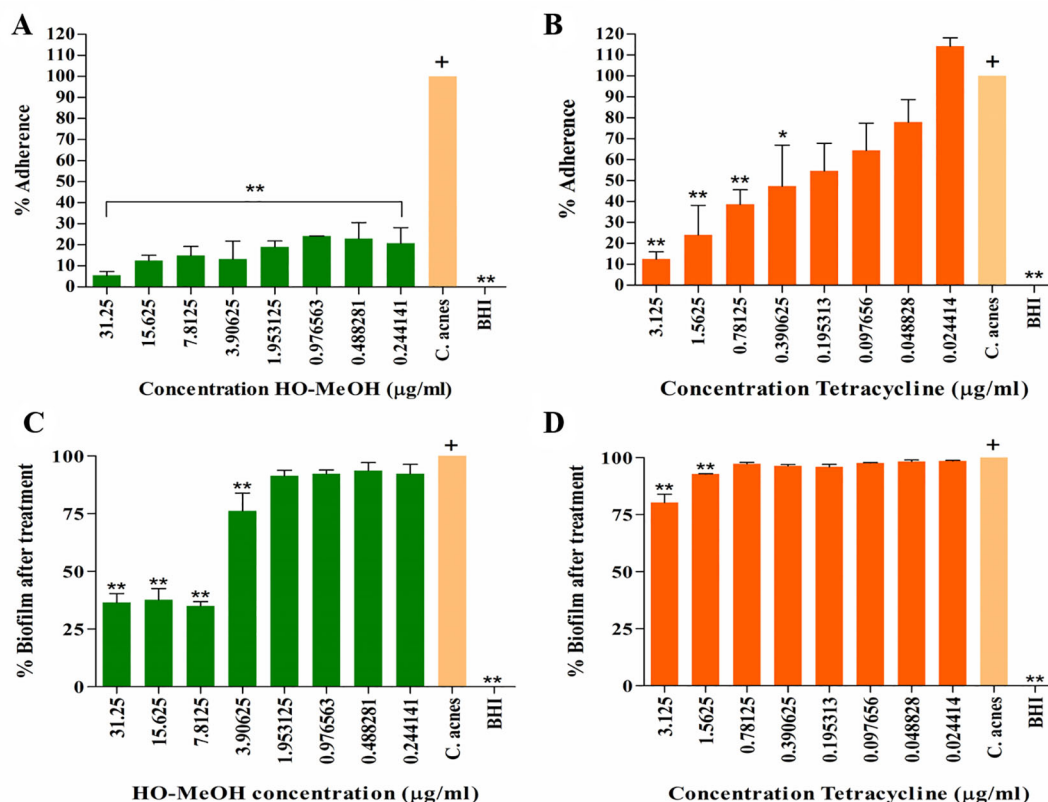


**FIGURE 1 |** The anti-adherence activity of the *Helichrysum odoratissimum* methanolic extract (**A**) and tetracycline (**B**) and the biofilm disruption activity of the *H. odoratissimum* methanolic extract (**C**) and tetracycline (**D**). \* $p < 0.05$ ; \*\* $p < 0.01$ . The "+" indicates the control column to which all the data sets were compared using the Dunnett's multiple comparison test.

adhesion and maturation remains unaffected by this antibiotic (Sivasankar et al., 2016).

Gram-negative and Gram-positive bacterial populations are known to cooperate, communicate, and grow symbiotically to form complex social communities in order to enhance invasion and persistence through a process known as quorum sensing. The biofilm structure forms an integral part of this process and is, therefore, an essential target to consider when developing acne therapies, considering the ineffectiveness of systematic antibiotics in this regard (Savoia, 2012). There was disruption of mature *C. acnes* biofilm at 31.25, 15.625, and 7.81  $\mu\text{g/ml}$  when compared to the untreated *C. acnes* control. The  $\text{IC}_{50}$  for the biofilm disruption was calculated to be  $7.65 \pm 0.60 \mu\text{g/ml}$  (Figure 8B). The extract also showed disruption of the *C. acnes* biofilm at a sub-inhibitory concentration of 3.91  $\mu\text{g/ml}$ , suggesting that the extract does not act only by killing cells within the biofilm but may have an additional role (Coenye et al., 2012) (Figure 1C). When compared with other extract tested against *C. acnes* biofilm disruption, *H. odoratissimum* showed prominent activity. A study by Chassagne et al. (2019) reported the biofilm eradication concentration ( $\text{MBEC}_{50}$ ) of *Ginkgo biloba* seed nut extract against *C. acnes* at 256  $\mu\text{g/ml}$  and an MIC of 64  $\mu\text{g/ml}$ .

The crystal violet staining method effectively allows for the quantification of biofilm biomass but is limited; however, by the inability to distinguish between live and dead cells (Peeters et al., 2008). Although the specific mechanism of biofilm disruption was not tested in this study, the results suggest that the biofilm disruption effect of HO-MeOH is most likely due to the bactericidal activity against cells within the biofilm. The majority of compounds possessing anti-biofilm activity are isolated from natural sources (Roy et al., 2018). A study by Cui et al. (2016) observed not only the inhibitory effect of the essential oil of *H. italicum* against biofilm formation but also its ability to eradicate biofilm structure of *S. aureus*. The essential oil showed better activity in both aspects when compared with the effect of major essential oil component, neryl acetate, alone. This suggested that the essential oil components act synergistically against biofilm formation and biofilm disruption. The HO-MeOH contains a number of volatile compounds identified through GC-MS, which could act synergistically resulting in the disruption of *C. acnes* biofilm. An amino-phloroglucinol, helichrytalicine B, isolated from *H. italicum* showed potent activity against the formation of *S. epidermidis* biofilms. Many *Helichrysum* species are abundant in  $\alpha$ -pyrone phloroglucinol derivatives, including *H. odoratissimum* which could be responsible for its biofilm eradication activity. Due to the ability of biofilm-forming bacteria to alternate between both single cell and biofilm states, it is important for agents to possess both strong anti-biofilm activity as well as antibacterial activity. This makes HO-MeOH a promising candidate as an anti-biofilm agent (Lourens et al., 2008; D'Abrosca et al., 2016). Tetracycline was less effective at disrupting established *C. acnes* biofilm. There was only significant biofilm disruption compared to the untreated *C. acnes* control at 1.56 and 3.125  $\mu\text{g/ml}$  (Figure 1D). Biofilm

structures are known to result in increased resistance to antibiotic activity; this could explain the ineffectiveness of tetracycline to reduce biofilm mass after treatment of the mature biofilm. Other tetracycline antibiotics (doxycycline and oxytetracycline), except minocycline, were not able to reduce biofilm biomass or exert bactericidal activity against *C. acnes* cells within the biofilm (Coenye et al., 2007). Biofilm formation varies between different bacterial phylotypes, ATCC 6919 has been classified as type IA<sub>1</sub>. This phylotype can produce higher amounts of biofilm biomass, possibly contributing to reduced efficacy of tetracycline (Kuehnast et al., 2018).

## Cytotoxicity on Human Keratinocytes and Murine Macrophages

The anti-proliferative effect of HO-MeOH was determined on human keratinocyte cells in order to determine non-lethal concentrations of the extract that could be investigated in subsequent hyper-keratinization and anti-inflammatory cell-based assays. Cell viability was normalized against the cell viability observed in the DMSO negative control. The  $\text{IC}_{50}$  of HO-MeOH on HaCaT viability determined to be  $167.00 \pm 27.95 \mu\text{g/ml}$  (Figures 2A and S9A). This is well above the MIC, suggesting that topical application of the extract at the MIC concentration should not affect HaCaT cell viability. Several *Helichrysum* species are traditionally used to treat inflammatory skin disorders and improve wound healing (Grčić et al., 2017). Other species in the Asteraceae family have also been traditionally reported to have this activity and is attributed to their ability to enhance keratinocyte proliferation and the remodeling of the skin extracellular matrix (Carvalho Jr. et al., 2018). There were obvious adverse effects on cell viability at 200 and 400  $\mu\text{g/ml}$ . However, at concentrations between 3.125 and 25  $\mu\text{g/ml}$  cell proliferation seems to be induced as compared to the negative control. The effects of HO-MeOH on human keratinocyte proliferation is, therefore, concentration sensitive. The anti-proliferative effect of HO-MeOH was determined in murine macrophages in order to obtain non-lethal doses of extract that could then be used to assess the nitric oxide inhibitory effects of the extract as well as the inhibitory effects on the expression of specific genes associated with inflammation. The cell viability was normalized against the negative DMSO vehicle control (0.625% v/v). The  $\text{IC}_{50}$  of HO-MeOH was  $61.29 \pm 10.51 \mu\text{g/ml}$  on RAW264.7 cells. The toxic inducer of DMSO (5% v/v) completely inhibited cell proliferation (data not shown) (Figures 2B and S9B).

## Interleukin-1 $\alpha$ Inhibition

The LPS-induced cytokine production was used as a control for IL-1 $\alpha$  production. The effects of HO-MeOH, together with *C. acnes* stimulation, was used to assess the anti-inflammatory activity of HO-MeOH in response to *C. acnes*-induced cytokine production specifically. The induction of HaCaT cells using heat-killed *C. acnes* showed a significant difference when compared to the untreated HaCaT cell control. The *C. acnes* caused an increase in IL-1 $\alpha$  from a basal concentration of  $298.10 \pm 20.88 \text{ pg/ml}$  to  $374.69 \pm 10.17 \text{ pg/ml}$ . A significant difference was also observed between the *C. acnes* treated cells

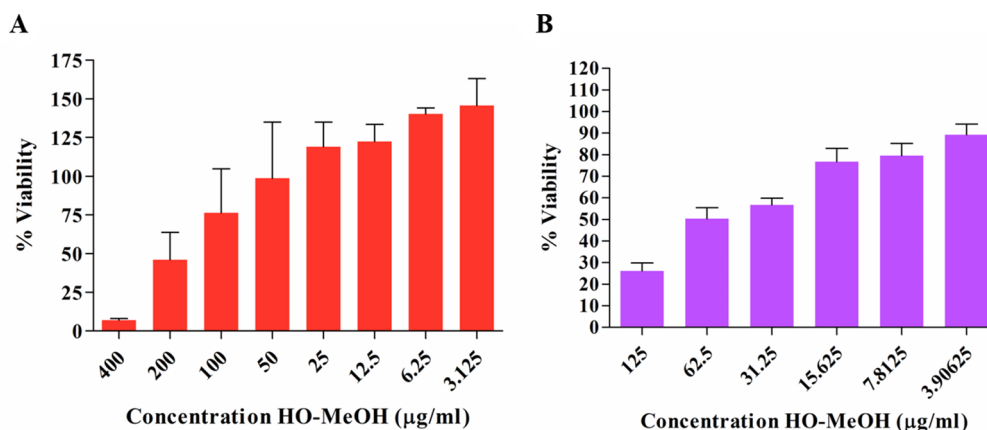


**FIGURE 2 |** Antiproliferative effects of the *Helichrysum odoratissimum* methanolic extract on human keratinocyte cells (HaCaT) (A) and murine macrophage cells (RAW264.7) (B).

and 100 μg/ml HO-MeOH, which reduced IL-1α protein levels to  $333.18 \pm 10.92$  pg/ml (Figure 3).

## Lipase Inhibition

The HO-MeOH extract exhibited an  $IC_{50}$  of  $157.50 \pm 6.85$  μg/ml against lipase activity (Figures 4A and S10). Tetracycline showed low levels of lipase inhibition even at the highest concentration

tested (Figure 4B). Previous studies have shown the ability of *C. acnes* lipase enzyme to use 2, 3-dimercapto-1-propanol tributyrates as a substrate, which suggests that the results obtained using lipase from *C. rugosa* would provide reliable inhibitory data for *C. acnes* lipase inhibition (Batubara et al., 2014). Previous reports of the activity of tetracyclines on lipase inhibition show similar results observed in this study. Tetracycline hydrochloride, chlortetracycline hydrochloride, and demeclocycline hydrochloride showed 76, 76, and 80% inhibition at 500 μg/ml, respectively. At 50 μg/ml, chlortetracycline hydrochloride and tetracycline hydrochloride showed 18 and 20% inhibition, respectively. Concentrations as high as 0.008 M (3.56 mg/ml) have only shown 89% inhibition (Hassing, 1971; Puhvel and Reisner, 1972). More recent studies have demonstrated similar results for tetracycline as a lipase inhibitor with  $IC_{50}$  as high as  $471.3 \pm 5.5$  μg/ml (Batubara et al., 2009). This study also tested the methanol extracts of several Indonesian plant species traditionally used for skin eruptions or acne and showed similar results. The methanol extracts of *Caesalpinia sappan*, *Curcuma longa*, *Curcuma xanthorrhiza*, *Goniothalamus macrophyllus*, and *Lepisanthes amoena* exhibited  $IC_{50}$  of  $150.0 \pm 1.0$ ,  $80.1 \pm 3.9$ ,  $274.5 \pm 5.7$ ,  $120.0 \pm 5.3$ , and  $151.7 \pm 3.5$  μg/ml, respectively, against *C. acnes* lipase. The use of HO-MeOH would, therefore, have a larger effect on prevention of sebum degradation by *C. acnes*, possibly preventing the formation of the glycerol nutrient source and release of free fatty acids, in turn, preventing *C. acnes* proliferation in the pilosebaceous unit and reducing inflammation caused by irritant free fatty acids.

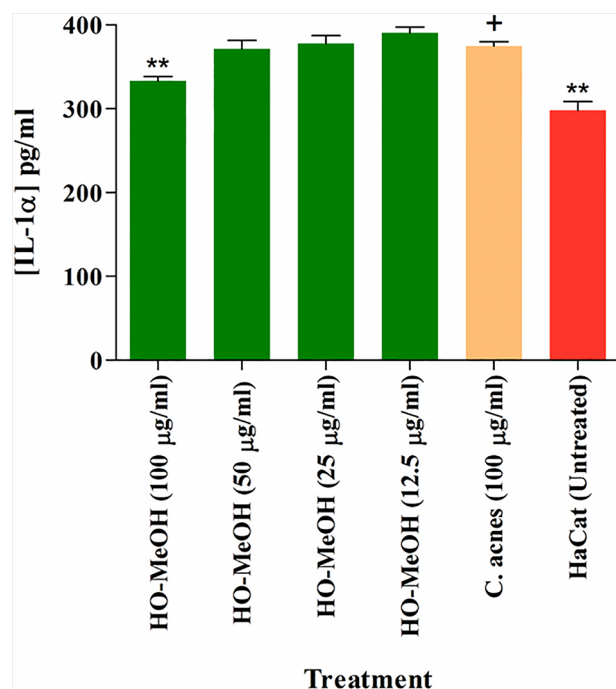


**FIGURE 3 |** Inhibition of interleukin-1α (IL-1α) protein levels in *Cutibacterium acnes*-induced human keratinocytes treated with the *Helichrysum odoratissimum* methanolic extract. \*\* $p < 0.01$ . The "+" indicates the control column to which all the data sets were compared using the Dunnett's multiple comparison test.

## Anti-Inflammatory Activity

### Inhibition of Pro-Inflammatory Cytokines

The effects of LPS and heat-killed *C. acnes* induction were assessed using several inflammatory marker cytokines including IL-1β, IL-6, IL-8, IL-10, IL-12p70, and TNF-α. The induction of HaCaT cells using LPS was used as a control for cytokine production. The effects of HO-MeOH, together with *C. acnes* stimulation, was used to assess the anti-inflammatory



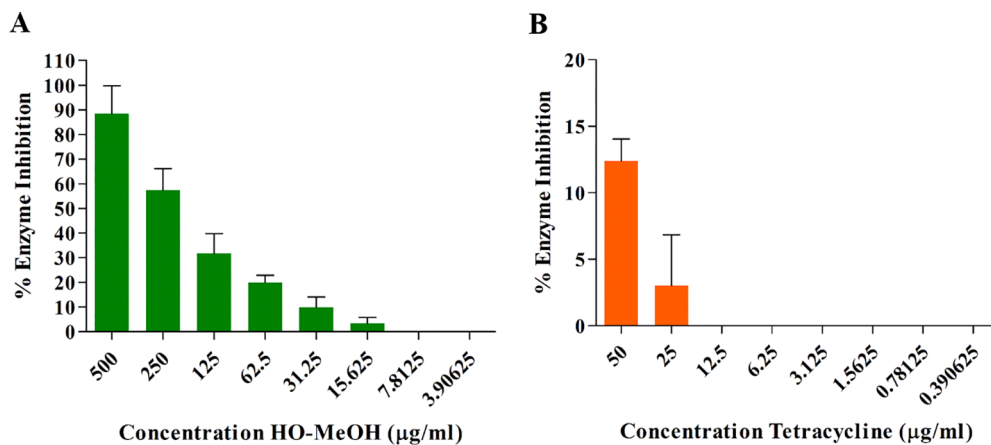


**FIGURE 4 |** Inhibition of *Candida rugosa* lipase activity by the *Helichrysum odoratissimum* methanol extract (A) and tetracycline (B).

activity of HO-MeOH in response to *C. acnes*-induced cytokine production specifically. The protein levels of IL-6 and IL-8 were found to be induced within detectable limits and were reported. The HaCaT cell viability observed for the treatment of cells was greater than 70%, except in keratinocytes treated with tetracycline, where 51.61% viability was observed (Figure 5A). This, therefore, suggests that any observed inhibition of IL-6 or IL-8 was not due to cytotoxicity against HaCaT cells for HO-MeOH (Wang et al., 2014). *C. acnes*-induced HaCaT cells resulted in significant increases of IL-8 when compared to the untreated cell control, which was not true for IL-6, even though levels of IL-6 were increased when compared to the untreated cell control (Figures 5B and S6). The HO-MeOH, tested at the MIC (7.81 μg/ml) exhibited 48.31% reduction in IL-8 protein levels from  $561.58 \pm 14.85$  to  $290.24 \pm 21.02$  pg/ml (Figure 5B). Tetracycline, in both cases had a stimulatory effect on IL-6 and IL-8 levels.

### Inhibition of Cyclooxygenase-II Activity

The COX-II inhibitory activity of HO-MeOH exhibited a dose-response with an  $IC_{50}$  of  $22.87 \pm 6.48$  μg/ml (Figures 6A and S11A). This was compared with the inhibition of Ibuprofen, a known inhibitor of COX-II activity with an  $IC_{50}$  of  $0.75 \pm 0.01$  μM (0.15 μg/ml) (Figures 6B and S11B). The GC-MS profile of the extract identified linoleic acid as one of the major constituents in the extract. This fatty acid has been previously reported to have COX inhibitory activity, with a higher selectivity toward COX-II. The reported  $IC_{50}$  values for linoleic acid were 94 μM (26.17 μg/ml) and 170 μM (43.33 μg/ml) for COX-II and COX-I, respectively (Ringbom et al., 2001). The HO-MeOH showed similar results to the ethanol extract of *Helichrysum kraussii*, which showed  $57.15 \pm 8.00\%$  inhibition at a concentration of 10 μg/ml. The positive control Ibuprofen, at the same concentration, inhibited  $90.17 \pm 3.12\%$  of COX-II activity (Twilley et al., 2017b). Ibuprofen in the current study,

exhibited similar COX-II inhibition, with 90.09% observed at 2.06 μg/ml (10 μM). The activity of arzanol, a prenylated phloroglucinol  $\alpha$ -pyrone compound from *H. italicum* has been identified as an inhibitor of PGE<sub>2</sub> production. The presence of these types of compounds has been identified in *H. odoratissimum* and could, therefore, be responsible for the observed COX-II activity (Lourens et al., 2008; Guinoiseau et al., 2013). The presence of benzothiazole was identified as one of the major constituents in the extract using GC-MS. Heterocyclic compounds, including those with the benzothiazole skeleton, have a vast range of pharmaceutical and biological activities, including anti-inflammatory activity. The presence of this compound and its derivatives could potentially contribute to the COX-II inhibitory activity (Yatam et al., 2018).

### Nitric Oxide Scavenging Activity and Intracellular Nitric Oxide Inhibition

The HO-MeOH extract exhibited NO with an  $IC_{50}$  of  $214.90 \pm 13.27$  μg/ml. The positive control vitamin C had an  $IC_{50}$  of  $35.24 \pm 7.85$  μg/ml (Table 3). The 2,2-diphenyl-1-picrylhydrazyl (DPPH) scavenging activity of the methanolic extract of *H. odoratissimum* (incorrectly identified as *Helichrysum dasyanthum* by Lourens et al., 2004) exhibited potent antioxidant activity with an  $IC_{50}$  of 12.33 μg/ml (Lourens et al., 2008), indicating its ability to scavenge free radicals. Several *Helichrysum* species have been investigated for their ability to scavenge free radicals using the DPPH model (Lourens et al., 2004; Albayrak et al., 2010). The nitric oxide scavenging activity of other *Helichrysum* species have also been tested. The aqueous leaf extract of *Helichrysum pedunculatum* exhibited 68% inhibition of NO radicals at 800 μg/ml. The aqueous extract of *Helichrysum longifolium* showed 31.71, 42.00, 62.28, and 64.96% inhibition at 200, 400, 600, and 800 μg/ml, respectively (Aiyegoro and Okoh, 2010). This data

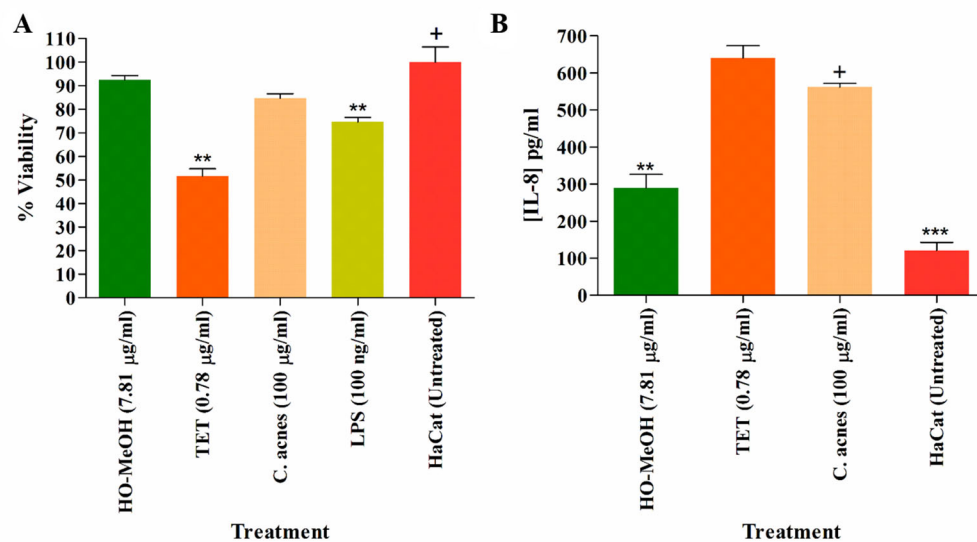


**FIGURE 5 |** The cell viability of human keratinocytes (HaCaT) **(A)**, inhibition of pro-inflammatory cytokine IL-8 **(B)**. \*\* $p < 0.01$ ; \*\*\* $p < 0.001$ . The "+" indicates the control column to which all the data sets were compared using the Dunnett's multiple comparison test.

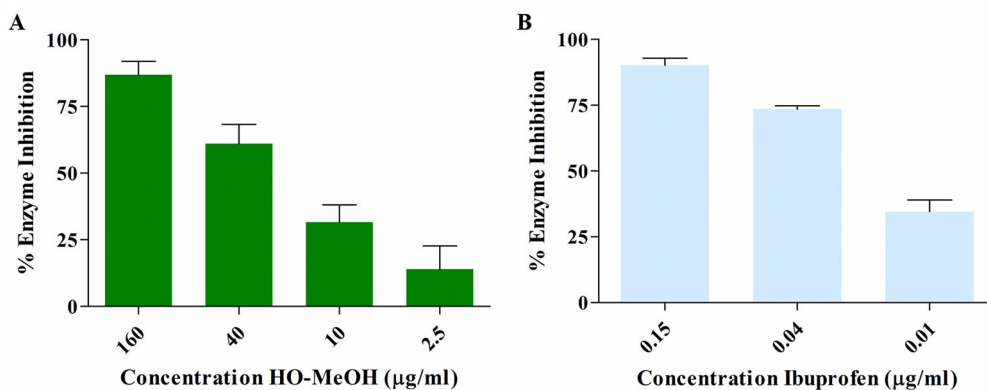
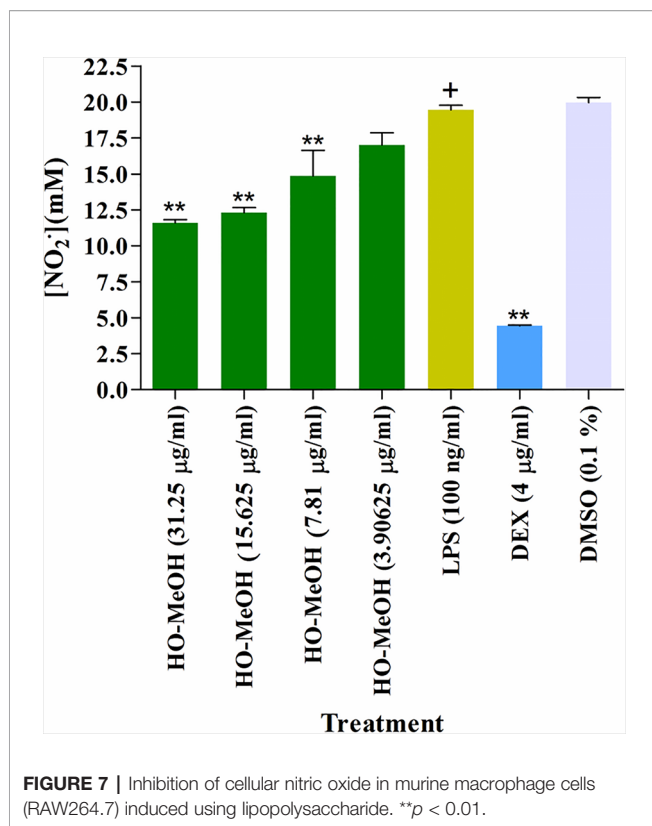


**FIGURE 6 |** Dose-dependent enzyme inhibition of cyclooxygenase II enzyme activity by the *Helichrysum odoratissimum* methanol extract **(A)** and ibuprofen **(B)**.

suggests that HO-MeOH is a more potent inhibitor of NO when compared to some other species of *Helichrysum* and was further investigated for its effects against intracellular NO production (Aiyegoro and Okoh, 2009).

The inhibition of cellular NO was tested using murine macrophages (RAW264.7) where induction of NO was achieved with treatment of the cells with LPS. The induction of NO by LPS is said to occur *via* activation of inducible iNOS and is quantitatively inducible in several cell types, including macrophages. The NO produced through the iNOS pathway are associated with many physiological processes of disease and

inflammation and is, therefore, an important target, considering that acne is a chronic inflammatory disorder (Lin et al., 2003). The inhibition of NO was determined through the concentration of nitrite ( $\text{NO}_2^-$ ). Inhibition of NO was compared with LPS-induced RAW264.7 cells. The HO-MeOH extract showed significant inhibition of NO at 7.81, 15.625, and 31.25  $\mu\text{g/ml}$ . The concentration of nitrite was reduced from 19.46  $\mu\text{M}$  in the LPS-stimulated cells to 14.86, 12.31, and 11.60  $\mu\text{M}$ , respectively. The positive control, dexamethasone showed significant inhibition of NO at 4  $\mu\text{g/ml}$  (10  $\mu\text{M}$ ). The negative control 0.1% DMSO showed no inhibitory effect on NO production, indicating that

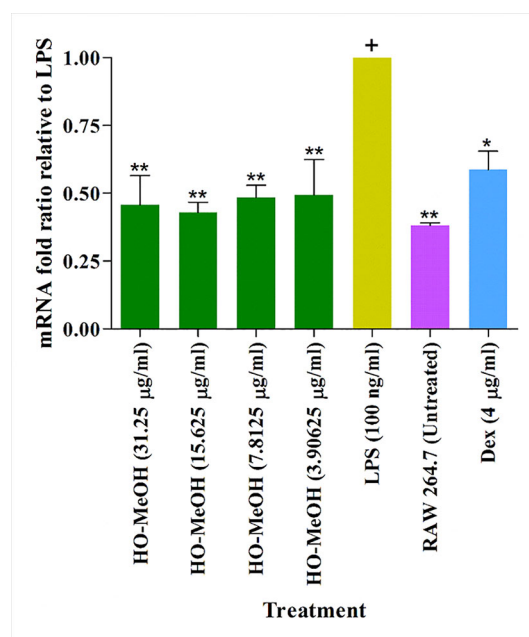


the observed inhibition was likely due to pre-incubation with HO-MeOH. The intracellular NO scavenging activity showed a reduction of 40.39 and 36.74% reduction in NO production levels at 31.25 and 15.625 µg/ml, respectively (Figure 7). The NO scavenging activity of HO-MeOH was similar for both these concentrations and correlated well with the intracellular inhibitory activity. Previous reports on the radical scavenging activity include potent DPPH scavenging activity of the ethanol extract with an IC<sub>50</sub> of 5.13 µg/ml (Twilley et al., 2017a). A study by Mao et al. (2017) highlighted the anti-inflammatory activity of flavonoids from *Helichrysum arenarium* in the prevention of inflammation-induced atherosclerosis. Flavonoids isolated from the methanolic flower extract of *H. odoratissimum* include 3,5-dihydroxy-6,7,8-trimethoxyflavone, 3-*O*-methylquercetin, and 4,2',4'-trihydroxy-6'-methoxychalcone (helichrysetin) (Van Puyvelde et al., 1989; Lourens et al., 2008). These constituents could potentially explain the anti-inflammatory activity of the HO-MeOH extract used in this study. The results warrant the future investigation of flavonoid-enriched fractions of *H. odoratissimum* for anti-inflammatory activity. The NO scavenging activity and intracellular NO inhibitory activity justified further investigation into possible mechanisms of this anti-inflammatory activity.

### Inhibition of Inflammatory Gene Expression

The use of murine macrophages (RAW264.7) in the investigation of anti-inflammatory activity of natural compounds is common practice. These cells behave much like

human macrophages, with the induction of LPS resulting in the activation of signal pathways and gene expression. The overexpression of both cyclooxygenase-II and inducible iNOS resulting in the formation of prostaglandin-E<sub>2</sub> (PGE<sub>2</sub>) and NO are among the most prominent effects of LPS induction (Ma et al., 2018). The gene expression of several inflammatory genes related to acne, including COX-II and iNOS, were investigated in LPS-induced RAW264.7 cells treated with HO-MeOH. The β-actin gene was used as the reference (housekeeping) gene. The gene expression levels of treated cells were normalized relative to the gene expression of β-actin. Cells induced with LPS only were set to 1 as the maximum level of overexpression. Therefore, values <1 indicated inhibition of gene expression and values >1 indicated gene overexpression relative to LPS stimulation. The melting curves and amplification plot indicated that there was no formation of primer-dimers with the PCR reaction. In an attempt to correlate gene expression data to the anti-inflammatory bioassays, only the COX-II and iNOS gene expression were reported. The HO-MeOH exhibited inhibition of COX-II expression. However, there was no significant difference between the COX-II expression levels in the HO-MeOH treatments when compared to those observed in LPS-induced expression. The positive control, dexamethasone exhibited a significant reduction in COX-II expression with a 2.63 reduction in fold change from 1 to 0.38 (Figure S7). On the other hand, the inhibition of NO observed in LPS-induced RAW264.7 cells treated with HO-MeOH is most likely due to



inhibitory gene expression of iNOS gene expression. The HO-MeOH extract showed significant reduction of iNOS expression at all concentrations with relatively consistent inhibition over the tested range (**Figure 8**). Chu et al. (2009) observed that the extracts of three Chinese herbs *Drynaria baronii*, *Angelica sinensis*, and *Cornus officinalis* had a greater inhibitory effect on the gene expression of iNOS as compared to that of COX-II. They also demonstrated that PGE<sub>2</sub> was inhibited to a lesser degree than that of NO, which correlated well with the results observed in the COX-II enzyme inhibition assay and the cellular NO inhibition assay. The HO-MeOH inhibited COX-II activity and consequently, the PGE<sub>2</sub> levels by 50% at a concentration of 22.87 µg/ml while 31.25 µg/ml caused a 59% reduction in NO. The results indicated that the HO-MeOH extract inhibited the functional COX-II enzyme, as opposed to the gene expression of this acute inflammatory biomarker. The pathogenesis of *C. acnes* should be a core target when developing acne therapies from natural sources, as the inflammatory cascade can often result in scarring of the skin.

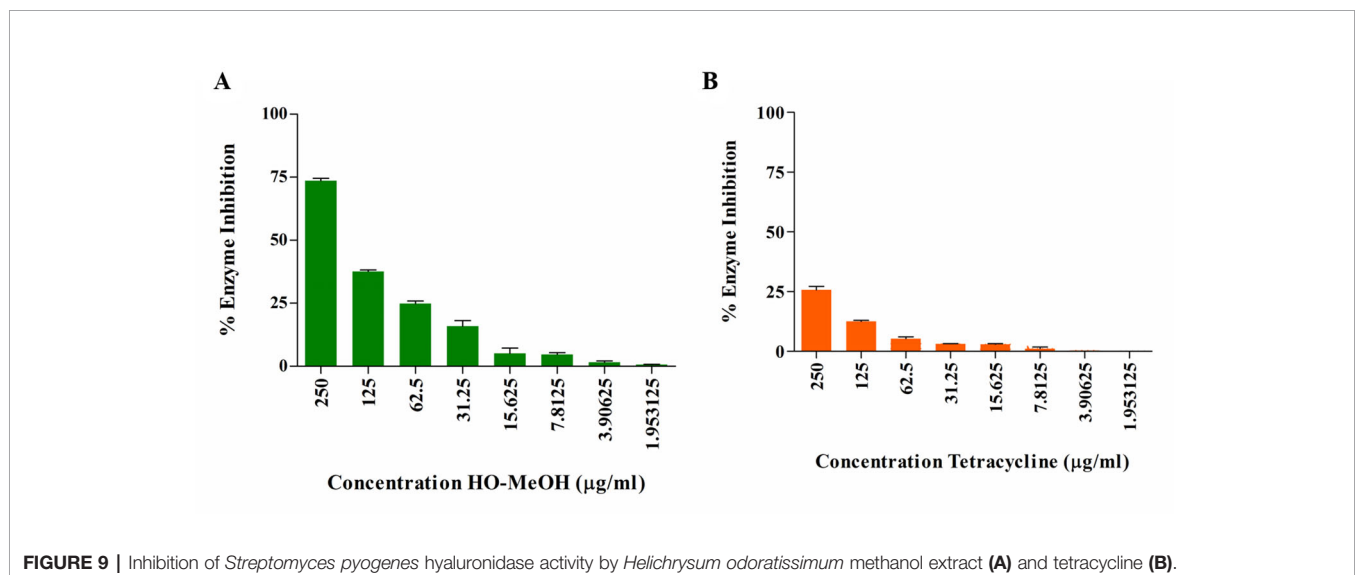
### Hyaluronidase Inhibition

Dose-dependent inhibition of HYAL activity was observed for HO-MeOH with an IC<sub>50</sub> of 145.45 ± 6.22 µg/ml (**Figures 9A** and **S12**). Tetracycline showed a dose-response inhibition of HYAL, with reduced inhibitory activity being observed with an IC<sub>50</sub> > 250 µg/ml (**Figure 9B**). There are not many reports on the inhibition of bacterial hyaluronidases, as many studies report on the inhibitors of bovine testes HYAL. Triterpenoid compounds glycyrrhizin and glycyrrhetic acid isolated from the root of *Glycyrrhiza glabra* have shown inhibition of *Streptococcus agalactiae* with IC<sub>50</sub> of 0.44 mM (362 µg/ml) and 0.06 mM (28 µg/ml), respectively. Inhibition was also observed against *Streptococcus equisimilis* HYAL activity with IC<sub>50</sub> of 1.02 mM (839 µg/ml) and 0.26 mM (122 µg/ml). Flavonoids rutin and silybin were also identified as inhibitors of *S. agalactiae* HYAL activity. The inhibitory activity of HO-MeOH, therefore, compares well with previously published data on bacterial

hyaluronidase inhibitors (Hertel et al., 2006). Considering that flavonoids and diterpenes have previously been isolated from *H. odoratissimum* it is not surprising that HO-MeOH showed inhibition of this enzyme. The use of *Streptococcus pyogenes* HYAL as a model for predicting the inhibitory effects of HO-MeOH on *C. acnes* HYAL is advantageous, as these HYALs share homology when comparing amino acid sequences. The HYAL type identified in several *C. acnes* is strain specific. Phylotypes of *C. acnes* belonging to type I<sub>A</sub> result in the production of larger fragments of HA whereas, those belonging to the type I<sub>B</sub> and II produce smaller fragments of more consistent sizes. Considering that HA fragments produced *via* HYAL activity are used as a nutritive source for *C. acnes* and can reduce the immune response during bacterial colonization, inhibitors of this enzyme should be considered advantageous in acne therapy (Nazipi et al., 2017). There are currently no identified acne therapies focused on hyaluronidase inhibition, which warrants further investigation into the isolation of constituents from HO-MeOH as hyaluronidase inhibitors.

### CONCLUSION

In conclusion, this study provides scientific validation for the traditional use of *H. odoratissimum* as a possible treatment for acne, based on direct antimicrobial effects as well as the inhibition of key targets in the pathogenic processes associated with the opportunistic pathogen, *C. acnes* in the progression of this skin disorder. The study identified the potent antimicrobial activity of the methanolic extract of *H. odoratissimum* against *C. acnes* and the anti-biofilm activity of this extract particularly affecting the initial step of bacterial adhesion. The study also identified the anti-inflammatory potential of *H. odoratissimum* inhibiting inflammatory cytokine IL-8, COX-II, and NO. The mechanism of action for NO inhibition was through the inhibition of iNOS gene expression. The hyaluronidase





inhibitory activity of *H. odoratissimum* indicated a potential source of bacterial hyaluronidase inhibitors, a key enzyme involved in bacterial spread and tissue injury, not only in *Cutibacterium* species but also other *Streptococcus* species. *C. acnes* has also been identified as a pathogen involved in joint infections in patients implanted with prosthetic medical devices. The anti-adhesion activity of the extract can perhaps be employed as a coating for medical devices prior to insertion for the prevention of joint inflammation.

## DATA AVAILABILITY STATEMENT

The datasets generated for this study are available on request to the corresponding author.

## AUTHOR CONTRIBUTIONS

MNDC conducted the study and compiled the manuscript. SK hosted MC in his laboratory and provided guidance with the RAW264.7 cell culture, MTT antiproliferative activity, intracellular NO, and gene expression work. LL provided guidance for the COX-II enzyme inhibition study. NL acted as the supervisor for the study and also provided a critical assessment and editorial guidance on the manuscript.

## REFERENCES

- Achermann, Y., Goldstein, E. J., Coenye, T., and Shirtliff, M. E. (2014). *Propionibacterium acnes*: from commensal to opportunistic biofilm-associated implant pathogen. *Clin. Microbiol. Rev.* 27 (3), 419–440. doi: 10.1128/CMR.00092-13
- Aiyegoro, O. A., and Okoh, A. I. (2009). Phytochemical screening and polyphenolic antioxidant activity of aqueous crude leaf extract of *Helichrysum pedunculatum*. *Int. J. Mol. Sci.* 10 (11), 4990–5001.
- Aiyegoro, O. A., and Okoh, A. I. (2010). Preliminary phytochemical screening and *in vitro* antioxidant activities of the aqueous extract of *Helichrysum longifolium* DC. *BMC Complement. Altern. Med.* 10 (1), 21–28.
- Akaber, M., Sahebkar, A., Azizi, N., and Emami, S. A. (2019). Everlasting flowers: phytochemistry and pharmacology of the genus *Helichrysum*. *Ind. Crops Prod.* 138, 1–21. doi: 10.1016/j.indcrop.2019.111471
- Albayrak, S., Aksoy, A., Sagdic, O., and Hamzaoglu, E. (2010). Compositions, antioxidant and antimicrobial activities of *Helichrysum* (Asteraceae) species collected from Turkey. *Food Chem.* 119 (1), 114–122. doi: 10.1016/j.foodchem.2009.06.003
- Asekun, O. T., Grierson, D. S., and Afolayan, A. J. (2007). Characterization of essential oils from *Helichrysum odoratissimum* using different drying methods. *J. Appl. Sci.* 7 (7), 1005–1008. doi: 10.3923/jas.2007.1005.1008
- Barroso, M. R., Barros, L., Dueñas, M., Carvalho, A. M., Santos-Buelga, C., Fernandes, I. P., et al. (2014). Exploring the antioxidant potential of *Helichrysum stoechas* (L.) Moench phenolic compounds for cosmetic applications: chemical characterization, microencapsulation and incorporation into a moisturizer. *Ind. Crops Prod.* 53 (2014), 330–336. doi: 10.1016/j.indcrop.2014.01.004
- Batubara, I., Mitsunaga, T., and Ohashi, H. (2009). Screening antiacne potency of Indonesian medicinal plants: antibacterial, lipase inhibition, and antioxidant activities. *J. Wood Sci.* 55 (3), 230–235.
- Batubara, I., Kuspradini, H., Muddathir, A. M., and Mitsunaga, T. (2014). *Intsia palembanica* wood extracts and its isolated compounds as *Propionibacterium acnes* lipase inhibitor. *J. Wood Sci.* 60 (2), 169–174. doi: 10.1007/s10086-013-1388-5

## FUNDING

The authors would like to thank the South African Research Chairs Initiative and the Indigenous Knowledge Systems Framework through the National Research Foundation (NRF) (Grant ID: 98334 & 105169) for funding the research.

## ACKNOWLEDGMENTS

The authors would like to acknowledge Ms. Magda Nel (H. G. W. J. Schweickerdt Herbarium) who helped with the plant identification, Dr. Lester Davids (University of Cape Town) for provision of the HaCaT cells, and Mrs. Sierra Smirnov for assisting Mr. MNDC with the work performed at the Plants for Human Health Institute. We acknowledge the LC-MS Synapt Facility (Department of Chemistry, University of Pretoria) for chromatography and/or mass spectrometry services run by Ms Madelien Wooding.

## SUPPLEMENTARY MATERIAL

The Supplementary Material for this article can be found online at: <https://www.frontiersin.org/articles/10.3389/fphar.2019.01559/full#supplementary-material>

- Boora, F., Chirisa, E., and Mukanganyama, S. (2014). Evaluation of nitrite radical scavenging properties of selected Zimbabwean plant extracts and their phytoconstituents. *J. Food Process.* 2014 (2014), 1–7. doi: 10.1155/2014/918018
- Bougatsos, C., Meyer, J. J. M., Magiatis, P., Vagias, C., and Chinou, I. B. (2003). Composition and antimicrobial activity of the essential oils of *Helichrysum kraussii* Sch. Bip. and *H. rugulosum* Less. from South Africa. *Flavour Fragr. J.* 18 (1), 48–51. doi: 10.1002/ffj.1152
- Burkhart, C. G., and Burkhart, C. N. (2007). Expanding the microcomedone theory and acne therapeutics: *propionibacterium acnes* biofilm produces biological glue that holds corneocytes together to form plug. *Am. J. Dermatol.* 57, 722–724. doi: 10.1016/j.jaad.2007.05.013
- Carvalho, Jr., A. R., Diniz, R. M., Suarez, M. A., Figueiredo, C. S., Zagnignan, A., Grisotto, M. A., et al. (2018). Use of some asteraceae plants for the treatment of wounds: from ethnopharmacological studies to scientific evidences. *Front. Pharmacol.* 9 (784), 1–11. doi: 10.3389/fphar.2018.00784
- Chassagne, F., Huang, X., Lyles, J. T., and Quave, C. L. (2019). Validation of a 16th Century Traditional Chinese Medicine use of *Ginkgo biloba* as a topical antimicrobial. *Front. Microbiol.* 10 (775), 1–13. doi: 10.3389/fmicb.2019.00775
- Choi, S. J., Hwang, J. M., and Kim, S. I. (2003). A colorimetric microplate assay method for high throughput analysis of lipase activity. *J. Biochem. Mol. Biol.* 36 (4), 417–420. doi: 10.5483/bmbrep.2003.36.4.417
- Chu, Q., Hashimoto, K. E. N., Satoh, K., Wang, Q., and Sakagami, H. (2009). Effect of three herbal extracts on NO and PGE2 production by activated mouse macrophage-like cells. *In Vivo* 23 (4), 537–544.
- Chukwudi, C. U. (2016). Ribosomal RNA binding sites and the molecular mechanism of action of the tetracyclines. *Antimicrob. Agents Chemother.* 60 (8), 4433–, 4441. doi: 10.1128/AAC.00594-16
- Coenye, T., Peeters, E., and Nelis, H. J. (2007). Biofilm formation by *Propionibacterium acnes* is associated with increased resistance to antimicrobial agents and increased production of putative virulence factors. *Res. In Microbiol.* 158 (4), 386–392. doi: 10.1016/j.resmic.2007.02.001
- Coenye, T., Honraet, K., Rossel, B., and Nelis, H. J. (2008). Biofilms in skin infections: *Propionibacterium acnes* and acne vulgaris. *Infect. Dis. Drug Targets.* 8 (3), 156–159. doi: 10.2174/1871526510808030156

- Coenye, T., Brackman, G., Rigole, P., De Witte, E., Honraet, K., Rossel, B., et al. (2012). Eradication of *Propionibacterium acnes* biofilms by plant extracts and putative identification of icariin, resveratrol and salidroside as active compounds. *Phytomedicine* 19 (5), 409–412. doi: 10.1016/j.phymed.2011.10.005
- Cui, H., Li, W., Li, C., and Lin, L. (2016). Synergistic effect between *Helichrysum italicum* essential oil and cold nitrogen plasma against *Staphylococcus aureus* biofilms on different food-contact surfaces. *Int. J. Food Sci. Technol.* 51 (11), 2493–2501. doi: 10.1111/ijfs.13231
- D'Abrosca, B., Buommino, E., D'Angelo, G., Coretti, L., Scognamiglio, M., Severino, V., et al. (2013). Spectroscopic identification and anti-biofilm properties of polar metabolites from the medicinal plant *Helichrysum italicum* against *Pseudomonas aeruginosa*. *Bioorg. Med. Chem.* 21 (22), 7038–7046. doi: 10.1016/j.bmc.2013.09.019
- D'Abrosca, B., Buommino, E., Caputo, P., Scognamiglio, M., Chambery, A., Donnarumma, G., et al. (2016). Phytochemical study of *Helichrysum italicum* (Roth) G. Don: spectroscopic elucidation of unusual aminophlorogucinols and antimicrobial assessment of secondary metabolites from medium-polar extract. *Phytochemistry* 132, 86–94. doi: 10.1016/j.phytochem.2016.09.012
- De Canha, M. N., Kishore, N., Kumar, V., Meyer, D., Nehar, S., Singh, B., et al. (2018). The potential of *Clausena anisata* (Willd.) Hook. f. ex Benth against *Propionibacterium acnes*. *S. Afr. J. Bot.* 119 (2018), 410–419. doi: 10.1016/j.sajb.2018.09.019
- De Medeiros-Ribeiro, C. A., Costa, A., Francesconi, F., Follador, I., and RocioNeves, J. (2015). Etiopathogeny of acne vulgaris: a practical review for day-todaydermatologic practice. *Surg. Cosmet. Dermatol.* 7 (3), 20–26. doi: 10.5935/scd1984-8773.2015731682
- De Rapper, S., Van Vuuren, S. F., Kamatou, G. P. P., Viljoen, A. M., and Dagne, E. (2012). The additive and synergistic antimicrobial effects of select frankincense and myrrh oils—a combination from the pharaonic pharmacopoeia. *Lett. In Appl. Microbiol.* 54 (4), 352–358. doi: 10.1111/j.1472-765X.2012.03216.x
- Dessinioti, C., and Katsambas, A. (2017). *Propionibacterium acnes* and antimicrobial resistance in acne. *Clinics In Dermatol.* 35 (2), 163–167. doi: 10.1016/j.clindermatol.2016.10.008
- Downing, D. T., Stewart, M. E., Wertz, P. W., and Strauss, J. S. (1986). Essential fatty acids and acne. *J. Am. Acad. Dermatol.* 14 (2), 221–225. doi: 10.1016/S0190-9622(86)70025-X
- Esposito, D., Chen, A., Grace, M. H., Komarnytsky, S., and Lila, M. A. (2014). Inhibitory effects of wild blueberry anthocyanins and other flavonoids on biomarkers of acute and chronic inflammation *in vitro*. *J. Agric. Food Chem.* 62 (29), 7022–7028. doi: 10.1021/jf4051599
- Falcocchio, S., Ruiz, C., Pastor, F. J., Saso, L., and Diaz, P. (2006). *Propionibacterium acnes* GdhA lipase, an enzyme involved in acne development, can be successfully inhibited by defined natural substances. *J. Mol. Catal. B Enzym.* 40 (3–4), 132–137. doi: 10.1016/j.molcatb.2006.02.011
- Fox, L., Csongradi, C., Aucamp, M., du Plessis, J., and Gerber, M. (2016). Treatment modalities for acne. *Molecules* 21 (8), 1063–1082.
- Grčić, N., Esch, S., Hensel, A., and Dias, A. C. P. (2017). Assessment of *Helichrysum* sp. extracts on *in vitro* keratinocyte proliferation and differentiation: potential use of plants for improved wound healing. *Zeitschrift für Phytotherapie* 38 (1), 7. doi: 10.1055/s-0037-1607159
- Gouveia, S., and Castilho, P. C. (2011). Characterisation of phenolic acid derivatives and flavonoids from different morphological parts of *Helichrysum obconicum* by a RP-HPLC-DAD(–)–ESI-MSn method. *Food Chem.* 129 (2), 333–344. doi: 10.1016/j.foodchem.2011.04.078
- Guinoiseau, E., Lorenzi, V., Luciani, A., Muselli, A., Costa, J., Casanova, J., et al. (2013). Biological properties and resistance reversal effect of *Helichrysum italicum* (Roth) G. Don. *Microb. Pathog. Strategies Combating Them: Science Technol. Educ.* 2, 1073–1080.
- Gundidza, M. G., and Zwaving, J. H. (1993). The chemical composition of the essential leaf oil of *Helichrysum odoratissimum* sweet from Zimbabwe. *J. Essent. Oil Res.* 5 (3), 341–343. doi: 10.1080/10412905.1993.9698235
- Han, R., Blencke, H. M., Cheng, H., and Li, C. (2018). The antimicrobial effect of CENIHC-Br against *Propionibacterium acnes* and its therapeutic and anti-inflammatory effects on acne vulgaris. *Peptides* 99, 36–43. doi: 10.1016/j.peptides.2017.11.001
- Hassing, G. S. (1971). Inhibition of *Corynebacterium acnes* lipase by tetracycline. *J. Invest. Dermatol.* 56 (3), 189–192. doi: 10.1111/1523-1747.ep12260792
- Hertel, W., Peschel, G., Ozegowski, J. H., and Müller, P. J. (2006). Inhibitory effects of triterpenes and flavonoids on the enzymatic activity of hyaluronic acid-splitting enzymes. *Arch. Pharm.* 339 (6), 313–318. doi: 10.1002/ardp.200500216
- Heyman, H. M., Senejoux, F., Seibert, I., Klimkait, T., Maharaj, V. J., and Meyer, J. J. M. (2015). Identification of anti-HIV active dicaffeoylquinic- and tricaffeoylquinic acids in *Helichrysum populifolium* by NMR-based metabolomic guided fractionation. *Fitoterapia* 103, 155–164. doi: 10.1016/j.fitote.2015.03.024
- Hofinger, E. S., Spickenreither, M., Oschmann, J., Bernhardt, G., Rudolph, R., and Buschauer, A. (2007). Recombinant human hyaluronidase Hyal-1: insect cells versus *Escherichia coli* as expression system and identification of low molecular weight inhibitors. *Glycobiology* 17, 444–453. doi: 10.1093/glycob/cwm003
- Hutchings, A., Scott, A. H., Lewis, G., and Cunningham, A. B. (1996). *Zulu Medicinal Plants: An Inventory* (Pietermaritzburg, South Africa: University of Natal Press).
- Javidnia, K., Miri, R., Soltani, M., and Khosravi, A. R. (2009). Essential oil composition of two Iranian endemic *Helichrysum* Miller. species (*H. leucocephalum* Boiss. and *H. artemisioides* Boiss. et Hausskn.). *J. Essent. Oil Res.* 21 (1), 54–56.
- Jeong, W. Y., and Kim, K. (2017). Anti-*Propionibacterium acnes* and the anti-inflammatory effect of *Aloe ferox* Miller components. *J. Herb. Med.* 9, 53–59. doi: 10.1016/j.hermed.2017.03.009
- Kosmadaki, M., and Katsambas, A. (2017). Topical treatments for acne. *Clinics In Dermatol.* 35 (2), 173–178. doi: 10.1016/j.clindermatol.2016.10.010
- Kotra, L. P., Haddad, J., and Mobashery, S. (2000). Aminoglycosides: perspectives on mechanisms of action and resistance and strategies to counter resistance. *Antimicrob. Agents Chemother.* 44 (12), 3249–3256. doi: 10.1128/AAC.44.12.3249-3256.2000
- Kuehnast, T., Cakar, F., Weinhäupl, T., Pilz, A., Selak, S., Schmidt, M. A., et al. (2018). Comparative analyses of biofilm formation among different *Cutibacterium acnes* isolates. *Int. J. Med. Microbiol.* 308 (8), 1027–1035. doi: 10.1016/j.ijmm.2018.09.005
- Kuiate, J. R., Amvam Zollo, P. H., Nguefa, E. H., Bessière, J. M., Lamaty, G., and Menut, C. (1999). Composition of the essential oils from the leaves of *Microglossa pyrifolia* (Lam.) O. Kuntze and *Helichrysum odoratissimum* (L.) Less. growing in Cameroon. *Flavour Fragr. J.* 14 (2), 82–84. doi: 10.1002/(SICI)1099-1026(199903/04)14:2<82::AID-FF780>3.0.CO;2-Z
- Kumar, B., Pathak, R., Mary, P. B., Jha, D., Sardana, K., and Gautam, H. K. (2016). New insights into acne pathogenesis: exploring the role of acne-associated microbial populations. *Dermatol. Sin.* 34 (2), 67–73. doi: 10.1016/j.dsi.2015.12.004
- Lall, N., Henley-Smith, C. J., De Canha, M. N., Oosthuizen, C. B., and Berrington, D. (2013). Viability reagent, Prestoblue, in comparison with other available reagents, utilized in cytotoxicity and antimicrobial assays. *Int. J. Microbiol.* 2013 (2013), 1–5. doi: 10.1155/2013/420601
- Lall, N., van Staden, A. B., Rademan, S., Lambrechts, I., De Canha, M. N., Mahore, J., et al. (2019). Antityrosinase and anti-acne potential of plants traditionally used in the Jongilanga community in Mpumalanga. *South Afr. J. Bot.* 126, 241–249. doi: 10.1016/j.sajb.2019.07.015
- Lawal, I. O., Grierson, D. S., and Afolayan, A. J. (2015). Phytochemical and antioxidant investigations of a *Clausena anisata* Hook., a South African medicinal plant. *Afr. J. Tradit. Complement. Altern. Med.* 12 (1), 28–37.
- Lin, H. Y., Juan, S. H., Shen, S. C., Hsu, F. L., and Chen, Y. C. (2003). Inhibition of lipopolysaccharide-induced nitric oxide production by flavonoids in RAW264.7 macrophages involves heme oxygenase-1. *Biochem. Pharmacol.* 66 (9), 1821–1832. doi: 10.1016/S0006-2952(03)00422-2
- Lourens, A. C. U., Reddy, D., Başer, K. H. C., Viljoen, A. M., and Van Vuuren, S. F. (2004). *In vitro* biological activity and essential oil composition of four indigenous South African *Helichrysum* species. *J. Ethnopharmacol.* 95 (2–3), 253–258. doi: 10.1016/j.jep.2004.07.027
- Lourens, A. C. U., Viljoen, A. M., and Van Heerden, F. R. (2008). South African *Helichrysum* species: a review of the traditional uses, biological activity and phytochemistry. *J. Ethnopharmacol.* 119 (3), 630–652. doi: 10.1016/j.jep.2008.06.011

- Lourens, A. C. U., Van Vuuren, S. F., Viljoen, A. M., Davids, H., and Van Heerden, F. R. (2011). Antimicrobial activity and *in vitro* cytotoxicity of selected South African *Helichrysum* species. *South Afr. J. Bot.* 77 (1), 229–235. doi: 10.1016/j.sajb.2010.05.006
- Ma, Y., He, Y., Yin, T., Chen, H., Gao, S., and Hu, M. (2018). Metabolism of phenolic compounds in LPS-stimulated RAW264.7 cells can impact their anti-inflammatory efficacy: indication of Hesperetin. *J. Agric. Food Chem.* 66, 6042–6052. doi: 10.1021/acs.jafc.7b04464
- Mabona, U., and Van Vuuren, S. F. (2013). Southern African medicinal plants used to treat skin diseases. *South Afr. J. Bot.* 87, 175–193. doi: 10.1016/j.sajb.2013.04.002
- Makrantonaki, E., Ganceviciene, R., and Zouboulis, C. (2011). An update on the role of the sebaceous gland in the pathogenesis of acne. *Dermato-Endocrinology* 3 (1), 41–49. doi: 10.4161/derm.3.1.13900
- Maksimovic, S., Tadic, V., Skala, D., and Zizovic, I. (2017). Separation of phytochemicals from *Helichrysum italicum*: an analysis of different isolation techniques and biological activity of prepared extracts. *Phytochemistry* 138, 9–28. doi: 10.1016/j.phytochem.2017.01.001
- Mao, Z., Gan, C., Zhu, J., Ma, N., Wu, L., Wang, L., et al. (2017). Anti-atherosclerotic activities of flavonoids from the flowers of *Helichrysum arenarium* L. MOENCH through the pathway of anti-inflammation. *Bioorg. Med. Chem. Lett.* 27 (12), 2812–2817. doi: 10.1016/j.bmcl.2017.04.076
- Mari, A., Napolitano, A., Masullo, M., Pizza, C., and Piacente, S. (2014). Identification and quantitative determination of the polar constituents in *Helichrysum italicum* flowers and derived food supplements. *J. Pharm. Biomed. Anal.* 96, 249–255. doi: 10.1016/j.jpba.2014.04.005
- Mathekg, A. D. M., and Meyer, J. J. M. (1998). Antibacterial activity of South African *Helichrysum* species. *South Afr. J. Bot.* 64 (5), 293–295. doi: 10.1016/S0254-6299(15)30903-0
- Mattii, M., Lovász, M., Garzorz, N., Atenhan, A., Quaranta, M., Lauffer, F., et al. (2018). Sebocytes contribute to skin inflammation by promoting the differentiation of T helper 17 cells. *British J. Dermatol.* 178 (3), 722–730. doi: 10.1111/bjd.15879
- Nagy, I., Pivarcsi, A., Koreck, A., Széll, M., Urbán, E., and Kemény, L. (2005). Distinct strains of *Propionibacterium acnes* induce selective human  $\beta$ -defensin-2 and interleukin-8 expression in human keratinocytes through toll-like receptors. *J. Invest. Dermatol.* 124 (5), 931–938. doi: 10.1111/j.0022-202X.2005.23705.x
- Nazipi, S., Stødikilde, K., Scavenius, C., and Brüggemann, H. (2017). The skin bacterium *Propionibacterium acnes* employs two variants of hyaluronate lyase with distinct properties. *Microorganisms* 5 (3), 57–72. doi: 10.3390/microorganisms5030057
- Nostro, A., Cannatelli, M. A., Crisafi, G., Musolino, A. D., Procopio, F., and Alonzo, V. (2004). Modifications of hydrophobicity, *in vitro* adherence and cellular aggregation of *Streptococcus mutans* by *Helichrysum italicum* extract. *Lett. In Appl. Microbiol.* 38 (5), 423–427. doi: 10.1111/j.1472-765X.2004.01509.x
- Nusbaum, A. G., Kirsner, R. S., and Charles, C. A. (2012). Biofilms in dermatology. *Skin Ther. Lett.* 17 (7), 1–5.
- Okamoto, K., Tamura, R., Tabara, K., Kitano, T., Kanayama, S., Kido, H., et al. (2016a). Keratolytic and comedolytic effects of topically applied benzoyl peroxide in hairless mice and rhino mice. *J. Dermatol. Sci.* 84 (1), 166. doi: 10.1016/j.jdermsci.2016.08.492
- Okamoto, K., Ikeda, F., Kanayama, S., Nakajima, A., Matsumoto, T., Ishii, R., et al. (2016b). *In vitro* antimicrobial activity of benzoyl peroxide against *Propionibacterium acnes* assessed by a novel susceptibility testing method. *J. Infect. Chemother.* 22 (6), 426–429. doi: 10.1016/j.jiac.2015.12.010
- Oliveira, R. A., Lima, E. O., Vieira, W. L., Freire, K. R. L., Trajano, V. N., Lima, I. O., et al. (2006). Study of the interference of essential oils on the activity of some antibiotic used clinically. *Rev. Bras. Farmacogn.* 16 (1), 77–82. doi: 10.1590/S0102-695X2006000100014
- Ottaviani, M., Camera, E., and Picardo, M. (2010). Lipid mediators in acne. *Mediators Inflamm.* 2010, 1–6. doi: 10.1155/2010/858176
- Peeters, E., Nelis, H. J., and Coenye, T. (2008). Comparison of multiple methods for quantification of microbial biofilms grown in microtiter plates. *J. Microbiol. Methods* 72 (2), 157–165. doi: 10.1016/j.mimet.2007.11.010
- Pereira, C. G., Barreira, L., Bijttebier, S., Pieters, L., Neves, V., Rodrigues, M. J., et al. (2017). Chemical profiling of infusions and decoctions of *Helichrysum italicum* subsp. *picardii* by UHPLC-PDA-MS and *in vitro* biological activities comparatively with green tea (*Camellia sinensis*) and rooibos tisane (*Aspalathus linearis*). *J. Pharm. Biomed. Anal.* 145, 593–603. doi: 10.1016/j.jpba.2017.07.007
- Portugal, M., Barak, V., Ginsburg, I., and Kohen, R. (2007). Interplay among oxidants, antioxidants and cytokines in skin disorders: present status and future considerations. *Biomed. Pharmacother.* 61 (7), 412–422. doi: 10.1016/j.biopha.2007.05.010
- Puhvel, S. M., and Reisner, R. M. (1972). Effect of antibiotics on the lipases of *Corynebacterium acnes in vitro*. *Arch. Dermatol.* 106 (1), 45–49. doi: 10.1001/archderm.1972.01620100033009
- Ramage, G., Tunney, M. M., Patrick, S., Gorman, S. P., and Nixon, J. R. (2003). Formation of *Propionibacterium acnes* biofilms on orthopaedic biomaterials and their susceptibility to antimicrobials. *Biomaterials* 24 (19), 3221–3227. doi: 10.1016/S0142-9612(03)00173-X
- Reininger, E. A., and Bauer, R. (2006). Prostaglandin-H-synthase (PGHS)-1 and-2 microtiter assays for the testing of herbal drugs and *in vitro* inhibition of PGHS-isoenzymes by polyunsaturated fatty acids from *Platycodi radix*. *Phytomedicine* 13 (3), 164–169. doi: 10.1016/j.phymed.2005.03.006
- Ringbom, T., Huss, U., Stenholm, Å., Flock, S., Skattebøl, L., Perera, P., et al. (2001). Cox-2 inhibitory effects of naturally occurring and modified fatty acids. *J. Natural Prod.* 64 (6), 745–749. doi: 10.1021/np000620d
- Rosenberg, M. (2017). Adhesion to hydrocarbons and microbial hydrophobicity - do the MATH. *FEMS Microbiol. Lett.* 364 (10), 1–3. doi: 10.1093/femsle/fnx069
- Roy, R., Tiwari, M., Donelli, G., and Tiwari, V. (2018). Strategies for combating bacterial biofilms: a focus on anti-biofilm agents and their mechanisms of action. *Virulence* 9 (1), 522–554. doi: 10.1080/21505594.2017.1313372
- Saric, S., Notay, M., and Sivamani, R. (2016). Green tea and other tea polyphenols: effects on sebum production and acne vulgaris. *Antioxidants* 6 (1), 2–17. doi: 10.3390/antiox6010002
- Savoia, D. (2012). Plant-derived antimicrobial compounds: alternatives to antibiotics. *Future Microbiol.* 7 (8), 979–990. doi: 10.2217/fmb.12.68
- Sibanda, T., and Okoh, A. I. (2007). The challenges of overcoming antibiotic resistance: plant extracts as potential sources of antimicrobial and resistance modifying agents. *Afr. J. Biotechnol.* 6 (25), 2886–2896.
- Silva, L., Rodrigues, A. M., Ciriani, M., Falé, P. L. V., Teixeira, V., Madeira, P., et al. (2017). Antiacetylcholinesterase activity and docking studies with chlorogenic acid, cynarin and arzanol from *Helichrysum stoechas* (Lamiaceae). *Med. Chem. Res.* 26 (11), 2942–2950. doi: 10.1007/s00044-017-1994-7
- Sivasankar, C., Maruthupandiyar, S., Balamurugan, K., James, P. B., Krishnan, V., and Pandian, S. K. (2016). A combination of ellagic acid and tetracycline inhibits biofilm formation and the associated virulence of *Propionibacterium acnes in vitro* and *in vivo*. *Biofouling* 32 (4), 397–410. doi: 10.1080/08927014.2016.1148141
- Swelankomo, N. (2004). *Helichrysum odoratissimum* (L.) Sweet [Online]. Available at: <http://www.plantzafrica.com/planthij/helichrysodor.htm> [Accessed 13/06/2018].
- Tepe, B., Sokmen, M., Akpulat, H. A., and Sokmen, A. (2005). *In vitro* antioxidant activities of the methanol extracts of four *Helichrysum* species from Turkey. *Food Chem.* 90 (4), 685–689.
- Twilley, D., Kishore, N., Meyer, D., Moodley, I., Kumar, V., and Lall, N. (2017a). The effect of *Helichrysum odoratissimum* (L.) sweet on cancer cell proliferation and cytokine production. *Int. J. Pharmacogn. Phytochem. Res.* 9 (5), 621–631. doi: 10.25258/phyto.v9i5.8138
- Twilley, D., Langhansova, L., Palaniswamy, D., and Lall, N. (2017b). Evaluation of traditionally used medicinal plants for anticancer, antioxidant, anti-inflammatory and anti-viral (HPV-1) activity. *South Afr. J. Bot.* 112, 494–500.
- Van Puyvelde, L., De Kimpe, N., Costa, J., Munyjabo, V., Nyirankuliza, S., Hakizamungu, E., et al. (1989). Isolation of flavonoids and a chalcone from *Helichrysum odoratissimum* and synthesis of helichrysetin. *J. Natural Prod.* 52 (3), 629–633. doi: 10.1021/np50063a025
- Van Vuuren, S. F., Suliman, S., and Viljoen, A. M. (2009). The antimicrobial activity of four commercial essential oils in combination with conventional antimicrobials. *Lett. Appl. Microbiol.* 48 (4), 440–446. doi: 10.1111/j.1472-765X.2008.02548.x
- Walsh, T. R., Efthimiou, J., and Dréno, B. (2016). Systematic review of antibiotic resistance in acne: an increasing topical and oral threat. *Lancet Infect. Dis.* 16 (3), 23–33. doi: 10.1016/S1473-3099(15)00527-

- Walters, C. E., Ingham, E., Eady, E. A., Cove, J. H., Kearney, J. N., and Cunliffe, W. J. (1995). In vitro modulation of keratinocyte-derived interleukin-1 alpha (IL-1 alpha) and peripheral blood mononuclear cell-derived IL-1 beta release in response to cutaneous commensal microorganisms. *Infect. Immun.* 63 (4), 1223–1228.
- Wang, N., Lv, J., Zhang, W., and Lu, H. (2014). Crucial role of TNF- $\alpha$  in UVB-induced apoptosis in the immortalized keratinocytes. *J. Dermatol. Clin. Res.* 2 (3), 1020–1027.
- Yani, V. V., Oyediji, O. A., Grierson, D. S., Afolayan, A. J., and Eloff, J. N. (2005). Chemical analysis and antimicrobial activity of essential oil extracted from *Helichrysum aureonitens*. *South Afr. J. Bot.* 71 (2), 250–252. doi: 10.1016/S0254-6299(15)30140-X
- Yatam, S., Gundla, R., Jadav, S. S., Reddy Pedavenkatagari, N., Chimakurthy, J., and Kedam, T. (2018). Focused library design and synthesis of 2-mercapto benzothiazole linked 1, 2, 4-oxadiazoles as COX-2/5-LOX inhibitors. *J. Mol. Struct.* 1159, 193–204. doi: 10.1016/j.molstruc.2018.01.060
- Zeraik, A. E., and Nitschke, M. (2012). Influence of growth media and temperature on bacterial adhesion to polystyrene surfaces. *Braz. Arch. Biol. Tehnol.* 55 (4), 569–576. doi: 10.1590/S1516-89132012000400012

**Conflict of Interest:** The authors declare that the research was conducted in the absence of any commercial or financial relationships that could be construed as a potential conflict of interest.

Copyright © 2020 De Canha, Komarnytsky, Langhansova and Lall. This is an open-access article distributed under the terms of the Creative Commons Attribution License (CC BY). The use, distribution or reproduction in other forums is permitted, provided the original author(s) and the copyright owner(s) are credited and that the original publication in this journal is cited, in accordance with accepted academic practice. No use, distribution or reproduction is permitted which does not comply with these terms.





# <sup>1</sup>H-NMR Metabolomics and LC-MS Analysis to Determine Seasonal Variation in a Cosmeceutical Plant *Leucosidea sericea*

Phophi Freda Sehlakgwe<sup>1</sup>, Namrita Lall<sup>2,3</sup> and Gerhard Prinsloo<sup>1\*</sup>

<sup>1</sup> Department of Agriculture and Animal Health, University of South Africa, Johannesburg, South Africa, <sup>2</sup> Department of Plants and Soil Sciences, Plant Science Complex, University of Pretoria, Pretoria, South Africa, <sup>3</sup> School of Natural Resources, University of Missouri, Columbia, MO, United States

## OPEN ACCESS

### Edited by:

Rudolf Bauer,  
University of Graz, Austria

### Reviewed by:

Kai Xiao,  
Second Military Medical University,  
China

Hyung-Kyoon Choi,  
Chung-Ang University, South Korea

### \*Correspondence:

Gerhard Prinsloo  
prinsg@unisa.ac.za

### Specialty section:

This article was submitted to  
Ethnopharmacology,  
a section of the journal  
Frontiers in Pharmacology

Received: 05 July 2019

Accepted: 17 February 2020

Published: 05 March 2020

### Citation:

Sehlakgwe PF, Lall N and  
Prinsloo G (2020) <sup>1</sup>H-NMR  
Metabolomics and LC-MS Analysis  
to Determine Seasonal Variation in a  
Cosmeceutical Plant *Leucosidea*  
*sericea*. *Front. Pharmacol.* 11:219.  
doi: 10.3389/fphar.2020.00219

*Leucosidea sericea* is an evergreen shrub belonging to the Rosaceae family with previous studies that indicated that *L. sericea* extracts exhibited strong anti-bacterial properties against *Propionibacterium acnes*, showing potential as a cosmeceutical. The plant is traditionally used as a vermifuge, as an astringent and to treat conjunctivitis. Commercial production is, however, not possible as no information is available on cultivation and the effect of external environmental factors such as seasonal variation on the medicinal properties of the plant. Seasonal variation was investigated and it was found that significant differences were observed between the anti-acne (*P. acnes*) activity of plant material collected in different seasons. The best activity was found in winter with a mean minimum inhibitory concentration (MIC) of 5.20  $\mu\text{g mL}^{-1}$  compared to spring at 26.04  $\mu\text{g mL}^{-1}$ . A <sup>1</sup>H NMR-based untargeted metabolomic analysis was used to determine the differences in the chemical profiles of plant samples collected in different seasons. Principal component analysis (PCA) showed clear separation of the seasons and a supervised orthogonal partial least square discriminant analysis (OPLS-DA) was used to determine the compounds that differentiated the spring from the winter samples. The contribution plot indicated a strong positive association with the NMR regions from  $\delta$  1.2–1.6, 3.3–4.1, and 6.8–8.0 ppm indicative of a compound with an aromatic ring. Different LC-MS analyses were used in conjunction with a compound database, MAGMa and CSIFingerID, which led to the identification of the compound 2-(4-ethoxyphenyl)-5,6,7,8-tetramethoxy-4H-1-benzopyran-4-one and also confirmed the presence of tangeritin, rutin, quercetin glucoside, and kaempferol glucosides as well as several other compounds previously identified from the plant. This compound similar in structure to the anti-microbial flavonoid tangeritin, was only present in the winter samples. It is therefore recommended that seasonal variation be closely monitored during cultivation and commercial harvesting, and that winter is the preferred harvesting season to obtain the best anti-acne activity.

**Keywords:** metabolomics, *Propionibacterium acnes*, seasonal, flavonoid, polymethoxy flavone, anti-bacterial, anti-acne, *Leucosidea sericea*

## INTRODUCTION

*Leucosidea sericea* Eckl. & Zeyh. is an evergreen dense shrub belonging to the family Rosaceae which includes the genus *Rosa*, poorly presented in South Africa with *L. sericea* the sole representative of the genus *Leucosidea*. The tree also occurs in mountainous areas near water at high altitudes of 1000 m in parts of Africa such as Zimbabwe and Lesotho. It is commonly known as “oldwood” (English), “ouhout” (Afrikaans), and “umTshitshi” in Zulu, and traditionally used as a charm to protect the inhabitants of homesteads, treat various ailments such as ophthalmia and intestinal worm infection, used as a vermifuge and astringent. The antioxidant, anti-inflammatory, acetylcholinesterase inhibitory activity and mutagenic activities have been investigated in different studies, although the cosmeceutical application is poorly researched with a single report on the anti-acne activity (Aremu et al., 2010; Sharma et al., 2014).

Acne is a common skin disease, affecting adolescent males and females, although it can present even in their twenties (Sinha et al., 2014). Topical retinoids, topical antimicrobials, isotretinoin and oral antibiotics are the most commonly used methods of treating acne, but even though there is a wide range of acne treatments, the response of acne to treatment varies considerably (Kim et al., 2008b). Additionally, bacterial resistance is a continuous challenge and plants therefore provide various opportunities to find new anti-acne agents (Chomnawang et al., 2007; Tsai et al., 2010; Sinha et al., 2014). The anti-acne activity for *L. sericea* was reported with a MIC value of  $15.62 \mu\text{g mL}^{-1}$  and the isolated active compound  $\alpha$ -kossin with an MIC value of  $1.95 \mu\text{g mL}^{-1}$  (Sharma et al., 2014), and therefore presents an opportunity as an anti-acne cosmeceutical.

Metabolomics is used in a wide range of applications such as plant breeding, assessment of crop quality, food assessment, toxicity assessment, nutrition assessment, medical diagnosis, assessment of disease status, pharmaceutical drug developments, gene-function elucidation, integrated systems biology, and technological advances in analytical chemistry (Moco et al., 2007). Untargeted metabolomics, provides a unique tool to investigate relatively unknown plants, to determine the effects of external stimuli such as season on the chemical profile, and associated biological activity. Since abiotic factors such as ultra violet light, temperature and biotic factors such as parasitism and pathogenic attack influence the development of complex metabolic compounds in plants, untargeted analysis ensure that all changes potentially be observed and included in quality assessment parameters (Hardy and Hall, 2012). A combination of different analytical techniques such as NMR and LC-MS provides support for the identification of changes in chemical profile and for the identification of compounds responsible for the altered biological activity.

Although *L. sericea* is used against various ailments, the phytochemical research on this plant is very limited and an untargeted NMR-based metabolomics and LC-MS analysis were used to investigate metabolite variation amongst seasons (winter, summer, spring, and autumn) in *L. sericea* leaves and how it affected the biological activity. LC-MS analyses were used

to identify the annotated compounds from the untargeted metabolomic analysis; as well as several known compounds and compounds not identified in the plant before. The changes in chemical profile and associated biological activity is proposed to be linked to an increase in concentration of a polymethoxy flavonol compound in winter, indicating the need for systematic research to determine optimum conditions for harvesting of material to obtain the best biological activity.

## MATERIALS AND METHODS

### Collection of Plant Material

Leaves of *L. sericea* were collected in four consecutive seasons namely; October 2013 (spring), January 2014 (summer), April 2014 (autumn) and June 2014 (winter) from uniform, healthy vigorous plants from the Clearwater Florida region, South Africa ( $26^{\circ}9'26''\text{S } 27^{\circ}54'10''\text{E}$ ) and compared to the voucher specimen PRU (119052) deposited at H. G. W. J. Schweickerdt Herbarium, Department of Plant Science, University of Pretoria, Pretoria. The collected leaves were then air-dried at room temperature, protected from direct sunlight. The dried leaves were ground into a fine powder and stored at room temperature in airtight containers protected from direct sunlight until analyses.

### Anti-acne Assay

The powdered plant material (3 g) were soaked in 30 mL of ethanol for 72 h and placed on a shaker at room temperature for extraction of the compounds for the anti-bacterial assay. The extracts were filtered and the filtrates were placed under laminar flow to evaporate the remaining solvent to produce around 10 mg of crude ethanol extract. The extract stock solution was prepared by weighing 2 mg of the ethanolic plant extract in a 2 mL Eppendorf tube. One mL of 10% DMSO (dimethyl sulfoxide-  $\text{C}_2\text{H}_6\text{OS}$ ) was added and sonicated at  $40^{\circ}\text{C}$  for 5 min, thereafter addition of 100  $\mu\text{L}$  of double distilled water ( $\text{ddH}_2\text{O}$ ). Minimum inhibitory concentration (MIC) values of ethanolic extracts of *L. sericea* samples were determined for anti-bacterial activity against *Propionibacterium acnes* using a serial dilution method (Eloff, 1998). Bacterial cultures of *P. acnes* were grown on Brain Heart Infusion agar [Merck SA (Pty) Ltd.] and transferred to Nutrient Broth [Merck SA (Pty) Ltd.] using a sterile inoculation loop. The OD (optical density) of the bacterial suspension was then adjusted to 0.132 at 600 nm using a Beckmann spectrophotometer, corresponding to 0.5 McFarland standard equating to  $10^8 \text{CFU mL}^{-1}$ . Tetracycline was used as a positive control (Sigma-Aldrich- Kempton Park, South Africa) prepared by adding 2 mg in 10 mL autoclaved  $\text{dH}_2\text{O}$ . A volume of 100  $\mu\text{L}$  was then added in a serial dilution method to give concentrations of 500– $3.96 \mu\text{g mL}^{-1}$  of the plant extracts and positive control wells in the sterilized 96-well plate. A bacterial suspension was included as a negative control and DMSO was used as a solvent control to make sure that bacterial inhibition was due to the sample activity and not the solvent vehicle.

The 96-well plates were incubated for 72 h at  $37^{\circ}\text{C}$  under anaerobic conditions in Anaerocult A [Merck SA (Pty) Ltd.] in the dark. Twenty  $\mu\text{L}$  of PrestoBlue was added to determine

the MIC values by visually observing the color change in the wells. Since PrestoBlue is a resazurin-based dye blue in color, it converts to resorufin (pink) in the presence of viable bacterial cells. The MIC values of the samples were defined as the lowest concentration of the plant extract that inhibits the conversion of PrestoBlue from blue to pink.

## Metabolomic Analysis

The same dried and grounded material used for the anti-acne assay was used for the NMR-based metabolomic analysis. An untargeted metabolomics analysis method was adapted (Maree and Viljoen, 2012; Mediani et al., 2012) and the plant material was subsequently extracted using a direct extraction method, where ethanol was replaced with methanol:water. Fifty milligrams of the dried leaves were weighed in 2 mL Eppendorf tubes and then extracted with 0.75 mL of deuterated methanol ( $\text{CH}_3\text{OH}-d_4$ ) and 0.75 mL of potassium dihydrogen phosphate ( $\text{KH}_2\text{PO}_4$ ) buffer in deuterated water ( $\text{D}_2\text{O}$ ) containing 0.1% (w/w) TSP (trimethylsilylpropionic acid sodium salt). The desired pH (6.0) was obtained adding NaOD (deuterated sodium hydroxide) to the buffer solution. The samples were then vortexed for 1–2 min at room temperature, sonicated at 30°C for 20 min and then centrifuged at 13 000 rpm for 20 min (Kim et al., 2010). The supernatant from each tube was then transferred into 5 mm NMR tubes where 32 scans were performed on a 600 MHz NMR spectrometer (Varian Inc., California, CA, United States).

The spectral data from NMR was processed using MestReNova software (9.0.1, Mestrelab Research Spain) where the spectral data from NMR was subjected to phase correction, baseline correction, referencing and normalizing after which the spectral intensities were reduced to integrated regions (bins) of equal width (0.04 ppm each) corresponding to the region of 0.04–10.00 ppm. The water peak (4.70–4.90 ppm) and methanol peaks (3.30–3.36 ppm) were excluded from the final data for further analysis (Mediani et al., 2012). The data from MestReNova was exported to Microsoft Excel for multivariate data analysis using SIMCA-P software (13.0, Umetrics, Sweden). The data was first analyzed using an unsupervised method known as principal component analysis (PCA), followed by a supervised model, and orthogonal partial least square discriminatory analysis (OPLS-DA). A scores plot and a contribution plot were used to determine sources of variation and the NMR values from the plots were then used in conjunction with databases and published literature for annotation. The permutation test with 100 permutations was performed for validation of the OPLS-DA model.

## Liquid Chromatography-Mass Spectroscopy (LC-MS)

Liquid Chromatography-Mass Spectroscopy was used in order to confirm the proposed compound annotated from NMR-metabolomics and chemometric studies as well as to confirm the presence of compounds previously identified in the plant. The dried leaf material was ground and 1 g was extracted with 1.5 mL MeOH (analytical grade, Sigma-Aldrich-Kempton Park, South Africa). Samples were sonicated in an ultrasonic

bath for 15 min and centrifuged for 15 min at 15 000 rpm. The supernatant was filtered through 0.2 micron syringe filters (Sartorius Minisart RC 4). Extractions were performed in triplicate for statistical processing.

## UHPLC Analysis

A Waters UHPLC coupled in tandem to a Waters SYNAPT G1 HDMS mass spectrometer was used to generate accurate mass data. Optimization of the chromatographic separation was done utilizing a Waters HSS T3 C18 column (150 mm  $\times$  2.1 mm, 1.8  $\mu\text{m}$ ) and the column temperature controlled at 60°C. A binary solvent mixture was used consisting of water (Eluent A) containing 10 mM formic acid (natural pH of 2.3) and acetonitrile (Eluent B) containing 10 mM formic acid. The initial conditions were 90% A at a flow rate of 0.4 mL min<sup>-1</sup> and were maintained for 1 min, followed by a linear gradient to 1% A at 35 min. The conditions were kept constant for 2 min and then changed to the initial conditions. The runtime was 40 min and the injection volume was 1  $\mu\text{L}$ . Samples were kept at 6°C in the Sample Manager during the analysis.

## Quadrupole Time-of-Flight Mass Spectrometry (q-TOF-MS) Analyses

A SYNAPT G1 mass spectrometer was used in V-optics and operated in electrospray mode to enable detection of phenolic and other ESI-compatible compounds. Leucine enkephalin (50 pg mL<sup>-1</sup>) was used as reference calibrant to obtain typical mass accuracies between 1 and 5 mDa (mDa). The mass spectrometer was operated in both ESI positive and negative modes with a capillary voltage of 2.5 kV, the sampling cone at 30 V and the extraction cone at 4.0 V. The scan time was 0.1 s covering the 50 to 1200 Dalton mass range. The source temperature was 120°C and the desolvation temperature was set at 450°C. Nitrogen gas was used as the nebulization gas at a flow rate of 550 L h<sup>-1</sup> and cone gas was added at 50 L h<sup>-1</sup>. MassLynx 4.1 (SCN 872) software was used to control the hyphenated system and to perform all data manipulation.

## Compound Annotation and Identification NMR Data

The important chemical shifts from the untargeted NMR-based metabolomic analysis, identified from the contribution plots, were compared to the chemical shifts of compounds in databases such as Chenomx (Version 8.3) and the Human Metabolome Database<sup>1</sup>. Candidate structures were compared with previously published literature.

## LC-MS Data

Automated chemical structure annotation and identification was obtained using MAGMa<sup>2</sup> to propose the most likely structure of the unknown compound based on the fragmentation pattern (Ridder et al., 2014, 2013). The fragmentation trees obtained from MAGMa were then transferred to CSIFingerID<sup>3</sup> to confirm

<sup>1</sup>[www.hmdb.ca/](http://www.hmdb.ca/)

<sup>2</sup><http://www.emetabolomics.org/magma>

<sup>3</sup><http://www.csi-fingerid.org/>

the identity based on the fragmentation pattern of the proposed compound. CSIFingerID calculates fragmentation trees from known reference spectra, fragmentation tree similarities as well as PubChem (CACTVS) and Klekota–Roth fingerprints.

The raw data was processed and extracted ion chromatograms (XICs) obtained based on the newly proposed unknown compound and known compounds found in published literature. The accurate mass data of each detected compound was submitted for elemental composition, double bond equivalence (DBE) as well as isotopic fit calculations. Compound identification was further enhanced by analyzing all samples with low and high collision energy settings of the collision cell. To minimize compound fragmentation a low energy setting of 3 eV was used, but to enhance fragmentation of molecules various collision energies between 10 and 40 eV were used (MSe). Fragmentation spectra were submitted to the NIST mass spectral library (Stein, 2014, Version 2.2 build Jun 2014) as well as the mass spectral libraries developed on the Synapt G1 system for identification of the compounds.

## RESULTS

The anti-acne assay achieved inhibitory activity at 3.90–31.25  $\mu\text{g mL}^{-1}$  which is comparable to previous reports by Sharma et al. (2014) at a MIC value of 15.62  $\mu\text{g mL}^{-1}$ . Better activity was, however, obtained in the colder seasons namely autumn and winter (Table 1).

Chenomx database and previously published data were used to annotate the main compounds in the plant extract (Table 2).

NMR-based metabolomic analysis was used to determine the extent of the chemical changes in the plants that affected the anti-acne activity as was obtained in Table 1. The unsupervised PCA revealed clustering of samples based on the season of collection. Autumn and winter samples grouped close to each other, separated from the summer and spring samples (Figure 1), indicating a similar chemical profile of the samples in winter and autumn when compared to the summer and spring samples. The tight clusters for the winter and autumn samples indicated minimal changes in the chemical profiles for the samples collected in these seasons. This is contrasted to the variation of the sample distribution for the spring and summer samples, which were not tightly clustered but spread out with a slight overlap between the samples, indicative of more variation in the chemical profiles of these samples. The very good description of the variation in the samples and the predictability of the model

is depicted in the  $R^2$  and  $Q^2$  values, respectively ( $R^2 = 0.977$  and  $Q^2 = 0.955$ ).

Since the best and lowest activity was achieved in winter and spring seasons, respectively, a supervised analyses was conducted using only the spring and winter samples (Figure 2). The OPLS-DA score plot clearly separated the spring from the winter samples with a very good description of the variation and predictability score for the model ( $R^2X = 0.914$  and  $R^2Y = 0.897$ ). Due to the good separation of the samples in the OPLS-DA analysis, a contribution plot was constructed to determine the important NMR regions contributing to the separation of the samples into the two clusters. For validation of the model, the permutation test with 100 permutations showed that the model is valid (Figure 3).

The contribution plot of the untargeted OPLS-DA analysis was used to locate the NMR regions of interest (Figure 4).

**TABLE 2 |** Annotated compounds in the methanolic water extracts analyzed using a 600 MHz NMR.

Compound	NMR values of extract (ppm)	Chenomx database (ppm)
Alanine	1.46	1.46
	1.47	1.47
Acetamide	2.00	2.00
	nd	6.79
	nd	7.52
Choline	3.19	3.19
	nd	3.50–3.52
	nd	4.04–4.07
Glycine	3.54	3.54
Fumarate	6.52	6.52
Isoleucine	0.99	0.99
	1.01	1.01
	nd	1.22–1.28
	nd	1.42–1.48
	nd	1.96–1.98
	nd	3.66
	nd	3.46
Sucrose	3.44	3.46
	nd	3.54–3.57
	3.64	3.67
	3.71–3.88	3.74–3.90
	4.01	4.04
	4.14	4.20
	4.16	4.22
	5.39	5.40
Xylose	5.40	5.41
	3.22	3.22
	3.42	3.42
	nd	3.60–3.69
	nd	3.90–3.94
	4.56	4.56
	4.58	4.58
	5.17	5.17
	5.18	5.18

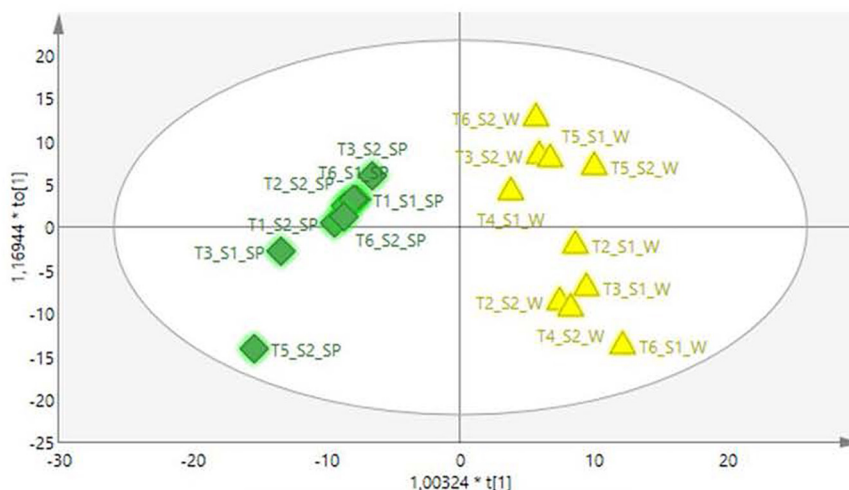
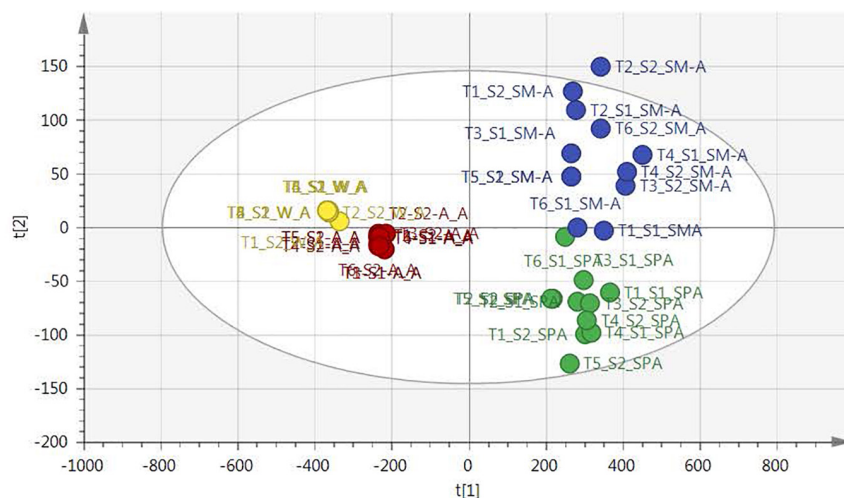
When peaks of the extract were too small to match to the peaks of the pure compound, they were denoted as not detected (nd).

**TABLE 1 |** MIC values of *L. sericea* extract against *Propionibacterium acnes* with MIC values in  $\mu\text{g mL}^{-1}$  for the four seasons.

Season	Mean ( $\mu\text{g mL}^{-1}$ )	Std. dev.
Spring	26.04	9.02398
Summer	20.83	9.02398
Autumn	7.81	0
Winter	5.20	2.25744

Each value represents the average of three replicates.





2-(4-ethoxyphenyl)-5,6,7,8-tetramethoxy-4H-1-benzopyran-4-one (**Figure 5**) and was further investigated using CSIFinger ID. The fragmentation pattern and intensities were submitted to CSIFinger ID to determine the possible compounds that could be linked to the pattern and intensities. The same compound was proposed and the proposed compound's NMR peaks were compared to the contribution plot as well as matched to the NMR profiles of the winter samples. The predicted NMR values of 2-(4-ethoxyphenyl)-5,6,7,8-tetramethoxy-4H-1-benzopyran-4-one<sup>4</sup> (Banfi and Patiny, 2008), the NMR values found in the sample as well as the published NMR peaks of tangeretin (Rashed et al., 2015) are provided in **Table 3**. Additionally the correlation values of the correlation matrix functionality of SIMCA was used to determine the correlation values of

<sup>4</sup><https://www.nmrdb.org>

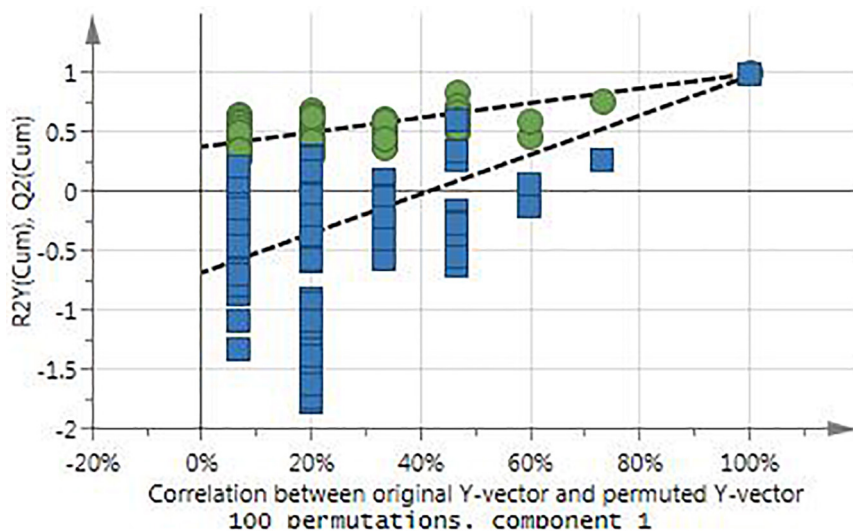


**FIGURE 3 |** Validation of the OPLS-DA model with the permutation test.

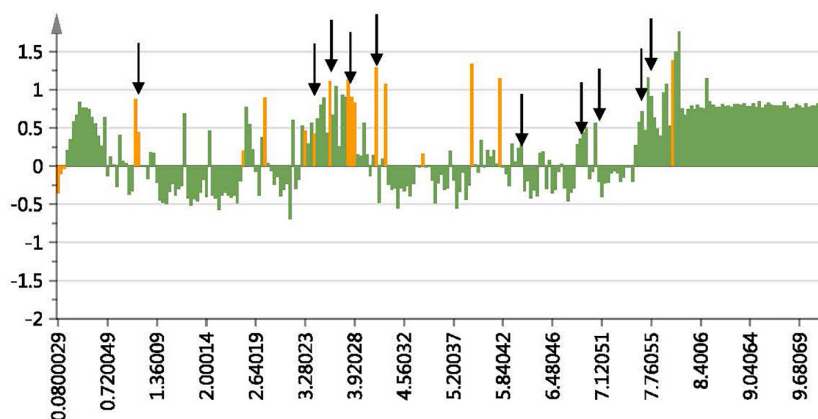


**FIGURE 4 |** Contribution plot showing NMR regions responsible for the separation of the winter samples from the spring samples. The positive bars indicate the NMR regions contributing to the separation of the winter samples. The arrows indicate the NMR regions of the proposed compound 2-(4-ethoxyphenyl)-5,6,7,8-tetramethoxy-4H-1-benzopyran-4-one at  $\delta$  1.29, 3.66, 3.80, 4.08, 6.35, 6.8, 6.88, 7.67, and 7.71 ppm.

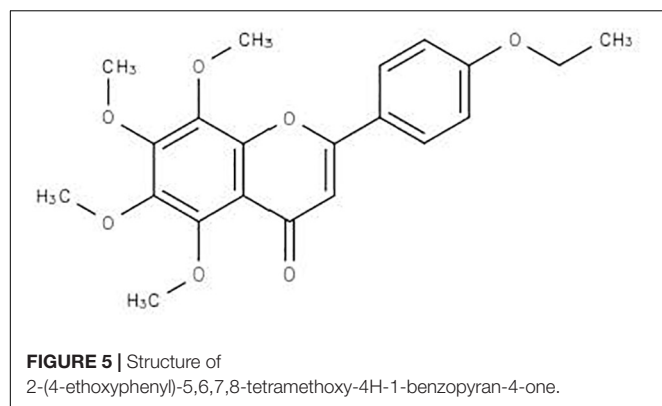
the peaks of the proposed compound and is also presented in **Table 3**.

The LC-MS analysis further identified 15 compounds from this plant, based on comparison with a compound database (**Table 4**). The list of compounds includes compounds that were previously identified from the plant such as  $\alpha$ -kossin, 3,5,7,3',4'-pentahydroxyflavone and tiliroside, as well as compounds not previously identified from this plant including compounds such as tangeritin, rutin, quercetin glucoside, and kaempferol glucosides (**Figure 7**).

## DISCUSSION

*Leucosidea sericea* was previously identified as a plant with good activity against *P. acnes* at  $15.62 \mu\text{g mL}^{-1}$  and the isolated active

compound  $\alpha$ -kossin with an MIC value of  $1.95 \mu\text{g mL}^{-1}$  (Sharma et al., 2014). Additionally 3,5,7,3',4'-pentahydroxyflavone was recently isolated from the methanol leaf extract of *L. sericea* with significant broad-spectrum antibacterial activity at  $1.95$ – $125 \mu\text{g mL}^{-1}$  (Pendota et al., 2018). This study investigated the effect of seasonal changes on the anti-acne activity of the leaf extracts using untargeted NMR-based metabolomics and subsequent LC-MS analysis. The winter samples provided the best anti-acne activity with a mean value of  $5.20 \mu\text{g mL}^{-1}$ , comparable to tetracycline (positive drug control) at  $3.90 \mu\text{g mL}^{-1}$ , also comparing well to previous reports (Sharma et al., 2014). This activity is, however, much better than anti-acne activity found in herbs such as rose (*Rosa damascene*), dzong (*Eucommia ulmoides* oliv.) and yerba mate (*Ilex paraguariensis*) with MIC values of 1 to  $2.5 \mu\text{g mL}^{-1}$  (Chomnawang et al., 2007; Kim et al., 2008b; Tsai et al., 2010). The winter samples,



however, presented better activity than the summer and spring extracts with much lower mean MIC values of  $26.04 \mu\text{g mL}^{-1}$  and  $20.83 \mu\text{g mL}^{-1}$ , respectively (Table 1). The activity of the summer extract corroborates with previous reports where *L. sericea* leaves inhibited *P. acnes* with MIC values of  $\leq 15.62 \mu\text{g mL}^{-1}$ . The autumn and winter extracts ( $7.81$  and  $5.20 \mu\text{g mL}^{-1}$ , respectively) therefore both showed increased activity to the previous reports, although not significantly different, and is an indication of the preparation of the plant for the colder months as better anti-bacterial activity has been obtained already in autumn. As the seasons progressed from spring to winter, the activity in winter and autumn improved significantly when compared to spring and summer samples. The improved activity from the warmer to the colder months could not be related to the previously identified anti-acne compounds, but to flavonoid-type compounds not detected in the spring and summer months. The effect of season has been investigated by numerous authors, as each plant reacts differently to seasonal changes and different metabolic pathways are responsible for production of the various secondary metabolites in both colder and warmer months (Prinsloo and Nogemane, 2018). Plants such as *Rosmarinus officinalis*, *Salvia fruticose*, and *Croton heliotropiifolius* contain higher concentrations of active compounds in summer and spring months (Lemos et al., 2015; Sarrou et al., 2016; de Alencar Filho et al., 2017). On the contrary many reports described increased activity and active compound levels in the colder months for example *Calamintha nepeta*, *Phillyrea angustifolia*, and *Thymus longicaulis* (Scognamiglio et al., 2014; Pacifico et al., 2015), whereas in some plants seasonal variation does not affect the chemical composition such as in *Vaccinium myrtillus* (Bujor et al., 2016). In this study, improved activity in colder months is an indication that the plant is preparing for colder seasons by increased production of anti-bacterial compounds, and therefore better activity was achieved in autumn and winter, even though activity in winter was superior at  $5.20 \mu\text{g mL}^{-1}$ . This study is the first report where the effect of season was determined on inhibitory activity of *L. sericea* against *P. acnes*.

The PCA provided an unsupervised overview of the metabolome of the plant leaves harvested in spring, autumn, winter and summer seasons, where variation was observed and samples similar in chemical profiles grouped together. The winter and autumn samples were clustered close together

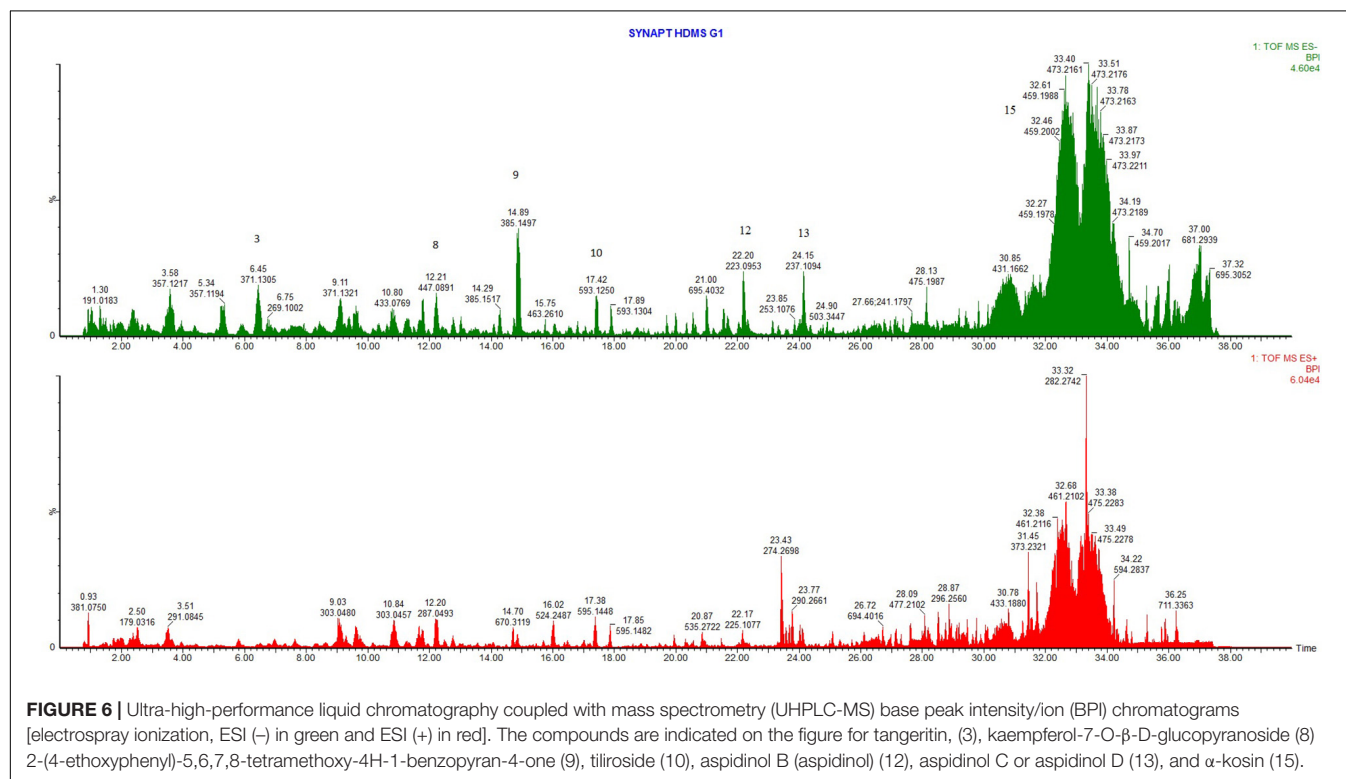
**TABLE 3 |** NMR values of 2-(4-ethoxyphenyl)-5,6,7,8-tetramethoxy-4H-1-benzopyran-4-one, the observed NMR values, the NMR values of tangeretin as well as the correlation values obtained from SIMCA.

H	Predicted (Banfi and Patiny, 2008)	Observed	Correlation values	Tangeretin (Rashed et al., 2015)
3	6.435 s	6.35 s	0.898	6.63 s
2'	7.533 ddd	7.67 d	0.789	7.85 d
3'	6.94 ddd	6.81 d	0.891	7.0 d
5'	6.94 ddd	6.88 d	0.897	7.0 d
6'	7.533 ddd	7.71 d	0.701	7.85 d
OCH <sub>3</sub>	3.831 s	3.81 s	0.831	4.07 s
OCH <sub>3</sub>	3.716 s	3.66 s	0.807	4.01 s
OCH <sub>3</sub>	3.838 s	3.67 s	0.833	3.92 s
OCH <sub>3</sub>	3.704 s	3.80 s	0.820	3.92 s
OCH <sub>3</sub>				3.86 s
OEth	4.177 q	4.08 m	0.857	
	1.277 t	1.29 t	0.855	

even though it was separated into different groups (Figure 1). The main compounds annotated in the extracts were alanine, acetamide, choline, glycine, fumarate, isoleucine, sucrose, and xylose, based on annotation using the Chenomx database and previously published data (Table 2). The tight clustering of the winter and autumn samples indicated low variation among these samples, whereas the loose grouping of the spring and summer samples indicated much more variation. Informed by the anti-acne results showing that the winter extracts have the best anti-bacterial activity at the MIC value of  $5.20 \mu\text{g mL}^{-1}$  and spring with the lowest activity at  $26.04 \mu\text{g mL}^{-1}$  (Table 1), these seasons were selected for a supervised OPLS-DA analysis to determine the difference in the chemical composition of the samples harvested in the different seasons (Figure 2). The OPLS-DA score plots clearly separated the spring from the winter samples, with a very good model prediction ability ( $R^2X = 0.914$  and  $R^2Y = 0.897$ ). Validation of the model was determined with the permutation test, performed with 100 permutations and indicated that the model is valid (Figure 3). Due to the clear separation of the samples, it was possible to construct a contribution plot of the winter samples (Figure 4), showing important contributing regions responsible for clustering of the samples. The aromatic ( $\delta$  6.1–8.0), sugar (3.3–4.2) and aliphatic regions ( $\delta$  1.2–1.3) were strongly associated with the winter samples. The peaks in these regions were compared with NMR profiles in Chenomx and Human Metabolome Database and also with previously published data. It was concluded that the regions corresponds very well to a flavonoid-type compound, which was confirmed with the use of LC-MS analysis. LC-MS analysis was imported to MAGMa, to determine the best possible fit to a structure which could be differentiated between the winter and spring samples. MAGMa is a highly acclaimed computational method annotating all fragmented compounds in LC-MSn data sets with candidate molecules taken from large chemical databases such as PubChem or the Human Metabolite Database. Based on an algorithm for candidate substructure annotation of multistage accurate mass spectral trees, provides candidates

**TABLE 4** | Compounds in *Leucosidea sericea*, indicating the mode [ESI (–) and ESI (+)], formula, mass and the retention time.

Compound	Formula	Mass	ESI (+)	ESI (–)	Mode and Rt (min)
1 3,5,7,3',4'-pentahydroxyflavone	C <sub>15</sub> H <sub>10</sub> O <sub>7</sub>	302.0427	303.0505	301.0348	ESI–; Rt 1.49
2 Procyanidin B1 and B2	C <sub>30</sub> H <sub>26</sub> O <sub>12</sub>	578.1424	579.1503	577.1346	ESI+/ESI–; Rt 2.36 and 3.50
3 Tangeritin	C <sub>20</sub> H <sub>20</sub> O <sub>7</sub>	372.1209	373.1287	371.1131	ESI–; Rt 6.45
4 5,7-dihydroxychromone	C <sub>9</sub> H <sub>6</sub> O <sub>4</sub>	178.0266	179.0344	177.0188	ESI–; Rt 8.55
5 Rutin	C <sub>27</sub> H <sub>30</sub> O <sub>16</sub>	610.1534	611.1612	609.1456	ESI+/ESI–; Rt 9.09
6 Quercetin glucoside	C <sub>21</sub> H <sub>20</sub> O <sub>12</sub>	464.0955	465.1033	463.0877	ESI+/ESI–; Rt 9.60
7 Kaempferol-3-O-rutinoside (Nicotiflorin)	C <sub>27</sub> H <sub>30</sub> O <sub>15</sub>	594.1585	595.1663	593.1507	ESI+/ESI–; Rt 11.81
8 Kaempferol-7-O-β-D-glucopyranoside	C <sub>21</sub> H <sub>20</sub> O <sub>11</sub>	448.1006	449.1084	447.0927	ESI+/ESI–; Rt 12.20
9 2-(4-ethoxyphenyl)-5,6,7,8-tetramethoxy-4H-1-benzopyran-4-one	C <sub>21</sub> H <sub>22</sub> O <sub>7</sub>	386.1366	387.1444	385.1287	ESI–; Rt 14.89
10 Tilioside	C <sub>30</sub> H <sub>26</sub> O <sub>13</sub>	594.1373	595.1452	593.1295	ESI–; Rt 17.44 or 17.91
11 Desaspidinol	C <sub>11</sub> H <sub>14</sub> O <sub>4</sub>	210.0892	211.0970	209.0814	ESI–; Rt 18.95
12 Aspidinol B (Aspidinol)	C <sub>12</sub> H <sub>16</sub> O <sub>4</sub>	224.1049	225.1127	223.0970	ESI–; Rt 22.20
13 Aspidinol C or Aspidinol D	C <sub>13</sub> H <sub>18</sub> O <sub>4</sub>	238.1205	239.1283	237.1127	ESI–; Rt 24.15
14 1-hydroxy-2-oxopomolic acid	C <sub>30</sub> H <sub>46</sub> O <sub>6</sub>	502.3294	503.3373	501.3216	ESI–; Rt 24.77 or 26.97
15 α-kosin	C <sub>25</sub> H <sub>32</sub> O <sub>8</sub>	460.2097	461.2175	459.2019	ESI–; Rt 32.67



ranked on the calculated matching score (Ridder et al., 2013, 2014). The polymethoxylated flavone 2-(4-ethoxyphenyl)-5,6,7,8-tetramethoxy-4H-1-benzopyran-4-one (**Figure 5**) achieved the highest matching score. The fragmentation tree of this compound was then transferred to CSIFingerID, which supported the proposed compound in MAGMa. Furthermore, the LC-MS analysis also showed difference in comparison of the height of the peak  $M/z$  386.137 of the winter and spring samples, confirming a difference in compound concentration, which was indeed in a higher concentration in the winter samples when compared to the spring samples. The compound, however,

was not isolated from the extract and the proposed compound should be isolated and subsequently confirmed with 2-D NMR and LC-MS analysis.

The extracted ion chromatograms (XICs) obtained based on the newly proposed unknown compound and known compounds was found in published literature. The accurate mass data, elemental composition, DBE as well as isotopic fit calculations matched the compounds as presented in **Table 4**. Fragmentation spectra were also submitted to the NIST mass spectral library (Stein, 2014, Version 2.2 build Jun 2014) as well as the mass spectral libraries developed on the Synapt G1



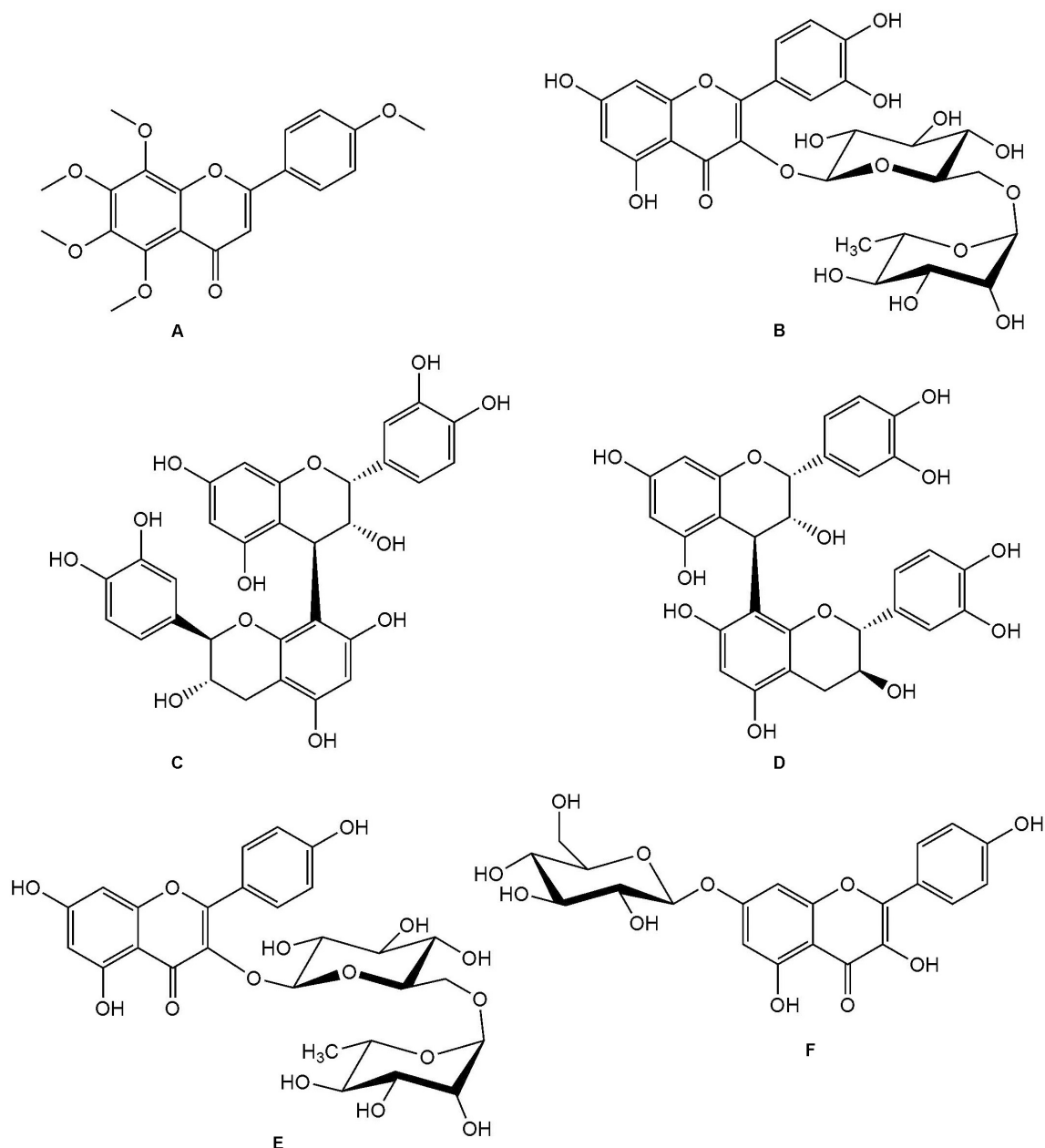


**FIGURE 7 |** Structures of compounds not previously isolated from *L. sericea*. **(A)** tangeretin; **(B)** rutin; **(C)** procyanidin B1; **(D)** procyanidin B2; **(E)** kaempferol-3-O-rutinoside (nicotiflorin); **(F)** kaempferol-7-O- $\beta$ -D-glucopyranoside.

system for identification of the compounds (Figure 6). The list of compounds includes compounds that were previously identified from the plant such as  $\alpha$ -kossin (15) (Sharma et al., 2014), 3,5,7,3',4'-pentahydroxyflavone, tilirosin (10), 1-hydroxy-2-oxopomolic acid, 5,7-dihydroxychromone (Pendota et al., 2018), aspidinol (12), and desaspidinol (Bosman et al., 2004). Compounds not previously identified from *L. sericea* includes-(4-ethoxyphenyl)-5,6,7,8-tetramethoxy-4H-1-benzopyran-4-one (9), tangeretin (3), rutin, quercetin glucoside and kaempferol glucosides (8) (Figure 7). Phloroglucinol derivatives

aspidinol and aspidin BB have also shown antibacterial (Pendota et al., 2018) as well as potent anti-acne activity (Gao et al., 2016).

Information on the compound 2-(4-ethoxyphenyl)-5,6,7,8-tetramethoxy-4H-1-benzopyran-4-one (both on structure elucidation and biological activity) is very limited and therefore information on the possible biological activity of the compound was derived from similar polymethoxylated flavones found in citrus, supported by the isolation of 3,5,7,3',4'-pentahydroxyflavone from *L. sericea* (Pendota et al., 2018).

Tangeretin and 2-(4-ethoxyphenyl)-5,6,7,8-tetramethoxy-4H-1-benzopyran-4-one are very similar compounds with only a difference of the ethoxy group substituted with a methoxy group in tangeretin. Hesperidin, nobiletin and derivatives are also very similar compounds found in citrus fruit and peel in tangerine, lemon and orange. Hesperidin was found to be the most predominant flavonoid in tangerine peel, followed by tangeretin and nobiletin (Ho and Kuo, 2014). Even though pharmacological activity such as neuroinflammatory activity, antibacterial, antifungal, antiaging, anti-tyrosinase, anti-acne, antiallergic, anticancer, anti-inflammatory and antiviral activity against the human respiratory syncytial virus (RSV) have been assigned to these compounds, it is known that these compounds individually often do not account for the activity of the extracts, and that these compounds in combination is responsible for the pharmacological activities observed (Kim et al., 2008a; Ho and Kuo, 2014; Rashed et al., 2015; Xu et al., 2015; Vargas et al., 2016; Adhikari et al., 2017; Hagenlocher et al., 2017). Additionally tangeretin and nobiletin also showed the best antibacterial activity against *Staphylococcus aureus*, *Microsporum canis*, *Escherichia coli*, *Trichophyton mentagrophytes* when tested against bacterial and fungal species when the peel extracts of *C. sinensis*, *C. limon*, and *C. reticulata* were tested, with antimicrobial activity also reported for these compounds in the leaf extract of *C. volkameriana* (Johann et al., 2007; Rashed et al., 2015). These two compounds are also the most effective compounds at inhibiting cancer cell growth of melanoma and lung (Rashed et al., 2015).

The essential oils of *C. obovoides* and *C. natsudaoides* were evaluated for their possibility as skin treatment when tested against *P. acnes* and *S. epidermidis*, exhibiting very good antibacterial activity against both bacteria with MIC values of 0.31  $\mu\text{L mL}^{-1}$  and 2.5–10  $\mu\text{g mL}^{-1}$ , respectively (Kim et al., 2008a). The anti-acne activity of *Citrus* species was further confirmed with essential oils of *C. limon* and *C. paradisi*, showing anti-acne properties against *P. acnes* (Zu et al., 2010) while essential oil of *C. aurantium* is known for its use in the treatment of acne (Sinha et al., 2014). *Citrus junos* was also investigated for its use in the cosmeceutical industry and the active compounds such as tangeretin and hesperidin were found to have anti-aging and anti-tyrosinase activity (Adhikari et al., 2017). Literature therefore provides ample evidence of the antibacterial activity of the polymethoxylated flavones, and although the activity of 2-(4-ethoxyphenyl)-5,6,7,8-tetramethoxy-4H-1-benzopyran-4-one has not been determined previously, the compound could possess very similar activity to the citrus polymethoxylated flavones such as tangeretin and nobiletin although it should be confirmed in biological assays.

## CONCLUSION

In conclusion, the leaf extracts of *L. sericea* inhibited the growth of *P. acnes* with a significant mean MIC value of 5.20  $\mu\text{g mL}^{-1}$  (comparable to the positive control tetracycline) for winter with lower activity during autumn, spring and summer. This report confirms the effect of external environmental stimuli

on the chemical profile and associated biological activity of plants, and in particular *L. sericea*. Untargeted NMR-based metabolomics was applied to successfully detect differences in the metabolome of the plant samples collected in different seasons. Multivariate data analysis (PCA and OPLS-DA) indicated a clear separation of samples according to seasons, corroborating the results obtained in the anti-acne assay. Subsequent analysis of the contribution plot, identified NMR regions in the aromatic, sugar and aliphatic regions, corresponding to a flavonoid-type structure. Following this, LC-MS, MAGMa and CSIFingerID were further used to propose the compound 2-(4-ethoxyphenyl)-5,6,7,8-tetramethoxy-4H-1-benzopyran-4-one as the compound responsible for the separation of the samples in the metabolomic analysis and better activity in winter. This compound is not very common and not well-researched, however, evidence of anti-bacterial activity is available for similar compounds such as tangeretin also indicating the possible antibacterial activity as was observed in the bacterial assay. UHPLC linked to LC-MS analysis was used to confirm the presence of 2-(4-ethoxyphenyl)-5,6,7,8-tetramethoxy-4H-1-benzopyran-4-one, tangeretin as well as compounds previously isolated from *L. sericea* such as  $\alpha$ -kossin, 3,5,7,3',4'-pentahydroxyflavone, tiliroside, and aspidinol. Future work should focus on isolation of the compound to confirm the structure of this relatively unknown compound 2-(4-ethoxyphenyl)-5,6,7,8-tetramethoxy-4H-1-benzopyran-4-one, and should further investigate the anti-acne activity of the compound and its possible synergistic effects with compounds such as kojic acid, tangeretin, aspidinol and 3,5,7,3',4'-pentahydroxyflavone, already identified from this plant which exhibited strong anti-bacterial activity.

## DATA AVAILABILITY STATEMENT

The dataset “*Leucosidea sericea* NMR seasons” for the metabolomic analysis of this study can be found in the Mendeley Library <http://dx.doi.org/10.17632/pyfh5ykgw.1>.

## AUTHOR CONTRIBUTIONS

PS conducted the research, analyzed and interpreted the data, and drafted the initial manuscript. NL provided assistance in conceptualization of the project and the anti-acne assays. GP conceptualized the research, assisted with the metabolomic analysis and interpretation of results, and finalized the manuscript for submission.

## FUNDING

The Department of Science and Technology of South Africa is thanked for funding.

## ACKNOWLEDGMENTS

Laboratory assistants and Prof. Paul Steenkamp are thanked for their assistance in the LC-MS, NMR, and anti-bacterial analysis.

## REFERENCES

- Adhikari, D., Panthi, V. K., Pangen, R., Kim, H. J., and Park, J. W. (2017). Preparation, characterization, and biological activities of topical anti-aging ingredients in a *Citrus junos* callus extract. *Molecules* 22:2198. doi: 10.3390/molecules22122198
- Aremu, A. O., Fawole, O. A., Chukwujekwu, J. C., Light, M. E., Finnie, J. F., and Van Staden, J. (2010). In vitro antimicrobial, anthelmintic and cyclooxygenase-inhibitory activities and phytochemical analysis of *Leucosidea sericea*. *J. Ethnopharmacol.* 131, 22–27. doi: 10.1016/j.jep.2010.05.043
- Banfi, D., and Patiny, L. (2008). Resurrecting and processing NMR spectra on-line. *Chimia* 62, 280–281. doi: 10.2533/chimia.2008.280
- Bosman, A. A., Combrinck, S., Roux-Van Der Merwe, R., Botha, B. M., and McCrindle, R. I. (2004). Isolation of an anthelmintic compound from *Leucosidea sericea*. *South Afr. J. Bot.* 70, 509–511. doi: 10.1016/S0254-6299(15)30189-7
- Bujor, O., Le, C., Volf, I., Popa, V. I., and Dufour, C. (2016). Seasonal variations of the phenolic constituents in bilberry (*Vaccinium myrtillus* L.) leaves, stems and fruits, and their antioxidant activity. *Food Chem.* 213, 58–68. doi: 10.1016/j.foodchem.2016.06.042
- Chomnawong, M. T., Surassmo, S., Nukoolkarn, V. S., and Grisanapan, W. (2007). Effect of *Garcinia mangostana* on inflammation caused by *Propionibacterium acnes*. *Fitoterapia* 78, 401–408. doi: 10.1016/j.fitote.2007.02.019
- de Alencar Filho, J. M. T., da, C., Araújo, L., Oliveira, A. P., Guimarães, A. L., Pacheco, A. G. M., et al. (2017). Chemical composition and antibacterial activity of essential oil from leaves of *Croton heliotropiifolius* in different seasons of the year. *Rev. Bras. Farmacogn.* 27, 440–444. doi: 10.1016/j.bjp.2017.02.004
- Eloff, J. N. (1998). A sensitive and quick microplate method to determine the minimal inhibitory concentration of plant extracts for bacteria. *Planta Med.* 64, 711–713. doi: 10.1055/s-2006-957563
- Gao, C., Guo, N., Li, N., Peng, X., Wang, P., Wang, W., et al. (2016). Investigation of antibacterial activity of aspidin BB against *Propionibacterium acnes*. *Arch. Dermatol. Res.* 308, 79–86. doi: 10.1007/s00403-015-1603-x
- Hagenlocher, Y., Feilhauer, K., Schäffer, M., Bischoff, S. C., and Lorentz, A. (2017). Citrus peel polymethoxyflavones nobletin and tangeretin suppress LPS- and IgE-mediated activation of human intestinal mast cells. *Eur. J. Nutr.* 56, 1609–1620. doi: 10.1007/s00394-016-1207-z
- Hardy, N. W., and Hall, R. D. (2012). *Plant Metabolomics: Methods and Protocols*. Totowa, NJ: Humana Press.
- Ho, S. C., and Kuo, C. T. (2014). Hesperidin, nobletin, and tangeretin are collectively responsible for the anti-neuroinflammatory capacity of tangerine peel (*Citri reticulatae pericarpium*). *Food Chem. Toxicol.* 71, 176–182. doi: 10.1016/j.fct.2014.06.014
- Johann, S., De Oliveira, V. L., Pizzolatti, M. G., Schripsema, J., Braz-Filho, R., Branco, A., et al. (2007). Antimicrobial activity of wax and hexane extracts from *Citrus* spp. peels. *Mem. Inst. Oswaldo Cruz* 102, 681–685. doi: 10.1590/S0074-02762007000600004
- Kim, H. K., Choi, Y. H., and Verpoorte, R. (2010). NMR-based metabolomic analysis of plants. *Nat. Protoc.* 5, 536–549. doi: 10.1038/nprot.2009.237
- Kim, S.-S., Baik, J. S., Oh, T.-H., Yoon, W.-J., Lee, N. H., and Hyun, C.-G. (2008a). Biological activities of Korean *Citrus obovoides* and *Citrus natsudaoides* essential oils against acne-inducing bacteria. *Biosci. Biotechnol. Biochem.* 72, 2507–2513. doi: 10.1271/bbb.70388
- Kim, S.-S., Kim, J.-Y., Lee, N. H., and Hyun, C.-G. (2008b). Antibacterial and anti-inflammatory effects of Jeju medicinal plants against acne-inducing bacteria. *J. Gen. Appl. Microbiol.* 54, 101–106. doi: 10.2323/jgam.54.101
- Lemos, M. F., Lemos, M. F., Pacheco, H. P., Endringer, D. C., and Scherer, R. (2015). Seasonality modifies rosemary's composition and biological activity. *Ind. Crop. Prod.* 70, 41–47. doi: 10.1016/j.indcrop.2015.02.062
- Maree, J. E., and Viljoen, A. M. (2012). Phytochemical distinction between *Pelargonium sidoides* and *Pelargonium reniforme* — A quality control perspective. *South Afr. J. Bot.* 82, 83–91. doi: 10.1016/j.sajb.2012.07.007
- Mediani, A., Abas, F., Khatib, A., Maulidiani, H., Shaari, K., Choi, Y. H., et al. (2012). 1H-NMR-based metabolomics approach to understanding the drying effects on the phytochemicals in *Cosmos caudatus*. *Food Res. Int.* 49, 763–770. doi: 10.1016/j.foodres.2012.09.022
- Moco, S., Vervoort, J., Moco, S., Bino, R. J., De Vos, R. C. H., and Bino, R. (2007). Metabolomics technologies and metabolite identification. *TrAC Trends Anal. Chem.* 26, 855–866. doi: 10.1016/j.trac.2007.08.003
- Pacifico, S., Galasso, S., Piccolella, S., Kretschmer, N., Pan, S., Marciano, S., et al. (2015). Seasonal variation in phenolic composition and antioxidant and anti-inflammatory activities of *Calamintha nepeta* (L.) Savi. *Food Res. Int.* 69, 121–132. doi: 10.1016/j.foodres.2014.12.019
- Pendota, S. C., Aremu, A. O., Po, L., Rárová, L., Dole, K., and Van Staden, J. (2018). Identification and characterization of potential bioactive compounds from the leaves of *Leucosidea sericea*. *J. Ethnopharmacol.* 220, 169–176. doi: 10.1016/j.jep.2018.03.035
- Prinsloo, G., and Nogemane, N. (2018). The effects of season and water availability on chemical composition, secondary metabolites and biological activity in plants. *Phytochem. Rev.* 17, 889–902. doi: 10.1007/s11101-018-9567-z
- Rashed, K., Said, A., Zheng, Y.-T., Tawila, A., Fouche, G., El-fiky, N. M., et al. (2015). Anticancer, Anti HIV-1 and antimicrobial potentials of methanol extract and non polar fractions of *Citrus volkameriana* leaves and phytochemical composition. *Res. J. Med. Plant* 9, 201–214. doi: 10.3923/rjmp.2015.201.214
- Ridder, L., Van Der Hooft, J. J. J., Verhoeven, S., De Vos, R. C. H., Bino, R. J., and Vervoort, J. (2013). Automatic chemical structure annotation of an LC-MSn based metabolic profile from green tea. *Anal. Chem.* 85, 6033–6040. doi: 10.1021/ac400861a
- Ridder, L., Van Der Hooft, J. J. J., Verhoeven, S., De Vos, R. C. H., Vervoort, J., and Bino, R. J. (2014). In silico prediction and automatic LC-MSn annotation of green tea metabolites in urine. *Anal. Chem.* 86, 4767–4774. doi: 10.1021/ac403875b
- Sarrou, E., Martens, S., and Chatzopoulou, P. (2016). Metabolite profiling and antioxidative activity of Sage (*Salvia fruticosa* Mill.) under the influence of genotype and harvesting period. *Ind. Crop. Prod.* 94, 240–250. doi: 10.1016/j.indcrop.2016.08.022
- Scognamiglio, M., D'Ambrosia, B., Fiumano, V., Golino, M., Esposito, A., and Fiorentino, A. (2014). Seasonal phytochemical changes in *Phillyrea angustifolia* L.: metabolomic analysis and phytotoxicity assessment. *Phytochem. Lett.* 8, 163–170. doi: 10.1016/j.phytol.2013.08.012
- Sharma, R., Kishore, N., Hussein, A., and Lall, N. (2014). The potential of *Leucosidea sericea* against *Propionibacterium acnes*. *Phytochem. Lett.* 7, 124–129. doi: 10.1016/j.phytol.2013.11.005
- Sinha, P., Srivastava, S., Mishra, N., and Yadav, N. P. (2014). New perspectives on antiacne plant drugs: contribution to modern therapeutics. *Biomed Res. Int.* 2014:301304. doi: 10.1155/2014/301304
- Stein, S. E. (2014). *Mass Spectral Database and Software Version 2.2. National Institute of Standards and Technology (NIST)*. Gaithersburg, MD: Scientific Instrument Services.
- Tsai, T. H., Tsai, T. H., Wu, W. H., Tseng, J. T. P., and Tsai, P. J. (2010). In vitro antimicrobial and anti-inflammatory effects of herbs against *Propionibacterium acnes*. *Food Chem.* 119, 964–968. doi: 10.1016/j.foodchem.2009.07.062
- Vargas, I., SAanz, I., Moya, P., and Prima-Yufer, E. (2016). Antimicrobial and antioxidant compounds in the nonvolatile fraction of expressed orange essential oil. *J. Food Prot.* 62, 929–932. doi: 10.4315/0362-028x-62.8.929
- Xu, J. J., Liu, Z., Tang, W., Wang, G. C., Chung, H. Y., Liu, Q. Y., et al. (2015). Tangeretin from citrus reticulata inhibits respiratory syncytial virus replication and associated inflammation in vivo. *J. Agric. Food Chem.* 63, 9520–9527. doi: 10.1021/acs.jafc.5b03482
- Zu, Y., Yu, H., Liang, L., Fu, Y., Efferth, T., Liu, X., et al. (2010). Activities of ten essential oils towards *Propionibacterium acnes* and PC-3, A-549 and MCF-7 cancer cells. *Molecules* 15, 3200–3210. doi: 10.3390/molecules15053200

**Conflict of Interest:** The authors declare that the research was conducted in the absence of any commercial or financial relationships that could be construed as a potential conflict of interest.

Copyright © 2020 Sehlagkwe, Lall and Prinsloo. This is an open-access article distributed under the terms of the Creative Commons Attribution License (CC BY). The use, distribution or reproduction in other forums is permitted, provided the original author(s) and the copyright owner(s) are credited and that the original publication in this journal is cited, in accordance with accepted academic practice. No use, distribution or reproduction is permitted which does not comply with these terms.



# Identification and Quantification of Bioactive Molecules Inhibiting Pro-inflammatory Cytokine Production in Spent Coffee Grounds Using Metabolomics Analyses

Khanh-Van Ho<sup>1,2</sup>, Kathy L. Schreiber<sup>3</sup>, Jihyun Park<sup>1</sup>, Phuc H. Vo<sup>1</sup>, Zhentian Lei<sup>4,5</sup>, Lloyd W. Sumner<sup>4,5</sup>, Charles R. Brown<sup>6</sup> and Chung-Ho Lin<sup>1\*</sup>

<sup>1</sup> Center for Agroforestry, School of Natural Resources, University of Missouri, Columbia, MO, United States, <sup>2</sup> Department of Food Technology, Can Tho University, Can Tho, Vietnam, <sup>3</sup> Cell and Immunobiology Core, University of Missouri, Columbia, MO, United States, <sup>4</sup> Metabolomics Center, University of Missouri, Columbia, MO, United States, <sup>5</sup> Department of Biochemistry, Bond Life Sciences Center, University of Missouri, Columbia, MO, United States, <sup>6</sup> Department of Veterinary Pathobiology, University of Missouri, Columbia, MO, United States

## OPEN ACCESS

### Edited by:

Namrita Lall,  
University of Pretoria, South Africa

### Reviewed by:

Amit Krishna De,  
Indian Science Congress Association  
(ISCA), India  
Subhash Chandra Mandal,  
Government of West Bengal, India

### \*Correspondence:

Chung-Ho Lin  
LinChu@missouri.edu

### Specialty section:

This article was submitted to  
Ethnopharmacology,  
a section of the journal  
Frontiers in Pharmacology

**Received:** 21 November 2019

**Accepted:** 19 February 2020

**Published:** 06 March 2020

### Citation:

Ho K-V, Schreiber KL, Park J, Vo PH, Lei Z, Sumner LW, Brown CR and Lin C-H (2020) Identification and Quantification of Bioactive Molecules Inhibiting Pro-inflammatory Cytokine Production in Spent Coffee Grounds Using Metabolomics Analyses. *Front. Pharmacol.* 11:229. doi: 10.3389/fphar.2020.00229

In this study, we assessed the anti-inflammatory properties of spent coffee grounds. Methanolic extracts of spent coffee grounds obtained from 3 Arabica cultivars possess compounds that exerted inhibitory effects on the secretion of inflammatory mediators (TNF- $\alpha$ , IL-6, and IL-10) induced by a human pro-monocytic cell line differentiated with PMA and stimulated with lipopolysaccharide (LPS). Our results indicated that the cytokine suppressive activities of the spent coffee ground (SCG) extracts were different among coffee cultivars tested. Hawaiian Kona extracts exhibited inhibitory effects on the expression of 3 examined cytokines, Ethiopian Yirgacheffe extracts reduced the secretion of TNF- $\alpha$  and IL-6, and Costa Rican Tarrazu extracts decreased the secretion of IL-6 only. Untargeted metabolomics analyses of SCG extracts led to the putative identification of 26 metabolites with known anti-inflammatory activities. Multiple metabolites (i.e., chrysin, daidzein, eugenol, naringenin, naringin, oxyresveratrol, pectolinarin, resveratrol, tectochrysin, theaflavin, vanillic acid, and vitexin rhamnoside) identified in the SCGs represent possible novel anti-inflammatory compounds. Of the 26 identified metabolites, the 12 compounds that had high relative intensities in all of the extracts were successfully quantified using liquid chromatography-tandem mass spectrometry analyses. Results from the targeted analyses indicated that caffeine and 5-caffeoylquinic acid (CQA) were the most abundant compounds in the SCG extracts. The contents of caffeine ranged from 0.38 mg/g (Ethiopian Yirgacheffe) – 0.44 mg/g (Costa Rican Tarrazu), whereas 5-CQA concentrations were in the range of 0.24 mg/g (Costa Rican Tarrazu) – 0.34 mg/g (Ethiopian Yirgacheffe). The presence of multiple anti-inflammatory compounds in SCGs provides a promising natural source for cosmetic and pharmaceutical industries.

**Keywords:** untargeted analysis, metabolomics, phenolics, anti-inflammatory, spent coffee grounds



## INTRODUCTION

Coffee, one of the most frequently consumed beverages, is the second greatest valuable commodity worldwide after petroleum (Murthy and Naidu, 2012). Approximately 6 million tons of spent coffee grounds (SCG), consisting of the solid residues produced during the brewing process, are produced annually on a global level (Getachew and Chun, 2017). The SCGs contain a rich source of amino acids, alkaloids, fatty acids, oils, polyphenols, minerals, and polysaccharides (Campos-Vega et al., 2015) and have been investigated for use as value-added products. The SCGs have been proposed to have a wide range of cosmetics application stemming from its phytochemical composition (e.g., phenolic acids, flavonoids, caffeine) (Campos-Vega et al., 2015). Other possible applications include fertilizers, absorbers, fillers and additives for polymer composites, supplements in animal feed, and biofuels (Givens and Barber, 1986; Castro et al., 2011; Park et al., 2016; Zarrinbakhsh et al., 2016; Moustafa et al., 2017; Ribeiro et al., 2017).

Coffee grounds were utilized as a folk medicine to treat dysentery, external wounds and inflammation (Hänsel et al., 1993). Native people also traditionally valued roasted coffee beans for medical purposes to treat anemia, edema, headaches, hepatitis, malaria, neuralgia, sleep disorders, and conditions of weakness (Hänsel et al., 1993; Rättsch, 2005). The SCGs are thought to exert multiple potential health benefits, but few studies have investigated the anti-inflammatory potential of these coffee residues. Ramalakshmi et al. (2009) reported no inhibitory effects of SCGs on expression of tumor necrosis factor (TNF)- $\alpha$  in the J774A.1 cell model system. In another study, López-Barrera et al. (2016) evaluated the effects of SCG fractions fermented by human gut flora on the cytokine secretion induced by lipopolysaccharide (LPS)-stimulated RAW 264.7 macrophages. This group reported that these SCG fractions significantly reduced the secretion of 3 cytokines [interleukin (IL)-1 $\beta$ , IL-10, and chemokine ligand (CCL) 17] out of the 40 examined cytokines/chemokines tested. The cytokine inhibition of the human gut fermented, unabsorbed SCG fractions were reported to be mediated primarily by short-chain fatty acids derived from dietary fiber (López-Barrera et al., 2016). In fact, multiple bioactive compounds in the SCGs (alkaloids and polyphenols) with known anti-inflammatory activities are potential sources of these cytokine suppressive effects. Similarly, bioactive compounds (e.g., caffeine, gallic acid, monocatecholquinic acids) identified in SCG have been reported to possess anti-inflammatory activities (Kim et al., 2005; Bravo et al., 2012; Hwang et al., 2014; Köroğlu et al., 2014). Despite these findings, the profiles of anti-inflammatory compounds in SCG from different coffee cultivars have not been adequately compared and characterized.

In this study, we described the inhibitory effects of SCG extracts derived from 3 Arabica cultivars on the expression of 3 inflammatory mediators (TNF- $\alpha$ , IL-6, and IL-10) using the human pro-monocytic cell line U-937. We subsequently identified and quantified the bioactive compounds in SCGs by metabolomics approaches. The integration of the cellular bioassay, untargeted chemical profiling, and targeted analyses is a powerful way to explore global activity metabolites

with known as well as unknown physico-chemical properties (Rinschen et al., 2019).

## MATERIALS AND METHODS

### Sample Preparation

Ground roast coffees from three Arabica cultivars including Costa Rican Tarrazu, Ethiopian Yirgacheffe, and Hawaiian Kona were purchased from Lakota Coffee Company (Columbia, MO, United States). Spent coffee grounds from these coffee cultivars were obtained from a coffee maker (Bunn VP17-2, Springfield, IL, United States) after brewing of the ground roast coffee for 5 min at 90°C. The SCG was immediately homogenized using a coffee grinder (CBG100S, Black + Decker, Beachwood, OH, United States). The homogenized samples (25 g wet weight, 78% water) were extracted in 100 mL of methanol (HPLC grade, Fisher Scientific, Pittsburgh, PA) twice and then sonicated at 10°C for 60 min as previously described in Ho et al. (2019). Subsequently, the methanolic extract was filtered through a 125 mm Whatman filter paper (GE Healthcare, Chicago, IL, United States) under SPE Vacuum Manifold (Visiprep<sup>TM</sup> SPE Vacuum Manifold, Sigma-Aldrich, United States), and then the supernatant was collected and stored at -20°C until analysis. The extract was allowed to thaw at room temperature, vortexed for 30 s, and then filtered through a 0.2  $\mu$ m syringe Anotop membrane filter (Whatman) prior to the analysis. For cellular assays, the resulting supernatant was evaporated until dryness under a flow of nitrogen. The dry extract was then resuspended with DMSO (Sigma-Aldrich, United States) at concentration of 5,000 mg/mL. Cytokine modulating activities of the extract were identified using BD<sup>TM</sup> cytometric bead array (CBA) kits (BD Biosciences, San Jose, CA, United States). For untargeted chemical profiling and targeted analyses, the extracts from each cultivar were injected in triplicate into ultra-high performance liquid chromatography coupled with high resolution mass spectrometer (UHPLC-HRMS) and HPLC with tandem mass-spectrometer (HPLC-MS/MS), respectively.

### Cell Culture and Differentiation Induction

The human monocyte cell line U-937 was obtained from American Type Culture Collection (ATCC) (CRL-1593.2, ATCC, Manassas, VA, United States). Cells were grown in complete Roswell Park Memorial Institute (RPMI) medium (RPMI 1640, ATCC) supplemented with 10% fetal bovine serum (FBS, Sigma-Aldrich) and 100  $\mu$ g/mL gentamicin at 37°C in a humidified incubator with 5% CO<sub>2</sub>. To induce differentiation of U-937 cells into macrophage-like cells, U-937 cells were seeded at  $2 \times 10^5$  cells/well in 96 well plates containing 50 nM of phorbol 12-myristate 13-acetate (PMA, Sigma-Aldrich) for 48 h (Rovera et al., 1979). Subsequently, the PMA-differentiated cells were washed twice and cultured in fresh growth media. The cells were incubated for an additional 18 h before pre-treatment with SCG extracts prepared from three cultivars. The SCG extracts were added in triplicate at 3 final concentrations (0.05, 0.5, and 5 mg/mL) for 2 h prior to stimulation with 1  $\mu$ g/mL

LPS (*Escherichia coli* 0127:B8, Sigma-Aldrich). Dexamethasone (Sigma-Aldrich), an anti-inflammatory agent known to inhibit cytokine secretion, was used as positive control at a concentration of 0.002 mg/mL. SCG extracts were resuspended in tissue culture-grade DMSO, and the highest concentration of DMSO in any sample was 0.1%. Therefore, a vehicle control of 0.1% DMSO was included in all experiments and served as a point of reference. After the addition of LPS for 22 h, the culture supernatants from each triplicate group were pooled, spun to remove cell debris, transferred to new tubes, and stored at -20°C until analysis.

## Cell Viability Analysis

MTT assays were performed to evaluate possible effects of the SCGs on cytotoxicity and/or cell loss. Briefly, cellular activity of mitochondrial dehydrogenase activity was measured using a colorimetric cell viability assay after removal of the supernatants. MTT substrate (Mosmann, 1983) was added to the cells in DMEM high glucose, phenol-red free media containing 1% FBS for 3 h at 37°C until formazan crystals were observed. Crystals were dissolved in acidified isopropanol, and samples were pipetted up and down several times to ensure that the crystals were completely dissolved before readings were taken. Absorbance was measured within 30 min after solvent addition using a BioTek ELx808 microplate reader (BioTek, Winooski, VT, United States). Formazan crystals were detected at a wavelength of 570 nm, and background absorbance was measured at 630 nm.

## Quantification of Cytokines/Chemokines Expression

A multiplex flow cytometric bead-based assay was used to quantitate the amount of secreted cytokines in the U-937 cells in the absence or presence of the SCG extracts. Multiple experiments were performed, and each cultivar was tested at 3 concentrations. Preparation of samples using the BD Cytometric Bead Array (CBA) human inflammatory cytokines kit was carried out according to the manufacturer's recommendations. For these studies, the analysis focused on a subset of inflammatory cytokines (TNF- $\alpha$ , IL-6, and IL-10) present in the kit. Triplicate samples were collected on a BD LSR Fortessa X-20 cell analyzer (BD Biosciences, San Jose, CA, United States) using instrument settings suggested by BD and optimized in each experiment. A cytokine standard curve was included in each experiment, and cytokine levels were calculated from a five-parameter logistic curve using a curve-fitting software.

## Untargeted Metabolomics Analyses to Putatively Identify Anti-inflammatory Molecules

The extracts were analyzed using an UHPLC system coupled to a maXis impact quadrupole-time-of-flight high-resolution mass spectrometer (Q-TOF) (Bruker Co., Billerica, MA, United States) operated in both negative and positive electrospray ionization modes with the nebulization gas pressure at 43.5 psi, dry gas of 12 L/min, dry temperature of 250°C and a capillary voltage of 4000 V, as described in Ho et al. (2018). The SCG

extracts obtained from 3 Arabica cultivars were separated using a Waters Acquity UHPLC BEH C18 column (2.1  $\times$  150 mm, 1.7  $\mu$ m particles size) at 60°C. The solvent system was 0.1% formic acid in water (A) and 100% acetonitrile (B). The gradient elution used started with a linear gradient of 95%: 5–30%: 70% eluents A: B in 30 min. Subsequently, the separation was followed by a linear wash gradient as follows 70–95% B, 95% B, 95–5% B, and 5% B at 30–33 min, 33–35 min, 35–36 min, and 37–40 min, respectively. The flow rate was 0.56 mL/min. Mass spectral data were collected automatically using a scan range from m/z 100 to 1,500 and auto-calibrated using sodium formate after data acquisition. Each coffee cultivar and methanol blank (served as a control) were analyzed in triplicate.

## Targeted Metabolomics Analysis to Determine Contents of Major Anti-inflammatory Molecules

Major metabolites that had high relative intensities across the SCG extracts were selected for absolute quantification of their contents using liquid chromatography-tandem mass spectrometry (LC-MS/MS) analysis with authentic standards. The LC-MS/MS analyses were performed using an HPLC system (Water Alliance 2695, Water Co., Milford, MA, United States) coupled to a Waters Acquity TQ triple quadrupole mass spectrometer operated in negative electrospray ionization mode with the nebulization gas pressure at 43.5 psi, dry gas of 12 L/min, dry temperature of 250°C and a capillary voltage of 1500 V. The compounds in the SCG extracts (20  $\mu$ L volume per injection) from three coffee cultivars were separated using a Phenomenex Kinetex C18 reverse-phase column (100  $\times$  4.6 mm; 2.6  $\mu$ m particle size, Torrance, CA, United States) at 25°C. The mobile phases were 0.1% formic acid in water (A) and 100% acetonitrile (B). The gradient elution used were 2% B, 2–80% B, 80–98% B, 2% B at 0–0.5 min, 0.5–7 min, 7.0–9.0 min, 9.0–15.0 min, respectively at a flow rate of 0.5 mL/min. MS detection was performed by MS/MS using the multiple reaction monitoring (MRM) mode. Waters IntelliStart optimization software was used to optimize collision, ionization energy, MRM and SIR (single ion recording) transition ions (molecular and product ions), capillary and cone voltage, desolvation gas flow, and collision energy. Waters Empower 3 software was used to analyze data. The concentrations of major anti-inflammatory compounds found in SCG extracts were determined based on a standard curve for each analyte generated using authentic standards of these compounds (purity > 95%, Sigma-Aldrich) at 8 concentrations (0.01, 0.025, 0.05, 0.1, 0.5, 1, 5, 10 ppm) in triplicate.

Assessment of the sensitivity of the analytical method was performed by calculating the limit of detection (LOD) and limit of quantification (LOQ). The LOD and LOQ for each compound were calculated by employing signal-to-noise ratios of three and ten. The extraction recover rates of the fortified internal standards colchicine and  $\beta$ -naphthylsulfate were used to determine the efficiencies of the extraction procedure. For the extraction procedure, 100  $\mu$ g of each internal standard was fortified. The recovery rates were greater than 95%.

## Data Processing and Statistical Analysis

Cell viability and cytokine concentrations were determined relative to control samples (in the presence of DMSO vehicle and without cultivars). Relative cell viability (%) was obtained by dividing the MTT absorbance of treated samples by those in control samples, and multiplying by 100. Relative cytokine secretions (%) were calculated by dividing the cytokine concentration of treated samples by those in control samples, and multiplying by 100. Relative cell viability, relative cytokine secretion, concentrations of anti-inflammatory compounds obtained from LC-MS/MS analysis were analyzed as a completely randomized design using PROC MIXED in SAS 9.4 (SAS Institute, Cary, NC, United States). The coffee extract (treatment) was the fixed effect and replication was the random variable. Differences between extracts were determined using Fisher's LSD at  $p < 0.01$ .

The UHPLC-MS data was analyzed based on the procedure described by Ho et al. (2019). First, the original LC-MS data files were converted to NetCDF format files and were uploaded to XCMS online platform<sup>1</sup> (Tautenhahn et al., 2012). The XCMS data were processed with parameters as follows: pairwise analyses between each coffee cultivar and the control (methanol) were conducted in centWave mode for feature detection (1  $m/z$  = 10 ppm, minimum peak width = 5 s, and maximum peak width = 20 s), an obiwarp method was selected for retention time correction (profStep = 1), chromatogram alignment was set as minfrac = 0.5, bw = 5, mzwid = 0.015, max = 100, minsamp = 1, adducts was optimized for UPLC/Bruker Q-TOF in both ESI(+) and ESI(-) and plant was selected for sample biosource for identification, and the unpaired parametric  $t$ -test (Welch  $t$ -test) was used for the statistical analysis. Metabolites of significant features ( $p < 0.01$  and intensity  $\geq 10,000$ ) were putatively identified based on the accurate mass of the molecular ions, referenced to METLIN metabolite mass spectral database containing over 1 million molecules<sup>2</sup> (Guijas et al., 2018). Metabolites with known to possess anti-inflammatory activities were used to predict anti-inflammatory compounds in each cultivar (Supplementary Table S1). To further characterize differences in profiles of anti-inflammatory compounds among examined coffee cultivars, partial least squares-discriminant analysis (PLS-DA) was performed via a web-based tool MetaboAnalyst (Chong et al., 2018).

## RESULTS

### Cell Viability Analysis

Cell viability assays were performed to address any potential cytotoxic effects of the SCG cultivars. A reduction in MTT absorbance could result from a loss of cell viability, a reduction in cell number, a decrease in mitochondrial activity, an inhibition of cytokine secretion, or a combination of these factors. The MTT viability assays were carried out immediately after the cell supernatants were collected. Dexamethasone, a known

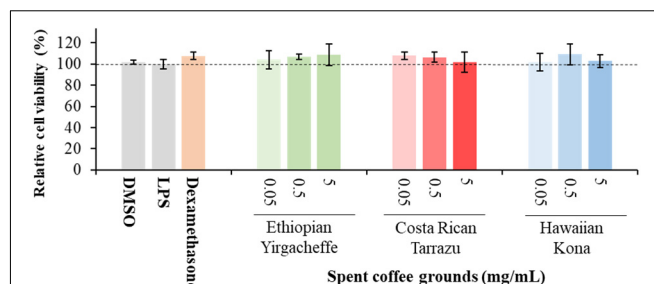


**FIGURE 1 |** Effect of DMSO, lipopolysaccharide (LPS), Dexamethasone, and spent coffee ground extracts on the viability of PMA-differentiated U-937 cells. DMSO, PMA-differentiated cells treated with 0.1% DMSO, no LPS, no coffee extracts; LPS, LPS and DMSO; coffee extracts, coffee extracts, DMSO and LPS; Dexamethasone, 0.2  $\mu$ g/mL dexamethasone, DMSO, and LPS. Mean  $\pm$  SEM.

inhibitor of cytokine secretion, was included as a positive control. Preliminary experiments using a wide range of DMSO concentrations indicated that DMSO did not affect U-937 cell number or viability as assessed by trypan blue exclusion (data not shown) at the concentrations used in this study, indicating that DMSO is not toxic under the experimental conditions. Therefore, a reduction in MTT absorbance in the presence of the cultivars would indicate a toxic effect of the cultivar rather than the vehicle.

The results shown in **Figure 1** illustrate that cell viability in all treatment groups (PMA-differentiated U-937 cells with the addition of SCGs, dexamethasone, LPS) was not significantly different compared to those in the control cultures (PMA-differentiated U-937 cells with DMSO but without LPS and SCG extracts). These results demonstrate that the SCG extracts and dexamethasone did not show any toxic effects on PMA-differentiated U-937 cells at any of the concentrations tested, and they were further examined for their effects on cytokine secretion.

### Impact of Spent Coffee Ground Extracts on Cytokine Secretion

Cytokine secretion was analyzed as a possible indicator of systemic inflammation using the U-937 model system. Secreted cytokine levels were measured in the absence or presence of SCG extracts, with the results expressed relative to control samples cultured with vehicle in the absence of SCG extracts. Three representative cytokines, TNF- $\alpha$ , IL-6, and IL-10, were chosen to reflect both anti-inflammatory as well as pro-inflammatory properties.

As shown in **Figures 2–4**, inclusion of Hawaiian Kona extracts in the cultures for 2 h prior to the addition of LPS reduced the levels of all 3 cytokines. This effect was dose-dependent, illustrated by a reduction in TNF- $\alpha$  secretion of 25.8, 29.9, and 60.5%, and in IL-6 levels by 32.1, 49.7, and 52.5%, at concentrations of 0.05, 0.5, and 5.0 mg/mL, respectively. TNF- $\alpha$  levels were reduced by 34.4 and 37.8% after pre-incubation of SCG extracts obtained from Ethiopian Yirgacheffe at concentrations of 0.5 and 5.0 mg/mL, respectively, but were not statistically different following pre-incubation with Costa Rican Tarrazu SCGs. A similar reduction in IL-6 levels was observed

<sup>1</sup> www.xcmsonline.scripps.edu

<sup>2</sup> http://metlin.scripps.edu



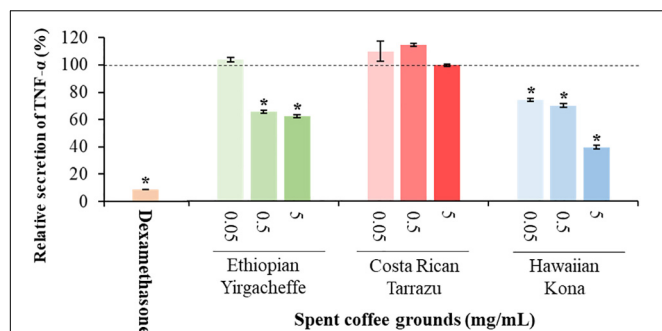


**FIGURE 2 |** Effect of spent coffee ground extracts on the secretion of TNF- $\alpha$  by PMA-differentiated, LPS-stimulated U937 cells. Dexamethasone was used at 0.2  $\mu$ g/mL as a positive control. (\*) Significant decrease ( $p < 0.001$ ) compared to PMA-differentiated, LPS-stimulated U937 cells in the absence of extract. Mean  $\pm$  SEM.

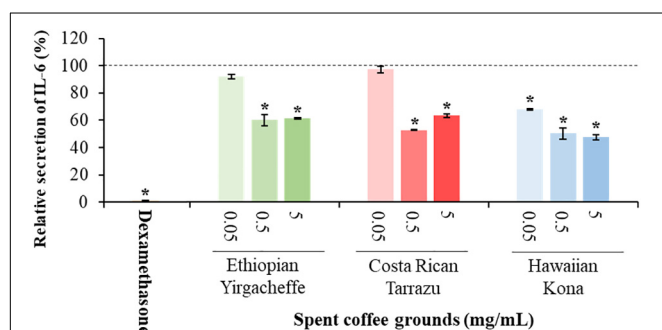


**FIGURE 3 |** Effect of spent coffee ground extracts on the secretion of IL-6 by PMA-differentiated, LPS-stimulated U937 cells. Dexamethasone was used at 0.2  $\mu$ g/mL as a positive control. (\*) Significant decrease ( $p < 0.001$ ) compared to PMA-differentiated, LPS-stimulated U937 cells in the absence of extract. Mean  $\pm$  SEM.

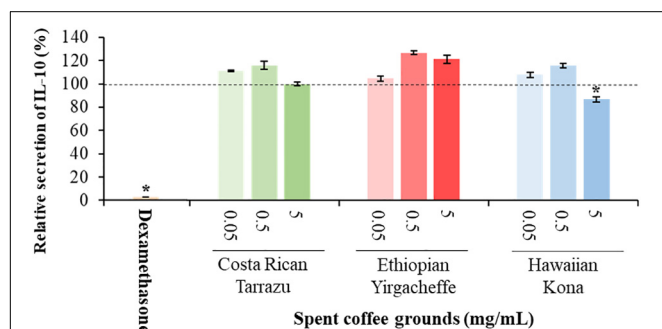


**FIGURE 4 |** Effect of spent coffee ground extracts on the secretion of IL-10 by PMA-differentiated, LPS-stimulated U937 cells. Dexamethasone was used at 0.2  $\mu$ g/mL as a positive control. (\*) Significant decrease ( $p < 0.001$ ) compared to PMA-differentiated, LPS-stimulated U937 cells in the absence of extract. Mean  $\pm$  SEM.

in cultures containing Ethiopian Yirgacheffe and Costa Rican Tarrazu extracts at the two highest concentrations of 0.5 and 5.0 mg/mL, with a decrease of 40.0, and 38.9%, and of 47.2 and 36.6%, respectively. No effect on IL-6 levels was observed at

the lower concentration of 0.05 mg/mL when U-937 cells were cultured with either extract. The effect on IL-10 secretion was minimal for all three SCG extracts, and the only minor effect noted was a 13.3% reduction after addition of the Hawaiian Kona extract at 5.0 mg/mL. Cytokine levels were reduced to over 90% for all 3 cytokines examined in the presence of the positive control agent dexamethasone, a known inhibitor of cytokine secretion.

## UHPLC-HRMS Analyses Revealed Anti-inflammatory Metabolite Profiles of the Spent Coffee Grounds

LC-MS fingerprints of anti-inflammatory molecules in the extracts were obtained from the liquid chromatography–high resolution MS (LC-HRMS) analysis. The UHPLC-HRMS data processed with XCMS Online resulted in 2,418 significant features in ionization positive mode and 162 features in the negative ionization mode. These features were annotated using METLIN metabolite database, which resulted in the putative identification of 26 metabolites with known anti-inflammatory activities (Supplementary Table S1). These metabolites included a alkaloid and polyphenolic compounds (Table 1). Twelve out of 26 anti-inflammatory metabolites that had high relative intensities across the SCG extracts of all coffee cultivars (Figure 5) were further selected for the absolute quantification of the concentrations in the SCG extracts by LC-MS/MS analyses with authentic standards (Tables 2, 3).

## LC-MS/MS Analyses Indicated Significant Differences in Anti-inflammatory Profiles of Three Coffee Cultivars

All 12 selected anti-inflammatory metabolites including caffeine, 5-caffeoylquinic acid (5-CQA), quinic acid, vanillic acid, caffeic acid, epicatechin, catechin, ferulic acid, 3-CQA, p-coumaric acid, p-hydroxybenzoic acid, gallic acid were found in Ethiopian Yirgacheffe extracts, while 10 out of 12 metabolites were detected in Costa Rican Tarrazu and Hawaiian Kona extracts (Table 3). The contents of these anti-inflammatory compounds in SCG vary among tested coffee cultivars. Caffeine, a methylxanthine alkaloid, was the most dominant compound in all examined coffee cultivars. The concentrations of caffeine were found to be the significant higher in Costa Rican Tarrazu ( $439.0 \pm 4.0$   $\mu$ g/g) and Hawaiian Kona ( $426.9 \pm 1.3$   $\mu$ g/g) than that in Ethiopian Yirgacheffe ( $384.5 \pm 1.1$   $\mu$ g/g). The most abundant phenolic compound in all examined coffee cultivars was 5-CQA. Ethiopian Yirgacheffe contained the richest abundance of 5-CQA ( $338.1 \pm 1.7$   $\mu$ g/g), followed by Hawaiian Kona ( $293.5 \pm 1.8$   $\mu$ g/g) and Costa Rican Tarrazu ( $236.7 \pm 1.5$   $\mu$ g/g). The abundance of quinic acid ranked second among the examined phenolic compounds. This compound was found to be at the highest amount in Costa Rican Tarrazu ( $238.3 \pm 0.5$   $\mu$ g/g), followed by and Hawaiian Kona ( $218.8 \pm 0.3$   $\mu$ g/g) and Costa Rican Tarrazu ( $207.4 \pm 0.5$   $\mu$ g/g). The contents of other compounds with an exception of 3-CQA were found to be present at the higher abundances in Ethiopian Yirgacheffe compared to other cultivars, while there were no significant



**TABLE 1** | Metabolites with known anti-inflammatory activities in spent coffee grounds from three Arabica cultivars via untargeted metabolomics analyses.

No.	Putatively identified compound	Retention time (min)	Theoretical mass	Exact mass	$\Delta$ ppm	Adducts	Predicted formula
1	3-Caffeoylquinic acid <sup>a,b</sup>	1.56	353.0866	353.0872	-1.70	[M-H]	C <sub>16</sub> H <sub>18</sub> O <sub>9</sub>
2	5-Caffeoylquinic acid <sup>a,b</sup>	2.24	353.0871	353.0872	-0.28	[M-H]	C <sub>16</sub> H <sub>18</sub> O <sub>9</sub>
3	3,5-Caffeoylquinic acid <sup>a</sup>	6.67	539.1162	539.1165	-0.56	[M + Na]	C <sub>25</sub> H <sub>24</sub> O <sub>12</sub>
4	Caffeic acid <sup>a,b</sup>	1.55	179.0348	179.0344	2.23	[M-H]	C <sub>9</sub> H <sub>8</sub> O <sub>4</sub>
5	Caffeine <sup>a,b</sup>	0.41	195.0881	195.0882	-0.51	[M + H]	C <sub>8</sub> H <sub>10</sub> N <sub>4</sub> O <sub>2</sub>
6	Catechin <sup>a,b</sup>	3.74	289.0697	289.0712	-5.19	[M-H]	C <sub>15</sub> H <sub>14</sub> O <sub>6</sub>
7	Chrysin <sup>a</sup>	20.28	255.0655	255.0657	-0.78	[M + H]	C <sub>15</sub> H <sub>10</sub> O <sub>5</sub>
8	Daidzein <sup>a</sup>	20.28	255.0655	255.0657	-0.78	[M + H]	C <sub>15</sub> H <sub>10</sub> O <sub>4</sub>
9	Epicatechin <sup>a,b</sup>	2.68	289.0708	289.0712	-1.38	[M-H]	C <sub>15</sub> H <sub>14</sub> O <sub>6</sub>
10	Eugenol <sup>a</sup>	5.55	165.0926	165.0916	6.06	[M + H]	C <sub>10</sub> H <sub>12</sub> O <sub>2</sub>
11	Ferulic acid <sup>a,b</sup>	2.67	193.0504	193.0501	1.55	[M-H]	C <sub>10</sub> H <sub>10</sub> O <sub>4</sub>
12	Gallic acid <sup>a,b</sup>	16.05	208.9846	208.9852	-2.87	[M + K]	C <sub>7</sub> H <sub>6</sub> O <sub>5</sub>
13	Naringenin <sup>a</sup>	5.29	271.0610	271.0606	1.48	[M-H]	C <sub>15</sub> H <sub>12</sub> O <sub>5</sub>
14	Naringin <sup>a</sup>	19.21	581.1843	581.1870	-4.65	[M + H]	C <sub>27</sub> H <sub>32</sub> O <sub>14</sub>
15	Oxyresveratrol <sup>a</sup>	13.65	407.1341	407.1342	-0.25	[M + H]	C <sub>20</sub> H <sub>22</sub> O <sub>9</sub>
16	p-Coumaric acid <sup>a,b</sup>	2.17	163.0403	163.0395	4.91	[M-H]	C <sub>9</sub> H <sub>8</sub> O <sub>3</sub>
17	p-Hydroxybenzoic acid <sup>a,b</sup>	0.76	139.0386	139.0395	-6.47	[M-H]	C <sub>7</sub> H <sub>6</sub> O <sub>3</sub>
18	Pectolinarin <sup>a</sup>	31.87	621.1827	621.1819	1.29	[M-H]	C <sub>29</sub> H <sub>34</sub> O <sub>15</sub>
19	Quercetin <sup>a</sup>	6.73	489.1359	489.1397	-7.77	[M-H]	C <sub>24</sub> H <sub>26</sub> O <sub>11</sub>
20	Quinic acid <sup>a,b</sup>	0.59	191.0562	191.0556	3.14	[M-H]	C <sub>7</sub> H <sub>12</sub> O <sub>6</sub>
21	Resveratrol <sup>a</sup>	7.71	229.0862	229.0864	-0.87	[M + H]	C <sub>14</sub> H <sub>12</sub> O <sub>3</sub>
22	Rutin <sup>a</sup>	13.65	407.1341	407.1342	-0.25	[M + H]	C <sub>20</sub> H <sub>22</sub> O <sub>9</sub>
23	Tectochrysin <sup>a</sup>	8.42	291.0627	291.0633	-2.06	[M + Na]	C <sub>16</sub> H <sub>12</sub> O <sub>4</sub>
24	Theaflavin <sup>a</sup>	13.01	565.1354	565.1346	1.42	[M + H]	C <sub>29</sub> H <sub>24</sub> O <sub>12</sub>
25	Vanillic acid <sup>a,b</sup>	3.70	335.0758	335.0767	-2.69	[M + H]	C <sub>16</sub> H <sub>14</sub> O <sub>8</sub>
26	Vitexin rhamnoside <sup>a</sup>	15.20	601.1539	601.1533	1.00	[M + Na]	C <sub>27</sub> H <sub>30</sub> O <sub>14</sub>

<sup>a</sup>Putative identification by UHPLC-HRMS. <sup>b</sup>Absolute concentrations were determined by LC-MS/MS with authentic standards.

differences in the contents of these compounds in Costa Rican Tarrazu and Hawaiian Kona. The concentrations of vanillic acid, caffeic acid, catechin, p-coumaric acid, p-hydroxybenzoic acid in Ethiopian Yirgacheffe were  $86.2 \pm 2.8 \mu\text{g/g}$ ,  $54.5 \pm 1.5 \mu\text{g/g}$ ,  $24.0 \pm 2.2 \mu\text{g/g}$ ,  $18.3 \pm 1.8 \mu\text{g/g}$ ,  $27.9 \pm 0.3 \mu\text{g/g}$ , respectively, while that of Costa Rican Tarrazu and Hawaiian Kona were  $53.9 \pm 1.3 \mu\text{g/g}$  and  $54.3 \pm 1.4 \mu\text{g/g}$ ,  $41.5 \pm 0.9 \mu\text{g/g}$  and  $43.4 \pm 0.5 \mu\text{g/g}$ ,  $1.9 \pm 0.3 \mu\text{g/g}$ , and  $1.4 \pm 0.3 \mu\text{g/g}$ ,  $0.7 \pm 0.1 \mu\text{g/g}$  and  $0.7 \pm 0.1 \mu\text{g/g}$ ,  $1.9 \pm 0.2 \mu\text{g/g}$ , and  $2.2 \pm 0.1 \mu\text{g/g}$ , respectively. Epicatechin and ferulic acid were not detectable in Costa Rican Tarrazu and Hawaiian Kona extracts, but were present in Ethiopian Yirgacheffe extracts at concentrations of  $37.2 \pm 1.5 \mu\text{g/g}$  and  $21.1 \pm 0.6 \mu\text{g/g}$ , respectively. No significant difference in the abundance of 3-CQA was found among all SCG extracts. This compound was found to be at minor levels in all three coffee extracts with its contents ranging from  $2.9 \pm 0.2 \mu\text{g/g}$  (Costa Rican Tarrazu) to  $3.9 \pm 0.5 \mu\text{g/g}$  (Hawaiian Kona).

To further characterize differences in anti-inflammatory profiles in SCGs obtained from different coffee cultivars, partial least squares-discriminant analysis (PLS-DA) were performed. A cross-validation method was utilized to evaluate model quality and resulting R<sup>2</sup> and Q<sup>2</sup> values were 0.99 and 0.97, respectively, indicating that the model was reliable. PLS-DA score plot with two principal components covered 99.3% of total variability of the data (Figure 6A), revealing significant differences

in anti-inflammatory profiles in SCG derived from different examined coffee cultivars. The first principal components (PC1) explained 89.3% of the total variability of the data, whereas the second principal components (PC2) accounted for 10.0% of the total variability of the data set. In the PLS-DA score plot, all 3 coffee cultivars were distributed separately along the PC1. Regarding the PC2, Costa Rican Tarrazu and Ethiopian Yirgacheffe relatively shared a similar pattern, and Hawaiian Kona differed from other cultivars. Variable importance in projection (VIP) analyses revealed 5-CQA, quinic acid, and caffeine were the most important compounds (Figure 6B). These compounds also were major compounds found in all tested cultivars (Table 3).

## DISCUSSION

Given the huge availability of SCGs, determination of bioactive compounds found within complex mixtures is an important step toward developing novel value-added byproducts that may potentially increase the sustainability of the coffee agro-industry (Kovalcik et al., 2018). In the present study, we demonstrated that methanolic extracts of SCGs possess compounds that exerted inhibitory effects on the secretion of inflammatory mediators (TNF- $\alpha$ , IL-6, and IL-10) induced in a human pro-monocytic cell line differentiated with PMS and stimulated with LPS. The

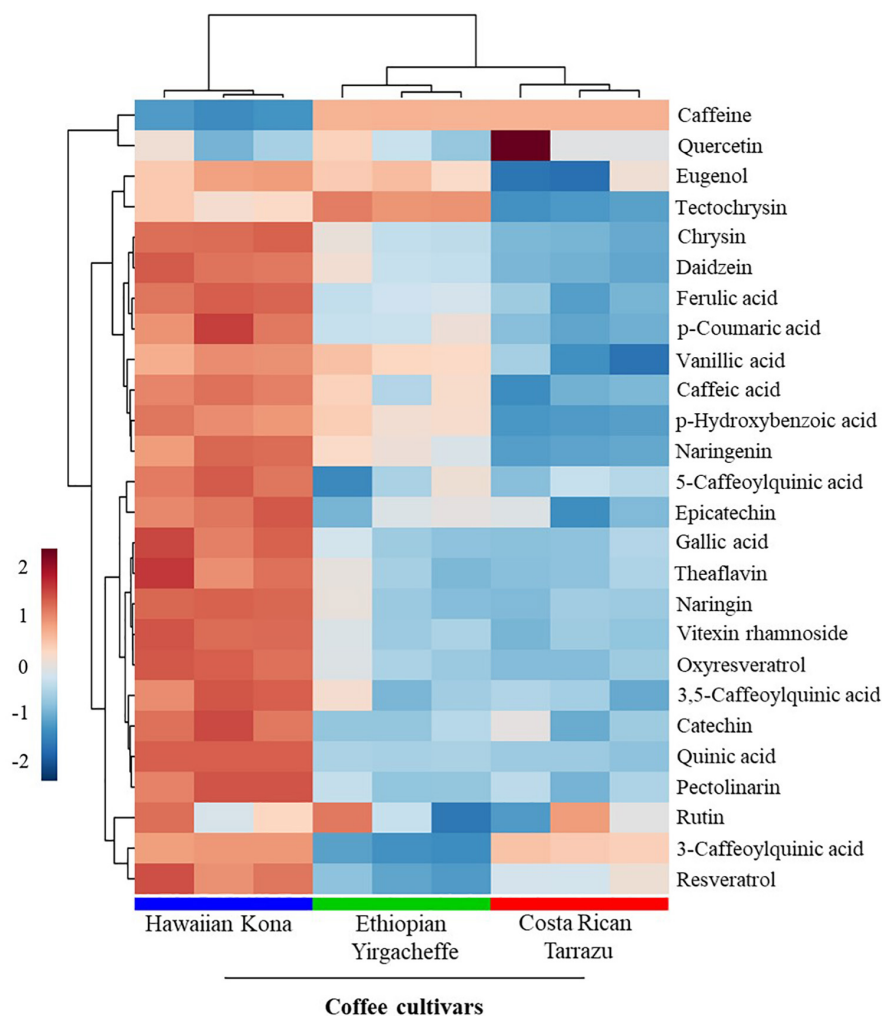


**FIGURE 5 |** Relative intensities of metabolites with known anti-inflammatory activities in spent coffee grounds. In the heatmap, red represents higher relative abundance, whereas blue represents lower relative abundance.

pro-inflammatory mediators TNF- $\alpha$  and IL-6 are key regulators of innate and adaptive immune responses, and they play a role in disease onset and persistence. As such, they offer potential therapeutic targets for the treatment of acute chronic diseases such as rheumatoid arthritis (Smolen and Aletaha, 2015). IL-10 is a potent immune-modulatory cytokine that has broad anti-inflammatory properties (O'Garra et al., 2008), including the inhibition of TNF production (Smallie et al., 2010). Our results indicated that the cytokine suppressive activities of SCG extracts were different among the coffee cultivars tested. Hawaiian Kona extracts affected the secretion of all 3 examined cytokines in the U-937 model system, whereas Ethiopian Yirgacheffe extracts reduced the secretions of TNF- $\alpha$  and IL-6 only and Costa Rican Tarrazu decreased the secretion of IL-6 only. Cell viability is similar in the absence and presence of all three SCGs extracts, demonstrating that the reduction in cytokine levels is not a result of direct toxic effects. It is possible that the varying levels of cytokine suppressive

activities among the Arabica cultivars arise from the differences in the composition and proportions of the anti-inflammatory compounds present in the different SCG extracts (Figure 6). The presence of multiple compounds in the cultivars also raises the possibility that different compounds in the same mixture may modulate each other's activity. For example, the overall cytokine concentration may be determined by a net balance between stimulatory and inhibitory activities. Likewise, there might be synergism between two inhibitory compounds, resulting in a more profound decrease in cytokine release. The involvement of multiple compounds on cytokine secretion might explain why Hawaiian Kona extracts exhibited inhibitory effects on all three cytokines, whereas the other cultivars had a more limited effect on cytokine secretion. Our findings suggested that SCG extracts from Hawaiian Kona have very distinct profiles of anti-inflammatory molecules and other metabolites as compared to the extracts from other cultivars (Figures 5, 6). The significant higher levels of the bioactive compounds with known

**TABLE 2 |** Molecular and product ions, retention times, linear correlation coefficients, LOD, and LOQ of anti-inflammatory compounds identified in spent coffee ground extracts.

Compound	Molecular ions (m/z)	Product ions (m/z)	Retention time (min)	Polarity	Linear equation <sup>a</sup>	Correlation coefficient (R <sup>2</sup> )	LOD <sup>b</sup> (μg/g)	LOQ <sup>c</sup> (μg/g)
5-Caffeoylquinic acid	353	191.04	5.71	ES-	$y = 96973x$	0.9963	0.043	0.142
Quinic acid	190.83	85	2.17	ES-	$y = 123139x$	0.9985	0.023	0.076
Vanillic acid	166.86	–	6.75	ES-	$y = 21505x$	0.9978	0.104	0.346
Caffeic acid	178.88	135	6.65	ES-	$y = 745425x$	0.9994	0.010	0.033
Epicatechin	288.63	109	6.54	ES-	$y = 22414x$	0.9912	0.084	0.279
p-Hydroxybenzoic acid	136.88	93	6.52	ES-	$y = 269043x$	0.9929	0.030	0.100
Catechin	288.65	109.2	6.31	ES-	$y = 18248x$	1.00	0.056	0.186
Ferulic acid	193	134.09	7.43	ES-	$y = 131247x$	0.9993	0.021	0.069
p-Coumaric acid	163.07	119	7.26	ES-	$y = 403050x$	0.9914	0.012	0.04
3-Caffeoylquinic acid	353	191	2.51	ES-	$y = 541946x$	0.9995	0.005	0.017
Gallic acid	169	125	2.48	ES-	$y = 234571x$	0.9862	0.005	0.016
Caffeine	195.01	137.9	6.28	ES+	$y = 2E-07x$	0.9842	0.002	0.007

<sup>a</sup>Linear equation indicate relationship between peak area of anti-inflammatory compounds and concentration in standard solutions. <sup>b</sup>LOD, limit of detection. <sup>c</sup>LOQ, limit of quantitation.

**TABLE 3 |** Polyphenols and caffeine (LC-MS/MS) contents (μg/g of dry weight) in spent coffee grounds.

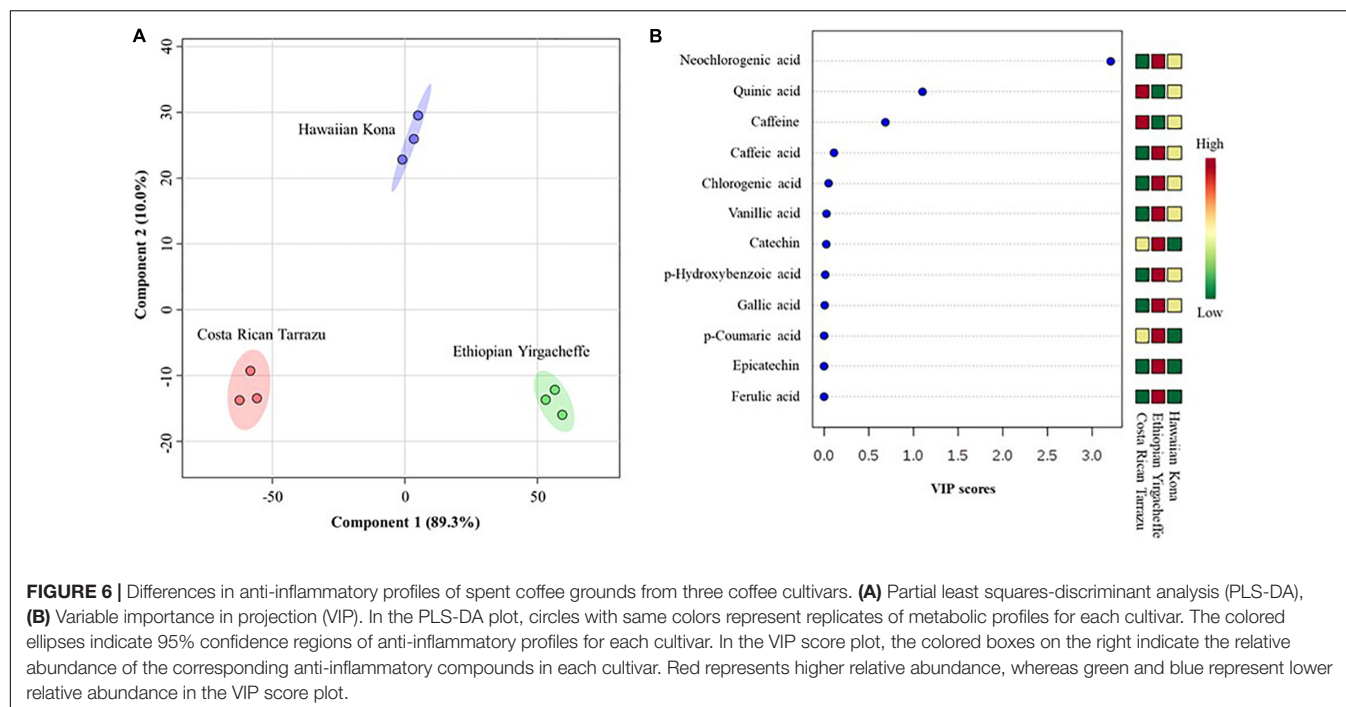
Polyphenols	Coffee cultivars		
	Ethiopian Yirgacheffe <sup>a</sup>	Costa Rican Tarrazu	Hawaiian Kona
5-Caffeoylquinic acid	338.1 ± 1.7 <sup>a</sup>	236.7 ± 1.5 <sup>c</sup>	293.5 ± 1.8 <sup>b</sup>
Quinic acid	207.4 ± 0.5 <sup>c</sup>	238.3 ± 0.5 <sup>a</sup>	218.8 ± 0.3 <sup>b</sup>
Vanillic acid	86.2 ± 2.9 <sup>a</sup>	53.9 ± 1.3 <sup>b</sup>	54.3 ± 1.4 <sup>b</sup>
Caffeic acid	54.5 ± 1.5 <sup>a</sup>	41.4 ± 0.9 <sup>b</sup>	43.4 ± 0.5 <sup>b</sup>
Epicatechin	37.2 ± 1.5	<LOD <sup>**</sup>	<LOD
p-Hydroxybenzoic acid	27.9 ± 0.3 <sup>a</sup>	1.9 ± 0.2 <sup>b</sup>	2.2 ± 0.1 <sup>b</sup>
Catechin	24.0 ± 2.2 <sup>a</sup>	1.9 ± 0.3 <sup>b</sup>	1.4 ± 0.3 <sup>b</sup>
Ferulic acid	21.1 ± 0.6	<LOD	<LOD
p-Coumaric acid	18.3 ± 1.8 <sup>a</sup>	0.7 ± 0.1 <sup>b</sup>	0.7 ± 0.1 <sup>b</sup>
3-Caffeoylquinic acid	3.9 ± 0.5	2.8 ± 0.0	3.7 ± 0.0
Gallic acid	3.1 ± 0.0 <sup>a</sup>	1.0 ± 0.0 <sup>b</sup>	1.1 ± 0.0 <sup>b</sup>
Total polyphenols	821.5 ± 5.7 <sup>a</sup>	578.6 ± 1.7 <sup>c</sup>	619.1 ± 0.7 <sup>b</sup>
Caffeine	384.5 ± 1.1 <sup>b</sup>	439.0 ± 4.0 <sup>a</sup>	426.9 ± 1.3 <sup>a</sup>

<sup>a</sup>All values are shown as mean ± SE (n = 3). In each row, different letter indicate significant differences (p < 0.01) among different spent coffee grounds. <sup>\*\*</sup>LOD, limit of detection.

anti-inflammatory activities in the Hawaiian Kona extracts (**Figure 5**), such as caffeine, 5-caffeoylquinic acid, and quinic acid might be directly or synergistically responsible for the inhibitory activities (**Table 3**). Furthermore, other materials (e.g., polysaccharides, ash, minerals) found in SCGs (McNutt and Quan, 2019) could be exerting an effect on IL-10 secretion in the U-937 model system. Cytokines are soluble factors that play a role in various steps of acute and chronic inflammation (Brenner et al., 2014). Taken together, our findings suggest that SCGs present a promising source of anti-inflammatory mediators for use in the pharmaceutical and cosmetic industries.

So far, only few studies have examined potential anti-inflammatory activities of SCGs in mouse cell line model systems. Ramalakshmi et al. (2009) evaluated SCG extracts derived from Arabia plantation and Robusta cherry, two varieties of graded coffee beans, on the expression of TNF-α in J774A.1 mouse cell

line. Their results showed that TNF-α levels were not suppressed following addition of these two extracts at the 3 concentrations tested (1, 3, and 10 μg/mL). Our results demonstrated inhibitory activity on TNF-α secretion in the human U-937 model system after pre-incubation with Ethiopian Yirgacheffe and Hawaiian Kona extracts. However, the effect was observed in our study using higher concentrations (500 and 5,000 μg/mL) of SCGs compared to those used in the Ramalakshmi et al. study. López-Barrera et al. (2016) evaluated the effects of SCG fractions fermented by human gut flora on the cytokine secretion in mouse RAW 264.7 macrophages stimulated with LPS. This group reported that out of the 40 cytokines/chemokines measured, the level of only 3 cytokines (IL-1β, IL-10, and CCL17) was significantly reduced. The cytokine inhibitory activity of the gut fermented, unabsorbed SCG fractions was mainly mediated by short-chain fatty acids derived from dietary fiber



(López-Barrera et al., 2016). Our results are consistent with other studies showing an effect of roasted coffee bean extracts on cytokine expression. Jung et al. (2017) investigated the role of different roasting levels (Light, Medium, City, and French roast) on the secretion of TNF- $\alpha$  and IL-6 in RAW 264.7 mouse cell line. Their findings showed that mRNA expression of TNF- $\alpha$  and IL-6 was reduced in the LPS-stimulated RAW 264.7 cells relative to control cells. In addition, the expression of TNF- $\alpha$  and IL-6 was decreased more as the roasting levels increased. An amount of inhibition comparable to that reported in our study was observed when the light roast coffee extract was tested at the highest concentration, 2 mg/mL, resulting in 42.9% and 36.7% inhibition of TNF- $\alpha$  and IL-6, respectively. The magnitude of this inhibition is comparable to that observed when Hawaiian Kona extracts were tested at 5 mg/mL, whereby a 60.5 and 52.5% reduction was found in TNF- $\alpha$  and IL-6 secreted protein levels, respectively.

Our results demonstrated a diverse range of the anti-inflammatory bioactive compounds in SCGs. In fact, 26 anti-inflammatory metabolites in the SCG extracts were putatively identified via untargeted metabolomics analyses and 12 anti-inflammatory compounds were successfully confirmed and quantified in SCG extracts by LC-MS/MS analyses with authentic reference standards (Tables 1–3). Among 26 anti-inflammatory metabolites, 12 compounds including chrysin, daidzein, eugenol, naringenin, naringin, oxyresveratrol, pectolinarin, resveratrol, tectochrysin, theaflavin, vanillic acid, and vitexin rhamnoside were the first report possibly present in SCGs, whereas other compounds have been documented as polyphenolic compounds in SCGs (Andrade et al., 2012; López-Barrera et al., 2016). Future research will focus on purification and characterization of compounds mainly driving the cytokine suppressive activities in SCGs.

Among the identified anti-inflammatory compounds, our results revealed that caffeine and 5-caffeoylquinic acid (5-CQA), a monocaffeoylquinic acid (CQA), were the most abundant compounds in the SCG extracts from all examined coffee cultivars. The contents of caffeine ranged from 0.38 mg/g (Ethiopian Yirgacheffe) – 0.44 mg/g (Costa Rican Tarrazu), whereas 5-CQA concentrations were in the range of 0.24 mg/g (Costa Rican Tarrazu) – 0.34 mg/g (Ethiopian Yirgacheffe). Caffeine is well-known as a signature compound in coffee and coffee byproducts. López-Barrera et al. (2016) reported that caffeine contents in Arabica SCG obtained from 2 roasted levels (medium and dark roasted) with Soxhlet extraction were approximately 0.4 mg/g, which roughly shared similar values of caffeine found in this study. However, Bravo et al. (2012) previously reported the contents of caffeine of Arabica SCG with Soxhlet extraction were in the range of 3.6–5.2 mg/g depending on the coffeemakers (filter, espresso, and plunger), which were > 9 times higher than the values observed in López-Barrera et al. (2016) and our study. Caffeoylquinic acids [monocaffeoylquinic and dicaffeoylquinic acids (diCQA)] have been documented as the most abundant phenolic compounds in spent coffee grounds (Campos-Vega et al., 2015), in which 5-CQA was the most abundant compound in SCGs obtained from both Arabica and Robusta varieties (Bravo et al., 2012). Bravo et al. (2012) reported that the contents of 5-CQA in Arabica spent coffee grounds obtained from different coffeemakers including filter, espresso, plunger were 3.6, 2.8, 2.5 mg/g respectively, which was 8–15 times higher than the values observed in our study.

Differences in the levels of bioactive compounds in SCG among different studies are likely due to the differences in coffee materials (coffee varieties, cultivars, geographic sources, growth



conditions), roasting processes and extraction preparation. Our results indicated that the SCGs obtained from 3 different Arabica cultivars differed on the contents of anti-inflammatory compounds (Table 3). In fact, the total phenolic compounds of SCGs were found to be highest in Ethiopian Yirgacheffe (0.82 mg/g), followed by Hawaiian Kona (0.62 mg/g), and then Costa Rican Tarrazu (0.58 mg/g). The concentrations of bioactive compounds in SCGs have been previously reported to be variable among coffee varieties. Arabica spent coffee grounds contained less caffeine than Robusta SCGs, but the contents of caffeoylquinic acids (i.e., 5-CQA, 4-CQA, 5-CQA, 3,4-diCQA, 3,5-diCQA, and 4,5-diCQA) in Arabica SCGs were higher than that in Robusta SCGs (Bravo et al., 2012). Furthermore, the amounts of bioactive compounds in SCGs have been previously documented to be highly dependent on extraction techniques and solvents. Many extraction methods (i.e., solid-liquid extraction, supercritical fluid extraction, Soxhlet extraction, and ultrasound, and microwave) with different solvents i.e., polar (methanol and ethanol), medium or non-polar (e.g., dichloromethane, ethyl acetate, hexane, supercritical fluids, subcritical water, deep eutectic and supramolecular solvents) have been utilized to maximize the recovery of bioactive compounds in SCGs (Mussatto et al., 2011; Andrade et al., 2012; Pavlović et al., 2013; Getachew and Chun, 2017; Yoo et al., 2018; Torres-Valenzuela et al., 2019). Spent coffee grounds defatted with petroleum ether (1:11, w/v) for 3 h at 60°C in a Soxhlet extraction system yielded the highest contents of total phenolic compounds, which ranged 18–22 mg 3-CQA equivalents/g SCG (Andrade et al., 2012). An increase in roasting levels of coffee beans significantly reduced the total phenolic compounds in SCGs. In fact, total phenolic compounds of SCGs derived from medium roasted coffee beans were 9.9 mg/g, while that of SCGs obtained from dark roasted coffee beans were 4.6 mg/g SCG (López-Barrera et al., 2016). Future efforts are ongoing to identify optimum roasting conditions that maximize the cytokine suppressive activities of the SCG extracts.

## CONCLUSION

Methanolic extracts of SCGs possessed cytokine inhibition on the human pro-monocytic cell line U-937. The cytokine suppressive effects and the contents of anti-inflammatory compounds in SCGs obtained from different Arabica cultivars were variable. Hawaiian Kona extracts showed the strongest inhibitory effect on the secretion of all 3 cytokines (TNF- $\alpha$ , IL-6, and IL-10), while Ethiopian Yirgacheffe extract reduced the secretions of TNF- $\alpha$  and IL-6 and Costa Rican Tarrazu only decreased the secretion of IL-6. Multiple (26) metabolites in the SCG extracts with known anti-inflammatory activities were identified via an untargeted metabolomics analysis. Targeted (LC-MS/MS) analyses resulted in the quantification of 12 metabolites that had high relative intensities in all of the extracts. Spent coffee grounds contain a wealth of anti-inflammatory bioactive compounds with caffeine and 5-CQA

as the most abundant compounds. Our findings indicate that SCGs could be promising sources of anti-inflammatory bioactive compounds that can be utilized for pharmaceutical and cosmetic industries.

## DATA AVAILABILITY STATEMENT

The datasets generated for this study are available on request to the corresponding author.

## AUTHOR CONTRIBUTIONS

C-HL and K-VH contributed to conception of the study. K-VH wrote the first draft of the manuscript. K-VH, KS, and C-HL designed the experiments. K-VH, KS, JP, and PV performed the experiments. K-VH and KS performed the analyses. KS, ZL, LS, and C-HL provided materials required for the experiments. All authors edited and approved the final version of the manuscript.

## FUNDING

This work was supported by the USDA/ARS Dale Bumpers Small Farm Research Center, Agreement number 58-6020-6-001 from the USDA Agricultural Research Service, Center for Agroforestry at University of Missouri, and Missouri Department of Agriculture Specialty Crop Block Grant Program (SCBGP) #16SCBGPMO0003. The Sumner lab and the MU Metabolomics Center have been graciously supported by several entities over the years for the development of natural products profiling and plant metabolomics. These specifically include support from the University of Missouri, The Samuel Roberts Noble Foundation, Bruker Daltonics GmbH, Agilent Technologies, US National Science Foundation (NSF)-JST Metabolomics for a Low Carbon Society #1139489, NSF MRI DBI #1126719, NSF RCN #1340058, and NSF MCB #1024976.

## ACKNOWLEDGMENTS

We would like to thank the Center for Agroforestry at University of Missouri, USDA/ARS Dale Bumpers Small Farm Research Center, and Missouri Department of Agriculture Specialty Crop Block Grant Program for supporting this research.

## SUPPLEMENTARY MATERIAL

The Supplementary Material for this article can be found online at: <https://www.frontiersin.org/articles/10.3389/fphar.2020.00229/full#supplementary-material>

## REFERENCES

- Andrade, K. S., Gonçalves, R. T., Maraschin, M., Ribeiro-do-Valle, R. M., Martínez, J., and Ferreira, S. R. (2012). Supercritical fluid extraction from spent coffee grounds and coffee husks: antioxidant activity and effect of operational variables on extract composition. *Talanta* 88, 544–552. doi: 10.1016/j.talanta.2011.11.031
- Bravo, J., Juainiz, I., Monente, C., Caemmerer, B., Kroh, L. W., De Peña, M. P., et al. (2012). Evaluation of spent coffee obtained from the most common coffeemakers as a source of hydrophilic bioactive compounds. *Int. J. Agric. Food Chem.* 60, 12565–12573. doi: 10.1021/jf3040594
- Brenner, D. R., Scherer, D., Muir, K., Schildkraut, J., Boffetta, P., Spitz, M. R., et al. (2014). A review of the application of inflammatory biomarkers in epidemiologic cancer research. *Cancer Epidemiol. Biomark. Prev.* 23, 1729–1751. doi: 10.1158/1055-9965.epi-14-0064
- Campos-Vega, R., Loarca-Pina, G., Vergara-Castañeda, H. A., and Oomah, B. D. (2015). Spent coffee grounds: a review on current research and future prospects. *Trends Food Sci. Technol.* 45, 24–36. doi: 10.1016/j.tifs.2015.04.012
- Castro, C. S., Abreu, A. L., Silva, C. L., and Guerreiro, M. C. (2011). Phenol adsorption by activated carbon produced from spent coffee grounds. *Water Sci. Tech.* 64, 2059–2065. doi: 10.2166/wst.2011.786
- Chong, J., Soufan, O., Li, C., Caraus, I., Li, S., Bourque, G., Wishart, D. S., and Xia, J. (2018). MetaboAnalyst 4.0: towards more transparent and integrative metabolomics analysis. *Nucleic Acids Res.* 46, W486–W494. doi: 10.1093/nar/kyk310
- Getachew, A. T., and Chun, B. S. (2017). Influence of pretreatment and modifiers on subcritical water liquefaction of spent coffee grounds: a green waste valorization approach. *J. Clean. Prod.* 142, 3719–3727. doi: 10.1016/j.jclepro.2016.10.096
- Givens, D., and Barber, W. (1986). In vivo evaluation of spent coffee grounds as a ruminant feed. *Agric. Wastes* 18, 69–72. doi: 10.1016/0141-4607(86)90108-3
- Guijas, C., Montenegro-Burke, J. R., Domingo-Almenara, X., Palermo, A., Warth, B., et al. (2018). METLIN: a technology platform for identifying knowns and unknowns. *Anal. Chem.* 90, 3156–3164. doi: 10.1021/acs.analchem.7b04424
- Hänsel, R., Keller, K., Rimpler, H., and Schneider, G. (1993). *Hagers Handbuch der Pharmazeutischen Praxis* (Berlin: Springer-Verlag), 926–940.
- Ho, K. V., Lei, Z., Sumner, L., Coggeshall, M., Hsieh, H. Y., Stewart, G., et al. (2018). Identifying antibacterial compounds in black walnuts (*Juglans nigra*) using a metabolomics approach. *Metabolites* 8:58. doi: 10.3390/metabo8040058
- Ho, K. V., Schreiber, K. L., Vu, D. C., Rottinghaus, S. M., Jackson, D. E., Brown, C. R., et al. (2019). Black walnut (*Juglans nigra*) extracts inhibit pro-inflammatory cytokine production from LPS-stimulated human pro-monocytic cell line U-937. *Front. Pharmacol.* 10:1059. doi: 10.3389/fphar.2019.01059
- Hwang, S. J., Kim, Y.-W., Park, Y., Lee, H.-J., and Kim, K.-W. (2014). Anti-inflammatory effects of chlorogenic acid in lipopolysaccharide-stimulated RAW 264.7 cells. *Inflamm. Res.* 63, 81–90. doi: 10.1007/s00011-013-0674-4
- Jung, S., Kim, M. H., Park, J. H., Jeong, Y., and Kov, K. S. (2017). Cellular antioxidant and anti-inflammatory effects of coffee extracts with different roasting levels. *J. Med. Food* 20, 626–635. doi: 10.1089/jmf.2017.3935
- Kim, S.-H., Jun, C.-D., Suk, K., Choi, B.-J., Lim, H., Park, S., et al. (2005). Gallic acid inhibits histamine release and pro-inflammatory cytokine production in mast cells. *Toxicol. Sci.* 91, 123–131. doi: 10.1093/toxsci/kfj063
- Köroğlu, Ö. A., MacFarlane, P. M., Balan, K. V., Zenebe, W. J., Jafri, A., Martin, R. J., et al. (2014). Anti-inflammatory effect of caffeine is associated with improved lung function after lipopolysaccharide-induced amnionitis. *Neonatology* 106, 235–240. doi: 10.1159/000363217
- Kovalick, A., Obruca, S., and Marova, I. (2018). Valorization of spent coffee grounds: a review. *Food Bioprod Process.* 110, 104–119. doi: 10.1016/j.fbp.2018.05.002
- López-Barrera, D. M., Vázquez-Sánchez, K., Loarca-Piña, M. G. F., and Campos-Vega, R. (2016). Spent coffee grounds, an innovative source of colonic fermentable compounds, inhibit inflammatory mediators in vitro. *Food Chem.* 212, 282–290. doi: 10.1016/j.foodchem.2016.05.175
- McNutt, J., and Quan, H. (2019). Spent coffee grounds: a review on current utilization. *J. Ind. Eng. Chem.* 71, 78–88. doi: 10.1016/j.jiec.2018.11.054
- Mosmann, T. (1983). Rapid colorimetric assay for cellular growth and survival: application to proliferation and cytotoxicity assays. *J. Immunol. Methods* 65, 55–63. doi: 10.1016/0022-1759(83)90303-4
- Moustafa, H., Guizani, C., and Dufresne, A. (2017). Sustainable biodegradable coffee grounds filler and its effect on the hydrophobicity, mechanical and thermal properties of biodegradable PBAT composites. *J. Appl. Polym. Sci.* 134, 1097–14628.
- Murthy, P. S., and Naidu, M. M. (2012). Sustainable management of coffee industry by-products and value addition - A review. *Resour. Conserv. Recycl.* 66, 45–58. doi: 10.1016/j.resconrec.2012.06.005
- Mussatto, S. I., Ballesteros, L. F., Martins, S., and Teixeira, J. A. (2011). Extraction of antioxidant phenolic compounds from spent coffee grounds. *Sep. Purif. Technol.* 83, 173–179. doi: 10.1016/j.seppur.2011.09.036
- O'Garra, A., Barrat, F. J., Castro, A. G., Vicari, A., and Hawrylowicz, C. (2008). Strategies for use of IL-10 or its antagonists in human disease. *Immunol. Rev.* 223, 114–131. doi: 10.1111/j.1600-065X.2008.00635.x
- Park, J., Kim, B., and Lee, J. W. (2016). In-situ transesterification of wet spent coffee grounds for sustainable biodiesel production. *Bioresour. Technol.* 221, 55–60. doi: 10.1016/j.biortech.2016.09.001
- Pavlović, M. D., Buntić, A. V., Šiler-Marinković, S. S., and Dimitrijević-Branković, S. (2013). Ethanol influenced fast microwave-assisted extraction for natural antioxidants obtaining from spent filter coffee. *Sep. Purif. Technol.* 118, 503–510. doi: 10.1016/j.seppur.2013.07.035
- Ramalakshmi, K., Rao, L. J. M., Takano-Ishikawa, Y., and Goto, M. (2009). Bioactivities of low-grade green coffee and spent coffee in different in vitro model systems. *Food Chem.* 115, 79–85. doi: 10.1016/j.foodchem.2008.11.063
- Rätsch, C. (2005). *The Encyclopedia of Psychoactive Plants: Ethnopharmacology and its Applications*. Park Street Press: South Paris, ME.
- Ribeiro, J. P., Vicente, E. D., Gomes, A. P., Nunes, M. I., Alves, C., and Tarelho, L. A. (2017). Effect of industrial and domestic ash from biomass combustion, and spent coffee grounds, on soil fertility and plant growth: experiments at field conditions. *Environ. Sci. Pollut. R.* 24, 15270–15277. doi: 10.1007/s11356-017-9134-y
- Rinschen, M. M., Ivanisevic, J., Giera, M., and Siuzdak, G. (2019). Identification of bioactive metabolites using activity metabolomics. *Nat. Rev. Mol. Cell Biol.* 20, 353–367. doi: 10.1038/s41580-019-0108-4
- Rovera, G., Santoli, D., and Damsky, C. (1979). Human promyelocytic leukemia cells in culture differentiate into macrophage-like cells when treated with a phorbol diester. *Proc. Natl. Acad. Sci. U.S.A.* 76, 2779–2783. doi: 10.1073/pnas.76.6.2779
- Smallic, T., Ricchetti, G., Horwood, N. J., Feldmann, M., Clark, A. R., and Williams, L. M. (2010). IL-10 inhibits transcription elongation of the human TNF gene in primary macrophages. *J. Exp. Med.* 207, 2081–2088. doi: 10.1084/jem.2010.0414
- Smolen, J. S., and Aletaha, D. (2015). Rheumatoid arthritis therapy reappraisal: strategies, opportunities and challenges. *Nat. Rev. Rheumatol.* 11:276. doi: 10.1038/nrrheum.2015.8
- Tautenhahn, R., Patti, G. J., Rinehart, D., and Siuzdak, G. (2012). XCMS Online: a web-based platform to process untargeted metabolomic data. *Anal. Chem.* 84, 5035–5039. doi: 10.1021/ac300698c
- Torres-Valenzuela, L. S., Ballesteros-Gómez, A., Sanin, A., and Rubio, S. (2019). Valorization of spent coffee grounds by supramolecular solvent extraction. *Sep. Purif. Technol.* 228:115759. doi: 10.1016/j.seppur.2019.115759
- Yoo, D. E., Jeong, K. M., Han, S. Y., Kim, E. M., Jin, Y., and Lee, J. (2018). Deep eutectic solvent-based valorization of spent coffee grounds. *Food Chem.* 255, 357–364. doi: 10.1016/j.foodchem.2018.02.096
- Zarrinbakhsh, N., Wang, T., Rodriguez-Urbe, A., Misra, M., and Mohanty, A. K. (2016). Characterization of wastes and coproducts from the coffee industry for composite material production. *Bioresources* 11, 7637–7653.

**Conflict of Interest:** The authors declare that the research was conducted in the absence of any commercial or financial relationships that could be construed as a potential conflict of interest.

Copyright © 2020 Ho, Schreiber, Park, Vo, Lei, Sumner, Brown and Lin. This is an open-access article distributed under the terms of the Creative Commons Attribution License (CC BY). The use, distribution or reproduction in other forums is permitted, provided the original author(s) and the copyright owner(s) are credited and that the original publication in this journal is cited, in accordance with accepted academic practice. No use, distribution or reproduction is permitted which does not comply with these terms.



# Biocompatible Nutmeg Oil-Loaded Nanoemulsion as Phyto-Repellent

Masturah Mohd Narawi<sup>1</sup>, Hock Ing Chiu<sup>1</sup>, Yoke Keong Yong<sup>2</sup>,  
Nur Nadhirah Mohamad Zain<sup>1</sup>, Muggundha Raoov Ramachandran<sup>3</sup>, Chau Ling Tham<sup>4</sup>,  
Siti Fatimah Samsurrijal<sup>5</sup> and Vuanghao Lim<sup>1\*</sup>

<sup>1</sup> Integrative Medicine Cluster, Advanced Medical and Dental Institute, Universiti Sains Malaysia, Penang, Malaysia,

<sup>2</sup> Department of Human Anatomy, Faculty of Medicine and Health Sciences, Universiti Putra Malaysia, Serdang, Malaysia,

<sup>3</sup> Department of Chemistry, Faculty of Science, Universiti Malaya, Kuala Lumpur, Malaysia, <sup>4</sup> Department of Biomedical Science, Faculty of Medicine and Health Sciences, Universiti Putra Malaysia, Serdang, Malaysia, <sup>5</sup> Craniofacial and Biomaterial Sciences Cluster, Advanced Medical and Dental Institute, Universiti Sains Malaysia, Penang, Malaysia

## OPEN ACCESS

### Edited by:

Gokhan Zengin,  
Selçuk University, Turkey

### Reviewed by:

Lei Chen,  
Fujian Agriculture and Forestry  
University, China  
Souaibou Yaouba,  
Université de Lorraine, France

### \*Correspondence:

Vuanghao Lim  
vlim@usm.my

### Specialty section:

This article was submitted to  
Ethnopharmacology,  
a section of the journal  
Frontiers in Pharmacology

**Received:** 01 July 2019

**Accepted:** 14 February 2020

**Published:** 17 March 2020

### Citation:

Mohd Narawi M, Chiu HI,  
Yong YK, Mohamad Zain NN,  
Ramachandran MR, Tham CL,  
Samsurrijal SF and Lim V (2020)  
Biocompatible Nutmeg Oil-Loaded  
Nanoemulsion as Phyto-Repellent.  
Front. Pharmacol. 11:214.  
doi: 10.3389/fphar.2020.00214

Plant essential oils are widely used in perfumes and insect repellent products. However, due to the high volatility of the constituents in essential oils, their efficacy as a repellent product is less effective than that of synthetic compounds. Using a nanoemulsion as a carrier is one way to overcome this disadvantage of essential oils. Nutmeg oil-loaded nanoemulsion (NT) was prepared using a high speed homogenizer and sonicator with varying amounts of surfactant, glycerol, and distilled water. Using a phase diagram, different formulations were tested for their droplet size and insect repellent activity. The nanoemulsion containing 6.25% surfactant and 91.25% glycerol (NT 6) had the highest percentage of protection (87.81%) in terms of repellent activity among the formulations tested for the 8 h duration of the experiment. The droplet size of NT 6 was 217.4 nm, and its polydispersity index (PDI) was 0.248. The zeta potential value was  $-44.2$  mV, and the viscosity was 2.49 Pa.s at pH 5.6. The *in vitro* release profile was 71.5%. When the cytotoxicity of NT 6 at 400  $\mu$ g/mL was tested using the MTS assay, cell viability was 97.38%. Physical appearance and stability of the nanoemulsion improved with the addition of glycerol as a co-solvent. In summary, a nutmeg oil-loaded nanoemulsion was successfully formulated and its controlled release of the essential oil showed mosquito repellent activity, thus eliminating the disadvantages of essential oils.

**Keywords:** nutmeg oil, repellent activity, *in vitro* release, nanoemulsion, *Aedes aegypti*

## INTRODUCTION

Zika virus recently spread to Malaysia, with six cases reported in September 2016 (Subramaniam, 2016). Zika virus, which is a mosquito-borne flavivirus that is closely related to the dengue virus, first appeared in Brazil and then spread to countries in Latin America (Subramaniam, 2016). Other mosquito-borne diseases such as yellow fever, dengue, and chikungunya also have become major health problems in tropical and subtropical countries (Adeniran and Fabiyi, 2012; Gupta et al., 2013). Hence, the use of insect repellent products is essential to prevent these diseases (Rocha-Filho et al., 2014). N, N-diethyl-3-methylbenzamide (DEET) is the synthetic main active ingredient in commercial mosquito repellent products, and it has excellent repellency against a wide range of

insects (Hang Chio and Yang, 2008). However, DEET poses health risks such as developmental toxicity in animals and environment (Iyer and Makris, 2010; Solomon et al., 2012).

With increased awareness of maintaining a green environment, biodegradable sources of mosquito repellent are widely promoted to replace chemical synthetic products that can have adverse effects on users (Maji and Hussain, 2009). Among available natural sources, essential oils from plants (Teng and Chen, 2017) are the preferred natural insect repellent because they contain rich sources of bioactive compounds, biodegrade to non-toxic products, and have less toxic on non-target organisms and the environment (Govindarajan, 2010; Lim et al., 2012; Assi et al., 2017). Plant essential oils are efficient insect repellents and provide direct protection to the user (Azeem et al., 2019). Although plant essential oils have been used in insect repellent products, their effectiveness is not significant (Bissinger and Roe, 2010). One possible reason could be that these products are characterized by uncontrolled release of the essential oil (such as, they either release too little or too much, with shorter duration of protection) (Solomon et al., 2012).

One potential way to solve the uncontrolled release problem is to encapsulate essential oils in nanoemulsions (Chen et al., 2020b). Preparation of a nanoemulsion involves mixing of two non-miscible liquids, such as oil and water, to produce spherical droplets with size ranging from 20 to 500 nm (San Martín-González et al., 2009). Their appearance is either transparent or slightly opaque (Sugumar et al., 2014). An additional constituent in nanoemulsions is surfactant, which acts as an emulsifying agent to decrease the interfacial tension between oil and water (Musa et al., 2013). Its presence prevents phase separation upon dispersion of the two immiscible liquids (Devarajan and Ravichandran, 2011). The stability of a nanoemulsion depends on its preparation. High energy emulsification provides intense disruptive forces to break up the mixture of oil, water, and surfactant into small droplets (Musa et al., 2013). Low energy emulsification involves the phase inversion method (Pant et al., 2014).

In this study, nutmeg oil-loaded nanoemulsion (NTs) systems were developed using glycerol, Montanov® 82 (non-ionic surfactant), and deionized water. We aim to investigate the effect of high energy emulsification of the system consisting nutmeg oil, together with physicochemical characteristics, the release study and mosquito repellent activity of the nutmeg oil-loaded nanoemulsion.

## MATERIALS AND METHODS

### Essential Oil and Standards

The essential oil, namely nutmeg oil (*Myristica fragrans*) was purchased from Imeltech Sdn. Bhd (Kuala Lumpur, Malaysia) with in-house code no. MF-004 (Batch no. NMO7956FT) and stored at the Herbarium Unit, Integrative Medicine Cluster, Advanced Medical and Dental Institute (IPPT).  $\alpha$ -pinene (Batch no. SHBB7538V, Sigma-Aldrich, St Louis, United States), safrole (Batch no. BCBH2795V, Sigma-Aldrich, Shanghai, China), and

terpinen-4-ol (Batch no. BCBF8537V, Sigma-Aldrich, Madrid, Spain) were used as standards for GCMS analysis.

### Animal and Test Organisms

Sprague Dawley (SD) rats were purchased from the Animal Research and Service Centre, Universiti Sains Malaysia (USM). Female *Aedes (Ae.) aegypti* and DEET were supplied by the Vector Control Research Unit (VCRU), USM.

### Nutmeg Oil-Loaded Nanoemulsions

The essential oil-loaded nanoemulsion method was adapted from Sakulku et al. (2009) with slight modifications. Briefly, a phase diagram of surfactant, co-solvent, and water representing an apex triangle was plotted. Ternary mixtures with varying concentrations of surfactant (Montanov® 82), co-solvent (glycerol), and double distilled water were prepared with a fixed nutmeg oil concentration (20% v/v). For each mixture, the total surfactant, co-solvent, and water summed to 100%. The mixture was emulsified using a high speed homogenizer (WT 130 hand-held homogenizer, Medigene, Selangor, Malaysia) at 18,000 rpm for 3 min. The formulation then was sonicated for 30 min using ultrasonicator cleaner (WUC-A10H, Wise Clean, Sonic Wise, California, United States) to obtain a submicron emulsion (Ragelle et al., 2012). Lastly, the formulation was centrifuged at 10,000 rpm for 15 min (Supermini Centrifuge, Hangzhou Allsheng Instruments CO., Ltd., Zhejiang Province, China). Visual observation was made immediately after centrifugation. Formulations with phase separation were rejected, whereas those without phase separation were chosen for particle size analysis. The desirable particle size was between 100 and 500 nm. The produced NTs were stored at 25°C until further use.

### Droplet Size and PDI

The particle size and PDI of the NTs were measured using the dynamic light scattering (DLS) technique at an angle of 173° and temperature of 25°C. This process was carried out using Zeta Nano-ZS apparatus (Malvern Instruments, Malvern, United Kingdom). Each NT sample was diluted with double distilled water until it reached the desired concentration, and all diluted samples were kept at a count rate of 150–300 k. Measurements were performed in triplicates.

### Mosquito Repellent Activity of NTs

#### Animal Ethics and Preparation of Animals

All animal procedures used were in strict accordance with animal care protocols, and all experimental protocols were approved by the Universiti Sains Malaysia Animal Ethics Committee [USM/Animal Ethics Approval/2013/(85) (441)]. SD rats (aged 8–10 weeks) were used for the insect repellent tests. The rats were kept at the Animal Research Facility, IPPT, USM under standard laboratory conditions for animals [temperature: 25 ± 2°C; relative humidity (RH): 55 ± 5%], with food and water provided and bedding replacement three times per week (Lim et al., 2012).

#### Test Organisms

The mosquitoes (*Ae. Aegypti*) were cultivated in the laboratory at constant temperature of 25–30°C and 80–90% RH at the VCRU,



USM. A Whatman (Maidstone, United Kingdom) filter paper was placed in a Petri dish filled with chlorine-free water, which then was placed in an adult female mosquito's cage. After eggs were laid, the Petri dish was removed and the eggs were allowed to hatch within 24 h. The newly hatched larvae were transferred into a rearing tray containing chlorine-free water and fed with a mixture of dog food, beef liver, yeast, and milk powder in the ratio of 2:1:1:1 w/w/w/w. Larvae were fed every day until pupation. At this stage, the pupae were separated from larvae and placed in a plastic cup with chlorine-free water in a mosquito cage. The plastic cup was removed from the cage when all adults had emerged. The adult mosquitoes were fed with vitamin B complex solution and 10% of sugar solution. Female adult mosquitoes of 5–7 days old were starved of blood for 24 h before being used in the repellent activity test.

### Repellent Activity

The mosquito repellent tests of the selected NTs were conducted using female mosquitoes and rats as the blood donor. This method was adapted from Oshaghi et al. (2003) with slight modification. A rat was placed in a customized cage. The rat's upper body (around 5 × 5 cm) was cleaned using ethanol and dried for 1–2 min before applying the NT. Approximately 1 mL of the NT was applied to the cleaned rat's body. Another rat was treated with DEET (positive control), and another with liquid paraffin (negative control). Each rat was then placed in a mosquito cage containing 50 female *Ae. aegypti* mosquitoes for first 10 min of every hour for a total of 8 h. The number of mosquitoes that landed on the rat (10 s) within each 10 min interval was counted and compared to the controls. Each test was performed in triplicates with a new batch of mosquitoes. The numbers of landings in treated and control tests (positive and negative) were recorded, and the mean percentage protection from mosquito landing was calculated. The percentage protection is defined as the average number of bites received by the subject in each test and was calculated using equation (1):

$$\text{Percentage protection} = \frac{(50 - \text{NL})}{50} \times 100 \quad (1)$$

Where 50 = number of mosquitoes in the cage and NL = number of landings.

## Characterizations of NTs

### Zeta Potential

The electrophoretic mobility and surface charge of each NT were measured by the frequency shift of scattered light at a 12° scattering angle using the Zeta Nano-ZS apparatus. Measurements were performed in triplicates.

### Transmission Electron Microscope (TEM) Analysis

Visualization of the morphology and structure of the NTs was carried out by TEM analysis (Ghozali et al., 2015). A drop (1 µL) of NT diluted with deionized water (1:200) was placed on a 300 mesh copper grid and left for 1 min. The excess liquid was drawn off with Whatman filter paper. The grid was kept inverted and a drop of 2% (w/w) phosphotungstic acid (PTA) was applied to

the grid for 10 s to negatively stain the sample. Excess PTA was removed by absorption on a Whatman filter paper. The grid was analyzed using a TEM Philips CM12 with Docu version 3.2 image analysis (Lim et al., 2013; Ayub et al., 2019).

### Viscosity and Flow Analysis

Viscosity measurement and flow analysis of the NTs were performed using a dynamic shear rheometer (Rheologica Viscotech, Tarragona, Spain). A 40 mm diameter of parallel plate geometry was attached to the instrument and calibrated with a gap width of 1 mm. Next, 1500 µL of the NT were pipetted onto the surface of the rheometer with the absence of bubbles. The rheometer was run with the shear rate ranging from 0.1 to 1000 s<sup>-1</sup> for 5 min, and the rate then was reduced from 1000 to 0.1 s<sup>-1</sup> over the course of 5 min.

### pH

The pH values of the NTs were determined directly using a calibrated pH meter (LIDA 92 series, Eutech Instruments Pte Ltd., Ayer Rajah Crescent, Singapore) at room temperature. The analyses were performed in triplicates.

## Release Study

### *In vitro* Release of Nutmeg Oil

The release study was conducted using Franz-type diffusion cells (Carbone et al., 2014). First, 1 mL of NT was loaded on a cellulose acetate membrane with 0.2 µm pore size and 25 mm diameter. Prior to sample loading, the membrane was soaked in isopropyl myristate for 1 h to mimic the lipophilic barrier of the stratum corneum. Next, the membrane was mounted on top of the cells with 25 mL of water-ethanol (50:50) in the receiving compartment. This was to allow the “sink” condition and sustain essential oil solubilization. This compartment was constantly stirred at 700 rpm at 32°C and equilibrated for 30 min before collecting the first sample. An aliquot of receptor medium (1 mL) was collected at 0 min, 30 min, and then every hour thereafter for 24 h during the study. At each sampling time point, the system was replenished with the same volume of fresh, preheated receptor medium. The collected samples were analyzed by gas chromatography-mass spectrometry (GC-MS) after extraction with hexane. This experiment was performed in triplicates. The essential oil release kinetics from NTs was investigated by fitting the release data into Higuchi's model, which can be expressed as:

$$Qt = kt^{0.5} \quad (2)$$

where  $Qt$  is the percent of essential oil released at a given time ( $t$ ) and  $k$  is the release rate.

### GC-MS Analysis

The collected samples from the release study were extracted using the liquid-liquid extraction technique for GC-MS analysis (Donsi et al., 2012). First, 1 mL of sample was dissolved in 5 mL of n-hexane and vortexed vigorously for 1 min. Sodium sulfate was added to the separated organic phase to remove the residual water. The GC-MS method was adapted from Lim et al. (2019). For sample analysis, 1 µL of diluted extracted sample in n-hexane

(1:1000) was auto injected in the splitless mode. The constituents in the essential oil were identified by comparison with the National Institute of Standard and Technology mass spectral library and presented as relative percentage of the total peak (Tan et al., 2014; Lim et al., 2015).

## Cytotoxicity Assay

### Cell Preparation

L929 cells (mouse fibroblast cells) were obtained from the American Type Culture Collection (ATCC). The preheated (37°C) culture vessel and medium were placed in a biosafety cabinet class II (ESCO Labculture®, Esco Micro Pte Ltd., Changi South Street, Singapore). The morphology of the cells was checked using an inverted microscope (CKX41 SE, Olympus, Tokyo, Japan). L929 cells were seeded in 75 cm<sup>2</sup> culture flasks that contained Dulbecco's modified eagle medium supplemented with 15% phosphate buffered saline (PBS), 5 mL penicillin streptomycin, and 5 mL L-glutamine. Next, the medium was aspirated and cells were washed twice with 5 mL PBS. Trypsin (5 mL) was added to disaggregate the cells, which then were incubated in a CO<sub>2</sub> incubator (Heraeus BB15, Thermo Scientific, Massachusetts, United States) at 37°C for 15 min. Then, 10 mL of warm medium were added to the cells after detachment to stop the trypsinization and to disperse the cells. The cells were centrifuged (Heraeus Megafuge 16 centrifuge, Thermo Scientific) at 1000 rpm for 5 min, and the supernatant was aspirated. Lastly, 5 mL of fresh warm medium was added and pipetted up and down with the pellet, then 50 µL of the cells were added to 50 µL of trypan blue to calculate the cell using hemocytometer (Yakop et al., 2018).

### Sample Dilution

For cell treatment, selected NT formulations were diluted with deionized distilled water in concentrations ranging from 50 to 400 mg/mL. The same procedure was repeated for DEET.

### 3-(4, 5-Dimethylthiazol-2-yl)-5-(3-Carboxymethoxyphenyl)-2-(4Sulfophenyl)-2H-Tetrazolium (MTS) Assay

L929 cells were seeded at  $3 \times 10^3$  cells/mL into 96-well plates containing 100 µL of medium (Hanan et al., 2018; Poobalan et al., 2018). Next, 50 µL of diluted NT and DEET at different concentrations were added to the cells. Cells were incubated for 48 h with untreated cells as the control. Each plate was then treated with 20 µL of MTS reagent, and absorbance was read at 490 nm after 4 h using a microplate reader (FLUOstar Omega, BMG LABTECH, Offenbury, Germany). Cell viability (%) was calculated using the following formula:

$$\text{Cell viability (\%)} = \frac{OD_{\text{sample}}}{OD_{\text{control}}} \times 100 \quad (3)$$

where *OD* is the absorbance from the microplate reader.

## Thermodynamic Stability Study

The preliminary stability of the NTs was evaluated at 24 h by centrifuging at 15,000 rpm for 15 min. Samples showing layer separation were eliminated. Samples without layer separation

were stored at  $25 \pm 2^\circ\text{C}$ ,  $60 \pm 2^\circ\text{C}$ , and  $4 \pm 2^\circ\text{C}$ . Droplet size and pH were measured at 1, 30, 60, and 90 d. The experiment was performed in triplicates.

## Statistical Analysis

Values were expressed as mean  $\pm$  standard deviation (SD). Differences among samples were examined using one-way analysis of variance. A difference was considered to be statistically significant at  $p < 0.05$ .

## RESULTS AND DISCUSSION

### Phase Diagram for NTs

A phase diagram of ternary mixtures with surfactant (Montanov® 82), co-solvent (glycerol), and double distilled water with nutmeg oil at a fixed concentration of 20% v/v was constructed (**Figure 1**). Each apex on the triangle representing the ternary system represents 100% of the component at that apex. The amount of surfactant used in the formulation ranged from 3.75 to 56.25%, that of glycerol ranged from 0.0 to 93.75%, and that of double distilled water ranged from 3.75 to 93.75%. In total, 296 formulations were constructed on the phase diagram. Visual observation was made immediately after the preparation of each formulation. Formulations that appeared as one phase were selected, and their average particle size was determined by the DLS technique using the Zeta Nano-ZS apparatus. Formulations with droplet size of  $\leq 500$  nm were selected as NTs for further testing (Pant et al., 2014).

**Table 1** shows the composition of the single phase nanoemulsions in the ternary system. NT 13 contained the highest percentage of surfactant (31.25%) and NTs 11, 14, and 15 had the lowest (3.75%). The amount of co-solvent in these NTs ranged from 93.17% (NT 15) to 15% (NT 3). NT 1 was formulated with 12.5% surfactant and 87.50% water, without any co-solvent.

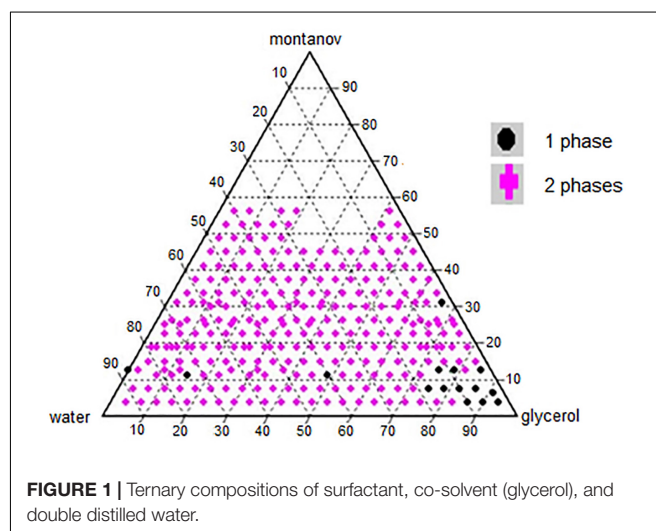


**FIGURE 1 |** Ternary compositions of surfactant, co-solvent (glycerol), and double distilled water.

**TABLE 1** | Composition of NTs.

Sample	% (v/v) of surfactant (Montanov® 82)	% (v/v) of glycerol	% (v/v) of H <sub>2</sub> O
NT 1	12.50	0.00	87.50
NT 2	12.50	75.00	12.50
NT 3	11.25	15.00	73.75
NT 4	11.25	48.75	40.00
NT 5	12.50	78.75	8.75
NT 6	6.25	91.25	2.50
NT 7	12.50	85.00	2.50
NT 8	7.50	75.00	17.50
NT 9	7.50	78.75	13.75
NT 10	7.50	82.50	10.00
NT 11	3.75	86.25	10.00
NT 12	7.50	86.25	6.25
NT 13	31.25	66.25	2.50
NT 14	3.75	90.00	6.25
NT 15	3.75	93.75	2.50

The construction of phase diagram is crucial to determine the single-phase boundary at each percentage of surfactant, co-solvent, and water with a fix percentage of nutmeg oil (20%) to yield a nanoemulsion in low free energy and thermodynamically spontaneous (Shakeel et al., 2008). The regions of the nanoemulsion in the phase diagram shown in **Figure 1** were marked after visual observation of the formulated samples to identify those that were monophasic, clear and transparent mixtures after stirring, sonication, and thermodynamic stability testing (Devarajan and Ravichandran, 2011).

A surfactant or emulsifying agent is important in formulating a nanoemulsion because it reduces interfacial energy between oil and the aqueous phase via formation of a layer around the droplets of the nanoemulsion and it provides a mechanical barrier to coalescence (Kotta et al., 2014). Hence, surfactants added to a water-in-oil system (nutmeg oil, water, and glycerol) increase the aqueous phase concentration due to micelle solubilization. In our study, nutmeg oil was attached to the hydrophobic region of the emulsifier micelle and transferred to the aqueous phase (Donsi et al., 2012). At high concentration of surfactant, smaller droplets of NT are formed, which decreases the interfacial tension between nutmeg oil and the aqueous phase (Wang et al., 2007). Phase separation of a nanoemulsion might occur at low concentration of surfactant due to incomplete coverage of surfactant to oil and aqueous phase (Musa et al., 2013). Therefore, identifying the optimal surfactant concentration was important for solubilizing the oil with micelle solutions with the maximum amount of surfactant at 10% to the oil ratio (Fernandez et al., 2004). Yuan et al. (2008) reported that the combination of Tween 20-Tween 40 (10%) and Tween 60–80 (6%) reached a plateau for droplet size of the nanoemulsion. This is because of full coverage by the excessive surfactant in the nanoemulsion system (Yuan et al., 2008). Tang et al. (2012) reported that the minimum droplet size of a nanoemulsion occurred when 5–6% concentration of Cremophore EL was used; further addition of surfactant led to an increase in droplet size

of the nanoemulsion (Tang et al., 2012). In our study, 7.5% was the maximum surfactant percentage that led to the formation of nano sized droplets with an acceptable PDI value. Once the nutmeg oil in the formulation has reached the saturation level (micelles), any addition of water and surfactant would not further dissolve. Excess free surfactant that is not adsorbed to the oil and aqueous interface would cause flocculation due to the increase of local osmotic pressure; this would cause the surfactants to “flow out” from the intervening liquid between the droplets, which in turn would lead to phase separation of the formulated samples (Jafari et al., 2007).

Glycerol acted as a co-solvent in this system to increase the viscosity of NTs and to decrease the droplet collision frequency (Chanasattru et al., 2007). Glycerol is added to the aqueous phase of a nanoemulsion to modify the bulk physicochemical properties of the formulated samples, such as density, viscosity, refractive index, interfacial tension, optimum curvature, and solubility of the surfactant in the aqueous phase (Saber et al., 2013). In our study, a high concentration of glycerol led to the nano formation of NTs (Saber et al., 2013).

## Droplet Size and PDI of Formulated NTs

The 15 formulations with single phase from the phase diagram were selected to determine their droplet size and PDI values using the DLS technique and a Zeta Nano-ZS apparatus. DLS measures the z-average mean of the nanoemulsion (Yuan et al., 2008). **Figure 2** shows the average droplet size and PDI of the selected samples. NT 6 exhibited the smallest droplet size (mean diameter 217.4 nm), and NT 13 had the largest droplet size (516.13 nm). As mentioned earlier, any NT with droplet size > 500 nm was rejected. Therefore, NT 13 was eliminated from further analysis. Formulations with droplet size in the range of 200 to 300 nm were NT 7 (266.17 nm), NT 8 (299.83 nm), NT 9 (299.13 nm), and NT 11 (288.1 nm). The rest of the formulations had droplet sizes between 300 and 400 nm. The appearance of NT 6 was slightly transparent because of its tiny droplet size. Although some of the NTs appeared cloudy, their droplet size was still in the nano range. Salvia-Trujillo et al. (2015) also reported that the droplet size of their nanoemulsion was still in the nano range despite a slightly turbid physical appearance.

The DLS technique measures the Brownian motion of the droplets, which is referred as the intensity-weighted average hydrodynamic diameter of the emulsion. Large droplets move more slowly than small ones. Sufficient dispersion of the nanoemulsion is required to reduce the multiple scattering effect of Brownian motion (Leong et al., 2009). Small droplets have a greater surface area than large droplets, thus more surfactant is needed to cover this greater area (Yuan et al., 2008). For this reason, the droplet size of NTs decreased with increasing percentage of surfactant due to adsorption of high amounts of oil and water. This led to the increased surface area and reduced interfacial energy, which provided the mechanical barrier to coalescence (Carbone et al., 2014).

Polydispersity index is an important measurement of homogeneity and stability of a formulated nanoemulsion. A small value of PDI indicates homogeneity and a narrow distribution of the nanoemulsion system (Sugumar et al., 2014). PDI values

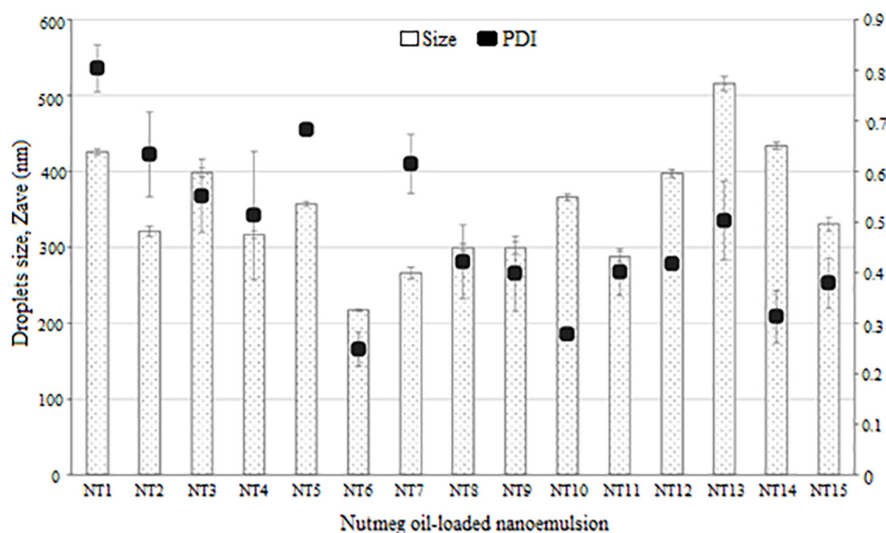


**FIGURE 2** | Droplet size and polydispersity index of NTs (mean  $\pm$  SD,  $n = 3$ ).

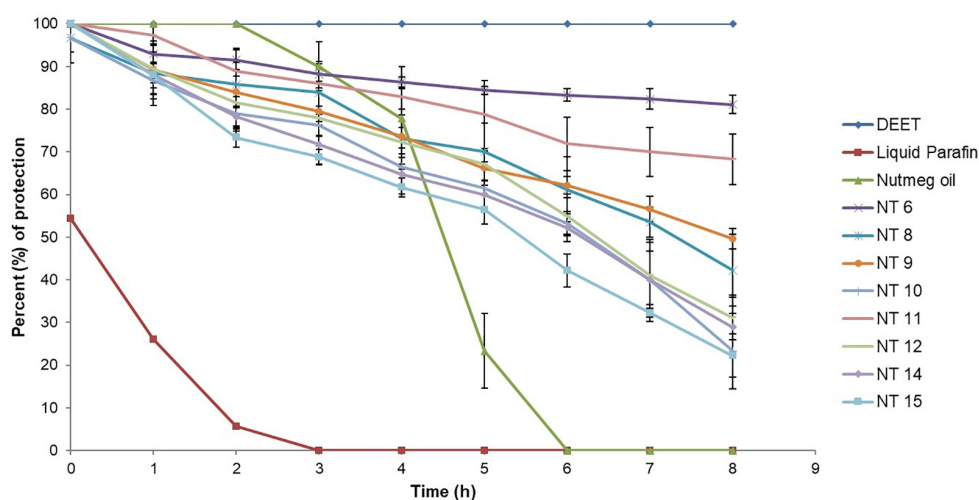


**FIGURE 3** | Mosquito repellent activity of controls, nutmeg oil, and selected NTs at hour intervals for the 8 h repellent test (Mean  $\pm$  SD,  $n = 3$ ).

range from 0 to 1 for width size distribution, where 0 indicates a monodispersed particle and  $>0.5$  indicates a broad distribution (Borhade et al., 2012). The formulations with PDI values  $< 0.5$  were NT 6 (0.248), NT 8 (0.421), NT 9 (0.398), NT 10 (0.278), NT 11 (0.401), NT 12 (0.418), NT 14 (0.313), and NT 15 (0.379). These eight formulations had low PDI values, which indicated they had a similar and narrow size distribution (stable and uniform) (Divsalar et al., 2012). Hence, they were chosen for use in the mosquito repellent test. In contrast, PDI values of NT 1, NT 2, NT 3, NT 4, NT 5, NT 7, and NT 13 were  $>$  than 0.5 and thus were eliminated from further study. High PDI values indicate an inhomogeneous and polydispersed distribution (Wissing and Müller, 2002). Polydispersity occurs when both large and small droplets are produced in a nanoemulsion system. When Ostwald ripening occurs, small droplets dissolve into the large droplets,

leading to increased droplet size (Wissing and Müller, 2002). This system is unstable, and phase separation occurs in such formulations after 24 h.

### Repellent Activity of the Selected NTs

Based on droplet size and PDI value, NT 6, NT 8, NT 9, NT 10, NT 11, NT 12, NT 14, and NT 15 were chosen for the mosquito repellent studies. These nanoemulsions did not show any phase separation after 24 h, indicating their stability. **Figure 3** shows the mosquito repellent activity of the selected NTs at every hour interval throughout the 8 h repellent test. The mosquito repellent activities of these NTs were compared with those of nutmeg oil, DEET (positive control), and liquid paraffin (negative control). At hour 0, nutmeg oil and NT 6, NT 9, NT 11, NT 12, NT 14, and NT 15 provided full protection (100%) for the subjects; NT



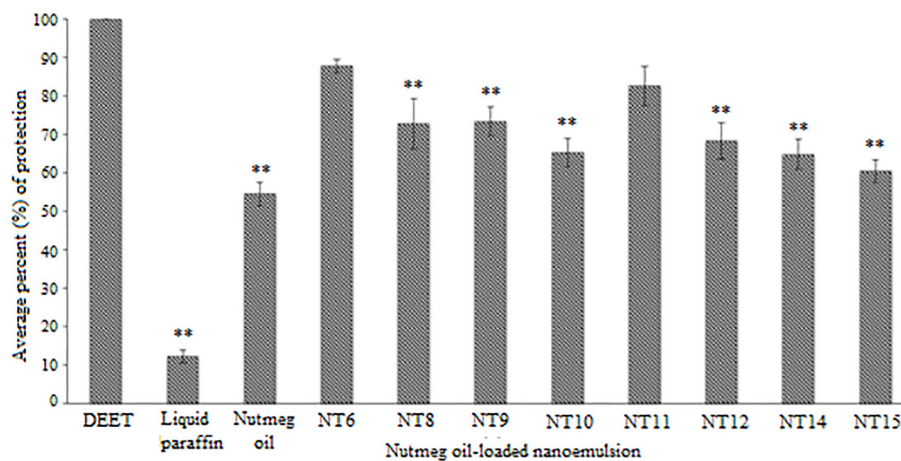


**FIGURE 4 |** Average percentage protection against mosquitoes provided by controls, nutmeg oil, and selected NTs for 8 h (Mean  $\pm$  SD,  $n = 3$ ). \*\*  $p < 0.01$  (Dunnett  $t$ -test).

8 and NT 10 provided 96.67% protection. Protection provided from hour 1 to hour 8 by NT 6 ranged from 92.94 to 81.09%, NT 8 (88.41 to 42.2%), NT 9 (89.35 to 49.57%), and NT 10 (86.67 to 23.33%). Protection provided by NT 11 and NT 12 ranged from 97.3 to 68.25% and 89.44 to 31.16%, respectively. NT 14 and NT 15 provided protection at 28.89% and 22.22% at hour 8, respectively.

**Figure 4** shows the average percent protection provided by the NTs to the test subjects throughout the 8 h test. NT 6 exhibited the greatest repellency (87.81%) and NT 15 was least effective (60.54%). Other NTs were recorded at 72.77% (NT 8), 73.41% (NT 9), 65.31% (NT 10), 82.65% (NT 11), 68.36% (NT 12), and 64.86% (NT 14). The average percent protection by nutmeg oil was 54.57%. The protection provided by NT 6 and NT 11 did not differ significantly compared to that of the control (DEET), whereas the other NTs were significantly less effective than DEET ( $p < 0.01$ ) (Rahman et al., 2015; Chong et al., 2018). In summary, NT 6 and NT 11 sustained their repellent activity every hour during the 8 h test. Therefore, these two NTs were selected for further characterization and the *in vitro* release study.

The selected formulated NTs exhibited higher percentage of protection compared to pure nutmeg oil. This proved that incorporating nutmeg oil into a nanoemulsion system could prolong the protection time. Although NT 6 and NT 11 could not provide greater protection than DEET (100% throughout the 8 h test), the toxicity of DEET should be taken into consideration. Natural essential oil-based repellent products are safe, pleasant to the user, and environmentally sustainable. The

duration of protection against arthropod bites is important too, as essential oils contain an abundance of volatile compounds (Maia and Moore, 2011).

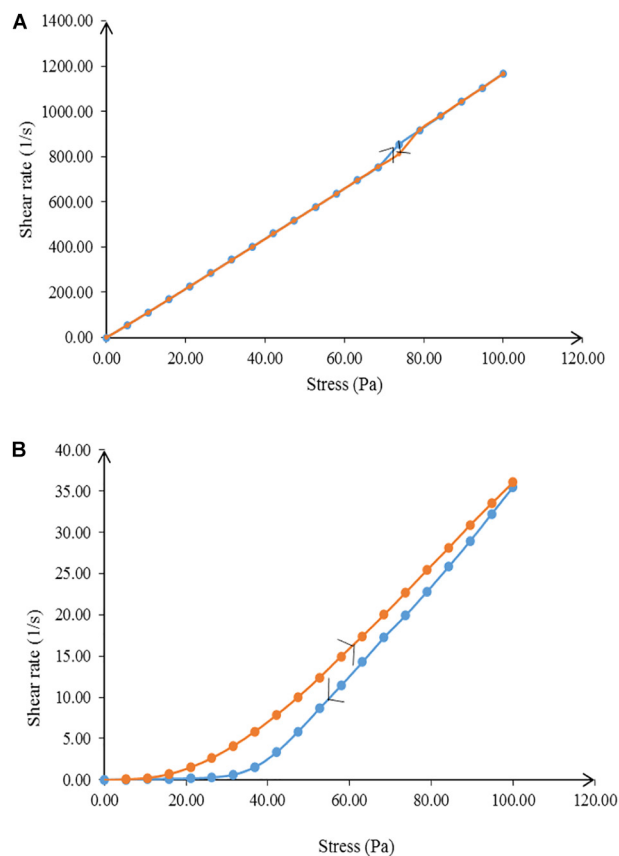


**FIGURE 5 |** Flow behavior of (A) NT 6 and (B) NT 11 from 0.00 to 100 Pa and from 100 to 0.00 Pa shear stress.

**TABLE 2 |** Zeta potential, average pH, and viscosity of NT 6 and NT 11 ( $n = 3$ ).

Formulation	Zeta potential (mV)	pH (mean $\pm$ SD)	Viscosity (Pa.s) at stress stress 100 Pa (mean $\pm$ SD)
NT 6	-44.20	5.60 $\pm$ 0.16	2.49 $\pm$ 0.49
NT 11	-62.90	5.30 $\pm$ 0.13	0.09 $\pm$ 0.02

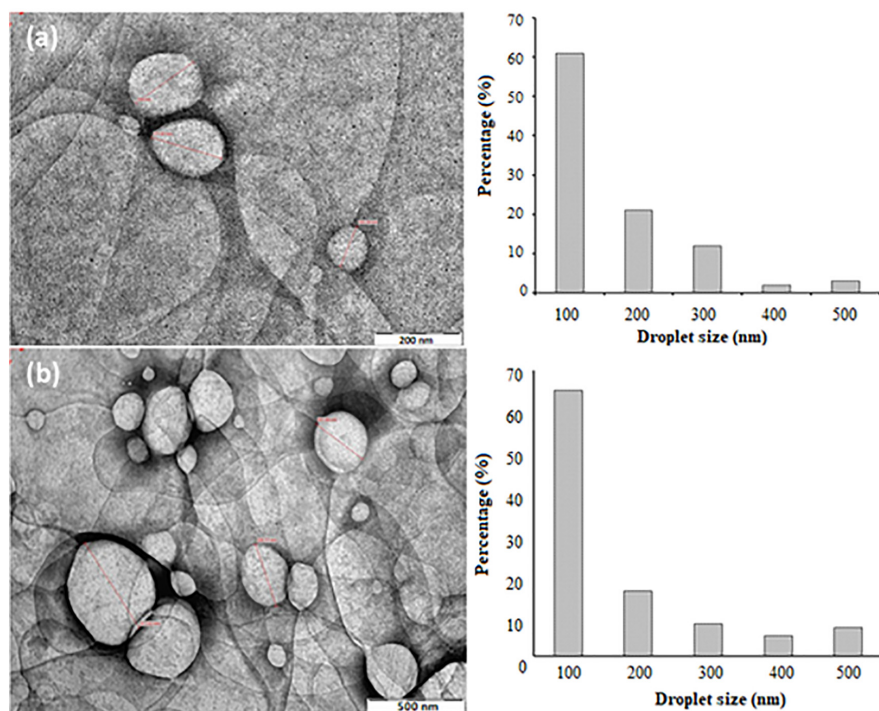


**FIGURE 6 |** TEM morphologies and size distributions of (a) NT 6 at 66,000 magnifications (b) NT 11 at 40,000 magnifications.

## Characterizations of NT 6 and NT 11

NT 6 and NT 11 were characterized for zeta potential, pH, viscosity, rheological behavior, and surface morphology. **Table 2** shows the data for zeta potential, average pH, and viscosity of NT 6 and NT 11. The surface charge of a nanoemulsion is characterized by zeta potential, where values  $>+30$  mV or  $<-30$  mV lead to repulsive forces between the droplets (Sari et al., 2015). The zeta potential values were  $-44.2$  and  $-62.9$  mV for NT 6 and NT 11, respectively. These high values indicated good physical stability of these nanoemulsion systems (Nuchuchua et al., 2009). High repulsive forces between the droplets of a nanoemulsion prevent aggregation in the system and provide good physical stability (Chanasattru et al., 2007). The amount of surfactant present is important because electrostatic repulsion is required to provide the surface charge for stabilization (Musa et al., 2013). Musa et al. (2013) reported that the negativity of zeta potential decreased when the amount of surfactant (lecithin) present was reduced. This repulsive electrostatic interaction between the droplets tends to hinder coalescence, thereby increasing the surface area between the droplets (Musa et al., 2013). In fact, different nanoemulsion system exhibits different particle size distribution. Nanoemulsion system of citronella oil exhibited lower droplet size with increasing surfactant concentration (but with higher glycerol concentration) (Sakulku et al., 2009). The droplet size distribution significantly determines the delivery of the system in terms of rate and the duration of release (Chen et al., 2019a,b). In this study, the negative zeta potentials recorded for NT6 and NT11 were obtained because of the presence of the non-ionic surfactant Montanov® 82.

The pH values of NT 6 and NT 11 were  $5.6 \pm 0.16$  and  $5.3 \pm 0.13$ , respectively. These pH values are suitable for topical administration to skin, as the pH of forearm skin is in the range of 4.2–5.9 (Borges et al., 2013). pH analysis is important to determine the stability and suitability of a product for topical application. In addition to pH, viscosity of a nanoemulsion is important for physical stability (Bali et al., 2010). Viscosities of

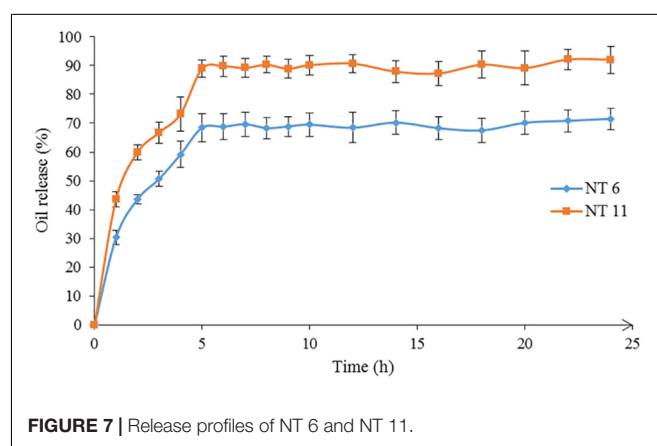


**FIGURE 7 |** Release profiles of NT 6 and NT 11.

**TABLE 3 |** *In vitro* release parameters of NT 6 and NT 11.

Formulation	J flux (mol dm <sup>3</sup> /cm <sup>2</sup> s)	R <sup>2</sup>	k Value (cm <sup>2</sup> s)
NT 6	0.00112	0.9981	$1.0049 \times 10^{-5}$
NT 11	0.00988	0.9866	$7.8143 \times 10^{-4}$

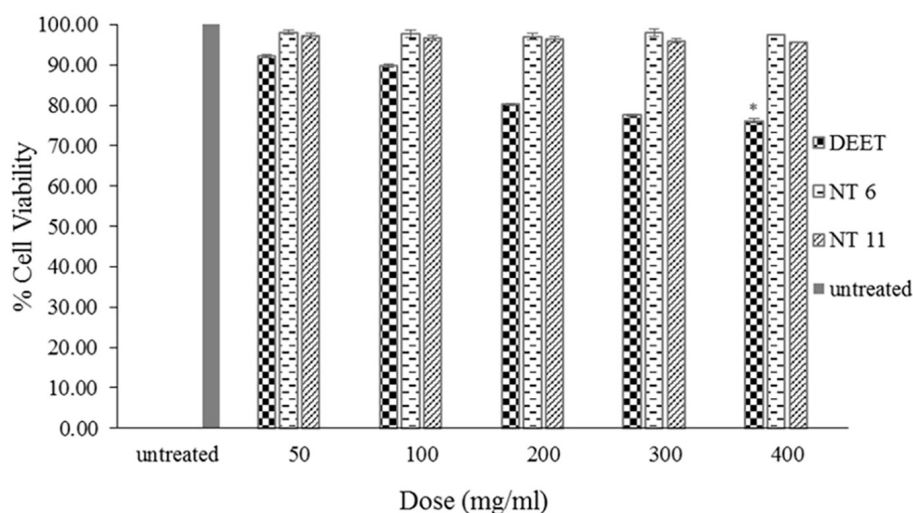


**FIGURE 8 |** Percentage cell viability of L929 cells after 48 h exposure to NT 6, NT 11, and DEET at different doses of treatment using the MTS assay (mean  $\pm$  SD,  $n = 3$ , \* $p < 0.05$  (LSD test)).

NT 6 and NT 11 at stress of 100 Pa were  $2.49 \pm 0.49$  and  $0.09 \pm 0.02$  Pa.s, respectively. These results show that glycerol plays a major role in increasing the viscosity of the nanoemulsion, as glycerol constitutes a greater percentage of NT 6 compared to NT 11 (Sakulku et al., 2009). In addition, the viscosity of NT 11 was less than that of NT 6 due to the water content (NT 11 > NT 6). A higher surfactant ratio traps water in the cross-linking chain of the surfactant, which causes high viscosity of the nanoemulsion (Ghosh et al., 2013).

Rheology, or flow behavior, is an important parameter for characterizing a nanoemulsion in terms of physical stability (Vasiljevic et al., 2006). The flow of a nanoemulsion affects the release and spreadability of the essential oil to the skin surface (Khurana et al., 2013). NT 6 exhibited non-Newtonian plastic behavior, whereas NT 11 showed Newtonian flow behavior (Figure 5) due to the difference in the water ratio. Varshosaz et al. (2013) stated that the coalescence of inner water droplets in the emulsion system gave effect on the behavior of the emulsion system. A nanoemulsion with low viscosity would not be adequate for an insect repellent product meant for topical skin application because it would tend to flow easily (Khurana et al., 2013). However, this problem was solved by the addition of glycerol as the co-solvent, which increased the viscosity of the formulation.

Transmission electron microscope is another important way to analyze the surface morphology of NTs, as it provides a high resolution view of the *in situ* structure of the nanoemulsion (Bali et al., 2010). Figure 6 shows the surface morphologies of NT 6 and NT 11 (stained by PTA). NT 6 and NT 11 appeared bright with dark circles around the droplets, and the NTs showed both regular and irregular spherical shapes.

Droplet size of NT 6 was smaller than that of NT 11. The droplet size distribution in NT 6 and NT 11 ranged between 100 and 500 nm, and this correlated well with the results from the Zeta Nano-ZS apparatus (Figure 6). This correlation is important

because the DLS measurement was performed via dilution of the nanoemulsion (Modi and Patel, 2011). The droplet size distribution of NT 6 and NT 11 showed the highest percentage at 100 nm (61% and 65%, respectively). Bali et al. (2010) also compared droplet size using two different approaches: TEM and photon correlation spectroscopy. TEM offers the advantage of providing high resolution for structures in the nano range, which cannot be detected by classical microscopy techniques (Salvia-Trujillo et al., 2013).

### ***In vitro* Release of Nutmeg Oil From NT 6 and NT 11**

The *in vitro* release of nutmeg oil from NT 6 and NT 11 was investigated for 24 h (Figure 7).  $\alpha$ -pinene (the major compound in nutmeg oil) was selected as the marker for this release study. The GCMS spectrum of the oil was published in Lim et al. (2019). Only 71.5% of nutmeg oil was released from NT 6 compared to 92.4% for NT 11. Release profiles of NT 6 and NT 11 fitted the Higuchi model and yielded  $R^2$  values of 0.9981 and 0.9866, respectively. NT 11 had higher flux and  $k$  value (release rate) than NT 6 (Table 3).

The release rate of an essential oil from a nanoemulsion is affected by viscosity, flow behavior, and water, surfactant, and co-solvent ratios in the nanoemulsion. NT 11 had a higher water ratio and exhibited higher flux and release rate compared to NT 6. Varshosaz et al. (2013) similarly reported that a metoprolol-loaded nanoemulsion (lecithin) with higher water ratio showed higher flux and release rate due to permeation enhancement of the desired compounds through cellulose acetate.

The slower release rate of NT 6 compared to NT 11 might be because NT 6 contained a higher percentage of surfactant (6.25%) compared to NT 11 (3.75%). Similarly, in a citronella oil-loaded nanoemulsion, the formulation containing 10% surfactant had a slower release rate compared to formulations with 2.5% and 5%

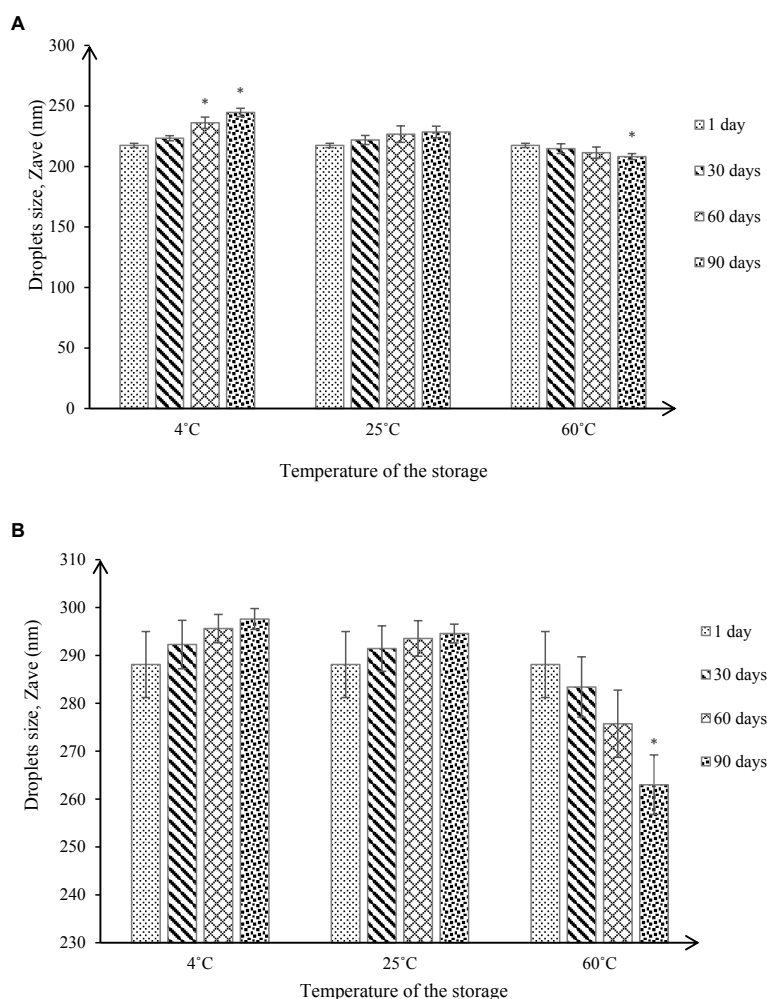


**FIGURE 9 |** Droplet size under different storage conditions throughout 90-day stability tests for **(A)** NT 6 and **(B)** NT 11 (mean  $\pm$  SD,  $n = 3$ ,  $*p < 0.05$ ).

surfactant (Sakulku et al., 2009). Therefore, surfactant content is an important factor affecting the release rate of an essential oil from a nanoemulsion system. In this study, the mobility of nutmeg oil and its release were easier at low surfactant percentage (i.e., NT 11). For NT 6, which contained a high level of glycerol, the release rate was lower because the glycerol caused the NT to be more viscous, which impacted the mobility of nutmeg oil in the carrier solution.

Despite its lower release rate, NT 6 showed greater mosquito repellent efficacy compared to NT 11. Sakulku et al. (2009) also reported that their citronella oil-loaded nanoemulsion with high percentage of glycerol and surfactant achieved a long duration of protection. These findings suggest that more viscous formulations prolong the protection time of repellent activity.

### Cytotoxicity of the NTs

Testing the safety of the NTs is important, as they are intended for use as a topical application for humans. The materials included in the formulation, such as nutmeg oil and surfactant, may cause some toxicity effect (due to the presence

of monoterpenes in nutmeg oil) (Shakeel et al., 2008). Therefore, NT 6 and NT 11 were subjected to cytotoxicity analysis using L929 MTS assays.

The cytotoxicity studies all were conducted using MTS assays (Chen et al., 2020a) with the same concentrations and cell lines (**Figure 8**). After 48 h of exposure to the formulations, the cell viabilities of the NT 6 group were 98.08% (50 mg/mL), 97.7% (100 mg/mL), 96.98% (200 mg/mL), 98.02% (300 mg/mL), and 97.38% (400 mg/mL). The NT 11 group exhibited cell viabilities at 97.1% (50 mg/mL), 96.81% (100 mg/mL), 96.36% (200 mg/mL), 96.02% (300 mg/mL), and 95.67% (400 mg/mL). The DEET group showed cell viabilities of 92.17% (50 mg/mL), 89.8% (100 mg/mL), 80.19% (200 mg/mL), 77.60% (300 mg/mL), and 76.16% (400 mg/mL), respectively. Comparison of results of the test compounds with those of L929 cell without treatment was made using the least significance difference (LSD) test. All samples showed no significance difference ( $p > 0.05$ ), except for DEET at the highest dose (400 mg/mL) ( $p < 0.05$ ).

These results indicate that NT 6 and NT 11 were not toxic to normal skin cells (Samad et al., 2018). In contrast,



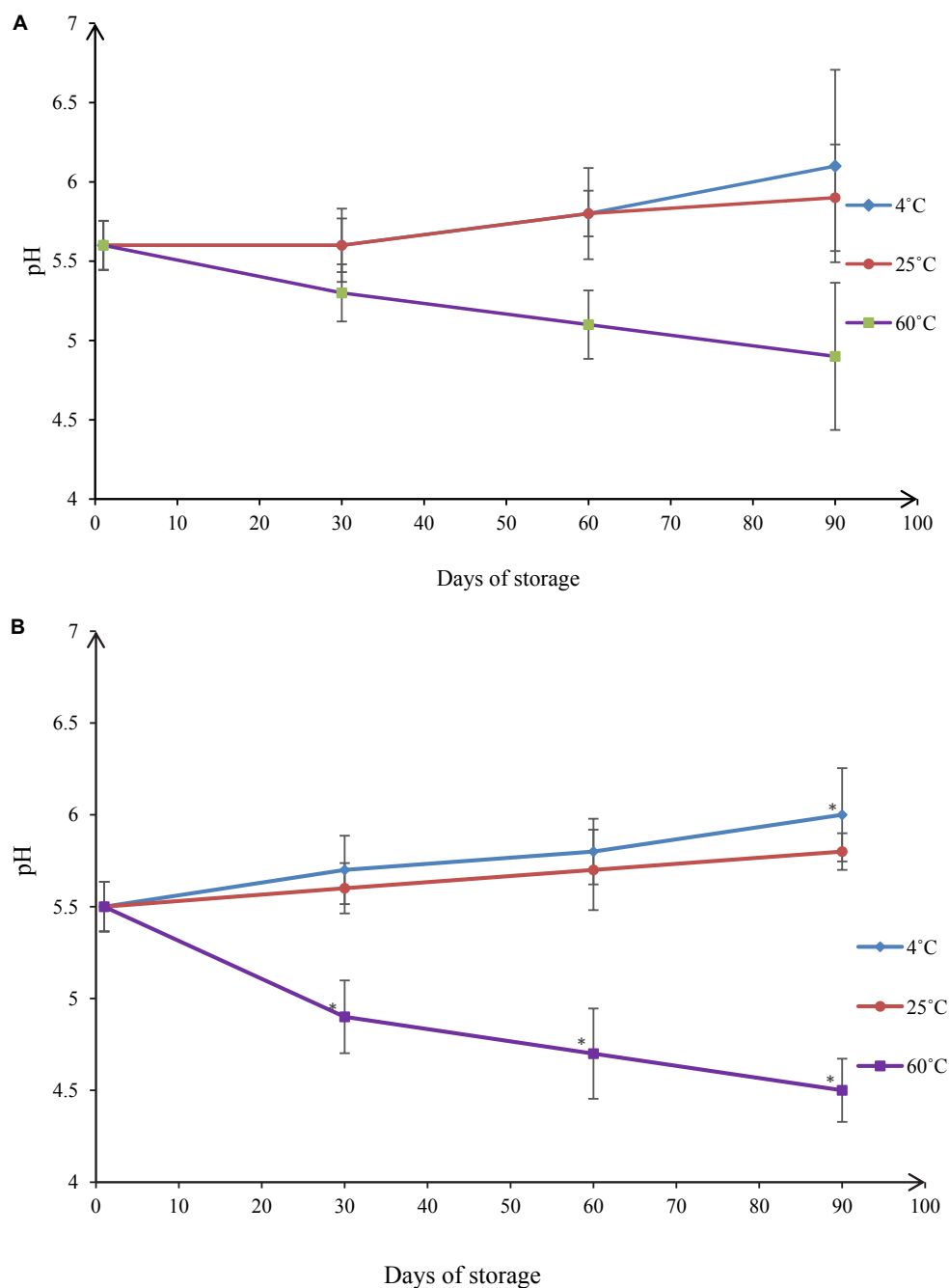


**FIGURE 10 |** pH values under different storage conditions throughout 90-day stability tests for **(A)** NT 6 and **(B)** NT 11 (mean  $\pm$  SD,  $n = 3$ , \* $p < 0.05$ ).

DEET at 400 mg/mL showed significant toxicity compared to the control. DEET is toxic to normal cell lines and causes skin eruption (Costanzo et al., 2007). The  $IC_{50}$  of the assay could not be determined because of low toxicity levels. Nerio et al. (2010) suggested that a low concentration of essential oil can reduce the toxicity and irritation effect. The amount of nutmeg oil (20%) used in the formulations in this study had no toxic effect on L929 skin fibroblast cells. Therefore, the formulated nanoemulsions

appear to pose no risk of skin irritation or toxicity for topical application.

### Stability of NT 6 and NT 11

The stabilities of NT 6 and NT 11 were measured based on droplet size and pH values at different storage temperatures (4°C, 25°C, and 60°C) and after 1, 30, 60, and 90 days of storage. Droplet size measurement (**Figure 9**) is a good indicator of

stability, as a rapid increase of particle size indicates low stability (Bernardi et al., 2011).

At 4°C, the droplet size of NT 6 increased from 217.4 to 223.37 nm after 30 days of storage, showing no significant difference ( $p > 0.05$  in droplet size increase compared to day 1). After 60 and 90 days of storage, the droplet size increased to 236.13 nm and 244.67 nm, respectively, which represented a significant difference ( $p < 0.05$ ) compared to day 1 (217.4 nm). At 25°C, the droplet size of NT 6 kept increasing to 221.9 nm after 30 days, 226.73 nm after 60 days, and 228.53 nm after 90 days of storage. However, these values were not significantly different from the droplet size on day 1. In contrast, droplet size decreased from 214.77 nm (30 days) to 211.4 nm (60 days) and 208.17 nm (90 days) at storage temperature of 60°C. Only the value after 90 days of storage was significantly different from that on day 1 ( $p < 0.05$ ).

For NT 11, droplet size at 4°C increased from day 1 (288.1 nm) to day 30 (292.27 nm), then to 295.6 nm and 297.6 nm after 60 and 90 days. The same trend occurred at 25°C of storage, where the droplet size increased from 291.43 nm (30 days) to 293.53 nm (60 days) to 294.51 nm (90 days). However, the increased values at both storage temperatures did not differ significantly from the droplet size at day 1 ( $p > 0.05$ ). The droplet size at 60°C decreased from day 1 (288.1 nm) to day 60 (275.33), but the values did not differ significantly ( $p > 0.05$ ). However, droplet size was 263 nm after 90, which was significantly smaller than droplet size on day 1 ( $p < 0.05$ ).

NT 6 and NT 11 stored at 4°C exhibited turbidity, but the formulation was transparent when stored at high temperature (60°C). An anti-HIV nanoemulsion formulation also appeared turbid at low temperature but transparent after storage at room temperature; this was due to coagulation in the nanoemulsion system at low temperature (Kotta et al., 2014).

For NT 6 and NT 11, the increased droplet size at storage temperatures of 4°C and 25°C was still within the acceptable range for a nanoemulsion (i.e.,  $\leq 500$  nm) (Pant et al., 2014), and phase separation was not observed throughout the storage period (Bernardi et al., 2011). These results indicate good stability in the nanoemulsion system. The significant increase in droplet size for NT 6 at storage temperature of 4°C after 60 and 90 days might be caused by Ostwald ripening, whereby small nanoemulsion droplets become larger. In addition, droplet aggregation by flocculation and coalescence between nanoemulsion droplets may occur (Rao and McClements, 2011).

pH monitoring is another way to assess the stability of a nanoemulsion (Figure 10). Changes in pH indicate a chemical reaction (Bernardi et al., 2011). pH values of NT 6 were 5.6 (day 1), 5.6 (day 30), 5.8 (day 60), and 6.1 (day 90) at 4°C. Values at 25°C were 5.6 (day 1), 5.6 (day 30), 5.8 (day 60), and 5.9 (day 90). These values did not differ significantly from those at day 1 ( $p > 0.05$ ). At 60°C, pH decreased to 5.3 (day 30), 5.1 (day 60), and 4.9 (day 90). The pH value at day 90 differed significantly from that at day 1 ( $p < 0.05$ ).

The pH values of NT 11 at 4°C storage temperatures were 5.5 (day 1), 5.7 (day 30), 5.8 (day 60), and 6.0 (day 90). At 25°C they were 5.5 (day 1), 5.6 (day 30), 5.7 (day 60), and 5.8 (day 90). For 4°C, the only significant difference detected was between the

values at day 90 and day 1 ( $p < 0.05$ ). No significant difference was detected between the control and any time point at 25°C ( $p > 0.05$ ). At 60°C storage temperature, the pH decreased from 5.5 to 4.5 over the course of 90 days, and the values at days 30, 60, and 90 all differed significantly from the value at day 1 ( $p < 0.05$ ).

These results show that the pH values of NT 6 and NT 11 were stable throughout 90 days of storage at temperatures of 4°C and 25°C. The range of reported pH values was acceptable for topical administration (5.4–6.9) (Borges et al., 2013). In summary, droplet size and pH of both NT 6 and NT 11 were stable at storage temperatures of 4°C and 25°C but not at 60°C. NT 6 and NT 11 are currently stored at the Herbarium Unit, Integrative Medicine Cluster, IPPT, USM with voucher numbers MF-004-NT6 and MF-004-NT11, respectively.

## CONCLUSION

Incorporating of essential oil using a nanoemulsion system can be used to control the release of the oil and prolong the insect repelling effect. In this study, nutmeg oil-loaded nanoemulsions were formulated and tested for their effectiveness as mosquito repellents.

Previous studies of nutmeg, basil, and peppermint oils and their combinations indicated that nutmeg oil was the best at providing protection against mosquitoes for SD rats. Therefore, nutmeg oil was used in this study to formulate essential oil-loaded nanoemulsions to develop an effective controlled release natural repellent formulation.

NT 6 and NT 11 formed desirable droplet sizes ( $< 500$  nm) with PDI values  $< 0.5$ . Zeta potentials of the NTs also were within the acceptable range ( $> -30$  mV). pH values ranged from 4.2 to 5.9, which is suitable for topical application. Viscosities of these NTs were affected by the amount of water and glycerol in the formulation. Release rates of nutmeg oil for NT 6 and NT 11 were  $1.0049 \times 10^{-5} \text{ cm}^2 \text{ s}$  and  $7.8143 \times 10^{-4} \text{ cm}^2 \text{ s}$ , respectively. The amount of surfactant used to produce NT 6 and NT 11 was less than 10%. The low percentage of surfactant used meets sensory, regulatory, and economic objectives. The preparation of NTs using a high speed stirring homogenizer and sonication tools produced stable nanoemulsion systems, which would be economically effective for larger scale production. In conclusion, NT 6 and NT 11 provided high mosquito repellent efficacy compared to nutmeg oil only and may prove to be useful alternatives for insect repellent products in the future.

## DATA AVAILABILITY STATEMENT

All datasets generated for this study are included in the article/supplementary material.

## ETHICS STATEMENT

All animal procedures used were in strict accordance with animal care protocols, and all experimental protocols were approved

by the Universiti Sains Malaysia Animal Ethics Committee [USM/Animal Ethics Approval/2013/(85) (441)].

## AUTHOR CONTRIBUTIONS

All the authors were involved in the designing of the experiments. Additionally, MM, HC, and NM conducted the experiments. MR, SS, YY, and CT analyzed and interpreted the data. VL and MM wrote the manuscript. VL supervised the entire study.

## REFERENCES

- Adeniran, O. I., and Fabiyi, E. (2012). A cream formulation of an effective mosquito repellent: a topical product from lemongrass oil (*Cymbopogon citratus*) Stapf. *J. Nat. Prod. Plant. Resour.* 2, 322–327.
- Assi, R. A., Darwis, Y., Abdulbaqi, I. M., Khan, A. A., Lim, V., and Laghari, M. H. (2017). *Morinda citrifolia* (Noni): a comprehensive review on its industrial uses, pharmacological activities, and clinical trials. *Arab. J. Chem.* 10, 691–707. doi: 10.1016/j.arabjc.2015.06.018
- Ayub, A. D., Chiu, H. I., Mat Yusuf, S. N. A., Abd Kadir, E., Ngali, S. H., and Lim, V. (2019). Biocompatible disulphide cross-linked sodium alginate derivative nanoparticles for oral colon-targeted drug delivery. *Artif. Cells Nanomed. Biotechnol.* 47, 353–369. doi: 10.1080/21691401.2018.1557672
- Azeem, M., Zaman, T., Tahir, M., Haris, A., Iqbal, Z., Binyameen, M., et al. (2019). Chemical composition and repellent activity of native plants essential oils against dengue mosquito, *Aedes aegypti*. *Ind. Crops Products* 140:111609. doi: 10.1016/j.indcrop.2019.111609
- Bali, V., Ali, M., and Ali, J. (2010). Study of surfactant combinations and development of a novel nanoemulsion for minimising variations in bioavailability of ezetimibe. *Colloids Surf. B Biointerfaces* 76, 410–420. doi: 10.1016/j.colsurfb.2009.11.021
- Bernardi, D. S., Pereira, T. A., Maciel, N. R., Bortoloto, J., Viera, G. S., Oliveira, G. C., et al. (2011). Formation and stability of oil-in-water nanoemulsions containing rice bran oil: in vitro and in vivo assessments. *J. Nanobiotechnol.* 9:44. doi: 10.1186/1477-3155-9-44
- Bissinger, B. W., and Roe, R. M. (2010). Tick repellents: past, present, and future. *Pestic. Biochem. Physiol.* 96, 63–79. doi: 10.1016/j.pestbp.2009.09.010
- Borges, V. R., de, A., Simon, A., Sena, A. R. C., Cabral, L. M., and de Sousa, V. P. (2013). Nanoemulsion containing dapson for topical administration: a study of in vitro release and epidermal permeation. *Int. J. Nanomed.* 8, 535–544. doi: 10.2147/IJN.S39383
- Borhade, V., Pathak, S., Sharma, S., and Patravale, V. (2012). Clotrimazole nanoemulsion for malaria chemotherapy. Part I: preformulation studies, formulation design and physicochemical evaluation. *Int. J. Pharm.* 431, 138–148. doi: 10.1016/j.ijpharm.2011.12.040
- Carbone, C., Campisi, A., Musumeci, T., Raciti, G., Bonfanti, R., and Puglisi, G. (2014). FA-loaded lipid drug delivery systems: preparation, characterization and biological studies. *Eur. J. Pharm. Sci.* 52, 12–20. doi: 10.1016/j.ejps.2013.10.003
- Chanasattru, W., Decker, E. A., Julian, and McClements, D. (2007). Inhibition of droplet flocculation in globular-protein stabilized oil-in-water emulsions by polyols. *Food Res. Int.* 40, 1161–1169. doi: 10.1016/j.foodres.2007.06.012
- Chen, L., Gnanaraj, C., Arulselvan, P., El-Seedi, H., and Teng, H. (2019a). A review on advanced microencapsulation technology to enhance bioavailability of phenolic compounds: based on its activity in the treatment of Type 2 diabetes. *Trends Food Sci. Technol.* 85, 149–162. doi: 10.1016/j.tifs.2018.11.026
- Chen, L., Lin, X., and Teng, H. (2020a). Emulsions loaded with dihydromyricetin enhance its transport through Caco-2 monolayer and improve anti-diabetic effect in insulin resistant HepG2 cell. *J. Funct. Foods* 64:103672. doi: 10.1016/j.jff.2019.103672
- Chen, L., Lin, X., Xu, X., Chen, Y., Li, K., Fan, X., et al. (2019b). Self-nano-emulsifying formulation of *Sonchus oleraceus* Linn for improved stability: implications for phenolics degradation under in vitro gastrointestinal digestion: food grade drug delivery system for crude extract but not single compound. *J. Funct. Foods* 53, 28–35. doi: 10.1016/j.jff.2018.12.009
- Chen, L., Lin, X., Xu, X., Wang, L., Teng, H., and Cao, H. (2020b). Anti-inflammatory effect of self-emulsifying delivery system containing *Sonchus oleraceus* Linn extract on streptozotocin-induced diabetic rats. *Food Chem. Toxicol.* 135:110953. doi: 10.1016/j.fct.2019.11.0953
- Chong, H. W., Rezaei, K., Chew, B. L., and Lim, V. (2018). Chemometric profiling of *Clinacanthus nutans* leaves possessing antioxidant activities using ultraviolet-visible spectrophotometry. *Chiang Mai J. Sci.* 45, 1–12.
- Costanzo, S. D., Watkinson, A. J., Murby, E. J., Kolpin, D. W., and Sandstrom, M. W. (2007). Is there a risk associated with the insect repellent DEET (N,N-diethyl-m-toluamide) commonly found in aquatic environments? *Sci. Total Environ.* 384, 214–220. doi: 10.1016/j.scitotenv.2007.05.036
- Devarajan, V., and Ravichandran, V. (2011). Nanoemulsions as modified drug delivery tool. *Pharm. Glob. Int. J. Compr. Pharm.* 2, 1–6.
- Divsalar, A., Saboury, A. A., Nabiuni, M., Zare, Z., Kefayati, M. E., and Seyedarabi, A. (2012). Characterization and side effect analysis of a newly designed nanoemulsion targeting human serum albumin for drug delivery. *Colloids Surf. B Biointerfaces* 98, 80–84. doi: 10.1016/j.colsurfb.2012.04.036
- Donsi, F., Annunziata, M., Vincenzi, M., and Ferrari, G. (2012). Design of nanoemulsion-based delivery systems of natural antimicrobials: effect of the emulsifier. *J. Biotechnol.* 159, 342–350. doi: 10.1016/j.jbiotec.2011.07.001
- Fernandez, P., André, V., Rieger, J., and Kühnle, A. (2004). Nano-emulsion formation by emulsion phase inversion. *Colloids Surf. A Physicochem. Eng. Asp.* 251, 53–58. doi: 10.1016/j.colsurfa.2004.09.029
- Ghosh, V., Mukherjee, A., and Chandrasekaran, N. (2013). Ultrasonic emulsification of food-grade nanoemulsion formulation and evaluation of its bactericidal activity. *Ultrason. Sonochem.* 20, 338–344. doi: 10.1016/j.ultsonch.2012.08.010
- Ghozali, S. Z. L., Lim, V., and Ahmad, N. H. (2015). Biosynthesis and characterization of silver nanoparticles using *Catharanthus roseus* leaf extract and its proliferative effects on cancer cell lines. *J. Nanomed. Nanotechnol.* 6:1000305. doi: 10.4172/2157-7439.1000305
- Govindarajan, M. (2010). Larvicidal and repellent activities of *Sida acuta* Burm. F. (Family: Malvaceae) against three important vector mosquitoes. *Asian Pac. J. Trop. Med.* 3, 691–695. doi: 10.1016/S1995-7645(10)60167-8
- Gupta, D. K., Chouhan, M., Mangalawat, S., and Gupta, R. (2013). A review on plant essential oils as mosquito repellent. *J. Curr. Sci.* 20, 741–747.
- Hanan, N. A., Chiu, H. I., Ramachandran, M. R., Tung, W. H., Mohamad Zain, N. N., Yahaya, N., et al. (2018). Cytotoxicity of plant-mediated synthesis of metallic nanoparticles: a systematic review. *Int. J. Mol. Sci.* 19:1725. doi: 10.3390/ijms19061725
- Hang Chio, E., and Yang, E. C. (2008). A bioassay for natural insect repellents. *J. Asia. Pac. Entomol.* 11, 225–227. doi: 10.1016/j.aspen.2008.08.002
- Iyer, P., and Makris, S. (2010). “Developmental and reproductive toxicology of pesticides,” in *Hayes’ Handbook of Pesticide Toxicology*, ed. R. Krieger, (San Diego, CA: Academic Press), 381–440. doi: 10.1016/B978-0-12-374367-1.00012-4
- Jafari, S. M., He, Y., and Bhandari, B. (2007). Optimization of nano-emulsions production by microfluidization. *Eur. Food Res. Technol.* 225, 733–741. doi: 10.1007/s00217-006-0476-9

- Khurana, S., Jain, N. K., and Bedi, P. M. S. (2013). Nanoemulsion based gel for transdermal delivery of meloxicam: physico-chemical, mechanistic investigation. *Life Sci.* 92, 383–392. doi: 10.1016/j.lfs.2013.01.005
- Kotta, S., Khan, A. W., Ansari, S. H., Sharma, R. K., and Ali, J. (2014). Anti HIV nanoemulsion formulation: optimization and in vitro-in vivo evaluation. *Int. J. Pharm.* 462, 129–134. doi: 10.1016/j.ijpharm.2013.12.038
- Leong, T. S. H., Wooster, T. J., Kentish, S. E., and Ashokkumar, M. (2009). Minimising oil droplet size using ultrasonic emulsification. *Ultrason. Sonochem.* 16, 721–727. doi: 10.1016/j.ultsonch.2009.02.008
- Lim, K. T., Lim, V., and Chin, J. H. (2012). Subacute oral toxicity study of ethanolic leaves extracts of *Strobilanthes crispus* in rats. *Asian Pac. J. Trop. Biomed.* 2, 948–952. doi: 10.1016/S2221-1691(13)60005-2
- Lim, V., Kiang Peh, K., and Sahudin, S. (2013). Synthesis, characterisation, and evaluation of a cross-linked disulphide amide-anhydride-containing polymer based on cysteine for colonic drug delivery. *Int. J. Mol. Sci.* 14, 24670–24691. doi: 10.3390/ijms141224670
- Lim, V., Mohd Narawi, M., Chiu, H. I., Tung, W. H., Tan, J. J., and Lee, C. K. (2019). Selected essential oils as repellents against aedes aegypti: validation of the bioconstituents using gas chromatography. *J. Essential Oil Bearing Plants* 22, 1058–1073. doi: 10.1080/0972060X.2019.1661796
- Lim, V., Yap, C., Chong, H., Shukkoor, M., and Priya, M. (2015). Antimicrobial evaluation and GC-MS analysis of *Strobilanthes crispus* ethanolic leaf extract. *Eur. J. Med. Plants* 10, 1–8. doi: 10.9734/ejmp/2015/20075
- Maia, M. F., and Moore, S. J. (2011). Plant-based insect repellents: a review of their efficacy, development and testing. *Malar. J.* 10:S11. doi: 10.1186/1475-2875-10-S1-S11
- Maji, T. K., and Hussain, M. R. (2009). Microencapsulation of *Zanthoxylum limonella* oil (ZLO) in genipin crosslinked chitosan–gelatin complex for mosquito repellent application. *J. Appl. Polym. Sci.* 2, 779–785. doi: 10.1002/app.29001
- Modi, J. D., and Patel, J. K. (2011). Nanoemulsion-based gel formulation of aceclofenac for topical delivery. *Int. J. Pharm. Pharm. Sci. Res.* 1, 6–12.
- Musa, S. H., Basri, M., Masoumi, H. R. F., Karjiban, R. A., Malek, E. A., Basri, H., et al. (2013). Formulation optimization of palm kernel oil esters nanoemulsion-loaded with chloramphenicol suitable for meningitis treatment. *Colloids Surf. B Biointerfaces* 112, 113–119. doi: 10.1016/j.colsurfb.2013.07.043
- Nerio, L. S., Olivero-Verbel, J., and Stashenko, E. (2010). Repellent activity of essential oils: a review. *Bioresour. Technol.* 101, 372–378. doi: 10.1016/j.biortech.2009.07.048
- Nuchuchua, O., Sakulku, U., Uawongyart, N., Puttipatkhachorn, S., Soottitantawat, A., and Ruktanonchai, U. (2009). In vitro characterization and mosquito (*Aedes aegypti*) repellent activity of essential-oils-loaded nanoemulsions. *AAPS PharmSciTech* 10, 1234–1242. doi: 10.1208/s12249-009-9323-1
- Oshaghi, M. A., Ghalandari, R., Vatandoost, H., Shayeghi, M., Kamali-Nejad, M., Tourabi-Khaledi, H., et al. (2003). Repellent effect of extracts and essential oils of Citrus limon (Rutaceae) and Melissa officinalis (Labiatae) against main malaria vector, Anopheles stephensi (Diptera: Culicidae). *Iran. J. Public Health* 32, 47–52.
- Pant, M., Dubey, S., Patanjali, P. K., Naik, S. N., and Sharma, S. (2014). Insecticidal activity of eucalyptus oil nanoemulsion with karanja and jatropa aqueous filtrates. *Int. Biodeterior. Biodegrad.* 91, 119–127. doi: 10.1016/j.ibiod.2013.11.019
- Poobalan, K., Lim, V. L., Kamal, N. N. S. N. M., Yusoff, N. A., Khor, K. Z., and Samad, N. A. (2018). Effects of ultrasound assisted sequential extraction (UASE) of Moringa oleifera leaves extract on MCF 7 human breast cell line. *Malaysian J. Med. Heal. Sci.* 14, 102–106.
- Ragelle, H., Crauste-Manciet, S., Seguin, J., Brossard, D., Scherman, D., Arnaud, P., et al. (2012). Nanoemulsion formulation of fisetin improves bioavailability and antitumour activity in mice. *Int. J. Pharm.* 427, 452–459. doi: 10.1016/j.ijpharm.2012.02.025
- Rahman, M. Z. F. A., Chong, H. W., and Lim, V. (2015). UV-visible metabolomics approach for the determination of selected adulterants in claimed premixed coffee. *Malaysian J. Med. Heal. Sci.* 14, 147–152.
- Rao, J., and McClements, D. J. (2011). Food-grade microemulsions, nanoemulsions and emulsions: fabrication from sucrose monopalmitate & lemon oil. *Food Hydrocoll.* 25, 1413–1423. doi: 10.1016/j.foodhyd.2011.02.004
- Rocha-Filho, P. A., Maruno, M., Oliveira, B., Bernardi, D. S., Gumiero, V. C., and Pereira, T. A. (2014). Nanoemulsions as a vehicle for drugs and cosmetics. *Nanosci. Technol. Open Access* 1, 1–4. doi: 10.15226/2374-8141/1/1/00105
- Saberi, A. H., Fang, Y., and McClements, D. J. (2013). Effect of glycerol on formation, stability, and properties of vitamin-E enriched nanoemulsions produced using spontaneous emulsification. *J. Colloid Interface Sci.* 411, 105–113. doi: 10.1016/j.jcis.2013.08.041
- Sakulku, U., Nuchuchua, O., Uawongyart, N., Puttipatkhachorn, S., Soottitantawat, A., and Ruktanonchai, U. (2009). Characterization and mosquito repellent activity of citronella oil nanoemulsion. *Int. J. Pharm.* 372, 105–111. doi: 10.1016/j.ijpharm.2008.12.029
- Salvia-Trujillo, L., Rojas-Graü, A., Soliva-Fortuny, R., and Martín-Belloso, O. (2015). Physicochemical characterization and antimicrobial activity of food-grade emulsions and nanoemulsions incorporating essential oils. *Food Hydrocoll.* 43, 547–556. doi: 10.1016/j.foodhyd.2014.07.012
- Salvia-Trujillo, L., Rojas-Graü, M. A., Soliva-Fortuny, R., and Martín-Belloso, O. (2013). Effect of processing parameters on physicochemical characteristics of microfluidized lemongrass essential oil-alginate nanoemulsions. *Food Hydrocoll.* 30, 401–407. doi: 10.1016/j.foodhyd.2012.07.004
- Samad, N. A., Nur, N., Nik, S., Kamal, M., Yahaya, N., Bin, M. Y., et al. (2018). Ethnobotanical, phytochemical, and pharmacological aspects of Melastoma sp. *Malaysian J. Med. Heal. Sci.* 14, 153–163.
- San Martin-González, M. F., Roach, A., and Harte, F. (2009). Rheological properties of corn oil emulsions stabilized by commercial micellar casein and high pressure homogenization. *LWT – Food Sci. Technol.* 42, 307–311. doi: 10.1016/j.lwt.2008.04.005
- Sari, T. P., Mann, B., Kumar, R., Singh, R. R. B., Sharma, R., Bhardwaj, M., et al. (2015). Preparation and characterization of nanoemulsion encapsulating curcumin. *Food Hydrocoll.* 43, 540–546. doi: 10.1016/j.foodhyd.2014.07.011
- Shakeel, F., Baboota, S., Ahuja, A., Ali, J., Aqil, M., and Shafiq, S. (2008). Nanoemulsions as vehicles for transdermal delivery of aceclofenac. *AAPS PharmSciTech* 8, 91–98. doi: 10.1208/pt0804104
- Solomon, B., Sahle, F. F., Gebre-Mariam, T., Asres, K., and Neubert, R. H. H. (2012). Microencapsulation of citronella oil for mosquito-repellent application: formulation and in vitro permeation studies. *Eur. J. Pharm. Biopharm.* 80, 61–66. doi: 10.1016/j.ejpb.2011.08.003
- Subramaniam, S. (2016). *Press Statement by Minister of Health Malaysia: Current Zika Situation in Malaysia 7th September 2016*. Available at: [http://www.moh.gov.my/english.php/database\\_stores/attach\\_download/337/450/](http://www.moh.gov.my/english.php/database_stores/attach_download/337/450/).
- Sugumar, S., Ghosh, V., Nirmala, M. J., Mukherjee, A., and Chandrasekaran, N. (2014). Ultrasonic emulsification of eucalyptus oil nanoemulsion: antibacterial activity against *Staphylococcus aureus* and wound healing activity in Wistar rats. *Ultrason. Sonochem.* 21, 1044–1049. doi: 10.1016/j.ultsonch.2013.10.021
- Tan, J. J., Azmi, S. M., Yong, Y. K., Cheah, H. L., Lim, V., Sandai, D., et al. (2014). Tualang honey improves human corneal epithelial progenitor cell migration and cellular resistance to oxidative stress in vitro. *PLoS ONE* 9:e96800. doi: 10.1371/journal.pone.0096800
- Tang, S. Y., Manickam, S., Wei, T. K., and Nashiru, B. (2012). Formulation development and optimization of a novel Cremophore EL-based nanoemulsion using ultrasound cavitation. *Ultrason. Sonochem.* 19, 330–345. doi: 10.1016/j.ultsonch.2011.07.001
- Teng, H., and Chen, L. (2017).  $\alpha$ -Glucosidase and  $\alpha$ -amylase inhibitors from seed oil: a review of liposoluble substance to treat diabetes. *Crit. Rev. Food Sci. Nutr.* 57, 3438–3448. doi: 10.1080/10408398.2015.1129309
- Varshosaz, J., Andalib, S., Tabbakhian, M., and Ebrahimzadeh, N. (2013). Development of lecithin nanoemulsion based organogels for permeation enhancement of metoprolol through rat skin. *J. Nanomater.* 2013, 1–10. doi: 10.1155/2013/139437
- Vasiljevic, D., Parojcic, J., Primorac, M., and Vuleta, G. (2006). An investigation into the characteristics and drug release properties of multiple W/O/W emulsion systems containing low concentration of lipophilic polymeric emulsifier. *Int. J. Pharm.* 309, 171–177. doi: 10.1016/j.ijpharm.2005.11.034
- Wang, L., Li, X., Zhang, G., Dong, J., and Eastoe, J. (2007). Oil-in-water nanoemulsions for pesticide formulations. *J. Colloid Interface Sci.* 314, 230–235. doi: 10.1016/j.jcis.2007.04.079



- Wissing, S. A., and Müller, R. H. (2002). Solid lipid nanoparticles as carrier for sunscreens: in vitro release and in vivo skin penetration. *J. Control. Release* 81, 225–233. doi: 10.1016/S0168-3659(02)00056-1
- Yakop, F., Abd Ghafar, S. A., Yong, Y. K., Saiful Yazan, L., Mohamad Hanafiah, R., Lim, V., et al. (2018). Silver nanoparticles Clinacanthus nutans leaves extract induced apoptosis towards oral squamous cell carcinoma cell lines. *Artif. Cells Nanomed. Biotechnol.* 46, 131–139. doi: 10.1080/21691401.2018.1452750
- Yuan, Y., Gao, Y., Zhao, J., and Mao, L. (2008). Characterization and stability evaluation of  $\beta$ -carotene nanoemulsions prepared by high pressure homogenization under various emulsifying conditions. *Food Res. Int.* 41, 61–68. doi: 10.1016/j.foodres.2007.09.006

**Conflict of Interest:** The authors declare that the research was conducted in the absence of any commercial or financial relationships that could be construed as a potential conflict of interest.

Copyright © 2020 Mohd Narawi, Chiu, Yong, Mohamad Zain, Ramachandran, Tham, Samsurrijal and Lim. This is an open-access article distributed under the terms of the Creative Commons Attribution License (CC BY). The use, distribution or reproduction in other forums is permitted, provided the original author(s) and the copyright owner(s) are credited and that the original publication in this journal is cited, in accordance with accepted academic practice. No use, distribution or reproduction is permitted which does not comply with these terms.



## OPEN ACCESS

### Edited by:

Namrita Lall,  
University of Pretoria, South Africa

### Reviewed by:

Sefirin Djiogue,  
University of Yaounde I, Cameroon  
SubbaRao V. Madhunapantula,  
JSS Academy of Higher Education  
and Research, India

### \*Correspondence:

Young Ho Kim  
ykh@cnu.ac.kr  
Young Ran Kim  
kimyr@jnu.ac.kr

<sup>†</sup>These authors have contributed  
equally to this work

### Specialty section:

This article was submitted to  
Ethnopharmacology,  
a section of the journal  
Frontiers in Pharmacology

**Received:** 13 October 2019

**Accepted:** 31 March 2020

**Published:** 23 April 2020

### Citation:

Park JU, Yang SY, Guo RH, Li HX,  
Kim YH and Kim YR (2020) Anti-  
Melanogenic Effect of *Dendropanax*  
*morbiferus* and Its Active Components  
via Protein Kinase A/Cyclic Adenosine  
Monophosphate-Responsive Binding  
Protein- and p38 Mitogen-Activated  
Protein Kinase-Mediated  
Microphthalmia-Associated  
Transcription Factor Downregulation.  
*Front. Pharmacol.* 11:507.  
doi: 10.3389/fphar.2020.00507

# Anti-Melanogenic Effect of *Dendropanax morbiferus* and Its Active Components via Protein Kinase A/Cyclic Adenosine Monophosphate-Responsive Binding Protein- and p38 Mitogen-Activated Protein Kinase-Mediated Microphthalmia-Associated Transcription Factor Downregulation

Jung Up Park<sup>1†</sup>, Seo Young Yang<sup>2†</sup>, Rui Hong Guo<sup>1</sup>, Hong Xu Li<sup>2</sup>, Young Ho Kim<sup>2\*</sup> and Young Ran Kim<sup>1\*</sup>

<sup>1</sup> College of Pharmacy and Research Institute of Drug Development, Chonnam National University, Gwangju, South Korea,

<sup>2</sup> College of Pharmacy, Chungnam National University, Daejeon, South Korea

*Dendropanax morbiferus* H. Lév has been reported to have some pharmacologic activities and also interested in functional cosmetics. We found that the water extract of *D. morbiferus* leaves significantly inhibited tyrosinase activity and melanin formation in  $\alpha$ -melanocyte stimulating hormone (MSH)-induced B16-F10 cells. *D. morbiferus* reduced melanogenesis-related protein levels, such as microphthalmia-associated transcription factor (MITF), TRP-1, and TRP-2, without any cytotoxicity. Two active ingredients of *D. morbiferus*, (10E)-9,16-dihydroxyoctadeca-10,17-dien-12,14-diynoate (DMW-1) and (10E)-(-)-10,17-octadecadiene-12,14-diyne-1,9,16-triol (DMW-2) were identified by testing the anti-melanogenic effects and then by liquid chromatography-tandem mass spectrometry (LC/MS/MS) analysis. DMW-1 and DMW-2 significantly inhibited melanogenesis by the suppression of protein kinase A (PKA)/cyclic AMP (cAMP)-responsive binding protein (CREB) and p38 MAPK phosphorylation. DMW-1 showed a better inhibitory effect than DMW-2 in  $\alpha$ -MSH-induced B16-F10 cells. *D. morbiferus* and its active component DMW-1 inhibited melanogenesis through the downregulation of cAMP, p-PKA/CREB, p-p38, MITF, TRP-1, TRP-2, and tyrosinase. These results indicate that *D. morbiferus* and DMW-1 may be useful ingredients for cosmetics and therapeutic agents for skin hyperpigmentation disorders.

**Keywords:** *Dendropanax morbiferus*, (10E)-9,16-dihydroxyoctadeca-10,17-dien-12,14-diynoate, anti-melanogenesis, tyrosinase, PKA/CREB, p-p38/p38, microphthalmia-associated transcription factor

## INTRODUCTION

*Dendropanax morbiferus* H. Lév, an endemic species in South Korea, has been used as an alternative traditional medicine for several diseases, such as headache, dysmenorrhea, infectious disorders, and skin disorders, for a long time (Jeong et al., 1995; Park et al., 2004; Lim et al., 2015). There are some reports that *D. morbiferus* shows anti-hyperuricemic, anti-amnesic, anti-obesity, immunomodulatory, and anti-inflammatory activities (Birhanu et al., 2018; Cho et al., 2018; Park et al., 2018a; Park et al., 2018b; Song et al., 2018; Sun et al., 2018b; Choo et al., 2019). The corresponding ingredients isolated from *D. morbiferus* leaves, such as 1-tetradecanol, dendropanoxide, rutin, gentisic acid, or oleifoliosides, have been reported to have diverse therapeutic potentials (Yu et al., 2012; Lee et al., 2013; Park et al., 2014; Park et al., 2017; Sun et al., 2018a). Recently, *D. morbiferus* is increasingly interested in functional materials in cosmetics. Several studies have reported that *D. morbiferus* and its components have diverse therapeutic potentials, such as anti-wrinkle, hair growth, and moisturizing effect (Lee et al., 2005; Deng et al., 2010; Lee et al., 2015; Park and Han, 2016). In addition, 1-tetradecanol, and  $\beta$ -sitosterol isolated from *D. morbiferus* were reported to possess anti-melanogenic effects (Lee et al., 2015). However, there are few studies about the anti-melanogenic activity of *D. morbiferus* and its components as a therapeutic potential herbal medicine. To further investigate the efficacy and mechanism of *D. morbiferus*, we evaluated its function on the anti-melanogenic effect in this study.

Melanin is produced from melanocytes in the epidermis by a pigmentation process called melanogenesis and it is the main factor determining the color of human skin, hair, and eyes (Riley, 2003; D'Orazio et al., 2013). In addition, melanin plays an important role in protecting the skin from ultraviolet (UV) radiation (Costin and Hearing, 2007; Brenner and Hearing, 2008). Moreover, abnormal accumulation of melanin on skin surface leads to various skin pigmentation disorders, such as dots, freckles, and post-inflammatory hyperpigmentation (Pillaiyar et al., 2018). Melanogenesis regulation is under a complex control. Tyrosinase, the main melanogenic factor in the biosynthesis of melanin, is a rate-limiting enzyme that catalyzes the hydroxylation of L-tyrosine to form tyrosine to 3,4-dihydroxyphenylalanine (DOPA) and oxidizes DOPA to produce DOPA-quinone (Slominski et al., 1988; Slominski et al., 2012). The main role of the melanin-synthesizing tyrosinase gene family (tyrosinase, TRP-1, and TRP-2) is to differentiate, proliferate, and accumulate melanin into melanocytes. Microphthalmia-associated transcription factor (MITF) is not only the main regulator of melanocyte proliferation, development, and survival but also a major

regulator of melanogenesis-related protein expression (Liu and Fisher, 2010; Kim et al., 2018b). cAMP-responsive binding protein (CREB) regulates the expression of MITF in melanosomes. The phosphorylation of CREB is regulated by the activation of cAMP/protein kinase A (PKA) cascades that are known to play main roles in melanin synthesis (Pillaiyar et al., 2017). The mitogen-activated protein kinase (MAPK) family proteins, including extracellular signal-regulated kinase (ERK) 1/2, c-Jun N terminal kinase (JNK) 1/2 and p38, are known to play crucial roles in melanogenesis (Wu et al., 2011; Pillaiyar et al., 2017). Melanin production can be triggered by a variety of factors, including  $\alpha$ -melanocyte stimulating hormone ( $\alpha$ -MSH), adrenocorticotrophic hormone (ACTH), and stem cell factor (SCF) (Chan et al., 2014). Specifically,  $\alpha$ -MSH is a key regulator in the biosynthesis of melanin and prompt expression of cAMP.

Here, we found that *D. morbiferus* inhibited tyrosinase activity and melanin formation in melanocytes. In the present study, we have investigated the molecular mechanisms of *D. morbiferus* on anti-melanogenic effects by testing MITF, TRP-1, TRP-2, cAMP, PKA/CREB, and p38 MAPK pathways. In addition, the active ingredients from *D. morbiferus* were identified by LC/MS/MS analysis.

## MATERIAL AND METHODS

### Chemical and Reagents

L-3,4-dihydroxyphenylalanine (L-DOPA),  $\alpha$ -melanocyte stimulating hormone ( $\alpha$ -MSH), and arbutin were purchased from Sigma-Aldrich Chemical Co. (St. Louis, MO, USA). Dulbecco's modified Eagle's medium (DMEM) was obtained from Welgene (DG, KR). Fetal bovine serum (FBS) and penicillin/streptomycin were purchased from Thermo Fisher Scientific (MA, USA). Lysis buffer and 3-(4, 5-dimethylthiazol-2-yl)-5-(3-carboxymethoxyphenyl)-2-(4-sulfophenyl)-2H-tetrazolium (MTS) were purchased from Promega (WI, USA). Antibodies specific to MITF, tyrosinase, TRP-1, TRP-2, p38, and GAPDH were purchased from Santa Cruz Biotechnology (CA, USA). Antibodies specific to PKA, CREB, ERK, JNK, p-CREB, p-PKA, p-p38, p-ERK, and p-JNK proteins were obtained from Cell Signaling Technology (MA, USA). Horseradish peroxidase-conjugated secondary antibodies were purchased from Jackson ImmunoResearch, Inc. (PA, USA). Western Bright™ ECL reagent was purchased from Advansta, Inc. (CA, USA). All other chemicals were used in analytical reagent grade.

### Preparation of the Water Extract From *D. morbiferus* Leaves and Its Fractions

*D. morbiferus* water extract (W-DP) and its ethyl acetate fraction (W-EA) were prepared using a method described previously (Park et al., 2018a). *D. morbiferus* leaves were obtained from Jangheung (JL, KR) and the origin of the herbal medicine was confirmed by Jeollanam-do institute of natural resources research (JL, KR). *D. morbiferus* leaves were extracted once with water at 100°C for 4 h. The filtered extract was

**Abbreviations:** ACTH, adrenocorticotrophic hormone; cAMP, cyclic adenosine monophosphate; CC, column chromatography; CREB, cAMP-responsive binding protein; DOPA, 3,4-dihydroxyphenylalanine; ERK, extracellular signal-regulated kinase 1/2; JNK, c-Jun N terminal kinase 1/2; MAPK, mitogen-activated protein kinase; MC1R, melanocortin type 1 receptor; MITF, microphthalmia-associated transcription factor; PKA, protein kinase A; SCF, stem cell factor; TRP-1, tyrosinase-related protein-1; TRP-2, tyrosinase-related protein-2; UV, ultraviolet;  $\alpha$ -MSH,  $\alpha$ -melanocyte stimulating hormone.

concentrated using a continuous vacuum evaporator (40°C, 670 mmHg) followed by lyophilization in a vacuum drier (770 mmHg). The crude water extract of *D. morbiferus* leaves (W-DP, 20 g) was suspended in water and successively divided with 3 x 1 L volumes of *n*-hexane, chloroform, ethyl acetate, *n*-butanol, and aqueous fraction, respectively. The fractions were concentrated using a rotary vacuum concentrator and dried in a 50°C dry oven for >48 h as described previously (Park et al., 2018a).

## Cell Cultures and Cell Viability Assay

Murine B16-F10 skin melanoma cells supplied by the Korea Cell Line Bank (SEL, KR) were maintained in DMEM supplemented with 1% penicillin/streptomycin and 10% FBS under an atmosphere of 5% CO<sub>2</sub> in a humidified 37°C incubator. To test cell viability, B16-F10 cells were cultured into 96-well plates (SPL Life Sciences Co., GG, KR) at a density of  $0.5 \times 10^4$  cells/well overnight. The cells were treated with W-DP at different concentrations with or without  $\alpha$ -MSH (200 nM) for an additional 72 h. The viability of B16-F10 cells was determined by MTS according to the manufacturer's instructions, and absorbance was read at 490 nm with an ELx808 ELISA microplate reader (BioTek Instruments, Inc., VT, USA).

## Intracellular Tyrosinase Activity

Intracellular tyrosinase activity was tested according to previously described method (Li et al., 2018). B16-F10 cells ( $1 \times 10^5$  cells/well) were treated with W-DP (0.03, 0.1, 0.3, 0.5 mg/ml), W-EA (0.01, 0.03 mg/ml), or arbutin (0.54 mg/ml) for 2 h, followed by addition with  $\alpha$ -MSH (200 nM) for 72 h. The cells were then lysed in a lysis buffer with protease inhibitor cocktail for 30 min at 4°C and centrifuged at 13,000 rpm for 10 min at 4°C. Proteins were quantified by using Bradford reagent and equal amounts of the lysates were treated with L-DOPA (2 mg/ml) in 96-well plates at 37°C for 2 h. The production of DOPachrome was measured using an ELISA microplate reader at an absorbance of 490 nm.

## Melanin Content Assay

B16-F10 cells ( $1 \times 10^5$  cells/well) were incubated into six-well plate (SPL Life Sciences Co., GG, KR) at 37°C overnight. B16-F10 cells were pretreated with W-DP (0.03, 0.1, 0.3 mg/ml), W-EA (0.01 mg/ml), or arbutin (0.54 mg/ml) for 2 h prior to stimulation with  $\alpha$ -MSH (200 nM) for 72 h. The cells were dissolved in 1 N NaOH with 10% DMSO for 1 h at 60°C. Total melanin lysates were transferred to a 96-well plate and the optical absorbance was measured at 405 nm using an ELISA microplate reader.

## Preparation of Active Compounds From *D. morbiferus*

Dried leaves and stems of *Dendropanax morbiferus* H. Lévy were purchased from the herbal company Hanna Arboretum, Goheung, Jeollanam-do, Korea and taxonomically identified by one of the authors (Prof. YHK). A voucher specimen (CNU 17002) was deposited at the Herbarium of the College of

Pharmacy, Chungnam National University. *D. morbiferus* (3.0 kg) were extracted with 10-fold volume of boiling methanol (10 L x 3) under reflux condition for three times. The methanol extract (470.0 g) was suspended in water and partitioned with *n*-hexane, CH<sub>2</sub>Cl<sub>2</sub>, EtOAc, and *n*-BuOH to yield *n*-hexane fraction, CH<sub>2</sub>Cl<sub>2</sub> fraction, EtOAc fraction, *n*-BuOH fraction, and aqueous fraction, respectively.

Column chromatography (CC) separations were performed using silica gels (SiO<sub>2</sub>; 70–230, 230–400  $\mu$ m particle size; Fuji Silysia Chemical Ltd., AIC, JP) and C<sub>18</sub> resins (75  $\mu$ m, Fuji Silysia Chemical Ltd., AIC, JP). Thin-layer chromatography (TLC) separations were performed using pre-coated silica gels 60 F254 and reversed-phase F254S plates (Merck, Darmstadt, Germany). The NMR spectra were recorded using a JEOL ECA 600 spectrometer (1H, 600 MHz; 13C, 150 MHz; JEOL Ltd, TKY, JP). High-resolution electrospray ionization mass spectra (HRESIMS) were obtained using an Agilent 6530 accurate-mass quadrupole-time of flight-liquid chromatography/mass spectrometry (Q-TOF LC/MS).

The EtOAc extract (21.8 g) was subjected to a silica gel column chromatography with a gradient of CHCl<sub>3</sub>–MeOH (60:1–0:1) to give ten fractions (Fr. EA1–EA10). Fraction EA3 (900.0 mg) was chromatographed on a silica gel column using a gradient of *n*-hexane–EtOAc (6:1–3:1) elution solvent to give eight subfractions (EA3A–EA3H), then subfraction EA3C (70.0 mg) was chromatographed on a reverse-phase column with a gradient of MeOH–water (9:1–1:0) to obtain three subfractions (EA3C1–EA3C3), subfraction EA3C1 (10.0 mg) was further chromatographed on a reverse-phase column with MeOH–water (3:1) to yield DMW-1 (5.3 mg). Subfraction EA3D (238.0 mg) was chromatographed on a reverse-phase column with a gradient of MeOH–water (3:7–1:0) to give eleven subfractions (EA3D1–EA3D11), then subfraction EA3D9 (13.6 mg) was further purified by a silica gel column chromatography with *n*-hexane–acetone (1:1) to yield DMW-2 (6.2 mg). (10E)-9,16-dihydroxyoctadeca-10,17-dien-12,14-diynoate (DMW-1): C<sub>19</sub>H<sub>26</sub>O<sub>4</sub>; viscous liquid; [ $\alpha$ ] –38.0° (c = 0.1, MeOH); HRESIMS ([M+NH<sub>4</sub>]<sup>+</sup> m/z 336.2167, calcd for 336.2175); 1D-NMR (CD<sub>3</sub>OD, 600 MHz), and 2D-NMR data (CD<sub>3</sub>OD, 600 MHz) (see **Supplementary Figure S2** and **Table S1**). (10E)-(–)-10,17-Octadecadiene-12,14-diyne-1,9,16-triol (DMW-2): C<sub>18</sub>H<sub>26</sub>O<sub>3</sub>; viscous liquid; [ $\alpha$ ] –32.6° (c = 0.1, MeOH); HRESIMS ([M+NH<sub>4</sub>]<sup>+</sup> m/z: 308.2219, calcd for 308.2226); 1D-NMR (CD<sub>3</sub>OD, 600 MHz), and 2D-NMR data (CD<sub>3</sub>OD, 600 MHz) (see **Supplementary Figure S3** and **Table S1**). Stock solutions of samples were diluted using phosphate buffered saline (PBS) or ethanol and filter-sterilized and then diluted with PBS for the working concentrations.

## Liquid Chromatography-Tandem Mass Spectrometry (LC/MS/MS) Analysis

Methanol (Sigma-Aldrich Chemical Co., MO, USA) and formic acid (Kanto, Chemical, TKY, JP) were used as LC/MS/MS gradient solvents. A Shimadzu HPLC system (KT, JP) consisted of a dual solvent pump LC-20A, an autosampler SIL-20AC, and a column oven Gemini C<sub>18</sub>. In addition, a mass



spectrometer Q-Trap 4000 (AB Sciex, Foster City, CA) was used for the separation and detection of the single compounds. In detail, the separation was carried out on a Gemini C<sub>18</sub> column (CA, USA) (5  $\mu$ m, 50 mm  $\times$  2.0 mm). The column was heated to 40°C under a flow rate of 0.3 ml/min with a stepwise elution from mobile phase A (0.1% formic acid in water) to mobile phase B (0.1% formic acid in acetonitrile) as follows. The linear gradient elution was set at 15–60% B for 1–4 min, 60% B for 5 min, and 15% B for 10–12 min. The injection volume was set at 10  $\mu$ l. The mass spectrometer was operated in positive Turbo Ion Spray mode and multiple reaction monitoring (MRM) scan mode. The instrumental mass parameters were set as follows: ion spray voltage 5500 V, curtain gas 20, GS1 60, GS2 60, and desolvation temperature (TEM) 500°C. First, we identified the full scan of mass spectra and product ion mass spectra of DMW-1 and 2. The mass transition of m/z 301.212 to m/z 55.2 was used for DMW-1, and m/z 273.213 to m/z 55.1 was used for DMW-2. AB Sciex Analyst software (version 1.5.2) was used for data integration.

The stock solutions of DMW-1 and 2 were prepared at a concentration of 100  $\mu$ M in methanol. The linear range of the calibration curve for DMW-1 and 2 was diluted in water at concentrations of 5, 20, 50, 200, and 500 ng/ml and used as a working standard. The stock solution of W-DP was prepared in water at concentrations of 10 and 50 mg/ml. The solutions were stored at 4°C.

### Cyclic AMP Assay

B16-F10 cells were cultured at a density of  $5 \times 10^4$  cells/well in 24-well plates for 24 h and pretreated with W-DP (0.1 mg/ml), W-EA (0.01 mg/ml), DMW-1 (10  $\mu$ M), or arbutin (0.54 mg/ml) for 2 h, followed by treatment with  $\alpha$ -MSH (200 nM) for 24 h. The cells were incubated with cell lysis buffer at  $-80^\circ\text{C}$  overnight, and then, the thawed lysates were harvested and centrifuged at 10,000 rpm for 10 min at 4°C. The cAMP levels in the lysates were measured by ELISA following the manufacturer's experimental protocols (R&D Systems, MN, USA).

### Western Blot Analysis

The target proteins were detected by Western blot analysis with specific antibodies. B16-F10 cells were cultured in 6-well plates at a density of  $1.5 \times 10^5$  cells/well and then incubated overnight. The cells were pretreated with W-DP (0.1 mg/ml), W-EA (0.01 mg/ml), DMW-1 (10  $\mu$ M), DMW-2 (10  $\mu$ M), or arbutin (0.54 mg/ml) for 2 h before stimulation with  $\alpha$ -MSH (200 nM) for 24 h. Then, cell lysates were harvested and centrifuged at 13,000 rpm for 10 min at 4°C. Equal amounts of the lysates were electrophoresed on 10% sodium dodecyl sulfate-polyacrylamide gel electrophoresis (SDS-PAGE) and transferred to polyvinylidene difluoride membranes (PVDF) (Millipore, MA, USA) at 400 mA for 2 h. The membranes were incubated with appropriate primary antibodies against MITF, tyrosinase, TRP-1, TRP-2, PKA, CREB, ERK, JNK, p-38, p-PKA, p-CREB, p-ERK, p-JNK, p-p38, or GAPDH at 4°C overnight. After being washed, the membranes were incubated with horseradish peroxidase-conjugated anti-rabbit or anti-mouse immunoglobulin

secondary antibodies for 1 h. Immunoreactive proteins were conducted using Western Bright™ ECL reagents and a C300 chemiluminescence imager (Azure Biosystems, Inc., CA, USA).

### Statistical Analysis

All experiments were repeated in at least three separate experiments. Statistical differences were evaluated using GraphPad Prism version 5.01 (San Diego, CA, USA). The results shown are representative experiments. We used one-way ANOVA for multi-group comparisons followed by a Tukey *post hoc* test;  $p < 0.05$  was considered statistically significant.

## RESULTS

### Effect of W-DP on Cell Viability, Tyrosinase Activity and Melanin Formation in $\alpha$ -MSH-Induced B16-F10 Cells

We studied the effect of W-DP on melanogenesis in B16-F10 melanoma cells. First, the cell viability was tested after treatment with various concentrations of W-DP in the presence or absence of  $\alpha$ -MSH. W-DP showed no cytotoxicity to B16-F10 cells (Figure 1A). Next, W-DP (0.03, 0.1, 0.3, 0.5 mg/ml) significantly reduced intracellular tyrosinase activity and melanin production in a dose-dependent manner (Figures 1B, C). In addition, the W-DP remarkably decreased the melanin contents in the cell pellets, which showed lighter colors (Figure 1D). These results suggest that W-DP decreases melanin synthesis through the downregulation of tyrosinase.

### Effect of W-DP on the Expression of Melanogenesis-Related Proteins in $\alpha$ -MSH-Induced B16-F10 Cells

We tested the inhibitory effect of W-DP on melanogenesis-related proteins by Western blot analysis. The expression levels of MITF and tyrosinase were significantly reduced by treatment with W-DP in a dose-dependent manner. TRP-1 and TRP-2 stimulated by  $\alpha$ -MSH were also simultaneously decreased by W-DP treatment (Figure 2). Our results suggest that its effect on melanin synthesis may be associated with the suppression of melanogenesis-related proteins such as tyrosinase, TRP-1, and TRP-2 through MITF inhibition.

### Structure Elucidation of DMW-1 and 2 in *D. moribiferus*

To identify the anti-melanogenic active constituents, we isolated 22 components from the ethyl acetate fraction (W-EA), which was separated from *D. moribiferus* by continuous fractionation (see Supplementary Figure S1). The crude water extract of *D. moribiferus* leaves was subjected to a succession of fractionation procedures and the W-EA showed the most significant inhibitory effects. We evaluated the effects of W-EA at various concentrations in  $\alpha$ -MSH-activated B16-F10 cells. W-EA significantly inhibited tyrosinase activity in a dose-dependent

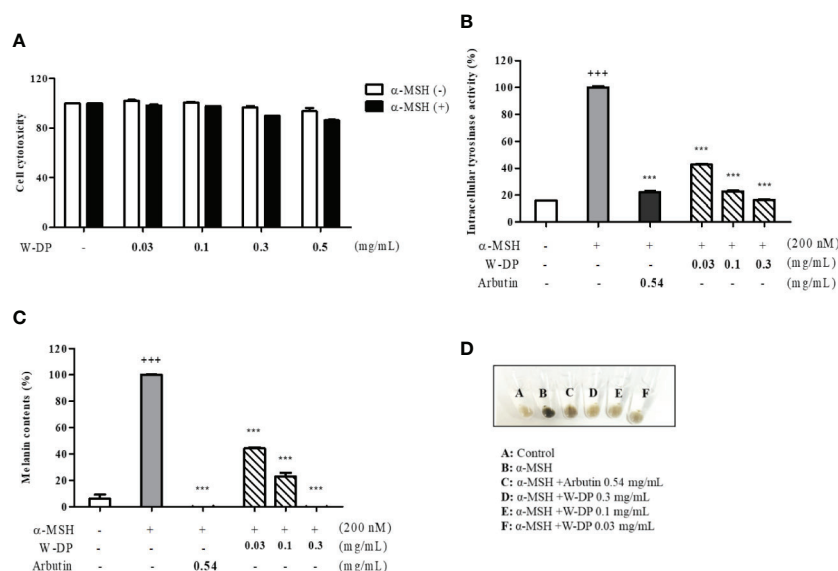


**FIGURE 1 |** Effect of W-DP on melanogenesis in  $\alpha$ -MSH-induced B16-F10 cells. B16-F10 cells pretreated with different concentrations of W-DP (0.03, 0.1, 0.3, 0.5 mg/ml) were incubated with or without  $\alpha$ -MSH (200 nM) for 72 h. **(A)** Cell viability was tested by MTS. **(B)** The cells were then lysed and quantified by using Bradford reagent. Equal amounts of the lysates were treated with L-DOPA (2 mg/ml) in 96-well plate at 37°C for 2 h. The production of DOPachrome was measured using an ELISA microplate reader at an absorbance of 490 nm. **(C)** The cells were dissolved in 1 N NaOH with 10% DMSO for 1 h at 60°C. Total melanin lysates were transferred to a 96-well plate and the optical absorbance was measured at 405 nm using an ELISA microplate reader. **(D)** Colors of the pellets indicated the change of melanogenesis from  $\alpha$ -MSH-induced B16-F10 cells. Data are expressed as the mean  $\pm$  SEM of three independent experiments. \*\*\* $P$  < 0.001 versus  $\alpha$ -MSH stimulation. \*\*\* $P$  < 0.001 versus the untreated control.

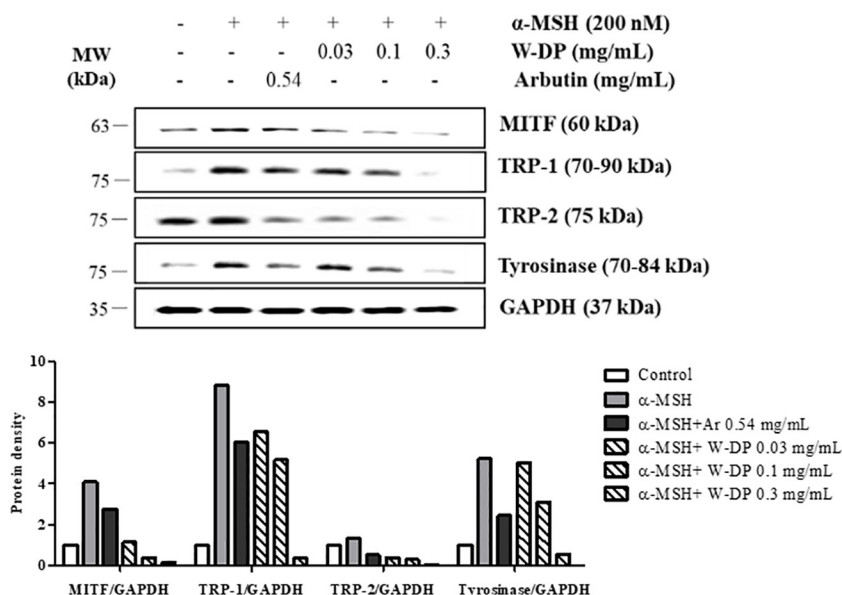


**FIGURE 2 |** Effect of *Dendropanax moribiferus* water extract (W-DP) on the expression of melanogenesis-related proteins in  $\alpha$ -MSH-induced B16-F10 cells. B16-F10 cells were pretreated with various concentrations of W-DP (0.03, 0.1, 0.3 mg/ml) or arbutin (0.54 mg/ml) for 2 h and then stimulated with  $\alpha$ -MSH (200 nM) for 24 h. The protein levels of MITF, tyrosinase, TRP-1, and TRP-2 were detected by Western blot analysis. Arbutin was used as a positive control, and GAPDH was used as the loading control. MITF, tyrosinase, TRP-1, and TRP-2 were analyzed and quantified using Azure Spot software.

manner. W-EA at the concentrations of ~0.001, 0.01, and 0.03 mg/ml showed 45%, 53%, and 65% inhibitory effects, respectively. W-EA was confirmed to be sufficiently effective even at a concentration of 0.01 mg/ml lower than 0.03 mg/ml. We showed the one concentration of W-EA results to compare the efficacy of single ingredients (data not shown). Of all isolated components, (10*E*)-9,16-dihydroxyoctadeca-10,17-dien-12,14-diynoate (DMW-1) and (10*E*)-(-)-10,17-octadecadiene-12,14-diyne-1,9,16-triol (DMW-2) significantly suppressed melanin contents in  $\alpha$ -MSH-induced B16-F10 cells (**Supplementary Table S2**). DMW-1 had a molecular formula of C<sub>19</sub>H<sub>26</sub>O<sub>4</sub> by HRESIMS ([M+NH<sub>4</sub>]<sup>+</sup> *m/z* 336.2167, calcd for 336.2175) and obtained as a viscous liquid (see **Supplementary Figure S2**). The <sup>1</sup>H-NMR spectrum showed signals for five olefinic protons at  $\delta$  6.34 (dd, *J* = 15.9, 5.7 Hz), 5.94 (ddd, *J* = 17.1, 10.2, 5.4 Hz), 5.79 (ddd, *J* = 15.9, 1.6, 0.9 Hz), 5.42 (d, *J* = 17.1 Hz), 5.22 (d, *J* = 10.2 Hz) and 4.96 (dd, *J* = 5.4, 1.1 Hz), two oxygenated methine protons at  $\delta$  4.96 (dd, *J* = 5.4, 1.1 Hz) and 4.13 (dtd, *J* = 7.2, 5.7, 1.6 Hz), and one methoxy proton at  $\delta$  3.76 (s). The <sup>13</sup>C-NMR spectrum revealed the presence of a carbonyl carbon at  $\delta$  176.0, four olefinic carbons at  $\delta$  151.9, 138.1, 116.6, and 108.4, four quaternary carbons at  $\delta$  82.2, 78.0, 74.0, and 70.6, two oxygen-bearing carbons at  $\delta$  72.4 and 64.0, and one methoxy carbon at  $\delta$  52.0 (see **Supplementary Figure S2** and **Table S1**). The above analyses suggested that DMW-1 should be a polyacetylene compound. The NMR results of DMW-1 were similar to those of the known DMW-2, except for a methoxy-carbonyl group (see **Supplementary Figure S3** and **Table S1**). DMW-1 and DMW-2 have a negative optical rotation value ([ $\alpha$ ] -38.0° and -32.6°), indicating the same relative configuration. The structures of DMW-1 and 2 components were identified by NMR spectroscopy and are shown in **Figure 3A**. DMW-1 and 2 were quantified in W-EA by LC/MS/MS analysis. The DMW-2 content (637 ng/ml) was dramatically higher than the DMW-1 content (87.1 ng/ml) in the W-EA fraction (**Figure 3B**). The

reaction times of DMW-1 and DMW-2 were 6.2 and 5.43 min, respectively.

## Inhibitory Effect of DMW-1 and 2 on Melanogenesis in $\alpha$ -MSH-Induced B16-F10 Cells

To examine the effects of DMW-1 and 2 on melanogenesis, B16-F10 cells were pretreated with two compounds and then stimulated with  $\alpha$ -MSH for 72 h. DMW-1 and 2 showed significant decreases in tyrosinase activity and melanin production. Notably, DMW-1 showed a better inhibitory effect than DMW-2 in B16-F10 cells. DMW-1 reduced the intracellular tyrosinase activity with an estimated IC<sub>50</sub> of 1.175  $\mu$ M and decreased the melanin accumulation with an estimated IC<sub>50</sub> of 1.221  $\mu$ M. The inhibitory effects of DMW-1 approached the effect of the reference compound arbutin (**Figures 4A, B**). As shown in **Figure 4C**, both compounds resulted in decreased melanin contents with lighter colors. Based on the above results, we studied whether DMW-1 and 2 could inhibit melanogenesis-related protein expression by Western blot analysis. DMW-1 and 2 remarkably decreased the protein expression levels of MITF, tyrosinase, and TRP-1 (**Figure 4D**). These results indicate that the anti-melanogenic effects of DMW-1 and 2 may be mediated by downregulating melanogenesis-related proteins.

## Effect of DMW-1 and 2 on the Phosphorylation Levels of PKA and CREB in $\alpha$ -MSH-Induced B16-F10 Cells

To investigate the effect of DMW-1 and 2 on cAMP-related signaling pathway, phosphorylation levels of PKA and CREB were analyzed by Western blot analysis. Compared to W-DP and W-EA, the phosphorylation levels of PKA and CREB proteins were markedly reduced by the treatment of DMW-1 and 2 in  $\alpha$ -MSH-induced B16-F10 cells. However, PKA and CREB levels

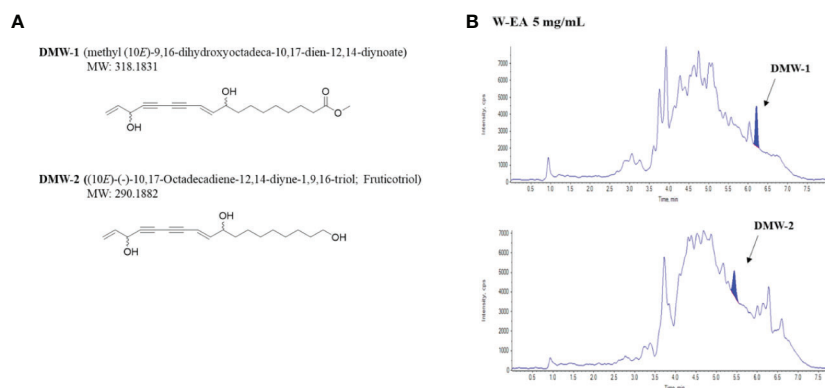


**FIGURE 3 |** Chemical structures and chromatograms of DMW-1 and 2. **(A)** Chemical structures of DMW-1 and 2 and **(B)** total ion chromatogram of DMW-1 and 2 in W-EA at 5 mg/ml. W-EA, ethyl acetate fraction.

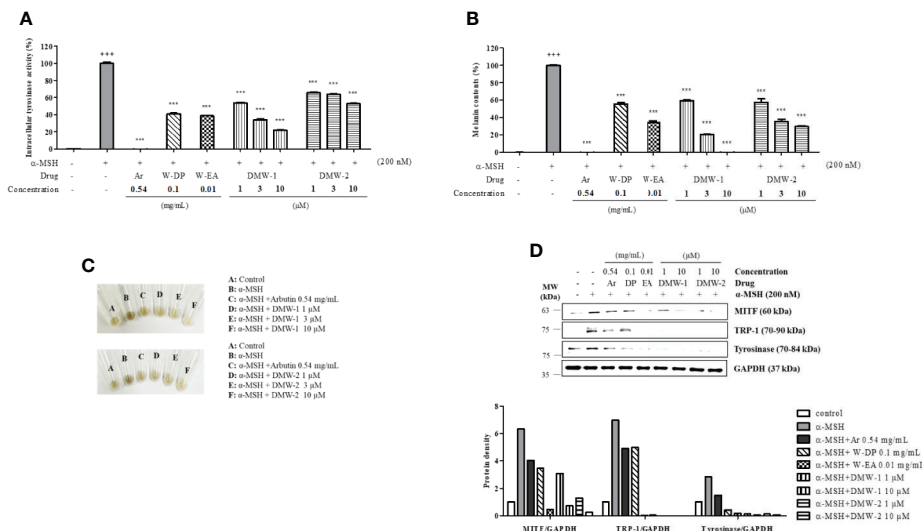


**FIGURE 4 |** Effects of DMW-1 and 2 on melanogenesis in  $\alpha$ -MSH-induced B16-F10 cells. B16-F10 cells ( $1 \times 10^5$  cells/well) were incubated into six-well plate at 37°C overnight. B16-F10 cells were pretreated with W-DP (0.1 mg/ml), W-EA (0.01 mg/ml), DMW-1 (1, 3, 10  $\mu$ M), DMW-2 (1, 3, 10  $\mu$ M), or arbutin (0.54 mg/ml) for 2 h prior to stimulation with  $\alpha$ -MSH (200 nM) for 72 h. **(A)** Equal amounts of the lysates were treated with L-DOPA (2 mg/ml) at 37°C for 2 h. The production of DOPachrome was measured at an absorbance of 490 nm. **(B)** The cells were dissolved in 1 N NaOH with 10% DMSO for 1 h at 60°C. Total melanin lysates were measured at an absorbance of 405 nm. **(C)** Colors of the pellets indicated the change of melanogenesis from  $\alpha$ -MSH-induced B16-F10 cells. **(D)** The expression levels of MITF, tyrosinase, and TRP-1 were determined by Western blot analysis, and the protein bands were quantified using Azure Spot software. GAPDH was used as the loading control. Data are expressed as the mean  $\pm$  SEM of three independent experiments. \*\*\* $P < 0.001$  versus  $\alpha$ -MSH stimulation. +++ $P < 0.001$  versus the untreated control. Ar, arbutin; W-DP, *D. moribiferus* water extract; W-EA, ethyl acetate fraction.

remained unchanged. DMW-1 showed a slightly greater inhibitory effect on the phosphorylation levels of PKA/CREB than DMW-2 in B16-F10 cells (Figure 5A). Moreover, the cAMP level accumulated in the lysates was evaluated using competitive ELISA. As shown in Figure 5B, DMW-1 decreased intracellular cAMP levels in a dose-dependent manner.

## Effect of DMW-1 and 2 on the Phosphorylation of p38 in $\alpha$ -MSH-Stimulated B16-F10 Cells

To further investigate whether DMW-1 and 2 exert anti-melanogenic effect through regulating the MAPK pathway, the phosphorylation levels of MAPKs were assayed by Western blot

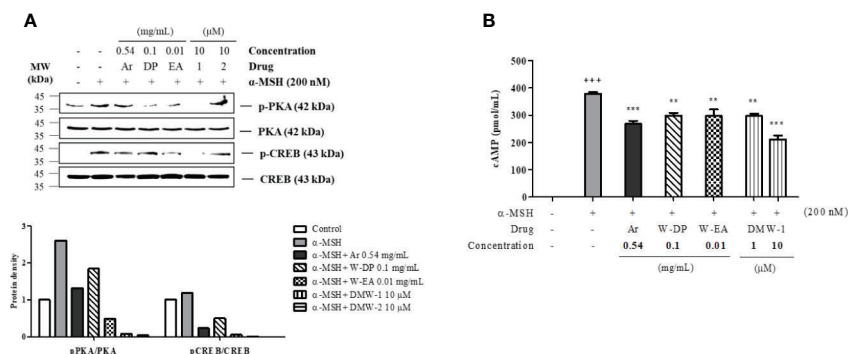


**FIGURE 5 |** Effects of DMW-1 and 2 on the phosphorylation levels of PKA and CREB in  $\alpha$ -MSH-induced B16-F10 cells. The cells were pretreated with W-DP (0.1 mg/ml), W-EA (0.01 mg/ml), DMW-1 (10  $\mu$ M), DMW-2 (10  $\mu$ M), or arbutin (0.54 mg/ml) for 2 h before stimulation with  $\alpha$ -MSH (200 nM) for 24 h. **(A)** The p-PKA and p-CREB protein levels were determined by Western blot analysis, and normalized to total PKA and CREB. The phosphorylation levels of PKA and CREB were analyzed and quantified using Azure Spot software. **(B)** The lysates were collected and cAMP levels were tested by ELISA. Data are expressed as the mean  $\pm$  SEM of three independent experiments. \*\* $P < 0.01$ , and \*\*\* $P < 0.001$  versus  $\alpha$ -MSH stimulation. +++ $P < 0.001$  versus the untreated control. Ar, arbutin; W-DP, *D. moribiferus* water extract; W-EA, ethyl acetate fraction.



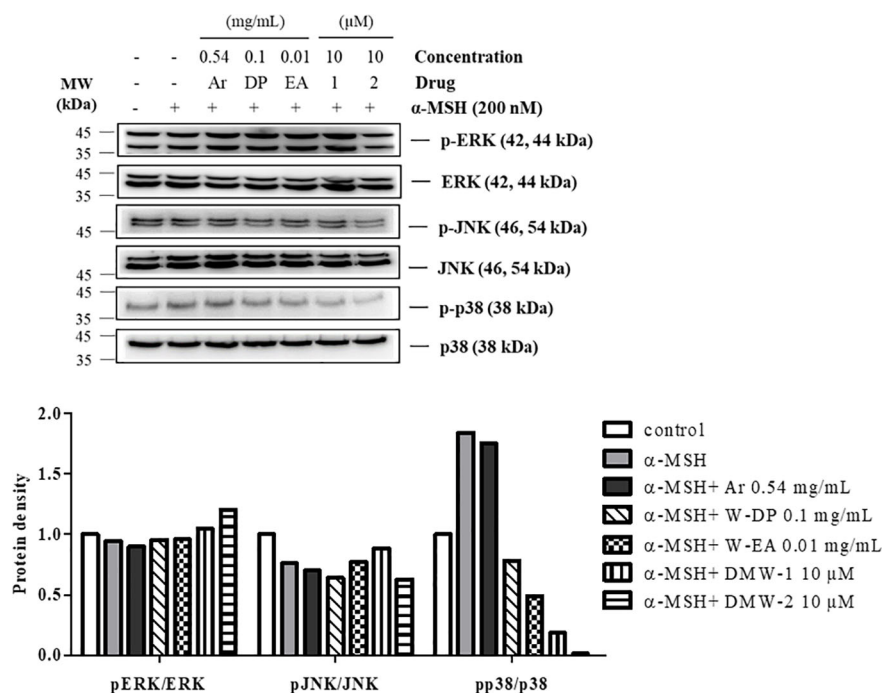


**FIGURE 6 |** Effect of DMW-1 and 2 on p38 phosphorylation in  $\alpha$ -MSH-stimulated B16-F10 cells. B16-F10 cells were pretreated with W-DP (0.1 mg/ml), W-EA (0.01 mg/ml), DMW-1 (10  $\mu$ M), DMW-2 (10  $\mu$ M), or arbutin (0.54 mg/ml) for 2 h before stimulation with  $\alpha$ -MSH (200 nM) for 24 h. Phosphorylation levels of ERK, JNK, and p38 were determined by Western blot analysis. Equal levels of proteins were confirmed using total ERK, JNK, and p38 antibodies. The protein bands were analyzed and quantified using Azure Spot software. Ar, arbutin; W-DP, *D. morbiferus* water extract; W-EA, ethyl acetate fraction.

analysis. As shown in **Figure 6**, DMW-1 and 2 significantly decreased p38 phosphorylation. In contrast, the phosphorylation levels of ERK and JNK proteins showed no increase after treatment with DMW-1 and 2 in B16-F10 cells. These data indicate that the anti-melanogenic activity of DMW-1 is associated with the decrease of p-p38 as well as p-CREB.

## DISCUSSION

There is an increasing interest in medicinal plants and their bioactive compounds for novel whitening therapies in recent years. Various cosmetic ingredients such as arbutin, kojic acid, and vitamin C have been used to inhibit hyperpigmentation (Ng

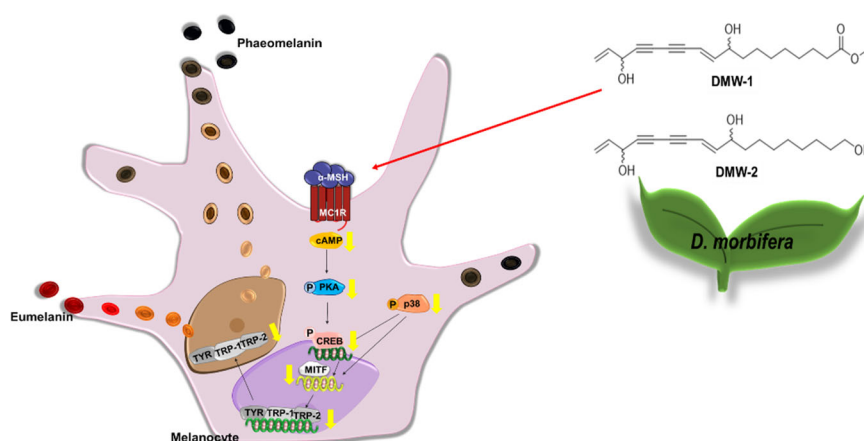


**FIGURE 7 |** Underlying potential mechanism of anti-melanogenesis of *D. morbiferus*. The anti-melanogenesis effect of *D. morbiferus* might be associated with downregulation of MITF. *D. morbiferus* and its active component DMW-1 significantly inhibited melanin formation by inhibition of melanogenesis-related proteins such as tyrosinase, TRP-1, and TRP-2. *D. morbiferus* and DMW-1 show multifunctional inhibitory activities on melanogenesis pathways via PKA/CREB- and p38 MAPK-mediated MITF degradation.

et al., 2014). We have studied to identify herbal medicines showing anti-melanogenic effects without cytotoxicity. To the best of our knowledge, this is the first report to demonstrate the anti-melanogenic effect of *D. morbiferus* leaves and its new single constituents. In this study, we investigated the underlying mechanisms of *D. morbiferus*-mediated anti-melanogenic effects and identified the active compounds. Interestingly, *D. morbiferus* significantly decreased melanin content in  $\alpha$ -MSH-induced B16-F10 cells (**Figure 1**). *D. morbiferus* did not show any cytotoxicity to B16-F10 cells (**Figure 1A**). Melanogenesis regulation is under complex control. Melanin synthesis can be regulated by the direct suppression of tyrosinase and by the downregulation of tyrosinase or other melanogenesis-related proteins. Here, we have investigated the molecular mechanisms of *D. morbiferus* on anti-melanogenic effects focusing on tyrosinase, TRP-1, TRP-2, MITF, cAMP, PKA/CREB, and p38 MAPK pathways. Interestingly, *D. morbiferus* markedly reduced the expression levels of MITF, TRP-1, TRP-2, and tyrosinase in a dose-dependent manner (**Figure 2**). Next, we isolated 22 components from ethyl acetate fraction of *D. morbiferus*. Of all the isolated components, DMW-1 and 2 significantly inhibited melanin contents in  $\alpha$ -MSH-induced B16-F10 cells (**Supplementary Table S2**). DMW-1 and 2 are polyacetylene-based compounds with similar structures (**Figure 3**), and their structural explanations are provided in the supplementary data (**Supplementary Figures S2 and S3 and Table S1**). Of all polyacetylene-based compounds, several studies have reported that (9Z,16S)-16-hydroxy-9,17-octadecadiene-12,14-dienoic acid has anti-obesity, anti-osteoclastogenic, antioxidant, anti-inflammatory, and anticomplement activities (Park et al., 2004; Kang et al., 2018; Kim et al., 2018a). The beneficial effect of (2Z,8Z)-matricaria acid methyl ester has been reported to inhibit tyrosinase activity (Luo et al., 2009). In this study, we confirmed that DMW-1 and 2 dramatically suppressed tyrosinase activity and melanin overproduction. Consistently, the expression levels of MITF, tyrosinase, and TRP-1 were remarkably decreased by DMW-1 and 2 (**Figure 4**). We found that DMW-1 and 2 dramatically inhibited melanogenesis through the downregulation of MITF and tyrosinase. DMW-1 showed significant inhibitory effect on melanogenesis, which indicated that the active compound was abundant in *D. morbiferus*. CREB regulates the expression of MITF in melanosomes and the phosphorylation of CREB is regulated by the activation of cAMP/PKA cascades that are known to play main roles in melanin synthesis (Pillaiyar et al., 2017). The inhibitory effect of DMW-1 on the phosphorylation levels of PKA and CREB was slightly greater than DMW-2 in B16-F10 cells, and DMW-1 significantly decreased intracellular cAMP levels in a dose-

dependent manner (**Figure 5**). Next, we examined the role of the MAPK signaling pathway in the effects of two chemical constituents on melanogenesis. DMW-1 and 2 significantly decreased p38 phosphorylation in B16-F10 cells. In contrast, the phosphorylation levels of ERK and JNK were not increased by the treatment of DMW-1 and 2 in B16-F10 cells (**Figure 6**). These results suggested that the PKA/CREB and p38-mediated signaling pathways were involved in melanin production and tyrosinase activity, which were affected by DMW-1. These results indicate that DMW-1 isolated from *D. morbiferus* has anti-melanogenic effect via PKA/CREB- and p38 MAPK-mediated MITF degradation.

In conclusion, *D. morbiferus* and its active component DMW-1 significantly inhibited melanin formation by inhibition of melanogenesis-related proteins such as tyrosinase, TRP-1, and TRP-2, without any cytotoxicity. *D. morbiferus* and DMW-1 show multifunctional inhibitory activities on melanogenesis pathways via PKA/CREB- and p38 MAPK-mediated MITF degradation (**Figure 7**). These results suggested that *D. morbiferus* and DMW-1 might be potential ingredients for application in cosmetics and therapeutic agents for skin hyperpigmentation disorders.

## DATA AVAILABILITY STATEMENT

The datasets generated for this study are available on request to the corresponding authors.

## AUTHOR CONTRIBUTIONS

JP was involved in the project design, carried out major experiments, and drafted the manuscript. SY and HL participated to extract the active compounds from *D. morbiferus* and reviewed the protocol. RG wrote and revised the manuscript. YRK and YHK conceived the project, provided reagents, and conceptual design, and wrote the manuscript. All authors read and approved the manuscript finally.

## SUPPLEMENTARY MATERIAL

The Supplementary Material for this article can be found online at: <https://www.frontiersin.org/articles/10.3389/fphar.2020.00507/full#supplementary-material>

## REFERENCES

- Birhanu, B. T., Kim, J. Y., Hossain, M. A., Choi, J. W., Lee, S. P., and Park, S. C. (2018). An in vivo immunomodulatory and anti-inflammatory study of fermented *Dendropanax morbiferus* Leveille leaf extract. *BMC Complement Altern. Med.* 18, 1-8. doi: 10.1186/s12906-018-2282-x
- Brenner, M., and Hearing, V. J. (2008). The protective role of melanin against UV damage in human skin. *Photochem. Photobiol.* 84 (3), 539-549. doi: 10.1111/j.1751-1097.2007.00226.x
- Chan, C. F., Huang, C. C., Lee, M. Y., and Lin, Y. S. (2014). Fermented broth in tyrosinase- and melanogenesis inhibition. *Molecules* 19 (9), 13122-13135. doi: 10.3390/molecules190913122

- Cho, S. S., Song, S. H., Choi, C. Y., Park, K. M., Shim, J. H., and Park, D. H. (2018). Optimization of the extraction conditions and biological evaluation of *Dendropanax moribifera* H. Lev as an anti-hyperuricemic source. *Molecules* 23 (12), 3313–3320. doi: 10.3390/molecules23123313
- Choo, G. S., Lim, D. P., Kim, S. M., Yoo, E. S., Kim, S. H., Kim, C. H., et al. (2019). Anti-inflammatory effects of *Dendropanax moribifera* in lipopolysaccharide-stimulated RAW264.7 macrophages and in an animal model of atopic dermatitis. *Mol. Med. Rep.* 19, 2087–2096. doi: 10.3892/mmr.2019.9887
- Costin, G. E., and Hearing, V. J. (2007). Human skin pigmentation: melanocytes modulate skin color in response to stress. *FASEB J.* 21 (4), 976–994. doi: 10.1096/fj.06-6649rev
- D'Orazio, J., Jarrett, S., Amaro-Ortiz, A., and Scott, T. (2013). UV radiation and the skin. *Int. J. Mol. Sci.* 14 (6), 12222–12248. doi: 10.3390/ijms140612222
- Deng, J. X., Kim, C. S., Oh, E. S., and Yu, S. H. (2010). First report of foliar blight on *dendropanax moribifera* caused by *alternaria panax*. *Mycobiology* 38 (4), 316–320. doi: 10.4489/MYCO.2010.38.4.316
- Jeong, B. S., Jo, J. S., Pyeo, B. S., and Hwang, B. (1995). Studies on the distribution of *Dendropanax moribifera* and component analysis of the golden lacquer. *Korean J. Biotechnol. Bioeng.* 10 (4), 393–400.
- Kang, M. J., Kwon, E. B., Ryu, H. W., Lee, S., Lee, J. W., Kim, D. Y., et al. (2018). Polyacetylene from *Dendropanax moribifera* alleviates diet-induced obesity and hepatic steatosis by activating AMPK signaling pathway. *Front. Pharmacol.* 9, 537–547. doi: 10.3389/fphar.2018.00537
- Kim, E. H., Jo, C. S., Ryu, S. Y., Kim, S. H., and Lee, J. Y. (2018a). Anti-osteoclastogenic diacetylenic components of *Dendropanax moribifera*. *Arch. Pharm. Res.* 41 (5), 506–512. doi: 10.1007/s12272-018-1033-3
- Kim, J. Y., Lee, E. J., Ahn, Y., Park, S., Kim, S. H., and Oh, S. H. (2018b). A chemical compound from fruit extract of *Juglans mandshurica* inhibits melanogenesis through p-ERK-associated MITF degradation. *Phytomedicine* 57, 57–64. doi: 10.1016/j.phymed.2018.12.007
- Lee, B. H., Choi, J. H., and Kim, H. J. (2005). Curing and thermal behaviors of Korean *Dendropanax Lacquer* made by acetone and wine spirit extraction methods. *Prog. Org. Coatings* 52 (3), 241–245. doi: 10.1016/j.porgcoat.2005.01.002
- Lee, J. W., Kim, K. S., An, H. K., Kim, C. H., Moon, H. I., and Lee, Y. C. (2013). Dendropanoxide induces autophagy through ERK1/2 activation in MG-63 human osteosarcoma cells and autophagy inhibition enhances dendropanoxide-induced apoptosis. *PLoS One* 8 (12), 83611–83617. doi: 10.1371/journal.pone.0083611
- Lee, S. Y., Choi, E. J., Bae, D. H., Lee, D. W., and Kim, S. O. (2015). Effects of 1-tetradecanol and  $\beta$ -sitosterol Isolated from *Dendropanax moribifera* Lev. on Skin Whitening, Moisturizing and Preventing Hair Loss. *J. Soc. Cosmet. Sci. Korea* 41, 73–83. doi: 10.15230/SCSK.2015.41.1.73
- Li, H. X., Park, J. U., Su, X. D., Kim, K. T., Kang, J. S., Kim, Y. R., et al. (2018). Identification of anti-melanogenesis constituents from *Morus alba* L. Leaves. *Molecules* 23 (10), 2559–2569. doi: 10.3390/molecules23102559
- Lim, L., Yun, J. J., Jeong, J. E., Wi, A. J., and Song, H. (2015). Inhibitory effects of nano-extract from *Dendropanax moribifera* on proliferation and migration of vascular smooth muscle cells. *J. Nanosci. Nanotechnol.* 15 (1), 116–119. doi: 10.1166/jnn.2015.8382
- Liu, J. J., and Fisher, D. E. (2010). Lighting a path to pigmentation: mechanisms of MITF induction by UV. *Pigment. Cell. Melanoma. Res.* 23 (6), 741–745. doi: 10.1111/j.1755-148X.2010.00775.x
- Luo, L. H., Kim, H. J., Nguyen, D. H., Lee, H. B., Lee, N. H., and Kim, E. K. (2009). Depigmentation of melanocytes by (2Z,8Z)-matricaria acid methyl ester isolated from *Erigeron breviscapus*. *Biol. Pharm. Bull.* 32 (6), 1091–1094. doi: 10.1248/bpb.32.1091
- Ng, L. T., Lin, L. T., Chen, C. L., Chen, H. W., Wu, S. J., and Lin, C. C. (2014). Anti-melanogenic effects of delta-tocotrienol are associated with tyrosinase-related proteins and MAPK signaling pathway in B16 melanoma cells. *Phytomedicine* 21 (7), 978–983. doi: 10.1016/j.phymed.2014.03.003
- Park, Y. M., and Han, J. S. (2016). A study on the utilization of *Dendropanax moribifera* Lev. leaf extract for material of functional cosmetics and hair growth products. *Asian J. Beauty Cosmetol.* 14 (3), 277–288. doi: 10.20402/ajbc.2016.0051
- Park, B. Y., Min, B. S., Oh, S. R., Kim, J. H., Kim, T. J., Kim, D. H., et al. (2004). Isolation and anticomplement activity of compounds from *Dendropanax moribifera*. *J. Ethnopharmacol.* 90 (2–3), 403–408. doi: 10.1016/j.jep.2003.11.002
- Park, S. E., Sapkota, K., Choi, J. H., Kim, M. K., Kim, Y. H., Kim, K. M., et al. (2014). Rutin from *Dendropanax moribifera* leveille protects human dopaminergic cells against rotenone induced cell injury through inhibiting JNK and p38 MAPK signaling. *Neurochem. Res.* 39 (4), 707–718. doi: 10.1007/s11064-014-1259-5
- Park, J. U., Kang, B. Y., Lee, H. J., Kim, S., Bae, D., Park, J. H., et al. (2017). Tetradecanol reduces EL-4 T cell growth by the down regulation of NF-kappaB mediated IL-2 secretion. *Eur. J. Pharmacol.* 799, 135–142. doi: 10.1016/j.ejphar.2017.02.002
- Park, J. U., Kang, B. Y., and Kim, Y. R. (2018a). Ethyl acetate fraction from *Dendropanax moribifera* leaves increases T cell growth by upregulating NF-AT-mediated IL-2 secretion. *Am. J. Chin. Med.* 46 (2), 453–467. doi: 10.1142/S0192415X18500234
- Park, S. Y., Karthivashan, G., Ko, H. M., Cho, D. Y., Kim, J., Cho, D. J., et al. (2018b). Aqueous extract of *Dendropanax moribifera* leaves effectively alleviated neuroinflammation and behavioral impediments in MPTP-induced parkinson's mouse model. *Oxid. Med. Cell. Longev.* 2018, 3175214–3175228. doi: 10.1155/2018/3175214
- Pillaiyar, T., Manickam, M., and Jung, S. H. (2017). Downregulation of melanogenesis: drug discovery and therapeutic options. *Drug Discovery Today* 22 (2), 282–298. doi: 10.1016/j.drudis.2016.09.016
- Pillaiyar, T., Namasiyayam, V., Manickam, M., and Jung, S. H. (2018). Inhibitors of melanogenesis: an updated review. *J. Med. Chem.* 61 (17), 7395–7418. doi: 10.1021/acs.jmedchem.7b00967
- Riley, P. A. (2003). Melanogenesis and melanoma. *Pigment. Cell. Res.* 16 (5), 548–552. doi: 10.1034/j.1600-0749.2003.00069.x
- Slominski, A., Moellmann, G., Kuklinska, E., Bomirski, A., and Pawelek, J. (1988). Positive regulation of melanin pigmentation by two key substrates of the melanogenic pathway, L-tyrosine and L-dopa. *J. Cell. Sci.* 89, 287–296.
- Slominski, A., Zmijewski, M. A., and Pawelek, J. (2012). L-tyrosine and L-dihydroxyphenylalanine as hormone-like regulators of melanocyte functions. *Pigment. Cell. Melanoma. Res.* 25 (1), 14–27. doi: 10.1111/j.1755-148X.2011.00898.x
- Song, J. H., Kang, H. B., Kim, J. H., Kwak, S., Sung, G. J., Park, S. H., et al. (2018). Antiobesity and cholesterol-lowering effects of *Dendropanax moribifera* water extracts in mouse 3T3-L1 Cells. *J. Med. Food.* 21 (8), 793–800. doi: 10.1089/jmf.2017.4154
- Sun, S., Kee, H. J., Jin, L., Ryu, Y., Choi, S. Y., Kim, G. R., et al. (2018a). Gentisic acid attenuates pressure overload-induced cardiac hypertrophy and fibrosis in mice through inhibition of the ERK1/2 pathway. *J. Cell. Mol. Med.* 22 (12), 5964–5977. doi: 10.1111/jcmm.13869
- Sun, S., Li, T., Jin, L., Piao, Z. H., Liu, B., Ryu, Y., et al. (2018b). *Dendropanax moribifera* prevents cardiomyocyte hypertrophy by inhibiting the Sp1/GATA4 pathway. *Am. J. Chin. Med.* 46 (5), 1021–1044. doi: 10.1142/S0192415X18500532
- Wu, L. C., Lin, Y. Y., Yang, S. Y., Weng, Y. T., and Tsai, Y. T. (2011). Antimelanogenic effect of c-phycocyanin through modulation of tyrosinase expression by upregulation of ERK and downregulation of p38 MAPK signaling pathways. *J. Biomed. Sci.* 18, 74–84. doi: 10.1186/1423-0127-18-74
- Yu, H. Y., Kim, K. S., Lee, Y. C., Moon, H. I., and Lee, J. H. (2012). Oleifolioside A, a new active compound, attenuates LPS-stimulated iNOS and COX-2 expression through the downregulation of NF-kappa B and MAPK activities in RAW 264.7 macrophages. *Evid. Based. Complement Alternat. Med.* 2012, 1–8. doi: 10.1155/2012/637512

**Conflict of Interest:** The authors declare that the research was conducted in the absence of any commercial or financial relationships that could be construed as a potential conflict of interest.

Copyright © 2020 Park, Yang, Guo, Li, Kim and Kim. This is an open-access article distributed under the terms of the Creative Commons Attribution License (CC BY). The use, distribution or reproduction in other forums is permitted, provided the original author(s) and the copyright owner(s) are credited and that the original publication in this journal is cited, in accordance with accepted academic practice. No use, distribution or reproduction is permitted which does not comply with these terms.

# Advantages of publishing in Frontiers



## OPEN ACCESS

Articles are free to read  
for greatest visibility  
and readership



## FAST PUBLICATION

Around 90 days  
from submission  
to decision



## HIGH QUALITY PEER-REVIEW

Rigorous, collaborative,  
and constructive  
peer-review



## TRANSPARENT PEER-REVIEW

Editors and reviewers  
acknowledged by name  
on published articles

## Frontiers

Avenue du Tribunal-Fédéral 34  
1005 Lausanne | Switzerland

**Visit us:** [www.frontiersin.org](http://www.frontiersin.org)

**Contact us:** [info@frontiersin.org](mailto:info@frontiersin.org) | +41 21 510 17 00



## REPRODUCIBILITY OF RESEARCH

Support open data  
and methods to enhance  
research reproducibility



## DIGITAL PUBLISHING

Articles designed  
for optimal readership  
across devices



## FOLLOW US

[@frontiersin](https://twitter.com/frontiersin)



## IMPACT METRICS

Advanced article metrics  
track visibility across  
digital media



## EXTENSIVE PROMOTION

Marketing  
and promotion  
of impactful research



## LOOP RESEARCH NETWORK

Our network  
increases your  
article's readership